DEVELOPMENTS IN PETROLEUM SCIENCE 18 B

# production and transport of oil and gas

SECOND COMPLETELY REVISED EDITION
PART B: gathering and transport

A.P. SZILAS

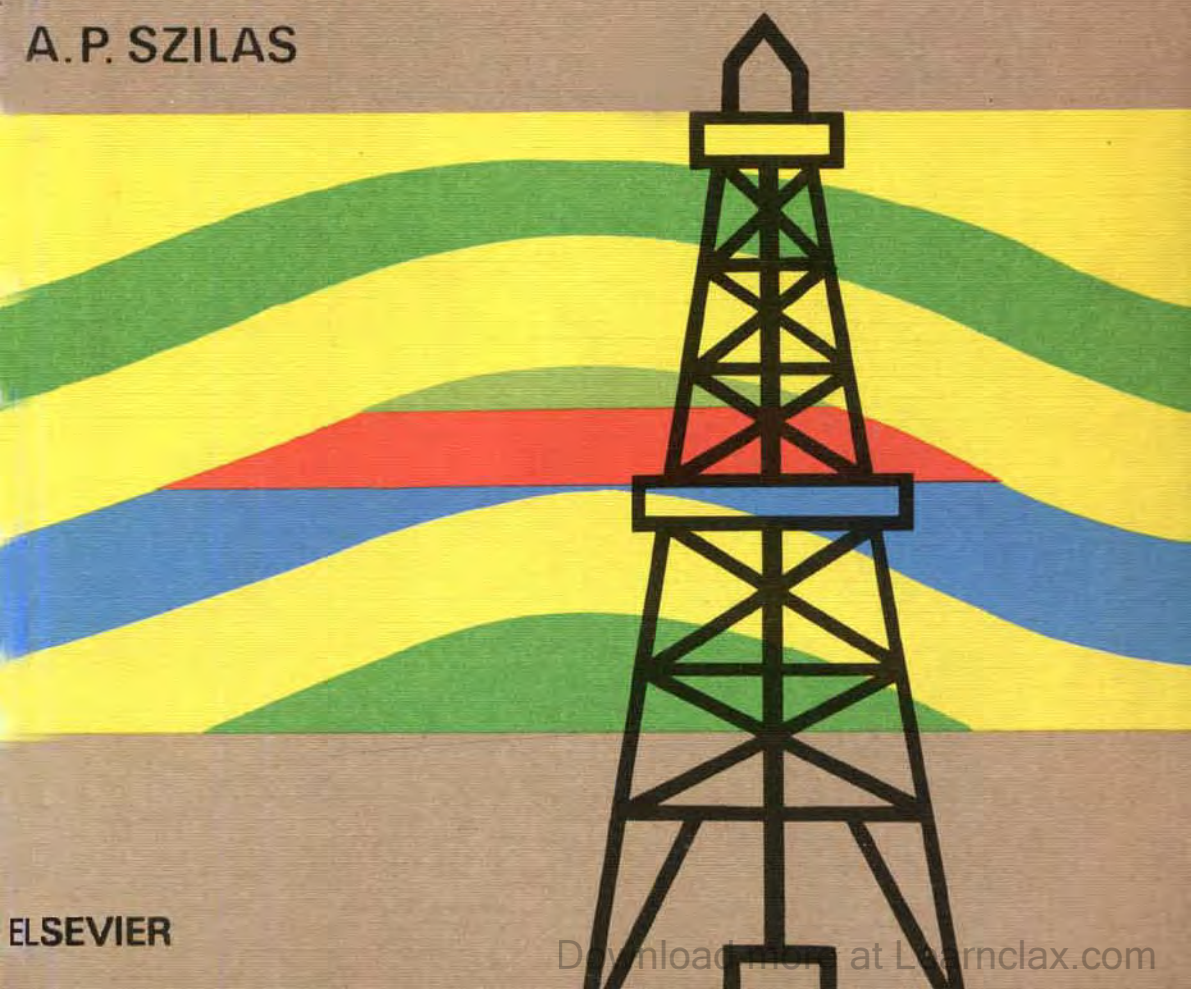

ELSEVIER

Developments in Petroleum Science, 18 B

# PRODUCTION AND TRANSPORT OF OIL AND GAS

## Second completely revised edition

### PART B

### Gathering and transportation

## DEVELOPMENTS IN PETROLEUM SCIENCE

**Advisory Editor: G. V. Chilingarian**

1. A. GENE COLLINS
GEOCHEMISTRY OF OILFIELD WATERS

2 W. H. FERTL
ABNORMAL FORMATION OF PRESSURES

3 A. P. SZILAS
PRODUCTION AND TRANSPORT OF OIL AND GAS

4 C. E. B. CONYBEARE
GEOMORPHOLOGY OF OIL AND GAS FIELDS
IN SANDSTONE BODIES

5 T. F. YEN and G. V. CHILINGARIAN (Editors)
OIL SHALE

6 D. W. PEACEMAN
FUNDAMENTALS OF NUMERICAL RESERVOIR SIMULATION

7 G. V. CHILINGARIAN and T. F. YEN (Editors)
BITUMENS, ASPHALTS AND TAR SANDS

8 L. P. DAKE
FUNDAMENTALS OF RESERVOIR ENGINEERING

9 K. MAGARA
COMPACTION AND FLUID MIGRATION

10 M. T. SILVIA and E. A. ROBINSON
DECONVOLUTION OF GEOPHYSICAL TIME SERIES IN THE
EXPLORATION FOR OIL AND NATURAL GAS

11 G. V. CHILINGARIAN and P. VORABUTR
DRILLING AND DRILLING FLUIDS

12 T. VAN GOLF-RACHT
FRACTURED HYDROCARBON-RESERVOIR ENGINEERING

13 F. JOHN FAYERS (Editor)
ENHANCED OIL RECOVERY

14 G. MOZES (Editor)
PARAFFIN PRODUCTS

15 O. SERRA
FUNDAMENTALS OF WELL-LOG INTERPRETATION
1. The acquisition of logging data

16 R. E. CHAPMAN
PETROLEUM GEOLOGY

17 E. C. DONALDSON, G. V. CHILINGARIAN and T. F. YEN
ENHANCED OIL RECOVERY
1. Fundamentals and Analyses

18 A. P. SZILAS
PRODUCTION AND TRANSPORT OF OIL AND GAS
Second completely revised edition

A. Flow mechanics and production
B. Gathering and transportation

Developments in Petroleum Science, 18 B

# PRODUCTION AND TRANSPORT OF OIL AND GAS

## Second completely revised edition

## PART B

### Gathering and transportation

by

**A. P. SZILAS**

*Professor of Petroleum Engineering*
*Petroleum Engineering Department*
*Miskolc Technical University for*
*Heavy Industries, Hungary*

**ELSEVIER**

**Amsterdam–Oxford–New York–Tokyo 1986**

Joint edition published by

Elsevier Science Publishers, Amsterdam, The Netherlands
and
Akadémiai Kiadó, the Publishing House of the Hungarian Academy of Sciences,
Budapest, Hungary

First English edition 1975
Translated by B. Balkay

Second revised and enlarged edition 1985 and 1986
Translated by B. Balkay and Á. Kiss

The distribution of this book is being handled by the following
publishers

for the U.S.A. and Canada

Elsevier Science Publishing Co., Inc.
52 Vanderbilt Avenue,
New York, New York 10017, U.S.A.

for the East European Countries, Korean People's Republic, Cuba, People's Republic of
Vietnam and Mongolia
Kultura Hungarian Foreign Trading Co., P.O.Box 149, H-1389 Budapest, Hungary

for all remaining areas

Elsevier Science Publishers
Sara Burgerhartstraat 25,
P.O.Box 211, 1000 AE Amsterdam, The Netherlands

**Library of Congress Cataloging Data**

Szilas, A. Pál.
Production and transport of oil and gas.

(Developments in petroleum science; 18B-)
Translation of Kőolaj és földgáztermelés.
1. Petroleum engineering. 2. Petroleum–Pipe lines.
3. Gas, Natural–Pipe lines. I. Title. II. Series.
TN870.S9413 1984 622'.338 84-13527
ISBN 0-444-99565-X (V. 2)
ISBN 0-444-99564-1 (Series)



Printed in Hungary

# Contents

This Page Intentionally Left Blank

## List of symbols and units for frequently used physical quantities

| | | |
|---|---|---|
| $a$ | temperature distribution or diffusivity factor | $m^2/s$ |
| $c$ | specific heat | |
| | per unit mass | J/(kg K) |
| | per mole mass | J/(kmole K) |
| $c$ | compressibility | $m^2/N$ |
| $d$ | diameter | m |
| $e$ | figure of merit of pipe | – |
| $g$ | acceleration of gravity | $m^2/s$ |
| $h$ | head loss of flow | m |
| $h$ | height, elevation difference | m |
| $h$ | specific enthalpy | J/kg |
| $k$ | equivalent absolute roughness | m |
| $k$ | specific cost of transportation | Ft/(kg km) |
| $k$ | heat transfer factor per unit length of pipe | W/(m K) |
| $k^*$ | heat transfer factor per unit surface | $W/(m^2 K)$ |
| $k_r$ | reflectivity factor | – |
| $k_{tr}$ | transmissivity factor | – |
| $l$ | length, distance from the origin | m |
| $n$ | number of moles of system | – |
| $n$ | exponent of exponential law | – |
| $p$ | pressure | Pa |
| $p_{pr}$ | pseudoreduced pressure | – |
| $p_r$ | reduced pressure | – |
| $q$ | volumetric flow rate | $m^3/s$ |
| $q_m$ | mass flow rate | kg/s |
| $r$ | radius | m |
| $s$ | wall thickness of pipe | m |
| $s$ | mixed slug length | m |
| $s_v$ | valve travel | m |
| $t$ | time, duration, period | s |

| | | |
|---|---|---|
| $v$ | flow velocity | m/s |
| $v$ | specific construction cost | Ft/m |
| $w$ | acoustic propagation velocity | m/s |
| $x_i$ | mole fraction of $i$th component of liquid | – |
| $y_i$ | mole fraction of $i$th component of gas | – |
| $z$ | compressibility factor | – |
| $z$ | geodetic head | m |
| $z_i$ | mole fraction of $i$th component of liquid-gas mixture | – |
| $A$ | cross-sectional area | $m^2$ |
| $A$ | depreciation cost | Forint/year |
| $D$ | rate of shear | 1/s |
| $E$ | modulus of elasticity | $N/m^2$ |
| $F$ | force, weight | N |
| $H$ | head capacity of pump | m |
| $K$ | cost | Forint/year |
| $K_i$ | equilibrium ratio of $i$th component in liquid-gas system | – |
| $L$ | length | m |
| $M$ | torque | N m |
| $M$ | molar mass | kg/kmole |
| $N$ | dimensionless number | – |
| $P$ | power | W |
| $Q$ | heat | J |
| $R$ | universal molar gas constant | J/(kmole K) |
| $R$ | volumetric ratio | – |
| $S$ | sign (flow direction indicator) | – |
| $S$ | mass fraction | kg/kg |
| $T$ | temperature | K, °C |
| $T_{pr}$ | pseudoreduced temperature | – |
| $T_r$ | reduced temperature | – |
| $V$ | volume | $m^3$ |
| $V$ | specific volume | $m^3/kg$ |
| $W$ | work, energy | J |
| $W'$ | specific energy content | J/N |
| $\alpha$ | flow constant | – |
| $\alpha_1$ | internal convection factor | $W/(m^2\ K)$ |
| $\alpha_2$ | external heat-transfer factor | $W/(m^2\ K)$ |
| $\alpha_T$ | temperature coefficient of oil density | $kg/(m^3\ K)$ |
| $\alpha_p$ | pressure coefficient of oil density | $s^2/m^2$ |
| $\varepsilon$ | volumetric rate | – |
| $\gamma$ | specific weight | $N/m^3$ |

| | | |
|---|---|---|
| $\eta$ | efficiency | – |
| $\kappa$ | ratio of specific heats | – |
| $\iota$ | melting heat of paraffin | J/kg |
| $\lambda$ | pipe friction factor | – |
| $\lambda$ | thermal conductivity factor | W/(m K) |
| $\mu$ | dynamic viscosity | Pa s |
| $\nu$ | kinematic viscosity | $m^2/s$ |
| $\xi$ | flow resistance factor (dimensionless pressure gradient) | – |
| $\rho$ | density | $kg/m^3$ |
| $\sigma$ | stress | $N/m^2$ |
| $\sigma_F$ | yield strength (of solid) | $N/m^2$ |
| $\sigma_B$ | tensile strength | $N/m^2$ |
| $\tau$ | shear stress | $N/m^2$ |
| $\Phi$ | heat flow | W |
| $\Phi^*$ | specific heat flow | W/m |

## FREQUENTLY USED SUBSCRIPTS

| Subscript | | Meaning | Example |
|---|---|---|---|
| *al* | allowable | $\sigma_{al}$ | allowable strength |
| *c* | clay | $S_c$ | clay fraction of soil kg/kg |
| *c* | critical | $p_c$ | critical pressure |
| ch | choke | $d_{ch}$ | diameter of choke |
| *e* | effective | $q_e$ | effective flow rate |
| *f* | pipe axis | $T_f$ | temperature in pipe axis |
| *f* | fluid | $q_f$ | fluid flow rate |
| *f* | friction | $\Delta p_f$ | friction pressure loss |
| *fL* | friction-laminar | $\Delta p_{fL}$ | friction pressure loss at laminar flow |
| *fT* | friction-turbulent | $\Delta p_{fT}$ | friction pressure loss at turbulent flow |
| *g* | gas | $M_g$ | molar mass of gas |
| *i* | inner | $d_i$ | inner pipe diameter |
| in | insulation | $T_{in}$ | insulation temperature |
| in | inflow | $\Delta p_{in}$ | pressure raise at inflow |
| *m* | mass | $q_{mg}$ | mass flow rate of gas |
| mol | molar | $V_{mol}$ | molar volume |
| max | maximum | $p_{max}$ | maximum pressure |
| min | minimum | $p_{min}$ | minimum pressure |
| *n* | normal, standard | $T_n$ | standard temperature |
| *o* | outer | $d_o$ | outer diameter, *OD* |
| *o* | oil | $\rho_o$ | density of oil |
| opt | optimum | $d_{opt}$ | optimum pipe diameter |

| | | | |
|---|---|---|---|
| $p$ | period | $t_p$ | time length of a period |
| $p$ | pressure | $\mu_p$ | dynamic viscosity at $p$ pressure |
| $r$ | relative | $\rho_r$ | relative density |
| re | reflected | $\Delta p_{re}$ | reflected pressure raise |
| $s$ | soil | $\lambda_s$ | thermal conductivity of soil |
| $sd$ | dry soil | $\lambda_{sd}$ | thermal conductivity of dry soil |
| $sw$ | wet soil | $\lambda_{sw}$ | thermal conductivity of wet soil |
| $st$ | steel | $c_{st}$ | specific heat of steel |
| tr | throughflow | $\Delta p_{tr}$ | pressure raise at throughflow |
| $w$ | water | $\mu_w$ | dynamic viscosity of water |
| Fo | Fourier | $N_{Fo}$ | Fourier number |
| Gr | Grashof | $N_{Gr}$ | Grashof number |
| $L$ | liquid | $z_L$ | mole fraction in liquid phase |
| Nu | Nusselt | $N_{Nu}$ | Nusselt number |
| Pr | Prandtl | $N_{Pr}$ | Prandtl number |
| Re | Reynolds | $N_{Re}$ | Reynolds number |
| $V$ | vapor, volatile | $z_V$ | mole fraction in vapor (gas) phase |
| $\Delta$ | difference | $\Delta p$ | pressure difference |
| $\bar{}$ | mean, average | $\bar{p}$ | average pressure |

*Remarks:*

a) list above does not contain
   — rarely used symbols, they are explained in the text,
   — indices signed by letters or figures if they denote serial number,
   — symbols of constants.

b) Indices are sometimes omitted for the sake of simplification if the denotation remains unambiguous.

CHAPTER 6

# GATHERING AND SEPARATION OF OIL AND GAS

## 6.1. Line pipes

### 6.1.1. Steel pipes

Steel pipes used in transporting oil and gas are either hotrolled seamless pipes or spiral or axially welded pipes, respectively. Pipes manufactured according to API Standards are used mostly by the oil- and gas-industry all over the world. On the basis of API Spec. 5L-1978 *Table 6.1 – 1* gives the main characteristics of the plain-end pipes of 1/8″ – 1 1/2″ nominal diameters. The main parameters of the pipes exceeding these sizes are given in *Table 6.1 – 2*. The table was constructed on the basis of API Spec. 5L – 1978, 5LX – 1978, 5LS – 1978, and 5LU – 1972. For each *OD* of the pipes the following data are given: the smallest and largest mass per length of the pipes (Column 3); the wall thickness (Column 4); the corresponding smallest and largest *ID*s (Column 5); and, besides, Table 6.1 – 2 shows that how many kinds of pipes of standard sizes manufactured according to the above specifications are available within the range of the given size limits (Columns 6 – 9). The tolerance of the *OD* depends both on the pipe-size and its mode of fabrication. The maximum admissible tolerance is ± 1 percent. The tolerance of the wall-thickness varies also depending on the pipe-size mode of fabrication. The maximum admissible tolerances range between +20 and −12·5 percents. Pipe ends are bevelled to facilitate butt welding. Unless there is an agreement to the contrary the bevel angle is 30° (tolerance +5° −0°) as measured from a plane perpendicular to the pipe axis. The height of the unbevelled pipeface, perpendicular to the axis should be 1·59 mm with a tolerance of ±0·79 mm.

Some characteristic data of these pipe materials and their strength are listed in *Table 6.1 – 3*. Threaded-end pipes for joining with couplings of 20 in (508·0 mm) or smaller nominal sizes are also made. These pipes are made however exclusively of steels of A – 25, A and B grades.

During the past two decades experts did their best to produce weldable steels of the highest possible strength for the oil- and gas-industry. *Figure 6.1 – 1* shows, after Forst and Schuster (1975), in a simplified form, that how the strength of the new standard pipe-materials increased in the course of the years. On the left side of the ordinate axis the standard grade can be seen while on its right the yield strength can be read in MPa units. The quality improvement during Period I is mainly due to the application of the micro-alloys, in Period II it was facilitated by a new type of thermo-mechanical treatment of the pipe steel, while in the third phase it was made

Table 6.1 – 1. Main parameters of API plain-end steel pipe line with *OD* from 10·3 – 48·3 mm (after API Spec. 5L – 1978)

| Nominal size, in. | *OD* $d_o$, mm | Specific mass $G$, kg/m | Wall thickness $s$, mm | *ID* $d_i$, mm | Test pressure for grade | | |
|---|---|---|---|---|---|---|---|
| | | | | | A | B | A25 |
| | | | | | bars | | |
| 1 | 2 | 3 | 4 | 5 | 6 | 7 | 8 |
| 1/8 | 10·3 | 0·36 | 1·73 | 6·8 | 48 | 48 | 48 |
| | 10·3 | 0·46 | 2·41 | 5·5 | 59 | 59 | 59 |
| 1/4 | 13·7 | 0·63 | 2·24 | 9·2 | 48 | 48 | 48 |
| | 13·7 | 0·80 | 3·02 | 7·7 | 59 | 59 | 59 |
| 3/8 | 17·1 | 0·85 | 2·31 | 12·5 | 48 | 48 | 48 |
| | 17·1 | 1·10 | 3·20 | 10·7 | 59 | 59 | 59 |
| 1/2 | 21·3 | 1·27 | 2·77 | 15·8 | 48 | 48 | 48 |
| | 21·3 | 1·62 | 3·73 | 13·8 | 59 | 59 | 59 |
| | 21·3 | 2·55 | 7·47 | 6·4 | 69 | 69 | 69 |
| 3/4 | 26·7 | 1·68 | 2·87 | 21·0 | 48 | 48 | 48 |
| | 26·7 | 2·19 | 3·91 | 18·9 | 59 | 59 | 59 |
| | 26·7 | 3·63 | 7·82 | 11·1 | 69 | 69 | 69 |
| 1 | 33·4 | 2·50 | 3·38 | 26·6 | 48 | 48 | 48 |
| | 33·4 | 3·23 | 4·55 | 24·3 | 59 | 59 | 59 |
| | 33·4 | 5·45 | 9·09 | 15·2 | 69 | 69 | 69 |
| 1 1/4 | 42·2 | 3·38 | 3·56 | 35·1 | 83 | 90 | 69 |
| | 42·2 | 4·47 | 4·85 | 32·5 | 124 | 131 | 90 |
| | 42·2 | 7·76 | 9·70 | 22·8 | 152 | 158 | 96 |
| 1 1/2 | 48·3 | 4·05 | 3·68 | 40·9 | 83 | 90 | 69 |
| | 48·3 | 5·41 | 5·08 | 38·1 | 124 | 131 | 90 |
| | 48·3 | 9·55 | 10·16 | 28·0 | 152 | 158 | 96 |

possible by the subsequent treatment of the pipe-steel before and after manufacturing the pipe. The increase in quality is of great economic importance. A pipeline of the same *ID* that can be operated on the same allowable working pressure is cheaper if it is constructed of pipes with smaller wall-thickness that are made of higher-strength steel. During a given period, for instance, while the unit-weight price of the pipe-steel, available in Hungary, ranged between 1 – 1·2, the relative value of the yield strength of these steels varied between 1 – 1·9. Since, according to Eq. 6.1 – 3, the allowable working pressure is directly proportional both to the wall-thickness (and that is why on the basis of $G = d\pi s\rho$ to the mass per length) and to the yield strength, the application of a better quality pipe-material is obviously more economical.

The specific transportation costs of both oil and gas decrease if the throughput to be transported is greater and the fluid or gas at the given throughput is carried through optimum size pipeline of comparatively great diameter. Application of

Table 6.1 – 2. Main parameters of API steel line pipes above $OD = 60.3$ mm (after API Spec. 5L-1978, 5LX-1978, 5LS-1978 and 5LU-1972)

| $OD$ $d_o$ | | Specific mass, $G$ | Wall thickness, $s$ | $ID$ $d_i$ | Number of sizes | | | |
|---|---|---|---|---|---|---|---|---|
| in. | mm | kg/m | mm | mm | 5L | 5LX | 5LS | 5LU |
| 1 | 2 | 3 | 4 | 5 | 6 | 7 | 8 | 9 |
| 2 3/8 | 60·3 | 3·02 | 2·11 | 56·1 | 11 | 11 | | |
| | | 13·45 | 11·07 | 38·2 | | | | |
| 2 7/8 | 73·0 | 3·68 | 2·11 | 68·8 | 12 | 12 | | |
| | | 20·39 | 14·02 | 45·0 | | | | |
| 3 1/2 | 88·9 | 4·51 | 2·11 | 84·7 | 12 | 12 | | |
| | | 27·67 | 15·24 | 58·4 | | | | |
| 4 | 101·6 | 5·17 | 2·11 | 97·4 | 12 | 11 | | |
| | | 18·62 | 8·08 | 85·4 | | | | |
| 4 1/2 | 114·3 | 5·84 | 2·11 | 110·1 | 17 | 16 | 17 | |
| | | 41·02 | 17·12 | 80·1 | | | | |
| 5 9/16 | 141·3 | 7·24 | 2·11 | 137·1 | 13 | | 11 | |
| | | 57·42 | 19·05 | 105·2 | | | | |
| 6 5/8 | 168·3 | 8·64 | 2·11 | 164·1 | 20 | 19 | 19 | 19 |
| | | 79·18 | 21·95 | 124·4 | | | | |
| 8 5/8 | 219·1 | 16·91 | 3·18 | 212·7 | 16 | 16 | 16 | 16 |
| | | 107·87 | 22·22 | 174·7 | | | | |
| 10 3/4 | 273·0 | 26·29 | 3·96 | 265·1 | 14 | 14 | 15 | 14 |
| | | 128·37 | 20·62 | 231·8 | | | | |
| 12 3/4 | 323·8 | 34·42 | 4·37 | 315·1 | 17 | 19 | 19 | 19 |
| | | 165·29 | 22·22 | 279·4 | | | | |
| 14 | 355·6 | 41·30 | 4·78 | 346·0 | 16 | 19 | 20 | 19 |
| | | 194·90 | 23·83 | 307·9 | | | | |
| 16 | 406·4 | 47·29 | 4·78 | 396·8 | 20 | 22 | 22 | 22 |
| | | 266·20 | 28·58 | 349·2 | | | | |
| 18 | 457·2 | 53·26 | 4·78 | 447·6 | 21 | 23 | 23 | 23 |
| | | 333·07 | 31·75 | 393·7 | | | | |
| 20 | 508·0 | 68·92 | 5·56 | 496·9 | 22 | 24 | 24 | 24 |
| | | 407·39 | 34·92 | 438·2 | | | | |
| 22 | 558·8 | 75·88 | 5·56 | 547·7 | 24 | 26 | 26 | 26 |
| | | 489·17 | 38·10 | 482·6 | | | | |
| 24 | 609·6 | 94·45 | 6·35 | 596·9 | 24 | 26 | 26 | 26 |
| | | 557·53 | 39·67 | 530·3 | | | | |
| 26 | 660·4 | 102·40 | 6·35 | 647·7 | 15 | 17 | 17 | 17 |
| | | 397·70 | 25·40 | 609·6 | | | | |
| 28 | 711·2 | 110·36 | 6.35 | 698·5 | 14 | 17 | 17 | 17 |
| | | 429·51 | 25·40 | 660·4 | | | | |
| 30 | 762·0 | 118·31 | 6·35 | 749·3 | 18 | 21 | 21 | 17 |
| | | 571·68 | 31.75 | 698·5 | | | | |
| 32 | 812·8 | 126·26 | 6·35 | 800·1 | 18 | 21 | 21 | 17 |
| | | 611·45 | 31·75 | 749·3 | | | | |

Table 6.1 – 2. cont.

| *OD* $d_o$ | | Specific mass, *G* | Wall thickness, *s* | *ID* $d_i$ | Number of sizes | | | |
|---|---|---|---|---|---|---|---|---|
| in. | mm | kg/m | mm | mm | 5L | 5LX | 5LS | 5LU |
| 1 | 2 | 3 | 4 | 5 | 6 | 7 | 8 | 9 |
| 34 | 863·6 | 134·22 | 6·35 | 850·9 | 18 | 21 | 21 | 17 |
| | | 651·22 | 31·75 | 800·1 | | | | |
| 36 | 914·4 | 142·17 | 6·35 | 901·7 | 18 | 21 | 21 | 17 |
| | | 690·99 | 31·75 | 850·9 | | | | |
| 38 | 965·2 | 187·05 | 7·92 | 949·4 | 19 | 19 | 19 | 15 |
| | | 730·76 | 31·75 | 901·7 | | | | |
| 40 | 1016·0 | 196·99 | 7·92 | 1000·2 | 19 | 19 | 19 | 15 |
| | | 770·53 | 31·75 | 952·5 | | | | |
| 42 | 1066·8 | 227·95 | 8·74 | 1049·3 | 18 | 18 | 18 | 14 |
| | | 810·30 | 31·75 | 1003·3 | | | | |
| 44 | 1117·6 | 238·90 | 8·74 | 1100·1 | 18 | 18 | 18 | 14 |
| | | 850·07 | 31·75 | 1054·1 | | | | |
| 46 | 1168·4 | 249·85 | 8·74 | 1150·9 | 18 | 18 | 18 | 14 |
| | | 889·84 | 31·75 | 1104·9 | | | | |
| 48 | 1219·2 | 260·78 | 8·74 | 1201·7 | 18 | 18 | 18 | 14 |
| | | 929·61 | 31·75 | 1155·7 | | | | |
| 52 | 1320·8 | 307·97 | 9·53 | 1301·8 | 15 | 15 | 17 | |
| | | 1009·15 | 31·75 | 1257·3 | | | | |
| 56 | 1422·4 | 331·83 | 9·53 | 1402·4 | 15 | 15 | 17 | |
| | | 1088·69 | 31·75 | 1358·9 | | | | |
| 60 | 1524·0 | 355·69 | 9·53 | 1505·0 | 13 | 13 | 17 | |
| | | 1168·23 | 31·75 | 1460·5 | | | | |
| 64 | 1625·6 | 379·55 | 9·53 | 1606·6 | 13 | 13 | 17 | |
| | | 1247·77 | 31·75 | 1562·1 | | | | |
| 68 | 1727·2 | 503·84 | 11·91 | 1703·4 | | | 14 | |
| | | 1327·31 | 31·75 | 1663·7 | | | | |
| 72 | 1828·8 | 568·71 | 12·70 | 1803·4 | | | 13 | |
| | | 1406·85 | 31·75 | 1765·3 | | | | |
| 76 | 1930·4 | 600·52 | 12·70 | 1905·0 | | | 13 | |
| | | 1486·39 | 31·75 | 1866·9 | | | | |
| 80 | 2032·0 | 710·19 | 14·27 | 2003·5 | | | 12 | |
| | | 1565·93 | 31·75 | 1968·5 | | | | |

spiral-welded steel-pipes is advantageous first of all for the construction of pipelines of big diameters. Table 6.1 – 2 shows that pipelines of 1727·2 – 2032·0 mm diameters are exclusively made by using this technology. In case of smaller diameters they are economical on the one hand because smaller wall-thickness is required than in case of the hot-drawn pipes, and on the other hand in case of the same geometrical parameters their allowable working pressure is higher than that of the axially welded pipes.

Table 6·1 – 3. Strength and composition of API steel line pipes
(after API Spec. 5L-1978, 5LX-1978, 5LS-1978, 5LU-1972)

| Grade | API Spec. | $\sigma_F$ MPa | $\sigma_B$ MPa | Alloying elements and impurities | Note |
|---|---|---|---|---|---|
| 1 | 2 | 3 | 4 | 5 | 6 |
| A 25 | 5L | 172 | 310 | C, Mn, Ph, S | |
| A | 5L, 5LS | 207 | 331 | C, Mn, Ph, S | |
| B | 5L, 5LS | 241 | 413 | C, Mn, Ph, S | |
| X-42 | 5LX, 5LS | 289 | 413 | C, Mn, Ph, S | |
| X-46 | 5LX, 5LS | 317 | 434 | C, Mn, Ph, S | |
| X-52 | 5LX, 5LS | 358 | 455[1]<br>496[2] | C, Mn, Ph, S | |
| X-56 | 5LX, 5LS | 386 | 489[1]<br>517[2] | C, Mn, Ph, S, Nb, V, Ti | |
| X-60 | 5LX, 5LS | 413 | 517[1]<br>537[2] | C, Mn, Ph, S, Nb, V, Ti | |
| X-65 | 5LX, 5LS | 448 | 531[1]<br>551[2] | C, Mn, Ph, S, Nb, V | only for welded pipes,<br>by agreement for<br>seamless pipes |
| X-70 | 5LX, 5LS | 482 | 565 | C, Mn, Ph, S | only for welded pipes<br>by agreement for<br>seamless pipes |
| X-80 | 5LU | 552 | 655<br>862 | C, Mn, Ph, S, Si | minimum value<br>maximum value |
| X-100 | 5LU | 689 | 758<br>931 | C, Mn, Ph, S, Si | minimum value<br>maximum value |

[1] For pipe diameter less than $d_o = 508$ mm, and for $d_o \geq 508$ mm, with wall thickness $s > 9{\cdot}5$ mm.
[2] For pipe diameter $d_o \geq 508$ mm, with wall thickness $s \leq 9{\cdot}5$ mm. Minimum elongation in 50·80 mm length

$$e = 7{\cdot}738 \times 10^9 \frac{A^{0{\cdot}2}}{\sigma_B^{0{\cdot}9}}$$

$A$ — cross-sectional area of wall, m$^2$; $\sigma_B$ — tensile strength, Pa.

The requirements concerning the quality of the pipe-materials are getting even higher due to the fact that more and more oil and gas wells are drilled in the arctic areas. The low temperatures, characteristic of these regions, considerably reduce the ductility of the pipe-materials. A parameter permitting the assessment of steel strength from this viewpoint is first of all, the critical or brittle-transition temperature established by the notch impact-bending test. The addition of Mn up to 2 percent will raise the yield strength of the steel and lower its brittle-transition temperature. A comparatively slight addition of Al (0·05 percent) will, however, raise the yield strength and substantially lower the brittle transition temperature at any Mn content *(Fig. 6.1.–2)*. That is why application of steel pipes containing small

amounts of Al is advantageous in cold environments. In the presence of Al finer grain structure develops (Haarmann 1970).

In order to decrease the material consumption and to achieve a greater allowable working pressure at the same time, new technologies were developed in France and in the German Federal Republic (Botkilin and Majzel' 1975). *Multilayer pipes.* A pipe is pulled into the other one. The inner pipe is of less yield strength, i.e. of weaker quality. The outer pipe is pre-stressed. One of the methods of producing this pipe combination is that the outer pipe is pulled upon the cold inner pipe in a warm state,

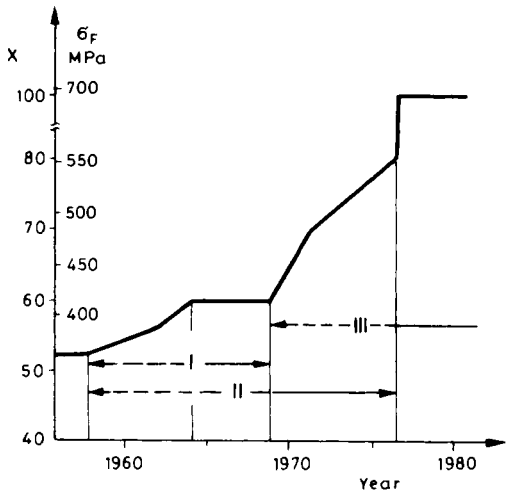


Fig. 6.1 – 1. Strength of standard pipe materials after Forst and Schuster (1975)

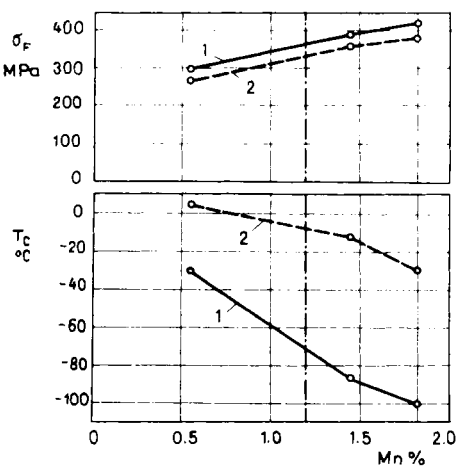


Fig. 6.1 – 2. Strength and brittle transition temperature of steel St 52.3 as affected by Mn content at low temperatures, at Al content of 0·05 percent (1) and 0·01 percent (2) after Haarmann (1970)

and in the course of cooling it shrinks. The other, more frequently applied, process is that the liner pipe is pulled on the inner pipe in a cold state and then a pressure, great enough to cause permanent deformation, is developed in the latter. *Pipes reinforced with wires.* Wires, having significantly more favourable strength parameters than those of the rolled plate, can be produced. Flat wires of this kind, with a thickness of one third of that of the pipe wall are winded round the pipe. Wires of $\sigma_F = 1422$ MPa yield strength are also applied. Pipelines of great diameters and small wall thickness may be deformed due to the expectable outside loading. In order to avoid this, instead of the greater wall thickness *stiffening rings* may be also applied.

### 6.1.2. Plastic pipes, plastic-lined steel pipes

Plastic pipe has been increasingly applied by the oil and gas-industry since the 1940s. It is applied first of all for the low-pressure transport of crude, gas and water. Plastic pipes have several *advantages* as compared to steel pipes. The density of the pipe material is smaller, thus its handling, storage, assembly and transport is simpler and easier, and the plastic pipes are resistant to both external and internal corrosion. Certain plastics have paraphobic properties preventing wax deposition which considerably reduces the cost of scraping when transporting waxy crudes. Their thermal and electrical conductivities are low. Because of these the maintenance costs of these pipelines are lower. The relative roughness of the inner surface of plastic pipes is low enough to be regarded as hydraulically smooth. Hence friction losses at any given throughput are lower than in steel pipes. The *drawbacks* of plastic pipes are as follows. The tensile strength of the pipe material is relatively small and it can even change significantly with the change of temperature, time and nature of loading (stationary, or fluctuating internal pressure). The thermal expansion coefficient is relatively high, it can be 15 times higher than that of steel. Their constancy of size, and resistance to physical influence including fire are slight.

Plastics used to make line pipes fall into two great groups: (1) heat-softened called thermoplastics and (2) heat-hardened called thermosetting resins. *Thermoplastic materials* are synthetic polymers which, in the course of the polymerization process, from short monomeric molecules become polymeric molecules of considerable length. The plastic in granulated or powder form is then pressed to the required size by applying extruders. Even in case of repeated heat treatment in the proper solvent they are still soluble and reformable and reusable again.

*Thermosetting plastics* or molding resins are formed in the course of the process of polycondensation of monomers. The uniting of monomers in this way is accompanied by some by-products such as water, $CO_2$ or ammonia. Pipes are made similarly to cast iron pipes, by static or centrifugal casting. Then the pipe is aged by applying chemical means or heat treatment. The material of the pipe already prepared cannot be reused. The relatively brittle pipe material is made more flexible by adding different additives, the most frequently applied type of which is fiber-glass. As far as thermoplastics are concerned, pipelines are made first of all from hard PVC (HPVC), shatterproof PVC (a mixture of PVC and chlorated

polyethylene, marked as PVC+CPE), and from hard polyethylene. The PVC (polyvinylchloride) is produced by polymerizing the vinylchlorid, a derivative of acetylene. Ethylene is the monomer of the polyethylene PE. Several versions of the above described basic plastics are manufactured and their physical parameters, due to the differences of the technologies and additives applied, may be different. *Table 6.1—4* (after Vida 1981) shows the main physical parameters of the above plastics

Table 6.1—4. Characteristics of Hungarian plastic pipe materials after Vida (1981)

| Type | Density, kg/m$^3$ | Tensile strength, MPa | Hardness, MPa | HB modulus of elasticity, MPa |
|---|---|---|---|---|
| | Standard | | | |
| | MSz 1425 | MSz 5546 | MSz 1421 | DIN 53457 |
| HPVC | 1420 | 59·3 | 102·3 | 810·4 |
| PVC+CPE | 1340 | 44·7 | 103·3 | 636·6 |
| HPE I | 900 | 21·2 | 44·7 | 187·8 |
| II | 890 | 19·3 | 36·1 | 162·5 |

used in Hungary. They are widely applied, first of all, in the gas industry where they are used for low-pressure gas-distribution. To illustrate the popularity of these pipes it is enough to mention that only in Europe pipelines made of HPVC totalling a length of 28 500 km were laid in 1978. Application of the gas pipelines made of HPE has considerably increased during the 1970s. In 7 countries of Western Europe 2·7 million metric tons were used in 1972, against 25·8 in 1979. A good overview concerning the parameters and existing standards of these pipelines is given by Müller (1977).

From the thermosetting plastics first of all the epoxy resins and the polyesthers are suitable for pipemaking. Polyesthers are polycondensation products of polyvalent alcohols (glycols, glycerins, etc.) with polyvalent acids (phthalic, maloic acid, etc.). Epoxy resins are produced by condensing diene with epichlor-hydrine in the presence of caustic soda. Depending on the technology and the applied additives several versions of these plastics are known. The API Specification 5LR—1972 describes pipes conducting oil, gas and industrial water, that are made of reinforced thermosetting resin (RTR) by centrifugal casting (CC) or filament wound (FW). Frequently fiber-glass is used as reinforcement, and thus the strength of the pipe material increases while its thermal conductivity and water absorption decreases.

The changes of the strength of the thermoplastics and resins due to temperature changes significantly differ. After Greathouse and McGlasson (1958) *Fig. 6.1—3* shows the change of the tensile strength with the temperature for two types of pipe material made of PVC and for two types of materials made of glass reinforced plastics. It can be clearly seen that the tensile strength of these latter materials is not smaller even at a temperature of 120 °C than at room temperature. There is a

peculiar change however in the allowable pressure in plastic pipeline with time. — *Fig. 6.1 – 4*, also after Greathouse and McGlasson, shows the increase in diameter of a PVC pipe in function of the loading period at different values of tangential, or hoop stress:

$$\sigma_t = \frac{p_i(r_i^2 + r_o^2)}{r_o^2 - r_i^2}.$$

We can see, that contrary to steel pipes, the process of diameter increase due to the internal overpressure is slow, and there is a critical hoop stress at which, if it is small enough, the increase in diameter ceases within a given period of time. If, however, $\sigma_t$ exceeds the critical value the pipe will go on swelling until it ruptures. Another important factor influencing the allowable internal overpressure of the pipes is that

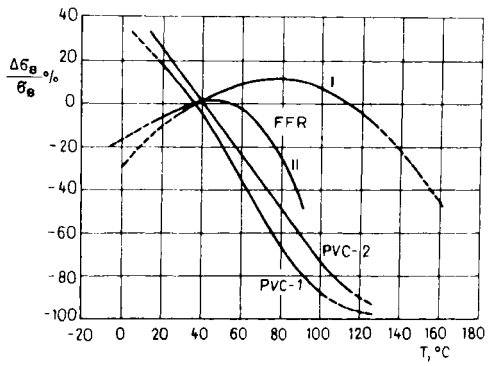


Fig. 6.1 – 3. Tensile strength of plastics v. temperature (Greathouse and McGlasson 1958)

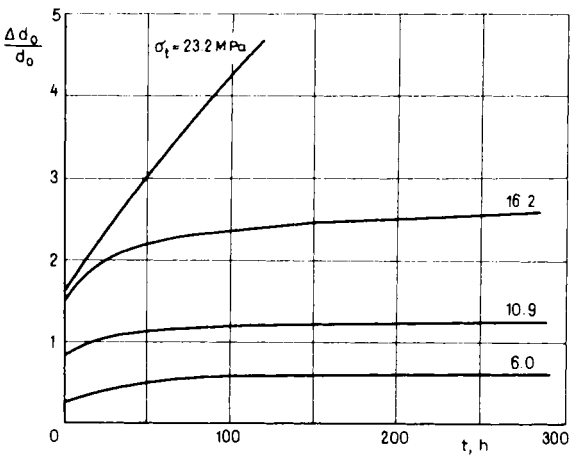


Fig. 6.1 – 4. Increase of diameter v. time of PVC-1 pipe (Greathouse and McGlasson 1958)

the pressure is constant, or changing, pulsating. Because of these specific features in several countries standards and specifications were compiled for the qualification of the plastic pipes. On the basis of the API Spec. 5LR *Table 6.1 – 5* shows the minimum strength characteristics of plastic pipe materials of different grades at temperatures of 23·0 °C and 65·6 °C. In each case here strength means hoop stress. The numbers after the R marking the different grades express the hoop stress in psi

Table 6.1 – 5. Minimum physical property requirements for reinforced thermosetting resin line pipe (RTRP) after API Spec. 5LR

| Property and test method | Grade | | | | | | | |
|---|---|---|---|---|---|---|---|---|
| | R-40 | | R-45 | | R-50 | | R-60 | |
| | 23·0 | 65·6 | 23·0 | 65·6 | 23·0 | 65·6 | 23·0 | 65·6 |
| | C | | | | | | | |
| Cyclic long term pressure* strength MPa | 27·6 | 27·6 | 31·0 | 31·0 | 34·5 | 34·5 | 41·4 | 41·4 |
| Cyclic short term pressure* strength MPa | 103 | 103 | 117 | 117 | 131 | 131 | 138 | 138 |
| Long-term static* MPa | 75·8 | 75·8 | 89·6 | 89·6 | 103 | 103 | 138 | 138 |
| Short-time rupture strength* (burst) MPa | 207 | 207 | 241 | 241 | 276 | 276 | 345 | 345 |
| Ultimate axial tensile strength MPa | 51·7 | 48·3 | 62·1 | 57·9 | 62·1 | 57·9 | 82·7 | 77·2 |
| Hydrostatic collapse strength MPa | 40·0 | 35·2 | 40·0 | 35·2 | 40·0 | 35·2 | 40·0 | 35·2 |

* Minimum hoop stress.

units in case of long-lasting cyclic loading. This value is given in the first line of the Table in MPa units. The standard pipe sizes according to this same specification are given in *Table 6.1 – 6.*

The favourable properties of the steel and plastic pipes are partly united in the plastic-lined steel pipe. Due to the plastic lining of the inside wall the pipeline becomes hydraulically smoother and thus, the throughput capacity increases. Wax does not adhere to the pipe wall, or, if it does, only to a much smaller extent. Internal corrosion ceases. No rust scale gets into the fluid stream and that is why the wear and tear of the measuring devices and pipe fittings decreases. The allowable working pressure of the pipe is determined by the parameters of the steel pipe. Polyethylene and epoxy resin are the most frequently used lining materials. Lining can be produced in the pipe mill, but older, already existing pipelines, especially gas pipes, can be also furnished with inside plastic lining. This latter process especially requires a special care and expertise. Against the external corrosion the outer surface of the pipes can be also coated with plastics.

Table 6.1 – 6. Dimensions and masses of RTRP pipes after API Spec. 5LR

| Nominal size $d_n$, in. | *OD* $d_o$, mm | *ID* $d_i$, mm | Total wall thickness $s_t$, mm | Min. reinforced wall thickness $s_{min}$, mm | Spec. max. $G_{nom}$, kg/m | Process of manufacture |
|---|---|---|---|---|---|---|
| 2 | 60·3 | 56·8 | 1·8 | 1·5 | 0·60 | FW |
| (2·375) | | 54·2 | 3·0 | 2·5 | 0·97 | FW |
| | | 50·7 | 4·8 | 4·2 | 1·77 | FW |
| | | 50·2 | 5·1 | 3·6 | 1·24 | CC |
| | | 47·6 | 6·4 | 4·3 | 1·86 | CC |
| | | 45·1 | 7·6 | 5·6 | 2·09 | CC |
| 2 1/2 | 73·0 | 69·5 | 1·8 | 1·5 | 0·76 | FW |
| (2·875) | | 63·4 | 4·8 | 4·2 | 1·97 | FW |
| | | 62·9 | 5·1 | 3·6 | 1·79 | CC |
| | | 60·3 | 6·4 | 4·3 | 2·17 | CC |
| | | 57·8 | 7·6 | 5·6 | 2·53 | CC |
| 3 | 88·9 | 85·3 | 1·8 | 1·5 | 0·89 | FW |
| (3·500) | | 84·8 | 2·0 | 1·8 | 0·97 | FW |
| | | 82·8 | 3·0 | 2·5 | 1·49 | FW |
| | | 78·7 | 5·1 | 3·6 | 2·09 | CC |
| | | 76·2 | 6·4 | 4·3 | 2·61 | CC |
| | | 73·7 | 7·6 | 5·6 | 3·13 | CC |
| 4 | 114·3 | 110·2 | 2·0 | 1·8 | 1·19 | FW |
| (4·500) | | 109·7 | 2·3 | 2·0 | 1·34 | FW |
| | | 108·2 | 3·0 | 2·5 | 1·94 | FW |
| | | 104·1 | 5·1 | 3·6 | 2·64 | CC |
| | | 101·6 | 6·4 | 4·3 | 3·57 | CC |
| | | 99·1 | 7·6 | 5·6 | 4·32 | CC |
| 6 | 168·3 | 162·7 | 2·8 | 2·5 | 2·53 | FW |
| (6·625) | | 160·2 | 4·1 | 3·6 | 3·87 | FW |
| | | 155·6 | 6·4 | 4·3 | 5·21 | FW |
| | | 153·0 | 7·6 | 5·6 | 6·18 | CC |
| | | 148·0 | 10·2 | 7·6 | 6·04 | CC |
| 8 | 219·1 | 212·2 | 3·4 | 3·2 | 2·98 | FW |
| (8·625) | | 209·9 | 4·6 | 4·1 | 5·66 | FW |
| | | 206·4 | 6·4 | 4·3 | 6·70 | CC |
| | | 203·8 | 7·6 | 5·6 | 8·04 | CC |
| | | 198·8 | 10·2 | 7·6 | 10·43 | CC |
| 10 | 273·1 | 264·4 | 4·3 | 3·8 | 6·26 | FW |
| (10·750) | | 261·9 | 5·6 | 5·1 | 8·68 | FW |
| | | 260·4 | 6·4 | 4·3 | 8·34 | CC |
| | | 257·8 | 7·6 | 5·6 | 9·98 | CC |
| | | 252·7 | 10·2 | 8·1 | 13·03 | CC |
| 12 | 323·9 | 313·7 | 5·1 | 4·4 | 8·94 | FW |
| (12·750) | | 312·7 | 5·6 | 5·1 | 10·43 | FW |
| | | 311·2 | 6·4 | 4·3 | 9·98 | CC |
| | | 308·6 | 7·6 | 5·6 | 11·92 | CC |
| | | 303·5 | 10·2 | 8·1 | 15·49 | CC |

### 6.1.3. Wall thickness of pipes

Though the formula applied for the calculation of the wall thickness of the pipelines used for the transportation of oil and gas is slightly different in the different countries (Csete 1980), the basis of these formulas is the same:

$$s = \frac{d_o \Delta p}{2e\sigma_{a1}} + s_1 + s_2 \qquad 6.1-1$$

where $\Delta p$ is the pressure difference prevailing across the pipe wall.

In case of steel pipelines $e$ means the figure of merit of weld seams. In case of seamless pipelines $e = 1$, while for axially welded pipelines $e = 0{\cdot}7 - 0{\cdot}9$.

For spiral-welded pipes, in Siebel's opinion (Stradtmann 1961) $e$ should be divided by the ratio $\sigma_\alpha/\sigma_\varphi$. $\sigma_\alpha$ is the tangential stress perpendicular to the seam while $\sigma_\varphi$ is the tangential stress in a cross section of the pipe perpendicular to the axis. In case of the commonly used spiral-welded pipes the pitch of the weld seam $\alpha$ is greater than 40° and then $\sigma_\alpha/\sigma_\varphi = 0{\cdot}8 - 0{\cdot}6$. The greater the $\alpha$ is, the smaller is the rate $\sigma_\alpha/\sigma_\varphi$. If $\alpha \geqq 40°$, then $\frac{e}{\sigma_\alpha/\sigma_\varphi} = 1$. It means that the locus of the least strength is not in the weld seam but in the steel sheet itself and Eq. 6.1 – 1 can be used by substituting $e = 1$.

The allowable stress is

$$\sigma_{al} = \frac{\sigma_F}{k} \qquad 6.1-2$$

where $\sigma_F$ is the yield strength and $k$ is the *safety factor*, a value greater than 1. According to the Hungarian specifications the following safety factors should be kept in mind in case of oil pipes and pipelines transporting petroleum products (1), and in case of pipelines transporting gas, and liquified gas (2):

| | (1) | (2) |
|---|---|---|
| a) Open country, ploughland, wood | 1·3 | 1·4 |
| b) At a distance of 100 – 200 m from inhabited areas, railroads, arterial roads, etc. | 1·5 | 1·7 |
| c) Within 100 m from same | 1·7 | 2·0 |
| d) In industrial and densely inhabited areas, under railroads, arterial roads and water courses | 2·0 | 2·5 |

In several countries instead of the safety factor its reciprocal value is used and it is called *design factor*. The value of this factor according to the standards in 12 countries having significant gas industry and summarized by Csete (1980) varies between 0·3 – 0·8. Thus, the matching reciprocal value, the safety factor is 3·3 – 1·25.

In Eq. 6.1 – 1 $s_1$ is a supplement due to the negative tolerance of the wall-thickness which, if considered, is 11 to 22 percent of the $s_0$ value calculated by the first term of

the equation. $s_2$ is a supplement added because of the corrosion and degradation and its value is max. 1 mm. From country to country it differs if $s_1$ and $s_2$ is considered in the course of the calculation of $s$. None of these values is prescribed in France, FRG, or in the USA. That is why a frequently used simpler version of Eq. 6.1 – 1 is

$$s = \frac{d_o \Delta p}{2e\sigma_{al}}. \qquad 6.1-3$$

$\sigma_F$ yield strength is the stress where the permanent deformation sets in so that in the course of the deformation the loading does not increase or vary. This phenomenon cannot be recognized in case of each metals and alloys. In this case the stress belonging to the 0·2 permanent deformation is considered to be the yield stress and instead of $\sigma_F$ it is marked with $\sigma_{0·2}$.

The allowable internal overpressure of the plastic pipe can be calculated by applying the ISO formula:

$$\Delta p = \frac{2\sigma_t s}{d_i}$$

where $\sigma_t$ hoop stress value can be taken from the relevant line of Table 6.1 – 5, $d_i$ is the average internal diameter *(ID)* that should be calculated from $(d_o - 2s)$.

*Example 6.1 – 1.* Find the required wall thickness of spiral-welded pipe of $d$ = 10 3/4 in. nominal size, made of X52 grade steel, to be used in a gas pipeline laid across ploughland and exposed to an operating pressure of 60 bars. From Table 6.1 – 2 the *OD* of the given pipe is 0·273 m. According to Table 6.1 – 3 $\sigma_F = 358$ MPa. By the above considerations, $k = 1·4$, and for spiral welded pipes $e = 1$. Hence by Eq. 6.1 – 3 the wall-thickness is

$$s = \frac{0·273 \times 60 \times 10^5}{2 \times 1 \times \frac{358 \times 10^6}{1·4}} = 3·20 \times 10^{-3} = 3·20 \text{ mm}$$

Table 6.1 – 2 shows the least standard wall thickness at 10 3/4 in, nominal size to be 3·96 mm. This thickness should be chosen.

## 6.2. Valves, pressure regulators

### 6.2.1. Valves

Valves used in oil and gas pipelines may be of gate, plug or ball, or globe type. All of these have various subtypes.

#### (a) Gate valves

The gate valve is a type of valve whose element of obstruction, the valve gate, moves in a direction perpendicular to both inflow and outflow when the valve is being opened or closed. Its numerous types can be classified according to several viewpoints. In the following we shall consider them according to their mode of closure. Typical examples are shown as *Figs 6.2 – 1 – 6.2 – 4*. Of these, 6.2 – 2 and 6.2 – 3 are conformable to API Std 6D – 1971. The main parts of a gate valve are termed as follows: handwheel *1*, stem *2*, gland *3*, stem packing *4*, bonnet *5*, bonnet bolts *6*, body *7*, wedge or disc *8*, and seat *9*. The element of obstruction in the valve shown as Fig. 6.2 – 1 is wedge *8*. This valve is of a simple design and consequently

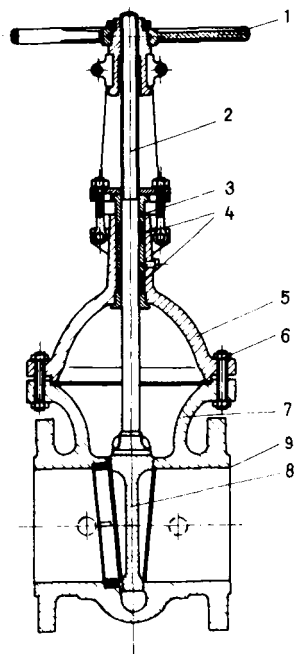


Fig. 6.2 – 1. Wedge-type rising-stem gate valve

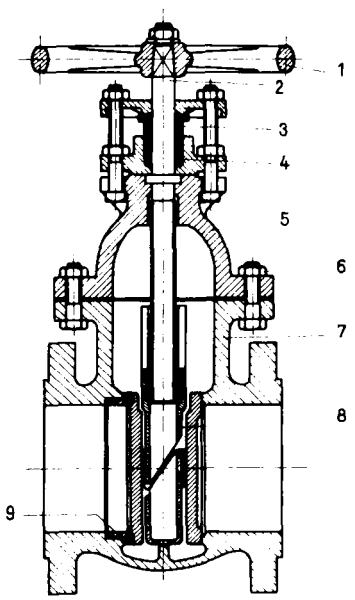


Fig. 6.2 – 2. Disk-type non-rising-stem gate valve, after API Std 6D-1971

rather low-priced, but its closure is not leakproof. First of all, it is difficult to grind the wedge to an accurate fit, and secondly, the obstructing element will glide on metal on closure; deposits of solid particles will scratch the surfaces and thus produce leaks. Fairly widespread earlier, this type of valve has lost much of its popularity nowadays.

The valve in *Fig. 6.2 – 2* is of the double-disk non-rising-stem type. Its tightness is much better than that of the foregoing type, because the two disks do not glide on the seats immediately before closure or after opening; rather, they move nearly at right angles to the same. The two elements of obstruction, machined separately, are more easily ground to a tight fit. The valve in *Fig. 6.2 – 3* is of the rising-stem, through conduit type with a metallic seal. It has stem indicator *1* as a typical structural feature. One of the advantages of this design is that the inner wall of the valve is exposed to no erosion even if the fluid contains solids. The elements of obstruction cannot wedge or stick. Overpressure in the valve is automatically released by safety valve *2*. Its drawback is that, owing to the metal-to-metal seal,

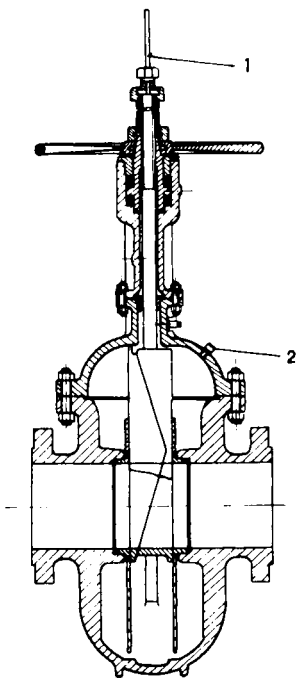


Fig. 6.2 – 3. Full-opening rising-stem gate valve, after API Std 6D-1971

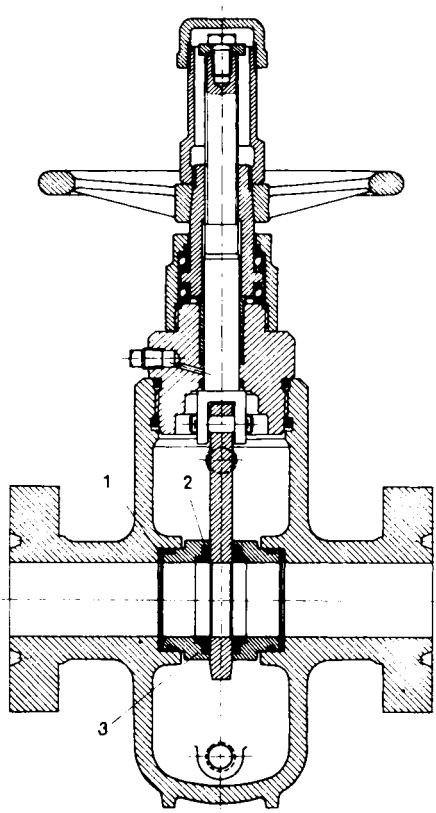


Fig. 6.2 – 4. Grove's G-2 full-opening floating-seat gate valve

tightness may not always be sufficient for the purposes envisaged in the oil and gas industry. Furthermore, the fit of the disks may be damaged by scratches due to solid particles. The biggest valves of this type now in use are made for 1000 mm nominal size and 66 bars operating pressure rating (Laabs 1969).

*Figure 6.2 – 4* shows a through conduit-type, non-rising-stem floating-seat valve. The so-called floating seats *3*, capable of axial movement, and provided with 0-ring seals *2*, are pressed against the valve gate by spring *1*. The pressure differential developing on closure generates a force which improves the seal. (Concerning this mechanism cf. the passage on ball valves in Section 6.2.1—(b).) Small solid particles will not cause appreciable damage to the sealing surfaces, but coarse metal fragments may. For high-pressure large-diameter applications, variants of this type of gate valve with the valve body welded out of steel plate are gaining in popularity.

The valves described above have either rising or non-rising stems. Rising stems require more space vertically. In a rising stem, the thread is on the upper part, likely to be exposed to the outer environment. In a non-rising stem, the thread is on the lower part, in contact with the well fluid. It is a matter of correctly assessing the local circumstances to predict whether this or that solution will more likely prevent damage to the threads. In rising-stem valves the handwheel may or may not rise together with the stem. In modern equipment, the second solution is current (cf. e.g. *Fig. 6.2 – 3*). Turning the stem may be effected directly, by means of a handwheel mounted on the stem (as in all types figured above), but also indirectly by transferring torque to the stem by a spur or bevel gear (*Figs 6.2 – 5* and *6.2 – 6*).

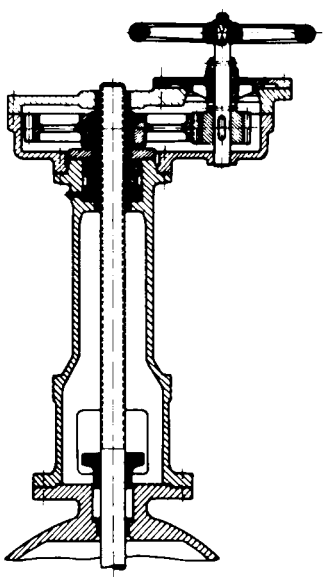

Fig. 6.2 – 5. Spur-gear gate-valve stem drive

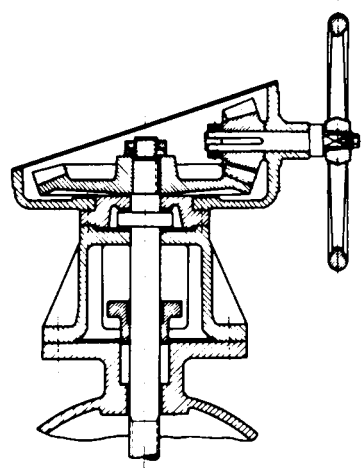

Fig. 6.2 – 6. Bevel-gear gate-valve stem drive

The valve may, of course, be power-operated, in which case the drive may be pneumatic, hydraulic or electric. *Figure 6.2 – 7* shows a rising-stem valve with electric motor and a bevel gear drive. Gate valves used in oil and gas pipelines usually have flange couplings, but in some cases plain-end valve bodies are used with flanges attached by welding, or threaded-end ones with couplings. At low operating pressures, the outer face of the flange, to lie up against the opposite flange,

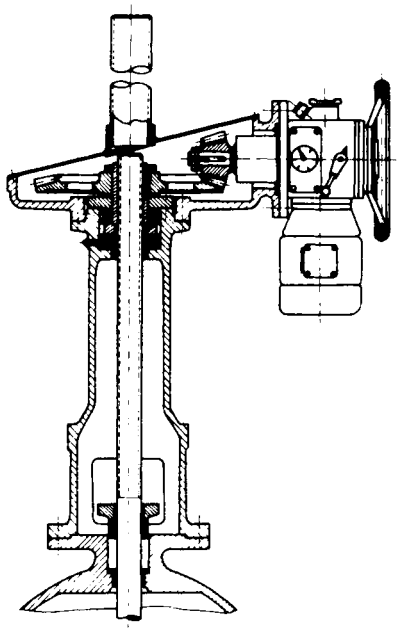

Fig. 6.2 – 7. Bevel-gear gate-valve stem drive, operated by electric motor

is either smooth or roughened. Ring gaskets used are non-metallic, e.g. klingerite. At higher pressures, it is usual to machine a coaxial groove into the flange, and to insert into it a metallic gasket, e.g. a soft-iron ring. — Operating-pressure ratings of gate valves range from 55 to 138 bars according to API Std 6D—1971. The standard enumerates those ASTM grades of steel of which these valves may be made. — Gate valves are to be kept either fully open or fully closed during normal operation. When partly open, solids in the fluid will damage the seal surfaces in contact with the fluid stream.

**(b) Plug and ball valves**

In these valves, the rotation by at most 90° of an element of obstruction permits the full opening or full closing of a conduit. The obstructing element is either in the shape of a truncated cone (plug valve) or of a sphere (ball valve). *Figure 6.2 – 8* shows

a plug valve where gland *1* can be tightened to the desired extent by means of bolts. There are also simpler designs. The contacting surfaces of the plug and seat must be kept lubricated in most plug valves. In the design shown in the Figure, lubricating grease is injected at certain intervals between the surfaces in contact by the

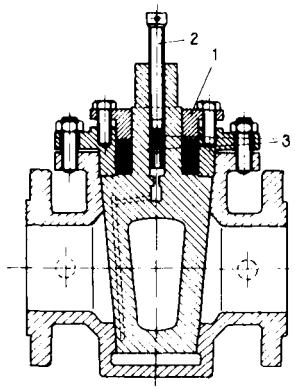


Fig. 6.2 – 8. Plug valve

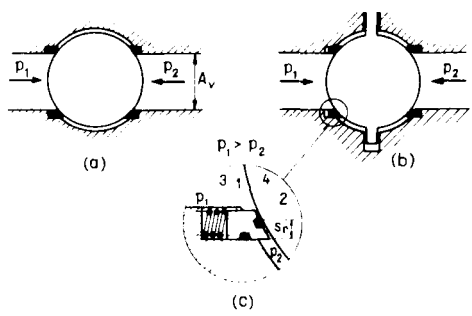


Fig. 6.2 – 9. Ball valve types, after Perry (1964)

tightening of screw *2*. Check valves *3* permit lubrication also if the valve is under pressure. Surfaces in contact are sometimes provided with a molybdene sulphide or teflon-type plastic lining. In full-opening plug valves, the orifice in the plug is of the same diameter as the conduit in which the valve is inserted. This design has the same advantages as a through conduit-type gate valve.

In the oil and gas industry, ball valves have been gaining popularity since the early sixties. They have the substantial advantage of being less high and much lighter than gate valves of the same nominal size, of providing a tight shutoff and of being comparatively insensitive to small-size solid particles (Belházy 1970). There are two types of ball valve now in use (Perry 1964) shown in outline in *Fig. 6.2 – 9.*

Solution (a) is provided with a floating ball, which means that the ball may be moved axially by the pressure differential and may be pressed against the valve seat on the low-pressure side. This latter seat is usually made of some sort of plastic, e.g. teflon. The resultant force pressing the ball against the seat is $F=(p_1-p_2)A_v$, that is, it equals the differential in pressure forces acting upon a valve cross-section equal to the pipe cross-section $A_v$. If $F$ is great, then the pressure on the plastic seal ring is liable to exceed the permissible maximum. It is in such cases that solution (b) will help. An upper and a lower pin integral with the ball will prevent pipe-axial

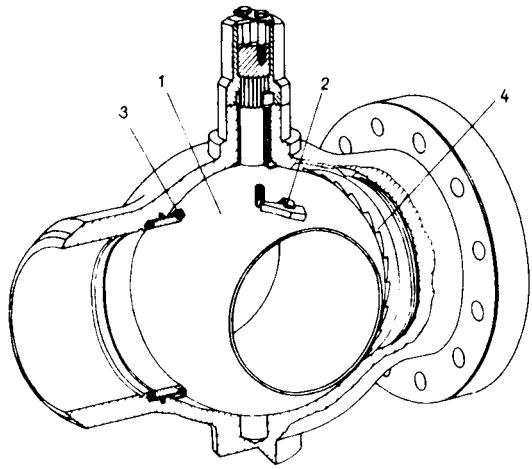


Fig. 6.2–10. Cameron's rotating-seat ball valve

movements of the ball. Sealing is provided by a so-called floating seat, exposed to two kinds of force. Referring to part (c) of the Figure, spring *3* presses metal ring *1* and the plastic O-ring seal *2* placed in a groove of the ring with a slight constant force against ball *4*. At low pressures, this in itself ensures sufficient shutoff. Moreover, it is easy to see that one side of surface $s_r d_t \pi$ is under a pressure $p_1$, whereas its other side is under pressure $p_2$. A suitable choice of ring width $s_r$ will give a resulting pressure force $(F_1-F_2)$ just sufficient to ensure a tight shutoff at higher pressures but not exceeding the pressure rating of the plastic O-ring.

*Figure 6.2–10* shows a Cameron-make rotating- and floating-seat ball valve. On each opening of ball *1*, seat *3* is rotated by a small angle against the pipe axis, by key *2* engaging the teeth *4* on the seat. This solution tends to uniformize wear and thereby to prolong valve life.

Ball and plug valves should be either fully open or fully closed in normal operation, just as gate valves should. The ball or plug can, of course, be power-actuated. Valve materials are prescribed by API Std 6D–1971.

### (c) Globe valves

The wide range of globe valve types has its main use in regulating liquid and gas flow rates. A common trait of these valves is that the plane of the valve seat is either parallel to the vector of inflow into the valve body, or the two include an angle of 90° at most. The element of obstruction, the so-called inner valve, is moved perpendicularly to the valve-seat plane by means of a valve stem. In the fully open position, the stem is raised at least as high as to allow a cylindrical gas passage area equal to the cross-sectional area of the pipe connected to the valve. A valve type in common use is shown in *Fig. 6.2 – 11*. The design of this type may be either single- or double-seat (the latter design is shown in the Figure). Single-seat valves have the advantage that inner valve and seat may be ground together more accurately to give

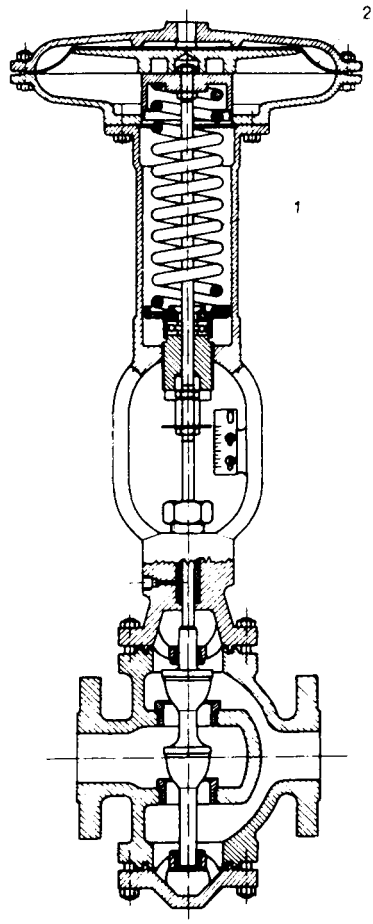


Fig. 6.2 – 11. Fisher's balanced diaphragm motor valve

a tighter shutoff. A high-quality valve should not, when shut off, pass more than 0·01 percent of its maximum (full-open) throughput. Double-seat valves tend to provide much lower-grade shutoff. The permissible maximum leakage is 50 times the above value, that is, 0·5 percent (Sanders 1969). The pressure force acting upon the inner valve of a double-seat valve is almost fully balanced; the forces acting from below and from above upon the double inner-valve body are almost equal. The force required to operate the valve is thus comparatively slight. The inner valve in a single-seat design valve is, on the other hand, exposed to a substantial pressure differential when closed, and the force required to open it is therefore quite great.

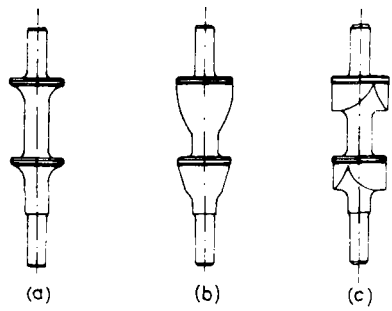


Fig. 6.2 – 12. Inner-valve designs

According to its design and opening characteristic, the inner valve may be quick-opening, linear or equal-percentage. Part (a) of *Fig. 6.2 – 12* shows a so-called quick-opening disc valve. It is used when the aim is to either shut off the fluid stream entirely or let it pass at full capacity ('snap action'). The characteristic of such a valve is graph (a) in *Fig. 6.2 – 13*. The graph is a plot of actual throughput related to maximal throughput v. actual valve travel related to total valve travel. Graph (a) shows that, in a quick-opening valve, throughput attains 0·8 times the full value at a relative valve travel of 0·5. The inner-valve design shown in part (b) of *Fig. 6.2 – 12* provides the linear characteristic of graph (b) in *Fig. 6.2 – 13*. In such a valve, a given throughput invariably entails a given increment in throughput. This type of regulation is required e.g. in fluid-level control where, in an upright cylindrical tank, a given difference in fluid level invariably corresponds to a given difference in fluid content. The inner-valve design shown in part (c) of *Fig. 6.2 – 12* gives rise to a so-called equal-percentage characteristic (part c, in *Fig. 6.2 – 13*). In a valve of this design, a given valve travel will invariably change the throughput in a given proportion. Let e.g. $q/q_{max} = 0{\cdot}09$, in which case the diagram shows $s_v/s_{max}$ to equal 0·40. If this latter is increased by 0·20 to 0·60, then $q/q_{max}$ becomes 0·2, that is, about 2·2 times the preceding value. A further increase in relative valve travel by 0·2 (that is, to 0·8) results in a relative throughput of 0·45, which is again round 2·2 times the foregoing value. This is the type of regulation required e.g. in controlling the temperature of a system. To bring about a unit change of temperature in the system

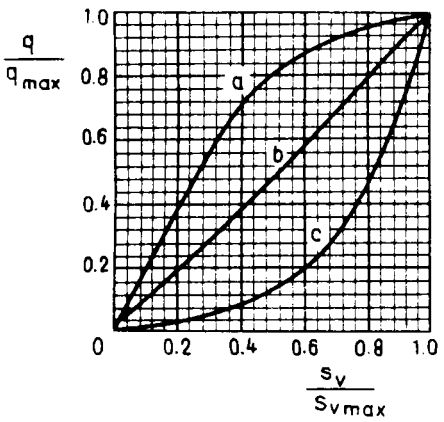


Fig. 6.2 - 13. Response characteristics of inner-valve designs

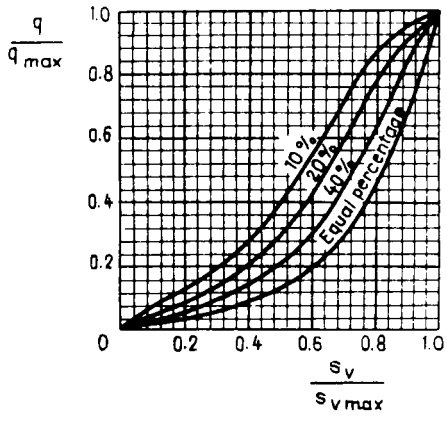


Fig. 6.2 – 14. Modified equal-percentage valve characteristics, after Reid (1969)

requires, say, 9 thermal units when the system is loaded at 90 percent but only 5 units if it is loaded at 50 percent (Reid 1969).

The above characteristics will strictly hold only if the head loss caused by the valve alone is considered; if, however, the flow resistance of the pipes and fittings attached to the valve is comparatively high, then increasing the throughput will entail a higher head loss in these. *Figure 6.2 – 14* (after Reid 1969) shows how an equal-percentage characteristic is displaced if the head loss in the valve makes up 40, 20 and 10 percent, respectively, of the total head loss in the system. The less the percentage due to the valve itself, the more the characteristic is distorted, and the less can the desired equal-percentage regulation be achieved. Throughput of a valve is usually characterized by the formulae

$$q_l = K_v \sqrt{\frac{\Delta p}{\rho_l}} \qquad 6.2-1$$

for liquids and

$$q_g = K'_v \sqrt{\frac{p_1^2 - p_2^2}{\rho_g T}} \qquad 6.2-2$$

for gas. $K_v$ and $K'_v$ are factors characteristic of the valve's throughput, equalling throughput under unity pressure differential (respectively, unity pressure-square differential in the case of gas). The $K$ factor will, of course, change as the valve travel is changed. In a good regulating valve, it is required that the $K_v$ (or $K'_v$) value obtaining at maximum throughput (at full opening) should be at least 50 times the value at the minimum uniform throughput permitted by the valve design (Reid 1969).

A widely used type of control valve is the Fisher-make double-seat spring-loaded motor valve of the normal-open type shown in *Fig. 6.2 – 11*. (This latter term means

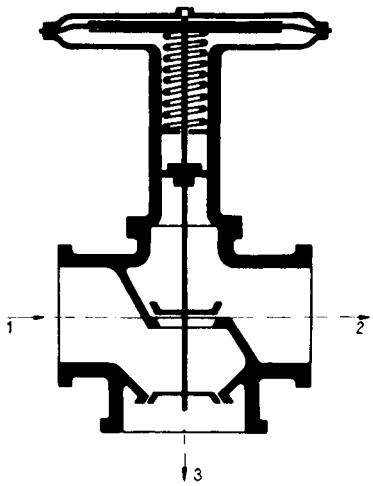


Fig. 6.2 – 15. Three-way two-position motor valve

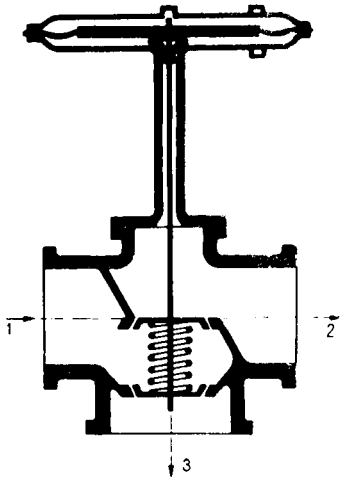


Fig. 6.2 – 16. Three-way three-position motor valve

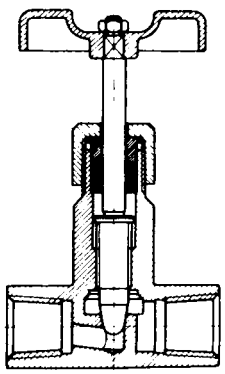

Fig. 6.2 – 17. Needle valve

that the valve is kept open by spring *1* when no actuating gas pressure acts upon diaphragm *2*.) The valve is two-way two-position, because it has two apertures (one inlet and one outlet), and the inner valve may occupy two extreme positions (one open and one closed).

Other diaphragm-type motor valves include the three-way two-position motor valve shown as *Fig. 6.2 – 15*. At zero actuating-gas pressure, the fluid entering the valve through inlet *1* emerges through outlet *2*. If gas pressure is applied, then the upper inner valve will close and the lower one will open, diverting fluid flow to outlet 3. *Figure 6.2 – 16* shows a three-way three-position motor valve. The diaphragm may be displaced by actuating-gas pressure acting from either above or below. At

zero actuating-gas pressure, the inner valves are pressed against their respective seats by the spring between them, and both outlets are closed. If gas pressure depresses the diaphragm, the upper inner valve is opened and the fluid may emerge through outlet *2*. If gas pressure lifts the diaphragm, the lower inner valve is raised

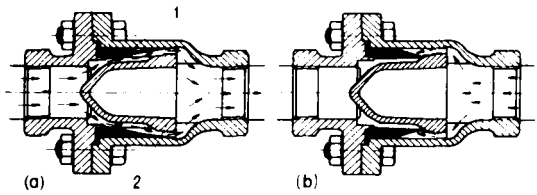


Fig. 6.2 – 18. Grove's 'Chexflo' check valve

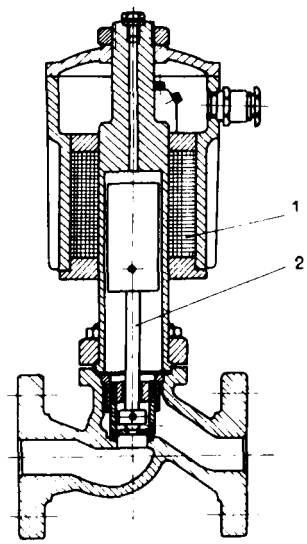


Fig. 6.2 – 19. MAW magnetic pilot valve

while the upper one is closed, and the fluid stream is deflected to pass through outlet *3*.

Of the host of special-purpose valves, let us specially mention the needle valve, one design of which, shown as *Fig. 6.2 – 17*, can be used to control high pressures in small-size piping of low throughput, e.g. in a laboratory. It is of a simple construction easy to service and repair.

Check valves permit flow in one direction only. *Figure 6.2 – 18* shows a Grove make 'Chexflo' type check valve. The tapering end of elastic rubber sleeve *1* tightly

Table 6.2 – 1. Advantages of various valve designs
(personal communication by J. Bognár)

| Design features | | Low head loss | Pipe scraping is possible | Long life | Tight shutoff | Ease of operation | Speed of operation | Applicability | | | Small space demand | Quick access |
|---|---|---|---|---|---|---|---|---|---|---|---|---|
| | | | | | | | | High pressure | Corrosive medium | Corrosive surroundings | | |
| Full opening | | × | × | | | | | | | | | |
| Seal of closing element | metallic | | | × | | | | × | | | | |
| | elastic | | | | × | | | | | | | |
| | mixed | | | × | × | | | × | | | | |
| Exchangeable seat | | | | | | | | | × | | | |
| Element of obstruction balanced | | | | | | × | | × | | | | |
| Stem turning on bearing | | | | | | × | | × | | | | |
| Inside-thread stem | | | | | | | | | | × | | |
| Outside-thread stem | | | | | | | | | × | | | |
| Bolted bonnet | | | | | | | | | | | × | |
| Ring-held bonnet | | | | | | | | | | | | × |
| Bolted stuffing box | | | | | | | | | | | × | |
| Thread stuffing box | | | | | | | | | | | | × |
| Level-operated | | | | | | | | × | | | | |
| Power-operated | | | | | | × | | | | | | |

embraces the cylindrical part of central core *2* if there is no flow in the direction shown in part (a) of the Figure. Even a slight pressure differential from left to right will, however, lift the sleeve from the core and press it against the valve barrel. The valve is thus opened. A pressure differential in the opposite sense will prevent flow by pressing the sleeve even more firmly against the core.

Actuating gas for diaphragm-controlled motor valves is often controlled in its turn by a pilot valve. *Figure 6.2 – 19* shows an electromagnetic pilot valve as an example. Current fed into solenoid *1* will raise soft-iron core *2* and the inner valve attached to it.

Valve choice is governed by a large number of factors, some of which have been discussed above. *Table 6.2 – 1* is intended to facilitate the choice of the most suitable design.

### 6.2.2. Pressure regulators

Gas and gas-liquid streams are usually controlled by means of pressure regulators without or with a pilot. A rough regulation of comparatively low pressures (up to about 30 bars) may be effected by means of automatic pressure regulators without pilot. These may be loaded by a spring, pressure or deadweight, or any combination of these. *Figure 6.2 – 20* shows an automatic regulator loaded by a deadweight plus gas pressure, serving to regulate the pressure of outflowing gas. Weight *1* serves to adjust the degree of pressure reduction. If downstream pressure is higher than desired, the increased pressure attaining membrane *3* through conduit *2* will depress both the diaphragm and the inner valve *4*, thereby reducing the flow cross-section and the pressure of the outflowing gas. If downstream pressure is lower than required, the opposite process will take place. Automatic pressure regulators have the advantage of simple design and a consequent low failure rate and low price, but also the drawback that, especially at higher pressures, they will tend to provide a rather rough regulation only. Control by the regulated pressure is the finer the larger the diaphragm surface upon which said pressure is permitted to act. A large diaphragm, however, entails a considerable shear stress on the free diaphragm perimeter. A thicker diaphragm is thus required, which is another factor hampering fine regulations.

A pilot-controlled pressure regulator is shown in outline in *Fig. 6.2 – 21* (Petroleum . . . *Field* 1956). The regulated pressure acts here on a pilot device rather than directly upon the diaphragm of the motor valve. Pressure of gas supplied from

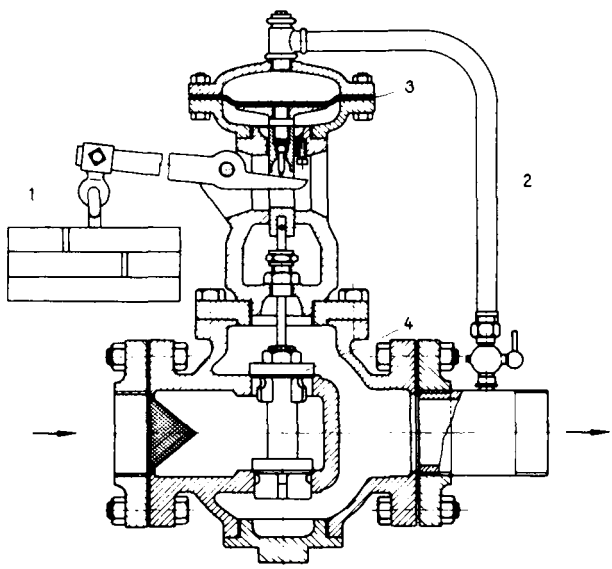


Fig. 6.2 – 20. Deadweight-loaded, automatic pressure regulator

a separate source is reduced to a low constant value by automatic regulator *1*. This supply gas attains space *3* through orifice *2* of capillary size. If vent nozzle *4* is open, then supply gas is bled off into the atmosphere. If downstream pressure increases, Bourdon tube *5* strives to straighten, thereby forcing the lower end of flapper *6* towards nozzle *4*. Gas pressure will therefore increase in space *3* above diaphragm *7* and the inner valve will travel downwards. Control sensitivity may be adjusted by displacing pivot *8*, whereas screw *9* serves to adjust the degree of pressure reduction.

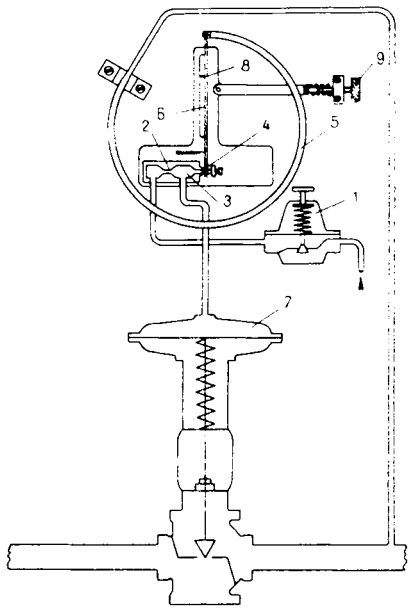


Fig. 6.2 – 21. Pilot-operated pressure regulator (Petroleum . . . *Field* 1956)

In pressure regulation, normal-open motor valves are often replaced by normal-closed ones. These latter may be of the type e.g. of the motor valve shown in *Fig. 6.2 – 22*, with the inner valve inserted upside down, that is, closing when pressed against the seat from below. Choice between the two options is to be based on a consideration of whether an open or a closed valve will cause less havoc, should the actuating-gas pressure fail. If the pressure conduit of the motor valve is hooked up to the upstream side, then the device will, without any further change, regulate the upstream pressure. If vent nozzle *4* (*Fig. 6.2 – 21*) is installed on the opposite side of flapper *6*, then control will be inverted, that is, pressure above the diaphragm will decrease as the controlled pressure increases. *Figure 6.2 – 22* presents the main modes of hookup of pressure regulators involving the usual types of pressure-loaded motor valve (after Petroleum . . . *Field* 1956; cf. also *Table 6.2 – 2*).

Table 6.2 – 2. Behaviour of main gas pressure regulator types

| | Controlled gas flow is | | | | | |
|---|---|---|---|---|---|---|
| | downstream | | | upstream | | |
| Control | direct | reverse | reverse | reverse | direct | direct |
| Downward valve travel will | close | open | close | close | open | close |
| On actuating-gas failure, valve will | open | close | close | open | close | close |
| On increase of controlled pressure, valve will | close | close | close | open | open | open |
| Type code | Ia | Ib | Ic | IIa | IIb | IIc |

*Figure 6.2 – 23* is a sketch of a Grove-make gas-dome-type pressure regulator. On installation of the valve, dome *1* is filled through conduits not shown in the Figure with gas at a pressure sufficient to exert upon diaphragm *2* a force bringing about the pressure reduction desired. This gas is trapped in the dome by means of needle valves. The lower surface of the diaphragm is exposed to the reduced pressure. It is primarily the pressure differential across the diaphragm that determines the position of inner valve *3*. The regulating action is improved by the gas space of the

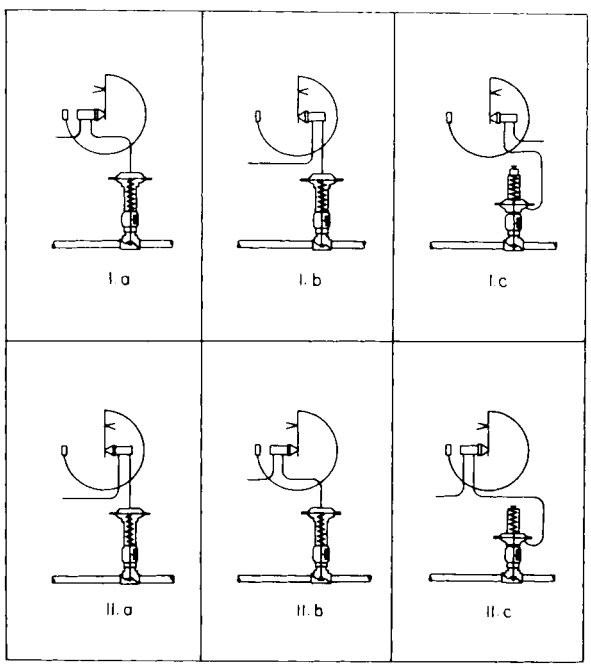


Fig. 6.2 – 22. Pressure-regulator hookups (Petroleum... *Field* 1956)

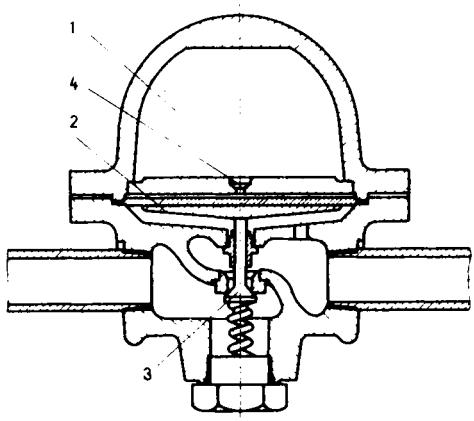


Fig. 6.2 – 23. Grove's gas-dome pressure regulator

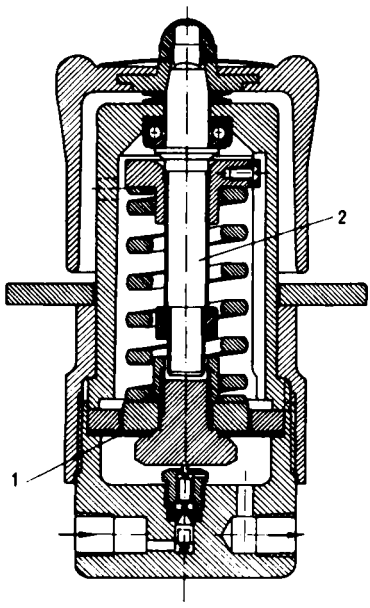


Fig. 6.2 – 24. Grove's M-16 type pressure regulator

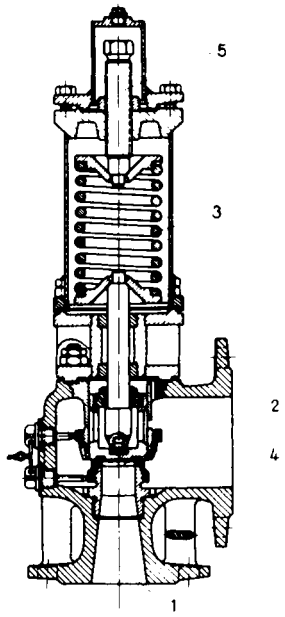


Fig. 6.2 – 25. Giproneftmash's SPPK-16 type spring-loaded safety valve

dome being divided in two by capillary *4*. If the controlled pressure rises above a certain maximum, a sudded pressure increase in the space below the capillary will occur and generate a considerable back-pressure. The great advantage of this type of reducing valve is its simplicity and reliability of operation. Its disadvantage is that the regulating pressure in the dome depends, of course, on ambient temperature. This design is therefore best suited for controlling low-rate gas flows in places of constant temperature.

The Grove Model 16 pressure regulator is likewise suited for controlling small gas throughputs (*Fig. 6.2 – 24*), e.g. to provide pressure-loaded motor valves with supply gas. The various sizes of this model can reduce the input pressure of round 70 bars to practically any pressure not less than 0·07 bar. Its operation resembles that of the gas-dome pressure regulator, the main difference being that diaphragm *1* is loaded by a spring adjusted by screw *2* rather than by the temperature-dependent pressure of gas in a dome.

Safety valves will blow off fluid or gas whenever pressure in the vessel containing them exceeds a given maximum. *Figure 6.2 – 25* shows a SPPK – 16 type Giproneftmash-make spring-loaded safety valve. If the force acting on valve disk *2* in the space connected with port *1* exceeds the downward force of spring *3*, the valve opens and permits the fluid to vent through outlet *4*. Opening pressure may be adjusted by modifying the spring force by means of screw *5*.

Most of the numerous other known types of pressure regulators and safety valves embody operating principles similar to those outlined above.

## 6.3. Internal maintenance of pipelines

On the walls of oil and sometimes also of gas pipelines, wax deposits will tend to form. Wax is composed of paraffin compounds, ceresin, asphalt and sand. The deposit reduces the cross-section open to flow, and its removal must therefore be provided for.

In case of gas pipelines two types of deposits, that may cause flow resistance must be taken into consideration. (i) Liquid hydrocarbons and water may condense in pipelines transporting gas. This liquid, which may contain solids, too, will reduce on the one hand the throughput capacity of the pipeline; on the other, liquid entering gas burners together with the gas may cause serious trouble. The accumulation of liquid in gas pipelines must therefore be prevented.

(ii) If the condensate, separated from the gas or water, is mixed with the lube oil of compressors, then this mixture, sticking to the pipe wall gathers dust and iron oxide particles, and thus, increases the roughness of the pipe wall and leads to its corrosion (VerNooy 1980b). By applying regular pipe scraping both of the above effects may be reduced.

Deposits are usually removed by means of scrapers (go-devils) or cleaning pigs inserted in the pipeline, at intervals depending on the rate of deposition, and moved along by the fluid or gas stream.

The go-devil (*Fig. 6.3 – 1*) is the type in longest use for cleaning the inner walls of oil pipelines. It is used up to nominal diameters of 12 in. Disks of leather or oil-resistant synthetic rubber mounted on plates *1* ensure 'piston action', the moving along of the scraper in the oil stream. Spring-loaded sawtooth rollers *2* ensure coaxial advance. The deposits are scraped off the pipe wall by spring-loaded blades

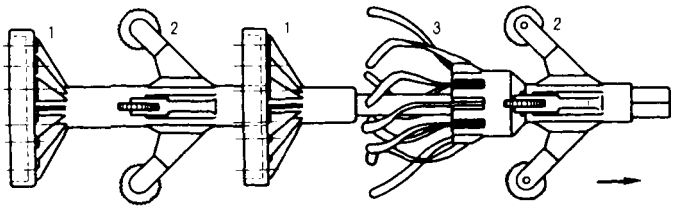


Fig. 6.3 – 1. Go-devil

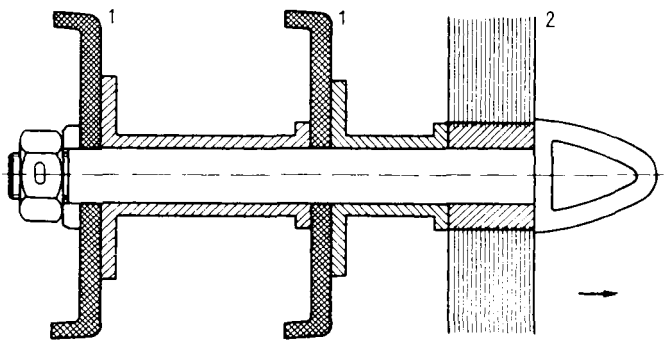


Fig. 6.3 – 2. General Descaling scraper for small-size pipelines

*3*. Certain scrapers are articulated, to help them negotiate sharp bends. This type of scraper has the drawback of having a large number of parts liable to break off in the pipe and cause all manner of trouble. In the scraper used for small-size pipes shown as *Fig. 6.3 – 2*, piston action is ensured by rubber cups *1*; scraping is performed by round wire brush *2*. In cleaning large-size pipelines, revolving pigs are used (*Fig. 6.3 – 3*). The front disk *3* of the scraper carrying piston cups *1* and round brushes *2* is provided with tangential jet nozzles through which a small amount of fluid may flow behind the scraper. The jets shooting from these nozzles make the pig rotate slowly, and help to loosen the deposit piled up by the advance of the scraper. Both effects reduce the hazard of the pig's seizing up in the pipeline.

The scraper, equipped with a conic packing and spring wire brushes, is of high cleaning efficiency (*Fig. 6.3 – 4*).

Stucking of scrapers may lead to operational problems. The main reasons for this are (i) the changing, and, from spot to spot, the extremely decreased pipe section, and

deformation in the pipe wall, respectively; (ii) the deposited layer on the pipe wall that is too thick, and too hard; and (iii) the wear, and possible break of the pipe scraper while passing.

In order to avoid the disorders, caused by the first two reasons enumerated above, the pipeline must be calipered. Before starting the operation of the pipeline, a plug, equipped with a metal disc on its face is used for calipering. Its diameter, in VerNooy's opinion, should be 92·5 percent of the *ID* of the pipeline. For the

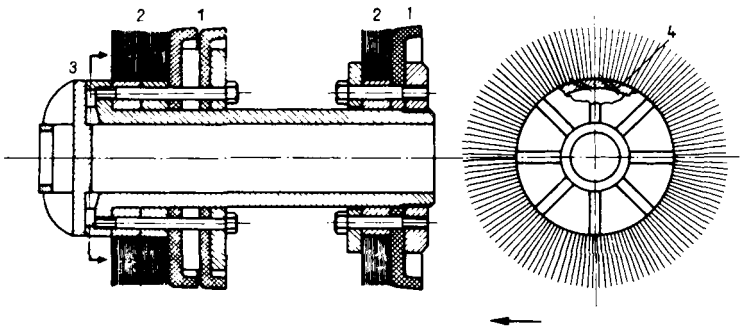


Fig. 6.3 – 3. General Descaling rotating scraper for large-size pipes

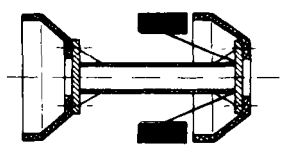

Fig. 6.3 – 4. Scraper with spring actuated wire brushes

measurement of the deformation, pipe wall thickness reduction, and deposition, in case of operating pipelines, the so-called caliper pig, can be used, that, while passing, records the parameters of the measured inside cross-section (VerNooy 1980a).

Scrapers may be used also to separate plugs of different liquids or plugs of liquid and gas ('batching') and it is also used for the removal of the liquid, settled in different sections of the gas pipeline.

If there is no wax deposit in the pipe, it is simpler, cheaper and less liable to cause trouble to insert a batching piston (pipeline pig) rather than a scraper. A pig of General Descaling make, GDSS 90 – 4 type is shown as *Fig. 6.3 – 5*. Its swab cups are made of neoprene. This pig will pass through any bend whose radius is at least half as great again as the pipe radius. Branch-offs of the same diameter as the mainline are no obstacle to its application. A pipeline batching ball serving also for the removal of liquids from gas lines is the Piball, likewise of GD make (*Fig. 6.3 – 6*).

The ball of synthetic rubber can be inflated with a liquid through valve 1 so that its diameter exceeds by 2 percent the *ID* of the pipe. Experiments have shown that the Piball removes all but 0·02 – 0·04 percent of the liquid in the pipe. Its advantages include longer life owing to its spherical shape and inflatability. It is compatible with

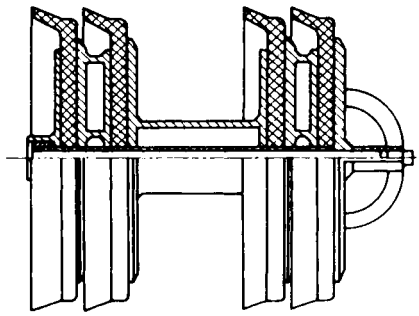

Fig. 6.3 – 5. General Descaling GDSS 90 – 4 pipeline pig

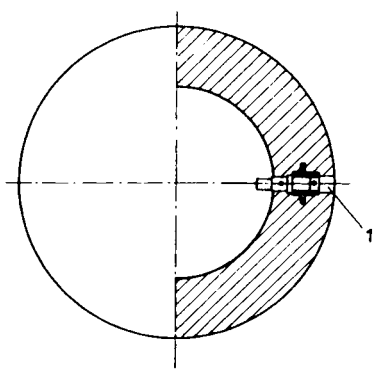


Fig. 6.3 – 6. General Descaling 'Piball'

lease automation and will readily pass through pipe fittings. Scrapers fitted with polyurethane blades, inflatable polyurethane pipeline balls and polyurethane-foam balls are also used; practical experience has shown these to be rather long-lived (Zongker 1969).

A fairly complete removal of liquid may be achieved by means of the so-called sypho-pig, shown schematically in *Fig. 6.3 – 7*. The device, fitted with four swab cups *1*, is pushed forward by dry gas in the pipeline. Part of the dry gas, entering through orifice *2*, passes through the tortuous paths indicated by arrows into chambers *3* and *4*, where it dries the pipe wall by evaporating the liquid film

adhering to it, and carries the vapour into chamber *5*. Liquid in chamber *5* is expelled by the gas through tube *6* and jetted through injectors *7* in front of the pig. The jets, causing turbulency in the liquid pushed forward by the pig, prevent solids from settling out of it and from seizing the pig (PLI Staff 1970). In some cases, balls or cylinders made of paraffin and asphalt kneaded together or of a substance slowly soluble in oil are also used for paraffin-removal.

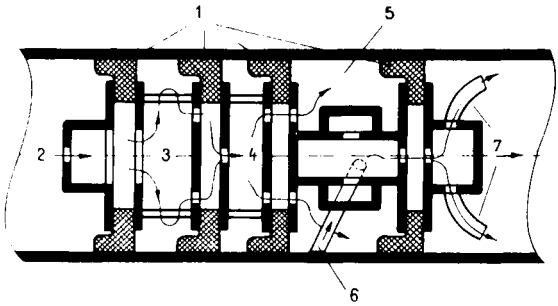


Fig. 6.3 – 7. Sypho-pig, after 'PLI Staff (1970)

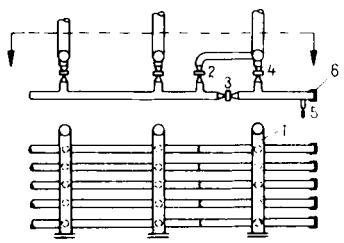


Fig. 6.3 – 8. Scraper trap in front of separator station

Scrapers are introduced into the flowlines of wells at the wellhead, and retrieved at scraper traps installed next to the separator station (*Fig. 6.3 – 8*). During the scraping operation, the well fluid is directed through gathering line *1* into the first separator, with valve *2* closed and valves *3* and *4* open. After the arrival of the scraper, valve *2* is opened; valves *3* and *4* are closed. The cut-off pipe section containing the scraper is bled off through relief valve *5;* the scraper can be removed after opening cover *6*. — *Figure 6.3 – 9* shows launching and receiving scraper traps installed at the beginning and at the end, respectively, of an oil pipeline. During normal operation, valves *1* and *2* of the launching trap [part (a) of the Figure] are closed, while valve *3* is open. After depressurizing through valve *4* the section cut off by valves *1* and *2*, cover *5* is removed and the scraper is inserted into oversize barrel *6*. After replacing cover *5*, valves *1* and *2* are opened and valve *3* is closed. Instead of

gate valves, handwheel-operated plug valves are often employed in these applications. The operation of the receiving scraper trap [part (b) of the Figure] is much similar to that of the launching trap. — Long pipelines are often provided with intermediate scraper stations (*Fig. 6.3 – 10*), where the worn scraper arriving on side *1* is retrieved and a new one is inserted on side *2* (cf. *Fig. 7.4 – 14*).

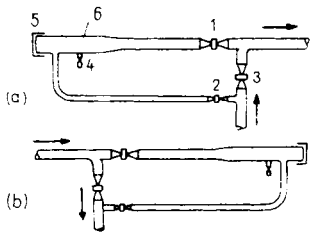


Fig. 6.3 - 9. Scraper traps at head and tail end of pipeline

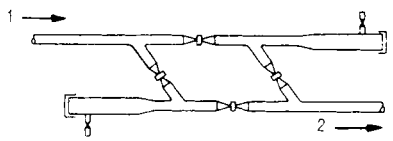


Fig. 6.3 – 10. Intermediate scraper trap on a pipeline

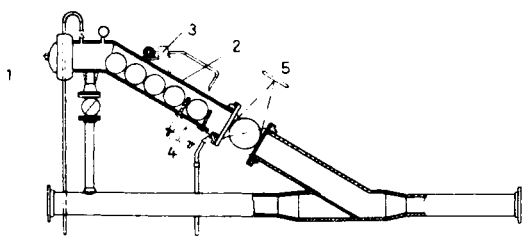


Fig. 6.3 – 11. General Descaling pipe ball feeder

Pipeline balls may be fed into the line by remote control. *Figure 6.3 – 11* shows the GD hydraulic ball feeder. After removal of cover *1*, several balls can be inserted into pipe section *2*. At the desired instant, a hydraulic control unit *3* (not shown in detail in the Figure) actuates release device *4* which lets a ball roll into the pipeline through open valve *5*. It is possible to monitor the passage of the ball through suitably chosen pipe sections. The sections in question are perforated and a fitting is installed in the perforation which includes a small feeler reaching radially into the flow section. The passing ball will touch the feeler; a device attached to this latter will mechanically or electrically signal the passage of the ball (cf. Section 7.2.3).

## 6.4. Separation of oil and gas

### 6.4.1. Equilibrium calculations*

The oil and gas composing the well fluid are usually separated in separators. A separator is essentially a vessel whose interior is kept at the prescribed separation pressure and temperature. Separator temperature is either determined by the temperature of the inflowing well stream and the ambient temperature, or adjusted by means of heating or cooling equipment. The prescribed separator pressure is usually maintained by a pressure regulator installed in the gas line of the separator. Oil and gas emerge from the separator through separate outlets. The composition and relative abundance of the separation products can be predicted either by laboratory tests, or — in a fair approximation — by theoretical considerations and/or using diagrams based on practical experience. In calculations based on auxiliary diagrams it is assumed that the well stream and the discharged oil and gas do not vary in composition with time; that separation is of the flash type; and that the system is in thermodynamic equilibrium at the given pressure and temperature. The calculations are based on the following three equations:

$$n = n_L + n_V \qquad 6.4-1$$

$$z_i n = n_L x_i + n_V y_i \qquad 6.4-2$$

$$K_i = \frac{y_i}{x_i} \qquad 6.4-3$$

$K_i$ is the equilibrium ratio of the $i$th component in the liquid-gas system. By Eq. 6.4 − 1, then, the total number of moles in the system equals the number of moles in the liquid and gas phases taken separately. By Eq. 6.4 − 2, the total number of moles of any component in the system equals the number of moles of that component taken separately in the liquid and gas phases. The above considerations imply

$$\sum_{i=1}^{m} x_i = \sum_{i=1}^{m} y_i = \sum_{i=1}^{m} z_i = 1 \qquad 6.4-4$$

Dividing both sides of Eq. 6.4 − 2 by $n$, we get

$$z_i = \frac{n_L}{n} x_i + \frac{n_V}{n} y_i .$$

Let $n_L/n = z_L$ and $n_V/n = z_V$; then

$$z_i = z_L x_i + z_V y_i . \qquad 6.4-5$$

By Eq. 6.4 − 4, the sum of the mole fractions of the components is unity, separately in the liquid and gas as well as in the entire liquid-gas system. By Eq. 6.4 − 5, the mole

* Largely after Amyx (1960)

fraction of a given component in the system equals the sum of its mole fractions in the gas and liquid phase, taken separately. Introducing $y_i$ and then $x_i$ from Eq. 6.4 $-3$, we get

$$x_i = \frac{z_i}{z_L + K_i z_V} \qquad 6.4-6$$

and

$$y_i = \frac{z_i}{z_L/K_i + z_V} . \qquad 6.4-7$$

These are the fundamental equations of equilibrium in separation.

In practice, separation is usually performed in several stages. Stages are series-connected, the last stage being the stock tank. Three-stage separation, for instance,

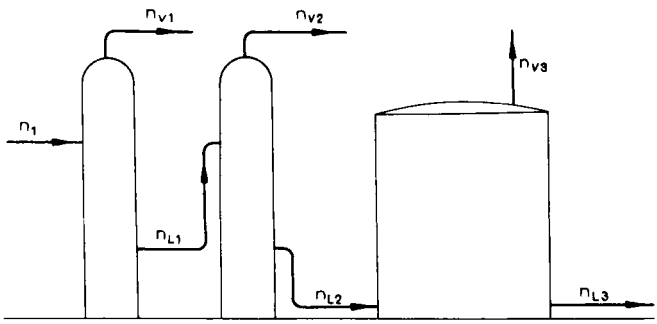


Fig. 6.4 – 1. Schematic diagram of three-stage separation

takes place in two separators and one stock tank (*Fig. 6.4 – 1*). The numerical suffixes attached to the symbols introduced above refer to the respective separator stages. The liquid discharged from the first separator enters the second separator. The mole number of this stream is

$$n_{L1} = z_{L1} n_1 .$$

The mole number of the liquid entering the third separator (which is the stock tank in the case considered) is

$$n_{L2} = z_{L2} n_{L1} = z_{L1} z_{L2} n_1 .$$

The mole number of the liquid obtained from the third separator is

$$n_{L3} = z_{L3} n_{L2} = z_{L1} z_{L2} z_{L3} n_1 .$$

The mole number of the gas discharged from the first separator is

$$n_{V1} = z_{V1} n_1 .$$

The mole number of gas discharged from the second separator is

$$n_{V2} = z_{V2} n_{L1} = z_{V2} z_{L1} n_1 .$$

The mole number of the hydrocarbon vapour discharged from the third separator (or simply evaporating from it, if the tank is open) is

$$n_{V3} = z_{V3} n_{L2} = z_{V3} z_{L1} z_{L2} n_1 .$$

In three-stage separation, the gas-oil ratio is generally the volume ratio of the gas discharged from the first two stages to the liquid collecting in the third stage (stock-tank oil), that is,

$$R = \frac{(n_{V1} + n_{V2}) V_{\text{mol}}}{n_{L3} \dfrac{M_{L3}}{\rho_{L3}}}$$

where $V_{\text{mol}}$ is the molar volume of the gas molecules in the standard state, in $m^3$/kmoles; $M_{L3}$ is the molar mass of the liquid collecting in the third stage, in kg/kmoles; and $\rho_{L3}$ is the density of the liquid collecting in the third stage, in $kg/m^3$. Dividing both the numerator and denominator of the above formula by $n_1$, we get

$$R = \frac{\dfrac{n_{V1} + n_{V2}}{n_1} V_{\text{mol}} \rho_{L3}}{\dfrac{n_{L3}}{n_1} M_{L3}} = \frac{(z_{V1} + z_{V2} z_{L1}) V_{\text{mol}} \rho_{L3}}{z_{L1} z_{L2} z_{L3} M_{L3}} \qquad 6.4-8$$

and for two-stage separation,

$$R = \frac{z_{V1} V_{\text{mol}} \rho_{L2}}{z_{L1} z_{L2} M_{L2}} . \qquad 6.4-9$$

The practical usefulness of equilibrium calculations depends first and foremost on the accuracy of the equilibrium ratios $K_i$. The equilibrium ratio of the $i$th component depends, in addition to separator temperature and pressure, also on the composition of the well fluid, and accurate values may only be expected from the laboratory testing of the fluid to be treated. The values of $K_i$ may, however, be determined in a fair approximation also by various methods based on auxiliary diagrams. The processes in current use relate the composition of the system to convergence pressure. It is assumed that if two systems of hydrocarbons agree as to convergence pressure, then the equilibrium ratios of their components will likewise be equal at the given pressure and temperature. Hence, in order to find $K_i$, it is necessary to know the convergence pressure of the system and the equilibrium ratios belonging to various convergence pressures. Determining in the laboratory the equilibrium ratios of the components of a given hydrocarbon system at various pressures and at a given temperature, one obtains families of curves similar to the two families shown in *Fig. 6.4 – 2*. These curves all end in one point, lying on the line $K = 1$ and characterized by a certain pressure. The pressure thus determined is the

apparent convergence pressure. It is 69 bars for the first family shown in the Figure, and 345 bars for the second (Amyx *et al.* 1960). If the laboratory experiment is performed at the critical temperature of the system, then the apparent convergence pressure agrees with the critical pressure. At any other temperature, convergence is merely apparent, because the system has its bubble point at a pressure lower than the

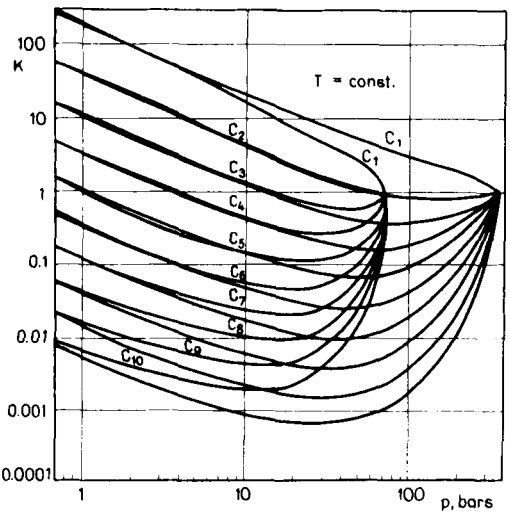


Fig. 6.4 – 2. Equilibrium ratios of components of hydrocarbon systems of 69 and 345 bars, apparent convergence pressure; from Natural Gasoline Association of America's *Equilibrium Ratio Data Book* (1957; used with permission of Natural Gas Processors Association)

apparent convergence pressure and there is just one phase instead of two at the point of convergence. In the zone between the critical pressure and the apparent convergence pressure, then, the equilibrium constant lacks a physical meaning: the corresponding curve sections and the point of apparent convergence itself are merely the results of extrapolation. The apparent convergence pressure of a given system of hydrocarbons can be determined by various means. Its importance is substantial especially at high pressures. At pressures below cca 7 bars, however, the system's composition, and hence, knowledge of its exact convergence pressure, lose much of their importance. Experiment has shown that in establishing the $K$ values required for calculating equilibria in low-pressure separators, a satisfactory accuracy will be achieved if convergence pressure is simply assumed to equal 345 bars (5000 psia). K-isotherms may be found in the NGAA *Equilibrium Ratio Data Book* (1957). *Figure 6.4 – 3* shows the $K$-isotherms of isobutane for an example.

In the usual laboratory-analysis report, it is usual to state the content or mole fraction of all components heavier than hexane by a single figure denoted $C_{7+}$ (heptane-plus). The composition of this mixture of hydrocarbons may vary widely,

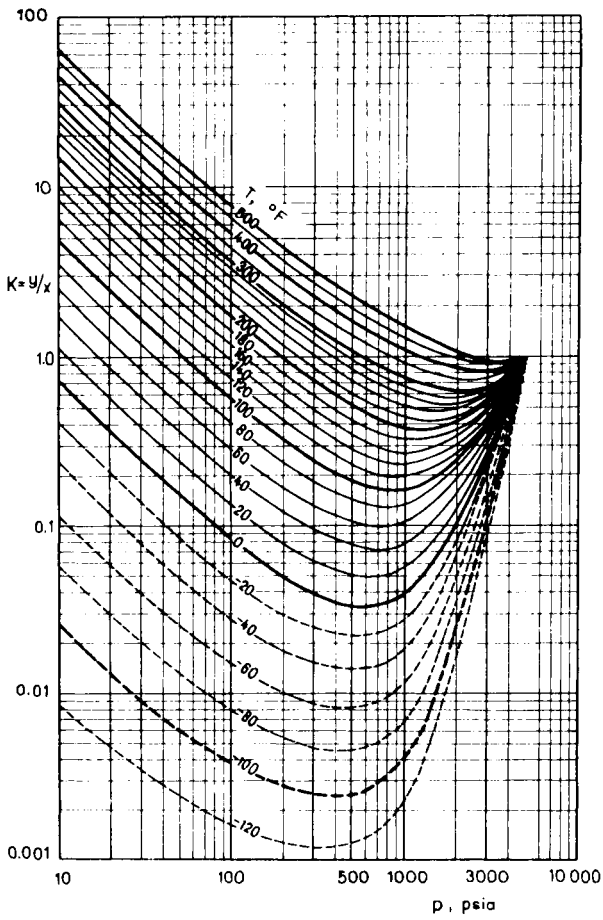


Fig. 6.4 – 3. Equilibrium ratios of isobutane at 5000 psia apparent convergence pressure; from Natural Gasoline Association of America's *Equilibrium Ratio Data Book* (1957; used with permission of Natural Gas Processors Association)

depending on the composition of the crude in hand. Since, however, the pressure curves and critical parameters of components heavier than hexane differ very little, the system may be satisfactorily characterized by a median $K$-value. The equilibrium ratios of this fraction can be estimated using the graphs in *Fig. 6.4 – 4* (after Katz and Roland in Amyx *et al.* 1960). Let us finally point out that, even though both the density and molar mass of the $C_{7+}$ fraction are required for equilibrium calculations, only one of the two data need be established in the laboratory, as the other one can be calculated using Cragoe's formula:

$$M = \frac{44{\cdot}29\rho}{1030 - \rho} \qquad 6.4-10$$

For the approximation of the equilibrium ratios, on the basis of the NGAA diagrams, numerical relations were elaborated by Canfield and Rowe. Canfield (1971) gives the $K_i$ equilibrium ratio of the $i^{th}$ component in the function of the following parameters: $p_{co}$ apparent convergence pressure; the $p/p_{co}$ pressure ratio and $T/T_{ci}$ temperature ratio; and the $z_{ci}$ critical deviation factor:

$$K_i = \frac{p_{co}}{p} \exp\left[ A_i B_i \left( 1 - \frac{p}{p_{co}} \right)^{0{\cdot}33\, T/T_{ci}} \right], \qquad 6.4-11$$

where

$$A_i = 8{\cdot}0272 - \ln p_{co} - 4{\cdot}4613 \frac{T_{ci}}{T} - 0{\cdot}1968 \left( \frac{T_{ci}}{T} \right)^3$$

and

$$B_i = 6{\cdot}3816 - 29{\cdot}0020\, z_{ci} + 35{\cdot}3443\, z_{ci}^2 .$$

The correlation, elaborated by Rowe (1978), is based on the fact, that, in case of a system characterized by a given convergence pressure, the logarithm of the

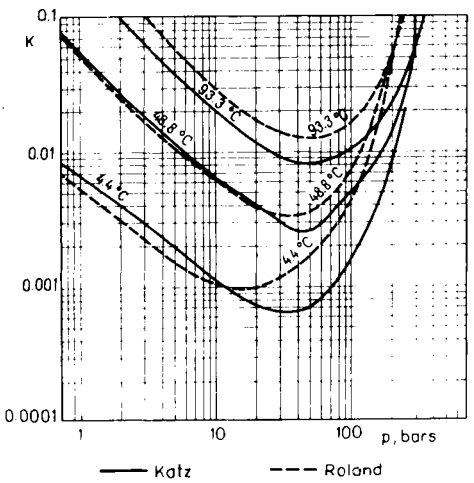


Fig. 6.4 – 4. Equilibrium ratio of $C_{7+}$, according to Katz and Roland (Amyx *et al.* 1960, p. 341; used with permission of McGraw-Hill Book Company)

equilibrium constants of the hydrocarbon components, at any constant pressure and temperature, changes in a linear way with the square of the critical temperature of the components.

Recently, to determine the phase equilibria of light hydrocarbons, several calculation methods, based on the equation of state, were elaborated (Kaufmann 1968; Starling 1973; Fussel and Yanosik 1978; Conrad and Gravier 1980). For hydrocarbon systems, containing also oil, development of such a system seems to be

Table 6.4 – 1. Physical parameters of hydrocarbons

| | Symbol | Unit | $CH_4$ | $C_2H_6$ | $C_3H_8$ |
|---|---|---|---|---|---|
| Molar mass | $M$ | $\frac{kg}{kmole}$ | 16·042 | 30·068 | 44·094 |
| Critical temperature | $T_c$ | K | 190·6 | 305·5 | 370·0 |
| Critical pressure | $p_c$ | bar | 46·4 | 48·8 | 42·6 |
| Critical density | $\rho_c$ | $kg/m^3$ | 161·9 | 203·1 | 226·2 |
| Critical molar vol. | $V_{mc}$ | $m^3/kmol$ | 0·09901 | 0·1480 | 0·1950 |
| Gas density (std) | $\rho_{gn}$ | $kg/m^3$ | 0·6750 | 1·265 | 1·855 |
| Gas density (rel.) | $\rho_{gr}$ | – | 0·554 | 1·038 | 1·522 |
| Liquid density | $\rho_l$ | $kg/m^3$ | 299·5* | 372·6 | 506·8 |

* Pseudo-gravity
Standard state is at $T_n = 15·6$ C, $p_n = 1·01$ bar

irrational, since the quantitative analysis and so the characterization of the crude in hand is rather complicated and expensive.

In case of the direct use of the NGAA curves the process of calculating the equilibrium at low pressure separation is, as follows:

Equilibrium calculation at low-pressure separation proceeds as follows: (i) The $K_i$ values for the prevailing temperature and pressure are read off the NGAA graphs for 345 bars convergence pressure, (ii) the equilibrium ratio of the $C_{7+}$ fraction is read off *Fig. 6.4 – 4*, (iii) a value for $z_V$ is estimated, and $x_i$ is calculated for each component using Eq. 6.4 – 6. (iv) If $\sum_{i=1}^{m} x_i$ is unity, then the assumed $z_V$ is correct, and so is, of course, $(1 - z_V) = z_L$. If $\sum_{i=1}^{m} x_i$ differs from unity, the calculation has to be repeated with a different $z_V$. Equilibrium calculations are usually performed by computer nowadays, thus bypassing the time-consuming successive approximation by pencil and paper. *Table 6.4 – 1* contains physical constants published by CNGA and NGAA for equilibrium calculations.

*Example 6.4 – 1.* With reference to the hydrocarbon system characterized by Columns 1 and 2 of *Table 6.4 – 2*, and assuming three-stage separation, (i) what are the compositions of the gas effluents of the individual separator stages? (ii) what will be the composition of the stock-tank oil collecting in the atmospheric-pressure stock-tank? (iii) what will be the 'useful' *GOR*, that is, the volume of gas discharged from the first two stages of separation per $m^3$ of stock-tank oil? Let separation temperature be 4 °C in all three stages, and let pressure be 6 bars in the first stage, 2·1 bars in the second, and 1·01 bar in the third. The standard state is at $p_n = 1·01$ bar and $T_n = 15·6$ °C.

The main results of the equilibrium calculation for the three separator stages are presented in *Tables 6.4 – 2 – 6.4 – 4*. The $K_i$ values were taken from the diagrams for 5000 psia convergence pressure of the NGAA Equilibrium Data Book; the values

(modified after CNGA and NGAA data)

| i-$C_4H_{10}$ | n-$C_4H_{10}$ | i-$C_5H_{12}$ | n-$C_5H_{12}$ | n-$C_6H_{14}$ | n-$C_7H_{16}$ | $C_{7+}$ |
|---|---|---|---|---|---|---|
| 58·120 | 58·120 | 72·146 | 72·146 | 86·172 | 100·198 | |
| 407·2 | 425·0 | 461·1 | 470·6 | 507·8 | 540·0 | |
| 36·6 | 38·0 | 33·2 | 33·5 | 29·9 | 27·4 | |
| 233·0 | 226·6 | 234·2 | 231·9 | 234·6 | 234·5 | |
| 0·2491 | 0·2578 | 0·3078 | 0·3109 | 0·3671 | 0·4270 | |
| 2·446 | 2·446 | 3·036 | 3·036 | 3·626 | 4·216 | |
| 2·006 | 2·006 | 2·491 | 2·491 | 2·975 | 3·459 | $M_i$ 28·96 |
| 561·9 | 582·3 | 623·1 | 629·0 | 662·5 | 686·5 | |

Table 6.4 – 2.
First separator stage; $p_1 = 6$ bars, $T_1 = 4\ ^\circ C$

| Component | $z_{i,1}$ | $K_{i1}$ | $z_{L1} = 0{\cdot}0742$, $z_{v1} = 0{\cdot}9258$ | |
|---|---|---|---|---|
| | | | $x_{i1}$ | $y_{i1}$ |
| 1 | 2 | 3 | 4 | 5 |
| $C_1$ | 0·7354 | 28·0 | 0·0283 | 0·7920 |
| $C_2$ | 0·1503 | 3·80 | 0·0418 | 0·1590 |
| $C_3$ | 0·0120 | 0·94 | 0·0127 | 0·0119 |
| i-$C_4$ | 0·0087 | 0·325 | 0·0232 | 0·0075 |
| n-$C_4$ | 0·0273 | 0·222 | 0·0976 | 0·0217 |
| i-$C_5$ | 0·0036 | 0·080 | 0·0243 | 0·0019 |
| n-$C_5$ | 0·0045 | 0·065 | 0·0335 | 0·0022 |
| $C_6$ | 0·0104 | 0·026 | 0·1059 | 0·0028 |
| $C_{7+}$ | 0·0478 | 0·0015 | 0·6327 | 0·0010 |
| Total: | 1·0000 | | 1·0000 | 1·0000 |

for $C_{7+}$ were read off *Fig. 6.4 – 4*. The composition of gas discharged from the three separator stages is given in Columns 5 of said Tables, whereas the composition of the stock-tank oil is given in Column 4 of Table 6.4 – 4. The useful *GOR* can be calculated using Eq. 6.4 – 8. In that relationship, the molar gas volume at the given parameters of state is

$$V_{\text{mol}} = \frac{R' T_n}{p_n} = \frac{8{\cdot}314 \times 288{\cdot}8}{1{\cdot}01 \times 10^5} = 0{\cdot}02377\ \text{m}^3/\text{mole} = 23{\cdot}77\ \text{m}^3/\text{kmole}\,.$$

Let us point out that the exact value of the molar gas constant in the SI system is $R = 8{\cdot}31433 \pm 0{\cdot}00044$ J/mole K. We have used the value 8·314, of sufficient accuracy for the task in hand. We have neglected $z_n$, the compressibility factor in the standard state, or have put it equal to unity.

For finding liquid density $\rho_{L3}$ we have used *Fig. 6.4 – 5*, which is Standing's nomogram (1952) transposed into the SI system. It furnishes density of a liquid

Table 6.4 – 3.
Second separator stage; $p_2 = 2{\cdot}1$ bars, $T_2 = 4\,^{\circ}C$

| Component | $z_{i2} = x_{i1}$ | $K_{i2}$ | $z_{L2} = 0{\cdot}9612$, $z_{V2} = 0{\cdot}0388$ | |
|---|---|---|---|---|
| | | | $x_{i2}$ | $y_{i2}$ |
| 1 | 2 | 3 | 4 | 5 |
| $C_1$ | 0·0283 | 78·0 | 0·0071 | 0·5533 |
| $C_2$ | 0·0418 | 10·5 | 0·0306 | 0·3210 |
| $C_3$ | 0·0127 | 2·60 | 0·0120 | 0·0311 |
| i-$C_4$ | 0·0232 | 0·840 | 0·0233 | 0·0196 |
| n-$C_4$ | 0·0976 | 0·560 | 0·0993 | 0·0556 |
| i-$C_5$ | 0·0243 | 0·200 | 0·0251 | 0·0050 |
| n-$C_5$ | 0·0335 | 0·150 | 0·0346 | 0·0052 |
| $C_6$ | 0·1059 | 0·060 | 0·1099 | 0·0066 |
| $C_{7+}$ | 0·6327 | 0·004 | 0·6581 | 0·0026 |
| Total: | 1·0000 | | 1·0000 | 1·0000 |

Table 6.4 – 4. Third separator stage; $p_3 = 1{\cdot}01$ bar, $T_3 = 4\,^{\circ}C$

| Component | $z_{i3} = x_{i2}$ | $K_{i3}$ | $z_{L3} = 0{\cdot}9798$, $z_{V3} = 0{\cdot}0202$ | |
|---|---|---|---|---|
| | | | $x_{i3}$ | $y_{i3}$ |
| 1 | 2 | 3 | 4 | 5 |
| $C_1$ | 0·0071 | 165·0 | 0·0016 | 0·2718 |
| $C_2$ | 0·0306 | 21·8 | 0·0215 | 0·4695 |
| $C_3$ | 0·0120 | 5·40 | 0·0110 | 0·0593 |
| i-$C_4$ | 0·0233 | 1·80 | 0·0230 | 0·0413 |
| n-$C_4$ | 0·0993 | 1·20 | 0·0989 | 0·1187 |
| i-$C_5$ | 0·0251 | 0·430 | 0·0254 | 0·0109 |
| n-$C_5$ | 0·0346 | 0·315 | 0·0351 | 0·0111 |
| $C_6$ | 0·1099 | 0·115 | 0·1119 | 0·0129 |
| $C_{7+}$ | 0·6581 | 0·0067 | 0·6716 | 0·0045 |
| Total: | 1·0000 | | 1·0000 | 1·0000 |

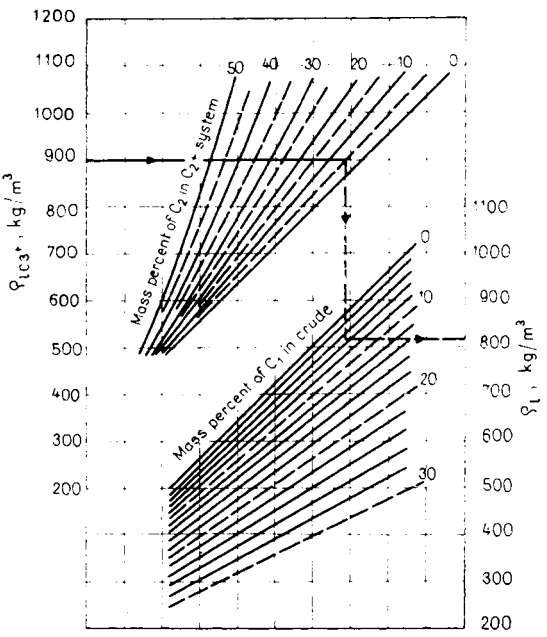


Fig. 6.4 – 5. Apparent density of crude containing methane and ethane, at $T = 15{\cdot}6$ C and $p = 1{\cdot}01$ bar, after Standing 1952 (reproduced by permission of the copyright owner – copyright © Chevron Research Company 1951; all rights reserved under the International Copyright Convention)

hydrocarbon containing $C_1$ and $C_2$. The starting data are listed in *Table 6.4 – 5*. The density of the liquid containing $C_{3+}$ is then,

$$\rho_{LC3+} = \frac{\sum_{i=3}^{7+} M_i x_{i3}}{\sum_{i=3}^{7+} \frac{M_i x_{i3}}{\rho_{Li}}} = 688 \text{ kg/m}^3.$$

The content of $C_2$ in the liquid $C_{2+}$ is 0·65 mass percent, and that of $C_1$ in the liquid $C_{1+}$ is 0·03 mass percent. Owing to the low values of $C_{1+}$ and $C_{2+}$, *Fig. 6.4 – 5* gives no deviation; that is, we may retain $\rho_{L3} = 688$ kg/m$^3$. From Table 6.4 – 5, $M_{L3}$ is 99·48 kg/kmole.

Introduced into Eq. 6.4 – 8, the data thus obtained give a *GOR* of

$$R = \frac{(0{\cdot}9258 + 0{\cdot}0388 \times 0{\cdot}0742) \times 23{\cdot}77 \times 688}{0{\cdot}0742 \times 0{\cdot}9612 \times 0{\cdot}9798 \times 99{\cdot}48} = 2185 \text{ m}^3/\text{m}^3.$$

If separator pressure exceeds 7 bars, or separator temperature is below $-5$ °C, then it will in general be necessary to determine the apparent convergence pressure

Table 6.4 – 5.

| Component | $x_{i3}$ | $M_i$ | $x_{i3}M_i$ | $\rho_{Li}$ | $\frac{x_{i3}M_i}{\rho_{Li}}$ |
|---|---|---|---|---|---|
| 1 | 2 | 3 | 4 | 5 | 6 |
| $C_1$ | 0·0016 | 16·04 | 0·03 | | |
| $C_2$ | 0·0215 | 30·07 | 0·65 | | |
| $C_3$ | 0·0110 | 44·09 | 0·48 | 506·8 | 0·0010 |
| i-$C_4$ | 0·0230 | 58·12 | 1·34 | 561·9 | 0·0024 |
| n-$C_4$ | 0·0989 | 58·12 | 5·75 | 582·3 | 0·0099 |
| i-$C_5$ | 0·0254 | 72·15 | 1·83 | 623·1 | 0·0029 |
| n-$C_5$ | 0·0351 | 72·15 | 2·53 | 629·0 | 0·0040 |
| $C_6$ | 0·1119 | 86·17 | 9·64 | 662·5 | 0·0146 |
| $C_{7+}$ | 0·6716 | 115·0 | 77·23 | 710·0 | 0·1088 |
| Total: | 1·0000 | $M_{L3}$ | 99·48 | | 0·1436 |

and to read the $K_i$s off the corresponding NGAA curve family. Since equilibrium calculations are rather time-consuming, it is recommended to find out beforehand whether two separate phases do exist at all at the temperature and pressure in question. If the well fluid is composed purely of hydrocarbons, this may be found out as follows. On reducing the temperature of the mix at a given pressure, the dew point ($E$) is reached first and the bubble point ($H$) is reached thereafter *(Fig. 6.4 – 6)*. If therefore, e.g. in so-called low-temperature separation, well fluid is introduced into the separator after cooling, it is necessary to examine whether the temperature before cooling is below the dew point and the temperature after cooling is above the bubble point. If both answers are yes, then the mix is two-phase in both cases and it

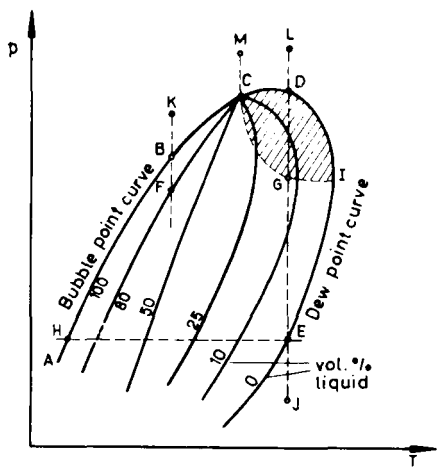


Fig. 6.4 – 6. Phase diagram of natural gas containing a significant amount of condensate

is worth while to perform the equilibrium calculation. At the *dew point*, one mole (say) of vapour keeps equilibrium with a liquid drop of evanescent size. Hence, in a very good approximation, $z_L = 0$ and $z_V = 1$, and by Eqs 6.4 – 4 and 6.4 – 6,

$$\sum_{i=1}^{m} x_i = \sum_{i=1}^{m} z_i / K_i = 1 . \qquad 6.4-12$$

If the value obtained is greater than unity, the mix is two-phase, because in order to make said value approach unity it is necessary to increase the $K_i$s and, by *Fig. 6.4 – 3*, this requires raising the temperature if the pressure is fixed. Now by *Fig. 6.4 – 6*, this is possible only if the mix is in the two-phase domain. At the *bubble point*, one mole (say) of liquid keeps equilibrium with a gas bubble of evanescent size. Hence, in a very good approximation, $z_L = 1$ and $z_V = 0$, and Eqs 6.4 – 4 and 6.4 – 7 yield

$$\sum_{i=1}^{m} y_i = \sum_{i=1}^{m} z_i K_i = 1 . \qquad 6.4-13$$

If the value of the equation is greater than unity, this means once more that the mix is two-phase, because in order to make said value approach unity it is necessary to reduce the $K_i$s; now, by *Fig. 6.4 – 3*, this requires lowering the temperature if the pressure is fixed, and by *Fig. 6.4 – 6* this is possible only if the mix is in the two-phase domain.

The well fluid often contains some water, too. It is necessary to keep in mind when performing calculations concerning such a fluid that *the common vapour pressure of immiscible liquids* is entirely independent of the proportion of the components in the liquid phase, being equal to the sum of the vapour pressures of the components, taken separately at the temperature considered.

*Example 6.4 – 2.* Find the vapour pressure of a water-pentane mix at 50 °C.

| Component | Vapour pressure bars |
|---|---|
| $H_2O$ | 0·12 |
| $C_5H_{12}$ | 1·60 |
| | 1·72 |

On heating this mix, the bubble point will occur at that temperature where the sum of the two vapour pressures equals the external pressure. The bubble-point temperature of the mix is, then, lower than that of any individual component (water-vapour distillation). It is often necessary to determine the temperature at which water starts to condense out of the hydrocarbon-water system (that is, to establish the dew point of the mixture.) Since each component generates its partial vapour pressure independently of the other components, the task is essentially to find the temperature at which the sum of partial pressures equals the vapour pressure.

Table 6.4 – 6.

| Component | $m$ kg | $M$ kg/mole | $n$ | $z$ | $p_{part.}$ 1·72$z$ MPa | $T_{ppart.}$ °C |
|---|---|---|---|---|---|---|
| 1 | 2 | 3 | 4 | 5 | 6 | 7 |
| $H_2O$ | 1·0 | 18 | 0·0555 | 0·285 | 0·49 | 80·9 |
| n-$C_5$ | 10·0 | 72 | 0·139 | 0·715 | 1·23 | 41·7 |
| | | | 0·1945 | | | |

*Example 6.4 – 3* (after Maddox 1963). What is the dew point at 1·72 bar pressure of vapour composed of one kg $H_2O$ and 10 kg n-pentane; which component will condense first? The calculation results are given in *Table 6.4 – 6*. On cooling from a higher temperature, the system will first attain 80·9 °C, and hence, water will condense at the dew point.

### 6.4.2. Factors affecting recovery in the separator*

#### (a) Separator pressure

*Figure 6.4 – 7* shows liquid recovery from a wellstream characterized in *Table 6.4 – 7*. It reveals that, e.g. at 70 bars pressure, one million $m^3$ of well fluid release 100 $m^3$ liquid $C_{7+}$. The curves show that, on increasing separator pressure, all components will at first condense to an increasing extent. The increment in condensate due to unity increase in pressure is highest in the case of methane and

Table 6.4 – 7.

| Component | $z_i$ |
|---|---|
| $C_1$ | 0·7118 |
| $C_2$ | 0·1503 |
| $C_3$ | 0·0478 |
| i-$C_4$ | 0·0104 |
| n-$C_4$ | 0·0343 |
| i-$C_5$ | 0·0096 |
| n-$C_5$ | 0·0114 |
| $C_6$ | 0·0092 |
| $C_{7+}$ | 0·0152 |
| Total: | 1·0000 |

* After Campbell (1955) and Whinery and Campbell (1958).

grows less as the molecular weight increases. The curves of components heavier than butane exhibit, however, peaks at which the liquid recovery is maximum for a given temperature, being reduced on further pressure increase by retrograde vaporization. This phenomenon is of considerable interest as regards the production of a liquid stable at atmospheric pressure. Graph *1* in *Fig. 6.4 – 8* is a plot v. separator pressure of liquid yield at a separator temperature of 27 °C; Graph *2* represents the volume of stock-tank oil stable at atmospheric pressure and 38 °C temperature, likewise v. separator pressure. The volume of stock-tank oil, composed largely of pentane and heavier components, will increase up to a pressure about of 41 bars to decrease again at higher pressures. A volume of liquid equal to the ordinate difference between the

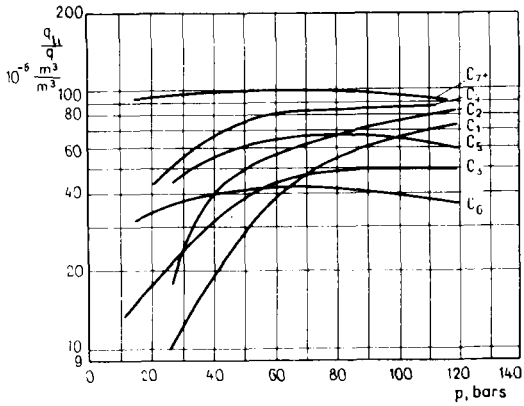


Fig. 6.4 – 7. Influence of pressure upon liquid recovery of components at $T = 27$ °C, after Campbell (1955)

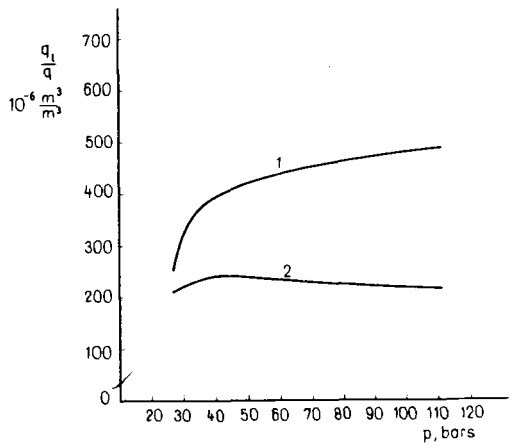


Fig. 6.4 – 8. Influence of pressure upon liquid recovery of separator at $T = 27$ °C, after Campbell (1955)

two graphs will evaporate in the tank at the given atmospheric temperature. Other well fluids separated at other temperature will give curves displaced against those given in the Figure, but their essential features will be same.

**(b) Separator temperature**

*Figure 6.4 – 9* gives yield curves for various hydrocarbons out of a given wellstream, for a pressure of 28 bars and various temperatures. The lower the temperature, the less will be the increment in $C_5$ and $C_6$ yield due to further decrease of temperature. The maximum recovery of $C_{7+}$ is at about 10 °C. — Graph *1* in *Fig. 6.4 – 10* represents the total relative liquid yield of the separator; Graph *2* represents the relative yield of stable liquid, capable of storage at atmospheric pressure; both v. separator temperature. Stable-liquid recovery is seen no to increase below about −10 °C. If the primary aim is to recover a maximum amount of stable liquid, temperatures between −1 and −10 °C will be preferred. Let us point out that at temperatures below +10 °C, the pentane and hexane content of the stable product will increase and this will result in a decrease of its gravity. If the primary aim is to increase the total liquid yield, e.g. in order to recover from the gas as much propane and butane as possible, then it may be preferable to lower the temperature even below −20 °C. Low-temperature separation, however, necessitates some special equipment that requires a considerable throughput to make it pay out. Separator temperatures higher than 30 °C are not be recommended as a rule.

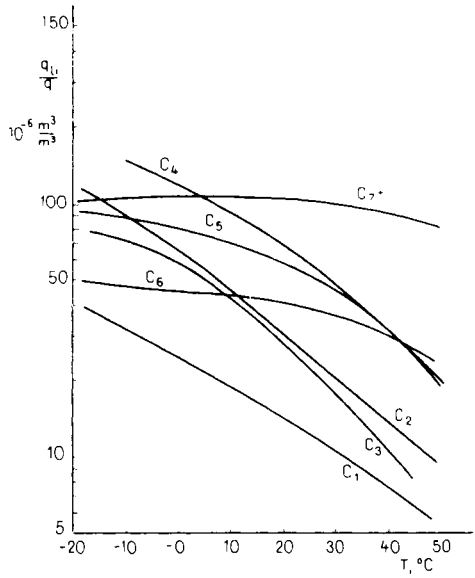


Fig. 6.4 – 9. Influence of temperature upon liquid recovery of components at $p = 28$ bars, after Campbell (1955)

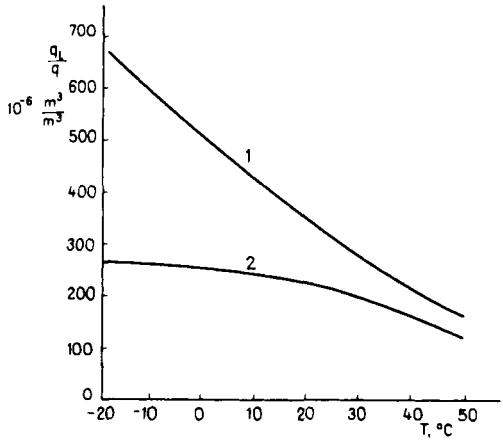


Fig. 6.4 – 10. Influence of temperature upon liquid recovery, at $p = 28$ bars, after Campbell (1955)

### (c) Composition of the wellstream

*Figure 6.4 – 11* is a plot of stable stock-tank oil yield v. tempeature, at two different separator pressures, for each of the three wellstreams characterized in *Table 6.4 – 8*. All three curves are seen to flatten out at temperatures below about $-7$ °C, and to become practically independent of temperature and pressure. Recovery of stable stock-tank oil is governed below temperatures of $-7$ °C largely by wellstream composition. The factor having the most profound influence on stable-liquid yield is the molar ratio of $C_{5+}$. Table 6.4 – 8 lists, in addition to the compositions of the three wellstreams marked *A*, *B* and *C*, also the absolute values

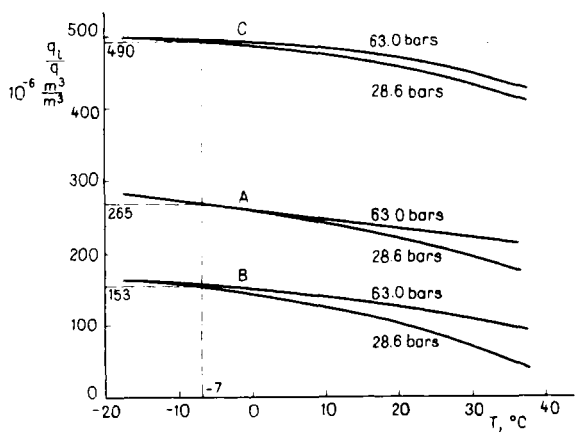


Fig. 6.4 – 11. Influence of composition upon liquid recovery, after Campbell (1955)

Table 6.4 – 8.

| Component | $z_i$ | | |
|---|---|---|---|
| | A | B | C |
| $C_1$ | 0·7118 | 0·7001 | 0·7354 |
| $C_2$ | 0·1503 | 0·1503 | 0·1503 |
| $C_3$ | 0·0478 | 0·0742 | 0·0120 |
| i-$C_4$ | 0·0104 | 0·0104 | 0·0087 |
| n-$C_4$ | 0·0343 | 0·0343 | 0·0273 |
| i-$C_5$ | 0·0096 | 0·0096 | 0·0036 |
| n-$C_5$ | 0·0114 | 0·0114 | 0·0045 |
| $C_6$ | 0·0092 | 0·0063 | 0·0104 |
| $C_{7+}$ | 0·0152 | 0·0034 | 0·0478 |
| Total: | 1·0000 | 1·0000 | 1·0000 |
| $z_{3+}$ | 0·1379 | 0·1496 | 0·1143 |
| $z_{3+\text{rel}}$ | 1·0 | 1·1 | 0·82 |
| $z_{5+}$ | 0·0358 | 0·0211 | 0·0627 |
| $z_{5+\text{rel}}$ | 1·0 | 0·59 | 1·8 |
| $\frac{q_L}{q}$ read off $10^{-6}\frac{m^3}{m^3}$ | 265 | 153 | 490 |
| $\frac{q_L}{q}$ read off-rel. | 1·0 | 0·58 | 1·8 |
| $\frac{q_L}{q}$ calc. $10^{-6}\frac{m^3}{m^3}$ | 272 | 152 | 492 |

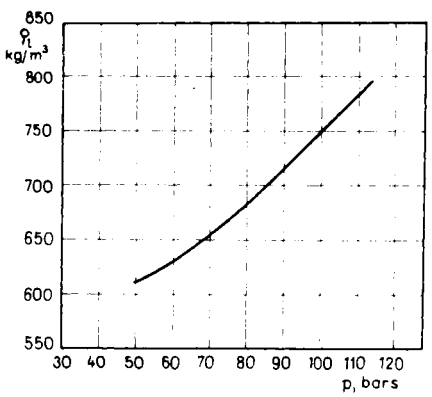


Fig. 6.4 – 12. Separator pressure ensuring maximum liquid recovery in the 21 – 27 °C temperature interval, after Campbell (1955)

of $z_{3+}$ and $z_{5+}$, and their values related to the yield for wellstream *A*. The relative stable-liquid yields of the three wellstreams are plotted in *Fig. 6.4 – 11*. The values at $-7$ °C, marked in the Figure by dashed lines, have also been listed in the Table. The yields related to the yield of fluid *A* are seen to agree pretty well with the relative values of $z_{5+}$. It is further apparent that $C_{3+}$ is not representative at all of stable-liquid yield. Stable-liquid yield to be expected on separation below $-7$ °C can be estimated by means of the formula

$$\frac{q_l}{q} = 8160 z_{5+} - 20. \qquad 6.4 - 14$$

The last row of Table 6.4 – 8 lists the values furnished by this formula for the three wellstreams *A*, *B* and *C*. There is a fair agreement with the $q_l/q$ values read off Diagram 6.4 – 11. Relationships characterizing recovery above $-7$ °C are more complicated. *Figure 6.4 – 12* is the plot of an empirical relationship furnishing the separator pressure ensuring maximum total liquid yield v. well-fluid gravity, for the temperature range between 21 and 27 °C.

### (d) Stage separation

In Sections (a), (b) and (c) we have analyzed the effects of temperature, pressure and wellstream composition, tacitly assuming two-stage separation with one separator and one stock-tank. If the number of separation stages is more than two,

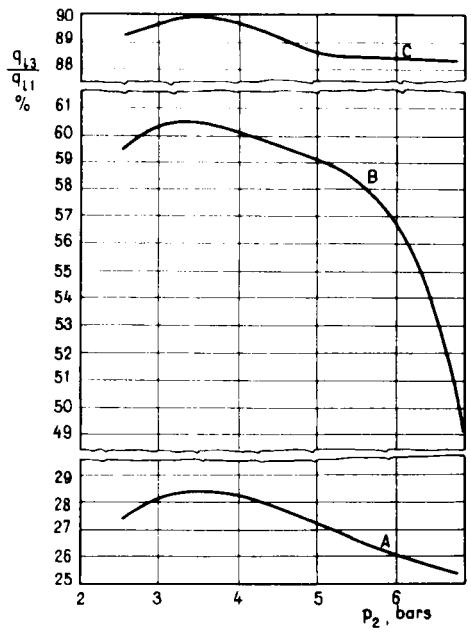


Fig. 6.4 – 13. Stable stock-tank oil recovery in three-stage separation, after Campbell (1955)

this will improve the recovery of stable stock-tank oil but diminish the total-liquid yield. Hence, evaporation loss in open tanks will be less after stage separation. Increasing the number of stages from two to three brings a considerable improvement. According to an investigation on 13 wells, the recovery of stable stock-tank oil was improved by 8 percent on an average (with a range from 3 to 22 percent). On increasing stage number from three to four, the improvement in recovery tends to be much less, and four-stage separation is not usually economical.

*Figure 6.4 – 13* shows what percentage of the liquid $q_{l1}$ discharged from the first separator stage (composition characterized in *Table 6.4 – 9*) will collect as stable oil ($q_{l3}$) in the stock tank as a function of second-stage pressure, provided first-stage pressure is 27·6 bars and third-stage pressure is 1·01 bar. Liquids *A* and *B* passing from the first-stage into the second derive from one and the same wellstream, but first-stage temperature was – 17·8 °C for liquid *A* and 26·7 °C for liquid *B*, resulting

Table 6.4 – 9.

| Component | $z_i$ | | |
|---|---|---|---|
| | (A) | (B) | (C) |
| $C_1$ | 0·1191 | 0·0826 | 0·1018 |
| $C_2$ | 0·2129 | 0·1060 | 0·0272 |
| $C_3$ | 0·1686 | 0·0986 | 0·0348 |
| i-$C_4$ | 0·0498 | 0·0403 | 0·0216 |
| n-$C_4$ | 0·1779 | 0·1634 | 0·0276 |
| i-$C_5$ | 0·0544 | 0·0713 | 0·0177 |
| n-$C_5$ | 0·0661 | 0·0924 | 0·0220 |
| $C_6$ | 0·0564 | 0·1130 | 0·7473* |
| $C_{7+}$ | 0·0948 | 0·2324 | |
| Total: | 1·0000 | 1·0000 | 1·0000 |
| $p_1$, bar | 27·6 | 27·6 | 27·6 |
| $T_1$, °C | – 17·8 | 26·7 | 26·7 |
| $q_{L1} \cdot 10^{-6} \frac{m^3}{m^3}$ | 658 | 293 | 131 |

* Hexane-plus

in a lower $C_{5+}$ content for *A*. *Figure 6.4 – 13* and Table 6.4 – 9 once more reveal stable-liquid recovery to be the better the higher the $C_{5+}$ content of the liquid entering stage two. The Figure reveals further that stable stock-tank oil yield is maximal in all three cases at the same, second-stage pressure of about 3·5 bars. Pressure in the first separator stage is limited by the maximum possible wellhead pressure or, more precisely, by the maximum incoming flowline pressure. Third-stage pressure is either atmospheric or is determined by the design features of the gas-gathering system. The only pressure that may be freely chosen within limits in

order to achieve maximum stable stock-tank oil yield is, then, the second-stage pressure.

The most favourable second-stage pressure can be determined either by in-plant experiment, time-consuming equilibrium calculations, or approximative calculations. Equilibrium calculations are to be carried out for numerous values of pressure, in the manner outlined in the foregoing section, which is a tedious procedure. The methods of approximation are more rapid but less accurate. Several such methods are known. In a rough approximation, second-stage pressure can be calculated from the relationship

$$p_2 = \sqrt{p_1 p_3}\,. \qquad 6.4-15$$

The $p_2$ furnished by this formula is usually higher than optimal.

A more accurate result for a low-molecular-weight gas-liquid mix can be obtained by a procedure which expresses second-stage pressure by one of two equations (Whinery and Campbell 1958). The first one is used when the relative molecular

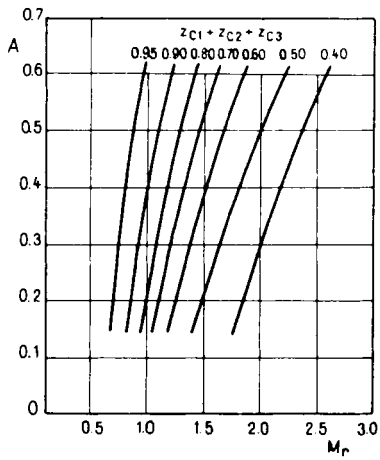


Fig. 6.4 – 14. Determining the $A$ factor, after Whinery and Campbell (1958)

weight $M_r$ of the well fluid, referred to air, is higher than 1, and the second one when it is lower than 1. The equations are for $M_r > 1$,

$$p_2 = 16\, A p_1^{0.686} + 2.96 \times 10^5 (A + 0.057) \qquad 6.4-16$$

and for $M_r < 1$,

$$p_2 = 8\, A p_1^{0.765} + 5.75 \times 10^5 (A + 0.028)\,. \qquad 6.4-17$$

The $A$ factor is plotted v. $M_r$ in *Fig. 6.4 – 14*. The procedure may be used if the third stage is atmospheric, in which case the result is accurate to within $\pm 5$ percent.

Table 6.4 – 10.

| Component | $z_i$ | $M$ | $1 \times 2$ |
|---|---|---|---|
| | 1 | 2 | 3 |
| $C_1$ | 0·40 | 16·01 | 6·40 |
| $C_2$ | 0·20 | 30·07 | 6·01 |
| $C_3$ | 0·10 | 44·09 | 4·41 |
| $C_4$ | 0·10 | 58·12 | 5·81 |
| $C_5$ | 0·10 | 72·15 | 7·22 |
| $C_6$ | 0·05 | 86·17 | 4·31 |
| $C_{7+}$ | 0·05 | 115·22 | 5·76 |
| Total: | 1·00 | | 39·92 |

*Example 6.4 – 4* (after Whinery and Campbell 1958). Let the well fluid be characterized by *Table 6.4 – 10*. Let first-stage pressure be 34·5 bars, and let the third stage be atmospheric. What is the most favourable second-stage pressure?

$$M_r = \frac{39{\cdot}92}{28{\cdot}96} = 1{\cdot}38$$

$z_{C1} + z_{C2} + z_{C3} = 0{\cdot}7$, and *Fig. 6.4 – 14* yields $A = 0{\cdot}421$. Since $M_r$ is greater than 1, we take Eq. 6.4 – 16;

$$p_2 = 16 \times 0{\cdot}421\,(34{\cdot}5 \times 10^5)^{0{\cdot}686} + 2{\cdot}96 \times 10^5(0{\cdot}421 + 0{\cdot}057) =$$
$$= 3{\cdot}47 \times 10^5 \text{ N/m}^2 = 3{\cdot}47 \text{ bars}.$$

### 6.4.3. Basic separator types

The compositions of the liquid and gas discharged from a separator differ somewhat from those predicted by calculation. In addition to the fact that calculation procedures based on auxiliary diagrams do not model real-life conditions quite accurately, this is due to the circumstance that the liquid will contain gas bubbles and the gas will contain mist. Of these, it is the liquid content of the gas that may cause trouble (in the transportation system). Modern separators are designed so that the mist content of the discharged gas be less than 0·1 g/m$^3$.

In most gas-liquid separators, the elements ensuring separation may be divided in three groups. (i) Means of rough separation. These serve to effect a first separation of liquid and gas, mainly by centrifugal force and the force of gravity. They include the inlet separating element, baffles, liquid passages, and that part of the separator between liquid surface and inlet (in vertical separators) or above the liquid level (in horizontal and spherical separators). (ii) Mist extractor. In order to separate mist not settled out by centrifugal force or gravity, a mist extractor is placed in the way of the gas stream. The mist extractor may be of the vane or coalescing-pack type, or it might be a hydrocyclone, often installed outside the separator body. (iii) Oil

collector. The liquids separated from the well-stream and condensed in the separator collect in the bottom part of the separator vessel. Liquid level is maintained within given limits by an LLC (liquid-level-control) device, in order to prevent gas from entering the oil outlet, and liquid from rising up to the elements mentioned above, and to ensure sufficient retention time for the gas bubbles to break out of the liquid.

Shapewise, separators may be vertical cylindrical, monotube or dual-tube horizontal, or spherical. In the sections below I shall describe typical examples for each of these.

**(a) Vertical separators**

The wellstream enters the vertical or upright cylindrical separator through an inlet installed at about two-thirds height. The inlet may be radial or tangential [(a) and (b) in *Fig. 6.4 – 15*]. Tangential inflow has the advantage that it exploits for separating liquid and gas a centrifugal force which may exceed the force of gravity

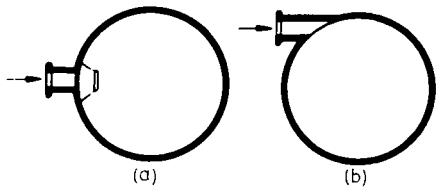


Fig. 6.4 – 15.

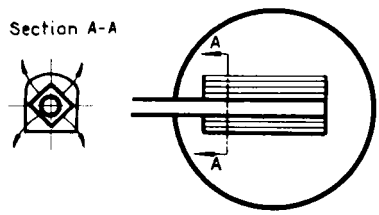


Fig. 6.4 – 16.

by up to two orders of magnitude: furthermore, the liquid will move in the separator in a spiral along the shell, while gas will rise in the central space along the separator axis. This considerably reduces the likelihood of contamination with mist as against the case of radial inflow. The inlet separating element shown in *Fig. 6.4 – 16*, a development on the radial-inflow idea, has lately been adopted by numerous makers of separators. Its use substantially promotes the separation of liquid and gas directly after inflow. *Figure 6.4 – 17* is a schematic diagram of a modern vertical separator. The wellstream enters separator *2* through inlet *1* and the separating element mentioned above. Liquid discharge is controlled by motor valve *5*,

operated by float *3* through pneumatic pilot *4*. Bobbing of the float is prevented by float shield *6*. Mist in the rising gas is extracted by vane-type device *7* from which it drips back into the separator space. Separator pressure is controlled by regulator *9*, installed in gas outlet *8*. Solids settling on the separator bottom can be removed through drain *10*. Overpressure protection is provided by spring- or dead-weight-loaded relief valve *11*. Numerous relief-valve designs are known, including the spring-loaded one in *Fig. 6.2 – 25*.

Valves providing full-capacity relief are usually rather large and therefore comparatively expensive. Safety relief of separators is therefore usually ensured by

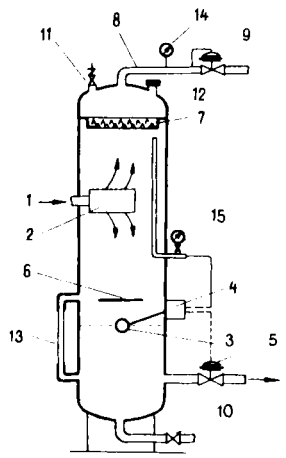


Fig. 6.4 – 17. Vertical separator

two devices: (i) a relief valve of comparatively small capacity, and (ii) a so-called rupture-disk safety head (*12*). If the overpressure in the separator is too great to blow off through the relief valve, then it will rupture a suitably dimensioned disk which opens an outlet of large enough size. A BSB make rupture-disk safety head is shown in *Fig. 6.4 – 18*. Disk *3* is sandwiched between flanges *1* and *2*. This double protection has the characteristic that the more frequent slight overpressures are blown off through the relief valve which closes again automatically as soon as separator pressure has returned to normal. Substantial overpressures cause disk rupture, after which it is necessary to close down the separator and to change the disk. Each separator is equipped with a gauge glass *(13* in *Fig. 6.4 – 17)*, and a manhole not shown in the Figure. Gas-outlet pressure is measured by gauge *14*, pressure below the mist extractor by pressure gauge *15*, installed on the actuating-gas line.

The float-type level sensor of the separator may actuate a regulator either mechanically or pneumatically. *Figure 6.4 – 19* shows a Fisher-make lever-type float-operated oil discharge valve (the float to be attached to the lever is not shown).

Pneumatic discharge-control valves tend to provide finer control, but they are more costly than the mechanical variety. The principle of a popular type of pneumatic control is illustrated by *Fig. 6.4 – 17*. In another design, the float is installed in a separate chamber connected with the separator space. This has the advantage that,

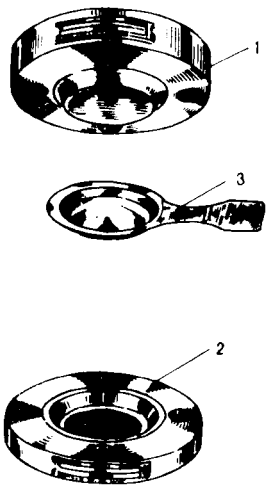


Fig. 6.4 – 18. BSB rupture-disk safety head

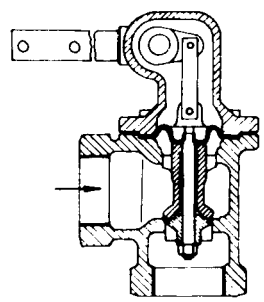

Fig. 6.4 – 19. Fisher's mechanical liquid level control

in case of float failure, the unit can be replaced without interrupting separator operation. A float-chamber type liquid-level controller of Fisher-make equipped with a pilot-operated pneumatic motor valve is shown in *Fig. 6.4 – 20*. If the liquid level is at middle height in float chamber *1*, pilot *2* feeds supply gas of about 1·6 bar pressure under the diaphragm of motor valve *3*. Liquid inflow and outflow rates of the separator are equal in this position. If inflow exceeds outflow, liquid level will rise in the float chamber. Lever *4* will rise and open valve *5*. Gas pressure will increase in the pilot and hence also under the motor-valve diaphragm, increasing

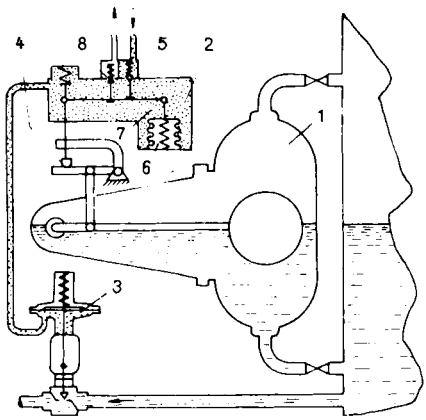


Fig. 6.4 – 20. Fisher's pilot-operated pneumatic float-chamber type liquid-level control

the opening of the inner valve in valve *3*. At the same time, bellows *6*, compressed by the increased outer pressure, depresses the right-hand hinge of lever *7* and through it closes supply-gas valve *5*. This stops the pressure increase under the motor-valve diaphragm. Valve opening will remain constant as long as liquid level remains at the same height. If it starts to decrease, then some of the gas is let out of the motor valve through bleed valve *8*, and the above-outlined process will take place in reverse.

**(b) Horizontal separators**

*Monotube horizontal separator (Fig. 6.4 – 21).* The stream enters the vessel through inlet *1*, to impinge tangentially upon the vessel wall. Separation of oil and gas is promoted by baffle plates *2*. Liquid level is controlled by discharge valve *4*, operated by float *3*. Gas is discharged through outlet *5*, liquid through outlet *6*. Pressure regulation, safety and other equipments are much the same as in vertical separators.

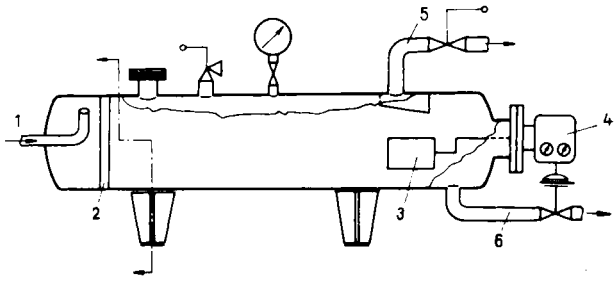


Fig. 6.4 – 21. Monotube horizontal separator

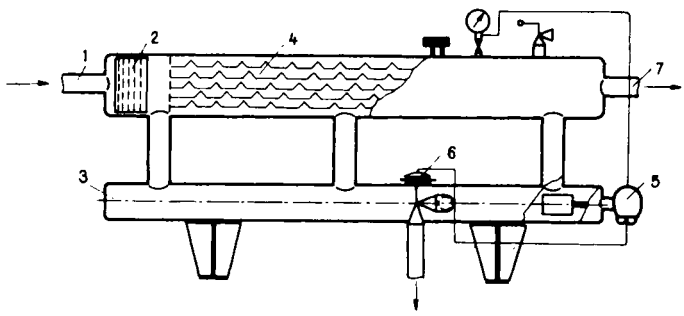


Fig. 6.4 – 22. Dual-tube horizontal separator

*Dual-tube horizontal separator (Fig. 6.4 – 22).* The wellstream enters the upper separator tube through inlet *1* and screen plates *2*. Part of the fluid flows through the first vertical conduit into lower tube *3*. The gas, still laden with mist, flows towards perforated vanes *4*. These promote the coagulation of the mist particles. The liquid phase thus formed may flow down the vertical conduits into tube *3*, from where it is discharged into the outlet through diaphragm motor valve *6* controlled by float-operated pneumatic regulator *5*. Gas is discharged through outlet *7*.

**(c) Spherical separators**

The separator shown in *Fig. 6.4 – 23* is provided with a bottom gas outlet. The wellstream enters through inlet *1*, to flow downward in the space bounded by spherical cap *2*. Oil collects in the bottom space. Its level is sensed by float *3* and its discharge through valve *5* is controlled by pneumatic pilot *4*. Mist is extracted in coalescing pack *6*. Gas is discharged through outlet *8* provided with pressure regulator *7*.

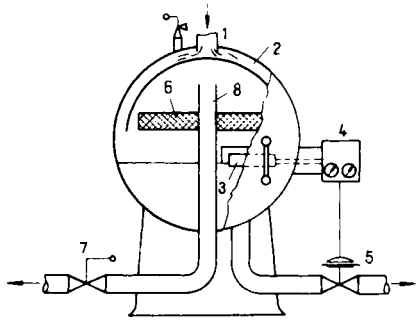


Fig. 6.4 – 23. Spherical separator

### 6.4.4. Separator selection

#### (a) Choice of the separator type

Vertical separators have the advantage of being insensitive to level fluctuations, and therefore permitting level control by simple means because, owing to the upright cylindrical shape, the liquid volume change per unit level change is slight, and, on the other hand, level changes will not affect gas-flow cross-section, nor, consequently, the mist content of the gas. They are therefore best suited for separating rapidly fluctuating ('heading') wellstreams. Floor space required per unit gas capacity is less than in the other types. Cleaning is relatively simple, which makes this type of separator suitable for handling sandy crudes, In the horizontal separator, gas capacity (that is, the number of standard volume units of gas that can be freed of liquid to the desired degree per unit of time) is greater for a given cylinder size than in the vertical separator. This is due to several circumstances. In the vertical separator, diameter must be sufficient to make the gas rise slower than the settling velocity of mist particles. Height is primarily determined by the space requirement of the elements described in Section 6.4.3—(a). Shell height of the current designs is, accordingly, about 3 m. Further increase in height will not improve gas capacity. — The capacity of horizontal separators increases with length. The wellstream entering the vessel will first lose the larger mist drops near the inlet. Mist particle size will gradually decrease from the inlet towards the gas outlet. The longer the separator the less will be the final mist-particle size, and hence, the mist content, of the gas effluent. (Particles below 0·01 mm size cannot be removed by settling alone.) The gas discharge does not meet the inflow, so that mist contamination is unlikely, which permits a higher flow velocity to be adjusted. The gas-liquid interface is comparatively extensive, so that the breakout of gas bubbles from the

Table 6.4 – 11. Advantages and drawbacks of separator types

| Separator type | | $I/q_g$* | Economy at high gas capacity, $q_g$ | Economy at high gas pressure | Mud, sand | Foaming oil | High-viscosity, freezing crude | Heading | Liquid level control | Portability | Installation, maintenance | $A/q_g$** |
|---|---|---|---|---|---|---|---|---|---|---|---|---|
| Vertical | | 3 | 2 | 3 | 2 | 3 | 2 | 2 | 1 | 3 | 2 | 1 |
| Horizontal | monotube | 2 | 1 | 1 | 3 | 1 | 1 | 3 | 4 | 2 | 1 | 4 |
| | dualtube | 2 | 1 | 1 | 3 | 1 | 3 | 1 | 2 | 2 | 1 | 3 |
| | sphere | 1 | 3 | 2 | 1 | 3 | 4 | 4 | 3 | 1 | 1 | 2 |

* First cost per unit gas capacity
** Floor space required per unit gas capacity

liquid takes rather a short time. The monotube horizontal separator is therefore smaller and cheaper than the vertical separator of the same gas capacity. The difference in cost is further increased if high-pressure separation is necessary, because a vertical separator of 3 m height, whose wall must be fairly thick to withstand high pressures, can be substituted by a longer horizontal vessel of less diameter and smaller wall thickness. — Dual-tube horizontal separators are more expensive than monotube ones, but the well-separated liquid and gas space prevent any subsequent mixing of the two phases, and the liquid level is always smooth. This is an advantage especially when handling light liquids. Heading of the well hardly affects separation efficiency. Both horizontal separator types are easier to install, handle and service than the vertical ones.

The main advantage of the spherical separator is that its first cost per unit gas capacity is least. It is to be preferred where well yields are comparatively low and uniform. It is easy to displace, install and clean. It requires little space especially in two-stage separation, because one sphere may be mounted on top of the other. *Table 6.4 – 11* serves to facilitate comparison of separator types' advantages and drawbacks. A lower rating means a greater advantage. (For choice primarily among horizontal separators see the work of Maher and Coggins 1969.)

**(b) Separator sizing**

Separator *ID* is determined in keeping with the above considerations by the desired gas capacity. This term means the maximum gas throughput that can be handled by the separator under the prescribed pressure and temperature with mist content kept below 0·1 g/m$^3$. Since internal design and differences in wellstream composition will both affect capacity, it is recommended to perform sizing on the basis of empirical formulae or procedures employing such formulae, as, e.g., Ch. K. Gravis' method (1960), adapted below to the SI system of units. Gas-capacity can be

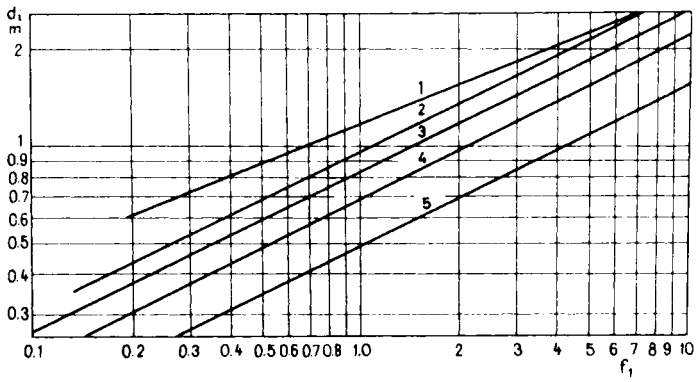


Fig. 6.4 – 24. Gas capacity factor of separators, after Gravis (1960)

read off *Fig. 6.4 – 24* in the knowledge of the capacity factor

$$f = f_1 f_l f_g f_h .$$

The gas-capacity base factor $f_1$ may be read off *Fig. 6.4 – 24* as a function of *ID* for separators of various type and length. $f_l$ is a liquid-density correction factor; its value is unity if $\rho_l = 848\ \mathrm{kg/m^3}$; $f_g$ is a gas-density correction factor, whose value is unity if

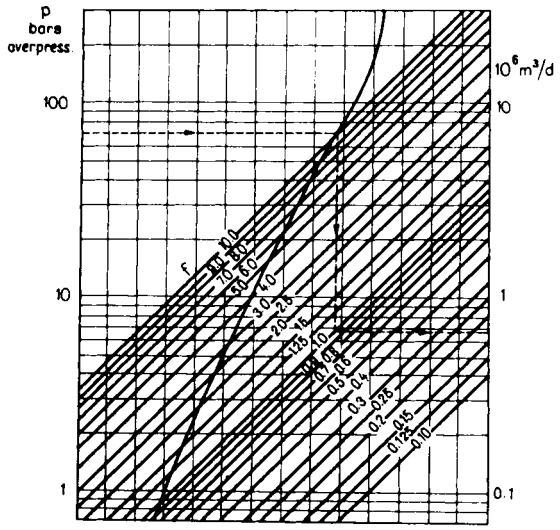


Fig. 6.4 – 25. Gas capacity of separators, after Gravis (1960)

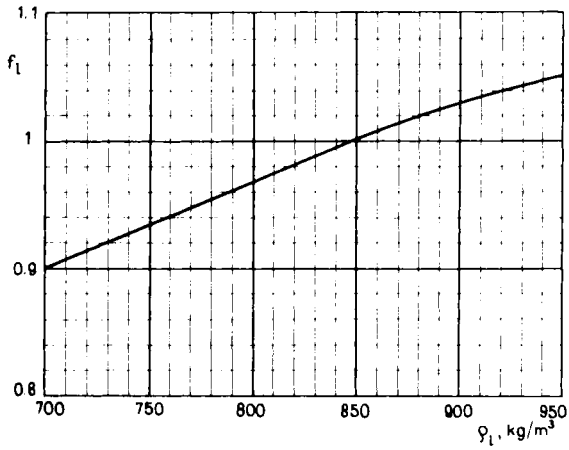


Fig. 6.4 – 26. Correction factor of liquid density, after Gravis (1960)

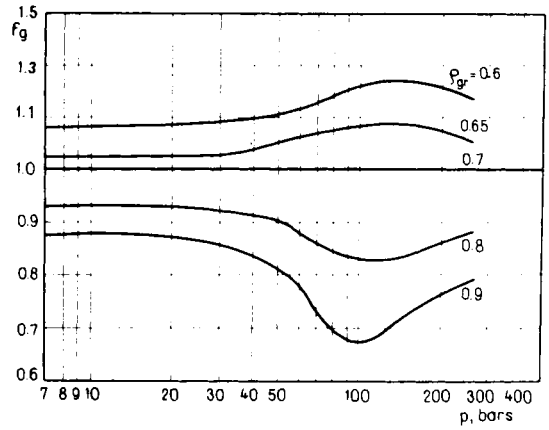


Fig. 6.4 – 27. Correction factor of gas density, after Gravis (1960)

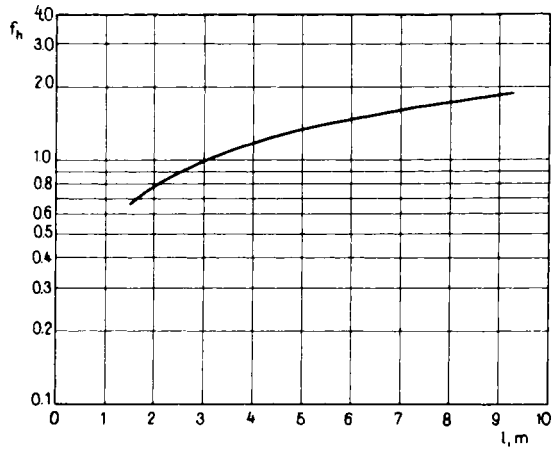


Fig. 6.4 – 28. Correction factor for horizontal-separator length, after Gravis (1960)

$\rho_{gr} = 0{\cdot}7$; $f_h$ is a vessel-length correction factor whose value is unity for any vertical or spherical separator and for horizontal separators of 3 m length. The values of these factors for conditions other than those stated above can be read off *Figures 6.4 – 26* to *6.4 – 28*. In the knowledge of $f$ and the required separator pressure $p$, the daily gas capacity can be read off *Fig. 6.4 – 25*.

Strictly speaking, the procedure assumes a separator temperature of 15·6 °C. Capacity is slightly less at higher and slightly more at lower temperatures. It is assumed that the pour point of the oil and the hydrate-formation temperature of the gas are both below separation temperature, foaming of the oil is average, and the inflow of wellstream is stabilized. For horizontal monotube separators, it is further

assumed that liquid takes up one-half of the inner space. In dual-tube separators, liquid is in the lower tube, the upper one being reserved entirely for gas. The gas capacity of a dual-tube horizontal separator is therefore approximately twice that of a monotube one of the same diameter.

*Example 6.4 – 5.* Find the gas capacity of a vertical separator if $d_i = 0{\cdot}9$ m, $p = 50$ bars, $\rho_l = 760$ kg/m$^3$, $\rho_{gr} = 0{\cdot}650$, and $h = 3$ m; from *Fig. 6.4 – 24*, $f_1 = 1{\cdot}18$; from *Fig. 6.4 – 26*, $f_l = 0{\cdot}94$; from *Fig. 6.4 – 27*, $f_g = 1{\cdot}05$; from *Fig. 6.4 – 28*, $f_h = 1$. The capacity factor is, then.

$$f = 1{\cdot}18 \times 0{\cdot}94 \times 1{\cdot}05 = 1{\cdot}16$$

From *Fig. 6.4 – 25*, $q_g = 650 \times 10^3$ m$^3$/d.

Retention time of oil is to be chosen so that the gas bubbles have sufficient time to break out of the oil. In non-foaming oil, this time is 1 to 3 min. Liquid space is the

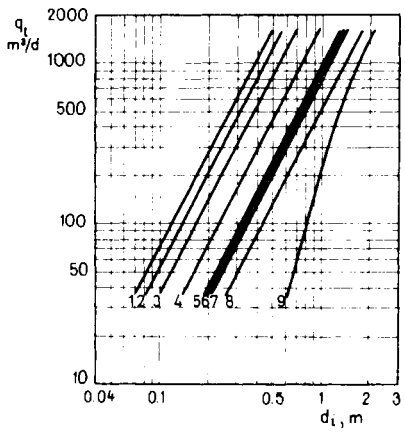


Fig. 6.4 – 29. Liquid capacity of separators, after Gravis (1960); *1* monotube horizontal, $h = 6{\cdot}1$ m; *2* dual horizontal, $h = 4{\cdot}6$ m; *3* dual horizontal, $h = 3{\cdot}0$ m, and monotube horizontal, $h = 6{\cdot}1$ m; *4* dual horizontal, $h = 1{\cdot}5$ m and monotube horizontal, $h = 3{\cdot}0$ m; *5* vertical, $h = 4{\cdot}6$ m; *6* monotube horizontal, $h = 1{\cdot}5$ m; *7* vertical, $h = 3{\cdot}0$ m; *8* vertical, $h = 1{\cdot}5 - 2{\cdot}3$ m; *9* spherical

space between the oil outlet and the level maintained by the regulator. If liquid-space volume is e.g. 0·16 m$^3$, and retention time is 1 min, then liquid capacity is $1440 \times 0{\cdot}16 = 230$ m$^3$/d. Liquid capacity as a function of *ID* can be estimated using *Fig. 6.4 – 29*. If the oil has a tendency to foam, retention time must be increased (even up to 20 min), and capacity is reduced accordingly. Foaming can be reduced considerably by adding to the wellstream small quantities of silicon (0·0017 – 0·025 ppm). Capacity increases up to 40 percent have been recorded (Nematizadeh 1969). This procedure will pay for itself especially if the aim to be achieved is a comparatively short-range temporary increase of capacity.

*Example 6.4 – 6.* Find, assuming an average tendency to foam, the liquid capacity of the separator described in the foregoing example, for a retention time of 1 min. *Figure 6.4 – 29* gives $q_l = 650\ m^3/d$.

The liquid discharge rate from the separator is determined jointly by the pressure differential between separator and tank and the flow resistance of the discharge line. When designing and installing the separator, it is to be ascertained that the maximum discharge rate determined by these factors be at least as high as the liquid capacity of the separator. The size of the lower tube of a dual-tube horizontal separator is determined by the prescribed retention time of the liquid: in practice, it is at least as large as the upper tube. The liquid level in spherical separators is usually about 13 cm below the horizontal median plane of the sphere.

If the wellstream is not stabilized (the well produces by heads or slugs or its production is intermittent), separators should be sized for the maximum instantaneous flow rate to be expected, rather than for the daily mean production rate. This is especially important when sizing spherical separators.

### 6.4.5. Special separators

#### (a) Cyclone separators

This a type of two-phase separator which ensures high-efficiency liquid separation without a mechanical mist separator, merely by a suitable flow-path design. *Figure 6.4 – 30* is the schematic diagram of a modern cyclone separator, after Barrett (1970). Tangentially entering through conduit *1*, and deflected into an approximately spiral flow path, the fluid descends between the vessel shell and bell baffle *2*; most of the liquid flows along the vessel wall into liquid space *3*. The gas

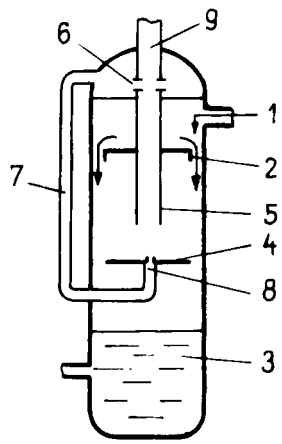


Fig. 6.4 – 30. Cyclone separator, after Barrett (1970)

vortex still containing mist rises through tube *5* above baffle *4*. The least-pressure point of the vortex is above the central orifice in plate *4*. Some of the mist particles in the gas impinge upon the lower surface of bell *2* and, coalescing, drip down into the liquid space. Most of the mist rising in tube *5* is thrown by vortex motion against the inner tube wall. Suction from the low-pressure centre generated above plate *4* sucks

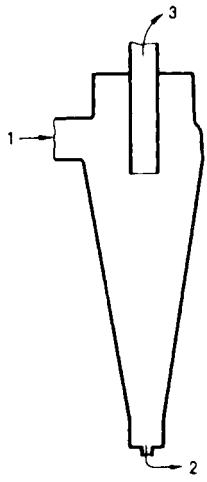


Fig. 6.4 – 31. DEMCO centrifugal separator

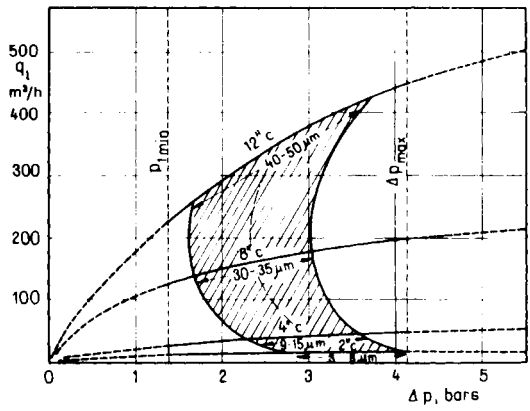


Fig. 6.4 – 32. Capacity of DEMCO centrifugal separators

this liquid through apertures *6* and conduit *7* to orifice *8*. The vortex rotating there blows the liquid towards the separator wall, where it may sink into the liquid space. Gas discharged through outlet *9* has 99·94 percent of its liquid content removed in this type of separator. There are also horizontal separators operating on this same

principle. The DEMCO centrifugal separator (sand trap) shown schematically in *Fig. 6.4 – 31*, serves to remove solid contaminants such as fine sand from liquids. Inflow is through conduit *1*. Solid particles, thrown against the conical shell, sink down along it to be drained through outlet *2*, whereas the pure liquid is discharged through outlet *3*. It is usual to connect several such units in parallel to an inlet and an outlet manifold. The separation capacity of a centrifugal separator of given size

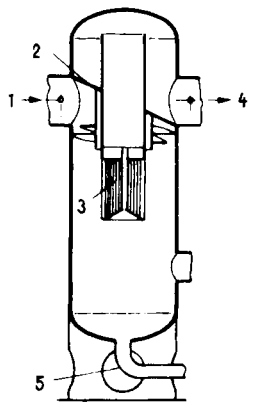


Fig. 6.4 – 33. MOKVELD separator

depends on the pressure differential between inlet and outlet and on the particle size of the solids to be separated. *Figure 6.4 – 32* is a capacity diagram of DEMCO separators. Separation efficiency is highest in the shaded domain. The separator will remove 90 percent of the solids of particle size indicated in the Diagram. In that domain $p_{1\,min}$ is the least recommended outflow pressure; $\Delta p_{max}$ is the maximum pressure difference to be applied.

*Figure 6.4 – 33* shows the MOKVELD separator (scrubber) serving to remove solid and liquid particles above 10 μm size. The primary fluid enters through inlet *1*. Gas flows downward below dividing plate *2*, and reaches outflow aperture *4* through baffles *3*. Liquid drops and solids removed from the turbulent gas are drained through conduit *5*. The scrubber will remove from 98 to 100 percent of the particles above 10 μm size.

**(b) Three-phase (oil-water-gas) separators**

In addition to oil and gas, the wellstream often contains substantial amounts of water. Water occurs either as a separate phase or in emulsion with oil. In the former case, so-called three-phase separators which separate oil from water as well as liquids from gas can be used to advantage.

The three basic types of three-phase separator are shown in *Figures 6.4 – 34* to *6.4 – 36*. Water is drained through a pilot-controlled valve operated by a float weighted

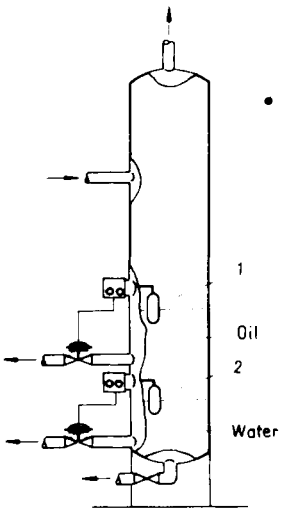


Fig. 6.4 – 34. Three-phase vertical separator, type (a); after Broussard and Gravis (1960)

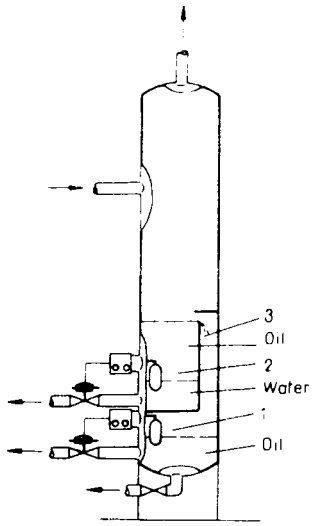


Fig. 6.4 – 35. Three-phase vertical separator, type (b); after Broussard and Gravis (1960)

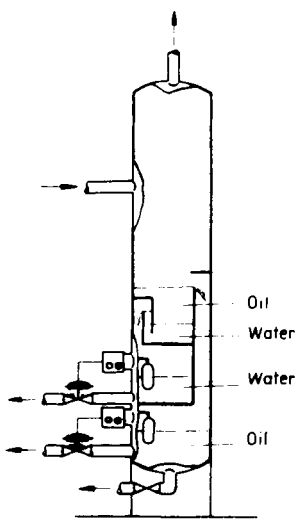


Fig. 6.4 – 36. Three-phase vertical separator, type (c); after Broussard and Gravis (1960)

so as to float at the water-oil interface. In type (a), oil and water levels are maintained by floats *1* and *2* alone. The gravity difference between water and oil is usually rather slight, and so is the differential buoyancy maintaining the weighted float at the water-oil interface. Sudden slugs of incoming liquid may make the floats bob up and down, which is detrimental to accurate level maintenance. This type is comparatively cheap and simple; the entire bottom space is available for settling; sand and mud deposits are comparatively easy to remove. In type (b) floats *1* and *2* are assisted in maintaining liquid levels by weir *3*. Settling space is, however, less than in type (a), and the internal fittings tend to hamper cleaning. In design (c), two separate liquid levels are maintained by weirs and floats, and there is no interface float. Water and oil collect in separate compartments. This has the advantage that, should any one of the float-operated level controls fail, water and oil will discharge separately, even though both will be mixed with gas. Its drawback is that the settling space is even smaller than in type (b), cleaning is cumbersome, and the entire device is rather expensive. Designs (b) and (c) above, as applied to spherical separators, are shown in *Figs 6.4 – 37* and *6.4 – 38*. In addition to the typical features of spherical separators, these have the advantage that, despite of the weirs in them, their cleaning is simpler than that of the corresponding vertical separators.

The emulsion treater made by NATCO is shown in *Fig. 6.4 – 39*. The emulsified water containing gassy crude, through pipe *1*, gets into heat exchanger *2*, where it is preheated. From here, it pours into separator *3* and, gas is carried from here through line *4*, while the emulsified crude, through pipe *5*, gets into chamber *6*. In heater *7* the liquid is heated to the necessary temperature by combustion gas, obtained by gas firing. The water thus separated is discharged through line *8*. The other liquid constituents, through the perforated baffle plates *9* are moving into the coalescing type mist extractor *10*, and then into the discharge port *11*. Here the pure oil flows into heat exchanger 2, and leaves the device through line *12*. By situating the port *14* of the syphon *13* the level of the water–oil boundary may be regulated. The pressure

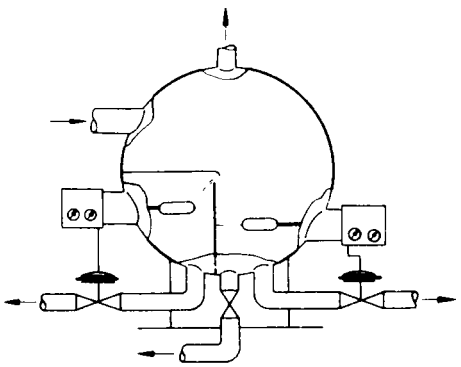

Fig. 6.4 – 37. Three-phase spherical separator, type (b); after Broussard and Gravis (1960)

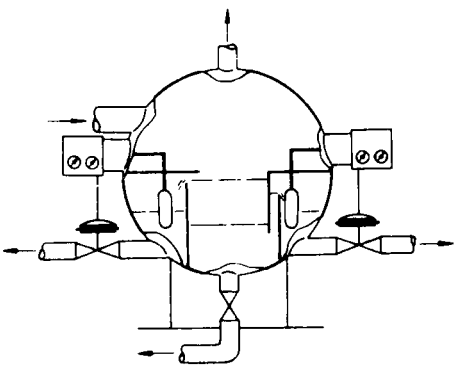

Fig. 6.4 – 38. Three-phase spherical separator, type (c); after Broussard and Gravis (1960)

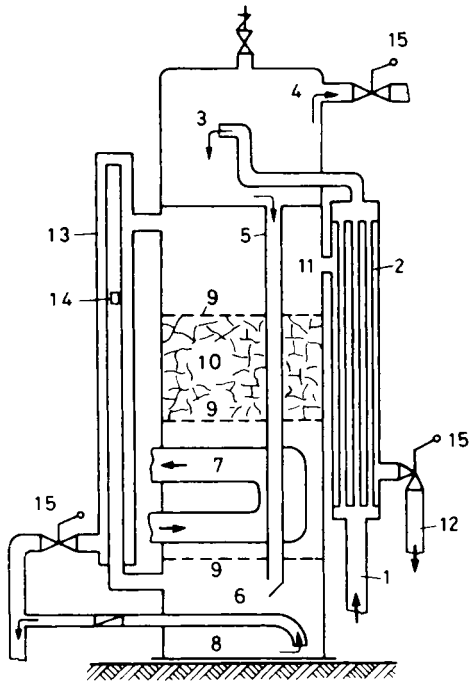


Fig. 6.4 – 39. NATCO emulsion treater

of the separator, a value, generally lower than 3·5 bars, may be adjusted by valves *15*. In order to facilitate emulsion treatment, chemicals may be also injected into the well stream before flowing into the separator.

**(c) Automatic metering separators**

Metering separators meter the weight or volume of the liquid discharge. Depending on whether the metered output is total liquids or oil and water separately, metering separators may be two- or three-phase. Different designs will have to be adopted according to whether the liquid and gas are easy to separate, or tend to form considerable foam, or the crude is of high-viscosity. Most metering separators measure the volume rather than the weight of the liquid discharge.

*Figure 6.4 – 40* after V. Smith shows a metering separator suitable for the two-phase separation of non-foaming oil (Frick 1962). The separator vessel is divided horizontally into two compartments, the upper one of which is the separator proper. Its design is essentially that of a conventional vertical separator (e.g. *Fig. 6.4 – 17*). The extreme positions of float *1* in the lower compartment (metering chamber) control by the intermediary of pilot *2* the valves *3* and *4*. Whenever the liquid level in the metering chamber is below upper float level *5*, valve *3* is open and valve *4* is

closed, and liquid may flow through conduit *6* from the upper compartment into the metering chamber. At the upper float level (position shown in dashed line), pilot *2* closes valve *3* and opens valve *4*. As soon as liquid level has sunk to the lower float level, valve *3* is re-opened and valve *4* is closed. The number of drainages of the metering chamber is recorded by counter *8*. This latter may also be equipped for a

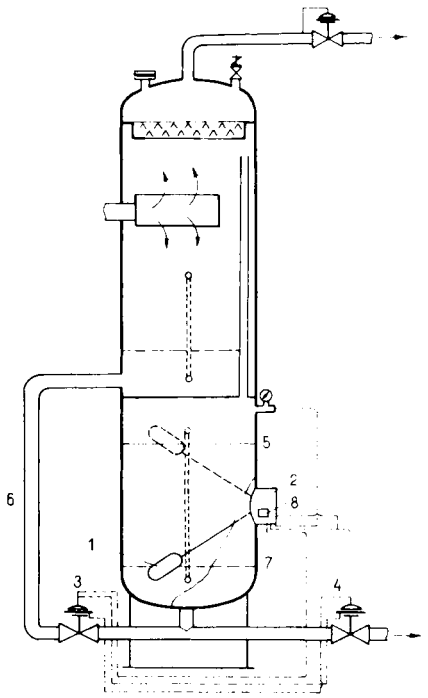


Fig. 6.4 – 40. Automatic metering separator, according to V. Smith; after Frick 1962, Vol. I, pp. 11 – 20 (used with permission of McGraw-Hill Book Company)

digital print-out of the metered liquid volume, by multiplication of the count with metering-chamber volume.

The separator in *Fig. 6.4 – 41* permits the automatic metering of low-capacity wells (McGhee 1957). The wellstream enters separator compartment *2* through inlet *1*. When discharge is inoperative, degassed oil drains through conduit *3* into metering chamber *4*. The rising oil level lifts steel-ball float into the position shown in the Figure. The ball in turn lifts lever pair *6 – 6* and pulls down stem *7*. This actuates pilot *8*, which makes supply-gas distributor feed gas through line *10* in order to close motor valve *11*. At the same time, pressure is reduced in line *12*, so that valve *13* will open. On discharge, the ball, sinking to the bottom of the chamber, depresses the lower lever *6*, and the pilot commands the gas distributor to close

valve *13* and to open valve *11*. Every downstroke of stem *7* is counted by counter *14*. The gas capacity of a separator of 0·3 m *ID* and 2 m height is about 6000 $m^3$/d.

*Portable separators* are used primarily around exploration wells and in single-well gathering and separating systems. These, too, may be two- or three-phase. They usually meter liquid by a positive-displacement or a dump type meter, and gas by an orifice meter. In three-phase separators, the separation of water from oil may be performed without heating (if the phases will separate readily) or with the aid of heating. In the latter case, a demulsifying chemical agent may or may not be added.

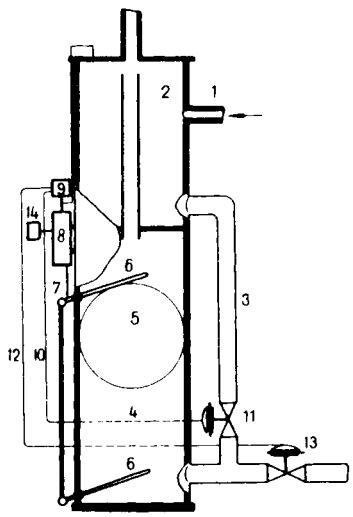


Fig. 6.4 – 41. Automatic metering separator for low-capacity wells, after McGhee (1957)

Heating may be direct gas-firing, or electrical. Separators may be upright or horizontal. In the following we shall restrict discussion to unheated horizontal portable separators, assuming that, if three phases are to be separated, water is entirely removed from oil by gravity alone during the liquid's stay in the separator. In the two-phase separator shown after J. D. Kimmel *(Fig. 6.4 – 42)*, liquid passes through a positive-displacement meter; the portable three-phase separator shown in *Fig. 6.4 – 43* (Frick 1962) is equipped for the dump metering of both oil and water. Separator tubes are 1·8 – 2·1 m long; diameters are 0·30 – 1·2 m. Maximum operating pressure is of 166 bars; maximum standard-state gas capacity is a round $500 \times 10^3$ $m^3$/d for two-phase, and a round $340 \times 10^3$ $m^3$/d for three-phase separation. Maximum liquid capacity is a round 750 $m^3$/d of oil for two-phase separation, and 750 $m^3$/d of oil plus 380 $m^3$/d of water for three-phase separation. The devices weigh 0·5 – 2 tons. When using a dump meter, the meter factor has to be determined in each new application, since owing to the gas content of the liquid and to the fact of metering being carried out at near-separator pressure and temperature,

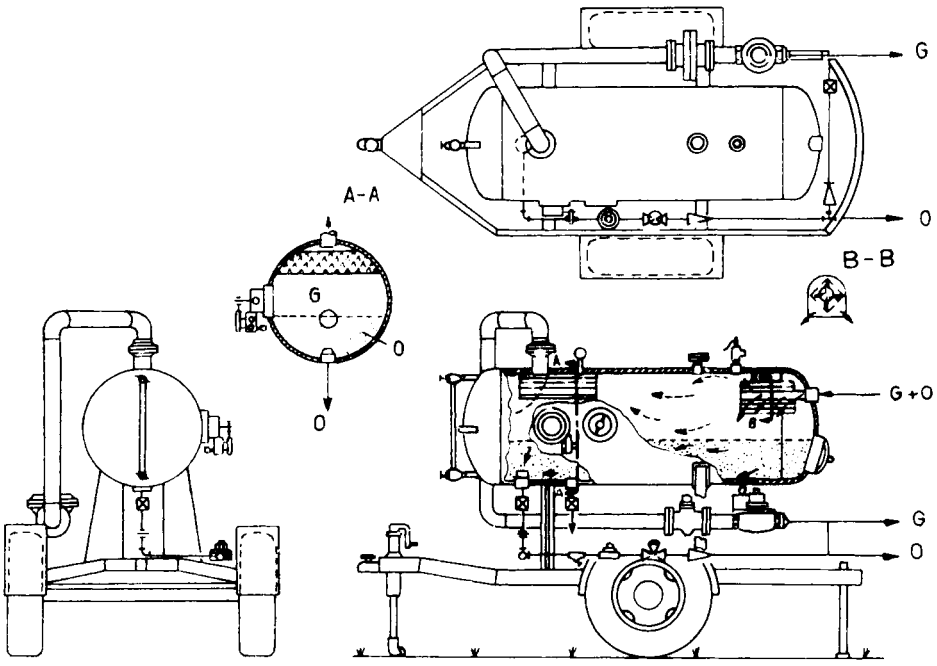


Fig. 6.4 – 42. Two-phase portable metering separator, according to J. D. Kimmel; after Frick 1962, Vol. II, pp. 29 (used with permission of McGraw-Hill Book Company)

standard-state volume will invariably differ from the metered volume. Moreover, a certain instrument error and some contamination of the liquid must also be reckoned with. The meter constant is always less than unity; that is, the volume reading is invariably greater than the standard-state volume of the liquid or the tank volume. Dump meters have the advantages that: (i) The correct operation of the meter is easy to verify; the meter is in good working order if it contains no deposits and is not deformed, and its valves open and close accurately. (ii) They are less sensitive to sand and other solids than positive-displacement meters. (iii) Metering accuracy is independent of throughput in the range from 0 to $q_{l\max}$. (iv) With gravity checks at intervals, they are suited also for the metering of foaming oil. (v) They can be serviced and repaired even with the separator onstream. (vi) Even if the control equipment fails, they will not meter gas as if it were liquid. Their drawbacks are: (i) First cost and installation cost are higher than in a positive-displacement meter. (ii) Metering is not continuous. (iii) Making the oil pass through the dump meter requires a non-negligible excess pressure in the separator. (iv) Deposits of wax will cause inaccurate metering. (v) Dump meters require more space and are heavier than positive-displacement meters. (vi) Especially if the oil is high-viscosity, the head loss due to metering is higher. Metering capacity depends on dump-vessel volume.

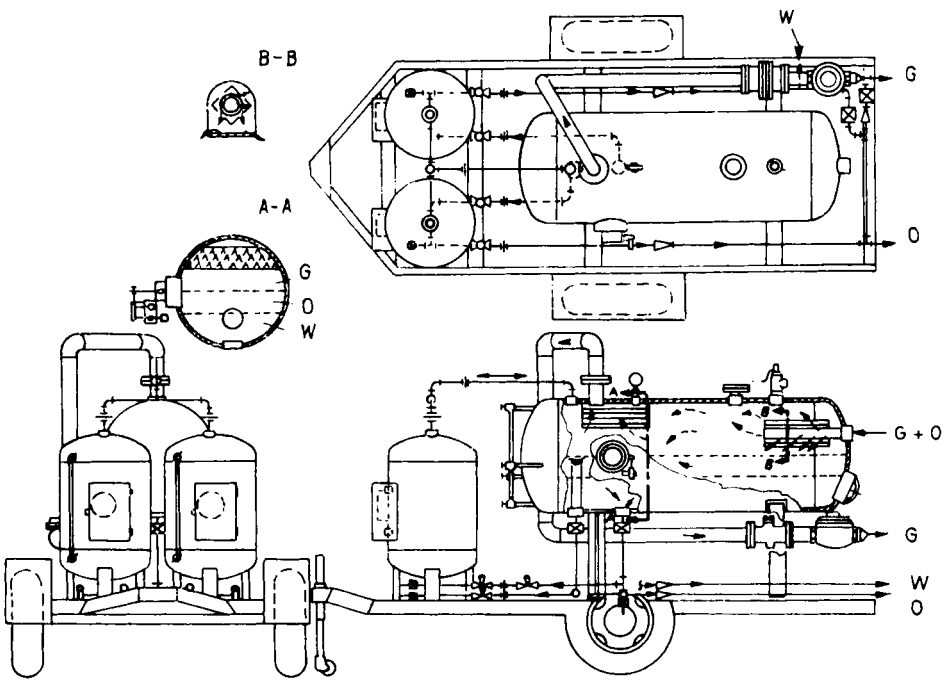


Fig. 6.4 – 43. Three-phase portable metering separator, according to J. D. Kimmel; after Frick 1962, Vol. II, pp. 29 (used with permission of McGraw-Hill Book Company)

Of the positive-displacement meters, nutation-disk type meters are most often employed for their simplicity, ruggedness, comparative width of measuring range and cheapness. They are, however, less accurate than oval-gear meters. Positive-displacement meters have the following advantages: (i) Liquid output and metering are continuous. (ii) These meters lend themselves also for the metering of high-viscosity oils. (iii) Pressure drop due to passage through the meter is negligible. (iv) Temperature compensation, that is, reduction of the metered volume to the standard-state volume is cheaper in most types than in a dump meter. Drawbacks include the following: (i) The liquid to be metered must be gasless. The meter will measure gas as if it were oil: indeed, fast changes in flow velocity due to gas slugs may damage or wreck the meter. (ii) Sand, mud, salt or any other solids are harmful to the meter and tend to falsify results. (iii) Accuracy is to be checked at intervals by means of a proving tank or a master meter. (iv) Accurate metering is restricted to a rather narrow output range (see also Section 6.6.3).

### 6.4.6. Low-temperature separation

If the wellstream is cooled to a low temperature before entry into the separator, separation will produce dry gas and a liquid rich in low-boiling-point hydrocarbons (condensate). The dew point of dry gas is lower, which makes it better suited for transportation in pipelines. If the liquid in the wellstream is of low boiling point in its entirety, then the liquid recovered will be raw gasoline rich in propane and

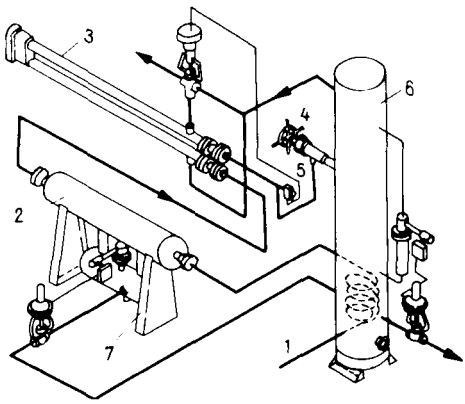


Fig. 6.4 – 44. Low-temperature separator, type a.1.1, after Frick (1962; used with permission of McGraw-Hill Book Company)

butane. Low-temperature separation, usually below $-5\,^{\circ}C$, is a comparatively recent procedure. Still, numerous variants have been devised. These may be divided in two large groups depending on whether the wellstream is cooled by its own near-adiabatic expansion, or by external means. The main technical difficulty to be overcome in low-temperature separation is that at the low temperature involved, combined with the pressure prevailing in the separator, gas hydrate will tend to form and, if nothing were done to forestall it, the separator would 'freeze up' pretty fast. In order to ensure continuous operation, various measures are taken to prevent freezing. In the following we shall further subdivide the two main types of low-temperature separation according to these measures.

According to E. C. Young, the main methods of low-temperature separation are as follows (Frick 1962). (a) Cooling is by expansion of the wellstream; (a.1) without hydrate inhibitor, (a.1.1) no external heating applied, (a.1.2) external heating applied; (a.2) with hydrate inhibitor, (a.2.1) without stabilization, (a.2.2) with stabilization; (b) cooling is by a refrigerant in a heat exchanger; (b.1) refrigerated by absorption; (b.2) refrigerated by compression.

Subtype (a.1.1). No inhibitor is added to the wellstream and no heating is employed to melt the hydrate. *Figure 6.4 – 44* shows equipment used for this purpose after Mapes (1960). Its main parts include inlet liquid separator *2*, gas-to-

gas heat exchanger *3*, and low-temperature separator *6*. The low-temperature separator itself is shown in more detail in *Fig. 6.4 – 45*. Wellstream enters through choke *1*. The solid hydrates freezing out of it collect on the vessel bottom. Outlets are: *2* for gas, *3* for liquid hydrocarbons, *4* for water. Solid hydrates are heated above decomposition temperature by warm wellstream flowing through coil *5*. Pressures

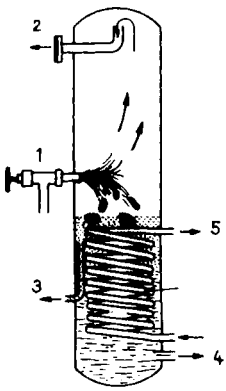


Fig. 6.4 – 45. Low-temperature separator, after Mapes (1960)

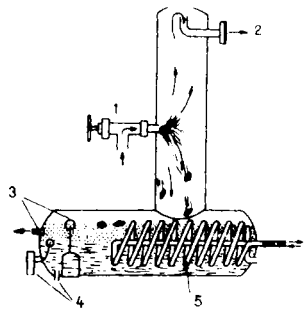


Fig. 6.4 – 46. Combined upright-horizontal low-temperature separator, after Mapes (1960)

and temperatures may e.g. be as follows: gas temperature upstream of choke, 30 °C; downstream of choke, 0 °C. Inflow temperature of heating wellstream, 50 °C; outflow temperature, 30 °C. Such cooling of the well fluid may ensured according to experience by letting the wellstream expand from 140 bars to, say, 5 or 10 bars. Low-temperature separators are not necessarily vertical: they may be horizontal, combined *(Fig. 6.4 – 46)*, or spherical as well. Referring once more to *Fig. 6.4 – 44*, the inflowing wellstream *1* is seen to be used in this setup to decompose hydrates collected at the separator bottom. The liquid is separated from the cooled well fluid in inlet-liquid separator *2*, for two reasons; one, to reduce the liability of the choke's freezing up; and two, gas is easier to cool if separated from the liquid of greater heat capacity, from which it could absorb more heat. The gas separated from the liquid then enters into heat exchanger *3* where it is cooled by the cold dry gas discharged from the separator to a temperature just above the hydrate-formation point upstream of the choke. This is achieved by regulating the quantity of dry gas passing through the heat exchanger by means of thermostat-controlled three-way motor valve *3*. This setup will function satisfactorily only if the heat delivered by the inflowing wellstream is sufficient to melt the gas hydrates at the separator bottom, and, on the other hand; if the temperature of the wellstream upstream of the choke is above the hydrate-formation point at the given pressure.

Subtype (a.1.2). Heat required to warm the wellstream and to decompose the gas hydrates collecting in the separator is taken from an external source. In this case, the gas-to-gas heat exchanger is replaced by a line heater. Gas is heated with either

steam or hot water in a heat exchanger, or part of the wellstream is passed through a coil in the liquid space of a boiler; the proportion of heated to unheated wellstream is controlled by the temperature upstream of the choke. The second solution is the more up-to-date. Gas hydrates are likewise decomposed by either water or steam taken from the boiler. This latter setup is illustrated by *Fig. 6.4 – 47*. The wellstream enters through conduit *1* to be divided by a three-way valve; part of it enters boiler *2*, to pass from there through choke *3* into combined separator *4*. Dry gas is discharged

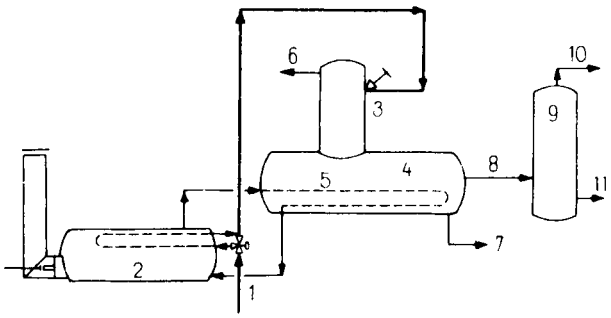


Fig. 6.4 – 47. Low-temperature separator, type a.1.2, after Mapes (1960)

through outlet *6*. Gas hydrates are heated to the required temperature by hot water circulating in conduit *5*. Water is drained through outlet *7*. Hydrocarbons are led through conduit *8* into second-stage separator *9*, where some gas can still be recovered from the liquid.

## 6.5. On-lease oil storage

### 6.5.1. Storage losses

Storage losses are comprised of leakage and evaporation loss. Leakage can be avoided if tank plates and fittings are tight and tanks are filled and emptied with proper care. Evaporation losses are due to the fact that the tank space above the stored crude is saturated with hydrocarbon vapours that will escape into the atmosphere. Evaporation losses fall into filling and breathing losses. Breathing is due to the daily fluctuation of tank temperature. Warming of the tank makes vapours expand, to escape partly into the atmosphere through the tank vents. On cooling, the tank will suck in air from the atmosphere. This process is further complicated by rain and other precipitations. Breathing loss is the higher the higher the vapour pressure of the product stored, the greater the temperature fluctuation, and the larger the vapour space. Filling losses will occur as the rising liquid level in a tank being filled expels the vapours contained in the vapour space. Evaporation has the following unwelcome consequences. (i) Hydrocarbon vapours escaping into the

atmosphere are lost for good, (ii) the light-fraction content, and hence, the value per ton, of the stored product decreases, (iii) the environment is polluted by the escaping vapours; moreover; (iv) an explosion hazard is created, and (v) the air entering the tank accelerates the corrosion of the inside tank wall.

Several ways to reduce or altogether stop evaporation losses are known. In order to assess the economy of the solution proposed, it is necessary to determine the losses, e.g. by closing all apertures of the tank into the atmosphere, save one, and by measuring the quantity and composition of the gas escaping through the remaining aperture over a longer span of time. For estimating evaporation losses of light hydrocarbons in big tanks, a procedure requiring no separate measurement has been devised (O'Brien 1951). The method is based on *Figs 6.5 – 1 – 6.5 – 3. Figure 6.5 – 1* shows Reid vapour pressures v. temperature for various hydrocarbons. As

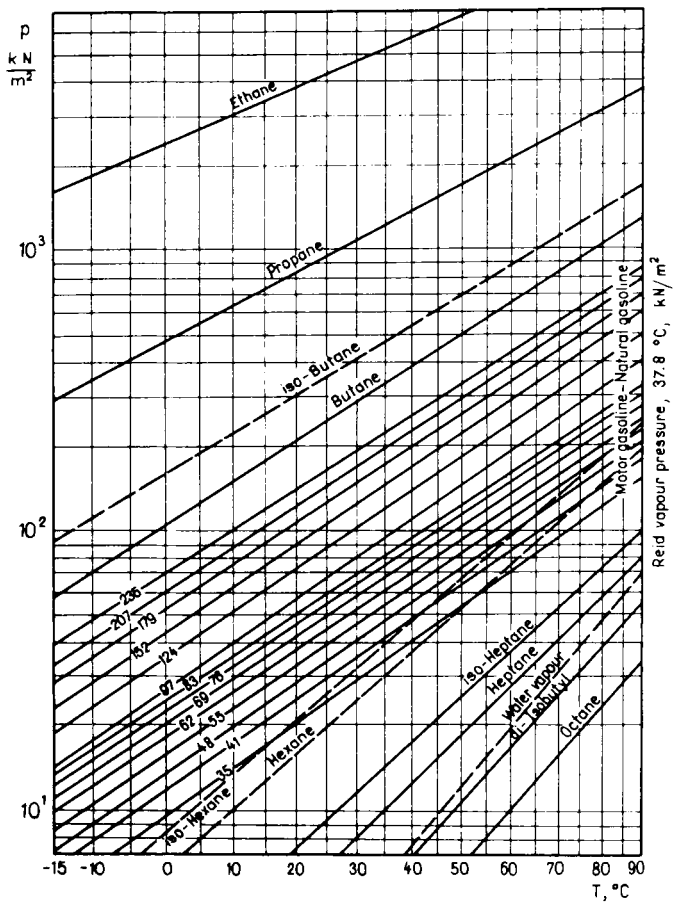


Fig. 6.5 – 1. Vapour pressures, after O'Brien (1951)

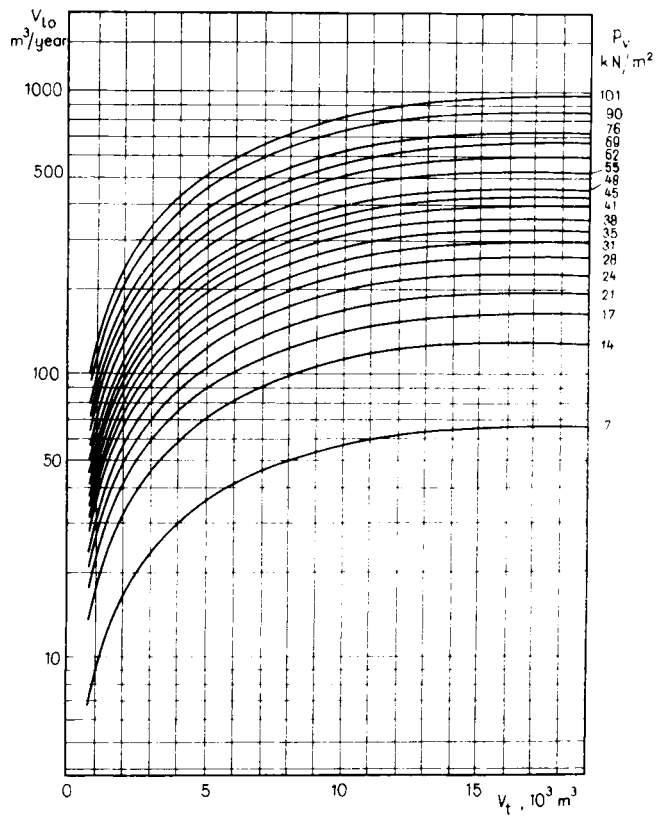


Fig. 6.5 – 2. Breathing loss, after O'Brien (1951)

regards evaporation loss, it is the surface temperature of the oils stored in the tank that is relevant. A statistic of data collected all over the USA has revealed surface temperatures to exceed mean annual temperatures by 5.5 °C on an average. *Figure 6.5 – 2* is a plot of breathing losses over one year v. tank volume, for various vapour pressures. In compiling this diagram tanks have been assumed to be painted a silvery colour and to be half full; the vapour space has been assumed to expand by 20 percent. *Figure 6.5 – 3* is a plot of filling loss v. tank volume for various vapour pressures. It has been assumed that the vapour escaping during filling has the same gasoline content as the vapour space. The tank is painted a silvery colour and is half-full on a long-term average.

*Example 6.5 – 1.* Find by O'Brien's method the breathing loss over one year and the filling loss during the filling of $10^6$ $m^3$ of liquid in a tank of 8700 $m^3$ capacity, if the liquid in the tank is gasoline of 90 kN/$m^2$ Reid vapour pressure and its mean surface temperature is 25 °C. By *Fig. 6.5 – 1*, vapour-space pressure is $p_v$ = 63 kN/$m^2$. Accordingly, breathing loss over one year is 485 $m^3$/year *(Fig. 6.5*

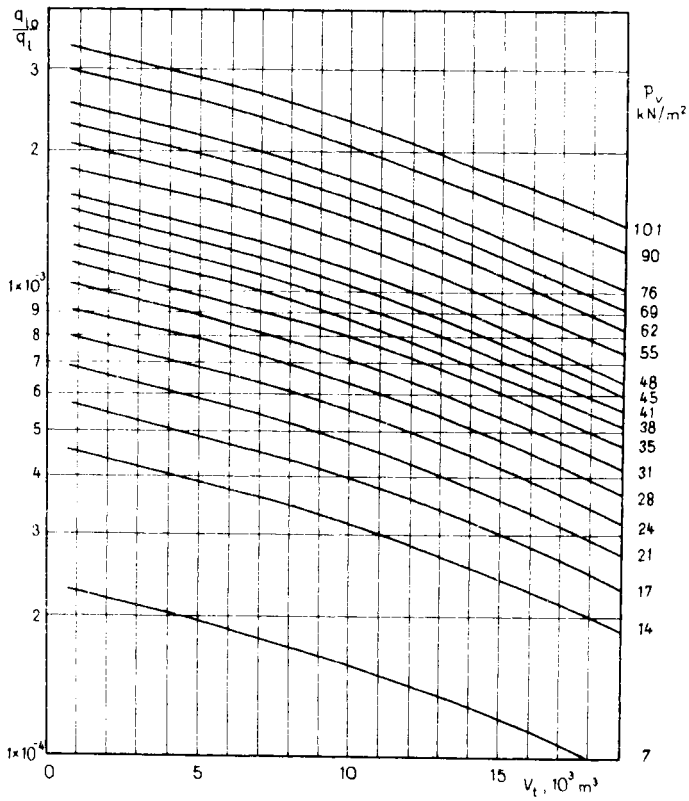


Fig. 6.5 – 3. Filling loss, after O'Brien (1951)

*– 2)*. By *Fig. 6.5 – 3*, the loss factor $q_{lo}/q_l$ is 0·00162, that is, 1620 m$^3$ for a liquid throughput of $10^6$ m$^3$.

Losses in an upright cylindrical tank may be reduced: (a) By keeping temperature fluctuations within limits. (i) The tank is painted a silvery or aluminium colour. Evaporation losses of a crude of 0·837 kg/m$^3$ gravity for tanks of different colours are listed in *Table 6.5 – 1*. (ii) The tank is partly or entirely covered with a heat-insulating layer. If covering is partial, it is applied to the tank roof. (iii) The tank is cooled by the evaporation of a sheet of water on the tank roof, or by sprinkling with water. A so-called water roof may reduce evaporation losses by 25 to 40 percent, sprinkling by more than 50 percent. (iv) The tank is built underground. An earth cover of 30 to 40 cm above the tank may prevent all breathing losses. (b) By closing the tank to the atmosphere, that is, by choosing a tank whose permissible internal pressure is higher than the vapour pressures that may arise. Evaporation losses will cease if pressure at the liquid surface is higher than the vapour pressure of the liquid. (c) By special tank-roof designs. (d) By means of vapour-recovery installations.

Table 6.5 – 1. Influence of colour to which tank is painted on breathing loss, for oil of 837 kg/m$^3$ gravity

| Colour of paint | Evaporation loss percent per year | Gravity after one year of storage |
|---|---|---|
| Black | 1·24 | 840·3 |
| Red | 1·14 | 839·7 |
| Grey | 1·03 | 838·6 |
| Aluminium | 0·83 | 838·1 |

### 6.5.2. Oil storage tanks

Oil tanks on a lease are installed partly at well testing stations, and partly at the central oil gathering station of the lease. They are usually made of steel sheet or concrete. Most of them are above-ground, but some are buried underground. Pits dug in the soil, as the simplest means of liquid storage, are used temporarily, if at all, next to exploration and after well blowouts. Oil-storage pits are to be dug in level ground, if possible. The pit walls and bottom are lined with stamped clay (cf. *Fig. 6.5 – 4*). In order to minimize seepage losses, a layer of water 10 – 15 cm high is poured

Fig. 6.5 – 4. Storage pit

in under the oil. Pits serving as mud pits or for the storage of fracturing fluid are first injected with a silicon compound and then with a polymer expanding in water. In such pits, seepage loss is less than 0·1 percent of the liquid volume stored (*Oil and Gas Journal* 1969). A similar treatment will reduce oil seepage, too.

The most widespread type of on-lease oil-storage tank is upright cylindrical, made of sheet steel. The sheet used is usually smooth, seldom corrugated. Smooth sheet is joined by bolting, riveting or welding. Bolted and riveted tanks can be taken apart without loss of sheet, and re-erected elsewhere. Welded tanks can be installed faster; they require less sheet for a given volume. However, their dismantling and re-erection entails a considerable loss of sheet. In welded tanks, rings are either butt- or lap-welded. (cf. *Fig. 6.5 – 5;* butt welds (a), telescopic lap-welds (b) and alternating-ring lap-welds (c)). Bottoms are flat; roofs are usually conical. The necessary wall thickness of upright cylindrical tank shells can be calculated in view of the maximum liquid pressure to be expected as

$$s = \frac{rp}{\sigma_{al}} = \frac{rh\rho_l g}{\sigma_{al} k} \qquad 6.5-1$$

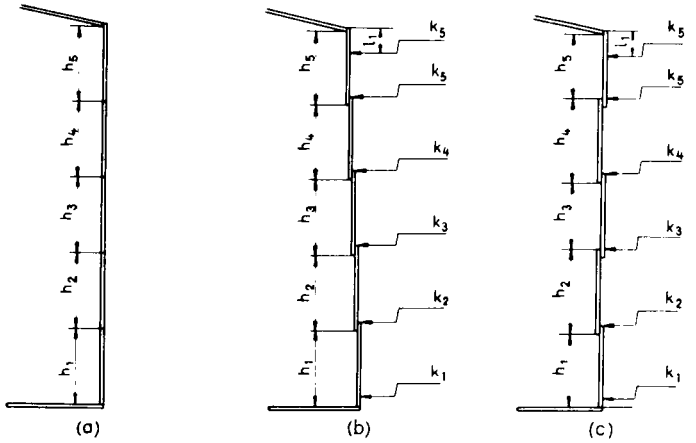


Fig. 6.5 – 5. Hoop welding patterns of tanks (Petroleum... *Oil* 1955)

where $r$ is radius, $h$ is the maximum height of liquid column in the tank, $\rho_l$ is the maximum liquid gravity to be expected, $\sigma_{al}$ is maximum permissible stress, and $k$ is a weld-seam factor.

*Example 6.5 – 2.* Let $h = 3$ m, $d = 5$ m, $\rho_l = 1000$ kg/m$^3$, $\sigma_{al} = 140$ MN/m$^2$. What wall thickness is to be chosen? – By Eq. 6.5 – 1,

$$s = \frac{2{\cdot}5 \times 3 \times 1000 \times 9{\cdot}81}{140 \times 10^6} = 5{\cdot}3 \times 10^{-4}\ \text{m} = 0{\cdot}53\ \text{mm}\,.$$

Providing the tank with the necessary rigidity and properly joining the sheets demand a wall thickness of 3 – 4 mm at least, depending on tank size and steel grade.

Up to about 600 m$^3$ capacity, tanks are made of sheet of constant thickness, determined by the above considerations, whereas larger tanks are telescoped (higher rings are made of thinner sheet). The quantity of metal needed to build a tank of given volume $V_t$ will be different for various height-to-diameter ratios. Metal volume is

$$V_{\text{me}} = d_i \pi h s_1 + \frac{d_i^2 \pi}{4}(s_2 + s_3)$$

and since

$$V_t = \frac{d_i^2 \pi}{4} h$$

we have

$$V_{\text{me}} = \pi s_1 h \sqrt{\frac{4V_t}{h\pi}} + \frac{V_t(s_2 + s_3)}{h}\,.$$

The least metal volume for a given tank volume may be determined by calculus. The derivative of $V_{me}$ with respect to $h$ is

$$\frac{dV_{me}}{dh} = \frac{\pi s_1}{2}\sqrt{\frac{4V_t}{h\pi}} - \frac{V_t(s_2+s_3)}{h^2}.$$

which implies that metal consumption will be a minimum if

$$\frac{h}{d_i} = \frac{(s_2+s_3)}{2s_1}. \qquad 6.5-2$$

Introducing this result into the above volume formula we get the most favourable tank height:

$$h_{opt} = \sqrt[3]{\frac{V_t(s_2+s_3)^2}{\pi s_1^2 k'}} \qquad 6.5-3$$

where $k'$ is the overlap factor. — It can be shown in similar way for telescoped tanks (Shishchenko and Apriesov 1952) that

$$h_{opt} = \sqrt{\frac{\sigma'_{al}(s_2+s_3)}{\rho g k'}} \qquad 6.5-4$$

where $\sigma'_{al} = \sigma_{al} k''$. The value of $k''$ ranges from 0·72 to 0·77. It accounts for strength reduction due to welding and riveting.

The optimal tank shapes given by the above formulae may be slightly modified by standard steel sheet sizes. On the other hand, as regards gauging the contents of a tank, it is better if the tank is taller, because a given error in level determination will cause the less error in volume, the slenderer the tank. In sizing tanks it should be kept in mind that tank weight per unit volume is the less the larger the tank *(Fig. 6.5*

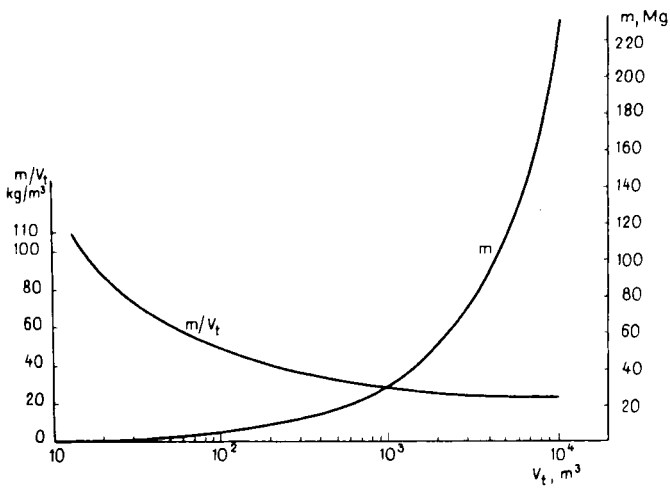


Fig. 6.5 – 6. Typical data of Soviet tanks, after Shishchenko and Apriesov (1952)

*– 6)*. It is therefore more economical, in so far as this is a prime consideration, to use a few big tanks than numerous small ones. Prescriptions concerning tanks are laid down in API Stds 12B, 12C, 12D and 12F. Aluminium tanks are treated in API Std 12G. Let us point out that tanks suitable for dismantling are not usually made in sizes larger than 1600 $m^3$. Larger tanks are of welded construction. Still, there is no objection to the making of small tanks by welding.

In most upright cylindrical steel tanks, vapour pressure above the liquid must not exceed 0·4 – 0·5 $kN/m^2$. For radially ribbed decks, this value may attain 0·2 – 0·5

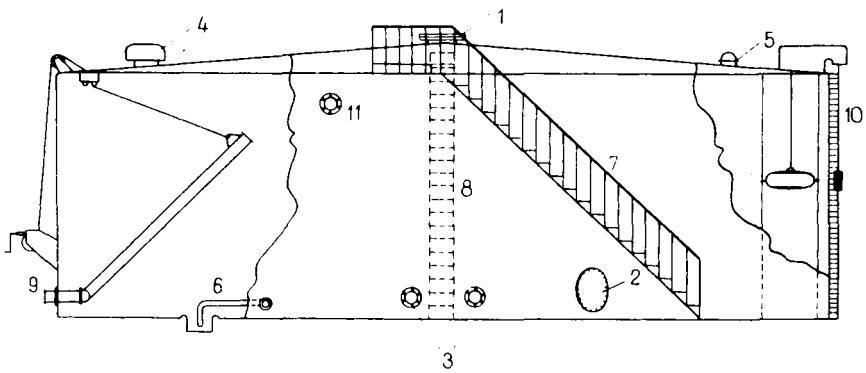


Fig. 6.5 – 7. Upright steel tank

bar, but such designs need substantially more steel. – If a tank is to withstand a higher pressure — a few bars, say — then a horizontal cylindrical shape is adopted. The cylindrical shell is closed on both ends by an ellipsoidal or spherical dome. Such tanks should be made in a shop and not on-site. For oils of particularly high vapour pressure, the spherical and spheroidal tanks usual in the storage of light distillation products should be employed. The fittings of upright cylindrical tanks are shown in *Fig. 6.5 – 7* as manhole on deck *1*, clean-out port on shell *2*, inlet studs *3*, breathing valve *4*, gauge hatch *5*, water drain *6*, outside ladder or stairs *7*, inside ladder *8*, drain stud, with swivelling suction pipe *9*, level gauge *10*, hookup to foam-type fire extinguisher *11*.

Breathing valves, installed on the roof apertures of tanks, open at 0·15 – 0·30 $kN/m^2$ pressure differential, both positive and negative. In the mechanical breathing valve shown as *Fig. 6.5 – 8*, valve *1* opens to overpressure in the tank, valve *2* opens to vacuum. Valve capacity depends on the maximum inflow/outflow rate of liquid into/from the tank (cf. Table 6.5 – 2, after Shishchenko and Apriesov 1952). In some instances, the gauge hatch is designed as a mechanical-type breathing valve *(Fig. 6.5 – 9)*; *1* is the datum level of liquid level gauging. Overpressure is released by the entire hatch cover pivoting about *2*; vacuum is compensated through disk valve *3*. In order to eliminate the hazard of the mechanical valves' sticking or seizing, hydraulic valves are used in some instances *(Fig. 6.5 – 10)*. Antifreeze liquid

poured in cup *1* will be raised in annulus *2* by overpressure and in annulus *3* by vacuum. This type of valve is designed so that the liquid will not be spilled out of annulus *2* or *3* until the maximum operating pressure of the mechanical valve has been exceeded. Breathing valves are often provided with flame arresters, in order to help localize tank fires. Breathing valves will reduce evaporation losses by 15 to 20 percent, depending on the nature of the crude stored.

*Figure 6.5 – 11* shows schematically two types of liquid-level gauge. The device in part (a) permits an approximate determination of liquid level. Line *2*, hanging float

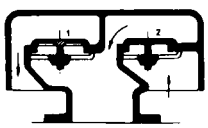

Fig. 6.5 – 8. Mechanical breathing valve after Shishchenko and Apriesov (1952)

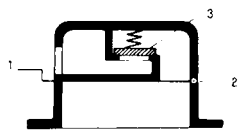


Fig. 6.5 – 9. Gauge hatch closed by mechanical breathing valve

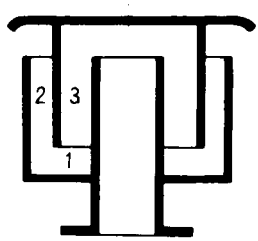


Fig. 6.5 – 10. Hydraulic safety valve

*1*, emerges through liquid-filled airlock *3* to pass in front of calibrated tape *4*. Index *5* will give an approximate reading of liquid level in the tank. Its purpose is to provide first-glance information to the operator rather than to permit accurate liquid-level measurement. In design (b), the bobbing of float *1* is limited by guide wires *2*, which makes for a higher accuracy in measurement. The perforated tape attached to the

Table 6.5 – 2. Diameters of mechanical breathing valves (after Shishchenko and Apriesov 1952)

| Pumping rate | Valve diameter |
|---|---|
| $m^3/h$ | mm |
| 0 – 50 | 50 |
| 50 – 100 | 100 |
| 100 – 200 | 150 |
| 200 – 400 | 200 |

float line is wound on meter drum *3*, whose number of revolutions will be proportional to the liquid level in the tank. Instrument dial *4* is calibrated directly in volume units. Line *2* and the perforated tape are tensioned by weight *5*. An automatic device permitting level gauging to better than 1 mm accuracy and compatible with a telemetering system is described in Wafelman (1969). By means of the swing pipe, oil can be extracted from any height within the tank. This permits us to separate oil layers of various degrees of contamination, or oil containing water, or

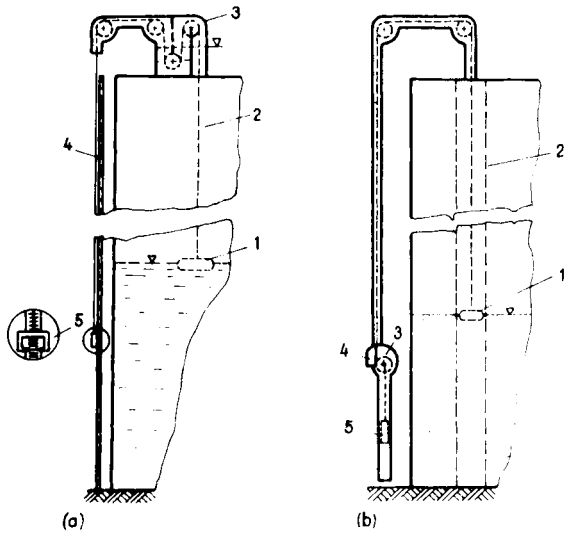


Fig. 6.5 – 11. Liquid level indicators, after Chilingar and Beason (1969)

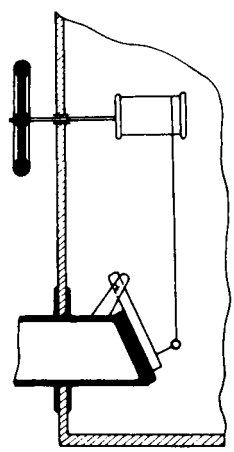

Fig. 6.5 – 12. Clap valve on fill conduit

other impurities. The inlet pipes of some tanks are fitted with clap valves, operating as back-pressure valves, that can be actuated from the outside *(Fig. 6.5 – 12)*. This has the advantage that broken-down valves in the fill line may be replaced without having to drain the tank. — Tanks may be provided with internal heating if the crude stored in them requires warming. Steam is generally used for heating.

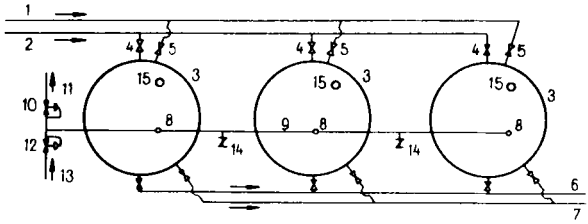


Fig. 6.5 – 13. Tank station

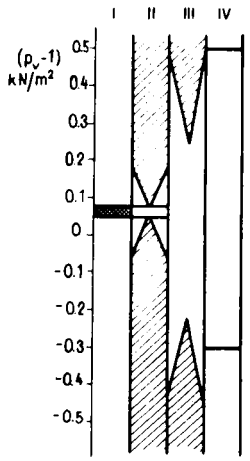


Fig. 6.5 – 14. Operation ranges of tank pressure regulating devices, modified after Chilingar and Beason (1969, p. 76; by permission of the authors and Elsevier Publishing Company)

Radiators may be plane or spiral, installed either near the bottom of the tank, or so as to heat the oil drained from the tank only (Pektyemirov 1951).

*Figure 6.5 – 13* shows the layout of a three-tank battery. Tanks *3* are filled through fill lines *1* and *2*. By manipulating valves *4* and *5*, any tank may be opened to the fill line. Oil is discharged from the tank through drain line *6*, which usually leads to the pump station. Water can be drawn off through line *7*. If the tank battery is manually operated, a means for the operator to see when oil starts to drain through the water drawoff must be provided. The vapour spaces of tanks are connected by vent line *9* hooked up to vertical pipes *8*, which permits the vapour expelled from

any tank being filled to enter the vapour spaces of the other two tanks, or a tank to suck in wet gas from the two other tanks when being drained. If gas pressure in the tanks nevertheless exceeds a certain value set on pressure regulator *10*, then the excess wet gas is bled off into a gathering line through conduit *11*. If one the other hand pressure in the vapour spaces drops below a value set on pressure regulator *12*, then this regulator admits dry gas from line *13* through vent line *9* into the vapour

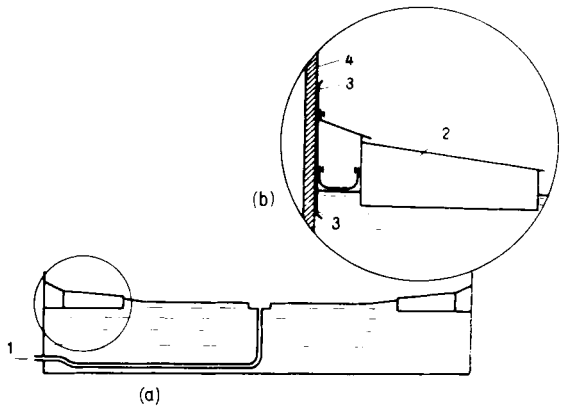


Fig. 6.5 – 15. McKenna's floating-deck tank

spaces of the tanks. If the gas stream required to adjust pressure in the tanks cannot be handled by regulators *10* and *12*, breather valves *14* enter into action. A further measure of safety is introduced by emergency relief valves *15*, which may be hydraulic or of some other design. It is essential that pressure regulators be matched to each other and to the permissible pressure ranges and gas flows to be expected. *Figure 6.5 – 14* (modified from Chilingar and Beason 1969) represents the pressure ranges covered by the various regulators and valves of the above-outlined system. Shaded width in each column is proportional to valve travel. In designing emergency relief valves it should be kept in mind that the volume of a hydrocarbon increases about 15 times on burning. It is this expanded gas stream that has to be released by the valve.

Little (1963) described a vapour recovery system where the vapour is drawn off the tanks at the central gathering station of an oil lease. Wet gas is passed through a scrubber and centrifugal compressor driven by a 22 kW electric motor. The system paid itself out in 76 days. — Tanks with special evaporation-reducing roofs are used primarily for the storage of light petroleum products, but their use may be justified also for comparatively light crudes. Several designs are known, of which the floating-roof tank is the one of particular interest for crude storage. The roof is not fixed to the tank side but floats on top of the liquid. There is practically no vapour space, and hence evaporation loss is either very low or nil, depending on the design. There are several solutions even within the group of floating-roof tanks. *Figure 6.5*

– *15,a* shows a circular-pontoon design. Rain falling on the roof is drained through pipe *1*. Several ways have been devised to seal the roof against the upright cylindrical shell. *Figure 6.5 – 15,b* shows one of these (McKenna make). The essential thing is that slide *3* mounted on roof *2* fit tank wall *4* as snugly as possible.

Experiments have been carried out to determine how the evaporation losses are influenced by the size and stuffing of the gap between the floating roof, and the inner tank surface (Jonker *et al.* 1977). It was found that the loss, due to evaporation, was the minimum when applying resilient packings at the bottom of the floating roof (shoe seals). A device as one of this kind is shown on *Fig. 6.5 – 15,b*.

When applying shoe seals, the fit does not influence the evaporation losses, unless, it exceeds 25 mm in maximum 5 percent of the tank perimeter. Evaporation losses may be further reduced by secondary seals.

## 6.6. Fluid volume measurement

In the practice of hydrocarbon production and transport it is important to measure the quantity of the oil, gas and water flowing and stored in and flowing out of the system both in view of process control and of commercial reasons.

Devices and techniques of measurement are widely discussed in several books, studies, standards and specifications. That is why we only try to give a summary here that may be important for production and transport engineers.

### 6.6.1. Measurement of crude volume in tanks

A traditional method to measure the volume of crude under standard conditions used to be the tank measurement, a method that is still applied in several countries. Tanks whose liquid content is determined by liquid-level gauging must be calibrated before use. Calibration may be performed either by calculation based on measurement of circumference and diameter, or directly by filling with known volume of water. Of the calculation methods, the one based on circumference measurement is the more accurate. In this method the circumference of every hoop is measured with a steel tape. In welded tanks, measurements are performed at one fifth of plate height below each horizontal weld seam, irrespective of the type of welding. The heights where measurements are to be carried out on riveted tanks are shown by the arrows in *Fig. 6.5 – 5*. Hoop height is measured for each constant diameter hoop. Sheet thickness $s$ must also be measured (the value adopted is the average of several measurements). If the measured circumference is $s_c$, and the number of overlaps is $n$, then approximate volume per unit height is

$$V = \frac{s_c^2}{4\pi} - \left( s_c s + b_1 s n + \frac{1}{2} b_2 s n \right) \qquad 6.6-1$$

with $b_1$ and $b_2$ identified in *Fig. 6.6 – 1*.

Accurate knowledge of tank volume demands the measurement also of the tank fittings that reduce or increase tank volume, or the establishment of their volume by calculation, with their elevation within the tank taken in due account. Tank volume is reduced by the inside ladder, the profiles joining wall to bottom, the ties between roof and floor, heating tubes, etc. The swivelling portion of the suction tube is usually left out of account. Tank volume is augmented by manhole domes, pipe studs, etc. Roughness of the tank bottom is usually accounted for by pouring in a

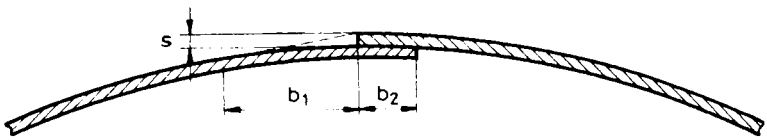


Fig. 6.6 – 1.

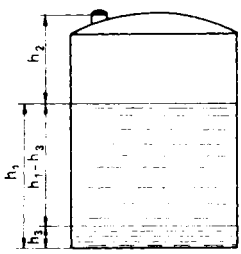


Fig. 6.6 – 2.

sheat of water of sufficient height to cover all unevennesses. Tanks of less than 80 $m^3$ nominal capacity should be at least two thirds full during measurement. When calibrating a tank with water, the tank is either gradually filled with, or gradually drained of, accurately known amounts of water. The results obtained are interpolated to yield capacity differences for each centimetre of level difference. This is a rather lengthy procedure if an accurate result is desired, and therefore it is used primarily to calibrate deformed tanks of irregular shape.

Tanks are calibrated (i) after installation or displacement, (ii) if tank fittings are changed, or (iii) if the tank gets deformed. The calibration results are transformed into a table which states cumulative tank volume for each centimetre from the bottom upward. Prescriptions in force concerning calibration are contained in API Std. 2551. Deformation of the shell of an upright cylindrical tank under load of the liquid in it has been described by mathematical formulae (Withers 1970).

The liquid content of a tank may be gauged in several ways. In earlier practice, gauging with steel tape was largely used. Two widespread methods of tape gauging are outage and innage measurement. Innage is measured by lowering a tape weighted with a bob to the tank bottom and, after having withdrawn it, recording the height to which it is wetted with oil ($h_1$; *Fig. 6.6 – 2*). The tank volume

corresponding to $h_1$ can be read off the calibration table. In outage measurement, the height corresponding to $(h_1+h_2)$ in the Figure is measured directly after calibration, and the datum level of measurement is marked on the gauge hatch. All subsequent measurements are referred to this datum. The tape with the bob here is now used to determine the height $h_2$ and the height of the oil column is calculated from the relationship $(h_1+h_2)-h_2=h_1$. This latter method is to be preferred if sediment is settled on the tank bottom.

The quantity of water separated at the tank bottom can be established by smearing the bottom end of the tape with a special paste or by hanging from it a bob calibrated in centimeters, with a strip of special paper stuck to it. The paper strip or paste will change its colour when coming in contact with water. The water volume corresponding to water level $h_3$ can be read off the calibration table.

The so-called actual oil volume established by gauging is to be corrected for two factors. First of all, the oil may contain dispersed, unseparated water, and, second, the volume of pure oil must, in the knowledge of actual temperature, be transformed to standard volume, or, in the knowledge of actual gravity, into mass. In order to check the purity of the oil, a sample must be taken in a manner prescribed by standards, and the water content of the sample and the gravity of the pure oil must be determined in the laboratory. The average temperature of the liquid in the tank must be similarly determined in a specified way. The relevant specifications can be found in API Stds 2543 – 2548.

Though due to its simple principle this volume measurement method is rather widespread, it is easy to prove that this method is neither accurate nor cheep. *Inaccuracy in the determination of the effective liquid volume* is caused (i) by the inaccuracy of the tank calibration; by the deformation of the tank after its calibration; by the sediments settled on the wall and bottom of the tank; and by the inaccuracy in the measurement of the level of the liquid, that is partly due to mistakes committed by the measuring personnel and partly to the wetting effect of the oil foam; (ii) by the inaccuracy in *determination of the water content.* Its main reasons are as follows: the interface of the water, separated and settled in the tank, with the oil is impossible to measure accurately; the water content of the emulsified oil is determined on the basis of tank samples. The water content of the sample differs from the average water content of the tank; and the determination of the water content from the tank fluid sample by applying centrifuging or distillation has its own mistakes in measurements and reading-off; (iii) *by the reduction of liquid volume:* If the water volume determined by the measurement is subtracted from the effective liquid volume, we obtain the pure oil volume stored in the tank, the so-called effective net oil volume. This volume must be corrected to standard temperature. Even this correction may be inaccurate, since the establishment of the average temperature of the bulk tank volume requires several measurements, and the value obtained differs from the real average; the density of tank oil changes with the change of temperature, and the rate of this change is different for different types of crudes; the constants of the equations describing this relations also have their own

errors. Due to the above reasons the net oil volume, or corrected volume, can be determined only with an accuracy of $\pm 1$ percent.

This process is very *expensive*. In order to increase the accuracy of level measurements tanks of comparatively smaller diameters are recommended. The same total storage volume is thus provided by a greater number of smaller volume storage tanks. This solution is, of course, more expensive than the application of smaller number of larger tanks (see Section 6.5.2). The total storage capacity of a given tank battery may be reduced in case the filling-up and emptying is not required because of the measurement.

This method of determination of oil volume *cannot be automated*. In spite of this fact, in certain countries, the liquid level in the tanks and thus the effective liquid volume is measured by instruments. This means is generally used for the purpose that the operator of the tank battery should be informed directly or by way of telemetry, that, into which storage tank the transported oil can be directed, and from which tank oil can be transported, respectively, and, approximatively how large is the tank battery's stock. All disadvantages can be avoided if the liquid volume, the quantity of the fluid is measured by a flow meter.

### 6.6.2. Dump meter

The dump meter is a small volume ($0{\cdot}04 - 4{\cdot}8\ m^3$) measuring tank, where the volume of liquid pumped through is automatically measured. In order to ensure the continuity of measurement generally two dump meters are applied. While one of

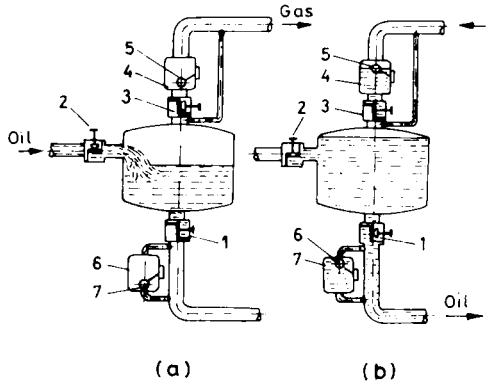


Fig. 6.6 – 3. Dump meter

them is filled, the other is emptied. The sketch of a dump meter instrument and its operation is shown in *Fig. 6.6 – 3*. On Figure (a) valve *1* is closed while valves *2* and *3* are open. The level of the oil flowing into the unit through valve *2* increases, till the float positioned in chamber *4* does not reach the top position. Then valves *2* and *3* close automatically, and valve *1* opens. The liquid drains till float *7* does not get in a

lower position in chamber *6*. Then the float directs the valves in starting position. The number of the drainages is measured by a counter. The range of the application of the dump meters is limited for some portable, skid-mounted well testers (Section 6.4.5 – (c)).

### 6.6.3. Fluid measurement by orifice meters

Measurement by orifice meters is first of all applied for metering the volume and quantity of gas, respectively. This method, however, is also suitable for measuring the mass or volume of fluids e.g. oil as well. In case of fluid flowing in the pipeline this device causes pressure drop by its orifice plate. Being aware of the pressure drop and some other physical parameters the standard volume, or the mass of the fluid flowing through the pipe during time $\Delta t$ can be calculated. *Fig. 6.6 – 4* shows the hookup of the formerly generally, today to less extent used mercury type orifice

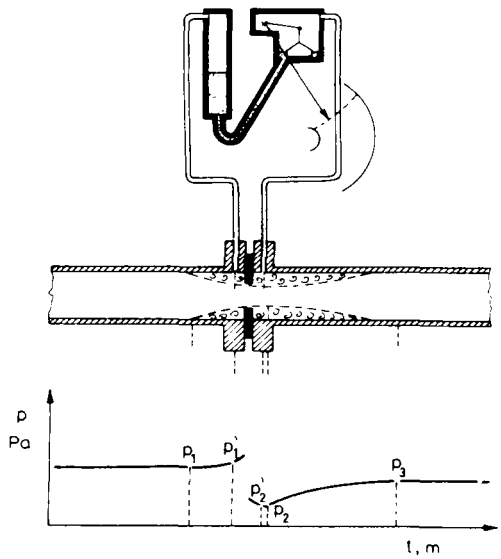


Fig. 6.6 – 4. Mercury type orifice meter

meter and the alteration of the flowing pressure along the surface of the pipe-wall caused by the orifice plate. Upstream and downstream of the orifice, the pressure considerably rapidly, changes. It is important, therefore, that the pressure measuring points should be standarized. In the case represented in the Figure it is obvious that the respective pressures are sensed and transmitted through the holes on the pipe flanges into the mercury-type instrument that records the pressure difference. There are other standardized measuring points too. According to ISO R

541 the mass flow rate is as follows:

$$q_m = 1{\cdot}111\alpha\varepsilon d_{ch}^2 \sqrt{\Delta p \rho_1}\,, \qquad 6.6-2$$

where $\alpha$ is the flow coefficient that will be discussed later on. The expansion factor $\varepsilon$ equals 1 in case if the density change of the fluid is negligible in the course of its flowing through the measuring device, i.e. generally in case of liquid flow. $d_{ch}$ is the diameter of the orifice, m; $\Delta p$ is the pressure difference caused by the orifice, Pa; $\rho_1$ is the actual density of the flowing fluid at flowing temperature and at $p_1$ upstream pressure at the orifice, kg/m$^3$.

In case of flow of vapours and gases, while measuring the pressure by flange taps, the expansion factor is

$$\varepsilon = 1 - (0{\cdot}41 + 0{\cdot}35\,\beta^4)\frac{\Delta p}{p_1}\frac{1}{\kappa} \qquad 6.6-3$$

where $\beta = d_{ch}/d_p$ and $\kappa$ is the ratio of specific heats. For other standard pressure measuring points the variables of the $\varepsilon$ formula are practically the same, while the form of the equation and the constants may differ.

The flow coefficient is

$$\alpha = \alpha'\left(1 + \frac{\beta A}{N_{Rep}}\right), \qquad 6.6-4$$

where $N_{Rep}$ is the Reynolds number calculated for the pipe section upstream of the orifice, while $A$ and $\alpha'$ are given by empirical equations depending on the place of the pressure measurement. For flange taps

$$\alpha' = f(\alpha_e\,,\ d_{ch}\,,\ A)$$

this is the stabilized value of $\alpha$ flow coefficient at high $N_{Rep}^{-5}$.

$$\alpha_e = f'(d_p\,,\ \beta)$$

where $\alpha_e$ is the flow coefficient and

$$A = f''(d_{ch}\,,\ d_p\,,\ \beta)\,,$$

thus the flow coefficient is

$$\alpha = F(d_{ch}\,,\ d_p\,,\ N_{Rep})\,. \qquad 6.6-5$$

This function is represented with a good approximation on *Fig. 6.6 – 5* which is valid, strictly spoken, for the corner taps only. It is visible that in case of relatively high Reynolds numbers, generally with values over $10^6$, the flow coefficient is a function of $\beta = d_{ch}/d_p$ only. At smaller values it is also a function of the Reynolds number, that, in turn, is the function of flow rate. From Eq. 1.1 – 2 it is obvious that for liquids

$$N_{Rep} = \frac{4}{\pi}\frac{q_m}{d_p \rho \nu}$$

and for gases

$$N_{\mathrm{Rep}} = \frac{4}{\pi} \frac{M}{R} \frac{q_n p_n}{T_n d_p \mu}$$

Since $q_m$ and $q_n$, respectively, are functions of the Reynolds number, the volume, or mass of the liquid throughput on the basis of the parameters, measured by the orifice meter can be calculated only by way of successive approximation, if the value of $N_{\mathrm{Rep}}$ is smaller than approx. $10^6$.

A former general practice for gas flow measurement, that is applied even today, is not the determination of the mass flow rate, but that of standard volumetric flow

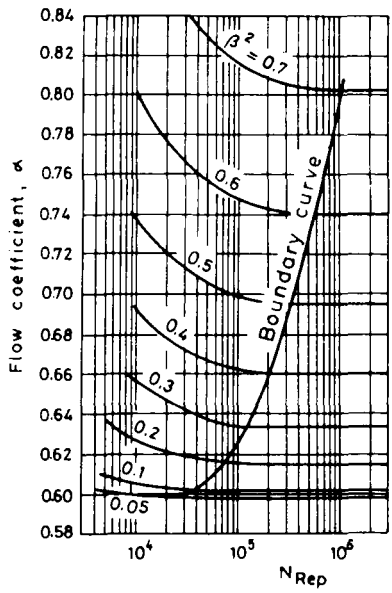


Fig. 6.6 – 5. The flow coefficient α after MSz 1709-67

rate, $q_n$. Considering the relation $q_m/\rho = q_n$ from Eq. 6.6 – 2, by applying the general gas law it is easy to obtain that

$$q_n = 1{\cdot}111\ \alpha\varepsilon d_{\mathrm{ch}}^2 \frac{T_n z_n}{p_n} \sqrt{\frac{R p_1 \Delta p}{M T z}}$$

and by substituting the value $R = 8314$ J/(kmol K)

$$q_n = 101{\cdot}3\ \alpha\varepsilon d_{\mathrm{ch}}^2 \frac{T_n z_n}{p_n} \sqrt{\frac{p_1 \Delta p}{M T z}}. \qquad 6.6-6$$

From the comparison of Eqs 6.6 – 2 and 6.6 – 6 it is obvious that for the determination of the mass flow rate $q_m$, two parameters should be measured ($\Delta p$ and

$\rho$), while for the calculation of standard volumetric flow rate, $q_n$, four ($p_1$, $\Delta p$, $M$ and $T$). This is one reason of spreading of the method of mass flow measurement. The condition of the application of this method is that the actual flow density should be measured with proper accuracy (Szeredai 1981). For the continuous measurement of the density of flowing medium with proper accuracy adequate methods developed only in the past decade. Such a solution is published in the Solatron Catalogue (1977). The essence of this method is that a small, transversally oscillating, body is immersed into the flowing fluid to be measured, the frequency of its oscillation changing with the density of the environment:

$$\rho = \frac{A}{f^2} + \frac{B}{f} + C,$$

where the density of the measured fluid is $\rho$. $f$ is the frequency of the oscillation, and $A$, $B$ and $C$ are constants. The obtainable accuracy of measurement is 0·1 – 0·3 percents, where the smaller value is relevant for liquids, and the greater one characterizes gases.

Each of the physical parameters may change during the measurement. The change of the pressure difference $\Delta p$ may be significantly large and rapid. The mass or volume of the gas throughput during $\Delta t$ time may be calculated both on the basis of recorded charts and digitally measured values, though the calculation must be fulfilled at relatively short $\Delta t$ time steps. The value of $\Delta t$ must be chosen so that the change in the measured physical parameters during this time should be negligible. On the basis of these considerations Eqs 6.6 – 2 and 6.6 – 6 can be written as

$$V_n = 1{\cdot}111\, d_{ch}^2 \sum_{i=1}^{n} \alpha\varepsilon \sqrt{\Delta p \rho_1}\, \Delta t \qquad 6.6-7$$

and

$$V_n = 101{\cdot}3\, d_{ch}^2 \frac{T_n z_n}{p_n} \sum_{i=1}^{n} \alpha\varepsilon \sqrt{\frac{p_1 \Delta p}{M T z}}\, \Delta t, \qquad 6.6-8$$

where $n$ stands for the number of time steps.

According to the measuring methods of the physical parameters, their recording and the calculation methods using the above data, several types of flow meters and measuring systems have been developed that can be classified into groups as follows:

(i) Individual instruments that record at least the pressure difference on chart. The gas volume must be manually computed on the basis of these charts. Pressure difference is measured with aneroid or with mercury type devices.

(ii) Individual instruments measuring the basic parameters at time intervals $\Delta t$. On the basis of the obtained results the flow rate during $t$ is calculated and the quantities for the period of $t = n \cdot \Delta t$ are summarized. The computing and summarizing device may be of mechanical, pneumatic and electric-electronic character.

(iii) Systems applying a joint computer-controlled unit by which the data groups belonging to several meter runs, are reported to a central computer, in intervals of $\Delta t$ periods and all the computing work is done by the computer centre. The computer may be a single-purpose machine of relatively small capacity, or a large capacity general unit that performs the gas volume calculation in part time.

For solving the quantity measurement problem of automated petroleum production and transport systems first of all units described in paragraph (iii) are suitable, while certain instruments of paragraph (ii) can be also applied; instruments described in paragraph (i), however, cannot be used for this purpose.

It should be noted that the inaccuracy of the measurement by applying orifice metering, in case of small Reynolds numbers, is comparatively high. According to *Figure 6.6 – 5* the greater the value of $\beta$ is the greater the Reynolds number, where the $\alpha$ curves are crossed by boundary curve, and the greater the slope of the curves is. That is why it is recommended that the diameter ratio should fall in the range of 0·2 – 0·7 and the pressure ratio $p_2/p_1$ should be higher than 0·75.

A frequent case is that for gas sales the heating value of the gas is considered and no gas mass, or standard volume of gas is sold but heat energy. In these cases, beside the parameters characterizing the gas mass, the heating value of the gas should be also constantly measured. For the measurement of the heating value several methods are applied (Yoho 1978).

According to a survey of the Gas Transport Committee of the World Gas Conference the accuracy of measurement ranges between 0·1 – 0·5 percents (*Report* ... 1976). Errors of more than 3 percent are reported from countries where pneumatic and mechanic equipments of average size are used. Errors of 0·1 percent magnitude were reported from certain West-European countries where at large export-purpose stations digital utilities are available. According to the same Committee for the measurement of gas volumes, the use of orifice meters is dominant all over the world. Several efforts are made to increase the measuring accuracy. It appears that there are means to increase the accuracy of even the individual measuring instruments, i.e. to improve several decades old methods (Laird 1981). Experience of the British Gas Corporation is reported by Rabone (1979) when he sums up the reasons for the widespread application of the orifice metering: the primary device is simple; great volumes may be measured with a relative good accuracy; its repeatability is good; no calibration is needed if the prescriptions are carefully followed; the instrument's changing is possible without stopping the gas flow; the slightly higher-than-designed gas rates can be measured without damaging the unit. Some of the main disadvantages of this type are that the measurement range, without changing the orifice plate, is comparatively small (cca. 1 : 10) and the pressure drop, occurring through the meter, may be relatively significant.

### 6.6.4. Critical flow power

A peculiar version of the orifice meter for gas volume measurement is the so-called critical flow prover. The measurement is based upon the principle that a lower than critical pressure ratio is developed by the orifice; the pressure and temperature of the gas stream passing through the device with sound velocity is measured and the actual gas flow rate is calculated using the above parameters. The basis of the relation used for the calculation is Eq. 1.4 – 122 valid for flow through a choke

$$q_n = 101{\cdot}3\, d_{ch}^2 \frac{p_1 T_n}{p_n} \alpha \sqrt{\frac{1}{M T_1} \frac{\kappa}{\kappa - 1} \left[ \left( \frac{p_2}{p_1} \right)^{\frac{2}{\kappa}} - \left( \frac{p_2}{p_1} \right)^{\frac{\kappa+1}{\kappa}} \right]} \ \mathrm{m^3/s}.$$

If the pressure ratio $p_2/p_1$ is smaller than the critical value then, considering Section 1.4.3 (a), the above equation can be simplified as follows:

$$q_n = \frac{k p_1}{\sqrt{T_1 M}} \ \mathrm{m^3/s}, \qquad 6.6-9$$

where $k$, at the given orifice type, practically depends on the choke size. The pressure upstream of the choke is $p_1$ ; $T_1$ is the temperature before the choke, and $M$ is the molar mass of the gas.

The critical flow prover is used, first of all, for the calibration of other, industrial gas flow meters and for the testing of flow rates of new gas wells. *Figure 6.6 – 6* shows

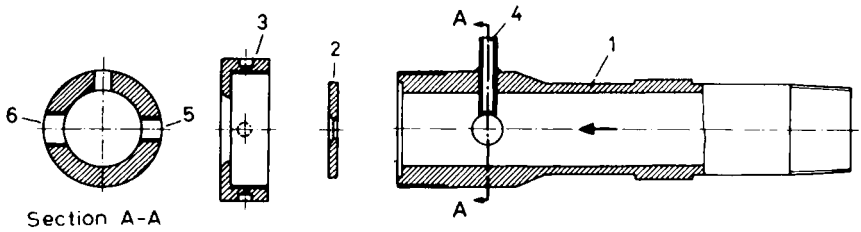


Fig. 6.6 – 6. Rawlins and Schellhardt's critical flow prover

the critical flow prover designed by Rawlins–Schellhardt and used for this latter purpose, in dismantled pieces (Szilas 1967). The measuring body *1* is mounted on the pipe end open to the atmosphere. To this the orifice plate *2* is fixed by cover *3*. The thermometer is placed in case *4* while the pressure gage is mounted in bore *5*. Hole marked *6* is closed by a valve.

### 6.6.5. Positive-displacement meters

In positive displacement meters, the liquid or gas enters a metering space of known capacity, confined by pistons or plungers of various design and performing motions of various types, and is then expelled therefrom. These meters may be

considered as hydraulic motors of high volumetric efficiency that adsorb energy from the passing fluid as is required to keep in motion the moving parts of the instrument. The effective volume of fluid is proportional to the number of strokes if the piston is reciprocating, or of revolutions if it is of the rotating type. The effective volume is, then, transformed in standard volume or mass. The parameters required to this procedure (pressure, temperature and density, respectively) are measured separately, similarly to the orifice metering, and the PD meters give automatically

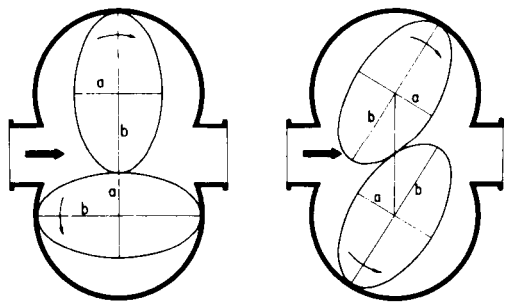


Fig. 6.6 – 7. Principle of oval-gear positive-displacement meter, after Reppisch (1958)

the corrected data. About 700 types of positive displacement meters are known. In the case of production and transport of oil and gas they are used first of all for oil quantity measurement, and the oval-gear meter is the most popular, the principle of which is shown in *Fig. 6.6 – 7* (Reppisch 1958). Every revolution of the pair of oval wheels provided with spur gears lets pass theoretically constant amount of liquid. Between the engaging gear-teeth of the two wheels, on the one hand, and the gearbox and the wheel sweeping by it, on the other hand, there are gaps of a few hundredths of millimeter width. Some of the liquid will pass unmetered through these gaps. At higher flow rates, pressure difference due to friction and flow resistance across the meter will increase, and so will leakage through the gaps, as an almost linear function of the pressure difference. Accurate metering requires knowledge of the relative leakage loss. The upper part *(a)* of *Fig. 6.6 – 8* shows pressure difference $\Delta p$ across an oval-gear meter, and leakage $\Delta q$, assumed to be proportional to $\Delta p$, v. the effective flow rate $q_e$ through the instrument. Part *(b)* of the Figure shows $\Delta q/q_e$ v. $q_e$ curve *(1)* (the percentage error of metering). In the ideal case of no leakage, the instrument will indicate the actual throughput (line *2*). In effect, however, actual throughput invariably exceeds by the leakage loss the volume indicated by the meter, if no measures to the contrary are taken. By suitable adjusting the variable gear ratio between oval gears and counter, however, displacing line *2* into the position of line *3*, so as to make the counter consistently indicate more oil by 0·25 percent than it would in the ideal case; the error is made zero where line *3* and curve *1* intersect, positive between the two points of intersection (that is, the indicated throughput will exceed the actual), and negative

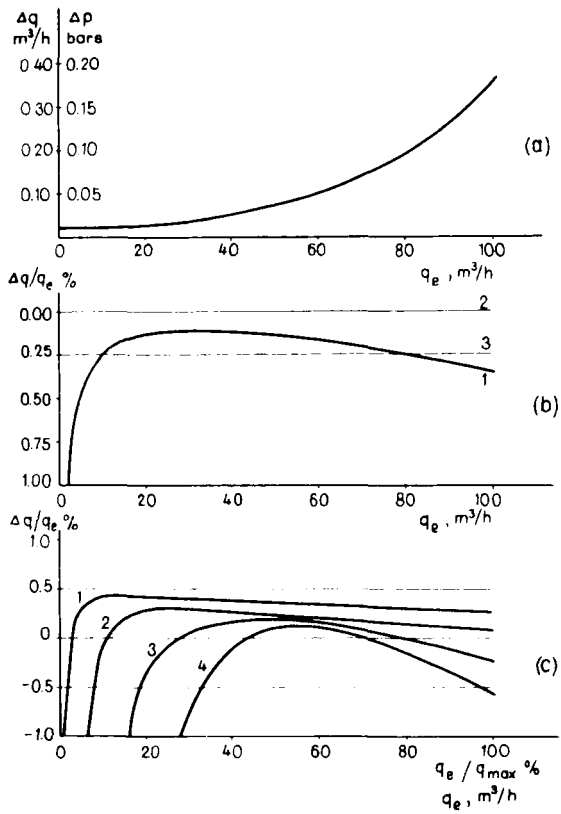


Fig. 6.6–8. Characteristics of oval-gear positive-displacement meter, after Reppisch (1958)

outside the two points of intersection. In the case shown, at throughputs of 6 – 100 $m^3/d$, the maximum error may be $\pm 0{\cdot}15$ percent. The error will be greater at low and high throughputs, and particularly heavy at very low throughputs. The leakage curve will, however, hold only for liquids of a given viscosity as, obviously, leakage loss depends not only on gap width but also on the viscosity of the liquid handled. Part *(c)* of the Figure shows the error curves for liquids of different viscosities at the same gear ratio. The viscosity, with the increasing numbers decreases. It is shown that (i) for liquids of different viscosities at the same flow rate the measurement error will be different; (ii) and also, that the same measurement error-limit can be achieved, in case of liquids of greater viscosity within greater, and in case of liquids of smaller viscosity within smaller ranges. — Exact results can be achieved, if flows of nearly constant viscosity and rate are measured and the calibration curves are determined using liquid of the given viscosity. Then even an accuracy of $\pm 0{\cdot}1$ percent may be achieved.

There are instruments that continuously sense the flowing temperature and correct the volume to standard temperature. The Bopp Reuther-type instrument (FRG), a positive displacement meter compensating for temperature is a device of this kind.

The accuracy of the net oil measurement may be significantly decreased, if water or gas bubbles, respectively, can be found in the measured oil. That is why the water content should be precisely measured, and getting of gas bubbles into the instruments should be prevented (see also Section 6.7.3 – (b)).

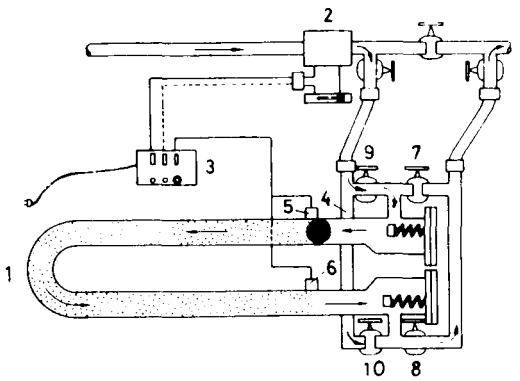


Fig. 6.6 – 9. Shell Pipe Line Co.'s ball-type meter prover

An extremely important task is the regular proving of measuring devices, that can be done in several ways. The specifications of the formerly widely used tank proving are described e.g. by ASME-API Code 1101. Nowadays the so-called ball type provers are used at an ever increasing rate. The principle of their operation is that the meter is connected with a prover of comparatively small volume in which the liquid rate can be determined with a great accuracy. An instrument of this type developed by the Shell Pipe Line Corp. is shown on *Fig. 6.6 – 9*. Liquid, passing through the unit, flows through measuring pipe *1* coated with epoxy resin, and the direction of its getting back into the pipeline is shown by arrows. The electronic pulse counter *3* of measuring unit *2* is turned on when ball *4* passes sensor *5*, and turned off when it attains sensor *6*. If valves *7* and *10* are opened, and valves *8* and *9* are closed at the same time, then the direction of flow in the measuring pipe becomes reversed, and the ball passes first indicator *6*, then indicator *5*. This flow, or ball motion, respectively, can be also applied for calibration. In order to achieve an exact calibration it is necessary that pulse frequency be high, the volume of the measuring pipe should be at least ten thousand times greater than the smallest possible volume (cca. 0·0038 l) determined by the number of pulses, and also its volume should be at least as great as the 0·5 percent of the greatest hourly throughput capacity of the measuring device. The specifications of the ball meter prover devices are described

in API Code 2531 (Komich 1973). Since these instruments are rather expensive, in order to decrease their costs, versions including no valves were also developed (O'Donnell 1973).

Beside its several advantages the positive displacement meter is liable to several errors as well, i.e. it is very sensitive as for the solid contaminations are concerned. It can cause the rapid wear of the instrument that may result in a rapid decrease in the accuracy of the measurement, in the stopping of the wheels, and even in their fracture. In these latter cases the liquid transport through the measuring instrument also ceases.

### 6.6.6. Turbine type flow meters

In a pipe-shaped instrument housing a turbine-like rotor is mounted that rotates at RPM proportional to the flow velocity of gas or liquid, passing through. Since the flow area is constant, in case of given temperature and pressure, the flow velocity is proportional to the effective flow rate, determined by the above parameters. The

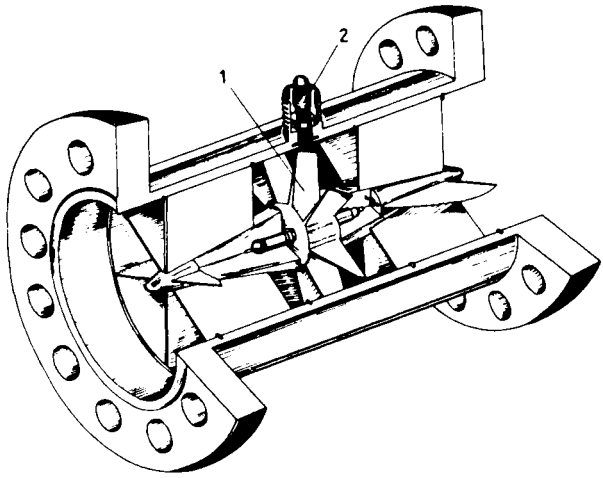


Fig. 6.6 – 10. Halliburton's turbine flow meter

characteristics of the rotating motion, in case of up-to-date devices, are transmitted, by way of electronic equipment, to the counter units producing digital signals. This method is applied in case of the Halliburton-type measuring turbine applying rotating magnets, that is shown on *Fig. 6.6 – 10*. Permanent magnet placed in turbine wheel *1* generates an alternating current in coil *2* the frequency of which is proportional to the turbine's RPM. Voltage peaks are counted by electronic pulse counters. The frequency of the impulses is proportional to the actual flow rate, while the total pulse number is proportional to the transmitted effective fluid volume. Here, the measurement error in the function of the flow rate is similar to that of

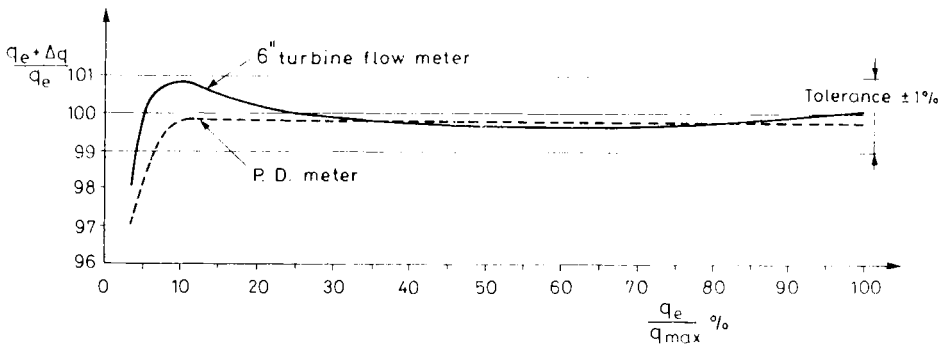


Fig. 6.6 – 11. Measurement accuracy of turbine flow meter

positive displacement meters (see former Chapter). *Fig. 6.6 – 11*, after Catalogue 350.1 of the American Meter Division, shows, in case of gas measurement the accuracy, expressed in percentages, in the function of the percentages of the recommended measuring capacity of the instrument. It is visible that the error in measurement of the effective volume is of a magnitude of 0·1 percent. Lehmann (1976) states that measurement error can be expressed by

$$\Delta q = A\left(1 - \frac{M}{q_e^2}\right) + (B - C) \cdot \left(1 - C\frac{v}{q_e}\right), \qquad 6.6 - 10$$

where $A$, $B$ and $C$ are instrumental constants; $M$ is the mechanical friction torque; and $v$ is the kinematic viscosity of the transported fluid. The first term of the formula characterizes the impact of friction upon the bearing that is rather small in case of modern devices. The second term stands for the liquid friction in case of higher than critical Reynolds numbers. By proper selection of $B$ and $C$ instrumental constants it can be achieved that, in a given viscosity range, in case of $N_{Re} > 3000$ values, this term should be negligible. Accurate measurement requires also the knowledge of the viscosity of the flowing medium.

The application of the turbine flow meter also supposes that the instrument should be preceded and followed by straight pipe sections, "meter runs" of undisturbed cross-sections. In order to eliminate the velocity components due to spin and vortices also straightening vanes are mounted into the inflow section. Specifications describing the standard application are described in AGA Committee Report No. 7 (Less 1980).

The starting time, required by the turbine flow meters, in order to measure the actual flow rate is only 5 – 10 ms, that is why the device is suitable to measure pulsating flow as well. At an average throughflow speed 10 m/s, the pressure drop is between 0·2 – 0·5 bars. The correction for standard volume or mass is carried out similarly as in the case of positive displacement meters.

The use of the turbine flow meters for the measurement of oil and gas is increasing. In case of oil flow measurement they replace PD meters. The primary advantage of

turbine flow meter is, that it is less sensitive to the solid contaminations, its wear is slower, and even if the rotor stops, it does not hinder the flow. Morse (1976) summarizes the results of experiments, carried out at seven oil fields for years, by which the aim was to determine which of the two measuring instruments can be used more efficiently for oils containing emulsion or solid contamination. The test result showed that, during the operating period, the repeatability of the positive displacement meters was $\pm 0{\cdot}81$ percent, while the same value for turbine meters is $\pm 0{\cdot}41$. The life of turbine flow meters proved to be eleven times longer, and the change of the meter factor during the testing period was half as much as that of the positive displacement meters.

Turbine flow meters are increasingly applied also for the measurement of large gas flow rates. An advantage as compared to orifice metering is that it rapidly adapts itself to the fluctuating flow rates and the measurement accuracy, in case of modern devices, may even reach 0·25 percent, if calibration is carried out at approximately the same pressure as that of the measurement. Several methods are applied for calibration. Wager (1977) is for the application of the critical flow prover equipped with a Venturi tube, since by this device even a measurement accuracy of 0·2 percent can be obtained. Most frequently, however, the series-connected master meters are used. For the calibration of oil measuring turbine flow meters, similarly to the positive displacement meters, ball provers are widely used. The largest device of this kind was developed in Japan, in 1974. Its capacity is $8000\,m^3/h$ while its repeatability is $\pm 0{\cdot}02$ percent. The meter proving process may be significantly simplified by applying the so-called European method, the essence of which is that calibration needs not be carried out for oils of each possible viscosity since one calibration is enough. Here, in the function of $q/v$, proportional to the Reynolds number, an universal error function is determined. The tests were carried out by using Sereg turbine meters (Sereg-Schlumberger 1978).

### 6.6.7. Other measurements

Measuring oil flow by any instruments it can occur that the stream contains water too, and the net oil flow rate can be determined only if the water content is also continuously measured, recorded. The most widely used device for this purpose is the capacitance type BS and W monitor. The dielectric constant of water is $30-40$ times higher than that of crude. This is the circumstance exploited in the method. In the monitoring loop shown in *Fig. 6.6 – 12*, a closed pipe *2* of length $s$ is installed coaxially in oil pipe *1*. The arrangement functions as a capacitor of length $s$, with wet oil as the dielectric. The capacitor (whose capacitance depends, besides the constant geometry of the arrangement, on the dielectric constant of the liquid) is hooked up to a resonant circuit. The eigenfrequency $f_n$ of the circuit depends on the water content of the liquid in the capacitor. This frequency is fed together with the constant frequency output $f_1$ of a generator into a mixing stage, and the beat frequency $(f_n - f_1)$ of the mixer is fed to a servo mechanism. This is designed so as to readjust the original frequency $f_n$ of waterless oil by turning a variable capacitor.

This turning, suitably amplified, serves as a measure of water content against an experimentally calibrated dial. Experience has shown this instrument to operate to about 50 percent water only. *Figure 6.6 – 13* after Wood (1958) shows the apparent electric resistivity and dielectric constant v. water content of a given grade of oil

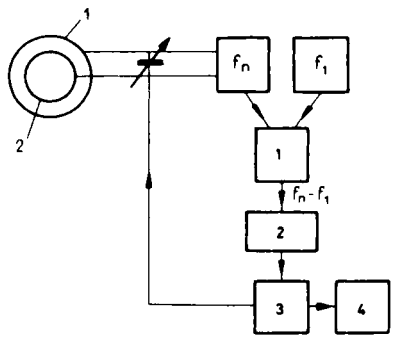


Fig. 6.6 – 12. Capacitance-type BS&W monitoring

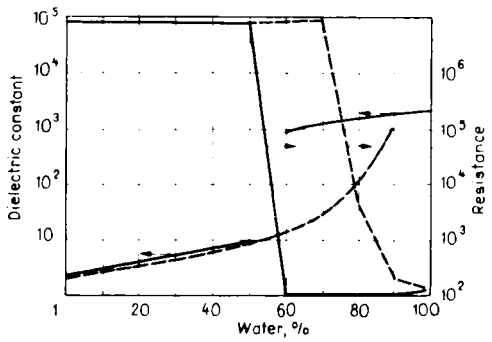


Fig. 6.6 – 13. Dielectric constant and resistance of a water-oil mix v. the water content, after Wood (1958)

mixed with an artificial brine of 9 weight percent salt content. The experiments were performed with *O/W* emulsions prepared respectively by fast and slow mixing (full and smooth dashed curves, respectively). Clearly, at about 50 – 60 percent water content the dielectric constant of fast-mixed emulsions takes a sudden jump with a concomitant drop in resistivity. In slow-mixed emulsions, the dielectric constant rises gradually, but resistivity takes a sudden drop between 70 – 80 percent. Similar phenomena are observed in mixes of other oils with brines of different concentration. The reason for this is that, at comparatively high water contents, the original *W/O* emulsion inverts into an *O/W* emulsion — earlier in fast mixes, later in slow ones — and salt water short circuits the capacitor cylinders.

Later investigations have shown the error of the capacitance-type BS and W meters to be significant, up to 7 percent. This has two main causes: the dielectric constant of water will be affected, first, by its content of clay minerals, especially montmorillonite, and, secondly, by the frequency used in the measurement. Scatter can be reduced considerably by employing a high frequency; 10 mcps seems the best (Thompson and Nicksic 1970). The accuracy of the measurement is considerably influenced by the quality of the emulsion (dropsize and distribution of the water).

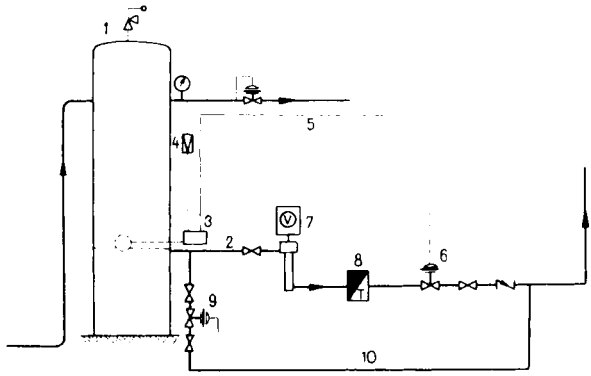


Fig. 6.6 – 14. Hookup of BS&W monitor downstream of separator, after Wood (1958)

The *B* and *W* monitor's accuracy is not indifferent to installation and hookup. *Figure 6.6 – 14* shows one of the most favourable hookups, immediately downstream of the separators. Liquid is discharged through line 2 from float-controlled separator *1*. Once the liquid in the separator has risen to the high level, control *3* supplies power gas taken from the gas-outlet reducer *4* through line *5* above the diaphragm of motor valve *6*, which opens the liquid discharge line. Water content is monitored by capacitance-type monitor *7;* liquid volume is metered by meter *8*. Bypass line *10* around the metering system can be remotely opened through remote-controlled motor valve *9*. The chart of the BS and W monitor is moved by the clockwork only when the separator is delivering liquid. The advantage of this hookup is that it provides continuous monitoring; pressure during discharge from the separator is constant; and the liquid is mixed rapidly and uniformly.

According to Wood, capacitance-type monitoring provides results close those of sampling from the stock tank, performed by the usual procedures but with the care befitting a calibration experiment. Samples taken from the flow line at the wellhead give widely divergent results, owing presumably to the frequent slug-type flow of the two phases, which tends to discredit this sampling procedure. Calibration of capacitance type *BS* and *W* monitors is outlined in Byers (1962 – 1963, Part 3).

Beside the above handled devices several other instruments were also used for the measurement of mass or volume of oil and gas. The practical importance and the

relative number of their application is small however. In the past decades devices measuring mass flow rate directly were supposed to face a bright future. Due to their sophisticated structure and high price, they are used only in a very limited rate. Among the most recent types first of all the vortex meter seems to be promising (Rabone 1979).

## 6.7. Oil and gas gathering and separation systems

The wellstreams of wells producing crude oil and natural gas are conveyed to centres located on the oilfield. A system comprising piping, pipe fittings and central facilities permits us to separate the liquid from the gas, to measure the quantity of both, to adjust their properties so as to fall within sales-contract and/or other specifications, and to transport them to the consumers or refineries. In the present chapter we shall follow the journey of gas up to where it is discharged from the separator, and that of oil to the intake of the pipeline's driver pump station. It will be assumed throughout that the water produced together with the crude can be removed by simple settling and that no special measures have to be taken to protect equipment from corrosion by the wellstream. Gathering and separating systems fall into three groups. All three types of system start at the well and end at the storage tanks of the oil pipeline or in the intake of the pipeline driver pump. The first group includes production systems of extremely high-capacity wells. Each well has its own facilities for separation and metering, possibly also for treatment. This setup is seldom economical. A more frequent type of system involves gathering and separating facilities permitting the common handling of several wellstreams. *Figure 6.7 – 1* shows a so-called well-centre system after Graf (1957). Individual wells *1* on the lease are connected to well centres *2*. Each wellstream is transported to the well centre in an individual flowline. At the well centres, the wellstreams at least of the

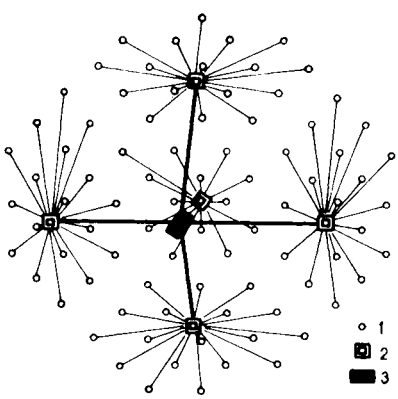


Fig. 6.7 – 1. Well-centre gathering system, after Graf (1957)

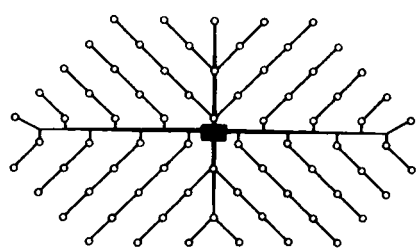

Fig. 6.7 – 2. Common-line gathering system, after Graf (1957)

wells selected for individual testing and metering are kept separate; their oil, gas and water rates are metered; then either the united wellstreams are transported as they are to the central gathering station *3* of the lease, or the gas separated at each well centre is introduced into the gas gathering line, whereas the liquid is forwarded to the central gathering station. In the third group (likewise after Graf 1957) several wells produce into a common flowline *(Fig. 6.7 – 2)*. Oil, gas and water production of individual wells are metered at intervals by means of portable well testers installed at the well sites. All other treatment takes place at the central station. Of the above-named three groups, the well-centre system is the most widespread and we shall restrict our following discussion to that system.

### 6.7.1. Viewpoints for designing gathering systems with well-testing centres

In outlining design principles for finding the most favourable gathering and separating system for any oil lease, we shall for the time being disregard whether the system in question is operated under manual control, by means of local automation, or by process control. Discussion shall be production-centred, and the decision as to which means of control is most efficient and most economical will be regarded as a separate subsequent task. The principles to be observed in designing are as follows. (a) The wellhead pressures of the wells should be as low as feasible. The resulting main advantages are: longer flowing life; lower specific injection-gas consumption in gas-lift wells; higher yield of wells produced with bottom-hole pumps in the last phase of production. (b) The hydrocarbon loss of the system should be a minimum. (c) The system should be easy to oversee as far as control and checking are concerned. This makes for disciplined production, and permits fast intervention in times of operating troubles. (d) Metering the individual and common oil, gas and water production of the wells and testing for impurities in the liquid produced should be ensured to the necessary accuracy. (e) When determining oil storage volume, the offtake rate to be expected is to be taken into consideration, together with interruptions in offtake due to breakdowns to be expected, as well as the settling time possibly required for the removal of water and impurities. (f) Expansion of facilities made necessary by the bringing in of further wells should require the least possible modifications to the existing installations; said modifications should be possible to achieve without disturbing the wells already in production. (g) Specific cost, referred to the volume unit of oil and/or gas produced, of installing and operating the system should be as low as possible. (h) Safety prescriptions should be meticulously observed.

The realization of these principles may raise the following, partly contradictory, viewpoints.

*ad* (a). (i) Head loss in the flowline between wellhead and separator should be as low as possible. Hence, sudden breaks in flowline trace and sudden changes in cross-section should be avoided; flowline size, length and trace should be chosen with a view to attaining minimum head loss; if the crude is waxy and/or sandy, measures

are to be taken to prevent the formation of bothersome deposits in the flowline and its fittings; in the case of high-viscosity or waxy crudes, reducing head loss may be achieved by heating the crude at the wellhead, heat-insulating the flowline, or injecting a friction-reducing chemical; if water is readily separated from the wellstream, it is recommended to install a water knockout next to each well. (ii) Separator pressure should be as low as possible. In order to keep it so, it is usually recommended to install separators higher than storage tank level at the well centres so as to make the oil flow by gravity from the separators into the tanks. The less the pressure needed to convey gas from the separator through the gathering line to the compressor station, the better. This can be achieved primarily by a gathering-line network of low flow resistance (big size, small aggregate length, efficient liquid knockout or scrubbing) and by using low-intake-pressure compressors.

*ad* (b). (i) Wellstreams from flowing wells of high wellhead pressure should be directed into a high-pressure separator; stage separation is recommended. (ii) The tank system should be closed if possible. (iii) Evaporation losses of open storage tanks, and (iv) oil and gas leaks should be kept at a minimum.

*ad* (c). Particularly in manually operated systems and those with local automation, care should be taken to concentrate all the gathering and separation facilities at the well centre and the central gathering station. In remote-controlled systems, designs ensuring the fast supply of meaningful information should be strived at. Information should be supplied both to the men working on the lease and to the remote-control centre.

*ad* (d). (i) The number of separators enabling individual wells to be tested at the well centre should be sufficient to permit measuring the oil, gas and water production of each well at intervals of 4 to 7 days. (ii) The number of common separators handling the wellstreams that are not separately metered should be composed of uniform units for each stage. The number of separators required is then determined by unit capacity. (iii) In on-lease gas metering, the accuracy of $\pm(1-2)$ percent of the orifice meter is adequate. The quantity of gas fed into a sales line or a transmission pipeline should be determined more accurately, if possible. (iv) If the liquid output is measured in the storage tanks at the well centres, then the number of so-called test tanks metering the liquid production of individual wells should agree with the number of test separators. Common tanks metering the production of the remaining wells should number at least two per centre. (v) For accounting within the lease it is usually sufficient to meter liquid at an accuracy of about 0·5 percent. It is desirable to meter oil delivered outside the lease at an accuracy of at least 0·2 percent.

*ad* (e). Optimum storage-tank volume may differ widely depending on the nature of the gathering, separation and transmission facilities. It is recommended in the usual case to have storage capacity for two-three days' production.

*ad* (f). Well centres are to be designed so that bringing wells in or off, and changing separator, tank or metering capacities might be achieved without affecting the equipment in operation. All the equipment and fittings of well centres within a lease

should be uniformed; fittings should be transportable to the well centre ready for installation, and it should be possible to install them without welding.

*ad* (g). (i) The mechanical production equipment of wells should be chosen, and phased during the productive life of the wells, so as to minimize specific production cost over the entire life of the lease. (ii) Gas from wells having a high wellhead pressure should be led at the lowest possible pressure loss into the compressor station. One and possibly two compressor stages may thus be saved temporarily. (iii) The number and location of well centres, as well as the location of the central gathering station, should be chosen so as to minimize total cost. (iv) Temporary piping should be joined by couplings. (v) Well-testing centres, usually hand-operated early in the life of the lease, should be devised so as to require the least possible modification when converting to automation. It is usually preferable to install an LACT (Lease Automatic Custody Transfer) system rather than a central gathering station early in lease life.

### 6.7.2. Hand-operated well-testing centres

When choosing the most suitable well centre design, several types may enter into consideration depending (i) on the nature of the wellstream to be handled, (ii) on the role to be assigned to the central gathering station, (iii) on the climatic conditions at the selected location. *Figure 6.7–3(a)* shows a type of tank station or well centre suitable for the handling of low-viscosity gaseous crudes containing no sand. Oil and gas separated from the crude are conveyed through flow lines *1* and fill lines *2* into test separators *3* or production separator *4*. Oil flows through line *5* into

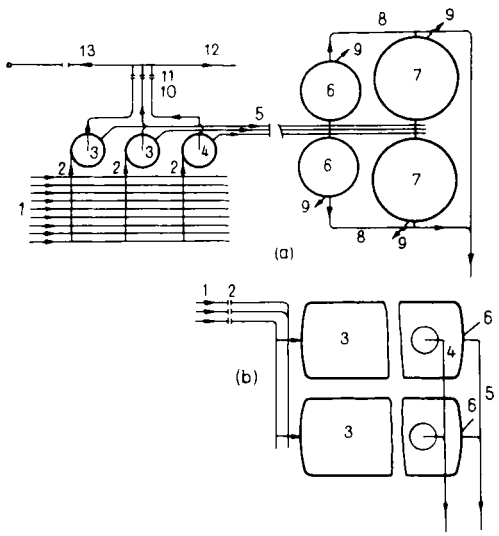


Fig. 6.7–3. Well centre for handling low-viscosity gaseous sand-free crude

metering tanks *6* or storage tanks *7*, which may be drained through lines *8*. Lines *9* serve for water drain. Tanks are upright cylindrical, so-called open sheet steel tanks. Separators discharge gas through lines *10* and orifice meter run *11* into gas gathering line *12*. Gas may also be vented or flared through line *13*. *Figure 6.7 – 3(b)* shows a schematic diagram of a 'closed' tank station or well centre. The separator-side layout is the same as above. Liquid discharged from the separators flows through lines *1* and orifice liquid meter run *2* into horizontal cylindrical closed tanks *3*. Hydrocarbon vapours enter through line *4* into the gas gathering line. Tank outlets are *4* for gas, *5* for oil and *6* for water.

Well fluid entering the separator is often heated in order to promote easier separation of gas and water and to prevent the formation of gas hydrate plugs in the separators and at the meters. Heating is by hot water or steam through a heat exchanger.

*Figure 6.7 – 4* is a detail of a well centre upstream of the tanks, used for the handling of low-viscosity sandless crudes, with two-stage separation and the evaporation loss to be expected in the open tanks reduced by vacuum stabilization (Scott 1965). The wellstreams enter the well centre through flowlines *1*. One wellstream is introduced into second-stage test separator *2*, of about 70 kN/m$^2$

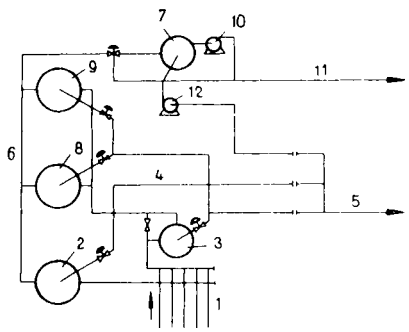


Fig. 6.7 – 4. Vacuum stabilization at well centre, after Scott (1965)

pressure, whereas the remaining wellstreams enter production separator *3*. Test separator *2* discharges gas through line *4* into the gas gathering line *5*, and liquid through line *6* into stabilizer *7*, which is under a vacuum of about 4 kN/m$^2$. The first-stage separator *3* discharges the common liquid production into second-stage separators *8* and *9*. These discharge oil into the stabilizer, and gas into line *5*. Gas separating in the stabilizer is fed by compressor *12* at the required pressure into gas line *5*. Pump *10* transports oil at an excess pressure of about 70 kN/m$^2$ through line *11* into the storage tank. Gas takeoff from the stabilizer column is continuous, whereas oil offtake is batchwise, because pump *10* (in a manner not shown in the Figure) circulates oil in the stabilizer until the liquid level in the vessel attains a predetermined height. Reflux is then stopped and discharge into line *11* is initiated.

This goes on until the liquid level drops to a predetermined height. The economy of this installation is revealed by the fact that, in the case discussed by Scott, the stabilizer paid itself out in 160 days. Economy is impaired by higher gas gathering line pressure, as this increases the power cost of gas compression.

In a Soviet type tank station used to handle gaseous, cut and sandy crudes (*Fig. 6.7–5*), wellstreams enter through flowlines *1* and fill lines *2* and *4* into production separator *3* or test separator *5*. Separators discharge liquid through vacuum separator *6* into cone-bottom storage tank *7*. Weighted float *8* at the oil-water

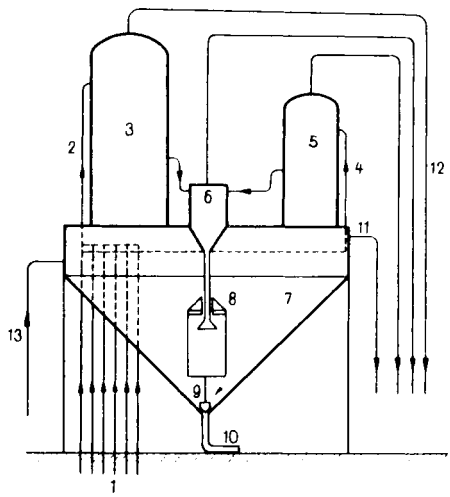


Fig. 6.7–5. Soviet well centre design for handling sandy crude

interface operates valve *9* which serves for the automatic drain of water and sand from the tank through line *10*. Pure oil is discharged through line *11*. Separators *3*, *5* and *6* deliver gas through line *12* and meter runs to the gas gathering line. The settled muddy sand can be slurried up with water introduced through pipe *13*.

The schematic layout of a tank station for handling waxy crudes low in gas and sand is shown as *Fig. 6.7–6*. Wellstreams enter through heated flowlines and distributors *2* into the test and production separators *3* and *4*. Oil is discharged through line *5*, the low gas production through *6*. The water drain is not shown in the Figure. Flowlines are usually heated with steam conveyed in internal or external, coaxial piping. Lines among tanks are conducted in covered concrete ducts sunk into the ground (dashed lines) that can be heated by the piping steam. — This design is suited also for handling high-viscosity oil low in gas and sand, whose pour point is lower than the ambient temperature. Heating the lines in these cases may not always be necessary.

*Figure 6.7–7* shows a gathering and separating system designed by Gidrovostokneft Institute of the USSR and employed in the Soviet Union. This system has

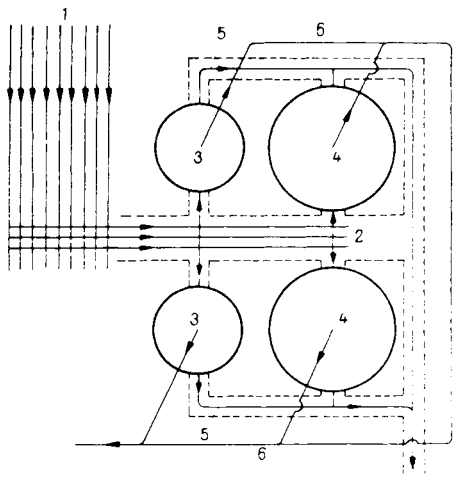


Fig. 6.7 – 6. Well centre for handling low-gas high-viscosity crude

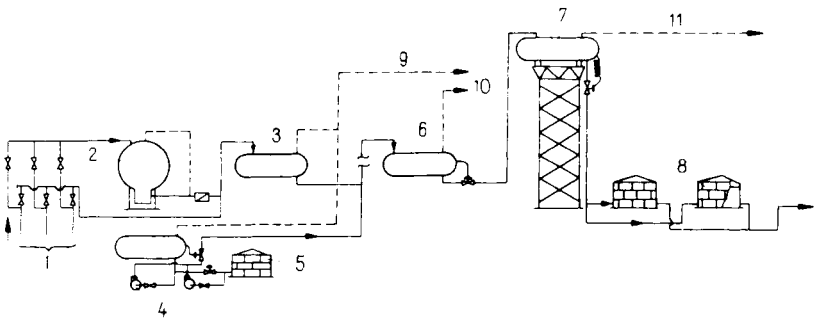


Fig. 6.7 – 7. Gathering and separating system of Gidrovostokneft (VNIIOEHG 1969)

the peculiarity that well centres perform first-stage separation only. The comparatively dry gas furnished by the separators is discharged into a gas gathering line; the liquid, which still contains significant quantities of gas, is conveyed to the central gathering station which is some 100 km away. This is where another two or, if the stock tank is also counted, three stages of separation take place. The main advantage of this system is that is permits centralization of a significant portion of the gathering and separating equipment for production spread over a vast area. In the solution shown in the Figure, flow lines *1* deliver wellstreams through metering units *2* into first-stage separator *3*. In the upper part of the Figure, separator pressure is sufficient to convey the liquid effluent to the faraway second-stage separator *6*. In the lower variant (with metering equipment not shown), pressure of separator *3* is insufficient to deliver the liquid to separator *6*, so that pump *4* and

tank *5* have been added at the well centre. Separator *6* delivers liquid to elevated third-stage separator *7* which in turn discharges into storage tanks *8*. Gas from each separator stage enters the gathering line of the gasoline recovery station through lines *9*, *10* and *11*.

Graf (1957) describes a simplified system in which no gas line emerges from well centres. Only the wellstream of the well being tested is being separated; the gas thus produced is vented or flared. The full output of the producing wells is conveyed by means of a screw pump to the central station. Any further separation and metering takes place at that station.

### 6.7.3. The automated system

Oilfield automation is a process that started a long time ago. The elementary tasks of oil production, gathering and separation have been handled for many a decade by equipment demanding no human intervention (liquid level controls in separators; gas pressure regulators, etc.). Early in the nineteen-fifties, a new wave of automation brought about the relatively rapid development of an automatic system termed LACT (Lease Automatic Custody Transfer), taking care of central oil gathering, treatment, metering and transmission (Resen 1957), as well as the development of automatic well testers (Saye 1958). The devices composing these systems were at first controlled by local automatisms, but connected systems were soon developed where metering results and the main situation parameters of peripheral units could be read off and recorded at a central control station. Even this system permitted substantial savings to be achieved. According to Wiess (*Oil and Gas Journal* 1964) the Gulf Coast Division of Sun Oil Company introduced centralized automation at this level on 19 leases, some of which were offshore. Some of the leases were already in production at the time, while the rest awaited development. The total cost of staggered automation was estimated at USA $ 500,000. This expenditure was balanced by three factors: (i) savings on investment (as against conventional equipment), (ii) increased sales income, and (iii) reduction of maintenance cost (*Table 6.7 – 1*). The Table shows that the increased income and the reduced maintenance cost together totalled USA $ 375,000 per year. Adding to this the difference in annual depreciation attributable to the reduction in investment cost we see that the investment of $ 500,00 paid itself out in slightly more than one year. By the late sixties, LACT had become so widespread that 60 – 70 percent of oil produced in the USA was treated and transferred to transport lines by this method. This phase of automation was followed early in the sixties by a second wave, represented by Computer Production Control (CPC).

The central computer acquires, records and processes all production, situation and safety data concerning the lease. In this off-line system, it is the dispatcher who, in the possession of the information presented by the computer, will intervene if necessary. Intervention will usually be by push-button-actuated remote control. As a stage of further development, on-line computer control was developed, where even intervention by remote control is initiated by the computer. Late in the sixties, after

Table 6.7 – 1. Savings due to automation of an oilfield

| Reduction in first cost | 1000 $ | % |
|---|---|---|
| Tanks | 303 | 50 |
| Piping and fittings | 36 | 6 |
| Other surface equipment | 137 | 23 |
| Offshore platform | 128 | 21 |
| Total | 604 | 100 |
| Annual increase in sales income | | |
| Reduction of oil gravity | 51 | 41 |
| More efficient use of equipment | 41 | 33 |
| Sale of tank vapours | 19 | 15 |
| Saving in gas power | 13 | 11 |
| Total | 124 | 100 |
| Annual reduction in maintenance cost | | |
| Payroll | 177 | 71 |
| Maintenance items | 48 | 19 |
| Transportation | 16 | 6 |
| Miscellaneous | 10 | 4 |
| Total | 251 | 100 |

the advent of third-generation computers employing integrated circuits, there were as many as 40 CPC systems operative on the various oil and gas fields of the world (Graf 1970). Production control by computer is considered a highly significant advance, "the biggest thing since rotary drilling in hydrocarbon production" (Pearson 1969). Its main advantages are reduced operating costs, reduced production downtime due to operating trouble, a more elastic and versatile optimization of production, and faster intervention in critical situations. All tasks that can be uniquely defined in the possession of all relevant information, and can be performed by the intermediary of remote-control-effectors, are set to CPC. This liberates most of the lease operators for tasks inaccessible to CPC; e.g. the operator opening and closing wellhead valves or handling scraping operations, or the gauger gauging liquid levels in tanks will become redundant, but the tasks of mechanics performing repairs and maintenance on production equipment will become more sophisticated and possibly more rewarding. No clerks recording production data and writing periodic reports will be required, but production experts and systems analysts analyzing the production processes recorded and giving instructions for new production targets will. Automatic operation will become much more flexible under the direction of computer programs than of local automatisms, as programs permit flexible adaptation to changes in requirements facing production without changing peripheral units. The Humble Oil and Refining Co. possesses, for instance,

500 process-control programs that are routinely used in all production units (Scott and Crosby 1970). Reduction of production downtime by fast intervention and more efficient trouble prevention may increase oilfield production by several percent (Harrison 1970). In the last decade, several descriptions of oil fields operated by CPC have been published. It appears from these that the system will prove economical for both big fields with some thousands of producing wells and smaller operators. A special analysis of where to employ automation, to what extent, and what degree of centralization to aim at is, however, indispensable in any particular case. Reports on automatic oil production control published in 1970 include in addition to the above-cited papers Bleakley 1970a, b; Burrell *et al.* 1970; Michie *et al.* 1970; Cox and Underrinner 1970; Chapin and Woodhall 1970; *World Oil* 1970; Martin 1970.

In the 1970s the CPC system became even more general. On the basis of several years' experience Shell accomplished a system, developed in Louisiana. The scheme of the computerized control system, with its centre in Houston, is shown, after Dunham (1977), in *Fig. 6.7–8*. The main controllers of the system are the field

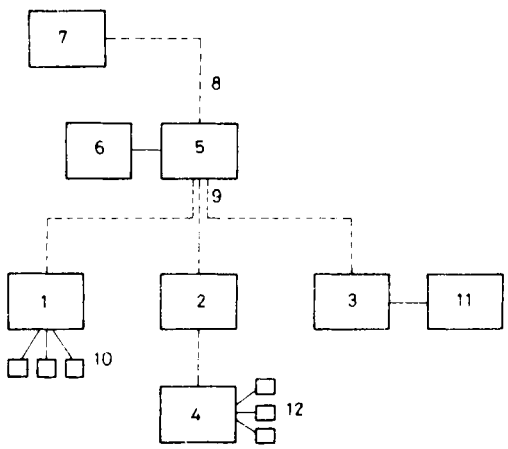


Fig. 6.7–8. Scheme of computerized control system, after Dunham (1977)

computers, *1*, *2*, *3* and *4*. Their tasks are first of all to collect field data, control the operation, and to indicate emergency situations. These computers are in on-line contact with the IBM VM/370 central computer *5*. The most important duty of this central unit is to store and analyze the input data, to prepare comprehensive reports, and to diagnose problems, occurring within the system. Each CPC program is developed in the centre, and they are regularly modified in accordance with the changing conditions and requirements. The complementaries of the central unit are computers *6* and *7*. Among the tasks of unit *6* we can mention the testing of the distributed system, program development, and the maintenance of the table and files. Computers *7*, corporated to the system, and located at a distance of about

16 kms, supply the engineering, accounting, and historical data through a line of 4800 bit/s transport capacity. The distance between the central and field computers may vary within a range of cca. 100 – 2400 km, and the signal transfer capacity of the lines 9 is 2400 bits/s.

Different devices are attached to the field computers. The remote terminals, and the telemetry system are marked by *10*. The satellite computer *11* makes possible the high speed input of data, and individual well control. The input–output station *12*, operated by remote control, and with man–machine terminals makes possible recording and card reading. If the relation between the central, and field computers are interrupted, these latter units are able to work independently. The introduction of the CPC system means, per month, and per well, an excess cost of $ 4 only.

In the following we shall be concerned with the peripheral production equipment of automated leases only. This equipment can be adapted to either human control or local automation or computer process control. The consideration on which this choice of subject is based is as follows. Development of a system of automatic production requires familiarity with three fields of endeavour. The first is oil and gas production. Specialists in this field will formulate production requirements. The second field is automation. Its specialists will supply and develop the hardware required for automatic operation. The third field is systems analysis and software preparation. Software is prepared by mathematicians on the basis of tasks formulated by production specialists, and complemented and updated to adapt it to changing conditions and advances in hardware. In the present book, we restrict discussion to the first field.

Let us point out that, in the first phases of developing (and, indeed, producing) an oilfield, it will rarely be possible to divine the optimal way of exploiting the field. A well-founded prediction of this will not be possible until the development is almost complete and the analysis of at least a shortish period of production has been performed. Specialists designing surface production equipment will have to gear their work to the production plans based on information acquired during these phases. This is when the definitive system may be designed, and the automation system can be chosen and realized. The final, most thoroughly automated system will thus be the product of step-by-step evolution from lesser to greater automation, governed throughout by the obvious aim that production equipment and automation elements once installed might be fitted at the least possible excess cost into the definitive system (Terris 1965).

### (a) Automated well centres

The purpose of an automated well centre is to carry out without direct human intervention the following tasks. (1) Cycling according to plan of intermitting wells. (2) Hookup according to plan of individual wells to the test or production separator. (3) Shutoff of wells in the case of metering or transmission system malfunction. (4) Separation of oil and gas composing the wellstreams. (5) Metering and recording of oil, gas and water production of wells being tested (possibly also of the entire set of

wells hooked up to the production separator), and possibly the reporting of information acquired to a processing centre. (6) Transmission of liquid and gas.

Carrying out tasks (1) – (3) requires a choice of valves and a sutiable hookup that will open or close under instructions from the program control or from malfunction warning equipment. Further required at each well is a flow-line shutoff actuated by pressure changes in the flowline, that will open or close the line, and possibly start up or shut down the installed production equipment.

*Figure 6.7 – 9* shows one of the possible layouts of an automatic tank station (Saye 1958). From flowlines *1*, wellstreams pass through motor valves *2* to be

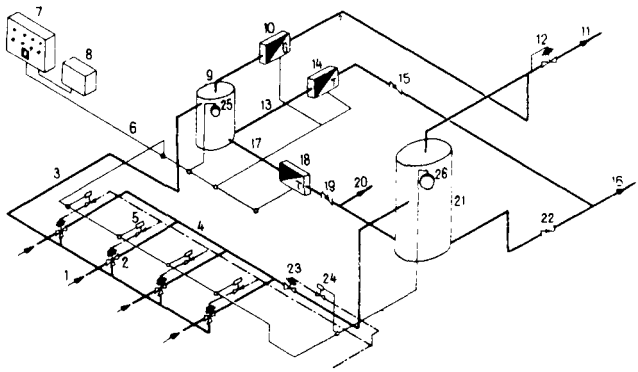


Fig. 6.7 – 9. Automatic well centre, after Saye (1958)

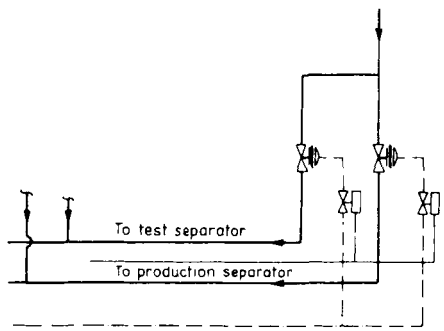


Fig. 6.7 – 10. Hookup of two-way two-position valves, after Saye (1958)

deflected either into line *3* and three-phase test separator *9*, or into line *4* and three-phase production separator *21*.

The diaphragm motor valves actuated by solenoid-operated pilots can be hooked up in different ways. In the design shown as *Fig. 6.7 – 10*, each flowline is branched,

and each branch carries a two-position two-way motor valve actuated by a solenoid-operated pilot. The valves are double seat, that is, pressure-compensated, and normal-closed as a rule. This design is used in connection with high-pressure wells, where opening and closing a non-compensated valve would require too much power. *Figure 6.7 – 11* illustrates the hookup of three-way, two-position motor

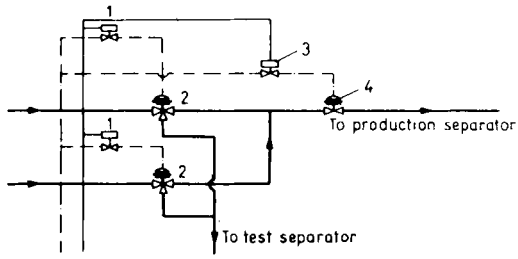


Fig. 6.7 – 11. Hookup of three-way two-position valves, after Saye (1958)

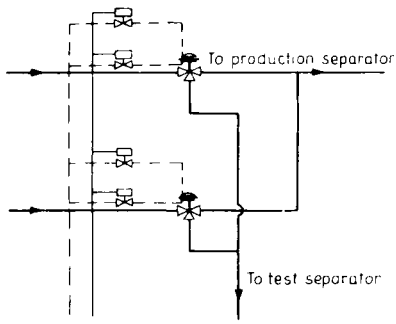


Fig. 6.7. – 12. Hookup of three-way three-position valves, after Saye (1958)

valves. The closing of pilot *1* opens motor valve *2* and directs the wellstream into the production separator. If the pilot feeds supply gas over the diaphragm of the motor valve, the wellstream is deflected towards the test separator. In this design, primarily suitable for comparatively low-pressure wellstreams, wells cannot be shut in one by one. In the case of system malfunction, all pilots close and all wellstreams are directed into the production separator. The inlet of this latter will automatically be closed by pilot *3* and motor valve *4*. *Figure 6.7 – 12* shows the hookup of three-way three-position valves. Deflection from the test into the production separator and conversely is controlled in each flowline by two solenoid-operated pilot valves feeding power gas above or below the motor valve diaphragms. If both pilots are closed, the motor valve will shut the well.

*Wellhead shut-in.* If the maximum allowable operating pressure of the flowline is higher than the pressure in the shut-in well, then opening and shutting in the well

can be performed at the tank station. In flowlines of low pressure rating, excessive pressure buildup can be forestalled by installing an electrical remote-control-valve at the wellhead. This solution is fairly costly, however, especially if the distances involved are great. It is more to the point to install on the wellhead a valve that will shut in the well if pressure passes an upper or lower (line rupture!) limit (cf. *Fig. 2.3 – 26* in Vol. A). In flowing and gas-lift wells, the safety device may be a pneumatically controlled motor valve, whereas in pumped wells pressure switches are employed. The pressure switch will cut the power supply to the prime mover (or cut the ignition circuit, if the prime mover is an internal-combustion engine) if pressure is too high or too low. Moreover, the pressure switch may control the opening or closing of a pneumatically or electrically operated wellhead shut-in valve.

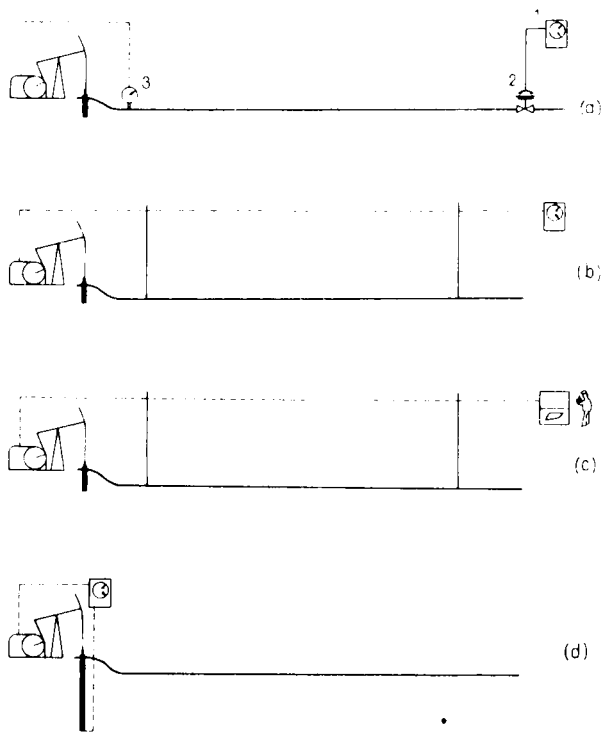


Fig. 6.7 – 13. Options of automating sucker-rod pumping

*Figure 6.7 – 13* shows as an example four ways of controlling the intermittent production of a well by sucker-rod pump. In (a), a centrally installed clockwork-type cycle controller *1* opens and closes valve *2*, likewise installed at the well centre. Whenever flowline pressure exceeds a certain limit, a pressure switch installed next to the well cuts out the prime mover. In (b), the centrally installed cycle controller

clockwork starts the prime mover by electric remote control. In (c), starting and stopping is initiated by an operator, who can also check pump operation by a dynamometer diagram transmitted to him on his call (this is a solution widespread in the Soviet Union). In (d), the pump is started by a clockwork cycle controller installed next to the well and stopped by a *BHP* sensing device. Setup (d) has the advantage that the duty cycle of the pump is controlled solely by the quantity of

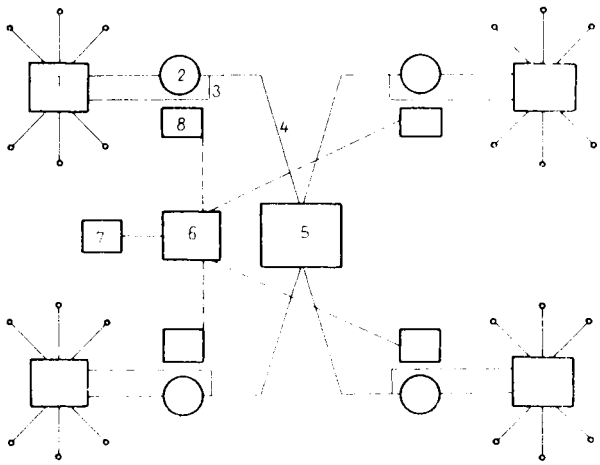


Fig. 6.7 – 14. Gathering system, after Saye (1958)

fluid accumulated in the well; also, the sensor, easy to install next to the well, will permit the recording of *BHP* and its changes, and hence supply the most relevant information concerning the correct adjustment of operation.

In the automatic tank station shown schematically as *Fig. 6.7 – 9*, the effluents of test separator *9* are metered by gas meter *10*, oil meter *14* and water meter *18*. Gas and oil discharged by production separator *21* are metered at the central station only. Pressure switches *25* and *26* send signals to process control *7* whenever separator pressures exceed a certain limit. If this happens in the test separator, then the control automatically reroutes the wellstream of the tested well into the production separator. If overpressure occurs in the production separator, then inflow is shut off by pilot *24* and motor valve *23*. This entails a pressure rise in the flowlines, as a result of which wellhead valves will shut in wells automatically (if flowlines are low-pressure-rated) and stop the prime movers of pumping units.

*Figure 6.7 – 14* illustrates a gathering system including one central metering and transmission station and four tank stations (Saye 1958). Production lines *3* bypassing metering equipment *2* at well centre *1* discharge all oil into gathering line *4* that delivers it to central station *5*. Central control *6* through substations *8* performs the cycling according to program of all wells and their alternative hookup to the test or production separator. Substations report metering results and other

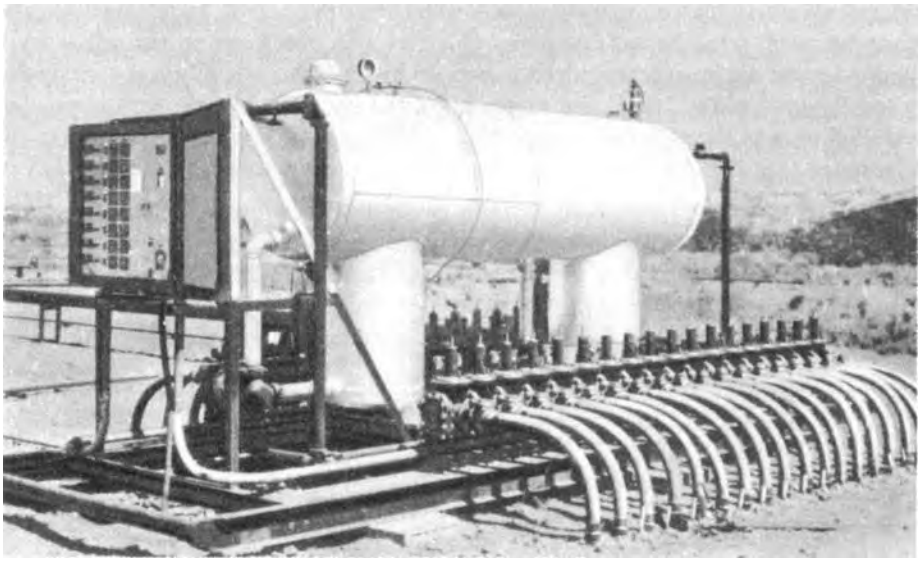

Fig. 6.7 – 15. Portable well tester of National Tank Co.

data to central recording facility 7. Oil metering by instrument usually obviates the need for the conventional tank batteries of well centres.

The dominant aim nowadays is for automatic well testers to be factory-made skid-mounted portable units whose installation should require just the time for connecting up the flowlines of wells and the oil, gas and water outlets, rather than 'do-it-yourself' facilities built in weeks and possibly months by the pipe-fitter gang on the lease. Portable well centres can be expanded by any number of new units as and when the increasing number of producing wells requires. Today's well testers may need no more horizontal space than a few $m^2$. *Figure 6.7 – 15* shows as an example the National Tank Co.'s portable automatic multi-well test unit.

**(b) Automatic custody transfer**

The prime purpose of a central gathering station in an oilfield is to separate most of the water, if any, from the crude flowing in from the well centres, to meter at a high accuracy the separated oil whose water content should not exceed a few tenths of a percent, and to deliver it to the inlet manifold of the transmission-line driver pump, or possibly into the storage tank of the pipeline 'in' pump. In certain cases, the crude is also stabilized at the central gathering station. Up to the mid-fifties, central gathering stations were conspicuous by a number of large tanks serving to store crude prior to transmission, and to gauge it by one of the procedures outlined in Section 6.6.1. A modern tank station of those times resembled *Fig. 6.5 – 13*.

Automatic gauging and transmission of crudes by the LACT system was first realized in 1954. As a result of this revolutionary step ahead, 60 – 70 percent of the crude produced in the USA was metered and transmitted by this means in 1960

(Scott 1967). In an LACT set-up, the watery crude enters through a dehydrator into the storage tank for pure oil. When the tank is filled to a certain level, and the transmission equipment is ready to receive oil, the crude stored in the tank is automatically transferred to the transmission equipment. After discharge from the tank, the BS&W (basic sediment and water) content of the crude is measured. If this is below the limit contracted for, then the oil is continuously metered into the receiving equipment of the transmission line. If BS&W exceeds the limit contracted for, then the crude is redirected from the storage tank into the dehydrator. In the first phases of evolution of LACT, some of the old tanks were retained and used as metering tanks. Crude was permitted to rise to a certain high level, after which it was pumped out until it sank to a certain low level. The tank volume between the two levels was accurately calibrated. The actual crude volume thus determined had to be corrected for water content and reduced to the standard state. In order to do so, it was necessary to establish the mean temperature of liquid in the tank, its actual gravity and its water content on outflow. The first LACT equipment built to perform all these tasks was installed by Gulf Oil Co. in 1954 (*Oil and Gas Journal* 1956). — Weir-type LACT equipment has the advantage that it can be installed in existing tanks that used to be controlled and gauged by hand; its correct operation can be checked at any time by manual gauging; also, the accuracy of measurement is not impaired by the presence of gas. Its disadvantage is that accurate metering depends on the correct functioning of a number of valves and floats; crude retention time may be long; paraffin deposits on the tank wall, and sediment settling out on the tank bottom, will reduce metering accuracy; liquid temperatures in the tank have to be established prior to every draining, and actual oil volumes have to be reduced to standard state by calculation; the system is open, so that significant evaporation losses may arise.

Today's LACT equipment is the result of fast, efficient evolution. The essential difference from early types is that oil is metered by positive-displacement meters rather than by draining known tank volumes, and meters will directly indicate or print out oil volumes reduced to standard state. *Figure 6.7 – 16* shows the layout of such a LACT system after Resen (1957). Crude arriving through line *1* from the automatic well tester is fed to dehydrator-demulsifiers. Pure crude is transferred from there into stock tank *3*. If level in *3* attains float $L_2$, valve $V_3$ opens and crude can pass through BS&W monitor *5* to valve $V_2$. If water content exceeds the limit contracted for, valve $V_2$ returns the oil into the demulsifier. If purity is satisfactory, supplementary transfer pump *7* is started; it will deliver oil sucked through strainer *6* into gas eliminator *8* and through it into the suction line of the main pump *13*. Oil is metered by positive-displacement meter *9* which, correcting the result for flow temperature, either shows on a dial the metered oil volume reduced to the steady state or transmits it to the control-centre. Sampler *10* automatically samples the outflowing oil, thus permitting to check BS&W content at intervals in the laboratory. Instead of the sampler, a BS&W check instrument may also be installed downstream of the positive-displacement meter. Bypass *11* (the calibration loop) that can be cut off by means of valves $V_4$ and $V_6$ can be replaced by a positive-

displacement meter prover in series with meter 9. This latter can be calibrated also by means of prover tank *14*; *4* is a safety-reserve tank whose presence is optional. The high accuracy (not less than 0·1 percent) of the system is due to the following circumstances. (i) Pressure regulator valve *12* ensures constant pressure downstream of the meter; the pump delivers at a nearly constant rate, and thus the leakage error of the positive-displacement meter may be kept at a minimum (cf. Section 6.6.3 – (c)). (ii) Strainer *6* removes solid impurities still present in the oil, thus preventing wear and malfunction of the meter. (iii) Oil pressure is raised slightly above stock-

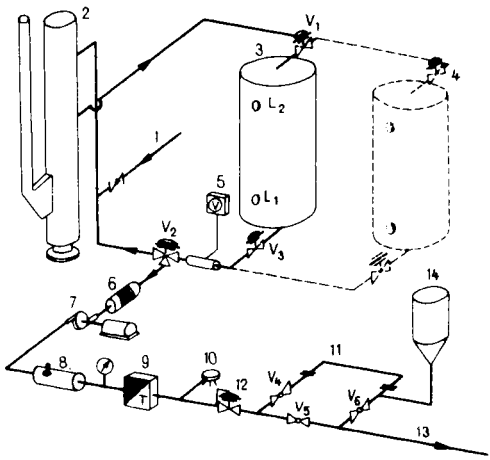


Fig. 6.7 – 16. Automatic central oil handling station with positive-displacement meter, after Resen (1957)

tank pressure by the transfer pump, and the oil may thus dissolve gas bubbles still present in it, if any. Degassing is facilitated also by gas eliminator *8*.

A schematic diagram of the strainer is shown as *Fig. 6.7 – 17*. The wire screen retains solid impurities. These are either sand grains produced together with the oil, or small, often sharp grains of tramp iron and metal that fall into the oil during its treatment. The schematic design of the gas eliminator is shown in *Fig. 6.7 – 18*. In this unit, the flow velocity of the crude drops to a value slightly lower than the critical rise velocity of gas bubbles, so that these may break out and accumulate in the dome of the vessel, depressing the oil level. When the float has sunk far enough, it permits the gas to escape into the atmosphere.

LACT systems with positive-displacement metering have the advantage over weir systems that they may be used in connection with closed, horizontal tanks, which permits to avoid evaporation losses. Another substantial advantage is that all equipment downstream of the stock tank can be portable, skid-mounted, permitting fast installation where required.

*Figure 6.7 – 19* is a diagram of one of the Jones and Laughlin S. D.'s portable LACT units. Once oil in the preparation tank has attained a certain high level,

switch *26* trips on and starts through switchgear *2* the electric motor driving pump *1*. When oil pressure has risen high enough, valve *11* opens and discharges oil into the pipeline. In its journey from the pump to the pipeline, the crude passes through strainer *3*, gas eliminator *4*, BS&W monitor *5*, three-way valve 7, meters *25* and *8*, valve *11*, and valve *12* closing off the calibration loop. If BS&W monitor *5* indicates on control panel *6* that BS&W surpasses the allowable maximum, then valve *7* diverts oil flow towards a treater. During discharge into the pipeline, electrical sampler *9* removes a small quantity of liquid and fills it into pressure-proof vessel *10*. The sample is agitated at intervals by means of manual mixer *10B*. Quantities for

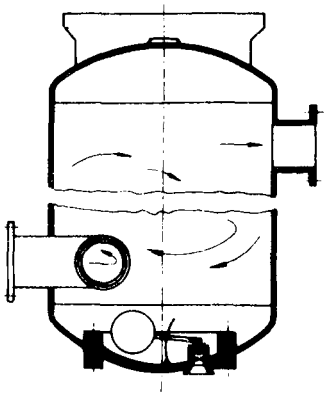

Fig. 6.7 – 17. Oil screen (Petroleum . . . *Oil* 1955)

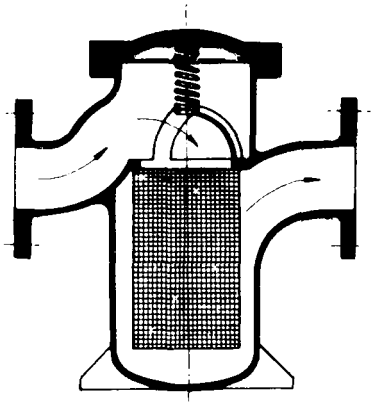

Fig. 6.7 – 18. Gas extractor (Petroleum . . . *Oil* 1955)

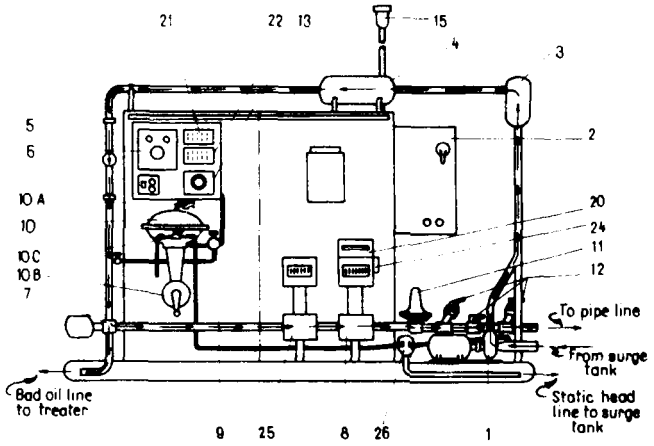


Fig. 6.7 – 19. Jones and Laughlin portable LACT equipment

laboratory analysis may be drained through four-way valve *10C*. The rest of the sample is discharged, by suitably turning valve *10C*, from tank *10* into the delivery pump, where it joins the main liquid stream. The unit is provided with auxiliary equipment that will shut off oil flow in the case of malfunctions, if the oil stream passing through the unit deviates from prescriptions, or if the daily or monthly limit of oil to be delivered has been attained. Transfer capacity of these portable units is 32 – 1300 $m^3$/d; their weight is 4·2 – 21 kN.

If the central LACT station receives crude from several leases, each sort of crude is fed to a separate LACT unit. Some units, however, are designed so as to be able to handle several inflows. Designing, installing and operation of LACT systems as well as requirements concerning accuracy of measurement and safety are treated in API Std 2502.

### 6.7.4. Design of field integrated oil production systems (FIOPS)*

Any system is the complex of interactive elements. Its determination is always arbitrary since no system exists upon which external forces or other systems do not exercise an impact. These impacts, however, in several cases can be considered as boundary conditions. Even the perception of the cooperation regularities of a relatively small number of elements may be useful. The mathematical modelling of the operation of small systems facilitates the best possible arrangement according to the requirements, and the determination of the optimum operating parameters of the so created complex, respectively. Unifying the smaller systems results in a new, larger, generally more complex system. The common operation of the original subsystems can produce new possibilities for a higher level optimization. This system enlarging procedure is synergistic if the economic gain obtained by the optimization of the enlarged system is greater than the sum of the gains of the subsystems optimized separately (Szilas 1980). For the time being the literature discusses only relatively smaller systems of oil producing equipment. A system like this may consist of the reservoir in the drainage area of *one* well, *one* producing well, the flowline and separator and their chokes, these elements making up the *production path*, or "*production spoke*". Its modelling for gasless oil is discussed in Section 2.2, while for gassy oil it is treated in Section 2.3. The Petroleum Engineering Department of the Miskolc Technical University for Heavy Industry studies the laws of a production system the main elements of which are hydrocarbon-bearing reservoirs, the total number of the wells, and the gathering, treating and transporting equipment on the surface. In order to simulate this production system the solution of the partial problems, discussed below, is necessary.

**(a) The design and location of optimum well producing systems**

(i) The producing rate, composition, and pressure of the fluid inflow from the reservoir into the well is changing with time. For a time the production from a well is going on by self flowing. Later on, the production rate, prescribed by the reservoir engineering project, can be usually achieved by artificial lifting equipment. Both the end of the flowing period, and the technically proper lift method that ensures the

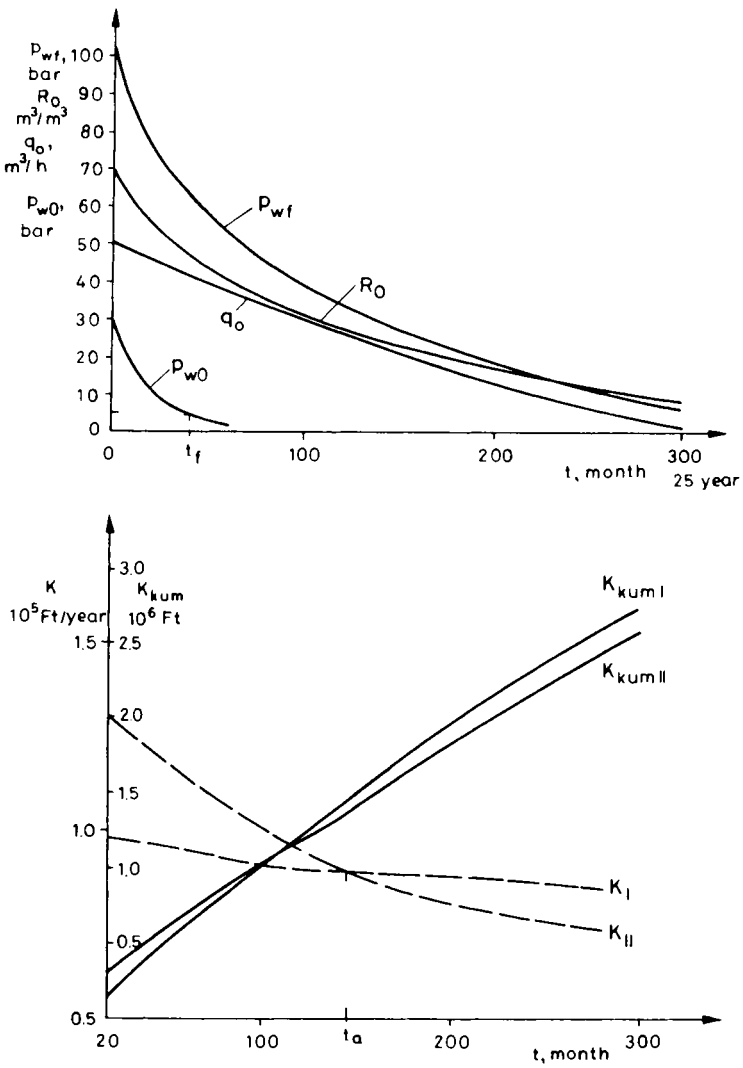


Fig. 6.7–20. Production and economic characteristics of a key-well (Szilas 1983)

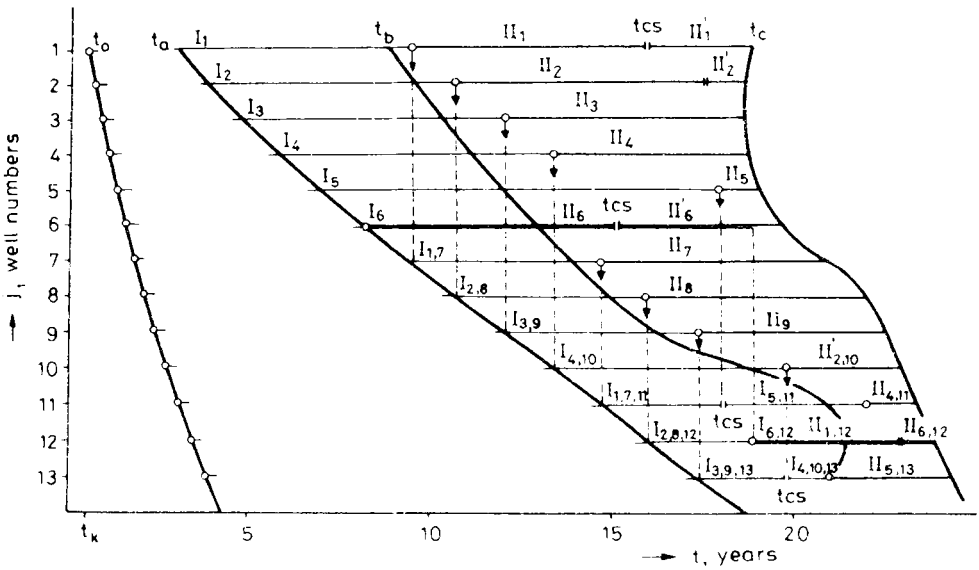


Fig. 6.7–21. Scheduling of production equipments (Szilas 1983)

most economical production in the total remaining production life, or in a given period, must be determined well by well. Such relations and computer programs have been developed by the Petroleum Engineering Department of the Miskolc Technical University for Heavy Industry. With the help of these relations and programs, on the basis of the reservoir engineering project, from well to well, and year by year, the specification of the technically suitable lifting method can be determined, including its operating point with the minimum operational cost, and also its value related to the production start timepoint. *Figure 6.7–20*, in the upper half of the diagram, shows the expected values of the characteristics valid for one well (key well) in the course of the production life on the basis of the reservoir engineering project, where $q_o$ is the liquid production rate, $R$ the gas oil ratio, and $p_{wO}$ the wellhead pressure and $p_{wf}$ the flowing bottom hole pressure. On the basis of the above data the lower section of the diagramme indicates that how the initial discounted production cost changes in case of optimally designed rod pumping (I), and in case of continuous gas lifting (II). Curves $K_{\text{kum I}}$ and $K_{\text{kum II}}$ show the cumulated production costs. It is also shown that before time $t_a$ rod pumping, while after it gas lifting is the more economical. The total cost for the whole production life in case of rod pumping is smaller by $\Delta K$ than it is in case of continuous gas lifting.

(ii) Considering the succession of the starting of the artificial lifting in the individual wells and also their production life, the location project must be designed. *Fig. 6.7–21* shows a project prepared for a small field, operating 13 wells, as an example (Szilas 1979). It is supposed that during the period of artificial production two types of lifting methods are applied, i.e. the method of rod pumping and

continuous gas lifting. $t_0$ line connects the moments of the beginning of the production of the wells, while $t_a$ connects the moments of ceasing of the flowing production. From this moment on up to $t_b$ production method I (rod pumping), and then method II (gas lifting) is the more economic. The numbers, given in the line of the single wells, tell us on which well, and when new production units must be mounted, or where they must be re-mounted if the production becomes unprofitable. Similar projects, developed for key wells should not be considered as rigid specifications, but only as estimations, since the details will be altered in the practice. This method helps us to determine that for the planned production of the wells when, what type and size and how many production units are necessary; what well service capacity must be turned for the installation; and how large is the expectable production cost. The application of the method shows that even in case of an oil field of average size (operating 50 – 100 wells) savings in the order of $1 million can be achieved, as compared to traditional practice.

### (b) Location of the units gathering, treating and transporting fluid streams from wells

The most favourable type and parameters of the well centres and central gathering station are those which take into account the rate and quality of the well streams, and the parameters and requirements of the production and utilization must be selected. The most favourable place of the well centres and central gathering station, and, moreover, the most advantageous trace of the flow lines and other transport lines belonging to the station, must be determined. Among the technically feasible solutions generally the versions requiring the lowest investment cost are considered as optimums. The planning method elaborated and programmed for computer by the Petroleum Engineering Department of the Miskolc Technical University for Heavy Industry is based upon dynamic programming (Gergely and Pancze 1982). It takes into consideration the well coordinates determined by the reservoir engineering project, the specifications concerning flow lines and transport lines, the type of the well centres, the terrain conditions of the oil field, the prohibited territories, the crossing of public utilities, and every significant cost components. The principle of optimization is as follows:

The number of the well centres to be set up should be $n_c$, the number of wells linked to the $i^{\text{th}}$ well centre is $n_{w(i)}$, the flowline cost of the $j^{\text{th}}$ well is $K_{f(i,j)}$. The investment cost of the transport line connecting the $i^{\text{th}}$ well centre with the central gathering station is marked with $K_{o(i)}$. The investment cost of other pipelines (gas gathering, water transporting pipes, etc.) should be $K_{e(m)}$ and their number is $n_e$. The component of the investment cost, independent of the number of the wells belonging to the gathering centres is $K_b$, while the cost depending on the number of the wells is $K_{v(i)}$. The investment cost of the surface gathering, treating and transporting devices is thus

$$K = \sum_{i=1}^{n_c} \sum_{j=1}^{n_{w(i)}} K_{f(i,j)} + \sum_{i=1}^{n_c} K_{o(i)} + \sum_{m=1}^{n_e} K_{e(m)} + \sum_{i=1}^{n_c} K_b + K_{v(i)}. \qquad 6.7-1$$

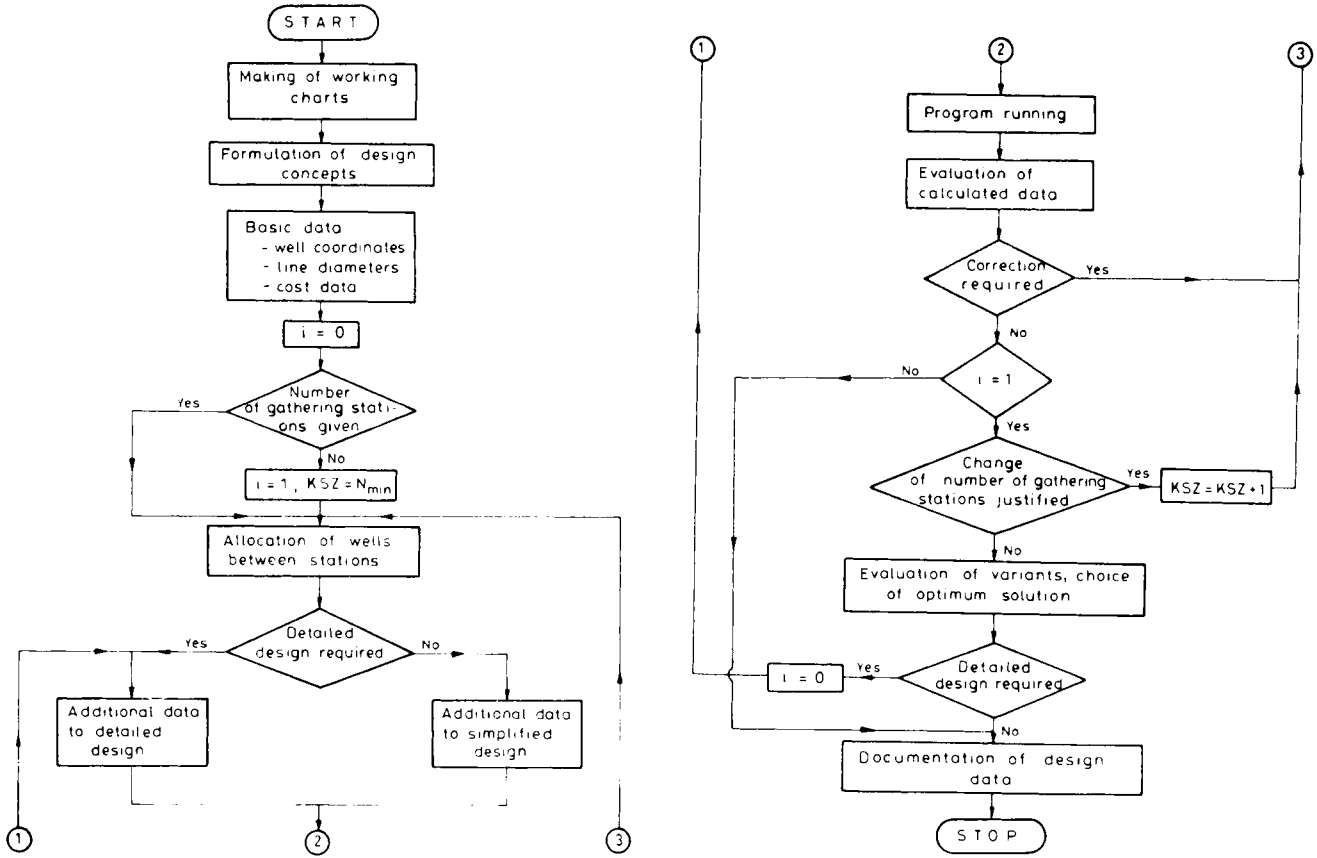


Fig. 6.7 – 22. Flow chart of gathering system planning, after Gergely and Pancze (1982)

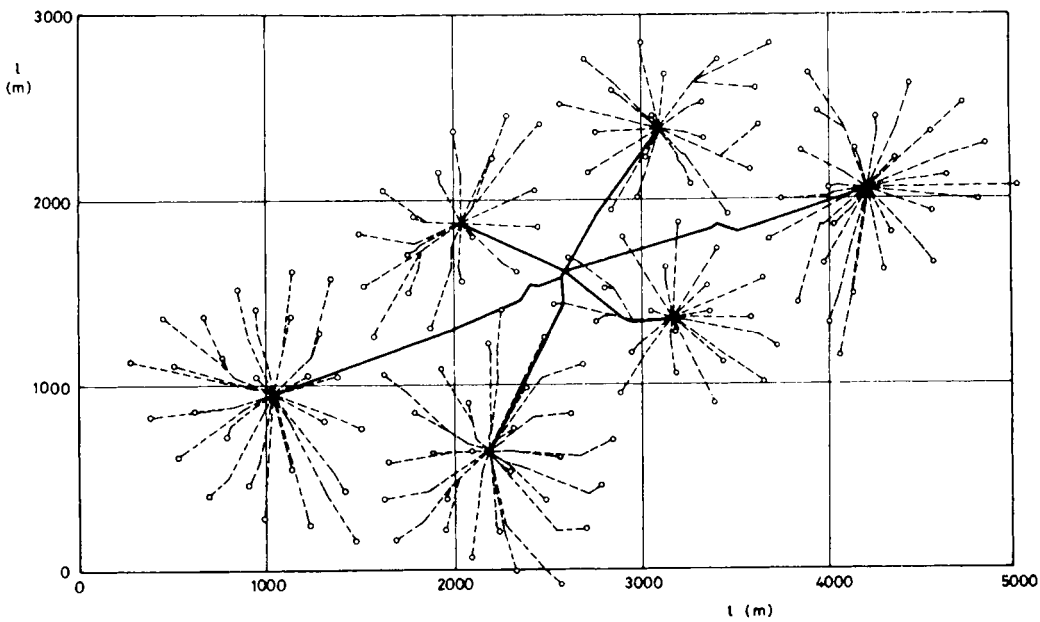


Fig. 6.7 – 23. Well centres and pipe line traces of the optimally located gathering system, after Szilas (1983)

The flow chart of the computation is shown on *Fig. 6.7 – 22.* The traces of the optimum project determined by the above method that considers the coordinates of 143 wells are shown by *Fig. 6.7 – 23.* By applying this design method, in the case examined, about 30 percent of the investment costs could be saved, as compared to the traditional location design procedures.

### (c) The production tetrahedron

From the enumerated production sectors the complete, above specified production system may be constructed. In the knowledge of the characteristics of this system the optimum solution can be found. The basis of the solution is the production tetrahedron shown on *Fig. 6.7 – 24* (Szilas 1983). The sketch shows the steps of principle and the linking of the sectors in the production system based on the reservoir engineering project. Integral parts of the system design are first the determination of the type and sizes of the optimum production units, then that of the gathering system; then the optimum location; and finally the determination of the optimum operating parameters. Interactions are indicated by arrows. Smaller arrows mean a smaller dependence. In order to decrease the number of iterations it is more effective to carry out the design work along the *1 – 2 – 3 – 4* graphs, as it is justified by the "big arrows". Reservoir engineering projects are considered as

independent, singular problems. The optimum system design must be determined for each reservoir engineering project version, and of them the best should be chosen.

The above method can be carried out if in the time of designing a necessary amount of data and information of proper accuracy is available. Obviously, the oil field will be more or less fully known at the end of the production life only. The rate of inaccuracy and insecurity of the information increases moving backwards in time. These realities, however, can be complied with (Szilas 1982a). That is why

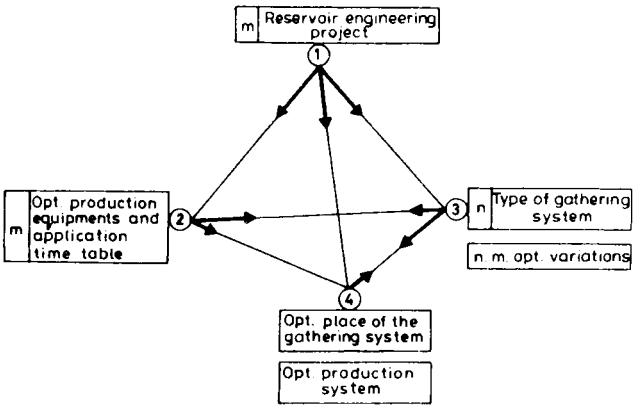


Fig. 6.7 – 24. The production tetrahedron, after Szilas (1983)

(i) the preliminary design must be started in the very first period of the development of the field. Being aware already of the initial information (well depth, well stream quality, productivity, reservoir pressure) several possibilities may be excluded;

(ii) concerning the extension of the field under development the engineer should obtain the possibly most accurate data at the earliest possible time from the geologist;

(iii) in order to facilitate the economical development, expansion or modification of the production system, well centres and oil transfer stations must be applied that are factory assembled, that can be joined by modular system and that, to a great extent, consist of skid mounted units;

(iv) it should not be neglected that the amount and accuracy of the information concerning the field, in the course of the production, increases. Such financial and investment policy should be introduced that, in case of possible further savings, facilitates the modification of the former projects during the production life.

CHAPTER 7

# PIPELINE TRANSPORTATION OF OIL

## 7.1. Pressure waves, waterhammer

Pressure wave may occur in pipelines transporting fluids if the velocity of the flowing liquid suddenly changes. The pressure wave propagates by the sonic velocity from the point of a leak or a device, initiating the change of pressure in both, or perhaps even more connecting pipeline branches. During propagation the wave's amplitude is reduced, damped, and perhaps it is even reflected. The pressure wave may be of positive character when a sudden decrease in the velocity of the flowing fluid may cause a rise in the pressure; and it may be also of negative character when the sudden rise in velocity of the fluid may result in dropping of pressure.

### 7.1.1. The reasons of the waterhammer phenomenon and its mathematical representation

Let us suppose that the pressure wave is analyzed by the epxerimental device represented by the sketch shown in *Fig. 7.1 – 1*. The most important part of this device is the horizontal pipeline, on the one end of which a tank of constant fluid level, $h = p/\rho g$, is mounted, while the other end is equipped with a gate wave. Let a steady flow with rate $q$ occur from the tank through the pipeline and the open gate valve, that gives a flow velocity $v$ in the pipe. Supposing that the viscosity of the fluid is negligible, the pressure line within a Cartesian coordinate system for length v. pressure will be a straight line that is parallel to the abscissa. The liquid is slightly compressible, i.e. this parameter corresponds to the properties of a real fluid. Let us suppose that the gate valve is shut down in an infinitely short period of time, and the development of the pressure wave is analyzed after this action.

The analysis of this phenomenon is facilitated by *Fig. 7.1 – 2* in which eight parts are shown, arranged in three columns and four lines. The two outer columns denote final states, while the column in the middle refers to moments when the pressure from moves at about the halfway of the pipeline. Within each part two diagrams are shown. The upper one represents the flow velocity in the function of the length. The height of the ordinate is proportional to the velocity change $v_o - 0 = \Delta v$. Flow occurs only in the field shaded with horizontal lines. The direction of flow is indicated by arrows. The lower diagram shows the pressure change in the function of length. The ordinate height of the vertically shaded field's territory is equivalent to the values of

$\Delta p$ waterhammer, pressure jump, pressure difference that can be computed from Eq. 7.1 – 1, a height that can be of a positive sign above the central line marking the $p$ tank pressure, or of a negative sign below it. At the moment, matching the "empty" field $(a)-1$, due to the sudden shut down of the gate walve a pressure jump of vertical face develops, the "face height" of which is $+\Delta p$. The front, in the direction marked by the great arrow, propagates towards the tank with acoustic velocity $w$. *Fig. (b) – 1* shows that to the right of the wave front the liquid is already quiet and here its pressure exceeds the hydrostatic pressure of the tank by $\Delta p$, while on the left-hand side the liquid flows toward the closed gate walve. *Fig. (c) – 1* shows that final situation when the pipeline is just filled with quiet liquid of $(p+\Delta p)$ pressure. Due to this excess pressure, from the moment suiting to empty field $(c)-2$, which is the same as for $(c)-1$, flow starts from the pipeline into the tank. *Fig. (b) – 2* shows the position of the front in a $t$ time after the beginning of the outflow. It can be seen that on the left of the front the liquid is flowing towards the tank, its pressure here decreases to the tank pressure. *Figure (a) – 2* shows that final state when in the complete pipe length fluid flows from the shut-down pipe end towards the tank, and

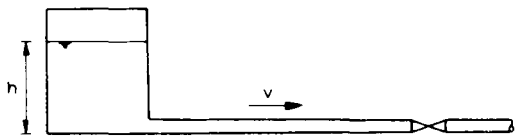


Fig. 7.1 – 1.

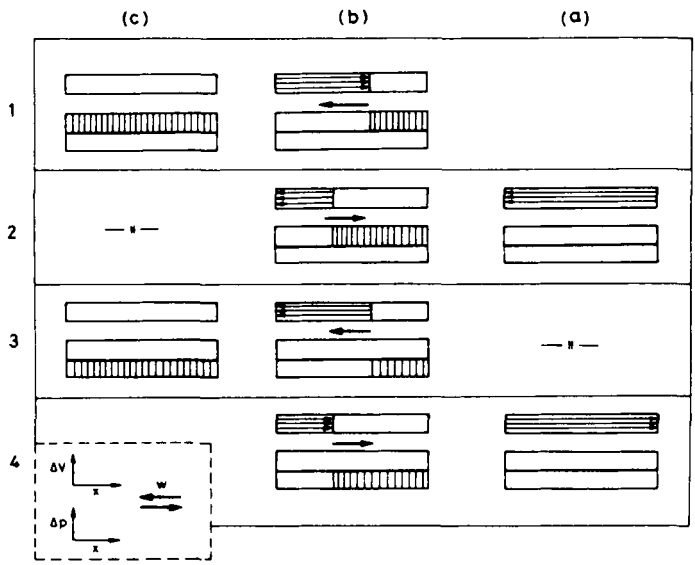


Fig. 7.1 – 2. Characteristic states of pressure wave propagation

the pressure of the liquid column in the pipeline equals $p$. No inflow occurs from the shutdown pipe end and that is why in the situation and moment of $(a)-2$, that is the same as in case of $(a)-3$, flow at the gate valve stops, and due to the impact of "flowing away" the pressure of the fluid decreases by $\Delta p$. *Figure (b) – 3* shows the position of the front after $t$ time. It can be read off that on the right-hand side the flow has already stopped, and its pressure is $(p-\Delta p)$. On the left-hand side the fluid still flows towards the tank, and here its pressure is equal to the pressure of the tank, $p$. In final situation $(c)-3$ the liquid is already in quiet in the total length of the pipeline, and its pressure is smaller than the pressure $p$ of the tank by $\Delta p$. Due to the occurring pressure difference flow starts from the tank towards the gate valve again. The situation after time $t$ is shown by *Fig. (b) – 4*. In this case the fluid, on the left-hand side of the front, flows again in the original direction with tank pressure, while on the right-hand side it is still in a quiet state, and here the pressure is smaller by $\Delta p$. In the end position, shown by *Fig. (a) – 4*, in the total length of the pipeline a fluid of $v$ velocity and $p$ pressure flows toward the shut-down gate valve. The first period of

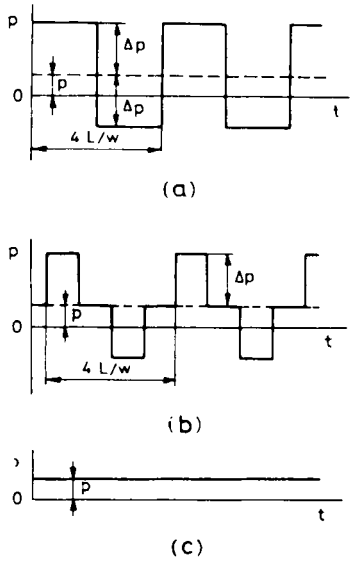


Fig. 7.1 – 3. Change of the pressure in selected points of the system characterized by Fig. 7.1 – 1.

the wave motion is, then, over, and the second period similarly to the first one begins.

Let us examine now how the pressure changes at certain selected points of the tank-pipeline-valve system in the function of time. After Thielen (1972b) on *Fig. 7.1 – 3* the $p-t$ relationship is shown at the closed gate valve (a), at the halfway of pipe-length (b), and at the tank (c). The period of the pressure wave in *Figs (a)* and *(b)* is $4L/w$. $L$ is the distance between the tank and the gate valve. The amplitude of the

pressure wave. $\Delta p$ may be computed from Eq. 7.1 – 1, and this value will not change for $2L/w$ length of time at the gate valve and for $L/w$ at the halfway. At the tank (c), the pressure is the same as the static pressure of the fluid, $p = h\rho g$.

For the calculation of the waterhammer pressure change due to sudden velocity change Allievy and Joukowsky recommended a formula derived from the momentum equation already at the beginning of the 20th century:

$$\Delta p = \rho \cdot w \cdot \Delta v \qquad 7.1 - 1$$

Pressure rise $\Delta p$ is directly proportional to the velocity drop $\Delta v$; the factor of proportionality is the product of the density of the fluid and the acoustic velocity in the fluid-filled pipeline, $\rho \cdot w$.

For several problems being important in practice the above equation does not offer solution. These are mainly as follows: (i) how the pressure changes at different points of the liquid transporting system; (ii) how the pressure change is influenced by the devices that are responsible for the change in the velocity of the fluid (e.g. valves, pumps), (iii) what is the impact of the physical parameters of the real fluids; and, finally (iv) how the configuration and elasticity of the pipeline system influence the

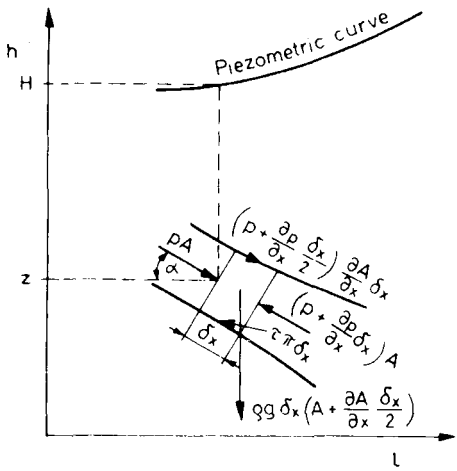


Fig. 7.1 – 4. Forces acting on fluid particle moving in $x$ direction, after Streeter and Wylie (1967)

process. Based on the research results of the past decades these questions can be answered with proper accuracy.

The up-to-date theories, modelling mathematically the pressure waves start from the relations valid for the transient flow of real fluids. A fundamental work, that is to be mentioned here, is published by Streeter and Wylie (1967). Supposing that the fluid flows in a channel of divergent cross-section shown on *Fig. 7.1 – 4*, the flow velocity in a cross-section perpendicular to the flow direction is constant, and due to the pressure change the system is submitted to elastic deformation. The forces acting on a fluid particle which moves in $x$ direction in a divergent channel are the

following: (i) pressure forces acting on the upstream and downstream cross sections and on the inclined faces of the tube, (ii) the $x$-component of the gravity force, (iii) the frictional force acting on the wall against of the motion. From the balance of forces the equation of motion can be obtained as

$$g\frac{\partial H}{\partial x}+\frac{\mathrm{d}v}{\mathrm{d}t}+\frac{\lambda v|v|}{2d}=0. \qquad 7.1-2$$

The equation of continuity can be interpreted with the help of *Fig. 7.1 – 5.* The channel was supposed to be slightly elastic. This hypothesis is valid for pipelines made of metal, cement, or other material where, due to the pressure impact,

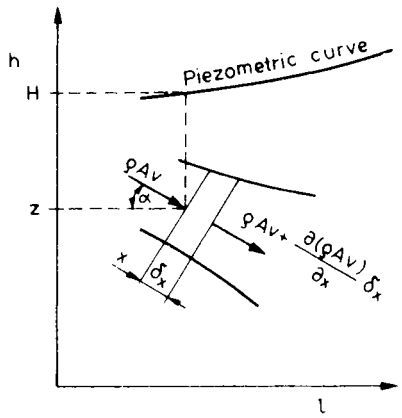


Fig. 7.1 – 5. Fundamental components of continuity equation, after Streeter and Wylie (1967)

relatively small elastic deformation occurs. The difference between the mass rates flowing in and out of the infinitesimal volume represented in the Figure equals the change of liquid mass bounded in the volume element. According to this consideration the basic equation for the continuity, in our case, can be derived as

$$\frac{w^2}{g}\frac{\partial v}{\partial x}+v\left(\frac{\partial H}{\partial x}+\sin\alpha\right)+\frac{\partial H}{\partial t}=0. \qquad 7.1-3$$

For the above cases equation

$$\frac{\partial p}{\partial x}=\rho g\left(\frac{\partial H}{\partial x}-\frac{\partial z}{\partial x}\right)=\rho g\left(\frac{\partial H}{\partial x}+\sin\alpha\right) \qquad 7.1-4$$

is also valid. After Thielen (1971), the propagation velocity of the pressure wave can be calculated by

$$w=\sqrt{\frac{1}{\rho\left(\frac{1}{E}+\frac{d_i}{s}\frac{1-\mu^2}{E_p}\right)}}. \qquad 7.1-5$$

While deriving this equation the pipeline was supposed to be of thin-wall type; the change in length of the underground pipeline was hindered by friction under surface due to the ground; while, at the same time the radial deformation was not influenced by the surrounding soil. Here $E$ is the fluid bulk modulus, $E_p$ is the pipe elastic modulus, $s$ is the pipe-wall thickness, and $\mu$ is the cross-section contractivity. Expression $\frac{d_i}{s}\frac{1-\mu^2}{E_p}$ can be denominated as the compressibility of the pipeline. Thielen (1971) discusses in detail the dependence of the above factors on temperature and pressure, and also offers relations and diagrams that may be used for computation.

From the above basic equations a calculation method may be derived, to numerically model the pressure wave by computer.

The equations of motion and continuity, Eqs 7.1 – 2 and 7.1 – 3 respectively, may be expressed as quasi-linear, hyperbolic, and partial differential equations, the two independent variables of which the pipe-length and time while the dependent variables are the head and velocity, where, in certain cases, the former is substituted by the pressure. By Streeter and Wylie (1967), these equations, by applying the method of characteristics, were transformed into four common differential equations. If the second term of little importance of the continuity equation is neglected, then the four differential equations are as follows:

$$\frac{q}{w}\frac{\mathrm{d}H}{\mathrm{d}t} + \frac{\mathrm{d}v}{\mathrm{d}t} + \frac{\lambda v|v|}{2d_i} = 0 \qquad 7.1-6$$

$$\frac{\mathrm{d}x}{\mathrm{d}t} = w \qquad 7.1-7$$

$$-\frac{q}{w}\frac{\mathrm{d}H}{\mathrm{d}t} + \frac{\mathrm{d}v}{\mathrm{d}t} + \frac{\lambda v|v|}{2d_i} = 0 \qquad 7.1-8$$

$$\frac{\mathrm{d}x}{\mathrm{d}t} = -w\,. \qquad 7.1-9$$

Briefly, the conjugate pairs of Eqs 7.1 – 6 and 7.1 – 7 is marked, as $C^+$ and the pair of Eqs 7.1 – 8 and 7.1 – 9 is called as $C^-$. Since $w$, in case of a given pipeline is constant, in the coordinate system $x$, $t$ Eqs 7.1 – 7 and 7.1 – 9 may be expressed by straight lines. These lines are the so-called characteristic lines of *Fig. 7.1 – 6*, along which Eqs 7.1 – 6 and 7.1 – 8 are valid. Obviously line $C^+$ corresponds to Eqs $C^+$, while line $C^-$ corresponds to Eqs $C^-$. If, then, values of $(v, H, t, x)_{A,B}$ at points $A$ and $B$ are known, then, by applying the four equations at point $P$ the values $(v, H, t, x)_P$ can be computed. For the sake of numerical solution the above relations should be transformed into finite difference equations. A grid of characteristics is now established in order to accomplish an orderly computer solution. A pipe of length $L$ is considered to be made up of $n$ equal reaches, $\Delta x = L/n$. On the basis $\Delta t$ can be determined by any difference equation that corresponds to Eqs 7.1 – 7 and 7.1 – 9.

Thus, by selecting the grid, and so the nodal points these equations are satisfied. Then, by difference equations, corresponding to differential equations 7.1 – 6 and 7.1 – 8, from the initial value, belonging to $A$ and $B$ points, the $v_p$ and $H_p$ values, at the moment $(t_o + \Delta t)$ and at the $\Delta x$ length valid in the midpoint between $A$ and $B$ points can be directly determined (see *Fig. 7.1 – 7*). At the points $i = 0$ and $i = n$, only one characteristic equation is available. It means, that at these points other $v - H$

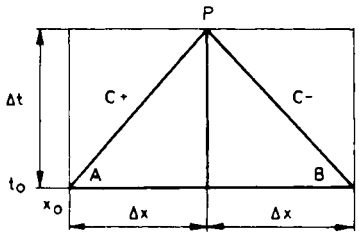


Fig. 7.1 – 6.

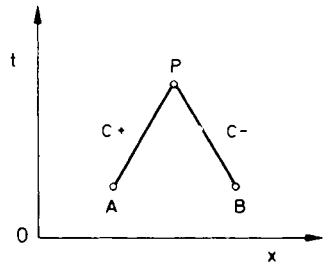


Fig. 7.1 – 7.

relations are needed in order to determine the boundary conditions. These can be edge or joint conditions. In the first case these are given by the $v - H$ parameters of tank or pump at the end of the pipeline. In the second case they are determined by the $v - H$ relation of the pipe-system containing a valve, or branching line.

The above conjugate differential equations can be solved also by applying other methods. Kublanovsky and Muravyeva (1970), e.g., use an implicite method. At the 2nd International Conference on Pressure Surges further new design methods were also discussed (Pipes and ... 1976).

### 7.1.2. Pressure wave in the transport system

In *Fig. 7.1 – 1* the pressure wave propagation was analyzed in a comparatively simple case, when on the one end of the pipeline a tank was mounted and on the other end a valve, and the pressure wave was initiated by the total and sudden stopping of the fluid flow. In reality, the formation of the pressure waves, and the transport system is much more complicated. In the section below, some cases of this sort, that are still relatively simple are treated.

On part (a) of *Fig. 7.1 – 8* as a pipeline is shown in which the velocity of the flowing fluid is decreased from $v_1$ to $v_2$ by the gate valve (Thielen 1972b). Supposing the flow to be frictionless, diagram $b$ and $c$ show the change in pressure, and flow velocity, respectively, in a short time $t$ after the partial closing. Against the flow direction, the pressure, before the gate valve, as compared to the steady state value (dashed line) increases, by a $\Delta p$ difference in pressure, and the wave front, supposed to be vertical spreads in the opposite direction to the flow with the acoustic velocity, $w$. Behind the gate valve the pressure is reduced by $\Delta p$, and this negative pressure wave propagates

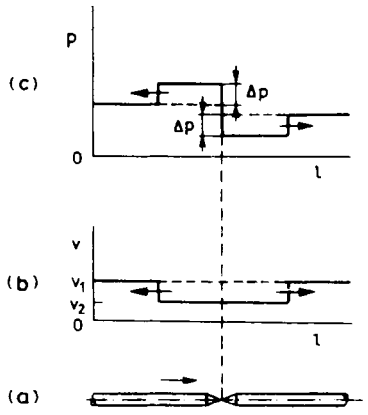


Fig. 7.1 – 8. Change of the pressure and velocity effected by the partial closing of the gate valve, after Thielen (1972b)

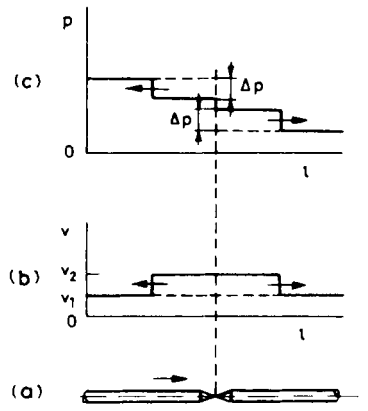


Fig. 7.1 – 9. Change of the pressure and velocity effected by the partial opening of the gate valve, after Thielen (1972b)

with the acoustic velocity in flow direction. From *Fig. (b)* it can be seen that, after the partial closure, the velocity is reduced by the same value in both pipe-sections, and this decrease, together with the wave front, spreads in two opposite directions. *Fig. 7.1 – 9* shows the same characteristics for the case, when a partially opened valve, mounted on the pipeline, is further opened. The positive velocity jump ($v_2 - v_1$), at the two sides of the gate valve, is the same, and, at the same time, at the two sides they propagate towards opposite directions (part *b*). The pressure change, $\Delta p$, upstream the gate valve is of negative, while downstream that is of positive sign (part *c*).

In the pipelines nodes, branches may occur. The waterhammer $\Delta p_{in}$ "inflowing" in any pipe section propagates in each jointed branch, its size however changes and becomes in the tested section $\Delta p_{tr}$. For describing this change Thielen (1972b) recommends the *transmissivity factor:*

$$k_{tr} = \frac{\Delta p_{tr}}{\Delta p_{in}}. \qquad 7.1-10$$

Each node can be considered a source of disturbance from which a certain part of the in-coming waterhammer, $\Delta p_{re}$ is reflected into the very pipe-section from the arrived $\Delta p_{in}$. The reflected pressure change can thus be characterized by the *reflectivity factor* that is determined by the formula

$$k_r = \frac{\Delta p_{re}}{\Delta p_{in}}. \qquad 7.1-11$$

According to Thielen, for multiple branching, the following relation is valid

$$k_{tr} = k_r + 1 \qquad 7.1-12$$

Pressure waves of positive or negative signs may occur at any point of the pipelines where the flow parameters change. Such change can be cuased by the change of inner diameter (perhaps only even by a change in the pipe-wall thickness) or by a change in fluid properties as in the case of slug transportation. The change, occurring at a pump station equipped with control valve, may be of special importance. *Fig. 7.1 – 10*, after Thielen and Bürmann (1973), shows, supposing

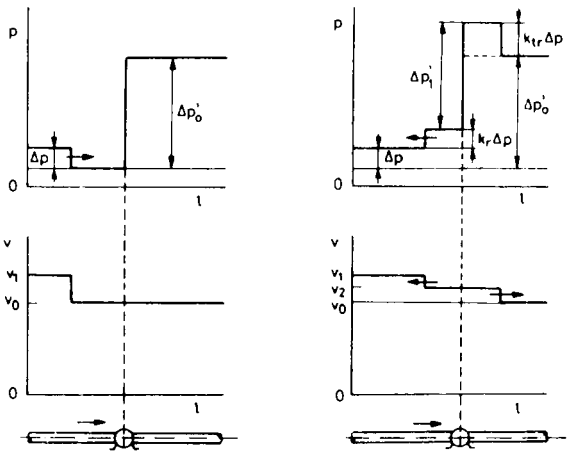


Fig. 7.1 – 10. Change of the pressure and velocity created by the flow through a pump, after Thielen (1972b)

inviscid flow, such change in velocity and pressure. On the left-hand side of the Figure (*a* group) the state is shown, when pressure jump of $\Delta p$ is approaching the pump station but has not reached it yet. Before the change the pump transports liquid of velocity $v_o$, the pressure of which, due to the power exercised by the pump, increases by a value of $\Delta p'_o$. After the arrival of the pressure wave (*b* group) the value of the difference of upstream-, and downstream pump pressures increases to $\Delta p'_1$. The transmitted waterhammer's value is $k_{tr} \cdot \Delta p$ while that of the reflected value is $k_r \cdot \Delta p$. The pressure rise of the inlet side is $(1 + k_r)\Delta p$. Considering that $w$, in Eq. 7.1 – 1, is of positive sign if pressure wave propagation coincides with the direction of the flow, and in contrary cases it is of negative sign, on the basis of the Figure it can be written that

$$\Delta p = \rho w (v_1 - v_o) \qquad 7.1 - 13$$

$$k_r \cdot \Delta p = -\rho w (v_2 - v_1) \qquad 7.1 - 14$$

$$k_{tr} \cdot \Delta p = \rho w (v_2 - v_o) \qquad 7.1 - 15$$

$$k_r + k_{tr} = 1 . \qquad 7.1 - 16$$

It should be noted that the sign of $k_r$ is of opposite character, as compared with the case valid for branching. From these relations it can be derived that the increased pressure difference is

$$\Delta p'_1 = \Delta p'_o - 2\Delta p + 2\rho w(v_2 - v_o). \qquad 7.1-17$$

This relation, together with Eqs 7.1 – 14 and 7.1 – 15 provide the possibility, in case characterized by *Fig. 7.1 – 10*, for computing the transmissivity and reflectivity factors on the basis of the values measured in the course of the pressure change. With proper alteration of the signs this computation method is also valid for negative pressure waves.

In each case discussed so far, the front of the pressure wave was considered to be of vertical face. This hypothesis would only be valid if the closure and opening were carried out within an infinitely short period of time. In reality, however, change takes place always in some finite $t$ period, and thus the face of the wave front is always modified. The generally skew profile can be approximated by several,

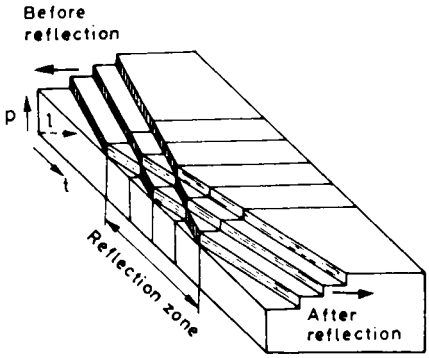


Fig. 7.1 – 11. Approximate determination of the skew pressure profile by vertical wave fronts, after Thielen (1972b)

vertical fronts. Thielen (1972b) shows an example valid for the tank-pipeline-gatevalve system, where the wavefront profile consists of three partial waves of vertical profile *(Fig. 7.1 – 11)*. He supposes that the total closure time of the gate valve is shorter than $t = L/w$, i.e. the time of propagation of the pressure wave from the valve to the tank. It is illustrated that first the lowermost, than the second, and third steps are reflected. The waves inflowing after each other do not modify each other but they are added.

### 7.1.3. Pressure waves in oil pipelines

In up-to-date oil pipelines where oil flows through series connected pipe sections from pump to pump instead of pump to tank, dangerous pressure wave may develop. In case of harmful pressure rise, and depression wave, respectively,

cavitation damaging the pump may occur. The speed of pressure increase of the stopped fluid flow may achieve the value of 10 bar/s; the pressure rise may be as great as 30 bars, and may propagate in the pipeline at a velocity of 1 km/s (Vladimirsky *et al.* 1976). The rate of pressure change may differ from the value that can be computed from relations valid for inviscid fluids. Another difference is that in the course of the propagation the size of the pressure change may be modified. Explanation for this phenomenon is given by Streeter and Wylie (1967). Its essence is as follows.

In *Fig. 7.1 – 12* characteristics described in Section 7.1.1 were supposed. The inviscid flow of the fluid from the tank into the pipeline is stopped within an

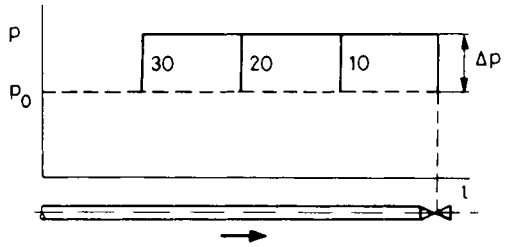


Fig. 7.1 – 12. Simulation I of pressure wave propagation, after Streeter and Wylie (1967)

infinitely short time by sudden closure of the gate valve. The vertical front of the pressure wave is shown at 10, 20 and 30 seconds after the closure. The pressure rise $\Delta p$ developed in this way is added to the original, horizontal pressure line of $p_0$ height, and in the course of propagation from right to left it remains unchanged.

Supposing a real fluid is flowing in horizontal pipeline the pressure line of the steady flow is kew with decreasing height in the direction of the flow. The pressure rise, due to waterhammer, is added to this value. During the propagation of its size, due to the capacitance effect of the pipeline, and the attenuation is modified. As for the first approach, let us suppose that the pressure rise, during the propagation period, remains unchanged, and it is added to the original steady state pressure line. This unreal case is shown in *Fig. 7.1 – 13*. After a sudden closure, first, the pressure upstream of the gate valve rises by a $\Delta p$ value that can be calculated from Eq. 7.1 – 1. After 10, 20 and 30 seconds it would pass through the indicated sections, if the original pressure line remains unchanged and the system would be rigid. In reality, the pipeline, due to the pressure rise expands to a small extent, the fluid is slightly compressible, and thus the line packing capacity of the pipeline increases. Due to this phenomenon the flow is going on with a reduced velocity for a time in the original direction, and the pressure upstream of the gate valve further increases.

The real situation is explained by *Fig. 7.1 – 14*. The initial pressure rise $\Delta p$, developing upstream of the gate valve after the sudden closure can be calculated from Eq. 7.1 – 1 here, too. When the pressure front propagates, with acoustic

velocity, against the direction of the original flow, then due to the capacity impact, described above, it meets a fluid flowing with the flow velocity of $v_x$, greater than 0. Thus the size of the waterhammer will be gradually decreasing by value of $\rho w(v_o - v_x)$. The real pressure rise along the pipeline is indicated by the dashed line, and this asymptotically approaches the steady state one. After covering a distance of $l_a$ the pressure rise equals zero. The upstream pressure $\Delta p$ before the closed gate valve

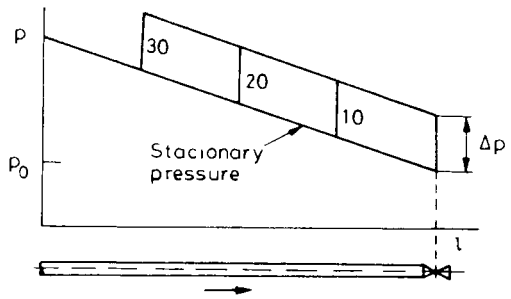


Fig. 7.1 – 13. Simulation II of pressure wave propagation, after Streeter and Wylie (1967)

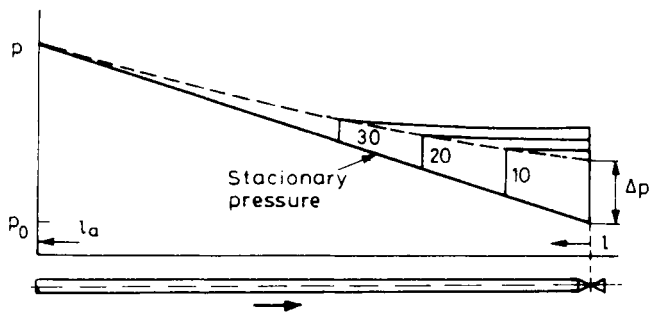


Fig. 7.1 – 14. Simulation III of the pressure wave propagation, after Streeter and Wylie (1967)

due to pressure equalization will further increase. The pressures, valid for 10, 20 and 30 seconds after the closure can be seen on the Figure. Though, in the description of the pressure jump and damping the viscosity, and so the friction of the fluid flow, are not indicated, they also play an important role in the birth of the phenomenon; the sloped pressure line of the steady state flow is the function of the friction pressure loss.

Because of the above described facts, as for the value computed from Eq. 7.1 – 1, the excess pressure rise before the suddenly closed gate valve, and the excess pressure decrease behind it can be quite high. Its rate must be considered at the structure design of the pipeline and fittings and at the design of safety devices. For computing the pressure change, several methods are described in the literature (see later).

In the previous section, basically, the reasons in the change of velocity were thought to be the opening and closure of valves. For the change in the velocity of the flowing fluid in the oil pipeline several other factors may be responsible, among which the most important are: the starting and stopping of pumps; the change in the energy supply of the pump driving motor; the instability of the head curve of the centrifugal pump; the normal operation of the piston pumps; the sudden change in the oil level within the tank; the vibrations within the pipe-system; and the sudden breaks, and leaks in the pipeline.

The relation between centrifugal pumps, and the pressure waves is of outstanding importance. The change in the performance of the centrifugal pumps may create, on the one hand, pressure waves, and on the other hand, the pressure waves, developing at other spots, are modified by the pumps while passing through them. This passing may cause damages, and even if damages do not occur, the pressure wave is modified, and this impact must be considered in the further modelling.

It must be noted that piston pumps may provoke pressure wave, however, the pressure waves, emerging upstream of these pumps do not pass through them. That is why a piston pump can be considered as a nodal point that divides the transporting system into inflow and outflow sections that are independent of each other.

In *Fig. 7.1 – 15*, after Thielen (1972b) pressure lines drawn with thick lines are shown that emerge in the inlet and outlet pipe sections joined to the pump station in

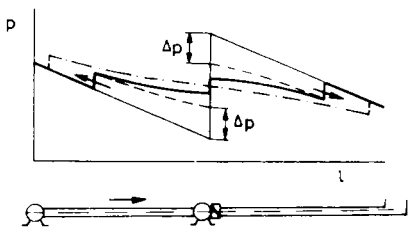


Fig. 7.1 – 15. Pressure wave evoked by the sudden closing of the pump station, after Thielen (1972b)

the case, if the centrifugal pumps suddenly stop, i.e. the pump station shuts down. The front of the pressure wave, in the given case, is steep. It shows that the closure must have been taken place in a very short time, but the sudden shut-down of the non-return valve, after the pump station, may play an important role, too. If the discharge head of the pump station, just shutting down, is higher than the twofold value of $\Delta p$ calculated From Eq. 7.1 – 1, the waterhammer develops on both sides of the pump station. In the pipe section before the pump the pressure increases, while in the section after it decreases; the two changes propagate into opposite directions. Upon the impact of the change on the two sides of the non-return valve the pressure difference decreases, then ceases. The valve, then, opens and the fluid flow starts in the original direction. The pressure line valid now is shown by a "dot and dash" line

in the Figure. If the outlet pressure of the shutting-down pump station is of a smaller value than that of the double of the waterhammer then the non-return valve does not shut down. The throttling impact of the shut-down pump, however, must be considered even in this case.

The maximum pressure, caused by the pressure rise due to the throttling, and closing, respectively, of the devices attached to the pipeline, is, for two reasons dependent on the slope of the pressure line, on the pressure gradient developing by steady state flow in the preceding section. On the one hand, the pressure gradient, in

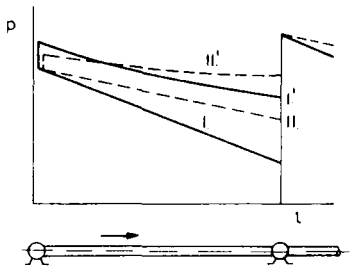


Fig. 7.1 – 16. Effect of the piezometric line on the shape of the pressure wave, after Thielen (1972b)

case of given pipeline and oil quality, is proportional to the flowing velocity, and so it determines the waterhammer and the occurring excess pressure that can be calculated from Eq. 7.1 – 1, while on the other hand it determines the suction pressure of the pump. Supposing that the pressure is constant at the beginning of the previous pipe section, the smaller the slope of the pressure line, the greater the steady pressure before the pump station. Line *I* of *Fig. 7.1 – 16* at flow rate $q_1$ represents the pressure line of the steady state flow (Thielen 1972b). Line *I'* shows the pressure wave front line developing at the shut-down of the second pump station. Let, in an other case, the transported stationary oil flow rate be $q_2 < q_1$. The steady state pressure line corresponding to this is *II*. At the sudden shut-down of the pump station the developing pressure jump line is *II'*. Though in this latter case the velocity of the stopped fluid flow, and thus the pressure jump is smaller, the absolute value of the pressure is greater in the upstream flow to the pump, after the stopping.

Among the reasons causing the pressure wave the starting and shut-down characteristics of the centrifugal pump are significant. After stopping, the energy supply to the driving motor pump operation does not stop immediately, but due to the kinetic energy stored the rotating parts are turning further for a time with a decreasing angular velocity. Due to this effect, at the entrance side a pressure wave of positive, and at the outlet side a pressure wave of negative sign develop. The amplitude and front profils of the pressure wave are fundamentally influenced by the characteristics of stopping. Several methods have been elaborated to compute the pressure-waves caused by the transient operation of the centrifugal pumps. Among

these procedures the method, elaborated by Streeter and Wylie (1974) may be considered outstanding that discusses the features of the pump stations located on offshore platforms. When determining the boundary conditions, the authors started from the data series of $q$ flow rate, $H$ discharge head, $M$ torque, and $n$ pump rpm, recommended by the manufacturers. Dividing the proper physical values valid at the start and stop by the recommended values we obtain $N_q$, $N_H$, $N_M$ and $N_n$ dimensionless numbers. By these parameters Equations

$$f_1(x) = \frac{N_H}{N_n^2 + N_q^2} \qquad 7.1-18$$

$$f_2(x) = \frac{N_M}{N_n^2 + N_q^2} \qquad 7.1-19$$

and

$$x = \pi + \text{arc tan}\frac{N_q}{N_n} \qquad 7.1-20$$

can be derived, and, by the relations $f_1(x)$ and $f_2(x)$ have to be calculated. The computed values may be connected with continuous lines, similarly to those, shown on *Fig. 7.1 – 17*. Supposing that at the start and stopping the characteristic change of the speed with time can be determined, or is known, the boundary conditions can be determined without bias. The authors also provide the computer program written in FORTRAN IV by the help of which the pressure waves, occurring in simple, or complicated systems consisting of pump, outlet-side valve, and pipeline can be simulated.

For simulating the deceleration of rotating masses in the pump Vyazunov and Golsovker (1968) offer a method. In *Fig. 7.1 – 18*, after Béres Deák and Filetóth (1975) the measured pressure and pressure changes, in the function of time, are shown at one of the pump stations of the Friendship Pipeline. In the Figure *a* stands for pressures of the outlet side, *b* denotes pressures at the suction side, while *c* is for the pressure changes at the outlet side. Two, parallel connected pumps were

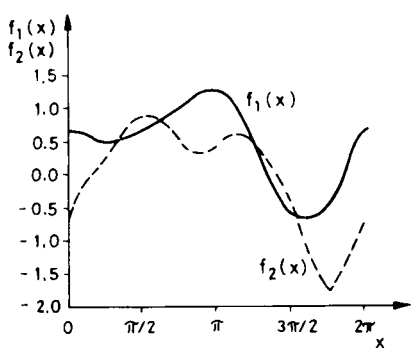


Fig. 7.1 – 17. Auxiliary diagram of Streeter and Wylie (1974)

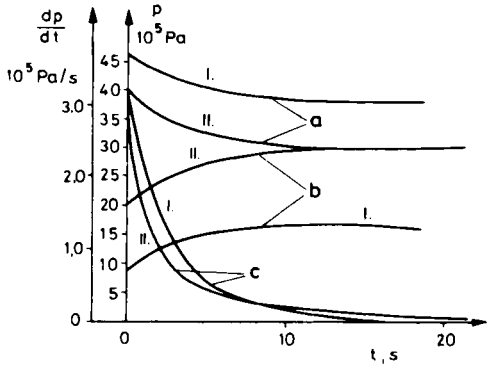


Fig. 7.1 – 18. Pressure lines at the pump station, after Béres Deák and Filetóth (1975)

operating at the station. The oil rate transported by one pump is 3500 $m^3/h$, while the two pumps together transported 4600 $m^3/h$. The diagram was plotted after the stopping of *one* pump. Before the measurements represented by curves *I* both pumps were in operation, while in case of curves *II* only one of the pumps worked.

Upon the centrifugal pumps both the pressure rise and the pressure depression caused by pressure wave may exercise a damaging effect. (i) First of all, in case of single suction pumps, the rapid change in pressure attempts to move the impellers suddenly in the axial direction and that may cause serious damages. That is why the pumps of great capacity are of double suction type. (ii) The pressure wave arriving at the pump station may cause the rapid shut-down of the non-return valve. Due to this effect the fluid flow stops, the pump may be overheated, the control stops the pump, and the damaging impact of the in-flowing pressure wave may increase. (iii) If the suction pressure, due to the depression decreases below the vapour pressure of the transported fluid, a vapour slug develops in the fluid, that getting into the pump may cause cavitation damages.

The negative pressure wave causing cavitation occurs due to the sudden rise of the flow rate, that is provoked, e.g. by the starting of the preceding pump station, or sudden opening of a gate valve. Mostly, it can be expected that the pipeline pressure sinks under the vapor pressure of the transported fluid, if the depression wave propagates in the direction of the fluid flow, i.e. in the direction of decreasing pressure. On hilly terrains, in case of normal operation, the minimum pressures may be expected at the terrain peaks. The probability of the development of the vapour slugs, due to depression waves is the highest at these spots. Since, before the vapour slug, at the descending terrain section the flow velocity of the fluid is greater than at the ascending side, the volume of the vapour slug is increasing for a time. Arriving in a section of greater pressure the slug "collapses", while the separated fluid masses flowing with different velocities of $v_1$ and $v_2$ "crash". The pressure rise

$$\Delta p = \frac{1}{2} \rho w (v_1 - v_2) \qquad 7.1-21$$

at the moment of disappearing of the cavity may be quite high, causing damages and leaks. A similar phenomenon may occur in the pump itself. The possibility of a depression wave must be always kept in mind at the suction side, when starting the pump operation.

Researchers, studying the laws of pressure waves, made an effort lately to represent graphically the pressure changes numerically determined previously by computers to facilitate the interpretation and location of this phenomenon. Techo (1976) describes a solution, at which the change of the pressure with length is printed, in the form of "letter-sketches", by making use of the usual print-out equipment of computers. An even more up-to-date method is described by Jansen and Courage (1977). Here the pressure wave corresponding to the different operation and boundary conditions is displayed first on a display, then it can be recorded in hard-copy form. By this method the operation of the designed oil-pipeline can be rapidly checked, and the most reliable solution can be selected.

## 7.2. Slug transportation

### 7.2.1. Mixing at the boundary of two slugs

The very same pipeline is often used for transporting several fluids of different quality in serial flow. The flowing fluid slugs, batches are mixing at the boundary developing between the two "pure" liquids, an increasing mixture slug during the flow. At one end of the interface the volumetric fraction of fluid $A$ is $\varepsilon_A = 1$, and this value, till the other end of the slug decreases to $\varepsilon_A = 0$. The volumetric fraction of fluid $B$ changes in the same way in the opposite direction. The mixing of the fluids raises difficulty both from the points of view of refining (if crude is transported), and of the utilization (if products are flowing in the pipeline). In each case, the allowed fraction $\varepsilon_{A,B}$ that fluids $A$ and $B$ may contain from each other can be determined. In an extreme case this value may be even zero. Being aware of the features and the permitted utilization concentration of the mixed slug it can be determined into which tank of the tank-farm belonging to the pipeline branches what quantity of pure, or mixed fluid should be directed. For crude transporting pipelines mixing means generally a smaller problem than for product transport. Knowledge of this phenomenon and its impact, however, is important in the first case, too.

The degree of mixing is significantly higher in case of laminar flow, as compared to the turbulent flow. The velocity distribution along the pipe-radius unambiguously justifies this phenomenon. According to the derivation by Yufin (1976), in a given case (pipe radius = 0·25 m; flow velocity = 1 m/s; friction factor = 0·02) the value of the diffusion factor is higher by $10^6$ in case of laminar than of turbulent flow. Transporting slugs, generally turbulent flow must be used.

The basic computing problem of the slug flow is the determination of the length of the mixed, contaminated slug at given parameters. Several relations by different authors could be cited. In the next section we introduce the essence of Weyer's equation and of its derivation based upon the works of earlier authors (Weyer 1962). Weyer characterizes the turbulent mixing with the equation of the molecular diffusion. His starting point is the known diffusion equation

$$\frac{\partial c}{\partial t} = k_d \frac{\partial^2 c}{\partial \bar{x}^2}, \qquad 7.2-1$$

where $c$ is the concentration changing along the flow path; $x$ is the fluctuating, axial displacement of a fluid particle in a long, straight pipe that can be described by the relation $x = X - ut$. Here $X$ is the net axial displacement of the particle in $t$ time after the start of the flow, while $u$ is the average flow velocity and $k_d$ is the diffusion coefficient. The solution of the above differential equation is

$$c = \frac{1}{2} - \frac{1}{2} \operatorname{erf}\left(\frac{x}{2\sqrt{k_d t}}\right), \qquad 7.2-2$$

where by the interpretation $y = \dfrac{x}{2\sqrt{k_d t}}$ the second member of the right hand side of the formula from the relation

$$\operatorname{erf} y = \frac{2}{\sqrt{\pi}} \int_0^y e^{-y^2} \, dy$$

on the basis of the Gauss-type error function can be computed. Let at one end of the interface the rate of $A$ oil be $\varepsilon$ while that of the $B$ oil be $(1-\varepsilon)$. At the other end of the contaminated slug the rate of $B$ oil is $\varepsilon$, and that of the $A$ oil is $(1-\varepsilon)$. Supposing that $c = 1-\varepsilon$, where $\varepsilon = 0{\cdot}95$ and $s = 2x$ then

$$\operatorname{erf} \frac{s}{4\sqrt{k_d t}} = 2\varepsilon - 1 . \qquad 7.2-3$$

Allowing the value $\varepsilon = 0{\cdot}95$ the equation can be transformed into a simpler form and from this the length of the mixed slug is

$$s = 4{\cdot}65\sqrt{k_d t} . \qquad 7.2-4$$

The $k_d$ diffusion factor was derived by Weyer on the basis of the turbulent velocity profile. He supposed that mass transfer takes place first of all in the radial direction. Due to the isotropic character of the turbulent flow, he also considered a mass transfer of smaller significance in axial direction, too. On this basis the diffusion factor is

$$k_d = 10{\cdot}1 \, v_* r , \qquad 7.2-5$$

where $v_*$ is the so-called frictional velocity that is the function of the shear stress, prevailing on the pipe wall, and the density:

$$v_* = \sqrt{\frac{\tau_r}{\rho}} . \qquad 7.2-6$$

The shear stress is

$$\tau_r = \frac{\lambda \rho \bar{v}^2}{8} , \qquad 7.2-7$$

where $\bar{v}$ is the average flow velocity; $\bar{v} = q/A$. Substituting Eqs 7.2 – 6 and 7.2 – 7, and the relation $r = d_i/2$ into Eq. 7.2 – 5 we obtain

$$k_d = 1{\cdot}79 \, d_i \bar{v} \sqrt{\lambda} . \qquad 7.2-8$$

This relation gives a shorter than real length for the mixed slug (Matulla 1972), and a theoretical mistake of the method is, that is neglects the increase of the mixing with the flow path. The relation offered by Austin and Palfrey (1963/64) seems to be more accurate. According to the authors the rate of the mixing, even in case of

turbulent flow, is significantly different above, and below of a critical value of $N_{Reb}$. This critical value is given by the relation

$$N_{Reb} = 10^4 \, e^{2{\cdot}75\sqrt{d_i}} . \qquad 7.2-9$$

Under the critical value the rate of mixing is greater and the length of the mixture can be calculated from equation

$$s = 18\,420\,(d_i L)^{0{\cdot}5} N_{Re}^{-0{\cdot}9} e^{2{\cdot}19\sqrt{d_i}} , \qquad 7.2-10$$

while above the critical value it is obtained from relation

$$s = 11{\cdot}75\,(d_i L)^{0{\cdot}5} N_{Re}^{-0{\cdot}1} . \qquad 7.2-11$$

For calculating the diffusion factor, Yufin (1976) describes several equations among which Asaturian's relation is

$$k_d = 17{\cdot}4\,\bar{v} N_{Re}^{2/3} , \qquad 7.2-12$$

where the average kinematic viscosity is obtained from equation

$$\bar{v} = \frac{v_A + 3v_B}{4} .$$

Subscript $A$ denotes the higher, while $B$ the lower viscosity fluids.

*Example 7.2–1.* Let us determine the mixed slug length in case of a pipeline of $d_i = 305$ mm and of 695 km length with the allowed value of $\varepsilon = 0{\cdot}95$. In the pipeline two light products whould be transported in serial flow slugs. The average kinematic viscosity of the two products is $\bar{v} = 0{\cdot}9 \times 10^{-6}$ m$^2$/s, the average flow velocity is $\bar{v} = 1{\cdot}652$ m/s, while the relative roughness of the pipe wall is $k/d_i = 2 \times 10^{-4}$.

The Reynolds number is

$$N_{Re} = \frac{\bar{v} d_i}{v} = \frac{1{\cdot}652 \times 0{\cdot}305}{0{\cdot}9 \times 10^{-6}} = 5{\cdot}60 \cdot 10^5 .$$

The friction factor, from Eq. 1.1–7 is

$$\frac{1}{\sqrt{\lambda}} = -2 \lg \left[ \frac{2{\cdot}51}{N_{Re}\sqrt{\lambda}} + \frac{k}{3{\cdot}71 d_i} \right] =$$

$$= -2 \lg \left[ \frac{2{\cdot}51}{5{\cdot}6 \times 10^5 \sqrt{\lambda}} + \frac{2 \times 10^{-4}}{3{\cdot}71} \right]; \lambda = 0{\cdot}0153 .$$

on the basis of Eq. 7.2–8

$$k_d = 1{\cdot}79 \times 0{\cdot}305 \times 1{\cdot}652 \sqrt{0{\cdot}0153} = 0{\cdot}112 ,$$

and according to Eq. 7.2–4

$$s = 4{\cdot}65 \sqrt{0{\cdot}112 \frac{695 \times 10^3}{1{\cdot}652}} = 1009 \text{ m} .$$

The critical Reynolds number, calculated by applying the Austin and Palfrey equation is

$$N_{Reb} = 10^4 e^{2.75\sqrt{0.305}} = 4.57 \times 10^4 .$$

Since $5.60 \times 10^5 > 4.57 \times 10^4$, the length of mixture can be computed from Eq. 7.2 − 11, i.e.

$$s = 11.75(0.305 \times 695 \times 10^3)^{0.5}(5.60 \times 10^5)^{-0.1} = 1440 \text{ m} .$$

In practice, several phenomena, related to the mixing of oil slugs can be found, the previous simulation of which can be important. Emphasized items are as follows:

(i) Between the two slugs, already at the initial stage of the flow in the pipeline, mixed slug occurs. The reason for this fact can be different. (1) With change of the crude type, the opening and shut-down of the valves need a definite time, on this account the two fluids are mixed already at the initial stage. (2) In pipelines on hilly terrains, during the shut-down period, the liquid of greater density being at a higher level, may sink down. (3) If it is not allowed that the two liquids following each other mix, even to the slightest extent, then a dividing slug, made of liquid of allowable quality must be created. The numerical simulation of these cases is given by Frolov and Seredyuk (1974a, b). From his relations it can be calculated that at a given time and determined spot what is the rate of mixing.

(ii) It often occurs that fluid A of the slug stream is transported only to tanks being at a given end-point of one branch, while fluid *B* is to be transported to the tanks of the tank-farm at the end-point of the main pipeline. Through the mixed slug "contaminating" liquid gets into both end-point tanks. The quality of the stored fluids may deteriorate to a damaging level. Vladimirsky *et al.* (1975) published a design method suitable to determine the concentration change of the mixed slug remaining in the pipeline. By applying this method the way of operation that prevents the undesirable quality deterioration may be planned.

(iii) If the flow is non-isothermal, the length of the mixed slug is greater than that of in case of isothermal flow. Chanisev and Nechval (1971) describe relations for the determination of mixing of oil slugs transported by spot heating.

(iv) The size of the mixed slug may be significantly influenced by the fluctuating velocity of the flow, the presence of the shut-down or open branches, and by-passes.

The length of the mixed section may be decreased if, between the two pure fluids, a dividing ball (so-called pipe-pig or gel slug) is applied (see Section 6.3). Their application, however, requires the building of proper input and output spots, and an other difficulty is raised by the passing through the booster pump stations (Matulla 1972). These difficulties may prove to be of small importance when because of the paraffin scraping input and output equipments are required, or, there is no booster pump station.

### 7.2.2. Scheduling of batch transport

If oil is carried in and out of the transport system in several places the design and optimization of the batch transport may be quite a complicated task. This applies especially to product transporting pipeline system carrying different products of several refineries to consumer centres (e.g. see Kehoe 1969). Scheduling a crude oil transporting system raises a smaller problem, since the fluid slugs to be transported here are relatively large, therefore the changes occur less frequently; the number of nodes in the pipeline system is generally smaller, and the transportation prescriptions are less rigorous. The scheduling procedure, however, is essentially the same as in the case of product pipeline system (Speur *et al.* 1975).

The task of systems transporting crude, in case of continental countries basically is, that they should carry the crude from the oil fields to the refineries. To this system lines of several oil fields may be joined, and through branching pipes the crude may be distributed among several refineries. If the quality of the crudes, originating from the different fields, is only slightly different regarding the hydraulic parameters of the transport and the requirements of the refineries, then, using prescribed parameters, the quantitative demands of the transportation must be satisfied only. If, however, the quality of the crudes to be transported from different fields significantly differs, and the crudes may not be transported in a mixture of homogeneous composition, then within the common transport sections slug transport is needed. Also, slug transport can be designed for pipelines, through which crudes of different qualities are transported from the shore-terminal to the refineries. The quality of the crudes, obtained on tankers, may differ from shipment to shipment.

There are three main design problems of the batch transport: a) the determination of the sequence of the slugs (batches) defined by the transport requirements; b) the numerical simulation of the flow; and c) the batch nomination sequencing.

First, generally monthly plans are prepared, considering the requirements of the consumers, and refineries, taking into account the available batches of the crude and using approximate flow and transport relations. On the basis of the above consideration the realizable monthly scheduling may be elaborated, that shows when, how many and what sort of crude should be injected into the system from different source points and at what time, what sort of and how much oil will be transported in different refineries. Scheduling for a shorter period, e.g. for a week or for ten days, can be carried out after this planning. At this stage already the hydraulic parameters of the transport system must be considered. This design process includes the solution of factual problems (which pump, when, from which tank and where should deliver; into which tank of the refinery what kind of crude, and at what time is pumped, etc.). Later on, the design is generally modified, since the real time of the injection of the crude batches, their volume may differ from the originally designed values, the pumps may fail, etc. By applying the parameters, differing from the designed ones, the operational plan must be modified in a very short time.

If, even the fact is considered, that the problem of transportation must be solved, regarding not only the technical feasibility but also the transport costs, i.e. an optimum operation must be designed, it is obvious that it can only be realized by applying computers.

In DeFelice's opinion (1976) the first problem to be solved by scheduling is the batch nomination sequencing. To each of the oil slug to be transported a code-name is given, that unambiguously expresses the shipper origin, source, product, grade, cycle requested and consignee of the volume specified. The first schedule is prepared by experimental relations obtained from the data of former transports. Several computerized design methods for precise hydraulic schedule are applied. One of these described by Techo (1976) is the so-called master-clock method. At this method a volume unit is taken, as the basis of the design, e.g. 1·5 $m^3$. Within the system checking points are determined. These are the spots on the pipeline (control-points) where some operation influencing the transport process occurs (e.g. terminals, initial sections of branches, etc.). Starting from a given situation, the

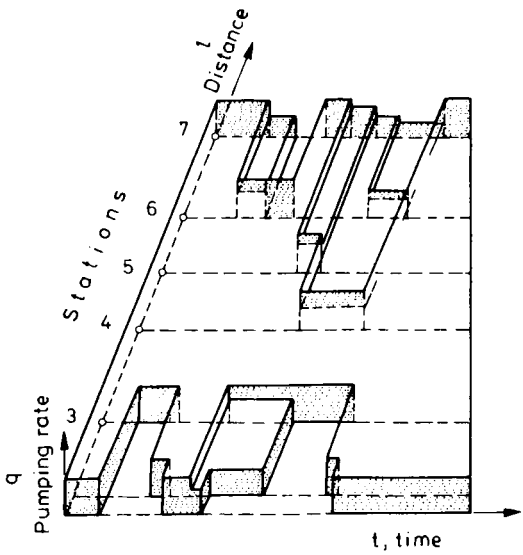


Fig. 7.2 – 1. Rate v. time diagram of batch transport, after Techo and Holbrook (1974)

element which is the nearest to any control point is chosen, and the time needed for reaching this point is calculated. At this moment the position of the slug elements is fixed, in relation to the control points, and the calculation is going on by applying the previous method. This method is relatively rapid and flexible, but its disadvantage is that it does not calculate the movement of the slug boundaries. After Techo and Holbrook (1974), in case of a product pipeline, the complexity of the slug motion, is well illustrated by a three dimensional diagram shown in *Fig. 7.2 – 1*,

where, in the function of time, the changes in the pump rates, at the pump stations are shown. Crosby and Baxter (1978) describe the main types of algorithms, on the basis of which computer programs are elaborated to increase the flexibility and capacity of the transporting system.

### 7.2.3. Detection of slug's borders

To deliver the pure fluids and the mixed slug into the designed tanks, it is necessary that the dispatcher should be continuously informed about the position of the slug boundaries, about the distance of these from the tail end points, and branches of the pipeline. In case of computerized control, the computer, on the basis of the input data, obtained by on-line flow meters, continuously computes the movement of the boundaries, and their momentary position, and these data are either visually, or digitally transmitted to the dispatcher. This method, however, is generally not accurate enough for controlling automated valve closing, or opening, and by these the transportation in proper direction and destination. That is why before the nodes of the pipelines, it is recommended to mount border detectors at given, predetermined intervals (e.g. distances of some 100 meters), and then at the occurrence of the change, signal is transmitted to the controlling centre, and/or, by on-line computer, valve openings and closures are automatically controlled. The boundary detector, in case of transporting without dividing device, directly measures the change in quality. Here, several methods are known. The instrument sensing the gamma irradiation and emission, indicates the change that, according to the oil qualities, the absorbed gamma-radiation, and thus the emitted radiation changes.

Zacharias (1969) describes an instrument operating on sonic principles. The sound velocity changes linearly with density. Into the oil, flowing in the pipeline, at certain intervals, sound impulses of great frequency are transmitted from the pipewall, and, between two previously determined surfaces, the propagation speed of the sound is measured. In case of two detectors method the dispatcher receives a warning signal while the slugborder passes the first detector, and the requested alteration in the direction of the flow is ordered while it passes the second detector. A density meter, complemented by simple comparator electronics, is also able to indicate slug boundaries.

Placing between the fluid slugs a dividing ball, perhaps pipe pig, the detectors show the passing of this device. By applying a mechanical dividing instrument, the rate of mixing can be reduced to 5 percent of the "without device" interface but the total prevention of this phenomenon is impossible. That is, the ball indicates the appearance of a fluid, the concentration of which may be determined by preceding calculations or tests. Changes in the flow direction should be ordered with this knowledge. For the detection, and signalling of the dividing ball, several methods were tested and applied. Yufin (1976) describes a mechanical signalling system. By the passing of the sphere a small cylinder penetrating radially into the pipeline is pushed out, and this signal is transmitted in an electric way. Speur and Jaques (1977)

describe an ultrasonic dividing detector. Here, the perforation of the pipeline is not necessary. On the outside wall of the pipeline a transmitter, operating with piezo-crystal, is attached and ultrasonic signals continuously are transmitted through the pipe. The signals, arriving at the other side of the pipe, are sensed by a receiver. At the moment, when a mechanical dividing instrument moves in the section, measured by the instrument, the intensity of ultrasonic signal significantly decreases. On this basis the dispatcher and/or the computer is informed about the passing of the fluid slug.

## 7.3. Leaks and ruptures in pipelines

Leaks, occurring in buried pipelines may be classified into two groups. The first group includes the big holes, caused by the rupture or break of the pipeline. They are mostly due to the too high internal pressure, or to external impact (earthquakes, landslides, the damaging operation of the bulldozers, etc.). It may be also promoted by ruptures, or fault of the pipeline that remained undetected during hydrostatic pressure test. Through ruptures and breaks of this type a relatively large oil volume pours out from the pipeline within a short time. The second group includes small leaks that develop generally due to corrosion in a longer period of time. Through these leaks a relatively small oil rate seeps into the soil. Between the two groups, holes and outflow of mean size practically do not occur (Kreiss 1972). Thus the main tasks of the leak detection are: (i) the checking of the integrity of the pipeline before starting its operation; (ii) the determination of the existence, and the locality of great leakages within a very short period of time; (iii) the recognition and location of small seepages, generally periodically. In the following section we discuss problems (ii) and (iii).

For the detection of the existence and the spot of the leaks in case of operating pipelines several methods have been elaborated. The most ancient method is the regular ranging over of the trace and its visual observation. Today, this operation is partly, or totally performed from vehicles (helicopters, planes). Particularly in case of great leaks and breaks the outpouring oil may cause considerable damages, that is why the aim is that the existence and locality of the rupture should be found in the shortest possible time after its induction. Beside the visual observation, systematic instrumental tests, and observation methods are also applied. Small leaks, caused by corrosion can be visually observed at the ranging only, if the seeping oil contaminates already the surface. In order to recognize the phenomenon in the shortest possible time the instrumental observation of this type of leakage should be also introduced. *Table 7.3 – 1*, after Takatsu, gives a survey of the instruments determining the existence, and sometimes also the place of the leaks. The symbols, used for the qualification are as follow: *1* to be applied in the first place; *2* is to be applied in the second place, or less suitable; *0* not suitable; + stands for instruments recommended in Japan; while – means that the device is officially not recommended for application in Japan. In the following part some methods of major importance are discussed. The interpretation of the type marks is shown on the Table.

Table 7.3 – 1. Leak detecting methods for pipeline after Takatsu and Sugaya (1977) with small modification

| Code | Detected parameter | Essence of the method | Small leak detection | Time for detection | | Leak location | Japanese stipulation code |
|---|---|---|---|---|---|---|---|
| | | | | during operation | during downtime | | |
| T/1 | Flow | a) Comparison of in- and outflowing crude rates | 1 | 1 | 0 | 0 | + |
| | | b) Comparison of differential value of flow rate difference between inlet and outlet point | 0 | 1 | 0 | 2 | – |
| T/2 | Pressure; $\frac{dp}{dx}, \frac{dp}{dt}$ | a) Measuring the change of hydraulic gradient | 0 | 1 | 0 | 2 | + |
| | | b) Negative pressure wave detection | 0 | 1 | 0 | 2 | – |
| | | c) Detection of differential pressure increase between block walves during downtime of pipeline and of | 1 | 0 | 1 | 2 | + |
| | | d) pressure drop in the pressurized section during downtime | 1 | 0 | 1 | 2 | – |
| T/3 | Noise | a) Detection of supersonic waves caused by leakage and of | 1 | 1 | 0 | 1 | – |
| | | b) elastic waves caused by leakage from outside of the pipe by noise meter | 2 | 1 | 2 | 2 | – |
| T/4 | Gas concentration | Detection of inflammable gas vaporized from spilled oil | 1 | 1 | 1 | 1 | + |
| T/5 | Air pressure | Detection of pressure drop of an air containing oil soluble tube dissolved by the spilled oil | 1 | 1 | 1 | 2 | – |
| T/6 | Impedance | Detection of change in impedance of oil soluble insulator dissolved by spilled oil | 1 | 1 | 1 | 1 | – |

Note: 1 means best method, 2 means good method, 0 means not advisable.

### 7.3.1. The detection of larger leaks

*Type T/1.* A rapid, and relatively simple detection is rendered by the so-called ERM system (Kreiss 1972). The essence of this method is that at the two end-points of the pipeline (or pipeline section) sensors are mounted which measure and transmit signals, directly proportional to the actual pumping rate. The signal device, e.g. may be two measuring probes, transmitting the pressure in the pipeline, or orifices, do not hindering line scraping, or an instrument, measuring the pressure differential at two ends of a pipe bend of small radius. The signals, measured at the ends of the pipeline are transmitted to a computer that continuously evaluates them. The derivative of the differences, in case of leaking, significantly change. After Kreiss (1972). *Fig. 7.3 – 1* represents two curves that can be defined by such a method. Curve *1* shows the difference between the liquid rates, inflowing at the starting point, and outflowing at the end point of the pipeline, respectively, i.e. the approximative liquid rate passing through the suddenly emerged leak; while curve *2* represents the total volume ratio of the ouflow liquid, as compared to the storage capacity of the pipeline, as a function of time. From the shape of curve *1* it can be read that this phenomenon includes three periods. In the first period, *a*, the outflowing liquid rate increases to a maximum value, and then it decreases to a certain value. This end value is determined by the parameters of the still operating pumps, and by those of the stationary out-flow through the leak. In period *b*, these parameters practically remain constant. At the beginning of period *c* pumping is stopped, and then the liquid pours out of the pipeline, which is supposed to be horizontal and closed at

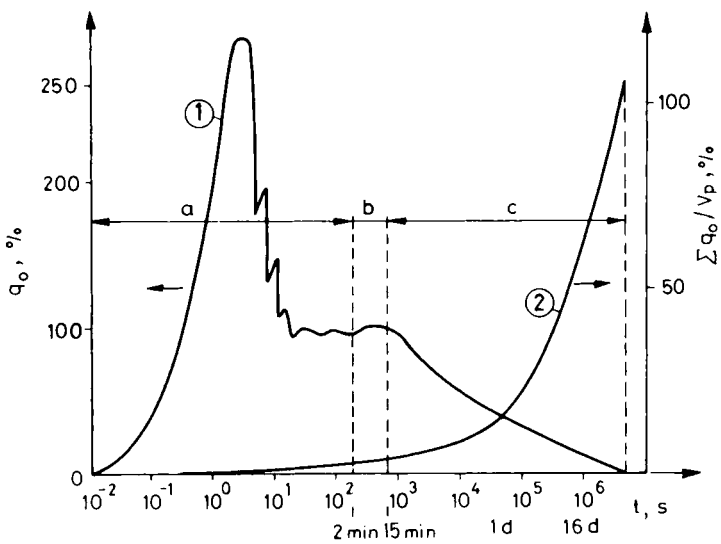


Fig. 7.3 – 1. Absolute and relative fluid volume in function of time flowing out through a leak, after Kreiss (1972)

both ends. The characteristic shape of curve *I* indicates the leak in 1 – 2 minutes after its occurrence, in spite of the fact that basic data used are not the exact volumetric rates but only signals proportional to them. In the method described by Cridner (1974), and Campbell (1975) *turbine flow meters are used for the measurement of in- and outflowing liquid rates*, the results obtained are comparatively exact, and the differences of measured data are recorded. Even in case of proper operation of the pipeline small fluctuation can be inspected *(Fig. 7.3 – 2)*. Differences may be

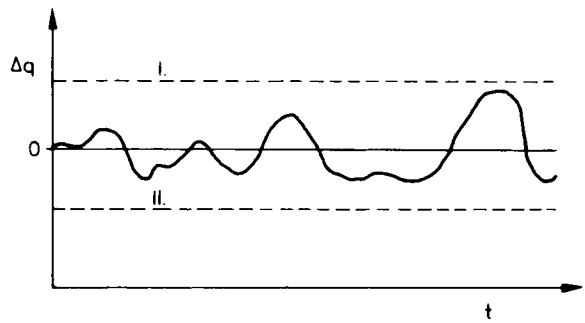


Fig. 7.3 – 2. The change of the fluid rate difference v. time existing between the pipeline inflow and outflow, after Campbell (1975)

attributed to the changes in temperature, pressure, and quality of the oil flowing in the pipeline, since due to the alteration of the above parameters the volume of the liquid, stored in the pipeline changes too. By experiments the upper, and lower limits of $\Delta q$ can be determined (lines *I* and *II*), i.e. the range within which the indicated fluctuation does not mean a damage in the pipeline. The midline of the recorded diagram is parallel to the abscissa, while its ordinate height corresponds to the point $\Delta q = 0$. If a large leak, or break occurs in the pipeline, the midline of the curve $\Delta q$ undergoes a one-directional change. Both the slope of the midline and the surpassing of the limit lines indicates leakage.

The pipe-break can also be indicated by *periodical mass balance* of the liquid volume flowing in the pipeline (Young 1975). Its essence is that the inflowing and outflowing liquid volume together with the temperature, pressure and density of the given pipeline, is measured for a predetermined short time, and, by strain gauges the tension in pipe is also determined. On the basis of these parameters, from time to time, it is automatically determined, if the difference in inflowing, and outflowing volumes at the pipe-ends is corresponding to the change in the oil volume contained in the pipeline. The procedure is accurate enough if the evaluation is carried out on the basis of a sufficiently great number of data. The speed of leakage sensing is the function of the frequency of measurement and evaluation. For this procedure a computer is needed and, as a whole, it is rather expensive.

*Type T/2.* By T/1 types, we obtain information only for the existence of leakages in the pipeline, but we do not receive information about the place of leakage, fracture or break. The location of the leakage, by observing, and evaluating of the pressure

waves, is possible (Thielen 1972a). Being aware of the parameters of the sound wave propagation in the pipeline, the time v. length curve of the negative pressure wave front which develops by the impact of outflowing liquid through an abruptly emerged leakage is previously determined and graphically represented (see also Section 7.1). In *Fig. 7.3 – 3(a)* two superpositioned diagrams of this kind are shown. In the function of pipeline-length, both of them show, between the $i$ and $k$ pressure testing points the arrival time of the pressure front, propagating in the pipeline,

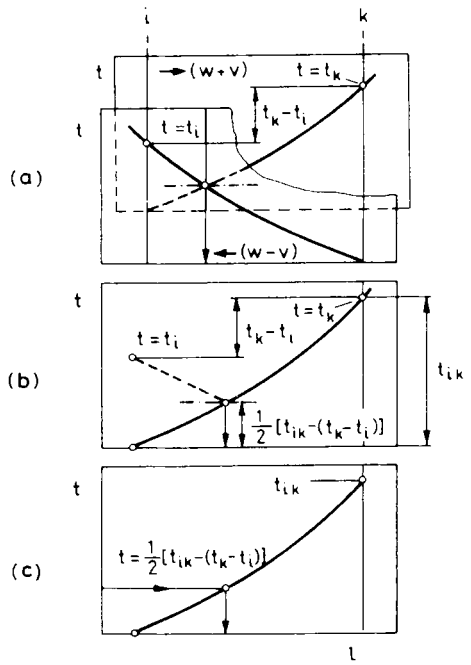


Fig. 7.3 – 3. The location of the leakage by pressure wave lines, after Thielen (1972b)

supposing that the pressure wave starts from a leak occurred at the other point of observation. The mirror image of the two curves is slightly different, since the propagation velocity towards the liquid flow direction equals $(w+v)$, while in opposite direction it is $(w-v)$. As a result of continuous telemetering we know the exact time of the arrival of the pressure wave to the $i$ and $k$ testing points, i.e. values $t_i$ and $t_k$. It can be, obviously, seen that if the above two curves, plotted on tracing paper, are placed upon each other so, that the testing points $i$ and $k$ should cover each other, and the two diagrams are vertically moved by the value of $(t_k - t_i)$, then the abscissa value of the intersection of the two lines determines the point of the break. The accuracy of this process hardly decreases, if, in the analysis of the bi-lateral pressure wave propagation, the flow velocity, $v$, is neglected. Excessive accuracy is often unnecessary, since the leakage, detected from the centre, is in most

cases seen by the service team sent to the spot, from distances of several hundred meters. In *Fig. (b)* is shown that, in practice, the location of the leakage, on the basis of the simplified curve, is performed by the help of the dashed line mirror curve. *Fig. (c)* shows the possibility of further simplification. Here, the point of the break is the abscissa value of that curve-point whose ordinate value is $0{\cdot}5[t_{ik}/(t_k - t_i)]$.

It can often be found that at certain sections of the pipeline oils of different quality are transported. Thus, it may occur that even between two pressure testing stations of the damaged pipe section, oil slugs of two different qualities flow. In such a case, the time v. length diagrams of the pressure wave, for both oil qualities, must be separately determined. By these curves and applying the above process two hypothetical break points are determined. The real break point will fall between the two calculated values. Being aware of the approximate place of the slug boundary at the moment of the break, the curves, time v. length may be made more accurate and thus, the location, if it is necessary, can be improved.

In spite of the fact that by applying the pressure wave method not only the place of leakage, but, obviously its occurrence may be also determined, the *T/1* processes are useful as well. The simultaneous application of different methods significantly increases the reliability of leak detection. In the Federal Republic of Germany, e.g., the simultaneous application of two independent methods is prescribed.

### 7.3.2. The detection of small leaks

*Type T/3.* The oil flowing out of the pipeline through a small leak and seeping into the soil generates sound. The flow being turbulent, a high frequency ultrasound develops that may be detected by instruments. Depending on the fact whether the measurement takes place outside or inside of the pipe wall, two types of solutions are known. In the first case, the detection and simultaneously the location of the leak is carried out by the help of a *contact microphone mounted on the outer surface of the pipe wall* sensing ultrasounds. Before the measurement, at certain points the soil is dug up and removed from the outside surface of the pipeline. If the leakage point is bracketed, then the next measurement is carried out at the midpoint between the two former test places. The first measurements were carried out by MAPCO in distances ranging from 1·2 – 9·6 km, and the accuracy of location was about 180 m (*Pipe Line...* 1973). In the other type of detection, pipe-pigs, *pistons, moving along together with the liquid stream* are inserted into the line, that are suitable for observing and recording ultrasounds. The signals are recorded on magnetic tape. After the bringing out of the piston, the location may be carried out on the basis of recorded velocity data of the pipe-pig and the recorded signals of outside mounted locators. In Karlsruhe, a significant amount of work was devoted to the determination of the conditions, among which, at the outflow of the oil through a small leak, ultrasonic signals of proper strengths can be obtained. It has been established that the intensity of the sound significantly depends on the cavitation occurring at the outflow, and on the stream being turbulent or not. The applicability range of this process was also determined (Naudascher and Martin 1975).

*Type T/6.* The "heart" of this process is an electric cable conducting alternating current. It consists of two metal wires insulated by a special material, soluble in oil. If this insulator is wetted by oil, or by any oil product, then it gets solved, the two metal wires get into contact, and by changing the resistance of the cable, in the monitor of the control station a warning signal appears. On the basis of the modified resistance, the leakage detector determines the distance where the short-circuit in the cable has taken place. The "Leak X" system, operating on the very same principle, is also suitable for indicating the damages caused by bulldozers (*Hydrocarbon*... 1973).

*Other process-types.* Location by pipe-balls (Gagey 1975). A rubber ball of a diameter exceeding the pipeline diameter by 1·5 percent is placed in the pipe, and this ball is transported by the flow for a distance of $A$. Then, the pumping is stopped, and the pressure of pipe-section $A$, and that of the remaining section $B$ is measured by a sensitive gauge. If leakage occurs in section $B$, then at an ideal case, supposing

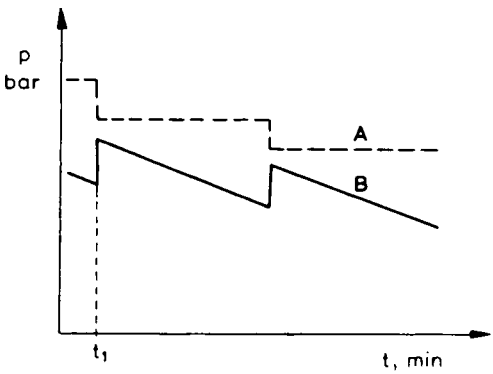


Fig. 7.3–4. Ideal pressure lines of leak location by pipe ball in isothermal flow, after Gagey (1975)

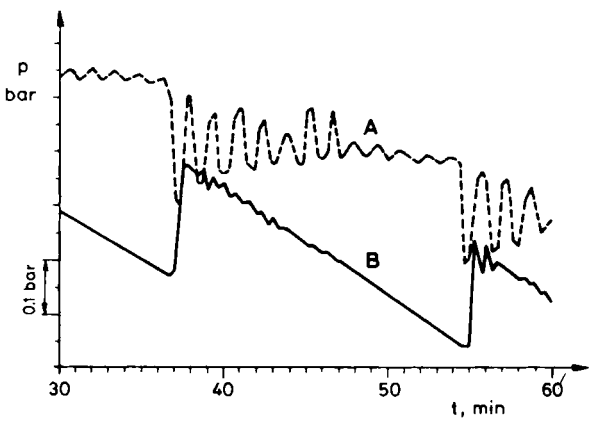


Fig. 7.3–5. Real pressure lines of leak location by pipe ball in isothermal flow, after Gagey (1975)

isothermal flow, pressure profiles, shown in *Fig. 7.3–4* are obtained. Pumping stopped at moment $t_1$. In section *A* the pressure remains unchanged, while in the section *B* it decreases continuously to the point, at which across the two sides of the ball a pressure differential of 0·1 – 0.5 bar, required for the moving the ball develops. Then the ball starts to move, and after covering a short distance it stops again. Due to this ball displacement, pressure in section *A* slightly decreases, and then remains

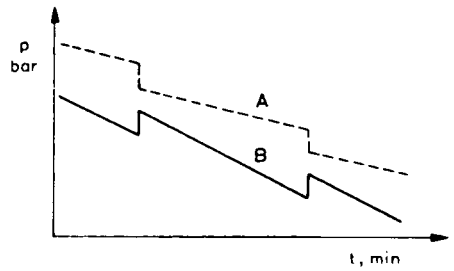


Fig. 7.3 – 6. Ideal pressure lines of leak location by pipe ball, after non isothermal flow (Gagey 1975)

constant. The pressure in section *B*, after a sudden, slight rise, decreases further continuously. In reality, due to the peculiar motion of the ball, getting stuck from time to time, the ideally straight pressure lines are modified. In *Fig. 7.3–5* real, measured pressure lines are shown. If, before the stopping, flow was not isothermal, then the theoretical pressure lines are similar to those, shown in *Fig. 7.3–6*. Because due to the cooling of the oil, the pressure in section *A* is also reduced. The rate of decrease in the pressure, however, is smaller here than in section *B*. If, after the first experiment, the ball is transported at a farther point of the pipeline, then other experiments, similar to the one described above, may be carried out, and so the spot of the leakage may be determined with an ever increasing accuracy. By this method even relatively small leaks can be well detected.

## 7.4. Isothermal oil transport

The temperature of the oil, flowing in a pipeline, generally varies along the length of the line. If, however, the viscosity of the crude is low, and the starting temperature does not significantly differ from soil temperature, then, for practical reasons, the flow may be considered isothermal.

### 7.4.1. Oil transportation with or without applying tanks

Main parts of the transporting system are the pipeline and the pump stations. If the oil is to be transported to a place located at a relatively small distance, then, one pump station at the head end point may prove to be sufficient. If, however, the pipeline is long then the building of several, so-called booster pump stations is

required. Formerly, at the booster stations, also cylindrical, vertical storage tanks of atmospheric pressure were used. The pump station in the head end $k$ of a pipeline section transported crude to the tanks of the tail end point $i$, and from these tanks the pumps of station $i$ sucked oil and transmitted it into the next section. The schedule of this solution is shown in *Fig. 7.4 – 1(a)*. The main advantage of this

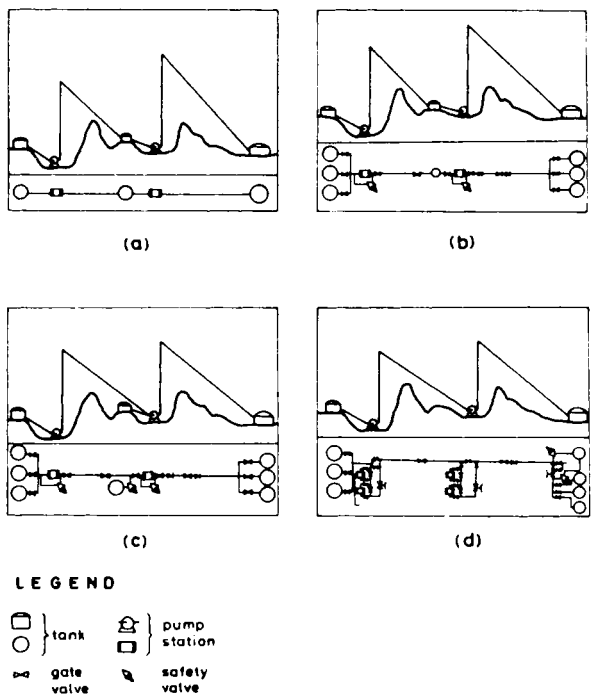


Fig. 7.4 – 1. Oil pipeline transport systems, after Hathaway (1972)

system lies in its simplicity and reliability. The tank farms of the booster stations ensure the elasticity of the transport rate, that is proportional to their storage capacity. The pipeline is the aggregate of hydraulically independent pipe sections. From this system the present method of transportation, operating with reservoirless booster stations had developed. The main stages of the development, after Hathaway (1972) are as follows. For different reasons (e.g. because of the installing scraper traps) mounting of gate valves on the pipeline became necessary. Already at this time, there existed the possibility that due to carelessness the gate valve remains closed at pump starting, and overpressure develops in the pipeline. In order to avoid harmful effects, in case of solution (b) shown in *Fig. 7.4 – 1*, at the pumps by-pass lines equipped with safety valves were mounted. If the pressure, after the pump, exceeded the allowed value, the valve opened, and a part of the oil flowed back

through the valve into one of the tanks of the station. The sketch of the first type of transport system with the booster stations (TBS) operating without storage tanks is shown in *Fig. (c)*. Since the suction pressure may also exceed the allowed value, another branch was installed upstream of the pump, through the safety valve of which the high-pressure oil could be led to a safety tank of relatively small storage capacity. One of the main conditions of the successful operation of TBS without storage tanks is that each pump station, within a very short period of time, should attain the same transport capacity, otherwise heavy positive or negative suction pressure changes may occur. In case of the up-to-date system, shown in *Fig. (d)* the protection against the harmful pressure surges is automatically provided. No safety tank is required. (The required safety equipments and control devices will be discussed, more in detail, in Section 7.5.)

The main advantages of the tankless TBS are the following: the vapour loss during the transport is smaller; the system is less incendiary; because of the lack of the tank farm and its equipment the investment costs are significantly lower; it can work without personnel, and especially, in case of unpopulated areas considerable additional costs may be spared; the greater leaks in the line are easier to detect because of the higher line pressure.

The disadvantages are, that the system requires a technically more advanced control system, and better trained personnel for periodical maintenance and checking; the transport capacity may decrease due to the fact that the oil must arrive at the pump with a higher than the bubble point pressure; any change in the parameters of the transporting process has an effect on the total length of the pipeline, and this, on the one hand may lead to dangerous pressure surges, on the other hand it requires the permanent co-ordination of the pump-station operation.

The pressure changes may be of two types. In the first group the relatively slow changes can be classified. These may be caused e.g. by the paraffin deposits on the inside pipe wall, or by the vapour caps developing at the top points of the pipeline. The change in these cases generally does not exceed the value of 0·1 bar/day. Rapid changes in pressure may originate, from the pressure surges due to the changes in transport parameters (see Section 7.1.1), or by batch transport. Flowing a slug interface through the pump, pressure change of even 10 bar/min order may occur. Against the damaging impacts of such changes in pressure only an automated control system may provide protection.

### 7.4.2. Design of fundamental transport operations

#### (a) Pressure traverse and maximum capacity of pipelines

Let the specific energy content of the flowing oil be $W_1(J/N)$ at the head end, and $W_x(J/N)$ at a distance of $l_x$ m from the head end. The decrease in specific energy content is equivalent to friction loss, i.e. it is

$$W_1 - W_x = \frac{p_1 - p_x}{\rho g} + \frac{v_1^2 - v_x^2}{2g} + z_1 - z_x = \frac{\Delta p_{fx}}{\rho g}. \qquad 7.4-1$$

Let us express the formula $\Delta p_{fx}/\rho g$ as $h_{fx}$, and substitute Eq. 1.1 – 1 to express $\Delta p_{fx}$, then we obtain

$$h_{fx} = \frac{\lambda v^2}{2gd_i} l_x = \xi_f l_x , \qquad 7.4-2$$

where the hydraulic, or friction gradient is

$$\xi_f = \frac{\lambda v^2}{2gd_i} \qquad 7.4-3$$

Substituting formula $v = \frac{q}{\frac{d_i^2 \pi}{4}}$ and the $g = 9{\cdot}81$ value we find that

$$\xi_f = 0{\cdot}0826 \frac{\lambda q^2}{d_i^5} . \qquad 7.4-4$$

Each term of Eq. 7.4 – 1 permits a twofold physical interpretation. They may be considered, on the one hand, as energy contents of a liquid body of unit weight, in $J/N$ units, and on the other, as liquid column heights in m, the density of the liquid being $\rho$.

The $p/\rho g$ term the specific external potential energy is equivalent to pressure head $h$ and the specific kinetic energy $v^2/2g$ to velocity head $h_v$, while the specific internal potential energy to the geodetic height, denoted by $z$. Neglecting the change in the specific volume of the flowing liquid, due to the change of pressure, in case of isothermal flow $v_1 = v_2$, i.e. the velocity head difference between two pipeline cross sections is zero. It means, that Eq. 7.4 – 1 can be expressed in the following, simpler form:

$$W_1 - W_x = h_1 - h_x + z_1 - z_x = \xi_f l_x . \qquad 7.4-5$$

In isothermal flow $\xi_f$ is constant, and therefore the specific energy content of the flowing oil, along the pipeline linearly decreases along the pipeline. On horizontal terrains $z_1 = z_2$, and thus Eq. 7.4 – 5 is further simplified, as

$$h_x = h_1 - \xi_f l_x , \qquad 7.4-6$$

i.e. the pressure head of oil, flowing in the pipeline, decreases linearly with distance along the pipeline.

The alteration of the components, characterizing the specific energy content, in case of pipelines laid on hilly terrains, is shown in *Fig. 7.4 – 2.*

*The pressure head $h_1$ at head end K required to move oil at a flow rate q* through pipe of *ID* $d_1$ laid over a given terrain can be determined as follows. Using Eq. 7.4 – 3 the gradient $\xi_f$ is calculated. *A* line with a slope corresponding to this gradient is drawn from tail end *V* to head end *K*. This is the pressure or piezometric traverse *1'* in *Fig. 7.4 – 2.* If this line intersects the ground profile, then the pressure traverse must be displaced parallel to itself until it will merely touch the ground profile (line

*l*). The initial pressure head $h_1$ is the above ground section of the ordinate at the head end *K*. It is recommended for satefy to augment $h_1$ by 30 – 50 m, with due attention to the reliability of the basic data. The point *M* where the pressure traverse is tangent to the ground profile is called critical. This is where the pressure head of the flowing liquid is least. Hydraulic gradient is greater between points *M* and *V* than between *K* and *M*. Consequently, if there is no throttling at the tail end, flow is free beyond the critical point and oil will arrive at atmospheric pressure at the tail

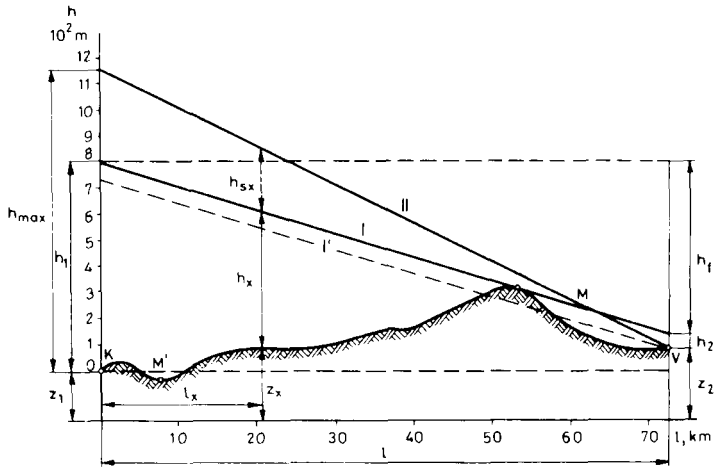


Fig. 7.4 – 2. Pressure traverse of pipeline laid over a hilly terrain

end tank. If throttling is applied at the tail end, the oil will have a pressure head of $h_2$ at the end point: *V* is usually above ground level, at the maximum possible liquid level of the tail-end tanks.

Another critical point as far as pipe strength is concerned may be valley point *M'*. It is necessary to calculate the pressure head *h* above *M* and find out whether pressure $p = h\rho g$ does not exceed the maximum allowable operating pressure of the pipeline. If the allowable pressure is exceeded, then pipes of greater wall thickness have to be applied or pressure reducing valves (see later) are to be installed.

*Example 7.4 – 1.* Let a pipeline of *OD* $d_o = 219{\cdot}1$ mm and *ID* $d_i = 209{\cdot}5$ mm ($s = 4{\cdot}78$ mm) be laid over the terrain shown in *Fig. 7.1 – 2*. The throughput at the temperature of transportation is $q = 150$ m³/h; $\rho = 830$ kg/m³; $v = 7{\cdot}5 \times 10^{-6}$ m²/s; $l = 72{\cdot}4$ km, and the equivalent roughness of the pipe is $k = 0{\cdot}2$ mm. Determine the pressure traverse and find the pump pressure $p_P$.

The Reynolds number is

$$N_{Re} = \frac{vd_i}{v} = 1{\cdot}273\frac{q}{d_i v} = 1{\cdot}273\frac{0{\cdot}04167}{0{\cdot}2095 \times 7{\cdot}5 \times 10^{-6}} = \qquad 7.4-7$$

$$= 3{\cdot}38 \times 10^4 .$$

Pipe relative roughness:

$$\frac{k}{d_i} = \frac{2 \times 10^{-4}}{0{\cdot}2095} = 9{\cdot}5 \times 10^{-4}.$$

From the Colebrook formula (Eq. 1.1 – 7) the friction factor is computed by iteration

$$\frac{1}{\sqrt{\lambda}} = -2 \lg \left[ \frac{2{\cdot}51}{3{\cdot}83 \times 10^4 \sqrt{\lambda}} + \frac{9{\cdot}5 \times 10^{-4}}{3{\cdot}71} \right]; \qquad \lambda = 0{\cdot}0253$$

By Eq. 7.4 – 4 the friction gradient

$$\xi_f = 0{\cdot}00826 \frac{0{\cdot}0253 \times 0{\cdot}04167^2}{0{\cdot}2095^5} = 0{\cdot}00899 \text{ m/m}.$$

The ordinate at $K$ corresponding to the intercept of the pressure traverse traced backwards from $V$ according to Eq. 7.4 – 5 is

$$h'_K = h_V + \xi_f l - (z_K - z_V) = 0 + 0{\cdot}00899 \times 72\,400 + 83 = 734 \text{ m},$$

where 83 m is the geodetic-head difference $(z_1 - z_2)$ between point $K$ and $V$. In the Figure, the pressure traverse in question is shown by dashed line $l'$. As it enters the ground, the head-end pressure head actually required is higher: it is obtained by displacing the pressure traverse parallel to itself, making it tangent to the ground profile at the point $M$. Accordingly $h''_K = 800$ m. For safety, let us augment this by 40 m, giving $h_K = 800 + 40 = 840$ m. The pressure head of the pump to be installed at point $K$ should then, be

$$p_P = h_K \rho g = 840 \times 830 \times 9{\cdot}81 = 6{\cdot}84 \text{ MPa}.$$

Assuming that *pumping station exists only at K head end, the greatest throughput of the pipeline* can be determined by the following procedure. Let us plot above the ground profile at $K$ the pressure head $h_{max}$ corresponding to the maximum allowable operating pressure of the pipe *(Fig. 7.4 – 2)*. Joining this point with $V$ (or with critical point $M$, if there is one) we obtain a pressure traverse whose slope corresponds to the maximum feasible pressure gradient $\xi_{fO\max}$. In the knowledge of this latter, the maximum oil throughput, $q_{O\max}$ can be determined as follows.

Let the two constants in Eq. 1.1 – 10 be $a = 0{\cdot}194$ and $b = 0{\cdot}189$. Then

$$\lambda = 0{\cdot}194 N_{Re}^{-0{\cdot}189}. \qquad 7.4-8$$

Introducing this into Eq. 7.4 – 4

$$\xi_f = 1{\cdot}53 \times 10^{-2} \frac{\nu^{0{\cdot}189} q^{1{\cdot}81}}{d_i^{4{\cdot}81}}, \qquad 7.4-9$$

whence

$$q = 10{\cdot}1 \frac{\xi_f^{0{\cdot}552} \cdot d_i^{2{\cdot}66}}{\nu^{0{\cdot}104}}. \qquad 7.4-10$$

Introducing into Eq. 7.4 – 10 the graphically determined value of $\xi_{fO\max} = \xi_f$ we may calculate $q_{O\max} = q$, the maximum liquid throughput of the pipeline if the only pump station is at the head end. The accuracy of the computation can be increased of the value of the friction factor, obtained from Eq. 7.4 – 8, is only considered as first approximation, and then the computation is continued by applying Eq. 1.1 – 7, i.e. the Colebrook formula. Eq. 7.4 – 4, similarly to the above by substituting the relation $v - q$, and the $g = 9{\cdot}81$, respectively, may be simplified to the following form:

$$\lambda_a q_a^2 = 12{\cdot}1 \xi_f d_i^5 , \qquad 7.4 - 11$$

where subscript $a$ refers to the above calculated approximate values. Knowing the value $q_a$ a more accurate Reynolds number, and from the Colebrook formula 1.1 – 7 a more accurate $\lambda_C$ friction factor can be computed. From Eq. 7.4 – 11 it follows that

$$\lambda_a q_a^2 = \lambda_C q_C^2$$

and from this relation the more accurately determined flow rate is

$$q_C = q_a \sqrt{\frac{\lambda_a}{\lambda_C}} . \qquad 7.4 - 12$$

The exact $q_{O\max}$ value is obtained after further iterations.

*Example 7.4 – 2.* Let us find the maximum throughput of the pipeline characterized in Example 7.4 – 1, if API standard pipe made of X-42 steel is used, and terrain belongs to category (a) characterized in Section 6.1 – 3, that is, the safety factor $k = 1{\cdot}3$; let $e = 1$. The pressure rating is calculated using Eq. 6.1 – 3. From Table 6.1 – 3, $\sigma_F = 289$ MPa, and hence by Eq. 6.1 – 2

$$\sigma_{al} = \frac{289}{1{\cdot}3} = 222 \times 10^6 \text{ Pa} .$$

The maximum allowable internal overpressure is

$$\Delta p = \frac{2e\sigma_{al}S}{d_o} = \frac{2 \times 1 \times 222 \times 10^6 \times 4{\cdot}78 \times 10^{-3}}{0{\cdot}2191} = 9{\cdot}69 \cdot 10^6 \text{ Pa}$$

$$\mathrm{h}'_{\max} = \frac{\Delta p}{\rho g} = \frac{9{\cdot}69 \times 10^6}{830 \times 9{\cdot}81} = 1190 \text{ m} .$$

Let us reduce this value by 40 m for safety. Hence, $h_{\max} = 1190 - 40 = 1150$ m. Plotting $h_{\max}$ at the point $K$ and joining it with $V$ we get pressure traverse II. Clearly, the pressure traverse passes above the critical ground-profile section, and the safety reserve of pressure is sufficient also from this point of view. The maximum pressure gradient is

$$\xi_{fO\max} = \frac{1150 - 83}{72\,400} = 0{\cdot}0147 \text{ m/m} .$$

The maximum liquid throughput by Eq.7.4 – 10 is

$$q_{O\max} = = 10{\cdot}1 \frac{0{\cdot}0147^{0{\cdot}552} \times 0{\cdot}2095^{2{\cdot}66}}{(7{\cdot}5 \times 10^{-6})^{0{\cdot}104}} = 0{\cdot}0525 \text{ m}^3/\text{s} =$$

$$= 189 \text{ m}^3/\text{h} .$$

Considering Eq. 7.4 – 7, the Reynolds number based on this pumping rate is

$$N_{\text{Re}} = 1{\cdot}273 \frac{0{\cdot}0525}{0{\cdot}2095 \times 7{\cdot}5 \times 10^{-6}} = 4{\cdot}25 \times 10^4$$

By Eq. 7.4 – 8

$$\lambda_a = 0{\cdot}194 \times (4{\cdot}25 \times 10^4)^{-0{\cdot}189} = 0{\cdot}0259$$

and according to Eq. 1.1 – 7

$$\frac{1}{\sqrt{\lambda}} = -2 \lg \left[ \frac{2{\cdot}51}{4{\cdot}25 \times 10^4 \sqrt{0{\cdot}0259}} + \frac{0{\cdot}2 \times 10^{-3}}{0{\cdot}2095 \times 3{\cdot}71} \right].$$

From this relation, by applying a short iteration we obtain that

$$\lambda_C = 0{\cdot}0243$$

By Eq. 7.4 – 12

$$q_i = 0{\cdot}0522 \sqrt{\frac{0{\cdot}0259}{0{\cdot}0243}} = 0{\cdot}0539 \text{ m}^3/\text{s} = 194 \text{ m}^3/\text{h} .$$

If, at this rate, we calculate again $N_{\text{Re}}$, and then $\lambda_C$, then we receive the previous 0·0243 value, i.e. $q_i = q_{O\max}$.

**(b) Increasing the capacity of pipelines by looping**

Even the maximum throughput $q_{O\max}$ of an existing pipeline may be insufficient to transport the required $q_O$ rate. One of the possibilities to increase the transport capacity of the existing pipe line is looping: a second line, a so-called twin line is laid alongside the original pipeline and is jointed to it. The twin line may be of two types: (i) new line of same length as old line but usually of different diameter (complete loop), (ii) new line shorter than old line but of the same *ID* (partial loop). Exceptionally, pipelines, that are shorter than the original ones, but are of greater internal diameter, are applied. The advantage of the shorter twin line of different diameter, as compared to the full length twin line, is that the transfer capacity of the system, by way of increasing its length may be further increased.

Solution (i) may be regarded as two independent pipelines with the size of the new line chosen so as to deliver a flow of $q_2 = q_1 - q_{O\max}$ under the original input pressure $h_{\max}$ between the points *K* and *V*. Owing to the identity of trace and of input and

output pressure the pressure gradient of the new line is the same as the maximum feasible gradient $\xi_{fO\max}$ of the existing line. $ID$ of the new line may be calculated by the following relation derived from Eq. 7.4 – 9

$$d_i = 0{\cdot}419 \frac{v^{0{\cdot}0393} q^{0{\cdot}376}}{\xi_f^{0{\cdot}208}}. \qquad 7.4-13$$

Supposing that $\xi_f = \xi_{fO\max}$ and $q = q_2$.

(ii) If the new line is to have the same $ID$ as the existing one, and $q_1 < q_{O\max}$, the length of the new line will be less than that of the existing one. The new line is usually laid beginning at either the tail or the head end of the old one. The choice between the two solutions is first of all determined by the ground profile (see later). A pressure traverse for the loop can be determined by the following consideration. When pumping at the prescribed rate $q_1 > q_{O\max}$, the pressure gradient in the single line section is $\xi_{f1} > \xi_{fO\max}$. By Eq. 7.4 – 9

$$\xi_{f1} = 1{\cdot}53 \times 10^{-2} \frac{v^{0{\cdot}189} q_1^{1{\cdot}81}}{d_i^{4{\cdot}81}}. \qquad 7.4-13/a$$

In the double section, the two pipes, of equal size, and subjected to the same head-end and tail end pressure, will both deliver oil at the rate $q_1/2$. The pressure gradient in this section is

$$\xi_{f2} = 1{\cdot}53 \times 10^{-2} \frac{v^{0{\cdot}189} \left(\frac{q_1}{2}\right)^{1{\cdot}81}}{d_i^{4{\cdot}81}}.$$

Dividing the first equation by the second and solving for $\xi_{f2}$, we get

$$\xi_{f2} = \xi_{f1} \left(\frac{1}{2}\right)^{1{\cdot}81} = 0{\cdot}285\, \xi_{f1}. \qquad 7.4-14$$

Equations 7.4 – 13/a and 7.4 – 14, due to the approximative character of the fundamental formulas, are only approximations. They are applied as a first approach and to form a basis for graphic solution. Graphic design is done by tracing a pressure traverse of slope $\xi_{f2}$ forward from head end $K'$ and another pressure traverse of slope $\xi_{f1}$ backward from tail end $V$, if the twin line is to be started at the head end. The new line is to extend to the point where the two traverses intersect. From the arrangement, shown in *Fig. 7.4 – 3*, it is obvious that, in order to avoid intersection with the ground profile, only the version, with the starting point $K$, can be realized. Because of the obtuse section due to the shape of the actual pressure traverses, and, also because of the approximate character of the hydraulic gradients, the length of the looped line must be determined more accurately by way of computation. The basis for this is the geometrical consideration that can be read off the Figure.

$$h = \xi_{fO\max} l = \xi_{f1}(l - l_x) + \xi_{f2} l_x$$

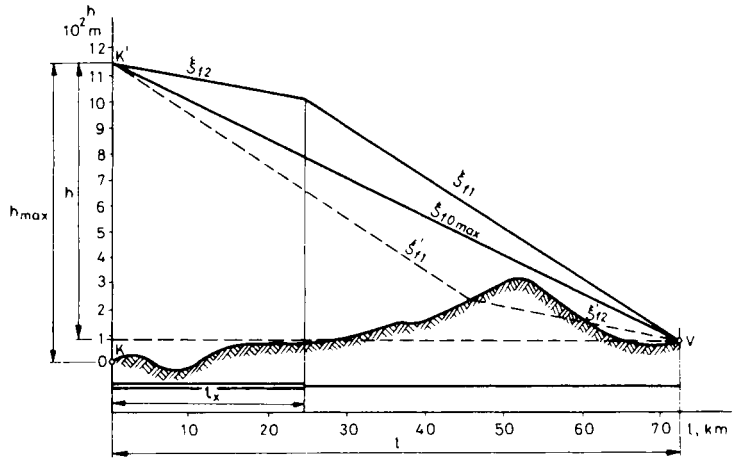


Fig. 7.4 – 3. Pressure traverse of twin (looped) pipeline

that is,

$$l_x(\xi_{f1}-\xi_{f2})=l(\xi_{f1}-\xi_{f0\max})$$

and from this relation

$$l_x=l\frac{\xi_{f1}-\xi_{f0\max}}{\xi_{f1}-\xi_{f2}}. \qquad 7.4-15$$

The exact friction factor for the gradients at turbulent flow in the transition zone may be computed by the Colebrook equation.

*Example 7.4 – 3.* Under the conditions stated in the previous example, existing pipeline capacity is to be increased to 227 $m^3/h$. A full length and a short length loop line are to be designed. (i) For a complete loop,

$$q_2=227-194=33\ m^3/h=0{\cdot}00917\ m^3/s\,.$$

By Eq. 7.4 – 13,

$$d_i=0{\cdot}419\frac{(7{\cdot}5\times10^{-6})^{0{\cdot}0393}\times(9{\cdot}17\times10^{-3})^{0{\cdot}376}}{(1{\cdot}47\times10^{-2})^{0{\cdot}208}}=0{\cdot}108\ m\,.$$

The next standard API pipe has $d_o=114{\cdot}3$ mm (= 4 1/2 in.) (see Table 6.1 – 2). For X-42 grade steel, with reference to Example 7.4 – 2,

$$\sigma_{al}=222\ MPa\,.$$

By Eq. 6.1 – 3

$$s=\frac{\Delta p d_o}{2e\sigma_{al}}=\frac{9{\cdot}69\times10^6\times0{\cdot}1143}{2\times1\times222\times10^6}=0{\cdot}0025\ m=2{\cdot}5\ mm\,.$$

The next standard pipe-wall thicknes according to API Spec. 5LX, is 3·18 mm, and hence, $d_i = 107{\cdot}9$ mm.

Increase of precision of the above result, by applying equations of greater accuracy is generally not required. According to Eq. 7.4 – 4, it is obvious that at the same pumping rate and flow gradient, between the computed approximate (*a* index!), and the true (*C* index !), referring to the friction factors, and pipe diameters, the following relation can be found:

$$d_{iC} = d_a \sqrt[5]{\frac{\lambda_C}{\lambda_a}}.$$

Thus the pipe diameter slightly depends on the value of friction factor, and the more accurate value of the latter may hardly influence the calculated, or, especially the nearest standard diameter of the pipeline.

(ii) In case of a partial loop according to Eqs 7.4 – 9 and 7.4 – 14, the approximate gradients are

$$\xi_{f1} = 1{\cdot}53 \times 10^{-2} \frac{(7{\cdot}5 \times 10^{-6})^{0{\cdot}189} \times 0{\cdot}06306^{1{\cdot}81}}{0{\cdot}2095^{4{\cdot}81}} = 0{\cdot}02036 \text{ m/m}$$

and

$$\xi_{f2} = 0{\cdot}285 \times 0{\cdot}02036 = 0{\cdot}005802 \text{ m/m}.$$

The length of loop line on the basis of the approximate gradients, expressed by both the graphic construction, and by Eq. 7.4 – 15 is

$$l_x = 72\,400 \frac{0{\cdot}02036 - 0{\cdot}0147}{0{\cdot}02036 - 0{\cdot}005802} = 2{\cdot}815 \times 10^4 \text{ m}.$$

If more accurate determination is needed, gradients $\xi_{f1}$ and $\xi_{f2}$ are to be computed by applying a more accurate friction factor relation. The Reynolds numbers, according to Eq. 7.4 – 7 are

$$N_{\mathrm{Re}(q)} = \frac{1{\cdot}27 \times 0{\cdot}06306}{0{\cdot}2095 \times 7{\cdot}5 \times 10^{-6}} = 5{\cdot}10 \times 10^4$$

and, calculated in the same way

$$N_{\mathrm{Re}(q/2)} = 2{\cdot}55 \times 10^4.$$

The friction factors, on the basis of Eq. 1.1 – 7, are

$$\frac{1}{\sqrt{\lambda_{(q)}}} = -2 \lg \left[ \frac{2{\cdot}51}{5{\cdot}1 \times 10^4 \sqrt{\lambda_{(q)}}} + \frac{0{\cdot}2 \times 10^{-3}}{0{\cdot}2095 \times 3{\cdot}71} \right]$$

and hence

$$\lambda_{(q)} = 0{\cdot}0238$$

similarly

$$\lambda_{(q/2)} = 0{\cdot}0266.$$

The flow velocities are

$$v_{(q)} = \frac{0{\cdot}06306}{\frac{0{\cdot}2095^2 \cdot \pi}{4}} = 1{\cdot}829 \text{ m/s}$$

and thus

$$v_{(q/2)} = 0{\cdot}9147 \text{ m/s}.$$

According to Eq. 7.4 – 3

$$\xi_{f(q)} = \frac{0{\cdot}0238 \times 1{\cdot}829^2}{2 \times 9{\cdot}81 \times 0{\cdot}2095} = 0{\cdot}01937 \text{ m/m}$$

similarly

$$\xi_{f(q/2)} = 0{\cdot}005414 \text{ m/m}.$$

So, by the Eq. 7.4 – 15 the more accurate length of the loop line is

$$l_x = 72\,400 \frac{0{\cdot}01937 - 0{\cdot}0147}{0{\cdot}01937 - 0{\cdot}005414} = 2{\cdot}423 \times 10^4 \text{ m}.$$

**(c) Location of booster stations**

The transport of a prescribed flow rate through a pipeline of given trace, and diameter must be carried out by applying the possibly least number of booster stations, thus reducing the investment cost of the pump stations to a minimum. This aim can be achieved by designing pump stations, the discharge pressure of which equals the greatest allowed internal overpressure of the pipeline, and the suction pressure is equal to the atmospheric tank pressure. The pressure profile slope, the flow gradient, between two pump stations is determined by the oil rate $q_1$ to be transported in the pipeline of a given diameter. The first pump station is located at the head end point, *K*. From the $h_{max}$, plotted here the pressure profile line corresponding to the pressure gradient is to be drawn up to the point, where the line would intersect the curve of ground profile augmented with the tank height. This intersection is the spot where the second pump station must be located. Here again, the $h_{max}$ is plotted, and the graphical design is to be continued, until the oil is transported to tail end point, *V*, by the last pump station. While applying this design method, it is supposed, that at the booster station storage tanks of atmospheric pressure are used (see *Fig. 7.4 – 4*). At tankless booster stations the suction pressure may not be lower than the bubble point pressure of the oil. Here, the stations will be closer to each other than in case of transporting systems applying tanks, and, so the number of stations will be greater.

*Example 7.4 – 4.* The transport capacity of the pipeline, described in the previous Example, must be increased to 340 $m^3/h$ by applying booster stations. The location of the pump stations with tanks is to be designed.

The Reynolds number for an oil flow rate of 340 $m^3/h = 0{\cdot}0945$ $m^3/s$, according to Eq. 7.4 – 7, is $7{\cdot}6 \times 10^4$. The friction factor, calculated from Eq. 1.1 – 7 is 0·0226. The

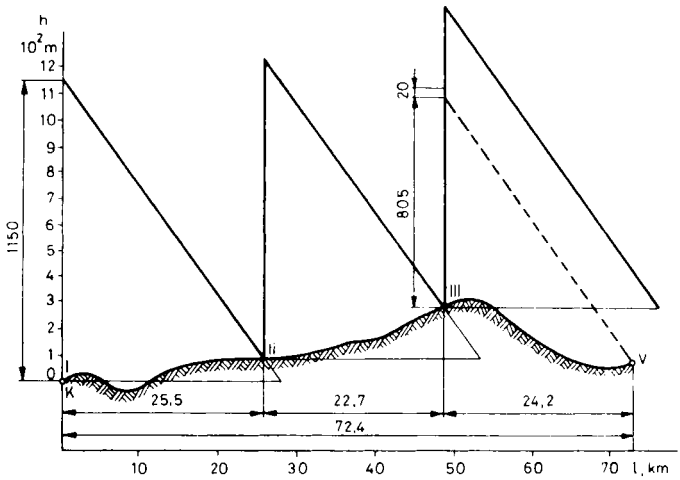


Fig. 7.4 – 4. Pressure traverse of pipeline with booster station

hydraulic gradient, by using Eq. 7.4 – 4 is

$$\xi_f = \frac{0{\cdot}0826 \times 0{\cdot}0226 \times 0{\cdot}0945^2}{0{\cdot}2095^5} = 0{\cdot}0413 \text{ m/m}.$$

The allowed maximum pressure head, according to Example 7.4 – 2, is 1150 m. Completing the design by using values of $\xi_f$ and $h_{max}$, from *Fig. 7.4 – 4* it can be seen that at pump station *III* the $h_{max}$ value is needlessly high. The discharge head required can be found by tracing a pressure traverse backward from point *V*, in which case the head in question is the height difference between the point *III* and the pressure traverse, and has a value of 805 m. Its value, increased for safety reasons by 20 m, is $h_{III} = 825$ m.

The transport system must carry oil generally in the whole year and sometimes of different qualities and flow rates. Even if the oil quality remains the same, its viscosity, together with the change in the soil temperature during the annual period, changes. Thus, the booster stations must be designed keeping the maximum throughput, and the occurring maximum viscosity values, always in mind. In case of hilly terrains it is to be checked that the forecasted smaller rates should be also transportable.

In *Fig. 7.4 – 5*, after Young (1960), the ground-profile of a tankless oil pipeline, and the station design traverses are shown. In the course of the design process it must be considered, that, due to the geodetic height of the terrain points, and to the hydrostatic pressure, respectively, how high is the possible maximum pressure head; what is the realizable minimum suction pressure and the minimum pressure at the critical highpoints, while considering the bubble point pressure. The design was started with rate $q_1$. On this basis the places of the tank stations, shown, are

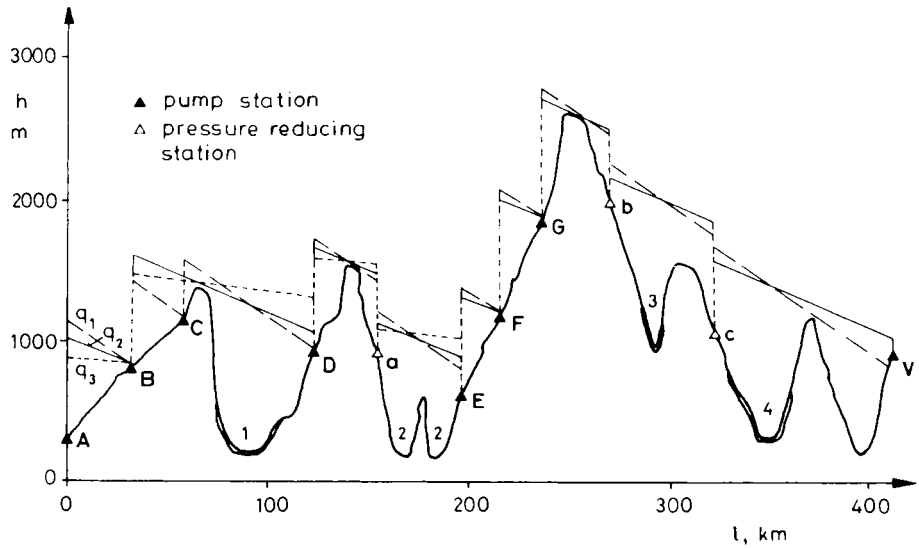


Fig. 7.4–5. Transport system planning in the case of hilly area, after Young (1960)

determined. In order to protect the low sections against overpressure, in valley *1* a thick walled pipe, marked with double line, in valley *2* pressure reducer station, marked *a*, and for the valley sections *3* and *4* the application of thick-walled pipes, and the building of the pressure reducing stations, *b*, and *c* was planned. At pump station *B*, the pump discharge pressure was reduced, otherwise the required pressure head of station *C* might have been too small. The version is irreal, since the pressure traverse at terminal *V* would show a "negative head", even in case of the highest maximum pressure that can be realized at pressure regulating station *c*. If the forecasted rate is smaller, the flow gradient is smaller too, and, sometimes only in principle, the pump stations can transport to a greater distance. The number of required stations, may be smaller than in case of higher rates. From the Figure it can be seen that, e.g. the transportation of a flow rate $q_2$, which is less than $q_1$, is realizable and for this task pump station *C* is not needed. In case of an even smaller flow rate $q_3$ on one hand, pump station *C* is needless too, on the other hand the version is irreal, since the minimum possible suction pressure before the pump station *E* is so large that the pipeline pressure in the valley section 2, would exceed the allowed value.

**(d) Optimum diameter and trace of the pipeline**

Most advantageous is the pipeline, that, between the given end-points, enables the transportation of the prescribed oil flow rate at the minimum transportation cost. The transportation cost consists of three cost components, differing in

character, and these are the depreciation costs of the investment, the maintenance plus operational costs, and the other, additional costs. In the next section, only the first two components will be considered, and their sums will be called, as direct costs. This simplification does not hamper the determination of the relative economic efficiency of several technical solutions, i.e. the choice of the version providing the minimum transportation cost. The total cost is proportionally greater with the third component. The consideration of this is justified if the costs of pipeline transport are compared to the transport costs of other methods e.g. to the costs of transporting by containers.

In order to determine the minimum value of the direct transportation costs, two problems must be solved: a) the determination of the optimum pipe diameter, and b) the designing of the optimum trace. Solving these problems, we suppose that the yearly oil transport is constant during the operational life of the pipeline. The real circumstances are generally more complicated. The pipeline is operating several decades long. If it transports only the production of a relatively known oil producing area, then the yearly throughput generally changes, but its rate may approximately forecasted. In such a case the pipe diameter is considered to be the optimum, at which the aggregate cost of the transportation is the lowest, considering the total transportation life. While designing it must be also considered, that from year by year, the oil volume will be transported possibly by pump stations of various numbers, and capacity. The situation may be further complicated, if the planned annual throughput is modified by unexpected circumstances, e.g. a new oil field is discovered, and its output should be transported also by the given pipeline. In such cases, starting from the existing transport system, we must design and realize a capacity increase that enables the reconstruction in the most economical way.

**(A) The optimum pipe diameter**

If the throughput to be transported annually is considered to be constant, then the optimum diameter of the pipeline can be determined by the following consideration. From *Fig. 7.4−6* it can be seen that in case of constant yearly throughput, the amortization cost $A$ increases with the increase in the pipe diameter, while the operational cost $B$ is reduced. The total cost of transportation, $K$, is obtained by summing the values of $A$ and $B$. The curve $K=f(d_i)$ has a minimum value. The pipe diameter $d_{i\,\mathrm{opt}}$, corresponding to this minimum point is the most advantageous, most economical.

$d_{i\,\mathrm{opt}}$ may be determined in one of two ways. a) Estimating costs for various pipe sizes, a plot similar to the one in *Fig. 7.4−6* is prepared and $d_{i\,\mathrm{opt}}$ is determined graphically. b) Optimum pipe size is calculated using a suitable mathematical formula, e.g. the one introduced by Smith–Brady–Donnell.

The total annual cost of transportation is

$$K = A_1 + A_2 + B_1 + B_2 . \qquad 7.4-16$$

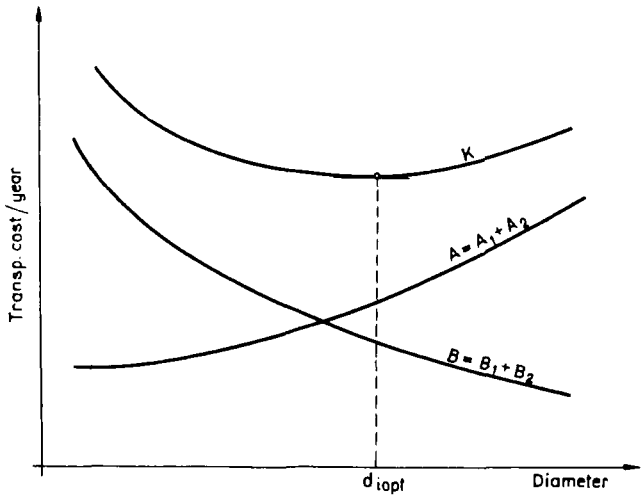


Fig. 7.4–6.

Here, depreciation $A_1$ is defined as

$$A_1 = (a_1 + a_2 d_i) l z_1 ,$$

where $a_1$ is a cost component independent of the pipe size, e.g. ditch cutting, and back filling within limits, and supervision in Ft/m. Ft being the abbreviation of the Hungarian monetary unit (Forint)*; $a_2 d_i$ is the cost component depending on the pipe size (pipe price, transportation to the site, welding, painting, insulation, pressure testing), $a_2$ is in Ft/m$^2$ units; $z_1$ is the annual depreciation rate of the ready-to-operate pipeline, and $l$ is the length of the pipeline in m.

The annual depreciation of a pump station is

$$A_2 = P b z_2 = \frac{q \rho g h b z_2}{\eta} , \qquad 7.4-17$$

where pump station output $P = \frac{q \rho g h}{\eta}$, W; $b$ is unit cost of the station, in Ft/W; $z_2$ is the annual depreciation rate of the pump station; and $\eta$ is the overall efficiency of the installation.

Using Eqs 7.4–2 and 7.4–9 we get

$$h = 1{\cdot}53 \times 10^{-2} \frac{v^{0{\cdot}189} q^{1{\cdot}81} l}{d_i^{4{\cdot}81}} .$$

* Other occurrencies, of course, can be used in these equations similarly.

Substituting this into Eq. 7.4 – 17 we find

$$A_2 = 1{\cdot}53 \times 10^{-2} \frac{q^{2{\cdot}81} \rho g v^{0{\cdot}189} b_2 z_2 l}{d_i^{4{\cdot}81}}. \qquad 7.4-18$$

The annual operating cost is

$$B_1 = Pcef,$$

where $c$ is the operating time over the year in s; $e$ is the specific energy consumption (J/J for electric motors and kg/J for internal compustion engines); $f$ is the unit price of power, or fuel (expressed in Ft/J, or Ft/kg).

Using the symbols introduced when deriving Eq. 7.4 – 18 we obtain

$$B_1 = 1{\cdot}53 \times 10^{-2} \frac{q^{2{\cdot}81} \rho g v^{0{\cdot}189} cefl}{\eta d_i^{4{\cdot}81}}. \qquad 7.4-19$$

The annual cost of maintenance $B_2$ may be considered constant. Let us replace the terms on the right-hand side of Eq. 7.4 – 16 by the above-defined expressions, and determine the derivative $\mathrm{d}K/\mathrm{d}(d_i)$. Putting the obtained relation equal to zero, and solving for the diameter we get, by the rules of calculus the pipe size that ensures the least cost of transportation

$$d_i = \sqrt[5{\cdot}81]{3{\cdot}18 \times 10^{-3} \frac{q^{2{\cdot}81} \rho g\, v^{0{\cdot}189} (bz_2 + cef)}{a_2 z_1 \eta}}. \qquad 7.4-20$$

In calculating optimal pipe size we have so far tacitly assumed the pipeline to operate without interruption, that is, at 100 percent exploitation. In reality, transportation is most often intermittent to a greater or lesser degree. The pauses in transportation provide the flexibility needed to handle excess output due to non-uniform production, breakdown etc., on the input side. A lower exploitation efficiency will, however, augment the specific cost of transportation. Transportation costs may be analyzed for various (constant) pipe sizes and variable throughput. Let us replace by the above defined expressions the terms of the right-hand side of Eq. 7.4 – 16. Let us contract the coefficients except $d_i$ and $q$ into constants denoted $C_i$; then we obtain relation

$$K = C_1 + C_2 d_i + C_3 d_i^{-4{\cdot}81} q^{2{\cdot}81}.$$

Let the length of the line be one km, and let us divide both sides of the equation by the annual oil throughput, $C'q\rho$. Let $K/C'q\rho = k$ denote the unit cost of transportation in Ft/(kg km) then

$$k = C_4 q^{-1} + C_5 d_i q^{-1} + C_6 d_i^{-4{\cdot}81} q^{1{\cdot}81}. \qquad 7.4-21$$

The relationship defines a set of curves, $k = f(q)_{d_i}$. The set in *Fig. 7.4 – 7* has been plotted, using a similar relationship. The ordinate is calibrated in terms of a relative specific transportation cost $k_{rel}$ referred to some base value (derived from a diagram

by Cabet 1966). In the Figure, the optimum sizes in the individual throughput ranges are indicated by separate lines. Clearly, the greater the desired throughput, the larger the optimum pipe size, and the loss the unit transportation cost. This family of curves cannot, of course be used directly in design work, as the constants in Eq. 7.4 – 21 will differ from case to case.

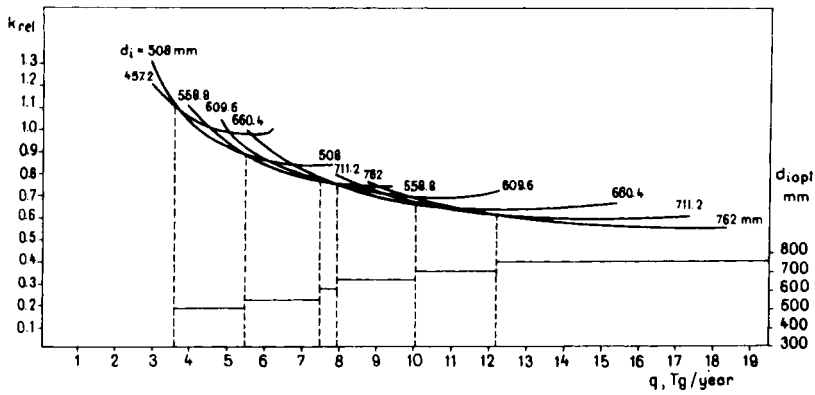


Fig. 7.4 – 7. Optimum pipe size v. throughput, after Cabet (1966)

*Table 7.4 – 1*, after R. Cabet (1966), lists the main cost components of the Le Havre–Paris pipeline, built in 1964. The depreciation costs and other financial expenses, here, are substantial.

Depreciation is in principle the annual decrease in the actual value of an installation. Book depreciation and actual depreciation often do not agree. Operating companies prefer book depreciation to be as high as possible. In France, for instance, the period for amortization prescribed by law is 30 years for buildings,

Table 7.4 – 1. Transportation cost components of the Le Havre–Paris oil pipeline (after Cabet 1966)

| Cost components | $10^6$ Francs | % |
|---|---|---|
| Depreciation | 6 534 | 30·7 |
| Debt servicing | 2 830 | 13·3 |
| Operating cost | 11 931 | 56·0 |
| Payroll | 4 035 | 18·9 |
| Power | 2 850 | 13·4 |
| Maintenance | 1 688 | 7·9 |
| Telecommunications | 275 | 1·3 |
| Others | 3 083 | 14·5 |
| Total | 21 295 | 100 |

20 – 25 years for pipes, 10 years for motors, pumps and five years for automation, and control equipment. In reality, however, since the introduction of cathodic protection, pipes have practically unlimited life. Even so, although the actual life of the equipment and fittings may be longer than the amortization periods mentioned above, these periods may nevertheless be technologically justified, as the progress of technology may make obsolete the equipment in use by putting on the market equipment and fittings more advanced both technically and economically. The relative depreciation (moral wear) of the existing installations will thus be accelerated.

### (B) The optimum trace of pipelines

In case of an underground pipeline of pre-determined diameter, made of steel of a given grade, the specific investment costs consist of two components. The first of these is the line cost for unit length, while the second component stands for the specific costs of digging the ditch, the laying of the pipeline, the backfilling, the clean-up operations, and the damages to be paid to the owner of the ground, concerned. Summarizing the different specific investment costs, from section to section of different lengths, along the selected trace, we obtain the total investment cost. The main factors, influencing the optimum trace with the possibly smallest investment cost, are the following: prohibited areas for pipeline laying (e.g. settlements, closed military areas); the undulation of the area; the increase of the pipe-wall thickness at the section passing through safety zones; the specific construction costs valid for soils of different types; the cost of the intersection of natural, or man-made lakes or rivers, marshes; damages; the requirements concerning the branching lines; and accessibility.

Before the designing of the trace of the pipeline a design map must be prepared that indicates all the parameters that may influence the construction costs of the pipeline. Previously, the trace on this map was plotted by the designers on personal considerations. Because of the high investment costs, the optimum version should be determined by applying computers. Such procedures, discussed in the literature may be classified as the network method, and as the method based on dynamic programming (Lesic 1973; Babin *et al.* 1972; Shamir 1971). Both from the aspects of the data preparation, and the running time on the computer, the procedure based upon dynamic programming proved to be the preferable one. In the next section the essence of the design method developed at the Department of Petroleum Engineering of the Miskolc Technical University for Heavy Industry, based on Kaufmann's procedure (1968) is discussed (Szilas *et al.* 1978).

The process can be interpreted by the help of *Fig. 7.4 – 8.* The head point of the pipeline, *A*, and the tail end-point, *O*, are given. The dashed lines $x_0 \ldots x_5$ are the border lines of areas of different specific construction costs. For the sake of lucidity, the boundaries of the prohibited areas and level lines of the ground are not indicated. The former will be referred to while explaining the next example, while the impact of the latter is shown by the cost indicating at the connecting lines. On the

boundary lines points are taken, the number and place of which are determined by the required accuracy. In the Figure these points are marked with symbol o. The first section, plotted between $x_0$ and $x_1$, corresponding to the fixed $A$ point and the assumed points of $B$, $C$, and $D$ may be a straight line section of $AB$, $AC$, or $AD$. The construction cost of the individual pipe section is obtained that the specific construction cost of the pipe is multiplied by the length of the pipe section. In the

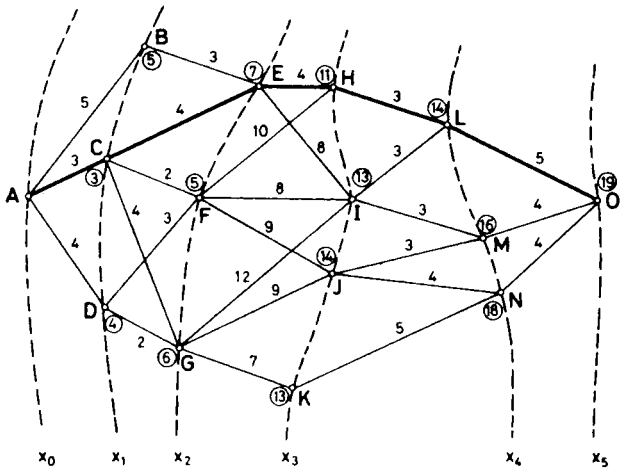


Fig. 7.4 – 8. Planning of the optimum trace of the pipeline

Figure these costs are indicated by the figures *5*, *3*, and *4* written beside the lines. In general, let us mark the construction cost of the individual pipe sections by the formula $v_i(x_{i-1}, x_i)$. Due to similar considerations, the construction costs of any pipeline, crossing the designated points, and connecting the points $A$ and $O$ may be calculated from

$$v_s(x_0, x_1, x_2, x_3, x_4, x_5) = v_1(x_0, x_1) + v_2(x_1, x_2) + v_3(x_2, x_3) + \\ + v_4(x_3, x_4) + v_5(x_4, x_5). \qquad 7.4-22$$

The determination principle of the trace of minimum cost is that each pipeline section must be optimum, i.e. of the minimum construction cost, on the one hand up to the point from which the section starts, and on the other hand, from this point till the end point of the section. Designing is to be carried out section by section, by applying boundary lines.

The line section of minimum cost between the boundaries $x_0$ and $x_1$ is

$$\text{MIN } v_1(A, X_1) = \min(5, 3, 4) = 3$$
$$X_1 = B, C, D,$$

where "MIN" means the "minimum" restriction referring to the mathematical formula, while "min" indicates that from the numerical values the smallest value is to be selected. $X_1$ designates the point on boundary line $x_1$.

The construction cost of the first, and second line sections between the boundaries $x_0$ and $x_2$ will be the minimum, if, between $A$ and $X_2$ points the traces of minimum cost are determined, and from the values obtained, the smallest is chosen, i.e. MIN $v_{1,2}(A, X_2)$. It is to be calculated as follows:

$$\begin{aligned} \text{MIN } v_{1,2}(A, E) &= \text{MIN } [(v_1(A, X_1) + v_2(X_1, E)] = \\ &= \min (5+3,\ 3+4,\ 4+\infty) = 7 \\ X_1 &= B, C, D \end{aligned}$$

$\infty$ sign was used where between the two actual points, because of prohibited areas pipelines may not be layed.

$$\begin{aligned} \text{MIN } v_{1,2}(A, F) &= \text{MIN } [(v_1(A, X_1) + v_2(X_1, F)] = \\ &= \min (5+\infty,\ 3+2,\ 4+3) = 5 \\ X_1 &= B, C, D \\ \text{MIN } v_{1,2}(A, G) &= [(v_1(A, X_1) + v_2(X_1, G)] = \\ &= \min (5+\infty,\ 3+4,\ 4+2) = 6\,. \end{aligned}$$

The minimum values corresponding to the proper points are encircled. The numerical value of

$$\text{MIN } v_{1,2,3}(A, H);\ -(A, I);\ -(A, J) \text{ and } -(A, K)$$

may be similarly determined. The minimum is

$$\text{MIN } v_{1,2,3}(A, X_3) = \text{MIN } v_{1,2,3}(A, H) = 11\,.$$

Considering the first four sections

$$\text{MIN } v_{1,2,3,4}(A, X_4) = \text{MIN } v_{1,2,3,4}(A, L) = 14\,.$$

Finally, for the total line length we can state

$$\begin{aligned} \text{MIN } v_{1,2,3,4,5}(A, O) &= \text{MIN } [(v_{1,2,3,4}(A, X_4) + v_5(X_4, O)] = \\ &= \min (14+5,\ 16+4,\ 18+4) = 19 \\ X_4 &= L,\ M,\ N\,. \end{aligned}$$

The minimum construction cost is determined by ACEHLO, the solid line in the Figure, the magnitude of which is 19 units.

It can occur with the trace, determined by the above method, that the pipe length is longer, or/and due to the level differences of the pipelines the demand for specific pumping power is greater than in case of other trace variants of greater construction costs. Such a case may occur first of all, if on the terrain, between the two end points, the level difference is very significant, or terrain spots of very high laying costs are present. Then, in order to achieve the determination of the optimum trace, further considerations, and calculations are needed.

The design method, discussed above, among the prevailing Hungarian conditions, decreases the construction cost of the pipeline, by 1·7 – 7·6 percent as compared to the traditional design method.

### (e) Selection of centrifugal pumps

For transportation of oil, generally horizontal axis multistage centrifugal pumps of radial double suction, and radial discharge are applied. The structure, and operation characteristics of the centrifugal pumps are discussed in several manuals. In this Chapter, only the peculiarities are discussed that are of outstanding importance, regarding the transportation of oil.

The characteristic diagrams of the operation of the centrifugal pumps, given by the manufacturers, are determined by using water. Curve $H$ in *Fig. 7.4 – 9* is the so-

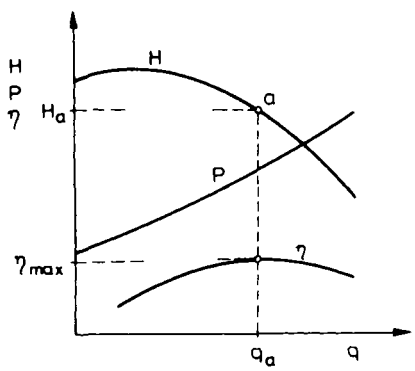


Fig. 7.4 – 9. Characteristic curves of centrifugal pump

called throttling curve representing the change in the (manometric) head, $H = \Delta p/\rho g$ in the function of the transported water flow rate, $q$. $\eta$ is the overall efficiency of the pumps, $\eta = \eta_m \eta_h \eta_v$, where $\eta_m$ comes from the friction of the seals, and bearings, and from the so-called "disc-friction" of the impellers rotating in the space, filled with liquid; $\eta_h$ is the hydraulic efficiency depending on the head losses of the fluid stream due to friction hitting and the change in the flow direction; $\eta_v$ is the volumetric efficiency. Curve $P$ gives the change in the power requirement of the pump, v. pumping rate.

The curves may be determined also by in situ tests, measurements. Among the operation parameters of the pump, the following relations may be determined:

$$\frac{H_1}{H_2} = \frac{n_1^2}{n_2^2}; \quad \frac{q_1}{q_2} = \frac{n_1}{n_2}. \qquad 7.4-23a, b$$

Thus, we may conclude the

$$\frac{q_1}{\sqrt{H_1}} = \frac{q_2}{\sqrt{H_2}} = \text{const}. \qquad 7.4-24$$

The efficiency curve has got its maximum. The pump should be selected so that its operating point would coincide with this best efficiency point *(BEP)*, corresponding to $\eta_{max}$.

By the affinity parabolas, expressing Eq. 7.4 – 24 in a graphic way, it can be determined on the one hand the congruent, head curve, at $n_2$ speed, of the pump where the original head curve was determined for $n_1$ speed, on the other hand, it can be constructed at what speed the given $q-H$ operating point may be realized. On *Fig. 7.4 – 10*, the head curve, represented by solid line is valid for the speed $n_1$. Knowing the *BEP* (a) determined by $q_{a1}$ and $H_{a1}$ the affinity parabola, intersecting it may be determined, and likewise the affinity parabolas, crossing points *b* and *c* may

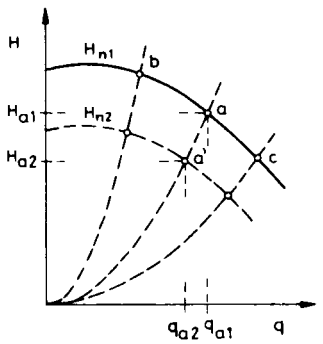


Fig. 7.4 – 10.

be also plotted. Points of the head curve, that are valid at the required $n_2$ speed may be obtained so, that we read off the intersection point coordinates $q_{a1}$, $H_{a1}$ belonging to *a* affinity parabola and speed $n_1$ head curve and from the relation, derived from Eq. 7.4 – 23

$$q_{a2} = q_{a1} \frac{n_2}{n_1}$$

we calculate the flow rate $q_{a2}$, whose corresponding affinity parabola point (*a'*) will be, one point of the $n_2$ head curve. In the same way, the other points of the new head curve, with the help of the affinity parabolas, may be plotted.

If, however, the $n_2$ speed is sought, by which an operating point, defined by the $q_{a2}$ and $H_{a2}$ values, may be achieved with the maximum possible efficiency, then supposed the coordinates of *BEP* are known at $q_{a1}$ from Eq. 7.4 – 23 it can be calculated that

$$n_2 = \frac{q_{a1}}{q_{a2}} n_1 .$$

The application ranges of the centrifugal pumps are well shown by the so-called iso-efficiency diagram *(Fig. 7.4 – 11)*. Beside the head curves, corresponding to different speeds (thicker solid line), some curves, indicating iso-efficiency (thinner solid line) are also shown.

The brake power, at each $q$, $H$, $n$ points of the area, is to be calculated from

$$P = \frac{q\rho gH}{\eta}. \qquad 7.4-25$$

A frequently accurring problem is that a rate, differring from that of the best efficiency point, generally a smaller rate, must be transported through the pipeline by the pump. *Fig. 7.4 – 12* shows the head curve of the pump ($H$), and the change of $H_v = h + h_f$ head loss v. rate at the pipeline flow. If, temporarily, a smaller rate than

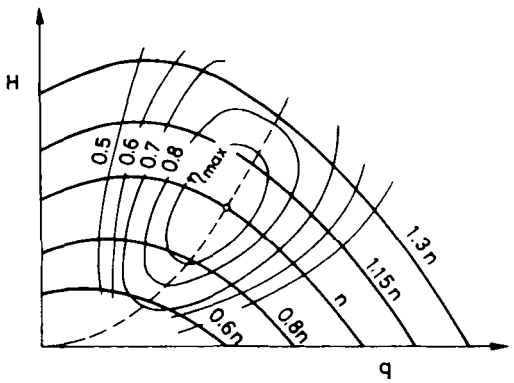


Fig. 7.4 – 11. Iso-efficiency curves of a centrifugal pump

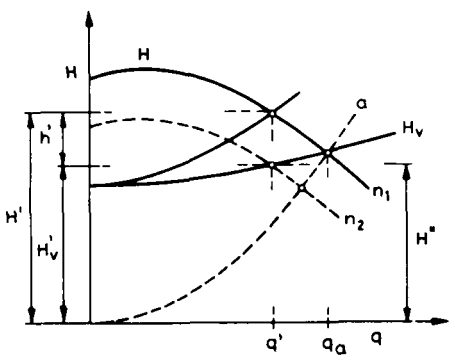


Fig. 7.4 – 12. Determination of the characteristics of the decreased delivery

the above value is to be transported, then two solutions are possible. One of them is, that the gate valve, adjusted after the pump on the pipeline, is throttled to the extent, that the $H'$ head, corresponding to the $q'$ rate should equal the sum of the line head loss, $H'_v$, and the $h'$ throttle loss. It is clear that a significant proportion of the pressure head, developed by the pump, is "uselessly" dissipated in this way. The

other alternative is that the required rate is achieved by a decreased pumping speed. If the speed is decreased from $n_1$ to $n_2$, the operating point $q'$, $H''$ remains close to the affinity parabola crossing $a$ point. The iso-efficiency curves, represented in *Fig. 7.4 – 11* show that this change is accompanied only by an insignificant decrease in the pump efficiency, and that is why it is generally much more economic than the control by throttling (Fishel and Howe 1979). After Liu (1981), about the energy

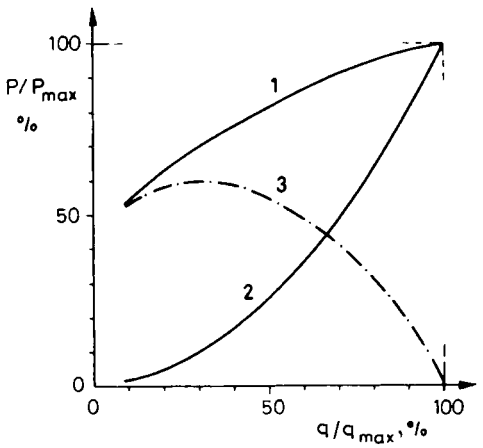


Fig. 7.4 – 13. Energy demand of rate control by throttling (1) and by rpm-alteration (2), after Liu (1981)

requirements of the two control methods information is given by *Fig. 7.4 – 13* that indicates the specific energy demand $P/P_{max}$, for transportation by throttling (curve *1*), and for transportation by decreased speed (curve *2*) in the function of $q/q_{max}$. Curve 3 shows the saving, if, instead of the throttling, transportation is accomplished, by change of speed.

It may occur that a greater rate is to be transported than the capacity of the existing pump. In such cases two, and less frequently more pumps are connected. The connection may be in parallel, or in series. In *Fig. 7.4 – 14* after Feizlmayr (1975), schemes of pump stations, applying parallel, and serial connections respectively are presented. The pumps of the station in part (a) are in parallel. The station is equipped with safety devices, such as valve and tank, and also with automatic scraper trap. In (b) station the pumps are in series, and here the change of the scraper is also possible. In both cases, the prime mover of the pumps is an asynchronous motor. The regulation of the rate is carried out by throttling.

In most cases the pumps in parallel are alike i.e. they can be characterized individually by the same head curve, transporting oil from a common suction line into a common discharge line. The resultant head curve may be plotted so that the double $q_x$ values of the original head curve are determined at different $H_x$ heads. The points, defined in this way, are connected by a solid line (see *Fig. 7.4 – 15*). The new

operating point is, thus, determined by the intersection of the system curve, $H_r$, and the resultant head curve ($H_{II}$). Accordingly, the corresponding rate will be always smaller than the double value of the rate transported by one pump, i.e. $q_{IIa} < 2q_{Ia}$. In case of crude oil pipelines the parallel connection is considered to be more advantageous, when the static portion of the flow losses is relatively high, i.e. the oil must be transported to "hill". In the opposite case (e.g. the dynamic loss is greater),

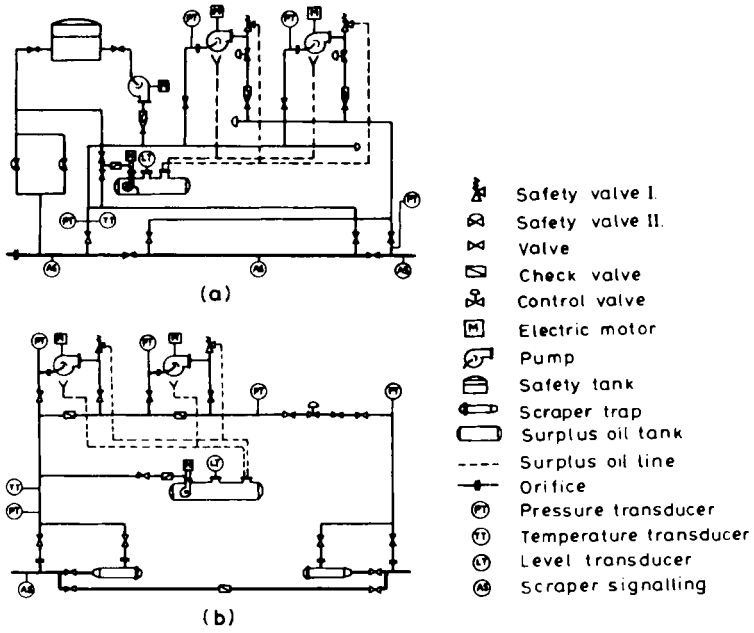


Fig. 7.4 – 14. Parallel and series connected oil transport stations, after Feizlmayr (1975)

the serial joining is the more advantageous. *Fig. 7.4 – 16* shows the original and resultant head curve of the series connected pumps. At any $q_x$ point the pressure head $H_{IIx}$ of the resultant curve is of double height, as compared to the original head curve $H_{Ix}$.

The peculiar, series connected first pump of the pump stations is special *booster pump*. This is generally placed at the deepest point of the area, occupied by tanks, and is a centrifugal pump of big capacity, and small head pressure. Its task is to pump the oil into the suction line of the transporting pump with a pressure, exceeding that of the vapour, and so it may prevent the cavitation damage in the main pump. The booster pump is also able to transport the oil from one tank into the other one, either for treating, or for safety reasons.

The prime movers of the pumps are generally the asynchronous electric motors with fixed, or adjustable speed, operated by alternating current. For the speed

adjustment several solutions are known. Liu (1981) describes a new, modern speed reductor, that is operated on hydraulic principles.

In cases, when the electric energy supply may not be ensured economically, but gas energy is available, first of all gas turbines are applied. Nowadays, Diesel engines are used only in case of relatively small capacities. For the selection of the prime movers, Wright (1981) offers practical criteria. In case of applying parallel connections the motors should be selected on the basis of the power requirement of the independent operation. Either corresponding to the disposition, or, due to the failure of one of the pump units it may occur that only one of the units operates.

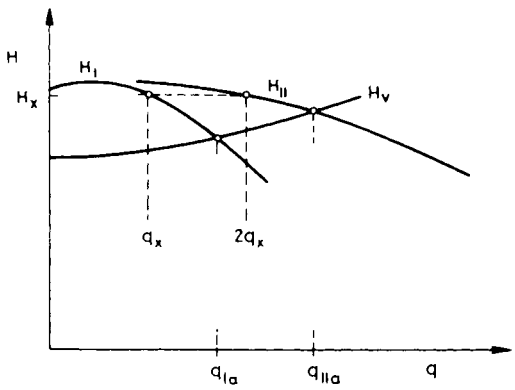


Fig. 7.4 – 15. Resultant head curve construction for parallel connected centrifugal pumps

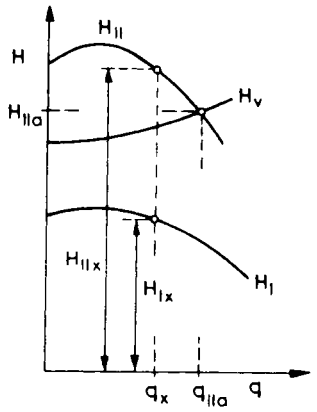


Fig. 7.4 – 16. Resultant head curve construction for series connected centrifugal pumps

All the above discussed problems are valid for both oil and water, supposing that the viscosity of the transported oil is constant. The head curves, given by the manufacturers for water, for oil of differing viscosity may not be, however, directly applied. Let us consider the specific energy transmitted by the ideal, frictionless fluid to be the pump's theoretical transportation head, and denote this value as $H_e$. The actual specific energy increase developing in the real fluid flow is $H$, that is smaller than the theoretical head by a head loss of $h'$, i.e.

$$H = H_e - h' .$$

Basically, the loss in the head consists of losses due to the friction and from drag. At the *BEP* of the pump this latter value may be neglected, and the head loss equals the product of a given energy loss factor, and the kinetic energy. Bobok (1972) indicated that this loss factor, simultaneously to the pipe friction factor, is the function of the Reynolds number, and the wall roughness. At a given rate consequently the smaller the actual head of the given pump is, the greater is the viscosity of the transported oil. Thus, the greater is the viscosity of the oil, the more downward the head curve, valid for the Newtonian oil of greater viscosity than the water, shifts.

No general solution is knonw, by which the head curve, measured at any pump for water, could be applyied for oil. The most often cited method is still that of A. J. Stepanoff's, that was developed on the basis of the experiments with solute casing pump without diffuser (Stepanoff 1948). By the pump water, and oils of 11 different viscosities were transported, the kinematic viscosity of which ranged between the values of $1 \times 10^{-6}$ and $1{\cdot}88 \times 10^{-3}$ m$^2$/s. The rpm of the pump ranged between 1240 and 1780, and the $n_q = nq^{0{\cdot}5}H^{\ 0{\cdot}75}$ value was 32–42. On the basis of his

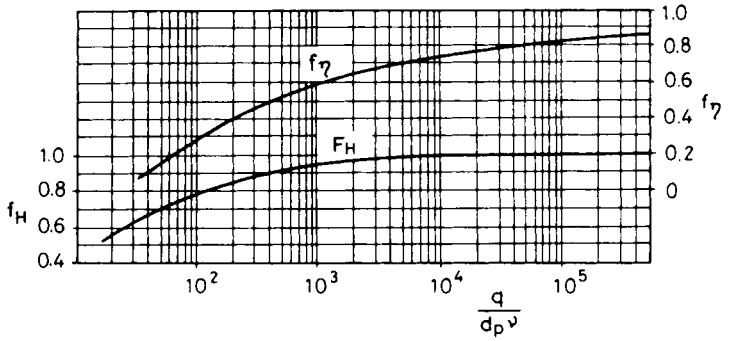


Fig. 7.4–17. Multiplication factors of oil transportation, after Stepanoff (1948)

experiments he determined the diagram, shown on *Fig. 7.4–17* that defines the multiplication factors $f_H$ and $f_\eta$ in the function of the formula $N_{Re} = q/(d_p \nu)$ that is proportional to the Reynolds number. $d_p$ is the impeller diameter of the pump. Moreover, he established that between the values valid for the water, $q_w$ and $H_w$, and those, valid for the oil of $\nu$ viscosity, $q_o$ and $H_o$ the following relation may be introduced:

$$\frac{q_w}{q_o} = \left(\frac{H_w}{H_o}\right)^{1{\cdot}5}. \qquad 7.4-26$$

By applying the above relations, the parameters of the operating point of the head curve valid for water may be converted for fluids of other viscosities. Since according to Falk (1967), with a good approximation, the zero-capacity head, $H_o$, is independent from the viscosity, i.e. it is constant, the head curve valid for the oil may be plotted between the points $q_o$, $H_o$ and $q_{ao}$, $H_{ao}$ with a good approximation. Anderson (1971) describes a nomogram, from which, in case of given $q$, $H$ and $\nu$, the correction factors $f_q$, $f_H$ and $f_\eta$ can be directly read.

*Example 7.4–5.* Let, at the *BEP* be $q_w = 1{\cdot}2$ m$^3$/min, $H_w = 100$ m, $\eta = 0{\cdot}8$, and $d_p = 300$ mm. Let us determine the transportation parameters for an oil of $\nu = 0{\cdot}76 \times 10^{-4}$ m$^2$/s viscosity and $\rho = 850$ kg/m$^3$ density:

$$N_{Re} = \frac{0{\cdot}02}{0{\cdot}3 \times 0{\cdot}76 \times 10^{-4}} = 877.$$

From *Fig. 7.4 – 17*

$$f_H = 0{\cdot}95 \quad \text{and} \quad f_\eta = 0{\cdot}58 .$$

On this basis

$$H_o = 0{\cdot}95 \times 100 = 95 \text{ m} \quad \text{and} \quad \eta_o = 0{\cdot}58 \times 0{\cdot}8 = 0{\cdot}46 .$$

According to Eq. 7.4 – 26

$$q_o = q_w \left(\frac{H_o}{H_w}\right)^{1{\cdot}5} = 0{\cdot}02 \left(\frac{95}{100}\right)^{1{\cdot}5} = 0{\cdot}0185, \text{ m}^3/\text{s}$$

and the power requirement determined by Eq. 7.4 – 25 is

$$P = \frac{0{\cdot}0185 \times 95 \times 850 \times 9{\cdot}81}{0{\cdot}46} = 3{\cdot}19 \times 10^4 = 31{\cdot}9 \text{ kW} .$$

In case of pseudoplastic fluids, corresponding to the power law, the Reynolds number is to be calculated by Eq. 1.3 – 15:

$$N_{\text{Repp}} = \frac{d_i^n \bar{v}^{(2-n)} \rho}{\mu'} \frac{8}{(6+2/n)^n} .$$

If the crude is thixotropic pseudoplastic it must be also considered, that after the storage in tank, i.e. after relaxation, or after flowing for a longer duration, that is, after a significant shear load period, does the oil get into the pump. The flow curves also change in the function of the shear time (see *Fig. 1.3 – 2*). From these curves the one, corresponding to the estimated shear time value, respectively the $\mu''$ and $n$ constants of the exponential equation simulating the above curve, must be substituted into the above relations.

In case of the characteristic curves of the pump, transporting oil, the possibility of the change in the viscosity of the oil must be also considered. The two main reasons for this are, that, on the one hand, the viscosity of the given quality oil may change due to temperature variations, and, on the other hand, the quality of the transported oil may change. The change in temperature may be temporary, or regularly expected. Temporary change may be caused by the temperature alteration of the oil, stored in tank at the first pump station, e.g. because of the modification in the treating technology. Regular alteration is caused by the seasonal change of the pipeline surrounding soil's temperature. During the summer warmer, while during the winter period colder oil gets in to the pumps. Shifts in the operating point may be also caused by the change of the $q - H_v$ system curve due to the alteration in flowing temperature.

The selection of the pump unit, and the control of its operation deserve special attention, if the pipeline transports oil slugs of different viscosities (Menon 1976). In *Fig. 7.4 – 18* three pairs of curves are shown. For all the three curves, $h$ means the heavy, and $l$ the light products (Diesel oil gasoline, resp.).

The curves *I* are valid for the same pump operating at $n$ speed. $H$ head is replaced by $\Delta p$ pressure difference. Curves *II* are the system curves of the pipe where, instead

of head loss $H_v$ pressure loss $\Delta p_v$ is represented. Curves *III* indicate the power of the prime movers, in the function of the transported flow rate. Curves *I* and *II* have four intersections, i.e. four operating points. At the *A* point heavy fluid flows in the pipeline, while light fluid in the pump. The pumped liquid rate is $q_A$, while the pressure increase, developed by the pump is $\Delta p_A$. The pump gradually fills up the pipeline with light product, and during this interval, the operating point slowly (e.g. during some hours) shifts from position *A* to *D*. At the *D* operating point the pump transports light liquid of $q_D$ rate, and the same quality of oil is moving in the pipeline.

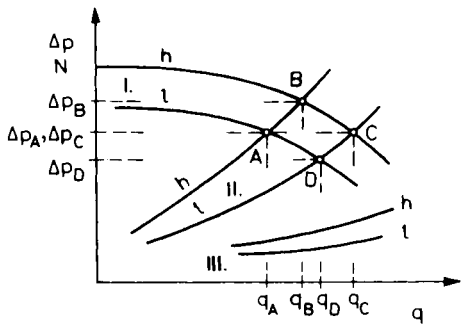


Fig. 7.4 – 18. Characteristic operating points of batch-transport, after Menon (1976)

The transportation parameters further change when heavy oil gets into the pump. In this case the operating point is suddenly shifted to *C* position. The discharge pressure raises to $\Delta p_C$, the rate to $q_C$ values and positive pressure wave may be generated. The operating point, *C*, is then gradually shifted since the pipeline is being filled up with heavy liquid. At the *B* operating point, the pump transports $q_B$ rate of the heavy liquid, and along the total pipeline this type of fluid flows. Further change may occur if light product gets into the pump. Then, the discharge pressure, supposing that the suction pressure remains the same, suddenly decreases by a value of $(\Delta p_B - \Delta p_A)$, and the transportation is continued with the parameters of the *A* operating point. Due to the rapid pressure change negative pressure wave may develop.

For transportation reasons the least favourable is the case when the flow resistance of the pipeline is the greatest, and the pressure increase developed by the pump is the smallest. This phenomenon occurs, when, in the total length of the pipeline heavy liquid of unfavourable flow behaviour is moving, while in the pump light liquid is still to be found. The pump is to be selected on the basis of $q$ and $\Delta p$ parameters of this operating point. If, by the pump selected in this way, a greater rate of light oil than the $q_A$ is to be transported, then it should be taken into consideration at the selection of the prime mover. The maximum transportable flow rate by the selected pump is $q_C$. The motor power corresponding to this value is $P_C$.

To fulfil the task that the selection, arrangement, and the operational capacity of the pumps should be optimum, is of extreme economic importance. Feizlmayr

(1975), while describing the Transalpine Pipe Line (TAL), says that the annular electric energy demand of the system, when fully developed, is about 100 million DM. By the optimum operation of the booster pump stations an annual 3·4 percent savings in electric energy were achieved, as compared to the previous non-optimized operation.

## 7.5. Isothermal oil transport system

The main parts of the transport system are the pipelines, the oil transport starting station, the booster stations, and the terminal. Their location, and, to a certain extent, their selection, is discussed in the previous Chapters. The main accessories and their tasks of the up-to-date oil transport systems with tankless booster stations will be discussed further.

Beside the pumps by-pass line with *check valve* is installed. It has to prevent that after the stopping of the transport a pressure greater than the allowed valve developes. In the upper section of *Fig. 7.5 – 1* (Feizlmayr 1975) the profile of a

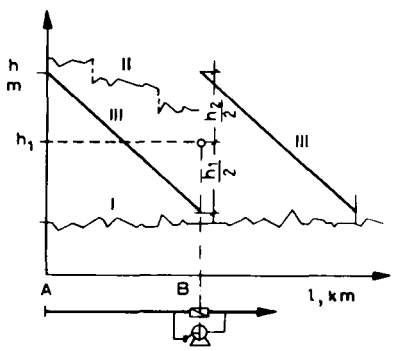


Fig. 7.5 – 1. Overpressure protection by check valve in approximately horizontal terrain, after Feizlmayr (1975)

pipeline, built on a near horizontal terrain (line *I*), the head curve of the allowed internal overpressure (line *II*); and the piezometric curve of the steady state flow (lines *III*) are plotted. At points *A* and *B* there are pump stations. Here, only station *B* is schematically denoted by a pump, and the line is furnished with check valve. If the flow stops, and the check valve, in the line, by-passing the pump *B*, closes, then the pressures in the *A – B* lines are equalized, and a pressure head, approximately equal to the average value, $h_1/2$, develops in it. This value is apparently smaller than the allowed values, determined by the *II* line. If no check valve were applied, the oil could flow back from the pipe section after *B* pump, and so, in unfavourable cases, the pressure at the suction side would exceed the allowed maximum value. In *Fig. 7.5 – 2* (after Feizlmayr 1975), pump stations *A* and *B*, set up on steep terrain are

shown. The task of the check valve, installed beside station *B*, is to prevent an overpressure in the section, following station *A*, after stopping the transportation. If the check valve fails, the oil, through safety valve *1*, flows into safety tank *2*.

*Figure 7.5 – 3* shows the characteristic curves of a given shorter section of TAL (Trans Alpine Pipeline), after Feizlmayr (1975). The marking of the lines is the same, as in case of the former Figure. Due to the great changes in the terrain, the piezometric curve slope, without pressure regulation, after *C* mountain peaks,

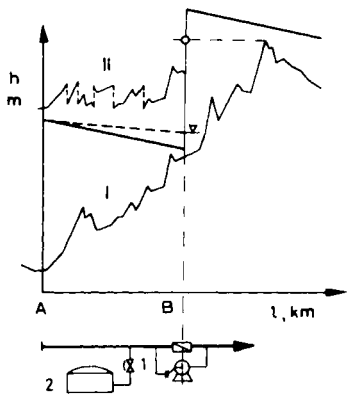


Fig. 7.5 – 2. Overpressure protection by check valve in hilly terrain, after Feizlmayr (1975)

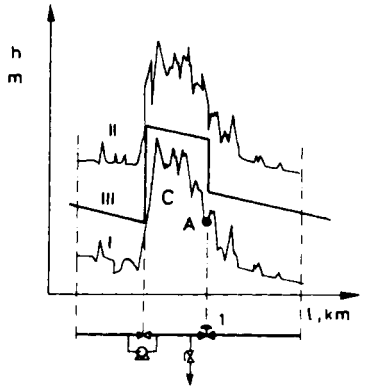


Fig. 7.5 – 3. Creation of the desired piezometric line by pressure regulator, after Feizlmayr (1975)

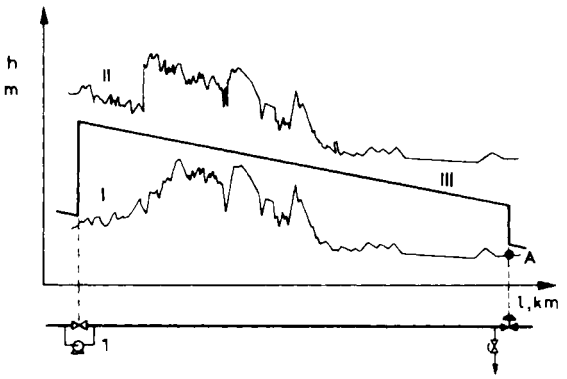


Fig. 7.5 – 4. Creation of the desired piezometric line by pressure regulator at the pipeline end section, after Feizlmayr (1975)

would be greater than the value of pressure curve *III*, required to ensure the flow rate, and for this reason, "non grata" free surface flow would develop (see Section 7.4.1). That is why, at the *A* point, *pressure regulator valves* are installed, that in the given pipe section provides the desired pressure curve slope. *Figure 7.5 – 4* shows the

last section of this very same pipeline. In order to avoid the open flow, at the *A* end-point pressure regulator valve is installed, which ensures the corresponding pressure gradient in the line section after pump *1*. Without this the flow would be open after several mountain peaks.

Generally, the pressure regulator valves do not offer protection against over-pressure, due to quick pressure waves. *Figure 7.5 – 5* shows a longer section of the TAL. At the low points, *A* and *B pressure limiting safety valves* denoted by *1*, are

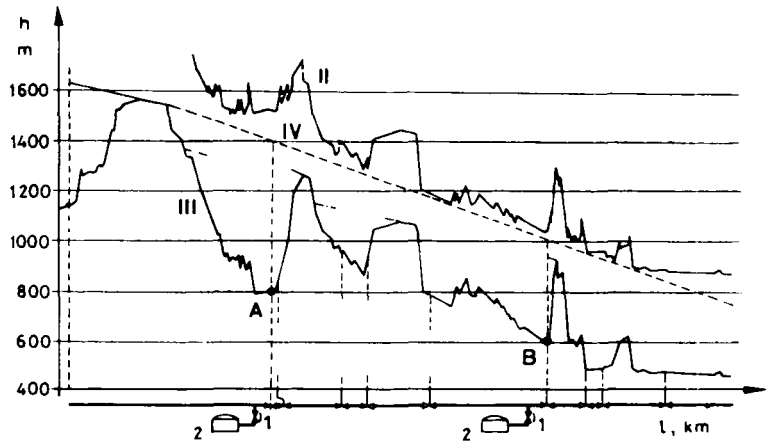


Fig. 7.5 – 5. Pressure regulation of a TAL pipe line section, after Feizlmayr (1975)

applied, that prevent pressures, higher than by the *II* line determined values, in the pipeline. The liquid rate responsible for the excess pressure is led into *safety tanks*, *2*.

Several types of the safety valves are known. The simplest devices of this group of instruments are spring loaded (e.g. see *Fig. 6.2 – 25*). Their disadvantage is that for their opening considerable excess-pressure is required, and their operation is also affected by the downstream pressure. The devices, equipped with pilot valves, accurately open, their operations is not influenced by downstream pressure, their functioning is, however, slow. The valves controlled by instruments (e.g. in *Fig. 6.7 – 9*), may be accurately set, and the prescribed pressure may be changed by remote control. Their operation however, requires external energy sources. The expansible tube type regulator, developed by Grove, seems to prove to be a rapid and reliable safety device requiring no external energy source (Cohn and Nalley 1980). One of its versions is planned to be applied to the oil pipelines of the USSR (*Pipe Line* ... 1979).

The scheme of the system is shown on *Fig. 7.5 – 6*. The pressure *1*, through the throttling valve *2*, acts upon bladder *4*, positioned in accumulator *3*, that separates the oil from the gaseous nitrogen above it in tank *5*. The pressure of this gas has an impact upon the bellows valve *6*, and the elastic flexo tube *7*, installed in it,

respectively. If the gas pressure is smaller than the pressure prevailing in line *8*, then the plastic pipe expands, and the oil from the pipeline, behind the core, through its slots *10* and *11*, flows into the safety tank installed following the *12* overflow line. The task of throttling valve *2* is to delay the impact of line pressure exerted on the outside wall of pipe *7*. On rapid pressure increase a pressure difference develops for a short time between the two sides of the pipe wall, resulting in the opening of the valve. If the pressure rise is of long duration the pressure difference between the two pipe surfaces is equalized, and the valve closes. *Fig. 7.5 – 7* shows how the line

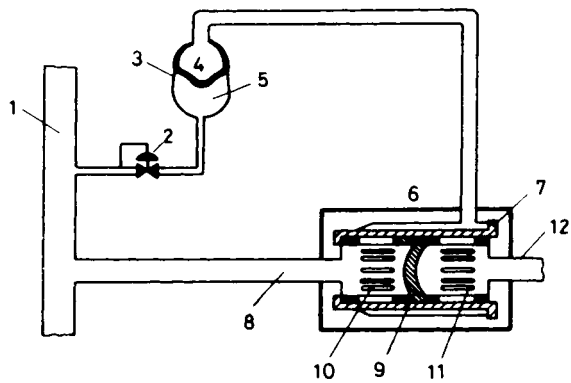


Fig. 7.5 – 6. Expansible tube type safety valve, after Cohn and Nalley (1980)

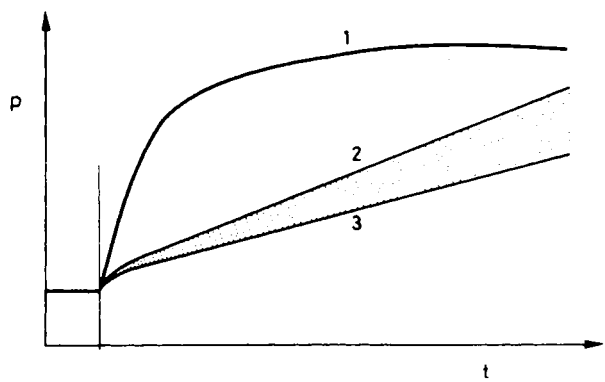


Fig. 7.5 – 7. Pressure lines with and without control, after Cohn and Nalley (1980)

pressure at the receiving pump stations, without safety valve, would change (curve *1*); and, within what maximum (curve *2*), and minimum (curve *3*) values, the pressure will rise due to the safety equipment.

In the prevention of pressures, smaller, or greater than the allowed values, the operation control equipment of the pump stations, has an important role. They

receive the signals from the gauges measuring the pressures at the suction, and discharge sides. If, at any pump station the section pressure is smaller than the allowed value, or the discharge pressure is greater, than the set value, the control unit stops first one of the pumps. Due to this, the intake pressure generally rises, and the discharge pressure is reduced. If the rate in the change is not sufficient, the next pump, or pumps, respectively are stopped by the control equipment. If with the first pump shut-down, pressure change in the desired direction does not occur at all, the

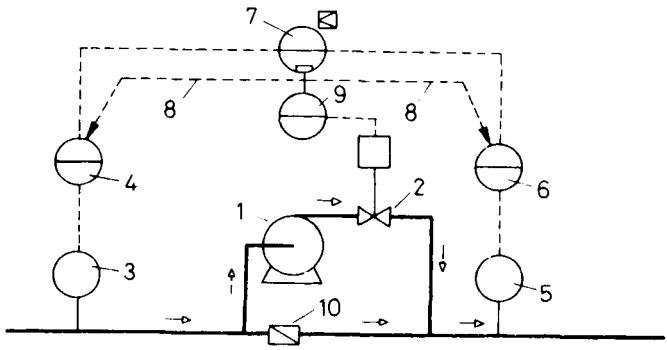


Fig. 7.5 – 8. Pressure control system of a one-pump station, after Cho *et al.* (1977)

alarm shut-down switch after a delay of 10 – 30 seconds stops every pump. A case of this sort may occur, e.g., when the pumps of the head station stop, or, the gate valve after the station gets closed.

In *Fig. 7.5 – 8* the configuration of a pressure control system, applied in the USA can be seen (Cho *et al.* 1977). The operating device, controlling the actions, is the *electrohydraulic throttling valve 2*, installed in the downstream of pump *1*. Check valve *10* is operated independently. The suction pressure is measured by gauge *3*, and the corresponding signals are transmitted to the direct acting controller *4*. Gauge *5* measures the discharge pressure of the pump, and transmits the corresponding signals to the reverse acting controller *6*. If the signals, observed by transmitter *3*, are smaller than the set point value, or the values measured by transmitter *5* are higher, signal selector *7* is alerted. This is connected to the two controllers and transmits the one with lower signals to the valve actuator. If the controllers fail valve *2* also closes. By unit *9* this valve can be manually also controlled. Motor overload could be similarly implemented. A reverse acting controller could be used, with a setpoint equal to the highest allowable current. The output of this would pass through signal selector *7* and would throttle the valve *2* if the motor current rose above the designated value.

*Figure 7.5 – 9* represents (after Cho *et al.* 1977), two series connected pumps at the booster station. At smaller rates one, while at higher rates two pumps transport. If, while operating the first pump, the second pump unit is also started, then the

developing of a pressure wave must be considered. To avoid this, in case of manual regulation, valve *2* is generally throttled before starting the pump, to reduce the pressure rise, due to the pressure surge. After starting the pump the valve is gradually opened. This solution, however, is characterized by a significant loss in energy. In case of programmable set point generator this loss in energy may be reduced. The scheme of this control unit is represented in *Fig. 7.5 – 10.* At stationary transport, with one pump, the parameters of *A* moment are valid. In that case the

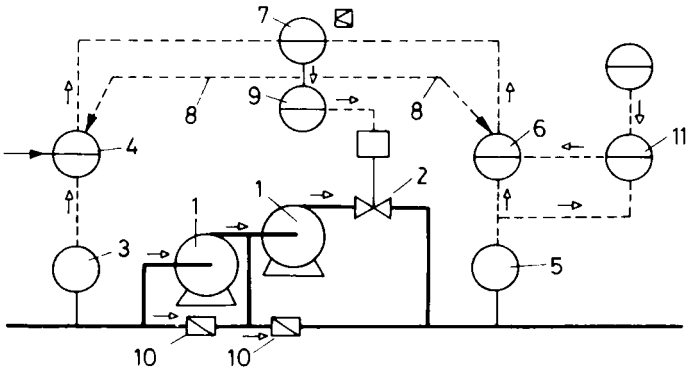


Fig. 7.5 – 9. Pressure control system of a two-pump station, with programmable starting, after Cho *et al.* (1977)

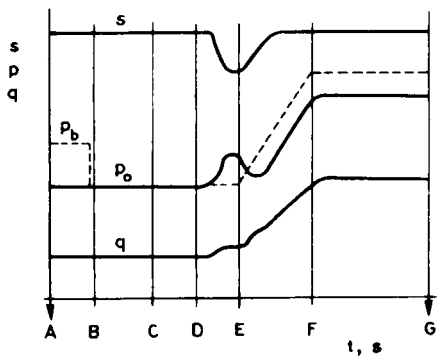


Fig. 7.5 – 10. The change of characteristics of series connected pumps with programmable starting v. time, after Cho *et al.* (1977)

adjusted pressure set point $p_b$ (dashed line) is slightly higher than the measured $p_0$ discharge pressure (solid line). Before starting the second pump, the set point generator is placed in track mode, and then, the set point decreases to the measured pressure (*B* moment). At *C* moment the set point generator is commanded to hold its present value and at *D* the second pump is started. In a short time the pump pressure

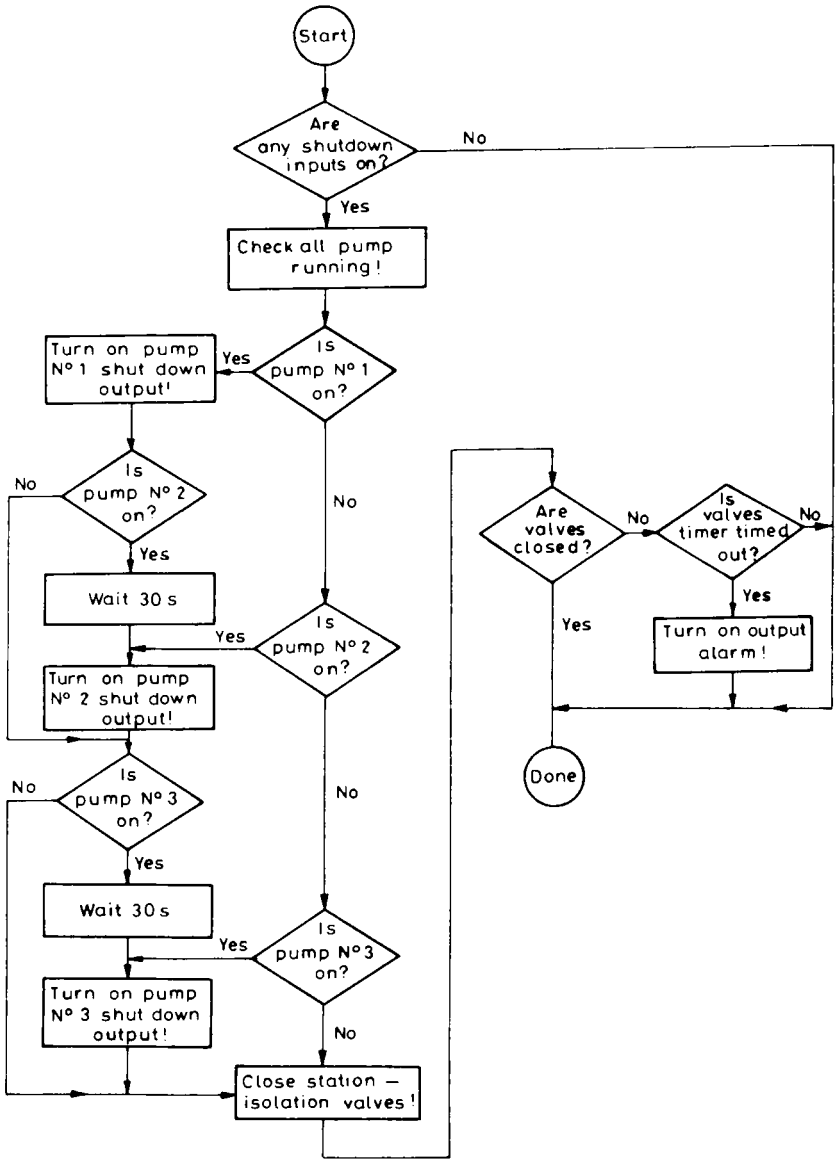


Fig. 7.5 – 11. Flow chart of centrifugal pumps' shut down process, after Muma and Henry (1976)

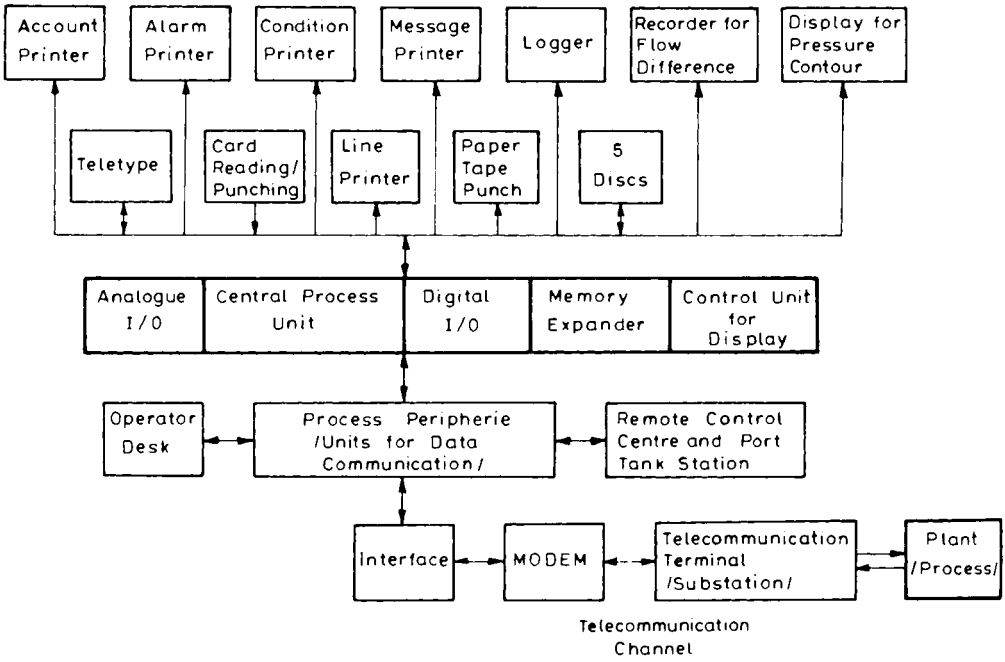


Fig. 7.5 – 12. Computer control's scheme of Europe's "Nord West Ölleitung", after Hoppmann (1976)

begins to increase above the set point value, and the off set causes the controller 6 *(Fig. 7.5 – 9)* to throttle valve *2*. The throttling minimizes the amplitude of the pressure wave. At moment *E*, after the pumping speed is great enough, the set point generator is placed in the ramp-up mode. The controller gradually opens the valve, and the rise at moment *F*, reaches the value, prescribed for the operation of the two pumps. In case of remote control the input signal to controller *4* may be also modified. The control valve is a floating seat full-bore ball valve with electrohydraulic actuator. The up-to-date devices entirely shut down within 3 s. Their parameters are of "equal percentage" (see Section 6.2.1 – (c)). Opening–closing hysteresis, proportional to pressure drop across the valve, must be here also considered.

The Continental Pipeline Co. improved the transport system of an existing 30 in. pipeline of 800 km length (Muma and Henry 1976). Under the control of the central, supervisory master computer, in a hierarchical system, a decentralized system was established, controlled by separate PLCs from pump to pump. The task included the starting-up of the motors, the starting, and shut down of the pumps in a given sequence, the control of the gate valves' operation, and alarm shut-down switches of the station. There are four programs elaborated for the control. As an example, *Fig. 7.5 – 11* shows the flow chart of the shut-down process of the pumps, including that of the gate valves of the stations.

There are several solutions for an up-to-date transport system (Szilas and Oláh 1978). Their common feature is that they are controlled by computers. A good example for a modern project is the north-west European pipeline (Nord West Ölleitung, i.e. NWÖ), that transports oil from the Wilhelmshafen port to six refineries (Hoppmann 1976). The length of the pipeline is 721 km, and it consists of pipe sections of 28″ and 40″ nominal diameters. The informations, flowing through the four wire communication channel (bandwidth ranges between 3000 – 3400 Hz), is received by computers of two systems. The IBM-1800 that belongs to the first has a core memory of 38 K, and 5 peripherical disc memories of 512 K. It works partly in on-line, and partly in off-line mode. The main off-line duties are quantity accounting, making statistics, disposition, planning of pump operation, determination of the load of the tanks, etc. It is used for solving on-line problems requiring relatively high computer capacity. The stored data are at the disposal of the off-line computing too. Such tasks are, among others, calculating the oil quantity balance on the basis of the tank content data, or, the visualization of the existent piezometric line of the pipeline on the computer display at 20 second cycles. The upstream and downstream pressures of the pumps and control valves, the curves, representing the maximum allowable pressures, and the geodetic profile are also visible.

The task of the two Siemens PR 320 computers belonging to the second system is the leak detection in on-line mode. Among the two units having 24 K core memory only one is working permanently. The other, stand-by computer is switched on by the dispatcher only in case of a failure, occurring in the operating unit. The computer, recognizing the leak on the basis of the telecommunicated pressure and rate data, is also able to locate the leak. *Figure 7.5 – 12* shows the scheme of the system, connected to an IBM machine, and also the prepared report types.

## 7.6. Non-isothermal oil transport

If oil viscosity is comparatively high and the temperature of the flowing oil differs appreciably from that of the line's environment, flow can no longer be regarded as isothermal. Pipelines transporting oil are most often buried in the ground. The thermal behaviour of the soil will accordingly affect the temperature of the flowing oil.

### 7.6.1. Thermal properties of soils

The temperature of soil of a given nature, undisturbed by human hand, is determined on the one hand by insolation, and on the other, by heat flowing from the interior of the Earth towards its surface. Insolation has a double period, a daily and a yearly one. The internal heat flow, due primarily to radioactive decay, is constant in a fair approximation at any geographical location. Its magnitude is less by about two orders of magnitude, in the depth range of 1 – 2 metres we are

concerned with, than the effects of insolation, and we shall accordingly disregard it in the sequel. Assuming the soil to be thermally homogeneous, temperature change per unit time is described by Fourier's differential equation

$$\frac{\partial T}{\partial t} = a_s \nabla^2 T \qquad 7.6-1$$

where $a_s$ is the temperature-distribution or diffusion factor defined by the relationship

$$a_s = \frac{\lambda_s}{c_s \rho_s}. \qquad 7.6-2$$

Assuming the surface to be level in an approximation sufficient for our purposes, the above equation describing temperature variations may be used satisfactorily also in its one-dimensional form,

$$-\frac{\partial T}{\partial t} = a_s \frac{\partial^2 T}{\partial h^2}. \qquad 7.6-3$$

Let us characterize the temperature change on the ground surface, that is, at $h = O$ by the relationship

$$\Delta T_O = \Delta T_{O_a} \sin \omega t$$

where $\omega = 2\pi/t_p$. The other symbols are identified in *Fig. 7.6 – 1*. Under physically meaningful initial conditions, Eq. 7.6 – 3 has the solution:

$$\Delta T_h = \Delta T_{O_a} \exp\left[-h\sqrt{\frac{\pi}{a_s t_p}}\right] \sin\left[\frac{2\pi t}{t_p} - h\sqrt{\frac{\pi}{a_s t_p}}\right]. \qquad 7.6-4$$

The extreme temperature fluctuation $\Delta T_{ha}$ at depth $h$ arises when the sine term equals unity, that is,

$$\Delta T_{ha} = \Delta T_{O_a} \exp\left[-\sqrt{\frac{h^2 \pi}{a_s t_p}}\right]. \qquad 7.6-5$$

This equation and *Fig. 7.6 – 1* reveal how the amplitude decreases with depth. Daily fluctuation is almost imperceptible at 1 m depth, being less than 0·1 °C in most cases. The yearly wave will cause measurable temperature changes to depths of 25 – 30 m, depending on the thermal properties of the ground. Beneath a depth of 30 m, temperature will be controlled solely by the terrestrial heat flow. *Figure 7.6 – 1* further reveals that the temperature wave *II* at depth $h$ is displaced in phase against the ground-surface wave. Phase shift is described by

$$\Delta t_p = \sqrt{\frac{t_p h^2}{4\pi a_s}}. \qquad 7.6-6$$

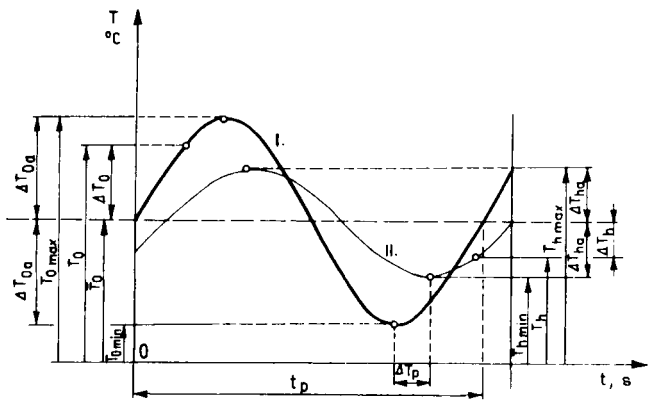


Fig. 7.6–1. Fluctuation in time of soil temperature

*Example 7.6–1.* Find the extremes of the daily temperature fluctuation and the phase shift at 0·3 and 1·0 m depth if $a_s = 4{\cdot}9 \times 10^{-7}$ m$^2$/s, and surface temperature varies from +22 to +2 °C. — In the notation of *Fig. 7.6–1*, surface amplitude is

$$\Delta T_{O_a} = \frac{T_{O\max} - T_{O\min}}{2} = \frac{22-2}{2} = 10\,^{\circ}\mathrm{C}.$$

By Eq. 7.6–5, the amplitude at depth 0·3 m is

$$\Delta T_{ha} = 10 \exp\left[-\sqrt{\frac{0{\cdot}3^2\pi}{4{\cdot}9 \times 10^{-7} \times 86\,400}}\right] = \pm 0{\cdot}75\,^{\circ}\mathrm{C}$$

whereas at depth 1·0 m it is

$$\Delta T_{ha} = \pm 0{\cdot}0018\,^{\circ}\mathrm{C}.$$

The mean temperature is, in a fair approximation,

$$\bar{T}_h = \bar{T}_O = T_{O\min} + \Delta T_{O_a} = 2 + 10 = 12\,^{\circ}\mathrm{C}.$$

Temperature extremes at 0·3 m depth are

$$T_{h\max} = \bar{T}_h + \Delta T_{ha} = 12 + 0{\cdot}75 = 12{\cdot}75\,^{\circ}\mathrm{C}$$
$$T_{h\min} = \bar{T}_h - \Delta T_{ha} = 12 - 0{\cdot}75 = 11{\cdot}25\,^{\circ}\mathrm{C}$$

at 1·0 m depth, they are

$$T_{h\max} = 12{\cdot}002\,^{\circ}\mathrm{C} \text{ and } T_{h\min} = 11{\cdot}998\,^{\circ}\mathrm{C}$$

that is, the fluctuation range at 1·0 m depth is evanescent. Phase shift at 0·3 m depth is stated by Eq. 7.6–6 to be

$$\Delta t_p = \sqrt{\frac{86\,400 \times 0{\cdot}3^2}{4 \times \pi \times 4{\cdot}9 \times 10^{-7}}} = 35{\cdot}5 \times 10^3\ \mathrm{s} = 9{\cdot}9\ \mathrm{h}.$$

Thermal conductivity of the soil depends on the conductivity of the soil matrix, on grain size distribution, on the bulk density of the dry soil, and on humidity. Makowski and Mochlinski, using an equation of Gemant, have developed a relationship describing the thermal conductivity of humid soil (Davenport and Conti 1971). They considered the dry soil substance to be made up of two grain size fractions: sand (0·002 – 2 mm particle size) and clay (less than 0·002 mm particle

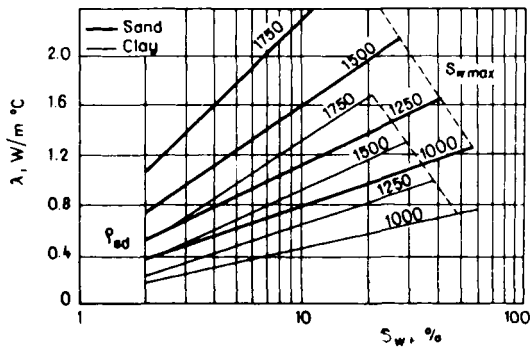


Fig. 7.6 – 2. Influence of water content upon thermal conductivity of sand and clay, after Davenport and Conti (1971)

size). Let the weight percent of clay be $S_c$ and the weight percent of humidity referred to the total dry substance be $S_w$. The thermal conductivity of the humid soil is, then,

$$\lambda_w = (A \lg S_w + B)\, 10^C \qquad 7.6-7$$

where $A = 0{\cdot}1424 - 0{\cdot}000465\, S_c$; $B = 0{\cdot}0419 - 0{\cdot}000313\, S_c$; $C = 6{\cdot}24 \times 10^{-4} \rho_{sd}$.

The determination of the temperature distribution factor requires knowledge of the bulk density and specific heat of the soil. In humid soil,

$$\rho_{sw} = \rho_{sd}(1 + 0{\cdot}01\, S_w) \qquad 7.6-8$$

and

$$c_{sw} = \frac{c_{sd} + 0{\cdot}01\, S_w c_w}{1 + 0{\cdot}01\, S_w} = \frac{c_{sd} + 41{\cdot}9\, S_w}{1 + 0{\cdot}01\, S_w}. \qquad 7.6-9$$

The simplification is based on the fact that the specific heat of water, $c_w = 1$ kcal/(kg K) = 4187 J/kg K. – Introducing the factors defined by the above equations into Eq. 7.6 – 2, we get for humid soil

$$a_{sw} = \frac{\lambda_{sw}}{\rho_{sw} c_{sw}} = \frac{A(\lg S_w + B)}{\rho_{sd}(c_{sd} + 41{\cdot}9\, S_w)}\, 10^C. \qquad 7.6-10$$

*Figure 7.6 – 2* is the diagram of Makowski and Mochlinski (in Davenport and Conti 1971) based on Eq. 7.6 – 7, and transposed into the SI system of units. It gives the thermal conductivity of humid soil v. percent humidity for sands and clays of

different bulk density. *Figure 7.6–3* (from the same source with modification), shows heat diffusivites v. percent humidity, likewise for sand and clays of different bulk density.

Various methods have been devised for determining the in situ thermal conductivity of undisturbed soil. Of these, we shall outline the transient needle-probe method after Makowski and Mochlinski (1956). The transient needle probe is an electrically heated device which can in effect be regarded as a linear source of

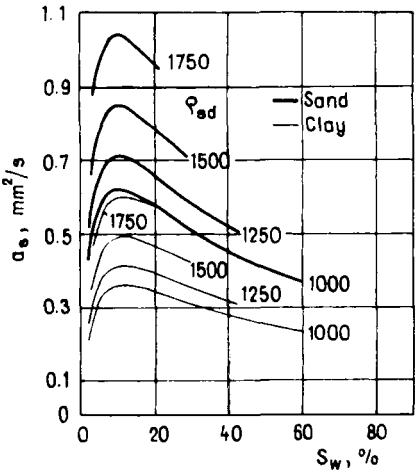


Fig. 7.6–3. Influence of water content upon temperature distribution factors of sand and clay, after Davenport and Conti (1971)

heat. It is inserted into a hole drilled in the soil at the place where the measurement is to be performed, and heated electrically so as to generate a heat flow of constant magnitude. Two thermocouples are attached to the outer, metallic sheath of the probe. They are used to establish its surface temperature at frequent intervals. It can be shown that if heat flow is constant, the temperature of the soil (on the outside of the metal sheath) at a distance equalling probe diameter $r$ from the linear heat source is given after the elapse of time $t$ by

$$T = \frac{\Phi^*}{4\pi\lambda_s r^2}\left[-\mathrm{EI}\left(\frac{r^2}{4a_s t}\right)\right].$$

If $r^2/4a_s t$ is low enough, that is, if $t$ is large as referred to $r^2/a_s$, then

$$\frac{1}{\lambda_s} = \frac{4\pi}{\Phi^*}\frac{T_2 - T_1}{\lg\frac{t_2}{t_1}} \qquad 7.6-11$$

that is, if heat flow $\Phi^*$ is constant, temperature varies as the logarithm of time. Plotting this relationship on log paper one obtains a straight line of slope $\Phi^*/4\pi\lambda_s$,

whence thermal conductivity can be calculated if $\Phi^*$ is known. In reality, steady heat flow will take some time to set in and the relationship will become linear after some time only. This time is, however, short enough (of the order of 10 s). In pipeline-industry practice, the equation is used in a modified form which takes into account that the thermal properties of the probe differ from those of the soil, and contains the electric current generating the heat flow — a directly measurable quantity — rather than the heat flow itself. The depth of penetration of the heat flow into the soil is a mere 20 – 30 mm, and so the measurement is to be repeated a number of times at any location in order to provide a meaningful mean value.

Thermal conductivity in the undisturbed soil is a function of instantaneous humidity, which is affected by the weather. Accordingly, it is necessary to take soil samples simultaneously with the probe measurements, and to determine on these the humidity of the soil, the bulk density of the dry substance, the clay-to-sand ratio and the specific heat. In the knowledge of these data and using Eqs 7.6 – 7 and 7.6 – 11, the thermal conductivity and diffusivity of the soil may be extrapolated to any humidity (Davenport and Conti 1971). A longer-term average diffusivity may be determined recording a full temperature wave on the surface and simultaneously at a depth of $h$ m below ground. Both Eqs 7.6 – 5 and 7.6 – 6 are suitable for calculating $a_s$ in the knowledge of temperature period $t_p$ and amplitude ratio $\Delta T_{ha}/\Delta T_{Oa}$ and phase shift $\Delta t_p$. — The temperature wave may be recorded over a full year, or over the duration of a shorter 'harmonic' wave.

### 7.6.2. Temperature of oil in steady-state flow, in buried pipelines

The flow temperature of oil injected into a pipeline will usually differ from soil temperature, the soil being mostly cooler than the oil. Assuming the heat flow pattern to be steady-state in and around the pipeline, the variation of axial oil temperature in the pipe can be determined along the pipeline as follows. Part of the potential energy of oil flowing in the pipeline, transformed into heat, will warm the oil. A relative increase in temperature will result also from the solid components' separating out of the oil. Oil temperature is reduced, on the other hand, by the transfer of heat from the pipeline into the lower-temperature environment.

In calculating the heat generated by friction let us assume the friction gradient along the pipeline to be constant on an average. A pressure-force differential $\Delta p d_i^2 \pi/4$ along a length $l$ of pipe generates heat in the amount $Q = \Delta p d_i^2 \pi l/4$. Neglecting the reduction in flow rate due to the increasing density of the cooling liquid, we have $l = vt$ and

$$v = \frac{q}{\frac{d_i^2 \pi}{4}}.$$

Using this relationship we may write up the heat generated by friction per unit of time over unit distance of flow:

$$\Phi^* = \frac{Q}{lt} = \frac{\Delta p}{l} q \,[\mathrm{W/m}]. \qquad 7.6-12$$

Let us assume that a temperature drop of 1 °C = 1 K causes the solidification of $\varepsilon$ kg of solids (to be called paraffin for simplicity) per kg of oil. Let the heat liberated by the solidification of 1 kg of paraffin be $\kappa$, in which case a temperature drop of 1 °C will liberate heat in the amount of $q\rho\varepsilon\kappa$, W/K in a liquid of gravity $\rho$ flowing at a rate $q$ per second; $\varepsilon$ and $\kappa$ are temperature-dependent, but we shall assume their mean values to be constant over the temperature range we are concerned with.

Let $k$ denote the heat flow per unit of time into the soil from a unit length of pipe per unit temperature difference, if the whole difference is $T_f - T_s$ (where $T_f$ is the axial temperature of the oil in the pipeline, and $T_s$ is the original soil temperature at the same depth). $k$ is the heat transfer coefficient per unit length of pipe, which we assume to be constant all along the line. The temperature of flowing oil will decrease by $\mathrm{d}T_f$ over a length $\mathrm{d}l$. The change in heat content of liquid flowing at the rate $q$ under the influence of this temperature difference equals the algebraic sum of the heat generated, on the one hand, and the heat lost to the environment, on the other, over an infinitesimal length of pipe $\mathrm{d}l$, that is,

$$q\rho c\,\mathrm{d}T_f = \Phi^*\,\mathrm{d}l + \varepsilon q\rho\kappa\,\mathrm{d}T_f - k(T_f - T_s)\,\mathrm{d}l \qquad 7.6-13$$

or, in a different formulation,

$$q\rho c\,\mathrm{d}T_f - \varepsilon q\rho\kappa\,\mathrm{d}T_f = \Phi^*\,\mathrm{d}l - kT_f\,\mathrm{d}l + kT_s\,\mathrm{d}l.$$

Let

$$q\rho c - \varepsilon q\rho\kappa = A \quad \text{and} \quad \Phi^* + kT_s = B.$$

Rearranging and writing up the integration, we have

$$\int \frac{A}{B - kT_f}\,\mathrm{d}T_f = \int \mathrm{d}l.$$

Solving this equation under the initial conditions $l = 0$, $T_f = T_{f1}$, and resubstituting the values of $A$ and $B$, the flow temperature at the end of a pipeline of length $l$ turns out to be

$$T_{f2} = T_s + \left(T_{f1} - T_s - \frac{\Phi^*}{k}\right) \exp\left[-\frac{kl}{q\rho(c + \varepsilon\kappa)}\right] + \frac{\Phi^*}{k}. \qquad 7.6-14$$

Let us point out that oil temperature will vary also radially in any cross-section of the pipeline. In turbulent flow, radial decrease is slight, but it may be significant in laminar flow. *Figure 7.6 – 4* shows one of the possible combinations of flow-velocity and temperature-distribution profiles after Chernikin (1958). Clearly, in this case the axial temperature $T_f$ of the oil is somewhat higher than the average temperature.

*Example 7.6 – 2.* Let the *ID* of the pipeline be $d_i = 0{\cdot}2$ m, and its length $l = 20$ km. Oil of gravity $\rho = 850$ kg/m$^3$ flows at a steady rate of $q = 100$ m$^3$/h through the

pipeline. Injection temperature, $T_{f1} = 50\,^{\circ}\text{C}$; soil temperature, $T_s = 2\,^{\circ}\text{C}$; $\Phi^* = 7$ W/m; $\bar{\varepsilon} = 3{\cdot}0 \times 10^{-3}$ l/°C; $\bar{c} = 1900$ J/(kg °C); $\bar{\kappa} = 2{\cdot}3 \times 10^5$ J/kg; $k = 2$ W/(m °C). Find the tail-end temperature $T_{f2}$ of the oil (i) assuming that paraffin deposition takes place over the entire temperature range of flow, (ii) assuming that paraffin deposition is negligible, and (iii) neglecting both the effects of paraffin deposition and friction loss.

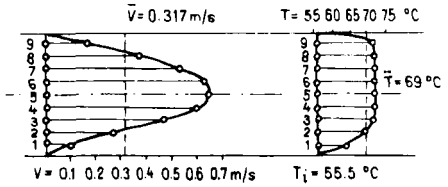


Fig. 7.6–4. Rate-of-flow and temperature traverses of oil flowing in a pipeline, after Chernikin (1958)

(i) By Eq. 7.6–14,

$$T_{f2} = 2 + \left(50 - 2 - \frac{7}{2}\right) \times$$

$$\times \exp\left[-\frac{2 \times 2 \times 10^4}{0{\cdot}0278 \times 850(1900 + 3{\cdot}0 \times 10^{-3} \times 2{\cdot}3 \times 10^5)}\right] + \frac{7}{2} = 28{\cdot}6\,^{\circ}\text{C}.$$

(ii) Assuming that $\varepsilon = 0$,

$$T_{f2} = 2 + \left(50 - 2 - \frac{7}{2}\right) \exp\left[-\frac{2 \times 2 \times 10^4}{0{\cdot}0278 \times 850 \times 1900}\right] + \frac{7}{2} = 23{\cdot}7\,^{\circ}\text{C}.$$

(iii) Assuming that $\varepsilon = 0$ and $\Phi^* = 0$,

$$T_{f2} = 2 + (50 - 2) \exp\left[-\frac{2 \times 2 \times 10^4}{0{\cdot}0278 \times 850 \times 1900}\right] = 21{\cdot}7\,^{\circ}\text{C}.$$

The heat of solidification of paraffin (Chernikin 1958) is rarely taken into account in practical calculations. It may, however, be of considerable importance, as revealed by Example 7.6–2. *Figure 7.6–5* is a diagram of heats of solidification v. melting temperature (after Grosse 1951) for various paraffins and other high-molecular-weight hydrocarbons. The latent heat of the components forming deposits in oil may, according to the data in the Figure, vary rather considerably depending on solid-phase composition. This enhances the importance of knowing the composition and/or thermal behaviour of the components solidifying within the pipeline's temperature range.

As a preliminary indication whether or not the heat generated by friction should be taken into account, the following rule of thumb may be helpful: heat generated by 100 bars of friction loss will raise the tail-end temperature of oil flowing in the pipeline by round 4 °C, irrespective of pipe size and throughput (Haddenhorst 1962).

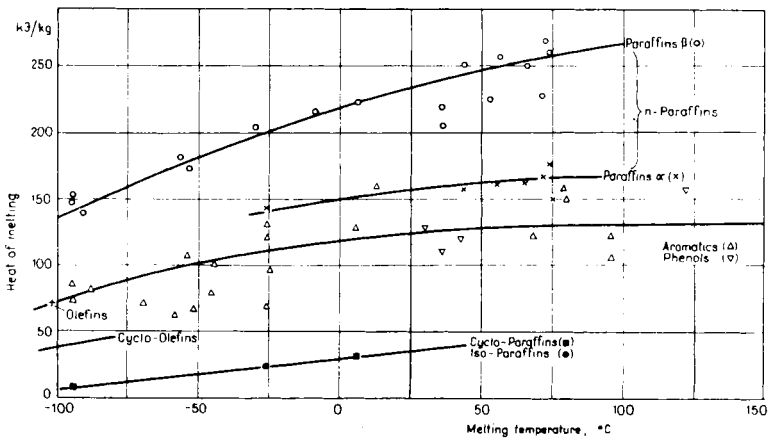


Fig. 7.6 – 5. Melting heats of solid hydrocarbons, after Grosse 1951 (used with permission of VDI-Verlag GmbH, Düsseldorf)

Equation 7.6 – 14 is most often used in the simplified form called Sukhov's equation in Soviet literature; it assumes $\varepsilon$ and $\Phi^*$ to be both zero:

$$T_{f2} = T_s + (T_{f1} - T_s) \exp\left(-\frac{kl}{q\rho c}\right). \qquad 7.6-15$$

### 7.6.3. The heat-transfer coefficient

In practice, the heat-tranfer coefficient is used in two forms. The factor $k^*$ expressed in W/(m$^2$ K) is heat flow from unit surface of pipe into the ground for unity temperature difference; $k$, in W/(m K) units, is the same for unit length rather than unit surface of pipe. The two factors are related by

$$k = \pi d k^*. \qquad 7.6-16$$

In pipelining practice, pipes are usually buried in the ground, laid in a ditch dug for the pupose, and covered with backfill. Assuming the soil to be homogeneous as to heat conductivity, the heat flow pattern for steady-state flow is described by the stream-lines and the orthogonal set of isotherms shown in *Fig. 7.6 – 6*. Next to the pipe, isotherms are circular in a fair approximation, with their centres the lower down on the vertical axis, the lower the temperature that they represent. In the case illustrated, and assuming that heat retention by the steel wall of the pipe is negligible, the heat transfer factor is

$$k = \frac{\pi}{\frac{1}{\alpha_1 d_i} + \frac{1}{2\lambda_{in}} \ln \frac{d_{in}}{d_o} + \frac{1}{\alpha_2 d_{in}}}. \qquad 7.6-17$$

The first term in the denominator describes internal convective thermal resistance, the second the effect of the thermal insulation applied to the pipe, and the third the thermal insulation by the soil itself.

*The first term in the denominator of Eq. 7.6 – 17*, the internal-convection factor $\alpha_1$, may be determined by one of several relationships. It equals the heat flow per unit wall surface, per unit temperature difference, from the pipe axis at temperature $T_i$ to

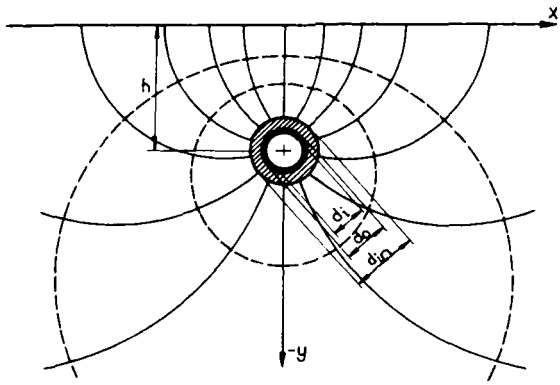


Fig. 7.6 – 6.

the pipe wall at temperature $T_f$. The relationships used are found to have the common property of starting from the Nusselt factor $N_{Nu}$:

$$\alpha_1 = N_{Nu} \frac{\lambda_f}{d_i}. \qquad 7.6-18$$

Heat transfer by convection has three typical cases, each of which corresponds to a zone of flow (Dobrinescu and Bulau 1969). These are: the turbulent zone at $N_{Re}$ above $10^4$, the transition zone for $N_{Re}$ between 2300 and $10^4$, and the laminar zone for $N_{Re}$ below 2300. In turbulent flow, according to Sieder and Tate,

$$N_{Nu} = 0{\cdot}027\, N_{Re}^{0{\cdot}8}\, N_{Pr}^{1/3} \left(\frac{\mu_f}{\mu_i}\right)^{0{\cdot}14} \qquad 7.6-19$$

where $\mu_f$ is the dynamic viscosity of oil at the pipe axis and $\mu_i$ is the same at the pipe wall.

For the zone of transition, Ramm proposes the following, extended formula:

$$N_{Nu} = 0{\cdot}027\, N_{Re}^{0{\cdot}8}\, N_{Pr}^{1/3} \left(\frac{\mu_f}{\mu_i}\right)^{0{\cdot}14} \left(1 - \frac{6 \times 10^5}{N_{Re}^{1{\cdot}8}}\right). \qquad 7.6-20$$

In the turbulent and transition zones, heat transfer by convection is rather significant, and so temperature differences between the pipe's axis and wall are not usually taken into account in these two zones. Heat transfer by convection is

significantly less in laminar flow; moreover, in liquid undergoing a forced motion, free convection currents will also form, which will modify the velocity profile. This modification is more significant in vertical than in horizontal flow strings, though. It is most expediently characterized in horizontal pipelines by the product of the Prandtl and Grashof numbers (Ford 1955):

$$N_{Gr}N_{Pr} = \frac{d_i^3 c\rho g\beta_T (T_f - T_i)}{\nu\lambda_f}. \qquad 7.6-21$$

For laminar flow, $N_{Nu}$ v. the product $N_{Gr}N_{Pr}$ can be determined using the Gill–Russell relationship illustrated by *Fig. 7.6 – 7* (Ford 1955). If the abscissa is greater than $5 \times 10^4$, then

$$N_{Nu} = 0{\cdot}184(N_{Gr}N_{Pr})^{0{\cdot}32}. \qquad 7.6-22$$

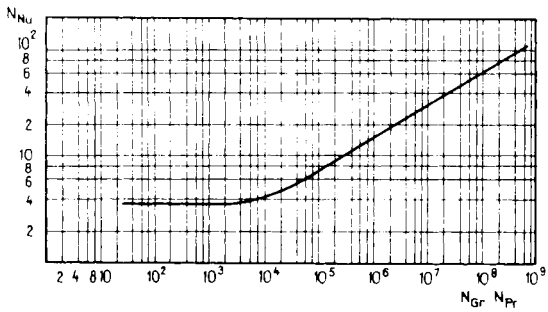


Fig. 7.6 – 7. Relationship $N_{Nu} = f(N_{Gr}N_{Pr})$ for finding $\alpha_1$, according to Gill and Russell; after Ford (1955)

Of the factors figuring in Eqs 7.6 – 21 and 7.6 – 22, specific heat $c$ and thermal conductivity $\lambda_f$ can be calculated using Cragoe's formula transformed into the SI system, by Dobrinescu and Bulau (1969):

$$c = \frac{762{\cdot}5 + 3{\cdot}38T}{\sqrt{\rho_4^{20}}} \qquad [\text{J/(kg K)}] \qquad 7.6-23$$

$$\beta_T = \frac{1}{2583 - 6340\,\rho_4^{20} + 5965(\rho_4^{20})^2 - T} \qquad [\text{1/K}] \qquad 7.6-24$$

$$\lambda_f = \frac{0{\cdot}134 - 6{\cdot}31 \times 10^{-5} T}{\rho_4^{20}}. \qquad [\text{W/(m K)}] \qquad 7.6-25$$

Furthermore

$$\rho_T = \rho_n - \alpha_T(T - T_n) + \alpha_p p. \qquad [\text{kg/m}^3] \qquad 7.6-26$$

The physical state of the oil would, at a first glance, be described in terms of the average temperature between the head and tail ends of the pipeline section.

According to Orlicek and Pöll (1955), however, heat transfer depends primarily on the nature and state of the liquid film adhering to the pipe wall. The correct procedure would consequently be to determine the physical parameters of the oil at the mean film temperature. No relationship suitable for calculating this temperature has so far been established, however. For practice it seems best to establish parameters for the mean wall temperature of the pipeline section examined. Viscosity depends markedly on temperature, less so on pressure in the range of oil transmission in pipelines. The $v = f(p, T)$ graphs state results of laboratory measurements. The temperature-dependence of viscosity in Newtonian liquids is best described by Walther's equation

$$\lg \lg (10^6 v + a) = b + c \lg T$$

$a$, $b$ and $c$ are constants depending on the nature of the oil; $a$ ranges from 0·70 to 0·95: putting it equal to 0·8 gives an accuracy sufficient for practical purposes. Hence,

$$\lg \lg (10^6 v + 0{\cdot}8) = b + c \lg T. \qquad 7.6-27$$

This equation implies that oil viscosity v. temperature will be represented by a straight line in an orthogonal system of coordinates whose abscissa ($T$) axis is logarithmic and whose ordinate (viscosity) axis is doubly logarithmic. This is the Walther–Ubbelohde diagram, whose variant conformable to Hungarian standard MSz – 3258 – 53 is shown as *Fig. 7.6 – 8*. In principle, two viscosity values determined at two different temperatures, plotted in this diagram, define a straight line representing the viscosity v. temperature function. In practice, it is indicated to measure viscosity at three temperatures at least, and to use the straight lines joining the three points plotted merely as an aid in interpolating between plots. It should be ascertained whether or not the oil exhibits anomalous flow behaviour at the lowest temperature of measurement, or evaporation losses at the highest. — Pressure tends to increase viscosity somewhat. According to Dobrinescu and Bulau (1969), dynamic viscosity at pressure $p$ is described by

$$\mu_p = \mu_a (0{\cdot}9789 + 0{\cdot}0261\, \rho_4^{20})^{1{\cdot}02p}. \qquad 7.6-28$$

This relationship gives a 13-percent increase in the viscosity of a 900 kg/m$^3$ density oil between atmospheric pressure and $p = 50$ bars.

*The second term in the denominator of Eq. 7.6 – 17* is proportional to the thermal resistance of the heat insulation about the pipe; in addition, to the nature of the insulator matrix, the thermal conductivity of the material as it is dependent primarily on pore volume and pore distribution. It is primarily the air in the pores that insulates. The thermal conductivity coefficient of air at room temperature ($\lambda_a$) is as low as 0·023 W/(m K). If temperature differences between different points of the hole wall make the air in the pores form conduction currents, then heat will flow through the pores by free convection in addition to conduction. The less the mean pore size, the less significant is convection. The resultant thermal conductivity of 'series-connected' small pores and the pore walls separating them is less than it would be for the same overall pore volume if the pores were larger. On the other

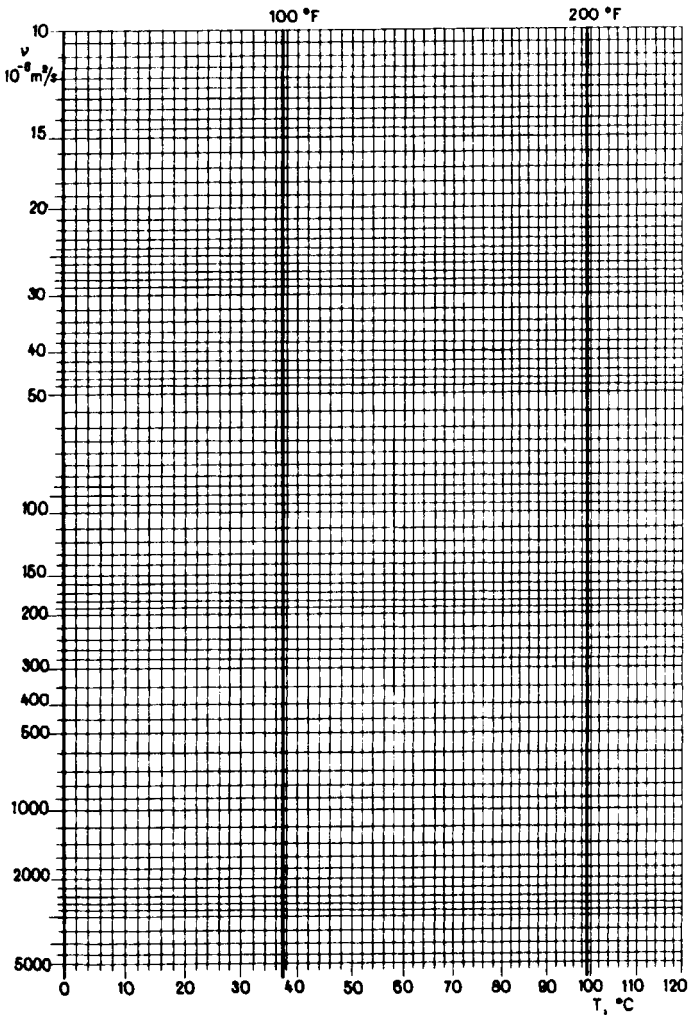


Fig. 7.6 – 8. Walther – Ubbelohde grid according to Hungarian Standard MSZ-3258-53

hand, the smaller the pores in a given matrix, the less the compressive strength of the insulator. Low-strength insulators will be crushed or pulverized by comparatively weak forces. Hence, reducing pore size in a given matrix is limited by the minimum requirement as to compressive strength. A material is a good thermal insulator if its conductivity is less than 0·08 W/(m K); if it contains no substance that corrodes the pipe; if it is chemically inert vis-à-vis air and water; if its compressive strength exceeds a prescribed minimum; if it keeps its properties over long periods of time; and if it can be fitted snugly against the pipe wall.

Table 7.6 – 1. Parameters of pipeline insulators (after Baleke 1949)

| Insulator | $\rho_{in}$ kg/m$^3$ | $\lambda_{in}$; W/(m K) at mean temperature °C | | | | | $\sigma_c$ bars |
|---|---|---|---|---|---|---|---|
| | | 0 | 20 | 50 | 100 | 150 | |
| Slag wool | 225 | 0·042 | 0·043 | 0·047 | 0·053 | 0·060 | |
| covered with galvanized sheet | 300 | 0·045 | 0·047 | 0·051 | 0·057 | 0·064 | 6 |
| Glass wool | 100 | 0·034 | 0·036 | 0·039 | 0·049 | 0·058 | – |
| covered with galvanized sheet | 375 | 0·035 | 0·037 | 0·041 | 0·050 | 0·059 | 6 |
| Burnt diatomaceous-earth bricks | | | | | | | |
| light | 370 | 0·070 | 0·072 | 0·075 | 0·081 | 0·088 | 3 – 4 |
| medium | 480 | 0·087 | 0·089 | 0·093 | 0·100 | 0·107 | 4 – 7 |
| heavy | 650 | 0·116 | 0·120 | 0·127 | 0·139 | 0·145 | 12 – 20 |
| Burnt diatomaceous-earth paste* | | | | | | | |
| light | 350 | 0·063 | 0·064 | 0·066 | 0·070 | 0·073 | 2 – 3 |
| medium | 500 | 0·075 | 0·078 | 0·081 | 0·085 | 0·088 | 2 – 3 |
| heavy | 700 | 0·104 | 0·108 | 0·116 | 0·125 | 0·129 | 3 – 4 |

* To be applied to hot pipeline only

Let us point out that water infiltrated into the pores will considerably impair insulation, since the thermal conductivity of water at room temperature is about 0·58 W/(m K), that is, about 25 times that of air. The exclusion of water from the insulator pores must therefore be ensured. This is achieved partly by choosing insulators with closed, unconnected pores, and partly by providing a waterproof coating. The main parameters of insulators most popular in earlier practice are listed in *Table 7.6 – 1*. The materials figuring in the Table are open-pored without exception, and must therefore be provided with a waterproof coating in every application. In the last decades, the use of polyurethane foam is on the increase. Shell Australia Ltd laid a 8-in. pipeline 56 km long, insulated with 51-mm thick polyurethane foam wound with polyethylene foil (Thomas 1965). Polyurethane foam is extremely porous (about 90 percent porosity) and light (about 34 kg/m$^3$). Pores are unconnected and filled with freon. Its heat conductivity is 0·016 – 0·021 W/(m K). It can be used up to a temperature of 107 °C. Insulation is usually applied in the pipe mill, but ends are left bare so as not to hamper welding. After welding, joins are insulated on-site with polyurethane foam, over which a prefabricated, pre-warmed polyethylene sleeve is slipped. On cooling, the sleeve contracts and provides a watertight seal. — Soviet pipeliners use a device that permits the on-site insulation with polyurethane foam of welded-together pipeline sections. The pipe, warmed to about 60 °C, is drawn through a foam-spraying

chamber. Correct size is ensured by a template fixed on the chamber wall (Zeinalov *et al.* 1968). High-grade heat insulation is expensive; it costs approximately as much again as the pipeline itself (Gautier 1970).

*The third term in the denominator of Eq. 7.6 – 17* describes the thermal resistance of soil surrounding the pipeline. Assuming the original undisturbed temperature of the soil at pipeline depth to be $T_s$, and the ground-surface temperature to be equal to this value, it can be shown that

$$\alpha_2 = \frac{2\lambda_s}{d_{in}\,\mathrm{ch}^{-1}\left(\frac{2h}{d_{in}}\right)}. \qquad 7.6-29$$

The approximation

$$\alpha_2 = \frac{2\lambda_s}{d_{in}\ln\frac{4h}{d_{in}}} \qquad 7.6-30$$

will be the better, the greater is $h/d_{in}$. In most practical cases, that is, at about $h/d_{in} \geqq 2$, the two formulae will furnish closely agreeing results; $d_{in}$ denotes the *OD* of the pipeline as installed, together with insulation and coatings. In the absence of such, $d_{in} = d_o$, the *OD* of the pipe. Determining the heat conductivity of the soil was discussed in Section 7.6.1. — In determining the heat transfer factor $k$ valid when the pipeline is operative, one should keep in mind that the porosity of the backfill is greater than that of the undisturbed soil, and that its thermal conductivity is consequently lower. A procedure accounting for this circumstance has been devised by Ford, Ells and Russell (Davenport and Conti 1971). The backfill will compact with time, and the effective heat-transfer factor will slightly increase in consequence. The heat transfer factor is affected by the wind, the plant cover, snow if any, soil moisture and the state of aggregation of water. Under a temperate climate, soil frost will rarely enter into consideration, but in permafrost regions it may play an important role. The way wind increases $k$, or the plant or snow cover decrease it, are too little known as yet to be evaluated in quantitative terms. The influence of soil moisture is known, however (it was discussed in Section 7.6.1). It is accordingly to be expected that the heat transfer factor will vary over the year as a function of soil moisture, influenced in its turn by the weather. *Figure 7.6 – 9* is a plot of $k^*$ factors measured over three years along three sections of the Friendship pipeline. It is seen that the factor is lowest in June, July and August, the hot dry months of a Northern hemisphere continental climate.

If the heat transfer factor $k$ is to be determined by calculation, and flow is laminar, then the computation of $\alpha_1$ requires the knowledge of the inside wall temperature $T_i$, too (cf. Eq. 7.6 – 21). Under steady conditions, heat flow from a one-metre pipeline section into the soil is

$$\Phi^* = k(T_f - T_s) = \alpha_1 d_i \pi (T_f - T_i) = \frac{2\pi\lambda_{in}(T_o - T_{in})}{\ln\frac{d_{in}}{d_o}} = \alpha_2 d_{in}\pi(T_{in} - T_s). \qquad 7.6-31$$

The inside and outside wall temperatures of steel pipe are taken to be equal, that is, $T_i = T_o$. The multiple equation 7.6 – 31 may be decomposed into three independent equations:

$$k(T_f - T_s) = \alpha_1 d_i \pi (T_f - T_i) \qquad 7.6-32$$

$$\alpha_1 d_i \pi (T_f - T_i) = \frac{2\pi\lambda_{in}(T_o - T_{in})}{\ln \frac{d_{in}}{d_o}} \qquad 7.6-33$$

$$\alpha_1 d_i \pi (T_f - T_i) = \alpha_2 d_{in} \pi (T_{in} - T_s) . \qquad 7.6-34$$

The relationship needed to determine $T_i$ is Eq. 7.6 – 32. The calculation can be performed by successive approximations. A value for $T_i$ is assumed first, and, using it, the physical parameters of the oil required to calculate $N_{Gr}N_{Pr}$ and $N_{Nu}$, are established. As a result. Eq. 7.6 – 18 will furnish a value for $\alpha_1$. Introducing this into Eq. 7.6 – 17, a $k$-value is calculated. Now Eq. 7.6 – 32 is used to produce another $k$-value, likewise using the previously determined $\alpha_1$. If the $k$s furnished by the two procedures agree, then the value assumed for $T_i$ is correct. If this is not the case, calculation has to be repeated with a different value for $T_i$. — Equation 7.6 – 33 or

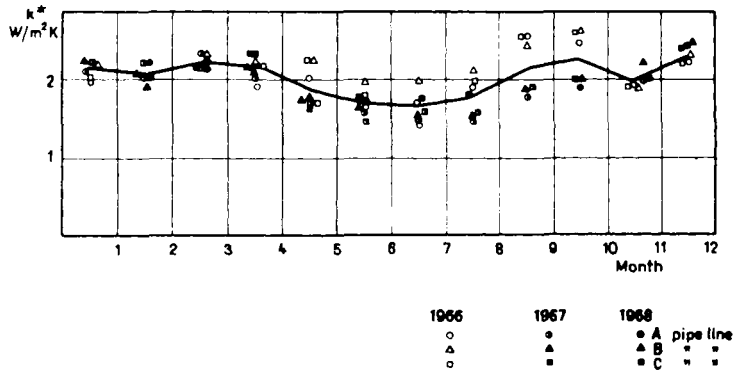


Fig. 7.6 – 9. Heat transfer factor v. time, after Rabinovich and Kuznetsov (1970)

7.6 – 34 may be employed, e.g. in possession of measured $T_{in}$ and $T_i$ values for a given pipeline, to calculate the thermal conductivity $\lambda_{in}$ of the insulation under operating conditions. This procedure permits us to verify whether the insulation provided has the effect aimed at, or whether it has deteriorated since its installation (Szilas 1966).

*Example 7.6 – 3.* Find the heat-transfer factor of a pipeline with $d_o = 0{\cdot}1143$ m, $d_i = 0{\cdot}1023$ m, $h = 1$ m. Variation of viscosity v. temperature for the oil of density $\rho_{20} = 887$ kg/m$^3$, flowing laminarly in the pipeline, is given in *Fig. 7.6 – 10*; $\lambda_s = 1{\cdot}76$ W/(m K), $T_f = 318{\cdot}4$ K, $T_s = 273$ K; the temperature coefficient of density, $\alpha_T = 0{\cdot}65$ kg/(m$^3$ K). — Let us assume that wall temperature $T_i$ is less by 9·5 K than oil

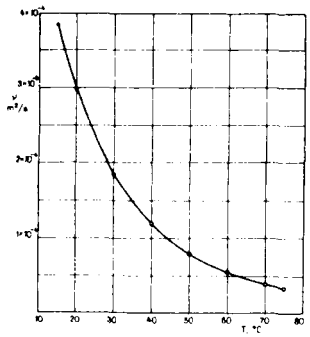

Fig. 7.6 – 10.

temperature $T_f$ (that is, $T_i = 308{\cdot}9$ K). Accordingly, the physical parameters of the oil are furnished by Eqs 7.6 – 23 — 7.6 – 26 as

$$\rho_T = 887 - 0{\cdot}65(308{\cdot}9 - 293) = 876{\cdot}7 \text{ kg/m}^3$$

$$c = \frac{762{\cdot}5 + 3{\cdot}38 \times 308{\cdot}9}{\sqrt{0{\cdot}887}} = 1918 \text{ J/(kg K)}$$

$$\beta_T = \frac{1}{2583 - 6340 \times 0{\cdot}887 + 5965 \times 0{\cdot}887^2 - 308{\cdot}9} = 7{\cdot}442 \times 10^{-4} \text{ K}^{-1}$$

$$\lambda_f = \frac{0{\cdot}134 - 6{\cdot}31 \times 10^{-5} \times 308{\cdot}9}{0{\cdot}887} = 0{\cdot}129 \text{ W/(m K)}.$$

From *Fig. 7.6 – 10*, the viscosity of the oil at 308·9 K (= 35·9 °C) is 1·423 $\times 10^{-4}$ m$^2$/s. By Eq. 7.6 – 21,

$$N_{Gr} N_{Pr} = \frac{0{\cdot}1023^3 \times 1918 \times 876{\cdot}7 \times 9{\cdot}81 \times 7{\cdot}442 \times 10^{-4}(318{\cdot}4 - 308{\cdot}9)}{1{\cdot}423 \times 10^{-4} \times 0{\cdot}129} =$$

$$= 6{\cdot}798 \times 10^6 .$$

Since $6{\cdot}798 \times 10^6 > 5 \times 10^4$, $N_{Nu}$ will be furnished by Eq. 7.6 – 22 as

$$N_{Nu} = 0{\cdot}184(6{\cdot}798 \times 10^6)^{0{\cdot}32} = 28{\cdot}26 .$$

By Eq. 7.6 – 18,

$$\alpha_1 = \frac{0{\cdot}129 \times 28{\cdot}26}{0{\cdot}1023} = 35{\cdot}66 \text{ W/(m}^2 \text{ K)}.$$

By Eq. 7.6 – 30,

$$\alpha_2 = \frac{2 \times 1{\cdot}76}{0{\cdot}1143 + \ln \dfrac{4 \times 1}{0{\cdot}1143}} = 8{\cdot}67 \text{ W/(m}^2 \text{ K)}.$$

Now the heat-transfer factor is, by Eq. 7.6 – 17,

$$k = \frac{\pi}{\frac{1}{35{\cdot}66 \times 0{\cdot}1023} + \frac{1}{8{\cdot}67 \times 0{\cdot}1143}} = 2{\cdot}448 \text{ W/(m K)}$$

whereas Eq. 7.6 – 32 yields

$$k = \frac{0{\cdot}1023 \times \pi \times 35{\cdot}66(318{\cdot}4 - 308{\cdot}9)}{318 \times 4 - 273} = 2{\cdot}400 \text{ W/(m K)}.$$

As a further approximation, let $T_i = 308{\cdot}7$ K, in which case Eq. 7.6 – 17 yields 2·449 W/(m K), and Eq. 7.6 – 32 yields 2·450, so that $k = 2{\cdot}45$ W/(m K) is accepted.

### 7.6.4. Calculating the head loss for the steady-state flow

#### (a) The oil is Newtonian

#### (A) Chernikin's theory

Equation 7.6 – 2 will hold for an infinitesimal length d$l$ of pipeline only, as the temperature of the oil flowing through the pipe may be considered constant, and so may, in consequence, also $\lambda$ and v:

$$\mathrm{d}h_f = \frac{\lambda v^2}{2gd_i}\,\mathrm{d}l. \qquad 7.6-35$$

Equation 1.1 – 10 may be used to express $\lambda$ also for laminar flow:

$$\lambda = a\left(\frac{1}{N_{Re}}\right)^b = a\left(\frac{\nu}{d_i v}\right)^b \qquad 7.6-36$$

where $a$ and $b$ are constants that, in laminar flow, depend on the flow type only. Substituting this expression of $\lambda$ and the expression

$$v = \frac{q}{\frac{d_i^2\pi}{4}}$$

into Eq. 7.6 – 35, we get

$$\mathrm{d}h_f = \beta\frac{q^{(2-b)}\nu^b}{d^{(5-b)}}\,\mathrm{d}l \qquad 7.6-37$$

where the constant coefficient is

$$\beta = \frac{4^{(2-b)}a}{2g\pi^{(2-b)}}.$$

Viscosity v. temperature in a Newtonian oil may be described over a limited temperature range also by Filonov's explicit formula

$$\nu = \nu_0 e^{-nT} \qquad 7.6-38$$

where $\nu_0$ is kinematic viscosity at 0 °C and

$$n = \frac{\ln \frac{\nu_I}{\nu_{II}}}{T_I - T_{II}},$$

where $\nu_I$ and $\nu_{II}$ are experimentally determined viscosities at the temperatures $T_I$ and $T_{II}$. Let us point out that $T$ is to be written in °C. $\nu_0$ may be considered as a fictive, extrapolated value. It has no physical meaning unless the oil is Newtonian at the temperature considered. At a distance $l$ from the head end of the pipeline, the temperature of the flowing oil is expressed by Eq. 7.6 – 15 as

$$T_f = T_s + (T_{f1} - T_s)e^{-ml}$$

where

$$m = \frac{k}{q\rho c}.$$

Introducing this into Eq. 7.6 – 38, we obtain

$$\nu = \nu_0 e^{-n[T_s + (T_{f1} - T_s)e^{-ml}]}.$$

Substituting this latter equation in Eq. 7.6 – 37, we get

$$\mathrm{d}h_f = \beta \frac{q^{(2-b)}\nu_0^b}{d^{(5-b)}} e^{-bnT_s} e^{-bn(T_{f1} - T_s)e^{-ml}} \mathrm{d}l. \qquad 7.6-39$$

Let $bn(T_{f1} - T_s) = B$, and

$$\beta \frac{q^{(2-b)}\nu_0^b}{d^{(5-b)}} e^{-bnT_s} = A$$

then

$$h_f = \int_0^l A e^{-Be^{-ml}} \mathrm{d}l.$$

Let $Be^{-ml} = u$; then, $e^{-ml} = u/B$. Hence,

$$l = -\frac{1}{m} \ln \frac{u}{B} \text{ and } \mathrm{d}l = -\frac{1}{mu} \mathrm{d}u.$$

Substituting the constants into this equation yields

$$h_f = -\frac{A}{m} \int_{u=B}^{B'} \frac{e^{-u}}{u} \mathrm{d}u.$$

Since

$$\int_{u=B}^{B'} \frac{e^{-u}}{u}\,du = \int_{u=B}^{\infty} \frac{e^{-u}}{u}\,du - \int_{u=B'}^{\infty} \frac{e^{-u}}{u}\,du = \mathrm{Ei}(-B') - \mathrm{Ei}(-B),$$

we have, in the original notation,

$$h_f = \beta \frac{q^{(2-b)} \nu_0^b}{d^{(5-b)}} e^{-bnT_s} \frac{1}{m} \times$$

$$\times \{\mathrm{Ei}[-bn(T_{f1} - T_s)] - \mathrm{Ei}[-bn(T_{f1} - T_s)e^{-ml}]\}.$$

Introducing the $\nu_0 = \nu_1 e^{nT_{f1}}$ implied by Eq. 7.6–38, and the

$$(T_{f1} - T_s)e^{-ml} = T_{f2} - T_s$$

implied by Eq. 7.6–15, we arrive at

$$h_f = \beta \frac{q^{(2-b)} \nu_1^b}{d^{(5-b)}} l \frac{e^{bn(T_{f1} - T_s)}}{ml} \times \qquad 7.6-40$$

$$\times \{\mathrm{Ei}[-bn(T_{f1} - T_s)] - \mathrm{Ei}[-bn(T_{f2} - T_s)]\}.$$

This equation may be contracted to read

$$h_f = \beta \frac{q^{(2-b)} \nu_1^b}{d^{(5-b)}} l \Delta_l \Delta_r \qquad 7.6-41$$

in which case, with reference to Eq. 7.6–37, it may be interpreted as the product of the pressure head loss of a liquid in isothermal flow whose viscosity is $\nu_1$ at the head end of the pipeline, of the correction accounting for cooling along the pipeline section $\Delta_l$ and of the radial temperature correction $\Delta_r$. In laminar flow, $\beta = 128/\pi g$, and $b = 1$; in turbulent flow, the corresponding values are 0·201/$g$ and 0·25, if friction factor $\lambda$ is determined using Eq. 1.1–4 (Chernikin 1958). In Eq. 7.6–41,

$$\Delta_l = \frac{e^{bn(T_{f1} - T_s)}}{ml} \{\mathrm{Ei}[-bn(T_{f1} - T_s)] - \mathrm{Ei}[-bn(T_{f2} - T_s)]\}$$

$\Delta_l$ is, then, the correction factor accounting for axial cooling. It shows how many times the head loss is increased owing to the fact that oil temperature gradually decreases from $T_{f1}$ to $T_{f2}$ during flow. $\Delta_r$ is the correction factor accounting for radial cooling. Its value would be unity if oil temperature were constant over any pipeline cross section. However, temperature in effect decreases from the pipe axis towards the wall (cf. e.g. Example 7.6–4), and hence mean viscosity in the pipe is higher than the axial viscosity. $\Delta_r$ accounts for this effect. Chernikin makes use of the Sieder–Tate relationship

$$\Delta_r = \varepsilon \left(\frac{\nu_i}{\nu_f}\right)^{\omega} \qquad 7.6-42$$

$v_i$ and $v_f$ are average viscosities of oil at the pipe wall and along the axis, respectively, at the arithmetic average of the head-end and tail-end temperatures of the pipeline section considered; $\varepsilon$ and $\omega$ are constants ($\varepsilon$ is 0·9 in laminar and 1 in turbulent flow; $\omega$ ranges from 1/3 to 1/4 in laminar and from 1/3 to 1/7 in turbulent flow). In pipelines transporting viscous crudes, the transition from laminar to turbulent flow may be expected at about $N_{Re} = 2000$.

Equation 7.6 – 41, suitable for comparatively fast calculation, has the following limitations. (i) In calculating the friction factor of turbulent flow, it employs the Blasius equation which refers to smooth pipe. Accuracy is easy to improve by introducing different constants $a$ and $b$ (cf. e.g. Eq. 7.4. – 8). (ii) Equation 7.6 – 38 is an approximate expression of the temperature-dependence of oil viscosity, valid over a rather limited temperature range only. (iii) Constants $\varepsilon$ and $\omega$ have rather broad ranges and therefore $\Delta_r$ cannot be determined to a desirable degree of accuracy.

**(B) Ford's theory (with modification)**

This procedure, more lengthy than the foregoing one, establishes the head loss of oil flowing in a pipeline by a finite-difference procedure. It permits us to account for the variation in $k$, and to use accurate friction-factor and viscosity values (Ford 1955). Below we shall present this method in a slightly modified form.

Starting from the initial axial oil temperature $T_{f1}$, we assume an axial temperature drop $\Delta T_f$ of a few °C to take over a place comparatively short, as yet unspecified length $l_1$ of pipe. It is assumed that the average temperature over this length of pipe is, in a fair approximation,

$$\bar{T}_{f1} = T_{f1} - 0{\cdot}5\Delta T_f . \qquad 7.6-43$$

Using Eqs 7.6 – 15, 7.6 – 17 and 7.6 – 30, it is possible to calculate the length $l_1$ over which the axial temperature drop is precisely $\Delta T_f$. In order to perform the calculation it is necessary to determine the heat transfer factor as indicated in Example 7.6 – 3 and, in the process, to find also the average wall temperature $T_{i1}$. Continuing the process, one obtains related values of $T_f$, $T_i$, $T_{in}$ and $l$, which permits plotting graphs of temperature v. length.

Viscosity values corresponding to the Reynolds number $N_{Re} = 2000$, characterizing the transition from laminar to turbulent flow, are calculated using Eq. 1.1 – 2; oil temperature $T_f$ corresponding to the 'critical' viscosity of the oil to be conveyed is then read off the corresponding $T-v$ graph. The point along the line where this temperature sets in will be where turbulent flow passes into laminar. In turbulent flow, as far as head loss calculations are concerned, pipeline cross-section temperature may be equated with $T_f$. In laminar flow, however, the temperature differential between pipe axis and pipe wall is so significant that the average of the two, which will in fact determine the behaviour of the crude (its effective viscosity first of all), has to be determined separately. It was found in practice that this is done most simply by reading said temperature off the experimentally established diagram

presented as *Fig. 7.6 – 11*, where it is plotted against the product of the Grashof and Prandtl numbers. In the knowledge of the diagram it is possible to establish the variation of corrected oil temperature $T_{fk}$ v. position along the pipe.

By the considerations outlined in Section 1.1, it is possible to find the density and friction factor corresponding to the temperatures $T_f$ (or $T_{fk}$) at the key points of both the turbulent and laminar flow sections along the pipe string. Planimetering

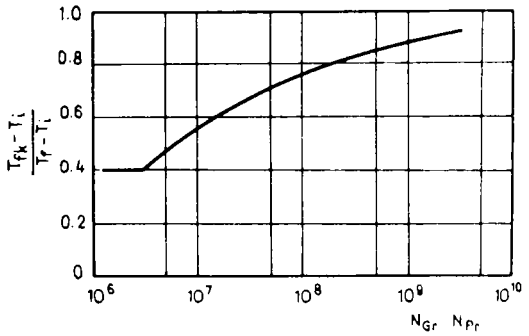


Fig. 7.6 – 11. Relationship for determining $T_{fk}$, after Ford (1955)

will furnish the mean values $\bar{\rho}$ and $\bar{\lambda}$ for both zones of flow. Substituting the relationship

$$v = \frac{q_m}{\frac{d^2\pi}{4}\bar{\rho}}$$

into Eq. 1.1 – 1, we obtain the friction loss as

$$\Delta p_f = \frac{8\,\bar{\lambda} q_m^2 l}{\pi^2\,\bar{\rho} d_i^5}. \qquad 7.6-44$$

Introducing the values of $\bar{\lambda}$ and $\rho$ we obtain the values $\Delta p_{fT}$ and $\Delta p_{fL}$, valid respectively for the turbulent and laminar zone. The full head loss is

$$\Delta p_f = \Delta p_{fT} + \Delta p_{fL}. \qquad 7.6-45$$

The calculation method is shown by the flow chart 7.6 – 12 (Szilas and Navratil 1978, 1981). $N_{\mathrm{Repp}}$ equals $N_{\mathrm{Re}}$ if the crude exhibits Newtonian flow properties.

*Example 7.6 – 4.* Find the friction loss in an uninsulated horizontal pipeline buried in the ground, if $d_i = 102{\cdot}3$ mm; $d_o = 114{\cdot}3$ mm; $k/d_i = 4 \times 10^{-4}$; $l = 9000$ m, $T_{f1} = 74$ °C; $T_s = 0$ °C; $h = 1$ m; $\lambda_s = 1{\cdot}76$ W/(m K); $\rho_{20} = 887$ kg/m$^3$; $q = 50$ m$^3$/h; $\alpha_T = 0{\cdot}65$ kg/(m$^3$ K), and crude viscosity varies with temperature as shown in *Fig. 7.6 – 10*. — Let $\Delta T_f = 4$ °C; the mean axial temperature $\bar{T}_{f1}$ of the first pipeline section is, then, $74 - 4/2 = 72$ °C. Let us find $N_{\mathrm{Re}}$ at this temperature. If it exceeds 2000, then

the flow is turbulent. In this case, in an approximation sufficient for our purposes, $\bar{T}_{fk1} = \bar{T}_{f1} = 72$ °C. Let us find $c$ for this temperature using Eq. 7.6 – 23, then, using Eq. 7.6 – 15, the length $l_1$ over which the crude's temperature drops to 70 °C from the initial 74 °C; $k$ is established using Eq. 7.6 – 17, under the assumption that $1/\alpha_1 = 0$. The procedure is continued until $N_{Re}$ attains the critical value of 2000. In the laminar zone of flow, this procedure is modified as follows. Starting from an inital axial temperature $T_{fn}$, one establishes the length of pipeline $l_n$ along which the axial temperature drops 4 °C. Here, the mean axial temperature equals $T_{fn} - 4/2$. To this value, an average wall temperature is arbitrarily assigned, then $k_n$ is calculated in the manner illustrated by Example 7.6 – 3, and $l_n$ is determined in the knowledge of $k_n$

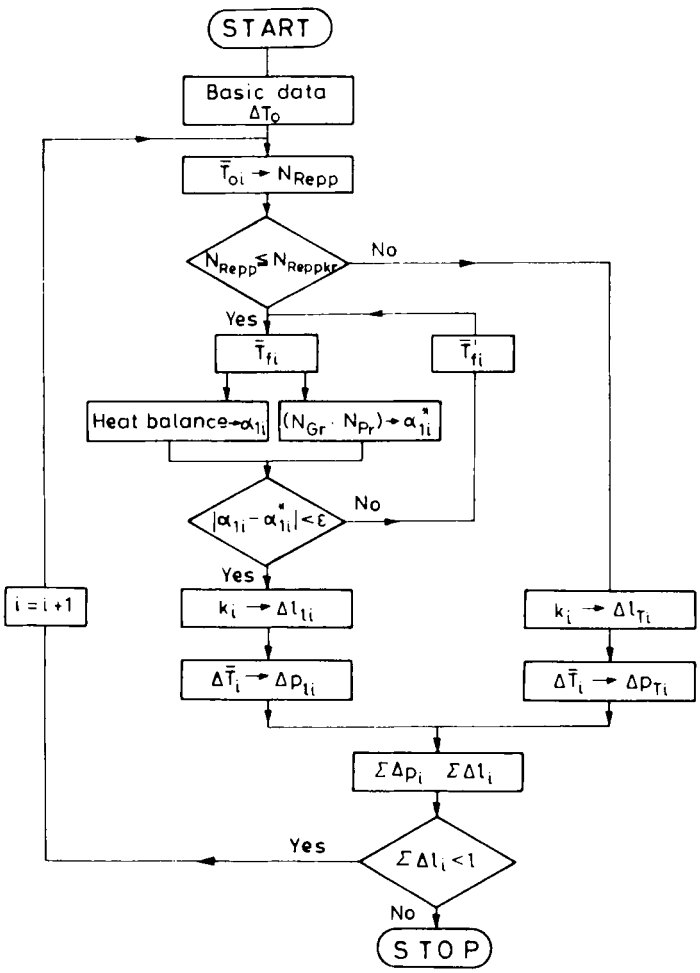


Fig. 7.6 – 12. Flow chart of pressure-loss calculation, after Szilas and Navratil (1978, 1981)

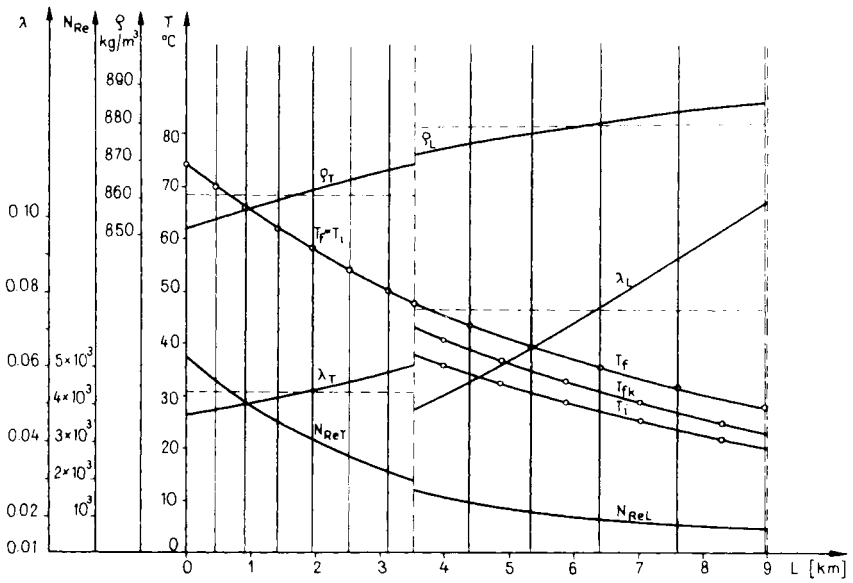


Fig. 7.6 – 13.

from Eq. 7.6 – 15. In a similar way, related values of $T_f$, $T_i$ and $l$ are calculated until $\Sigma l$ attains or exceeds 9000 m, the full length of the pipeline.

Making use of *Fig. 7.6 – 12*, $T_{fk}$ is determined for each pair of $T_f$ and $T_i$ calculated for the laminar zone. *Figure 7.6 – 13* is a plot of temperatures $T_f$, $T_i$ and $T_{fk}$ v. distance from the pipeline's head end, and of oil gravity $\rho$ at the temperatures $T_f$ and

Table 7.6 – 2.

| Serial number | $T_{fn} - T_{f(n+1)}$ | $\bar{T}_{fn}$ | $T_{fkn}$ | $T_{in}$ | $\rho_n$ | $\nu_n$ |
|---|---|---|---|---|---|---|
| | K | K | K | K | kg/m³ | $10^{-4}$ m²/s |
| 1 | 347 – 343 | 345·0 | – | 345·0 | 853·2 | 0·361 |
| 2 | 343 – 339 | 341·0 | – | 341·0 | 855·8 | 0·413 |
| 3 | 339 – 335 | 337·0 | – | 337·0 | 858·4 | 0·474 |
| 4 | 335 – 331 | 333·0 | – | 333·0 | 861·0 | 0·546 |
| 5 | 331 – 327 | 329·0 | – | 329·0 | 863·6 | 0·633 |
| 6 | 327 – 323 | 325·0 | – | 325·0 | 866·2 | 0·736 |
| 7 | 323 – 320·4 | 321·7 | – | 321·7 | 868·4 | 0·837 |
| 8 | 320·4 – 316·4 | 318·4 | 313·6 | 308·7 | 873·6 | 1·16 |
| 9 | 316·4 – 312·4 | 314·4 | 309·6 | 305·1 | 876·2 | 1·38 |
| 10 | 312·4 – 308·4 | 310·4 | 305·6 | 301·6 | 878·8 | 1·65 |
| 11 | 308·4 – 304·4 | 306·4 | 301·6 | 298·1 | 881·4 | 1·97 |
| 12 | 304·4 – 300·4 | 302·4 | 297·7 | 294·6 | 883·9 | 2·37 |
| 13 | 300·4 – 296·4 | 298·4 | 294·1 | 291·3 | 886·3 | 2·82 |

$T_{fk}$. The mean density found by planimetering is $\bar{\rho}_T = 861{\cdot}1$ kg/m$^3$ in the turbulent section and $\bar{\rho}_L = 879{\cdot}4$ kg/m$^3$ in the laminar section. The $N_{Re}$ and $\lambda$ values at the key points, at temperatures $T_f$ and $T_{fk}$, are likewise plotted in *Fig. 7.6 – 13*. The mean values of $\lambda$ have also been planimetered; they are $\bar{\lambda}_T = 0{\cdot}0432$ in turbulent and $\bar{\lambda}_L = 0{\cdot}0654$ in laminar flow.

Friction loss in the turbulent section is

$$\Delta p_{fT} = 1{\cdot}95 \times 10^6 \text{ N/m}^2$$

and in the laminar section

$$\Delta p_{fL} = 4{\cdot}46 \times 10^6 \text{ N/m}$$

The full friction loss is, then,

$$\Delta p_f = 6{\cdot}41 \times 10^6 \text{ N/m}^2 .$$

All the other relevant intermediate results of the calculation are listed in *Table 7.6 – 2*.

**(b) The oil is thixotropic-pseudoplastic**

If the flow of the pseudoplastic oil through the pipeline is isothermal, the friction pressure drop, can be calculated by the relations, described in Section 1.3.5. If the oil is not only pseudoplastic but thixotropic too, the shape of the flow curves, serving as a basis for the calculation of the pressure-loss, changes with the shearing time (see *Fig. 1.3 – 2*). The flowing pressure loss, for this period of time, may be calculated by the isochronal curves (Ritter and Baticky 1967). The time $t_s$, required for the stabilization is generally of a magnitude of 10 minutes. From this, it is obvious, e.g.

| $N_{Gr} N_{Pr}$ | $N_{Re\,n}$ | $\lambda_n$ | $\alpha_{1n}$ | $k_n$ | $c_n$ | $\Delta l_n$ | $\Sigma \Delta l_n$ |
|---|---|---|---|---|---|---|---|
| $10^6$ | – | – | W/(m$^2$ K) | W/(m K) | J/(kg K) | m | m |
| – | 4972 | 0·0378 | – | 3·11 | 2047 | 450 | 450 |
| – | 4341 | 0·0392 | – | 3·11 | 2033 | 473 | 923 |
| – | 3769 | 0·0410 | – | 3·11 | 2019 | 500 | 1423 |
| – | 3259 | 0·0428 | – | 3·11 | 2005 | 529 | 1952 |
| – | 2806 | 0·0448 | – | 3·11 | 1990 | 563 | 2515 |
| – | 2405 | 0·0469 | – | 3·11 | 1976 | 602 | 3117 |
| – | 2061 | 0·0493 | – | 3·11 | 1964 | 420 | 3537 |
| 6·866 | 1512 | 0·0423 | 35·76 | 2·45 | 1935 | 858 | 4395 |
| 5·567 | 1268 | 0·0505 | 33·52 | 2·42 | 1920 | 948 | 5343 |
| 4·467 | 1060 | 0·0604 | 31·32 | 2·38 | 1906 | 1059 | 6402 |
| 3·545 | 883 | 0·0725 | 29·13 | 2·34 | 1892 | 1197 | 7599 |
| 2·773 | 733 | 0·0873 | 27·00 | 2·30 | 1878 | 1378 | 8977 |
| 2·135 | 614 | 0·1042 | 24·86 | 2·24 | 1865 | 23 | 9000 |

that if $t_s = 25$ min, and the flow velocity $v = 1$ m/s, the flow behaviour of the oil may change before covering a distance of $25 \cdot 60 \cdot 1 = 1500$ m, and then they get stabilized. During this period, the starting value of the apparent viscosity, and so that of the flow gradient, decreases to a stabilized smaller value. For this reason, with a relatively short pipeline, the use of the isochronal flow curves may be justified. If the length is of 10 – 100 km magnitude, however, the accuracy of the pressure loss calculation is insignificantly influenced by the fact, that, the flow gradient is higher in the first section of 1 – 2 km length than in the following one. That is why, at long-distance pipelines, the pressure loss is calculated using steady-state flow curves. The flow gradient is constant along the pipeline at isothermal flow, similarly to that of Newtonian fluid flow.

At non-isothermal flow, essentially the procedure, described in Section 7.6.4 – (a, b) is used for pressure loss calculation. A slight modification is needed however because, in order to determine the convection factor, $\alpha_1$ (Eq. 7.6 – 18), the Nusselt coefficient must be determined as a function of the kinematic viscosity (Eq. 7.6 – 21). For pseudoplastic crudes, instead of this the apparent viscosity, valid for the given shear rate should be used.

### 7.6.5. Temperature of oil in transient flow, in buried pipelines

In the foregoing sections we have assumed the heat flow about the buried pipeline to be steady. This is the case if the pipeline carries a crude of inflow temperature, flow rate and physical parameters constant over a comparatively long span of time, and the temperature of the soil outside the warmed-up envelope about the pipeline is subject to no change. Strictly speaking, this condition is never satisfied. If, however, departure from the steady state is comparatively slight, procedures outlined in Sections 7.6.2 and 7.6.4 remain applicable.

In numerous cases of considerable practical interest, however, deviation from the steady state may be sufficient to make the steady-state relationships unsuited for even an approximate description of the situation. Transient heat-flow situations of this nature will tend to arise primarily in the following cases: (i) when starting up a hot pipeline: the hot oil flowing into the pipeline that, initially, is as cold as the ground, will gradually warm the environment; (ii) flow in the pipeline is stopped and then started again; (iii) flow rates in the pipeline are subject to fluctuations, (iv) the nature and hence the thermal properties of the crude transported are subject to fluctuations. Any meaningful attempt at solving these problems requires the knowledge of the relationships characterizing the processes of warming and cooling. These will permit the calculation of pressures arising on start-up and restarting, and the variation of said pressures with time.

Numerous models and calculation methods have been devised to describe the transient heat-flow and liquid-flow situations and to solve partial problems all subsumed under the above-stated general problems. To mitigate the complications caused by the large number of variables involved, simplifying assumptions have been introduced, and, as a result of these, individual models may rather

substantially differ from one another. The first attempts at a synthesis have been published, but the development of theories readily applicable in practice has not by far been accomplished as yet. One publication to be given special mention is Tugunov's academic thesis (Tugunov 1968), which summarizes 39 papers written on the subject by the author and his co-workers. Similarly interesting syntheses were presented at the Symposium on 'Waxy crudes in relation to pipeline operations' (London, November 1970). Some of the lectures presented were concerned with transient-flow problems (Davenport and Conti 1971). It seems, however, too early yet to attempt a synthesis of the results achieved so far in the scope of the present book. In the following I propose to present a transient model which describes the temperature changes of flow v. length and time in a pipeline shut down after steady-state flow (Szilas 1968).

It is assumed that (i) the pipeline is embedded in an infinite half-space filled with soil homogeneous as to thermal behaviour, (ii) the temperature of the soil in contact with the pipeline can be described by the Chernikin model (1958) based on the linear-heat-source theory of Carslaw and Jaeger (1947). — The solution referred to has been used by Chernikin to characterize oil temperatures in non-insulated pipelines, neglecting the difference between the thermal behaviour of oil and soil. In the following I shall derive the 'cooling model' for an insulated pipeline. Let us assume that, at a given instant $t$, oil temperature is constant all over a certain cross-section of the pipeline, including also the steel pipe cross-section; that is, $T_f = T_o$, where suffix $o$ refers to the *OD*.

Heat flowing through the wall of unity-length pipe into the cooler ground over an infinitesimal length of time $\mathrm{d}t$ reduces the temperature of oil and steel by $\mathrm{d}T$:

$$\left[\frac{d_i^2\pi}{4}\rho_f c_f + \frac{(d_o^2 - d_i^2)\pi}{4}\rho_{st}c_{st}\right]\mathrm{d}T_o = -k(kT'_o - T'_{in})\,\mathrm{d}t$$

where the symbol $T'$ refers to the transient nature of the process. The heat transfer factor is, after the necessary changes to Eq. 7.6 – 17:

$$k = \frac{\pi}{\frac{1}{2\lambda_{in}}\ln\frac{d_{in}}{d_o}}.$$

Let

$$\frac{\pi}{4k}[d_i^2\rho_f c_f + (d_o^2 - d_i^2)\rho_{st}c_{st}] = A\,.$$

Then, after rearranging,

$$A\left[\frac{\mathrm{d}T_o}{T'_o - T'_{in}}\right] = -\mathrm{d}t\,. \qquad 7.6-46$$

Cooling will affect not only oil temperature $T'_o$, but also the outer surface temperature $T'_{in}$ of the insulation. It is to describe this change that we shall make use of the Carslaw–Jaeger–Chernikin relationship. Let $P_1$ be the image of the projection of the linear heat source on a plane perpendicular to it *(Fig. 7.6 – 14)*; then the

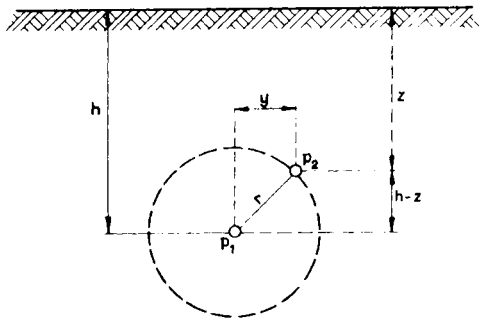


Fig. 7.6 – 14.

difference in temperature between point $P_2$ lying in the plane of projection and defined by the coordinates $y$ and $z$ and the undisturbed soil will be

$$T'_o - T_s = \frac{\Phi^*}{4\pi\lambda_s}\left\{\mathrm{Ei}\left[-\frac{h^2}{r^2}\frac{1}{N_{\mathrm{Fo}}}\right] - \mathrm{Ei}\left[-\frac{1}{4N_{\mathrm{Fo}}}\right]\right\}. \qquad 7.6-47$$

If $t = \infty$, then the Equation reduces to the following form valid for steady-state flow:

$$T_o - T_s = \frac{\Phi^*}{2\pi\lambda_s}\ln\frac{2h}{r}. \qquad 7.6-48$$

Now making use of Eqs 7.6 – 47 and 7.6 – 48,

$$\frac{T'_o - T_s}{T_o - T_s} = \frac{1}{2\ln\dfrac{2h}{r}}\left\{\mathrm{Ei}\left[-\frac{h^2}{r^2}\frac{1}{N_{\mathrm{Fo}}}\right] - \mathrm{Ei}\left[-\frac{1}{4N_{\mathrm{Fo}}}\right]\right\}$$

where

$$N_{\mathrm{Fo}} = \frac{a_s t}{r^2}$$

is the Fourier factor. In a given pipeline, that is, if $h$, $r$, $\lambda_s$, $\rho_s$ and $c_s$ are given, this reduces to the simpler form

$$\frac{T'_o - T_s}{T_o - T_s} = \kappa$$

where

$$\kappa = \mathrm{f}(t) = \frac{1}{2\ln\dfrac{2h}{r}}\left\{\mathrm{Ei}\left[-\frac{h^2}{r^2}\frac{1}{N_{\mathrm{Fo}}}\right] - \mathrm{Ei}\left[-\frac{1}{4N_{\mathrm{Fo}}}\right]\right\}. \qquad 7.6-49$$

This relationship, in the form given here, describes the process of warming up. In the case of cooling down after steady-state flow, on the other hand,

$$\frac{T'_o - T_s}{T_o - T_s} = 1 - \kappa$$

that is,

$$T'_o = (1-\kappa)\,(T_o - T_s) + T_s\,. \qquad 7.6-50$$

Chernikin used this relationship to determine the surface temperature of an 'oil cylinder' of radius $r$. He assumed the difference in thermal properties between oil in a non-insulated pipeline and the surrounding soil to be negligible. In an insulated pipeline, this relationship seems suited to determine the external temperature of the insulation, that is,

$$T'_{in} = (1-\kappa)\,(T_{in} - T_s) + T_s\,. \qquad 7.6-51$$

If this expression of the external, variable temperature $T'_{in}$ of the pipeline is introduced into Eq. 7.6 – 46, then this latter furnishes the time variation of the temperature of oil enclosed in an insulated pipeline. The complicated nature of this relationship made us adopt the following simplified method for solving it. The relationship $\kappa = f(t)$ for a given case can be plotted graphically using Eq. 7.6 – 49. The individual sections of the curve thus obtained are approximated well enough by a relationship of the form

$$\kappa = a + b \ln t\,. \qquad 7.6-52$$

Introducing this relationship into Eq. 7.6 – 51, and the result into Eq. 7.6 – 46, we get

$$A\,\frac{\mathrm{d}T_o}{T'_o - B + C \ln t} = -\mathrm{d}t \qquad 7.6-53$$

where

$$B = (1-a)\,(T_{in} - T_s) + T_s$$

and

$$C = b(T_{in} - T_s)\,.$$

The general solution of Eq. 7.6 – 53 is

$$T'_o = B - C \ln t + \left\{C\,\mathrm{Ei}\left[\frac{t}{A}\right] + c\right\} e^{-\frac{t}{A}} \qquad 7.6-54$$

where $c$ is the constant of integration. The initial condition of $T'_o = T_o$ if $t = 0$ gives the particular solution

$$T'_o = B - C \ln t + \left\{C\,\mathrm{Ei}\left[\frac{t}{A}\right] + T_o - B - C(0{\cdot}5772 - \ln A)\right\} e^{-\frac{t}{A}}\,. \qquad 7.6-55$$

This relationship permit us to calculate the variation of temperature $T'_o = T'_f$ v. the time $t$ elapsed after shutdown of the pipeline, at any pipeline section situated at distance $l$ from the head end of the line.

*Figure 7.6 – 15* shows the time variation of the temperature of oil enclosed in an insulated pipeline. In plotting these curves using Eq. 7.6 – 55 we have assumed the temperature prevailing during steady-state flow to be 70 °C at the instant

of shutdown. Furthermore, $\rho_f = 968$ kg/m$^3$; $\alpha_T = 0{\cdot}55$ kg/(m$^3$ K); $T_s = 0$ °C; $d_i = 0{\cdot}273$ m; $d_o = 0{\cdot}292$ m; $d_{in} = 0{\cdot}392$ m; $h = 1{\cdot}1$ m; $\lambda_{in1} = 0{\cdot}035$ W/(m K) (glasswool); $\lambda_{in2} = 0{\cdot}019$ W/(m K) (polyurethane foam).

Using Eq. 7.6 – 55 to establish cooling curves at various pipeline sections and plotting the oil temperatures belonging to given cooling times $t$ v. position along the pipeline one obtains a family of $T'_o = f(l)_t$ curves. The family shown in *Fig. 7.6 – 16* includes the curve for steady flow at $t = 0$, calculated using Eq. 7.6 – 15. Oil has been assumed to flow in the pipeline characterized above, except that steel is merely wrapped in tar paper against corrosion. The initial inflow temperature is $T_{o1} = 70$ °C and further, $q_m = 12{\cdot}5$ kg/s, and $l = 11{,}200$ m. Cooling is seen to be rather rapid in the

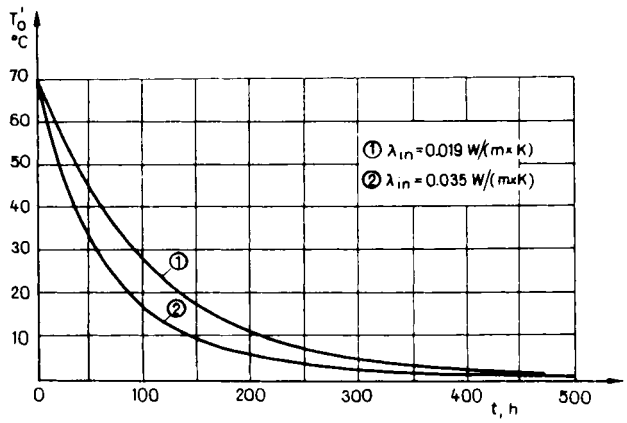


Fig. 7.6 – 15. Temperature v. time of oil shut-in in an insulated pipeline (Szilas 1968)

first few hours, and to slow down rather considerably thereafter. The original cooling rate is reduced to 44 percent after the first day, but the undisturbed soil temperature is not attained even in 30 days.

Warming of a cold pipeline by hot oil flowing in it will be discussed largely after Davenport and Conti (1971). Hot oil introduced into a cold line cools much faster, of course, than it would in steady-state flow in a warmed-up pipe. The heat-transfer factor valid for such situations may be several times the factor for the steady state. Pumping time until steady heat flow sets in may be found in a fair approximation for an uninsulated pipeline buried in the ground by comparing steady-state and transient Nusselt numbers.

Universally valid is that

$$N_{Nu} = \frac{k^* d_o}{\lambda_s} = \frac{k}{\lambda_s \pi}, \qquad 7.6-56$$

where $k^*$ is expressed from Eq. 7.6 – 16.

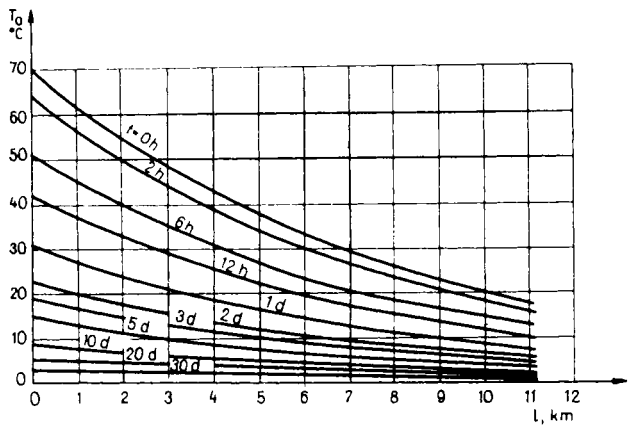


Fig. 7.6 – 16. Temperature traverses of oil shut-in in a pipeline, at various instants, after shut-in (Szilas 1968)

If only the heat insulating effect of the soil is considered, then in case of steady-state heat flow, using Eq. 7.6 – 30

$$k = \alpha_2 d_o \pi = \frac{2\pi\lambda_s}{\ln \frac{4h}{d_o}}. \qquad 7.6-57$$

Substituting this equation into formula 7.6 – 56 the Nusselt-number valid for steady-state is obtained:

$$N_{Nu} = \frac{2}{\ln \frac{4h}{d_o}}. \qquad 7.6-58$$

For transient heat flow, the following relation is valid:

$$N'_{Nu} = 0{\cdot}362 + \frac{0{\cdot}953}{N_{Fo}^{0{\cdot}33}}, \qquad 7.6-59$$

where the Fourier number is

$$N_{Fo} = \frac{a_s t}{d_o^2}. \qquad 7.6-60$$

If $t_s$ is the time required for achieving the steady-state heat flow, then $N_{Nu} = N'_{Nu}$ and from Eqs 7.6 – 58, 7.6 – 59 and 7.6 – 60 it follows that

$$t_s = \left[ \frac{0{\cdot}953}{\frac{2}{\ln \frac{4h}{d_o}} - 0{\cdot}362} \right]^3 \frac{d_o^2}{a_s}. \qquad 7.6-61$$

Example 7.6 – 5. Let us calculate that how much time is required to attain the steady-state heat flow, if $d_o = 0{\cdot}292$ m; $h = 1{\cdot}1$ m; $a_s = 0{\cdot}86 \times 10^{-6}$ m$^2$/s.

Putting the above values into Eq. 7.6 – 61 we get

$$t_s = \left[ \frac{0{\cdot}953}{\frac{2}{\ln \frac{4 \times 1{\cdot}1}{0{\cdot}292}} - 0{\cdot}362} \right]^3 \frac{0{\cdot}292^2}{0{\cdot}86 \times 10^{-6}} =$$

$$= 1{\cdot}62 \text{ Ms} = 18{\cdot}8 \text{ days.}$$

In reality, the hypothesis of the infinite half-space will not model the actual heat flow too accurately after the heat flow issuing from the pipeline has attained the ground surface. Heat loss will exceed the calculated value by 10 to 15 percent thereafter. The heat flow pattern will change, however, very slowly, and the time it takes to attain the steady state is infinite in principle. The accuracy of $\lambda_s$ is not as a rule better than 10 percent. Accuracy is not, then, impaired any further if the above relationship is considered to hold also for the steady state.

Flow in pipelines is not usually interrupted long enough for the oil in the pipe to cool down to the undisturbed soil temperature. On restarting, then, the initial temperature is higher than the undisturbed soil temperature, and it takes less time to attain the steady or a near-steady state. Finding this time for an uninsulated pipeline may be performed by the following consideration. We prepare a family of curves similar to that in *Fig. 7.6 – 16* for the case under consideration. Each curve of the family will be represented in a fair approximation by a 7.6 – 15-type equation. These equations will differ only as to the value of $k$, but even $k$ will be constant all along a given curve. Putting $q\rho = q_m$, and $c = c_o$, one may write up for any curve

$$k = \frac{\ln \Delta T_1 - \ln \Delta T_2}{l} q_m c_o \qquad 7.6 - 62$$

where $\Delta T = T - T_s$.

Knowing the duration of cooling one may pick out that curve from *Fig. 7.6 – 16* which will hold when flow is restarted. It is necessary to calculate the time it would take for the oil flowing in the pipe to attain this state if pumping hot oil were started through an entirely cold environment. In order to find it, we use Eq. 7.6 – 62 to determine the $k$ value corresponding to the actual cooling curve and then Eq. 7.6 – 56 to determine the transient $N_{Nu}$; Eq. 7.6 – 59 is then used to calculate $N_{Fo}$ and Eq. 7.6 – 60 to find the equivalent pumping time. This is the reduction in the time needed to attain steady heat flow against the case when pumping is started at the undisturbed soil temperature.

### 7.6.6. Startup pressure and its reduction

#### (a) The oil is Newtonian

A pipeline may in principle be warmed up simply by pumping into it the high-viscosity crude to be transported. This would, however, require long pumping, often of unjustified duration. Accordingly, the cooled-down pipe is usually flushed first with hot light oil and the high-viscosity crude is not introduced until the line has sufficiently warmed up. Pressure conditions in the warming-up pipeline can be

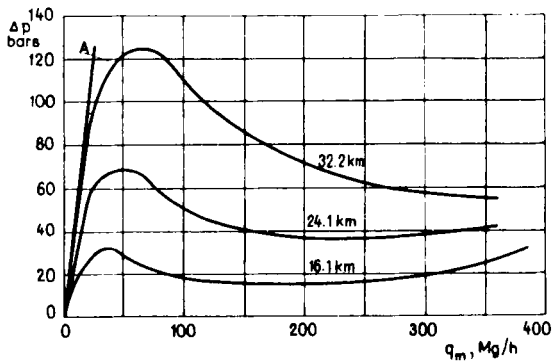


Fig. 7.6 – 17. Friction loss v. throughput at various lengths of 12-in. pipeline, after Ford (1955)

described by Ford's method, which is based on relationships referring to the steady state (Ford 1955).

*Figure 7.6 – 17* shows pressure v. throughput graphs of high-viscosity crudes flowing in 12-in. pipelines of different length. Any point on the curves states the pressure drop of steady flow at the rate $q_m$ chosen in the pipeline of the given length. Inflow temperature of the oil is round 66 °C in each line, and soil temperature is 4 °C. All three curves exhibit peak pressure drops at comparatively low throughputs. After this peak, the driving-pressure requirement decreases first, to increase again at higher throughputs. Assuming initial temperature to be constant, these curve shapes are due to the following: (i) greater throughputs entail higher friction losses in isothermal flow (line $O-A$), (ii) the increase in mean oil temperature reduces viscosity which in turn reduces friction loss. At low throughputs, oil temperature hardly differs from soil temperature, and flow is laminar as a rule. The friction loss can be derived from Eqs 1.1 – 1 and 1.1 – 3 as

$$\Delta p_f = k''_L q_m \qquad 7.6-63$$

that is, a linear function of throughput. This is the relationship illustrated by line $0-A$, tangent to the 32·2-km curve. — At infinite throughput, the average oil temperature equals the inflow temperature. Flow may in that case be assumed

turbulent, and on the basis of Eqs 1.1 – 1 and 1.1 – 10 we get

$$\Delta p_f = k''_T q^{(2-b)} \qquad 7.6-64$$

where $b < 1$. The right-hand ends of the curves in *Fig. 7.6 – 17* approach the line defined by this equation as an asymptote. In plotting any point of these curves we have assumed flow to be steady state. The steady state is not attained instantly, however. Let us assume that a throughput of 100 Mg/h is conveyed through the 24·1-km line. Let us now increase this throughput to 150 Mg/h. At first, the increase in throughput will hardly raise the average temperature of the oil above the preceding steady-state value. Assuming flow to be laminar, a throughput increased by half requires a driving pressure increased by half, that is, pressure drop will suddenly increase from 51 to 76 bars. As time goes on, the average temperature increases gradually, and as a result, $\Delta p_f$ decreases to and stabilizes at about 40 bars.

It follows from the above considerations that pressure drop on startup is invariably higher than that shown in the Figure, the deviation being the higher, the greater the ratio between the throughput to be attained in one step and the steady throughput shown in the Figure. It is when the step $\Delta q$ is infinitesimal that the values in the Figure prevail. Even in this — unrealistic — case it is apparent, however, that startup requires more pressure than steady-state flow. For instance, conveying 350 Mg/h of oil through the 32·2-km line entails a pressure drop of 55 bars, but startup will require a peak pressure of at least 124 bars. If for a delivery pressure of 1 bar the pump can exert 56 bars pressure at most, then this equipment will deliver 14 Mg/h of oil throughput at most. It is therefore fundamental that, if the pipeline is to be heated with the oil to be conveyed, the pump must be chosen so as to be able to deliver the peak pressure. In order, furthermore, to make startup fast enough, it is desirable that the pump should exceed said peak by 20 – 25 percent at least.

*Figure 7.6 – 17* further reveals the pressure change to be expected when steady flow is reduced. Let e.g. the steady throughput through the 24·1-km line be 150 Mg/h, and let us reduce this flow to 100 Mg/h. In the first instants of reduction, the temperature of oil flowing in the pipeline will not change; hence, by Eq. 7.6 – 63, pressure drop will suddenly decrease by one-third, from 40 to round 27 bars. Owing to the lower flow rate, however, the mean oil temperature will gradually decrease and stabilize at a lower value, while the pressure loss climbs to 54 bars. — Reducing the startup or peak pressure may be achieved by several means. At a point somewhere along the pipeline, a booster or a heater station or both can be installed. Let us assume that the operating conditions characterized by *Fig. 7.6 – 17* prevail and that a booster-heater station is installed at the middle of the 32·2-km line, that is, at a distance of 16·1 km from both ends. If the intermediate station is used to heat the oil to be conveyed to the inflow temperature of the head end (66 °C), then the line may be considered as comprising two 16·1-km segments, whose behaviour is characterized by the lowermost curve in *Fig. 7.6 – 17*. Peak pressure drop will, then, be 31 bars as opposed to the preceding 124 bars. Even if pumping at the intermediate station is avoided, peak pressure will not exceed $2 \times 31 = 62$ bars. Once the line is

warmed up, heating at the intermediate station may be ceased (and so may pumping, if any). The peak pressure drop to be attained by heating but no pumping at the intermediate station in the 32·2-km line does not significantly exceed the pressure drop of conveying 350 Mg/h of oil in steady flow. If intermediate heating is unfeasible, peak pressure may be reduced by intermediate pumping alone. In the 32·2-km line, this requires a booster pump of round 70 bars pressure. The booster station will, in order to halve the pressure differential, be installed not halfway along the line, but at a distance of about 23 km from the head end.

We have tacitly assumed so far that startup is performed by pumping the same quality crude as is to be conveyed in the steady state. This would, however, often render startup too slow; other, lower-viscosity liquids are used for startup in these cases, such as a light oil or water. Lower viscosity reduces the pressure drop against what is to be expected with the high-viscosity crude; that is, at the maximum allowable operating pressure of the pipe, throughput will be higher and heating will accordingly be faster. If the startup liquid is water, heating is accelerated also because the specific heat of water is more than twice that of oil. The drawback of this method is that, on closing down the line, the pipe has to be flushed with the low-viscosity liquid, and the transmission of this latter requires a substantial amount of power. Economy is improved if the water can be put to some use at the tail end, or if the line must at intervals carry light oil anyway.

The startup pressure can be reduced by electric heating of the pipeline cooled down (cf. SECT-system in Section 7.6.7).

**(b) The crude is thixotropic-pseudoplastic**

Let us create a $\Delta p$ pressure difference between the final cross-sectional areas of gelled crude cylinder being in a horizontal pipe of $d_i$ diameter and $l$ length. Due to this effect, at the inside pipe wall, shear stress $\tau_1$ arises and the balance of forces may be expressed as follows:

$$\frac{d_i^2 \pi}{4} \Delta p = d_i \pi \tau_i l$$

and, hence, the prevailing shear stress at the wall is

$$\tau_i = \frac{d_i}{4} \frac{\Delta p}{l}. \qquad 7.6-65$$

The relation is also valid for any $d$ diameter value, smaller than $d_i$, and thus, by substituting $d_i = 2r$, the shear stress on the cylindrical surface of $r$ radius is

$$\tau = \frac{r \Delta p}{2l}. \qquad 7.6-66$$

That is, the shear stress changes linearly v. radius. In the axis of the pipe it equals zero, while at the pipe wall it attains the maximum value expressed by Eq. 7.6–65.

Let us assume that a rigid walled pipe of $l$ length and $d_i$ internal diameter is filled by gelled thixotropic pseudoplastic oil without void, and between the two ends of the section $\Delta p$ pressure difference is achieved by injecting Newtonian crude at the head end. If the injected liquid rate is small, the deformation of the paraffin network of the gelled oil will be insignificant and elastic, but essentially it remains, and through its leaks the injected, and the inter-lattice oil, according to Darcy's law, is filtrating (Verschuur *et al.* 1971). The complete gelled plug begins to move, if the pressure gradient, $\Delta p/l$, is increased to the extent, where, the maximum $\tau_i$ shear stress on the pipe inner surface, will equal $\tau_e$ the yield stress of the crude, valid for the actual temperature. The gradient, then, on the basis of Eq. 7.6 – 65, will be

$$\frac{\Delta p}{l} = \frac{4\tau_e}{d_i}.$$

Due to the shear stress $\tau_i = \tau_e$, the paraffin lattice of the gel breaks in the very thin liquid film along the pipe wall, within which the crude remains gelled. Along the pipe wall, coated by paraffin in oil suspension, the gel slug slides with a rather small

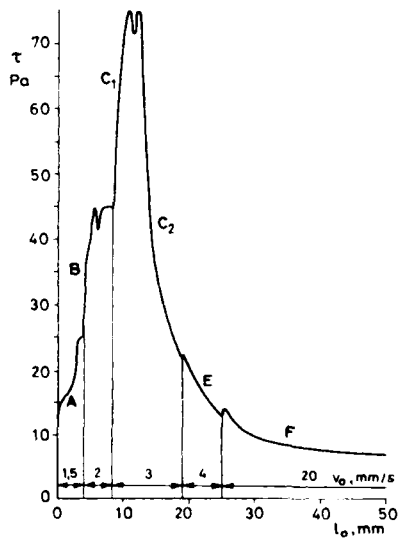


Fig. 7.6 – 18. Degradation of a gel-plug's paraffin lattice, after Verschuur *et al.* (1971)

resistance. In case of increasing flow velocity the paraffin network of the gel slug is gradually destructed, degraded. *Figure 7.6 – 18* shows the diagram as a result of experiments of Verschuur *et al.* (1971). The above process was simulated in laboratory. The diagram gives the shear stress for different $v_o$ injection velocities, in the function of the displaced oil length, $l_o$. It can be seen that at a relatively small injection velocity (diagram sections *A* and *B*), the shear stress is stabilized at a maximum value, that is the greater, the greater is the injected oil rate. During this

period, at the tail and of the experimental pipe, paraffin free oil seeps. $C_1$ part of the $C$ section is similar to the former. After achieving the maximum shear stress, at the tail end first gelled oil at nearly constant shear stress, then along curve $C_2$, paraffin in oil suspension at decreasing shear stress flows out. According to curves $E$ and $F$, further increase of the injected rate do not significantly influence the rate of destruction.

The process in pipelines of industrial size, while the oil is cooling and the flow is starting, significantly differs from that described above. The main reasons are:

(i) The *compressibility of the crude plug* in the pipeline. The oil body is compressible for two reasons: on the hand, the crude itself, as a liquid, or gel, is slightly compressible. On the other hand, the gelled crude does not continuously fill out the space in the pipeline. The compressibility of the crude, $c_o$ (that is about $7{\cdot}5 \times 10^{-10}\ m^2/N$), and its elasticity constant, $E_o = 1/c_o$, respectively may be determined exactly by laboratory tests. A much more difficult task is, however, the determination of the void fraction volume of the crude in the pipeline. The primary reason for its formation is, that, after stopping of the flow, the specific volume of the cooled oil is smaller than that of the warm oil. The void volume will be relatively significant, if, during the cool-down process, no extra outward liquid "makeup" is injected into the pipeline. Verschuur et al. carried out experiments with a pipeline of 888 m length, and 0·2 m internal diameter. They found, that the void fraction of the

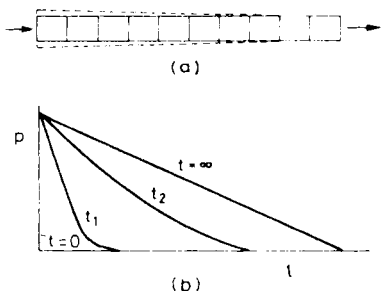


Fig. 7.6 – 19. Pressure wave propagation during gelled oil starting, after Perkins and Turner (1970)

cooled thixotropic pseudoplastic oil could be put to 2 percent, if during the cool-down process the pipe ends were closed. Due to this the compressibility of the oil plug has raised to a 250 times higher value. While calculating the void volume, occurring during the cool-down process, it should be also considered that during the cooling-down the internal pressure of the pipeline generally decreases, and, also for this reason, the pipe diameter, and its storage volume become smaller. The compressibility factor of the pipe is

$$c_p = \frac{d_i(1-\nu^2)}{sE_p}, \qquad 7.6-67$$

where the pipe wall thickness is $s$, $E_p$ is the elasticity modulus of the pipe material, and $v$ is the Poisson number. The void volume is also decreased by the fact that the specific volume of the crude, due to the pressure drop, slightly increases.

The startup pressure is decreased by the compressibility of the crude and the pipeline. Upon the impact of the "starting oil", pumped into the pipeline the oil plug does not begin to move along the whole pipe length, and the lattice degradation does not start along the total length, at the same time, but only gradually. First, due to the oil compression, and pipe expansion, a displacement resulting in the partial,

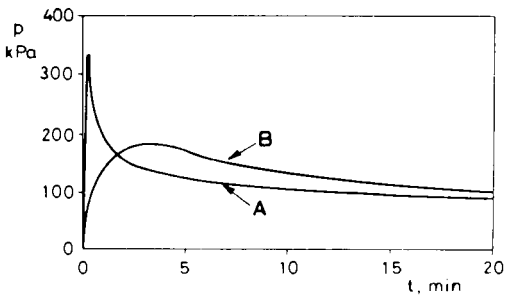


Fig. 7.6 – 20. Startup pressure v. time at rigid walled (A) and at elastic pipe line (B), after Perkins and Turner (1970)

or total degradation of the lattice, will develop in the first, $l_1$ section of the pipe. The great, initial static shear stress is replaced by a smaller, remanent shear stress. A large portion of the start-up pressure is, thus, preserved for degrading the gel-slug, positioned in next pipeline section $l_2$. *Figure 7.6 – 19*, after Perkins and Turner (1970) shows, how the pressure wave propagates during the start-up *(Fig. a)*, and how great will be the pressure v. length at different $t$ moments calculated from the beginning of the startup *(Fig. b)*. In *Fig. 7.6 – 20*, after the same above authors, it is shown how the startup pressure v. time changes at a given oil rate, when the pipe is rigid walled (curve *A*), or when the pipe is elastic (curve *B*). The startup-pressure reducing effect of the elastic system is visible.

(ii) In the pipeline the cooling effect spreads from outside to inside. This process is assumed to create a laminated structure, parallel to the pipe wall. Little is known about the shape and size of the cavities, and their distribution in the pipe may be rather diversified. In the unmoving paraffin network of a given cooling gel section the liquid oil necessarily moves, seeps. If the seepage velocity is rather high, that can be expected first of all in case of rapid cooling, then the space lattice will be more or less destroyed by the flow. Due to this, the yield stress of the gelled oil sections decreases. The factors, influencing this phenomenon, were analyzed among laboratory conditions, by Verschuur *et al.* (1971).

(iii) *Figure 1.3 – 4* shows that the yield stress is exponentially increased v. the decrease in the temperature. In the case shown in the Figure, its magnitude increases to a ten times higher value, while the temperature of the oil decreases from 18 °C to

8 °C. For the reason that the cooling down propagates from outside to inside in the pipeline, the yield stress along the radius decreases till the time, the temperature of the total pipeline content will be equal to that of the surrounding soil. That is why, in case of a non-totally cooled-down pipeline, the startup pressure can be equal with a yield stress prevailing in $r_e < r_i$ radius.

(iv) So far it has been tacitly assumed that the paraffin lattice of the gel, filling out the pipe, is of isotropic character before the degradation. Research, carried out quite

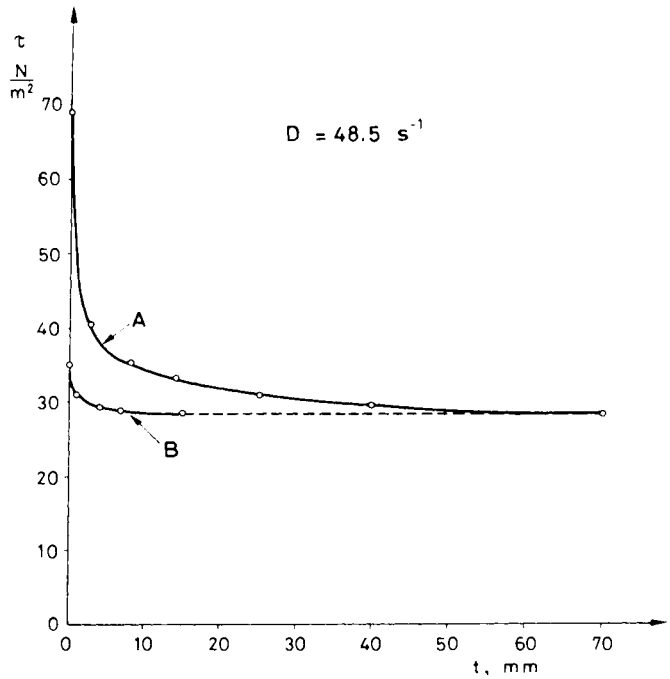


Fig. 7.6 – 21. Degradation of the original paraffin lattice (A) and the same procedure, after relaxation (B) (Szilas 1981, 1984)

recently, however, has pointed out that the lattice of the cooling oil "remembers" the previous flow, and, in case of formerly laminar flow, the lattice density, perpendicular to the flow direction, may be smaller, than parallel to it (gridshell theory; Szilas 1981, 1984). This latter value can be equal to the yield stress obtained among laboratory conditions. *Figure 7.6 – 21* shows that how the shear stress, at constant shear rate, changes v. time, performing the measurement with rotoviscometer. Curve A shows the result of the first measurement, while curve B was determined by using the same sample after a relaxation period of 12 hours. It can be seen that the initial shear stress, valid at 0 shear time, and belonging to a given shear rate (injection rate) is smaller in the second case.

Due to the above listed phenomena the startup pressure of the industrial pipelines may be significantly smaller than the calculated value, based on the yield stress $\tau_e$, measured among laboratory conditions and using Eq. 7.6 – 67. So far no relation is known by which for each case, and with a proper accuracy, among the given conditions the startup pressure may be forecasted. By applying Eq. 7.6 – 67 only the theoretically possible maximum value may be calculated. For industrial design experiments are required among real circumstantes. The qualitative knowledge of the phenomena, however, occurring during the cooling down of the pipeline, can give us a good base to influence the industrial factors for the sake of startup pressure decrease.

It may be found that the conditions of the cooling down, and restarting is impossible to be controlled to the extent so, that the starting pressure should be low enough. In other words, it may occur that the gelled oil along the total pipe length would not start, in spite of exerting the maximum internal overpressure. In such a case, methods, reducing the startup pressure, are to be employed. Methods of this kind are as follow:

(i) Due to mixing *additives, modifying the pipe lattice* to the oil, not only the flowing gradient is reduced (see Section 7.7.3), but also the static shear stress (yield stress) of the oil. This method, if applyied only for reducing the startup pressure, is rather expensive, since the additive, in case of normal operation, is to be continuously injected. Its great advantage is that it is totally safe, and the oil treatment accessories requires small space. That is why it is extremely advantageous in case of transporting oil from offshore field's platforms. This method is used, e.g. at the off shore Bombay High Field, where the oil, treated with additives, is transported to the shore through a pipeline nearly of 200 km length, and 700 mm in diameter.

(ii) The compressibility of the oil significantly increases if *gas is mixed to it*. The startup pressure may be reduced even by only a few percent of gas content. This accounts for the fact, that after the stopping of wells, producing high pour point gassy oils, for the restarting of the flow in the flow line, in certain cases, small startup pressures are needed only.

The disadvantage of this method is, that the presence of the free gas, according to the two-phase flow laws, increases the flow gradient (see Section 1.4.2), and thus, the specific energy demand of the transport is increased, while the transport capacity of the pipeline is reduced. In certain cases, injection of gas, that due to the oil pressure will dissolve in the oil, may be advantageous. The flow, in case of normal operation, remains of single phase character. After stopping, however, due to the pressure reduction, the gas goes out of the solution, and thus, increases the compressibility of the pipe fluid.

(iii) The startup pressure may be realizable, relatively small, if no temperature drop in the pipeline is allowed, or the cooled-down oil is *heated*, respectively. For both purposes the line-heating, described in Section 7.6.7 is suitable, and for oil pipelines, first of all, it is the SECT system.

(iv) The reduction of the startup pressure of the untreated crude is possible by the sectional startup, that requires proper pipeline accessories. Before establishing

them, it should be experimentally determined, how long is the line length $l_s$ from which the gelled oil, by applying the allowable maximum line pressure, may be still started. According to *Fig. 7.6 – 22*, section by section of $(l_s - \Delta l)$ length, the represented set ups should be accomplished. The flow, with a very small flow rate, is to be started by the standard station pump, at the head end point. The oil, from $(l_s - \Delta l_1)$ length pipe section, through open gate valve *1*, discharges into the small-size starting tank *2*. Gate valves *3* and *5* are closed. As the startup pressure is sufficiently

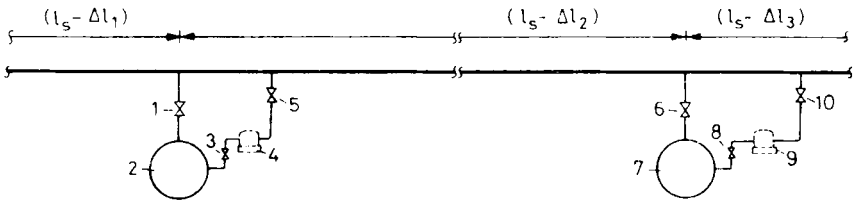


Fig. 7.6 – 22. Hookup of the section by section starting

reduced, i.e. the gel structure is degreaded in the first starting section, gate valve *6* is opened, and *1* is closed. The transportation, by the pump in the head end, is continued with the same low rate. The oil flow starts in the second pipe section $(l_s - \Delta l_2)$, and for a short period of time oil pours in tank 7. The startup procedure should be continued similarly until the oil will be moving along the total pipeline. The rate can be gradually increased thereafter to the value of continuous operation. By applying skid mounted pumps *(4, 9)* the oil, conveyed into the starting tanks, and perhaps mixed with solvents, may be reinjected through open gate valves *3, 5*, and *8, 10*, respectively, into the pipeline. The distance between the service stations $(l_s - \Delta l_i)$, while approaching the end points, gradually decreases. Its reason is, that the length $\Delta l_i$ is, due to the greater remanent shear stress and consequently to the greater starting pressure gradient v. length increasing. This method is recommended first of all if at the ambient temperature the oil is still transportable.

### 7.6.7. Pipelines transporting hot oil

Heating oil to reduce its flowing pressure drop may be performed either by spot or line heating. In spot heating, oil is heated either before entering into a pipeline section, or at booster stations. In this type of transporting, temperature will decrease downstream of the heater, even if the heat flow is steady-state. In line heating, the oil is heated all along the pipeline. This solution is restricted usually to shorter pipelines. The axial temperature of the oil does not change v. the pipe length.

One of the possible arrangements of a *spot-heating* system is shown schematically on *Fig. 7.6 – 23*. Oil stored in tank 1 is heated by steam circulating in heat-exchange coils, to a temperature $T_{ta}$, lower than the start-up temperature of the pipeline, $T_1$, but sufficient to permit the oil to flow to pump *3*. This latter drives the oil through

heat-exchanger *4* into pipeline *6*. Heat absorbed in *4* and power dissipated in the pump will heat the oil from $T_{la}$ to $T_1$. Steam heating the coils in the tanks and in heat exchanger *4* is produced in boiler *5*. At the delivery end, oil enters tank *7*. At the end of the delivery period, pump *3* sucks light oil from tank *2* to flush out the high-viscosity crude; during shut-down, the line stays filled with the non-freezing liquid. On re-starting the flow, the cool pipe and its environment are heated with light oil, taken from tank *2*, and heated before injection, and the heating oil then is driven to tank *8* at the receiving station. During the break in the transport of the high-viscosity crude, the light oil is returned by pump *9*, through line *6*, into tank *2*.

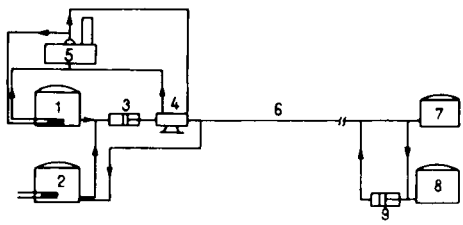


Fig. 7.6 – 23. Oil transmission system with spot heating

The economics of a pipeline, transporting hot oil, will be rather considerably affected by the breaks. These breaks may be due to several causes. While planning the pipeline operation, it is necessary to reckon with the variations in the throughput expected of the line v. time. A pipeline is often started up even before the oil field it is to serve has been fully developed; the yearly production is less than the expected peak. Referring again to Diagram 7.6 – 17, it is necessary to consider the way the lowering of throughput effects the pressure drop in the pipeline. For instance, considering the diagram of the 24·1 km line, one sees that in the throughput range from 150 to 350 Mg/h, the pump discharge pressure will hardly change. In the 32·2 km line, on the other hand, transporting 150 Mg/h of oil requires about one and half as high a pump pressure again as transporting 350 Mg/h. If the maximum allowable working pressure of the pipeline is less than the 88 bars to be expected at the throughput of 150 Mg/h, then continuous transport is out of the question. The higher pumping rate, resulting in a lower pressure drop, can be achieved only by intermittent operation.

Further to be provided are the means permitting the possibly fast and low cost restarting of the flow after unforeseen breaks and malfunction. With reference to the family of cooling curves in *Fig. 7.6 – 16*, it is easy to see that, after any interruption the pump pressure needed for re-starting is the less, the sooner the high-viscosity crude in the pipeline is displaced by light oil. As an example, *Fig. 7.6 – 24* (Ells and Brown 1971) shows, how in a given case the pump pressure varies v. time if the displacement of the crude in pipe with light oil is started immediately after the interruption (curve *1*), and after a delay of six hours (curve *2*).

The equipment and operation of spot heating are to be designed, so as to keep the cost of transporting the given quantity of oil over the given pipeline as low as possible. The number of technically feasible variants is so high that no theory, taking into account of all factors, influencing the choice of the optimum solution, has so far been put forward. There are, however, methods that permit optimization of individual parameters. For instance, Tugunov (1968) published a procedure for finding the optimum thermal insulation of a pipeline. He assumes the head-end, and tail-end temperatures of the flow, and the length diameter of the pipeline, to be

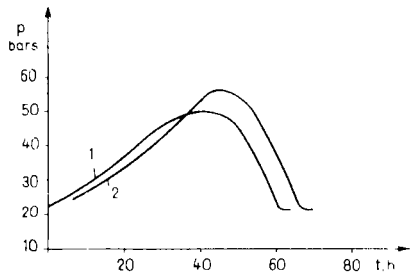


Fig. 7.6 – 24. Starting pressure v. time, after Ells and Brown (1971)

known, and the oil to be Newtonian. His variables are the heat insulation to be provided, and, accordingly, also the number of the intermediate heater stations. Westphal (1952) compares the economy of the operation of insulated, and uninsulated pipelines of a given size, and various rates of throughput. He finds that, in the case considered, uninsulated pipe will be more economical at comparatively low throughputs, and vice versa.

Jablonsky devised a procedure for finding the optimum head-end temperature of oil. $T_{opt}$ is that temperature, at which the aggregate cost of heating and pumping is the lowest. He assumed heat transfer factor $k$ to be constant along the pipeline. Abramzon (1968) solved the same problem for variable $k$, whereas Muradov and Mametklychev (1970) accounted also for the latent heat, liberated by the solidification of the paraffin.

As an example for a modern spot-heated hot-oil pipeline, let us cite the one built by Getty Oil Co., one of the largest of its kind (O'Donnell 1968; Griffith 1970). The uninsulated 20-in. underground line of 280 km length transports 26,000 $m^3$ of crude per day. Tankage is restricted to the head-end station. At the booster stations, there are heaters, pumps and accessories only. The total pump power is 9·3 MW; the aggregate heating power is 59 MW. The line is operated by a Motorola type process control which acquires and processes 250 measurement and position data every 15 s. The control ensures the correct delivery temperature; it governs according to program and records the transmission of various batches of oil; controls the opening and closure of the right valves when scrapers pass booster facilities, the programwide operation of screw pumps on startup, the cut-in of safety equipment,

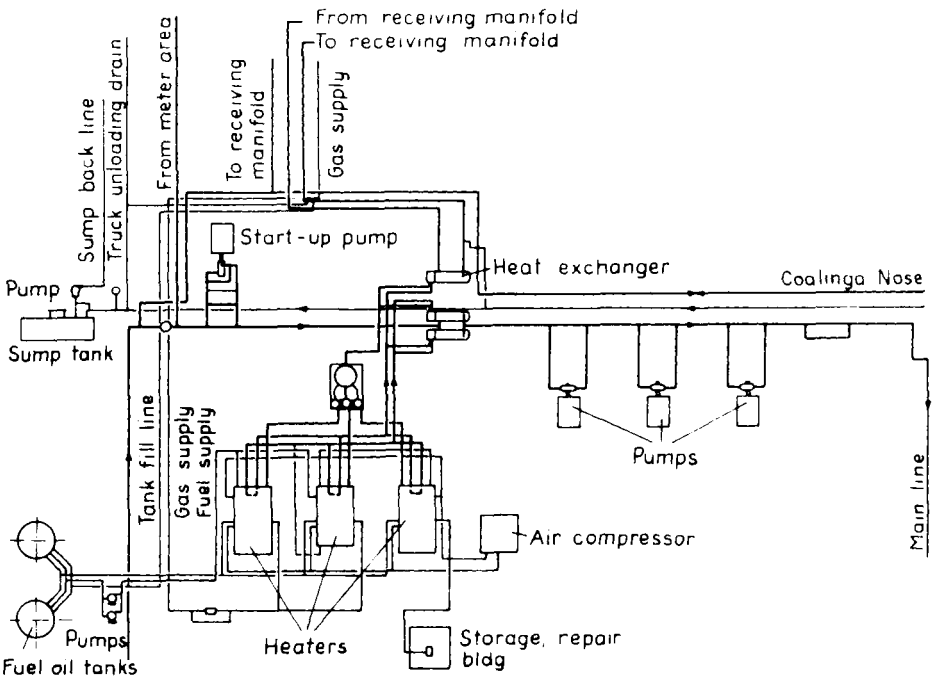


Fig. 7.6 – 25. Coaling station, outgoing facilities, after O'Donnell (1968)

and a number of other automatic operations. *Figure 7.6 – 25* shows the outgoing facilities at the Coalinga station; while in *Fig. 7.6 – 26* the schematic layout of a booster station can be seen (O'Donnell 1968).

For spot-heated pipelines, the possibility of the removal of the gelled crude is to be ensured. The removal may take place section by section, similarly to the process described, referring to *Fig. 7.6 – 22.*

In *line heating*, heat may be supplied by hot water, steam, and electricity. In the two former cases, the heating medium will flow in pipes, parallel to the oil pipeline. The heating pipe may be either coaxial, within or without the oil pipe; or parallel to it on the outside *(Fig. 7.6 – 27)*. The advantage, in the first case *(Fig. a)* is that the temperature of the outer pipe-wall is lower and heat loss is, consequently, reduced, but the oil line cannot be scraped. If the heater line is non-coaxial (*c*, *d*), heat transfer from heater line to the oil line is worse but the size of the oil pipe may be less for a given pressure drop. The use of heater lines is restricted, as a rule, to short pipelegs (less than 1 km in length). *Table 7.6 – 3* (after Pektyemirov 1951), helps in choosing the number and size(s) of heater lines. A modern way of insulating the parallel heating arrangement is discussed by Eichberg (1970). The 3-in. pipe is provided with two parallel heater lines of 1 1/2″ in size, conveying hot water. The common insulation is a polyurethane foam wrapping under a common PVC-foil sheat.

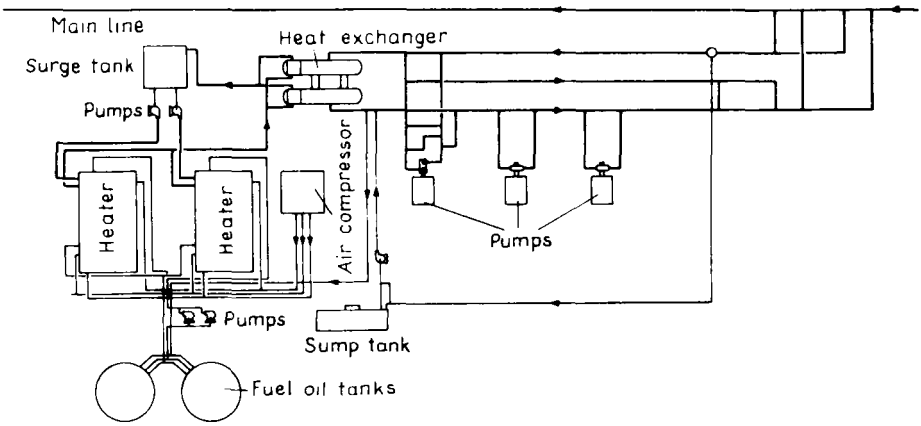


Fig. 7.6 – 26. Booster pump and heating station, after O'Donnell (1968)

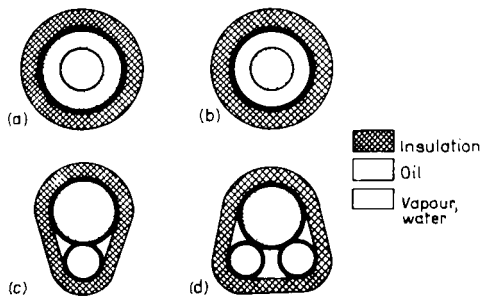


Fig. 7.6 – 27. Line heating designs

Directly after installation on the pipe ensemble, this latter can be fastened finally, and for good, by a sort of zip fastener developed on the foil sheath.

During the past decade the *SECT*(skin electric current tracing) *system*, elaborated in Japan, and applied there in the industrial practice for the first time in the 1970s, is increasingly applied in the oil industry all over the world. Formerly the method was used for heating of relatively short pipelines, transporting high viscosity crude from the port to the refinery, or high viscosity products from the refinery to remote storage stations. By now, it may be also applied, safely, and economically, for heating long-distance pipelines, if introducing electric energy is possible at maximum 15 km intervals. The schematic diagram of the system is shown on *Fig. 7.6 – 28*. On the outer wall of the pipeline *1*, one or more heating pipes *2* of parallel axis and 6 – 38 mm internal diameter are welded, within the pipeline, a *3* copper cable of 8 – 60 $mm^2$ cross-section insulated with plastics (heat resistant PVC, polyethylene, sylicon rubber, teflon) is positioned. The cable is attached to the heater pipe section's

tail ends *4*. From power unit *5*, alternate current is led into the system. The current through the cable flows into the heating pipe wall, and the circuit is closed through the wire *6*. The interference of the electromagnetic fields, surrounding the cable and heater line, results in a so-called skin effect. Due to this, the electric current, conducted by the heater pipe, propagates through a tight annular cross section. Inner diameter of it is equal to the inner diameter of heater pipe; the outer diameter is only 0·1 mm larger. Other parts of the pipe, such as the external cylindrical

Table 7.6 – 3. Compatible sizes of oil pipe and of steam pipe used to heat it (after Pektyemirov 1951)

| Oil pipe size in, | Steam pipe | |
|---|---|---|
| | number | size, in. |
| 2 – 3 | 1 | 1/2 |
| 4 – 5 | 1 | 3/4 |
| 6 | 1 | 3/4 – 1 |
| 8 | 2 | 3/4 |

surface, are free of electricity. In the small current conducting cross-sections considerable heat develops, appearing first of all in the wall of the pipe, that, through the welds, propagates to the external wall of the oil-line, and to its content. In order to achieve the required heating, the necessary voltage drop is 300 – 700 V/km, and the amount of the current is 50 – 200 A/km. The transmitted heat power is 15 – 20 W/m (Ando and Kawahara 1976). The pipeline is schematically shown in *Fig. 7.6 – 29*. The oil transport line *1* and cable *2*, surrounding heating line *3* are covered by a common heat insulating polyurethane coating, that, in order to protect against water and mechanical damages, is coated by polyethylene pipe *5*. The pipeline, due to the oil flow, and because of the high voltage power transmission line in the vicinity, may de slightly filled up with some static electricity, that is why the system is grounded (see *7* in *Fig. 7.6 – 28*). According to Ando and Kawahara, the actually

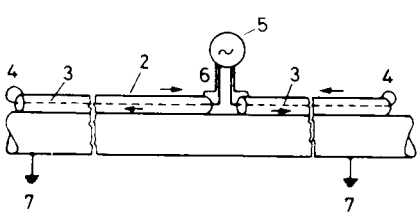


Fig. 7.6 – 28. Scheme of the electric outfits of the SECT system, after Ando and Kawahara (1976)

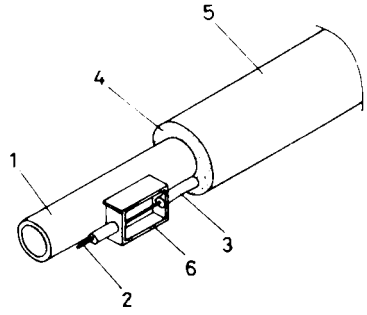


Fig. 7.6 – 29. The structure of the SECT pipe line, after Ando and Kawahara (1976)

measured voltage difference between the external pipe wall and the soil is only 100 $-200$ mV, and through the grounding wire a current of $10-200$ mA passes. The mounting and replacement of the cable without damaging the heat insulation, and later without disturbing the soil, may be realized by applying the "pull-boxes", *6*, as shown in *Fig. 7.6 – 29.*

The SECT system proved to be economical. Its economy, as compared to the steam heating, increases with the pipeline's length, where it is to be applied. In Japan, the heating cost is merely 30 percent of the cost of steam heating for 3700 m length. System SECT may be also applied for heating oil field flow lines and transport lines carrying high pour point crude. Myers (1978) furnishes technical and economic data about field trials, where, beside the SECT, other electric heating methods were also used. SECT proved to be the more economical in each case, if the oil pipe diameter exceeded 3 inches, and at each diameter, where the length of the pipeline exceeded 1650 m, respectively. In Europe, an oil pipeline, heated by the SECT system, was built first in 1979. This pipeline of 24 inches diameter transports oil from a port on the Adriatic see to a refinery of 4·7 km distance (Galati *et al.* 1979).

Advantages of the SECT system are: (i) below 70 °C, heating cost is usually smaller than at any other methods; (ii) it works automatically fulfilling precisely the temperature prescriptions either while heating up gelled oil or at continuous oil transport; (iii) it requires practically no maintenance.

## 7.7. Methods of improving flow characteristics

### 7.7.1. Heat treatment

Flow behaviours of thixotropic, pseudoplastic crudes are discussed in Section 1.3.1. To improve the flowing behaviour of these crudes heat treatment uses the feature, that the macrostructure of the solidified paraffins can be very different depending on the rate of cooling. At relatively high temperatures, $80-90$ °C, all the paraffins are in solution. If the subsequent cooling is rapid several, independent paraffin crystals develop, that, at a terminal temperature of about 20 °C, usually do not unite to form a connected space lattice. The flow properties of this dispersed system may be much more favourable, than that of the oil, in which the paraffin, due to the slow cooling, forms a more connected space lattice. The macrostructure of the paraffin is also influenced by the fact, whether the oil, while cooling, is in rest or it is moving. Laboratory experiments show, that, due to the mixing, during the cool-down process, paraffin of less connected space lattice, i.e. oil of more favourable flow behaviour develops.

While cooling the character of the developed disperse system is significantly influenced by the malthene content of the oil too. This waxy oil ingredient consists of heteropolar molecules of rather varied composition, which adhering to the dissolved paraffin crystals, prevent their further growth, and hinder the development of connected space lattices. Their impact is influenced by their chemical

composition and amount. Furthermore they exert a very characteristic influence on the flow properties of the crude during a "reheating and cooling" procedure. This will be further discussed below.

The *Fig. 7.7 – 1* shows the results of the experiments, performed at the Department of Petroleum Engineering of the Miskolc Technical University for Heavy Industry (Hungary). The crude from Algyő field (Southern Hungary) of 20 °C

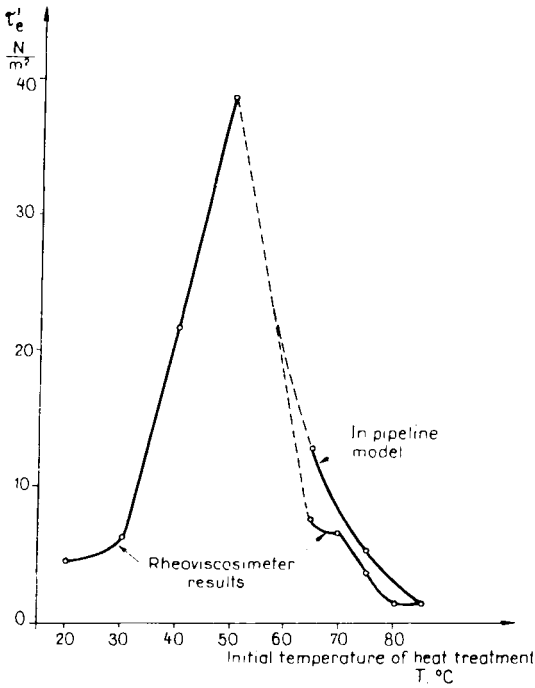


Fig. 7.7 – 1. Influence of starting temperature of heat treatment upon apparent yield stress, after Szilas *et al.* (1978)

temperature originally was treated at first in standstill by heating to various temperatures, then cooling back to 20 °C at a constant rate, and thereafter the static shear stress was measured. The Figure shows that the flow behaviour, characterized by the above mentioned parameter, significantly changes with the end-temperature of the re-heating. It will significantly worsen before reaching the value of 50 °C; at higher temperatures improvement can be seen, but only at a temperature of 70 °C we attain the flow properties of the original untreated oil. In case of re-heating to 80 – 85 °C, the static shear stress was lower, as compared to the original, untreated value.

Similar result is obtained, if, for the characterizing of the flow properties other rheological parameters, e.g. the apparent viscosity, corresponding to some given

shear rate, are selected. The so-called *critical reheating peak temperature*, offering the worst flow properties, may change from crude by crude. In the course of our experiments we found 50 °C to be the most frequent, but occasionally significantly higher values, such as 70 °C, were also measured. This phenomenon appears only in the case, if, beside the praffin, also resinuous components exist in the crude. The probable explanation for this may be, that the malthene molecules, as described above, join the paraffin crystals only in the course of a process of cooling down from a relatively high temperature. This occurs at the first cooling during the production process too. On reheating, the relatively light homologues of the composite crystals of the paraffin melt, and the associated malthene molecules liberate again. These, however, due to the previous binding, have lost their activity, and can regain it only at a relatively high temperature. The inactive malthene molecules are, in the course of cooling from relatively small reheating temperature, unable to prevent the dissolved paraffin molecules from joining the existing space lattice fractures, and thus a space lattice, more connected than the previous one, and an oil of worse flow properties develops. *Table 7.7 – 1* presents the results of laboratory experiments, where the sensitivity of different Hungarian crudes for heat treatment was examined. For characterizing the flow behaviour, the $\mu_r$ relative apparent viscosity,

Table 7.7 – 1. Effect of heat treatment on several Hungarian crudes

| Name of crude | Slow cooling without mixing | | Slow cooling with mixing | | Fast cooling without mixing | | Fast cooling with mixing | |
|---|---|---|---|---|---|---|---|---|
| | $\mu_a$, P | $\mu_{rb}$ | $\mu_{ra}$ | $\mu_{rb}$ | $\mu_{ra}$ | $\mu_{rb}$ | $\mu_{ra}$ | $\mu_{rb}$ |
| | 1 | 2 | 3 | 4 | 5 | 6 | 7 | 8 |
| Szank I | 13·8 | 1·04 | 0·77 | 0·79 | 1·03 | 1·09 | 0·70 | 0·78 |
| Szank II | 0·14 | 2·42 | 0·91 | 1·86 | 0·86 | 2·14 | 0·80 | 1·36 |
| Tázlár | 31·6 | 1·42 | 0·92 | 1·10 | 0·94 | 0·97 | 0·52 | 0·86 |
| Kiskunhalas I | 0·77 | 5·31 | 1·00 | 3·84 | 1·24 | 4·84 | 1·00 | 4·21 |
| Kiskunhalas II | 3·05 | 1·33 | 1·00 | 1·00 | 0·43 | 0·94 | 0·33 | 1·22 |

determined at 10 °C, and at $D = 145{\cdot}5\ s^{-1}$ shear rate, was selected. The adjective "relative" here means, that the apparent viscosity values are, in each case related in every line to the $\mu_a$ values of column 1, measured after a slow cooling without mixing. The value for slow cooling was 0·95 °C/min, while the same value for rapid cooling 2·20 °C/min. $\mu_{ra}$ denotes the "relative" value, achieved by continuous cooling, while $\mu_{rb}$ gives the relative value obtained after a "reheating to 50 °C and cooling" treatment. The impact of the rapid, and slow cooling, and that of the re-heating can be seen. Re-heating generally worsens the flow properties. The best flow properties develop by "rapid cooling and mixing" (column 7), while the worst ones by "slow cooling, without mixing" (column 2).

Being aware of the fact that the flow properties of the crude, due to the temperature, and shear history, may significantly change, is of great importance.

This knowledge may be directly used for industrial improvement of flow properties. Besides, it indicates, that also independently of our intentions, in the course of production, transport, and storage, the flow behaviour may change. Rheological measurements, the results of which may serve as a basis of the calculation of pressure loss, may be carried out only with representative samples, where the temperature and shear history is the same as that of the oil to be transported.

Both from the points of view of the laboratory-scale history simulation, and the heat treatment, performed in order to improve the flow properties, it is important to determine the minimum and maximum efficient values for cooling speed. Maximum efficient cooling speed, expressed in °C/min units, is the limit value, above which the flow properties cannot be improved any more, while the minimum cooling speed is the value under which the flow properties already may not be worse. The above cooling speed values, occurring in practice range from 1 to 3 °C/min. In the knowledge of these limits, on the one hand, the time, required for the laboratory simulation of the flow history may be shortened, and, on the other hand, while designing the heat treatment process, the cooling speed, that enables us to achieve the most favourable flow properties by using the minimum cooling energy, may be determined.

By means of calculation it is generally impossible to determine the flow properties of a mixture of different thixotropic pseudoplastic crudes from the parameters of the basic oils. Beside the chemical composition of the components, the rate of their heat treatment, the temperatures of the components, and the difference in their temperatures before mixing play also an important role. The expectable flow properties may only be determined by measuring samples prepared by laboratory simulation of real shear and temperature history and mixing circumstances.

In certain cases simulation may be even more difficult, since the physico-chemical properties of the sample, during stopping or storage, may change. This phenomenon is called "aging", and is assumed to be related to changes in the chemical composition.

The first commercial application of heat treatment took place at Nahorkatiya and Moran, in India (*Oil and Gas Journal* 1963). Even today these are the largest heater-treater stations, described in literature, and they are modernized continuously (Chandrasekharan and Sikdar 1970). The main parameters of the production and transport of the two oilfields, and the Nahorkatiya plant will be discussed as follows.

At Nahorkatiya, the crude whose pour point ranges from 29 to 34 °C and whose paraffin content is 15·4 percent, is transported through a 16″ pipeline of 402 km length to a refinery where part of it is refined; the rest is transported through a 14″ line to another refinery at a distance of 765 km from the first one. The first line segment was designed for a yearly throughput of 2·75 Tg, the second for a throughput of 2·0 Tg year. The lowest soil temperature at pipe depth 1·2 – 1·8 m is 18 °C. Heat treatment is required between October and April. It entails a significant improvement in flow behaviour. Typically, at 18 °C temperature and a shear rate of 13 $s^{-1}$, the apparent viscosity is 0·6 Pas in untreated oil, and 0·1 Pas in treated oil.

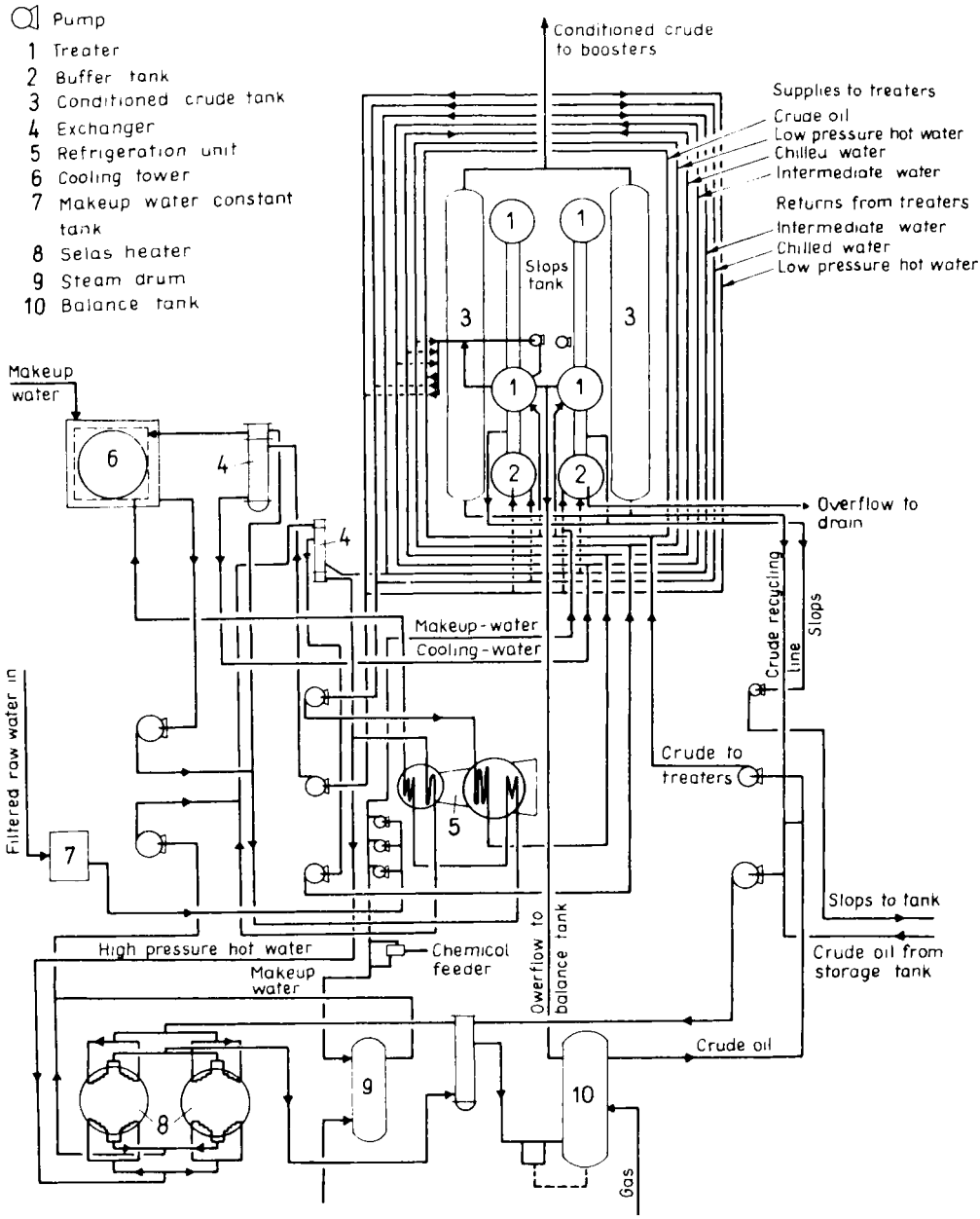


Fig. 7.7 – 2. Nahorkatiya crude heat treater station (Chandrasekharan and Sikdar 1970)

The Nahorkatiya crude heat treater plant is shown as *Fig. 7.7–2* after Chandrasekharan and Sikdar (1970). The crude is heated in gas-fired heat-exchangers to between 90 and 95 °C. Subsequent cooling to 65 °C is effected in heat exchangers, using crude to be preheated as the coolant. In the next step, the static crude is chilled with water to 18 °C. Each of the 36 treater tanks is an upright cylindrical tank 6·1 m high, and of 9·2 m of diameter; each tank contains 127 one-inch chilling tubes. It is the cooling water that flows in the tubes, and the crude that occupies the space between them. Stationary cooling takes place in the following steps. The empty tank is filled with crude, which is chilled by the circulation of cold water at a rate of 0·6 °C/min. After cooling to 18 °C, the crude is pumped to a storage tank, and the tubes are used to circulate hot water, which again rises the tank temperature to 65 °C. This melts the deposited paraffin and prepares the tank for the reception of another batch of crude. These heating and cooling operations are performed by means of five water circiuts, each separate from the others. (i) High-pressure hot water heated with gas to 145 °C and held under sufficient pressure to keep it below its bubble point is used to heat low-pressure hot water and to regenerate the concentrated lithium bromide coolant of the absorption cooler. (ii) Low-pressure hot water is used to heat the treaters to 65 °C after the chilling period. (iii) "Intermediate" water is used to cool oil in the first phase of cooling. It is kept at a temperature of 30 °C by "cooling" water cooled in a cooling tower. (iv) Cold water is used to chill the crude to 18 °C in the treater tanks. This water is cooled to 14 °C in an absorption refrigerator. (v) Cooling water, circulated in an open circuit including a cooling tower, is used to cool the intermediate water. The 324 valves of the treating plant are controlled by an electric Flex-o-Timer. The water circuits are controlled by a programme controller which adjusts the required temperatures. The procedure, because of requiring a great investment, is rather expensive. That is why in India now a cheaper solution is being designed that provides continuous heat treatment during the flow (Mukhopadhyay 1979).

### 7.7.2. Solvent addition

The mixing together of two crudes, or products, comparatively low in malthenes, differring from each other in flow behaviour, will result in a mixture whose flow properties will usually fall between the properties of the two components. It is possible to improve, by this means, the flow behaviour of high-paraffin, high viscosity gelling crudes, e.g. by the addition of lower viscosity crude, or a liquid product, such as gazoline, kerosene, or diesel fuel. Attempts have been made at predicting the behaviour of mixtures starting from those of the components. No laws of general scope have been derived as yet, but important research was carried out to determine empirical relationships (Aliev *et al.* 1969).

The effect of the solvent upon the continuous transport can be determined by measuring the flow curves of high viscosity crudes and those of the mixture at various temperatures, and from the results, in the way, described in Section 1.3.5, the change of the pressure gradient v. throughput at different temperatures is to be

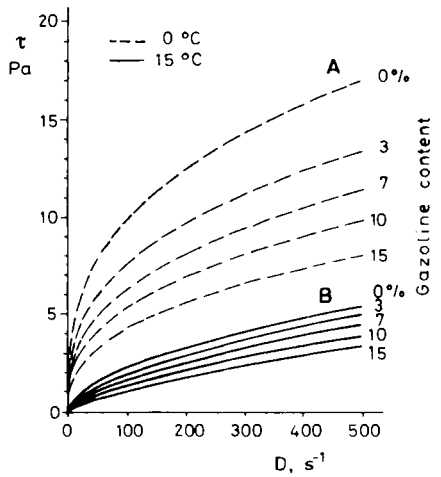


Fig. 7.7 – 3. The effect of condensate on the flow curves of Algyő-crude, after Szilas and Navratil (1978, 1981)

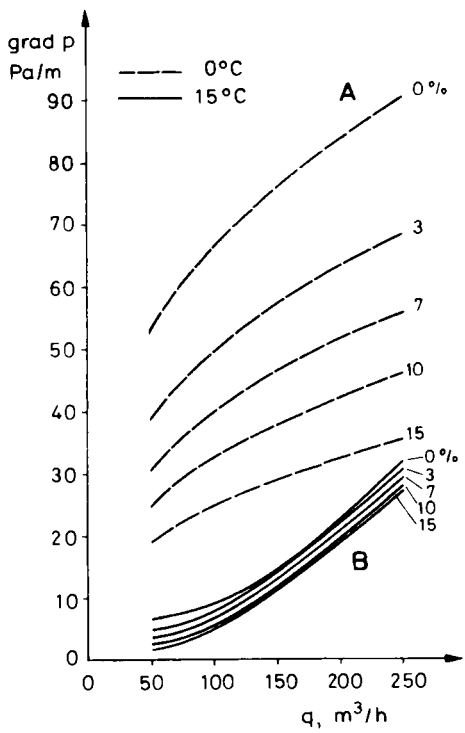


Fig. 7.7 – 4. Isothermal flow gradient in a $d_i = 0{\cdot}3$ pipe line for oil flow curves characterized by Fig. 7.7 – 3 (Szilas and Navratil 1978, 1981)

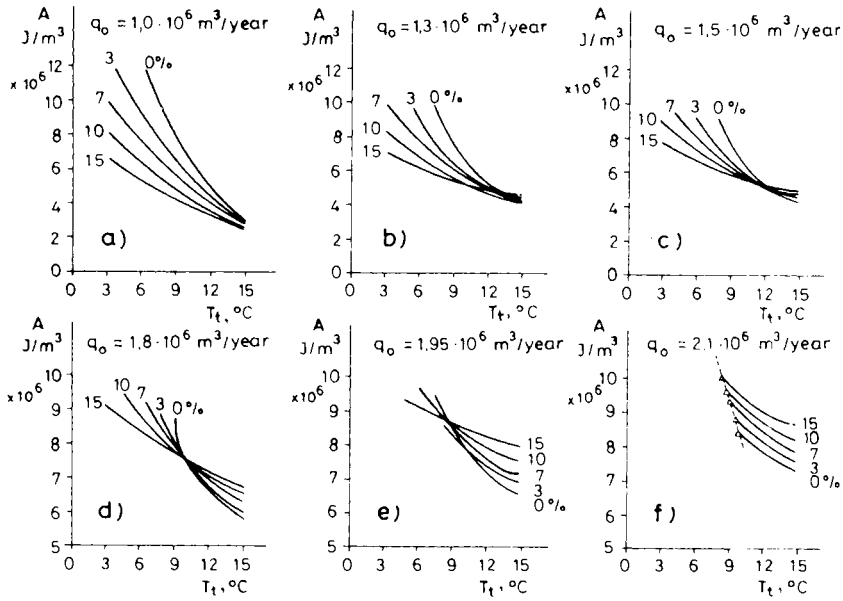


Fig. 7.7 – 5. Specific energy demand of non isothermal, solvent using oil transport under different operating conditions, after Szilas and Navratil (1978, 1981)

calculated. *Figure 7.7 – 3* shows the steady state flow curves of an Algyő crude, mixed with natural condensate at temperatures of 0 and 15 °C.

*Fig. 7.7 – 4* shows the flow pressure gradients of the same fluids while passing through a pipeline of 0·30 m *ID*. It can be seen that the flow curves of the basic crude, and that of the mixture are of pseudoplastic character. Due to adding the condensates the friction pressure loss is reduced. The rate of this reduction in case of crudes of lower temperature, i.e. of worse flow property, is greater.

The mixing of the additives to the basic crude will cause upon the flow pressure drop two effects of opposite character. On the one hand, it increases the flow rate and, therefore, in case of unchanged other parameters, the flow pressure loss increases too; on the other hand, it creates better flow properties by which this loss is reduced. Obviously, there is a given rate of the solvent at which the decrease in the flow pressure loss is the greatest. Values below and above this rate increase the flow pressure loss. The summarized effect of the influencing parameters are well shown by *Fig. 7.7 – 5*. The specific energy demand, after Szilas and Navratil (1978, 1981) was calculated for a pipeline of 162 km length and 0·305 m diameter, from formula

$$A = \frac{\Delta p q_m}{q_o \eta}, \quad \text{J/m}^3$$

where $\Delta p$ is the flowing pressure loss; $q_m$ is the volumetric rate of the mixture, while $q_o$ is that of the original crude; $\eta$ is the efficiency of the centrifugal pump. It was

assumed that the pipeline was laid horizontally, with an axis 1·2 m below the surface. The head end temperature of the oil, in each case, was 42 °C, the thermal conductivity factor of the soil 2·0 W/(m K), and the allowable maximum pressure loss in the pipeline was 58 bars. It was also assumed that the maximum time exploitation factor was 0·96. The six parts of the Figure show the specific energy demand of the stabilized, non-isothermic flow in the function of soil temperature at different yearly liquid throughputs. In each Figure, the flow energy demand of five different flow behaviour oils are plotted by using the flow curves of *Fig. 7.7 – 3*. The numerals beside the curves show the percentage of the solvent v, the transported crude. According to *Fig. 7.7 – 5 (a)*, at a relatively small yeary throughput, the specific energy demand, at any temperature is the smaller, the greater is the rate of solvent. In case of greater throughputs, however, in Figs *(b) – (e)*, an inversion

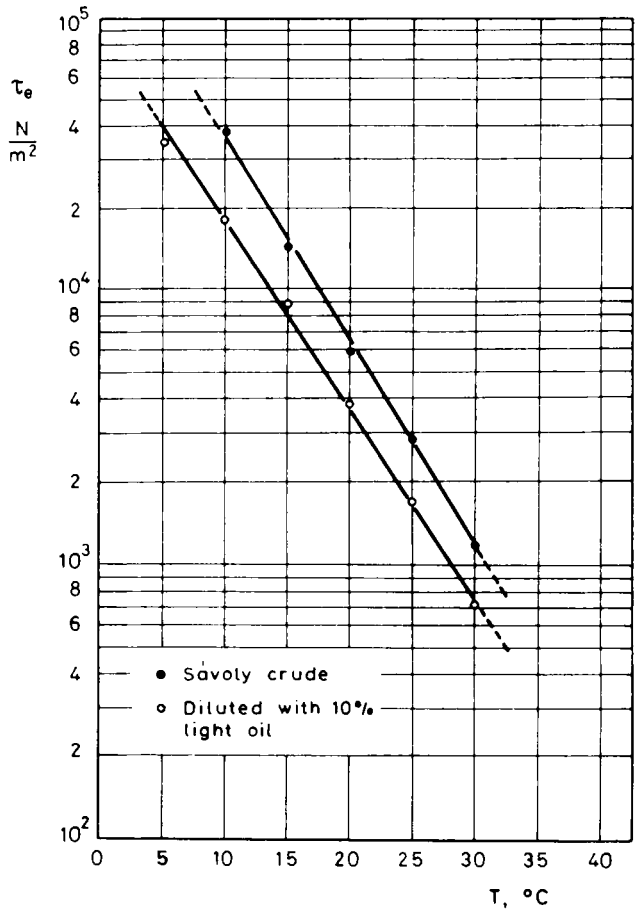


Fig. 7.7 – 6. Effect of the solvent addition on the Sávoly-crude's apparent yield stress

temperature appears. For lower soil temperatures the previous statement remains valid, i.e. the greater is the condensate content of the crude, the smaller is the specific energy demand of the transport. At a temperature, higher than the *inverse value*, the situation changes. First only the curve, corresponding to the greatest solvent rate raises above the curve of the untreated crude *(Fig. b)*, then gradually, the same phenomenon follows for the curves, corresponding to smaller condensate contents, and they are arranged in an inverse order. In *Fig. (f)* the inversion point has already disappeared, and only the sections of the curves, valid for higher soil temperature can be seen. Their pressure losses at lower soil temperature would exceed the

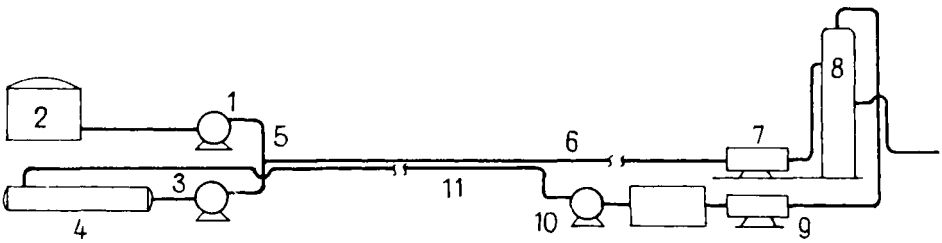


Fig. 7.7 – 7. Transport of diluted crude

maximum allowable values, 58 bars. These boundary values are shown by the triangles, connected by dashed lines. This Figure demonstrates too, that on the one hand, with an increase in the solvent content the specific energy demand of the transportation also increases, and, on the other hand, lower is the soil temperature, at which the prescribed rate of crude can be transported.

It also indicates that at smaller yearly yields the flow improving features of the additives prevail, while at greater yields the volume increasing effect dominates. The reason for this is, that the greater is the throughput, the greater is the flowing temperature, resulting in more favourable flow behaviour of the basic crude. The effect of the solvent, reducing viscosity, is, thus, relatively small. The other reason is that the pipeline section in which turbulent flow exists with pressure loss nearly proportional to the square of flow rate at greater throughputs is longer, contrary to the laminar section, where the pressure loss is proportional to the first power of the rate (Section 1.1).

Due to the effect of the solvent, the static shear stress or apparent yield stress (AYS) $\tau'_e$ is also reduced. In *Fig. 7.7–6* the change of AYS of curde from Sávoly (Hungary) v. temperature, and the same relationship for the same oil, after adding a 10 percent of light oil is represented. It can be seen that, due to the solvent, $\tau'_e$ considerably decreases.

The economics of this method is considerably improved if the solvent is an unrefined product (raw gasoline, low viscosity crude) produced in the vicinity of waxy crude, which can be handled together with the crude after arrival at the refinery. Costs are higher if no natural solvent is available, and the solvent used has

to be recovered by reboiling after delivery, and returned to the head end of the pipeline. The schematic diagram of a transmission system of this sort is shown on *Fig. 7.7 – 7* (Szilas 1966).

Pump *1* sucks high-viscosity crude from storage tank *2*. Pump *3* sucks solvent from horizontal tank *4*. The two pumps inject the two liquids in the prescribed proportion through mixing throat *5* into pipeline *6*. The mixed oil is heated at the delivery and in heat exchanger *7*, and the solvent is evaporated in tower *8*. The evaporated fraction is cooled, and liquified in heat exchanger *9*, and returned by pump *10* through line 11 into tank *4*. The mixing ratio of the crude and solvent is to be matched according to the changing ground temperature.

### 7.7.3. Chemical treatment

Flow parameters can be improved by adding certain chemicals to the crude. The chemicals, in question, belong to two distinct groups. The first group includes compound that enter and modify the paraffin lattice during the cooling of the crude. The compounds of the second group constitute solvates in the oil, and, assuming a preferred orientation, parallel to the main direction of flow, prevent the radial displacement of liquid particles in turbulent flow, thus reducing the energy dissipation due to impulse exchange.

*Lattice-modifying additives* include the so-called P-inhibitors. Molecules of this inhibitor adhere to the edges or dislocations of the paraffin-crystals, formed during

Table 7.7 – 2.
Flow parameters of a crude, untreated and treated with a 0·15% solution of ECA 5217 (after Brod *et al.* 1971)

| Flow parameters at 4 °C | Oil | |
|---|---|---|
| | untreated | treated |
| ASTM upper pour point, °C | 21 | 6 |
| Plastic viscosity, $Ns/m^2$ | 0·112 | 0·058 |
| Static shear stress, $N/m^2$, measured with | | |
| rheoviscosimeter | 32 | 0·43 |
| TAL pipe model | 35 | 1·0 |

the cooling of the crude. Their effect is similar to that of the natural malthenes. This results in most of the paraffin forming minute crystal grains, owing to the reduction in the adhesion affinity between paraffin particles, and in the tendency to form aggregates (Price 1971). According to Price, the *P*-inhibitors found to be useful in practice, belong to two groups of chemical compounds, notably ethylene copolymers, and higher polymers. In this latter, the main chain of the polymer has side chains of *n*-paraffins. Both types of compounds are anchored by these side chains to the paraffin lattice.

Of the additives tried out in European practice, the best known ones bear the code designations ECA 841 and ECA 5217 (Brod *et al.* 1971). ECA 841 is a paste at room temperature; it dissolves readily in aromatic solvents such as benzene, and its homologues. ECA 5217 is jelly, or paste-like at room temperature; it dissolves well in these solvents, too. Both compounds are presumably esthers with metacrylate type polymer chains attached to them. The effects of the two compounds were investigated both in the laboratory and in the field. *Table 7.7 – 2* shows that how the flow behaviour of a 4 : 1 mixture of an African and Middle-East crude was modified

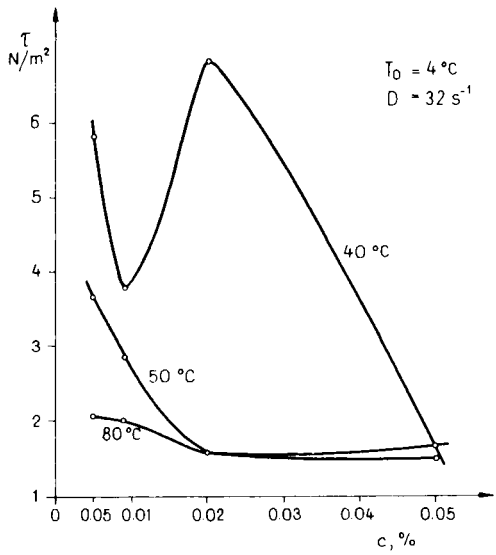


Fig. 7.7 – 8. Influence of P-inhibitor ECA 841 upon shear stress in Algyő crude

by the addition of 0·15 percent ECA 5217. The improved properties, achieved by the additive were retained even after a storage period of 25 days in a tank.

The extent, to which flow properties are improved by the additives, depends on concentration and temperature. *Fig. 7.7 – 8* summarizes the results of experiments with ECA 841, performed at the Petroleum Engineering Department of the Miskolc Technical University for Heavy Industry (Hungary). The points, plotted, were established for Algyő crude at 4 °C temperature, and 32 $s^{-1}$ shear rate, using a Haake rotary viscometer. The parameter is the temperature at which the inhibitor was added. The shear stress at a given concentration of additive is seen to be the less (within the range of concentrations examined), the higher is the temperature of addition. This is explained by the nature of the adsorption mechanism. The additive is the more effective, the less the separated paraffin in the oil at the time when the additive is added, and, hence, the smaller size the structures formed by the paraffin crystals. The difference, in shear stress between 40 and 50 °C, is considerable.

Minimum shear stress was almost identical in the three cases. This value was ensured by adding just 0·02 weight percent ECA 841 at temperatures of 50 and 80 °C, whereas 0·05 percent was required to obtain the same effect at 40 °C.

Laboratory tests are needed to decide which of the additives is efficient for a given crude, what is the optimum concentration and the optimum mixing temperature taking into account the economy too. Measuring the flow curves of the selected samples we can calculate the pressure gradient curves similar to those shown on *Fig. 7.7—4* and so the friction pressure loss valid at given industrial transport parameters. It should be noted that the efficiency of the additives does not increase proportionally to the concentration. At several examined cases optimum efficiency could be achieved at relatively small, 0·025—0·05 percent of concentration.

In the oil production and transport practice several methods are known by which the adhesion of the paraffin on the inner wall of the pipe, dissolved from the crude, may be partially, or fully prevented. A group of these methods, in order to achieve the prescribed aim, uses chemicals. Fulford (1975) describes investigations, where the efficiency of this type of chemicals was determined by laboratory-scale flow experiments. He found that the optimum values were achieved with five ethylene co-polymers of different composition. We may assume that these chemicals may modify the space lattice, and thus, their mechanism of operation is very similar to that of the *P*-inhibitors.

It was in 1954 that drag reduction in both Newtonian and non-Newtonian fluids under the influence of certain additives was first observed. Experience has shown the most effective *drag reducers* to be long straight-chained lyophilic polymers. In polar liquids, e.g. water, the most effective molecules are those which include polar groups such as the carboxy group. One such compound is CMC (carboxy-methyl-cellulose). These macromolecules form solvates in the fluid to which they are added (Elperin *et al.* 1966). In the oil industry, drag-reducing additives are added mainly to the water-based injection fluids of hydraulic formation fracturing. Lescarboura *et al.* (1970) describe that both laboratory and field experiments were carried out in Oklahoma in order to determine, that, for decreasing the frictional pressure loss in the light oil, and Diesel oil, respectively, what additive, and to what a proportion, may be efficient. The additives tested included the high-molecular-weight hydrocarbon polymer of code designation CDR, and several variants of a polysobuthylene, called Vistanex. At a given concentration, these additives were found to be the more effective, the more readily they solvate in the fluid to be treated. The presence of polymers may reduce the drag in turbulent flow in two ways. In the flowing liquid, the elastic macromolecules arranged parallel to the flow direction hinder the radial movement of the flowing liquid's particles, and adsorb and temporarily store the energy that would otherwise get dissipated by impulse exchange (Pruitt *et al.* 1965). The other effect, involved, is that some of the macromolecules will adhere to the pipe wall, and reduce its relative roughness (White 1964). The presence of the polymers augments the apparent viscosity of the transported liquid, and imparts non-Newtonian properties even to Newtonian

fluids. A very comprehensive survey of the different ideas concerning the effect of the different additives is given by Hoyt (1972).

The pressure drop to be expected in a pipeline cannot be predicted on the basis of flow curves determined by means of rotary viscometer. That is due to two factors. One, the rotation viscometer will not evaluate the influence of pipe roughness. Two, according to certain hypotheses (Elperin *et al.* 1966) flow in the pipe may arrange the polymer molecules so, that their concentration will differ from the axis to the pipe wall. Wang (1972) carried out flow experiments in laboratory size pipelines. He wanted to find, that how the two types of friction reducing additives would change the friction factor, valid for the clean basic oil. The equation, derived on the basis of his experiments, is practically a generalized version of the Prandtl–Kármán equation, 1.1 – 6

$$\frac{1}{\sqrt{\lambda}} = 2 \lg N_{Re} \sqrt{\lambda} - 0{\cdot}8 + B\,, \qquad 7.7-1$$

where $B$ is the factor of the friction loss reducing additive, that can be obtained from the formula:

$$B = 0{\cdot}288\, B_{max} \lg (7{\cdot}4\tau_w/\tau_{wc})\,. \qquad 7.7-2$$

$B_{max}$ is the maximum value of $B$ factor, realizable by the given additives, that can be determined by laboratory-scale pipeline experiments, in the function of the factor $(\mu_m - \mu_b)/\mu_m$ that includes the dynamic viscosities of the basic oil, and the mixture. The viscosity of the mixture, $\mu_m$ is always higher than that of the basic oil, $\mu_b$, and its magnitude is proportional to the concentration. Its value may be measured by extrusion viscometer. $\tau_w$ is the shear stress, prevailing at the pipe wall, and $\tau_{wc}$ is the shear stress prevailing at the pipe wall, that develops if factor $B$ is just the half of the value of $B_{max}$. The application of the above relation requires laboratory experiments, that are not available for every designers. The knowledge of an equation, from which the expected effect of the additive may be approximately calculated, may be, thus, important too. Such relation is described by Lescarboura *et al.* (1970).

Strictly, this procedure holds only for the fluids and additives tested, but it will give a rough idea of what to expect with other fluids and additives, and permits to estimate the extent of drag reduction. Laboratory experiments were performed in one-in. pipe of 3·7 m length, in a flow velocity range from 0·6 – 4·9 m/s. These were succeeded by field experiments in 45 km of 8″ and 51·5 km of 12″ line respectively. It was found that the drag reduction $\Delta p_{dr}/\Delta p_o$ due to a given additive in a given fluid depends on the additive concentration $c_{dr}$, flow velocity $v$, and pipe diameter $d_i$. The drag reduction due to the additive, termed CDR, in the 8″ and 12″ pipes tested (and, in a fair approximation, all over the pipe size range from 4 – 16″) is

$$\frac{\Delta p_{dr}}{\Delta p_o} = \frac{2{\cdot}19\, v - 1}{\dfrac{c_{dr} v}{0{\cdot}32 c_{dr} - 30{\cdot}9} + \dfrac{1000}{76{\cdot}6 + 0{\cdot}098 c_{dr}}}\,, \qquad 7.7-3$$

where $c_{dr}$ is the additive concentration in parts per million ($10^{-6}$ m$^3$/m$^3$).

*Example 7.7 – 1.* Find the percent drag reduction in light oil flowing at 2·3 m/s velocity with CDR added in a proportion of 1000 ppm. Equation 7.7 – 3 yields

$$\frac{\Delta p_{dr}}{\Delta p_o} = \frac{2{\cdot}19 \times 2{\cdot}3 - 1}{\dfrac{1000 \times 2{\cdot}3}{0{\cdot}32 \times 1000 - 30{\cdot}9} + \dfrac{1000}{76{\cdot}6 + 0{\cdot}098 \times 1000}} = 0{\cdot}30,$$

that is, drag reduction due to the additive amounts to 30 percent.

By Eq. 7.7 – 3, drag reduction increases with increasing flow velocity. The maximum to be expected in practice is 50 – 60 percent. One thing to be given proper attention in choosing an additive is that the "strength" of the polymer molecule must be sufficient, that is, it must not be degraded by the buffeting it receives in the flowing liquid. Drag-reduction efficiency decreases as degradation proceeds.

### 7.7.4. Oil transport in a water bed

A fairly large number of the publications since 1950 have contained theoretical considerations and experimental data concerning the common transport of oil and water in the same pipeline. These publications assert if during flow the phase in contact with the pipe is the water rather than the oil, and the oil remains enclosed in

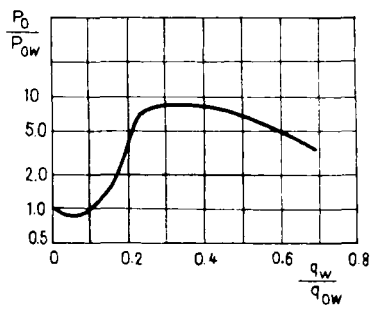


Fig. 7.7 – 9. Power to drive pure crude and crude in water bed v. water content, after M. E. Charles

a sort of water sheath, then the drag of flow and the driving power required may be significantly less even though the throughput is increased by the addition of the water. *Figure 7.7 – 9*, a plot of M. E. Charles' experimental data, shows the pressure needed to pump the oil alone, referred to the pressure demand of the oil-water mixture, v. the water content of the mixture (Szilas 1966). The pressure reduction factor is seen to attain a maximum of about 9 for a water cut of 0·3 – 0·4. The practical application of this idea was hampered by the fact that the two phases, flowing together, tend to form highly unstable flow patterns: it was especially in pipelines, laid over hilly terrain that the two phases were least likely to flow the way they were expected to.

In the last years, the common transport of oil and water was attempted in a different way, in the form of "oil-in-water" emulsions prepared by adding surface-active additives to the water. The viscosity of this type of emulsion is independent of oil viscosity. Laboratory tests by Rose and Marsden (1970) showed that the viscosity of the emulsion is best described by the Richardson formula

$$\mu_{ow} = \mu_w \exp\left[ a \frac{q_o}{q_{ow}} \right] \qquad 7.7-4$$

where $a$ is a constant.

In the cases investigated, the viscosity of the emulsion was much lower than that of the oil. At $q_o/q_{ow} = 0{\cdot}5$, drag was one ninth of the drag of oil alone.

Important research, in this field, was carried out by Soviet experts, who experimented in long pipelines with Mangyshlak crude and heavy fuel oil, respectively, in emulsion with water treated with sulphonol, being the pipeline length 3·6 km, and the diameter 152 mm. A relationship suitable for calculating a valid friction factor for the common flow of the two phases was given by Guvin and Stepanyugin (1970a) as

$$\lambda_{ow} = \frac{0{\cdot}390 R_\sigma^{-1{\cdot}13} \left( \dfrac{q_o}{100\, q_{ow}} \right)^{n_1}}{(245 A^{1{\cdot}10} N_{Reow})^{n_2}}, \qquad 7.7-5$$

where

$$R_\sigma = \frac{\sigma_{ow}}{\sigma_o + \sigma_w}; \quad A = \frac{\mu_w^2}{\mu_{ow} \sigma_{ow} d_i};$$

$$N_{Reow} = \frac{v_{ow} d_i}{\nu_w};$$

$$n_1 = 3{\cdot}50(1 - 3{\cdot}82 R_\sigma)^2; \quad n_2 = 1{\cdot}75(1 - 3{\cdot}82 R_\sigma).$$

The relationship shows the friction factor to be independent indeed of the flow properties of the oil phase. The influence of temperature is very slight: it will merely change the viscosity of the additive-treated water. Investigations showed the active material to coat the water–oil interface and the pipe wall. Adsorption takes place in some 30 min.

Using the flow equations thus derived, a calculation procedure was developed permitting the optimization of the transmission cost (Guvin and Stepanyugin 1970b). *Figure 7.7 – 10* shows optimum $q_o/q_{ow}$ ratios for various length of pipeline v. annual throughput, calculated by this method. Clearly, the greater the throughput is, the higher is the optimal relative water content. For a given throughput of oil, $(q_o/q_{ow})_{opt}$ is the less, the longer the pipeline is. *Figure 7.7 – 11* shows the optimum pipe size, likewise v. oil throughput. The optimum size for a given length is the larger the greater the throughput is, and, for a given throughput, it is the smaller, the longer the pipeline. In both Figures the numbers on the graphs indicate the pipeline length in thousand-kilometre units.

At the delivery end, the emulsion must, of course be treated, and the water must be removed. In order to prevent pollution of the environment, it is necessary to add to the water a chemical that biologically neutralizes, or decomposes the surface-active additive (Guvin and Stepanyugin 1970a, b).

In accordance with the remarks, referring to *Fig. 6.6 – 13*, in case of relatively high water content, exceeding the 60 percent, from the mixture of water and crude, without any additives, "natural" oil-in-water emulsion may develop. Knowing this phenomenon, high-viscosity crude is produced and transported at the Nagylengyel

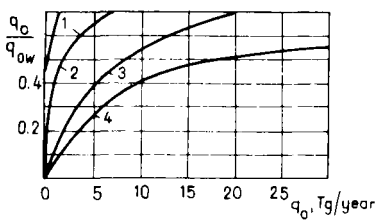


Fig. 7.7 – 10. Optimum *O/W* ratio of transmission in a water bed, after Guvin and Stepanyugin (1970b)

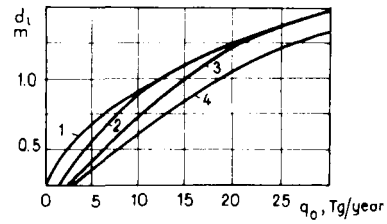


Fig. 7.7 – 11. Optimum pipe size of transmission in a water bed, after Guvin and Stepanyugin (1970b)

field (Hungary) so, that the water is led into the annulus of the sucker rod-pumped wells.

In order to reduce the flow pressure drop, in the Soviet Union, aqueous solution of certain polymers is injected in the pipelines transporting crude. It is assumed that the inner wall of the pipeline is partially, or fully coated by the solution, and, the desired effect is attained in this way (Poraiko and Vasilenko 1975).

Oil that is solid at the flow temperature in the pipeline can be transported in suspension in water. The oil grains have been shown to concentrate along the pipe axis, whereas the fluid next to the pipe wall is practically pure water. The drag, accordingly, is slight. The suspension is thixotropic–pseudoplastic. The flow in the pipeline is influenced by the slippage of the water "sheath", shear rate, shear duration, and flow temperature (Lamb and Simpson 1963). The transport of oil suspended in water was first employed in Indonesia, in 1962. The schematic diagram of the transmission system is shown in *Fig. 7.7 – 12*. The oil of about 41 °C pour point, containing 33 percent paraffin, is transported at a rate of 2 Tg/year in a 20″ line of 238 km length from the Tandjung field to the Balik Papan refinery. This method permitted the decrease in apparent viscosity at a flow velocity of 0·7 m/s from $10^2$ Pas to 0·4 Pas; 70 percent of the fluid is gelled oil; the rest is water (Lamb and Simpson 1963).

Design have been prepared, and experiments have been performed, respectively, in order to carry the crude, cooled under the pour point temperature, in liquid hydrocarbons instead of water. Theoretically, it can be carried out in more than one way. In the course of a distillating process, the waxy crude may be separated, on the

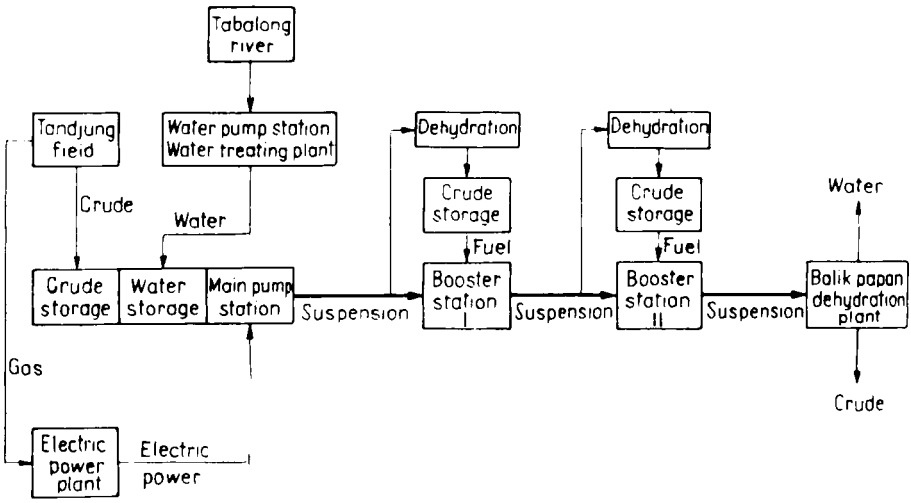


Fig. 7.7 – 12. Tandjung pipeline, after Lamb and Simpson (1963)

one hand, to paraffin-rich heavy oil, and paraffin free light product, on the other. The cooled down, solid and granulated heavy phase, after being introduced into the liquid phase, may be transported in the form of a coarse suspension. The solution of the solid oil grains, by coating with a chemical, non-soluble in oil, may be reduced. A study describes a possible alternative, for the Alaska pipeline according to which the gelled crude granulate could be transported in liquified natural gas (*Pipe Line Industry*... 1975).

CHAPTER 8

# PIPELINE TRANSPORTATION OF NATURAL GAS

Pipelines, transporting natural gas, depending on the task to be performed may be classified into several groups, that, in most cases are the following:

a) gas gathering pipelines of the gas fields between the wells and separators;
b) gas gathering pipelines between the separators and the gas processing plant;
c) high-pressure gas transmission pipelines between the gas processing plants and the consumption districts;
d) middle-pressure gas distribution pipeline system between the tail end of the transmission pipeline and the intake point of the low-pressure gas distribution system;
e) low-pressure gas distribution system between the middle-pressure intake point, and the consumers.

Through the flowline, belonging to the a) category, depending on the quality of the produced gas, dry or wet gas is transported, i.e. the flow may be of one-, or two-phase character. In the narrow sense the above statement refers to the fluids produced from the gas wells, but in a broader sense the well stream of oil well may be also considered wet gas. The flow lines, transporting from the individual wells are generally independent of the other lines, and the flow pressure drop may be calculated, as described in Sections 1.2 and 1.4.2, respectively. *Figure 8 – 1(a)* is the schematic representation of the gathering system consisting of flow lines and separators.

The pipelines of the (b) category through, independent lines, or connected, but usually not looped pipeline systems transmit generally gases of small liquid content. The flow, in most cases, can be considered to be steady state. The flow pressure drop can be calculated as described in Sections 1.2 and 1.4.2, respectively. Its schematic diagram is shown by *Fig. 8 – 1(b)*. In pipelines (a) and (b) the temperature change is considerable enough to significantly influence the liquid-gas rate. In the course of accurate calculation both factors (liquid-gas rate; temperature) must be considered.

The main transport line is relatively long, and the operating pressure is quite high, 10 – 70 bars in Hungary. At its tail point(s) regulator stations are erected that passes the gas, by the prescribed pressure, into the gas distribution pipeline system. Its scheme is shown by *Fig. 8 – 1(c)*. At the intake point, and, in some cases at intermediate point, or points along the pipeline, the gas flow of the required pressure

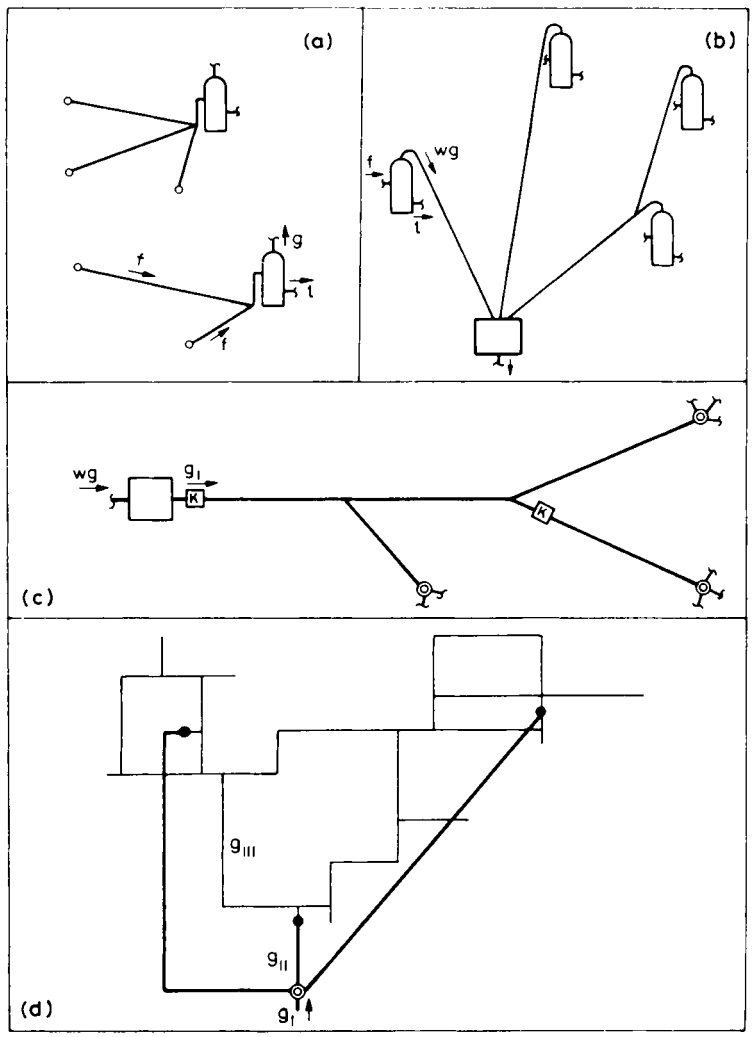


Fig. 8 – 1. Fundamental types of gas transporting systems

and rate is achieved by applying compressors. Except for the first, relatively short initial section of the pipeline the flow is of near soil temperature, and can be considered isothermal.

Through the regulator stations of the middle-pressure (max. 10 bars) pipeline network the gas is passed into the low-pressure distribution system, the operation pressure of which is less than 0·1 bar in Hungary. On *Fig. 8–1(d)* a three-way middle pressure gas distribution system, and a low-pressure looped distribution network can be seen. On this latter, the service pipelines for the gas consumers are not marked. In a fair approximation the flow is isothermal and of soil temperature. It may occur, first of all in case of industrial consumers, that they are directly linked to the middle-pressure network.

In pipeline c) the flow is often not stabilized. The fluctuations in consumption lead to so-called slow transients.*

The period of consumption fluctuation is generally some hours long. The estimation of the operating conditions of the existing, or designed pipelines is impossible using steady state flow equations. For simulation the transient flow further equations and calculation methods are required.

Usually, the low-pressure gas distribution system is multiple connected and looped. Middle- and high-pressure pipeline systems sometimes may be also looped. In such networks the numerical simulation of the flow parameters (pressure, flow rate, time) is complicated, that is why the calculation is carried out by computers.

The petroleum engineer, dealing with the production of oil and natural gas, and with the transport of processed fluids from the field, rarely faces tasks concerning the flow in looped gas lines and transient flow. Such numerical simulations and the solution of designing and dimensioning problems is generally the task of the gas engineer dealing with the transport and distribution of gas. For this reason, these problems will be discussed here only to the extent, that the petroleum engineers should know the corresponding characteristics, and could formulate the problems to be solved to the gas engineer with a wide knowledge.

## 8.1. Physical and physico-chemical properties of natural gas

In the following we shall be concerned only with those physical and physicochemical properties that affect the transmission of gas in pipelines; even those properties will be discussed only in so far as they enter into the relevant hydraulic theories.

* Last transients are the pressure waves created by the rapid change in the flow velocity that propagate by the sonic velocity (see Section 7.1, valid for the liquids). These pressure waves, here, while discussing the gas flow, will not be treated.

### 8.1.1. Equation of state, compressibility, density, gravity

It is the gas laws or, in a broader scope, the equations of state concerning natural gas that describe the interrelationships of pressure, specific volume and temperature, all of which may be subsumed under the notion '$pVT$ behaviour' of the gas. Natural gas is not ideal, and the deviation of its behaviour from the ideal gas laws is seldom negligible and occasionally quite considerable. For the purposes of practical calculations, those equations describing the $pVT$ behaviour of real gases are to be preferred that account for deviation from ideal-gas behaviour by a single correction factor, based on a consideration valid for any gas. Such a consideration is the *theorem of corresponding states*, expressed in terms of state parameters reduced to the critical state: this theorem states the existence of a function of the reduced state parameters, $f(p_r, V_r, T_r)=0$, that is valid for any gas. The $pVT$ behaviour of natural gas can be described in terms of an equation of state corrected by the compressibility factor $z$:

$$pV=z\frac{R}{M}T \qquad 8.1-1$$

where $V$ is the specific volume valid at pressure $p$ and temperature $T$; $R$ is the universal gas constant, whose rounded-off value is 8314 J/(kmole K). Any given gas is characterized by its specific gas constant, or simply gas constant,

$$R'=\frac{R}{M}. \qquad 8.1-2$$

By the theorem of corresponding states, the compressibility factors $z$ of two gases are equal if the reduced state parameters of the two gases are equal, that is, if the gases are in the same corresponding state. Reduced pressure is

$$p_r=p/p_c$$

and reduced temperature is

$$T_r=T/T_c.$$

In the case of gas mixtures, reduced parameters of state are to be replaced by the pseudo-reduced parameters $p_{pr}$ and $T_{pr}$ defined in terms of the pseudocritical pressure and temperature $p_{pc}$ and $T_{pc}$, both depending on gas composition, as follows:

$$p_{pr}=p/p_{pc} \qquad 8.1-3$$

and

$$T_{pr}=T/T_{pc}. \qquad 8.1-4$$

If gas composition is known, $p_{pc}$ and $T_{pc}$ can be determined by applying the principle of additivity or — usually at a lower accuracy — using empirical diagrams. Additivity means that molar mass, pseudocritical pressure and pseudocritical temperature of a mixture can be added up from the respective parameters of the

components, combined with their molar fractions or volume fraction:

$$M = \sum_{i=1}^{n} y_i M_i$$

$$p_{pc} = \sum_{i=1}^{n} y_i p_{ci}$$

$$T_{pc} = \sum_{i=1}^{n} y_i T_{ci} .$$

The accuracy of this calculation is usually impaired by the circumstance that, in the composition of the gas, the relative abundance of the heaviest components is given by a single figure denoted $C_{n+}$. The critical parameters are usually put equal to those of the component $C_{n+1}$; if e.g. the combined heavy fraction is $C_{6+}$, then it is taken into account with the critical parameters of heptane, $C_7$. This is, of course, an approximation whose accuracy depends on the actual composition of the combined heavy fraction.

*Example 8.1 – 1.* Find the molar mass and pseudocritical parameters of state at a pressure of 88 bars and 280 K temperature of the wet natural gas whose composition is given in Columns (1) and (2) of *Table 8.1 – 1.* The physical constants

Table 8.1 – 1.

| Components of natural gas | $z_i$ | $M_i z_i$ | $T_{ci} z_i$ | $p_{ci} z_i$ |
|---|---|---|---|---|
| | | kg/kmol | K | $10^5$ Pa |
| 1 | 2 | 3 | 4 | 5 |
| Methane | 0·790 | 12·67 | 150·7 | 36·67 |
| Ethane | 0·100 | 3·01 | 30·5 | 4·89 |
| Propane | 0·055 | 2·43 | 20·3 | 2·34 |
| i-Butane | 0·010 | 0·58 | 4·1 | 0·36 |
| n-Butane | 0·015 | 0·87 | 6·4 | 0·57 |
| n-Pentane | 0·024 | 1·73 | 11·3 | 0·81 |
| $CO_2$ | 0·001 | 0·04 | 0·3 | 0·08 |
| $N_2$ | 0·005 | 0·14 | 0·6 | 0·17 |
| Total: | 1·0000 | 21·47 | 224·2 | 45·90 |

of the gas components are listed in Table 6.4 – 1. The calculation whose details are given in Columns (3), (4) and (5) of Table 8.1 – 1, furnishes $M = 21{\cdot}5$ kg/kmole. By Eqs 8.1 – 3 and 8.1 – 4,

$$p_{pr} = \frac{8{\cdot}8 \times 10^6}{4{\cdot}59 \times 10^6} = 1{\cdot}92$$

and

$$T_{pr} = \frac{280{\cdot}0}{224{\cdot}2} = 1{\cdot}25\,.$$

*Figure 8.1 – 1* permits us to read off pseudocritical pressures v. pressure and pseudocritical temperatures v. temperature for hydrocarbon gases of various molar mass.

*Example 8.1 – 2.* Find using *Fig. 8.1 – 1* pseudoreduced parameters of state for a gas of molar mass $M = 21{\cdot}5$ at the pressure and temperature stated in the foregoing example. — *Figure 8.1 – 1* furnishes $p_{pc} = 4{\cdot}61$ MPa and $T_{pc} = 223$ K. — By Eqs 8.1 – 3 and 8.1 – 4,

$$p_{pr} = \frac{8{\cdot}8 \times 10^6}{4{\cdot}61 \times 10^6} = 1{\cdot}91$$

and

$$T_{pr} = \frac{280}{223} = 1{\cdot}26\,.$$

The results furnished by the two procedures are in approximate agreement, but more substantial deviations may occur in other cases. Empirical diagrams other than *Fig. 8.1 – 1* have been published (e.g. Stearns *et al.* 1951).

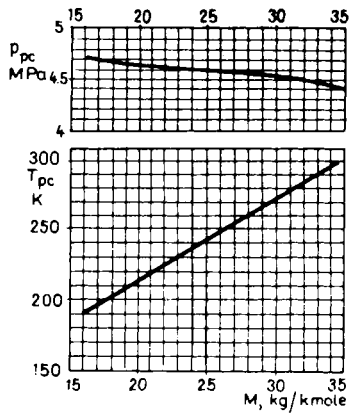


Fig. 8.1 – 1. Pseudocritical parameters of natural gas v. molar mass (from Katz 1959, p. 111; used with permission of McGraw-Hill Book Company)

The compressibility factor $z$ can be determined most accurately by laboratory experiments on $pVT$ behaviour. If no $z = f(p, T)$ diagram based on experiment is available, then $z$ is determined as a function of the reduced state parameters out of empirical diagrams or relationships. One of the best-known empirical diagrams is that of Standing and Katz (1942; *Fig. 8.1 – 2*). For the pseudoreduced parameters $p_{pr} = 1{\cdot}92$ and $T_{pr} = 1{\cdot}25$ of Example 8.1 – 1, it furnishes $z = 0{\cdot}64$.

Many authors derived and published equations for numerical simulation of Standing Diagram curves. The main task was to find suitable methods for the rational use of the diagram for computer calculations. The more advantageous a calculation method is the higher its accuracy and the shorter the computer running

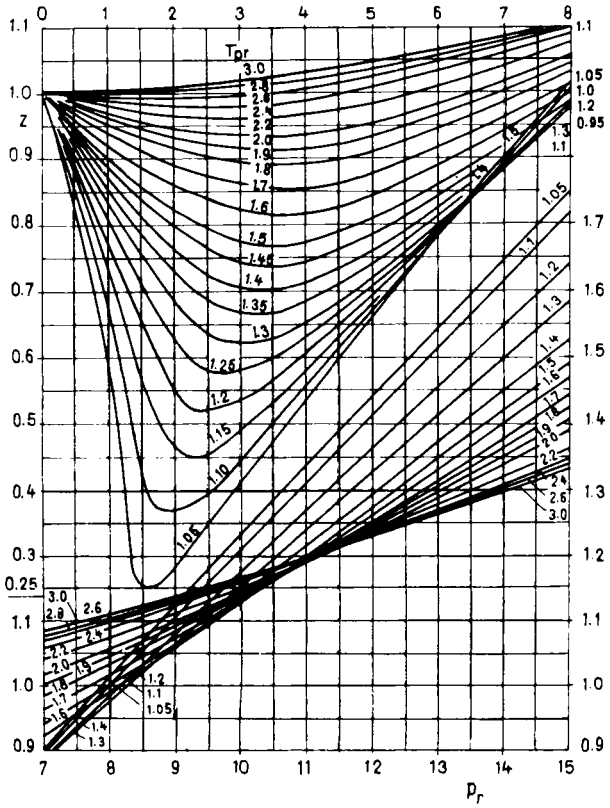


Fig. 8.1 – 2. Compressibility factor of natural gas v. pseudo-reduced parameters of state, after Standing (1952; reproduced by permission of the copyright owner—copyright © Chevron Research Company 1951; all rights reserved under the International Copyright Convention)

time is. Takács (1976) gives a survey about the use of equations of nine different authors and compares their accuracy and running time.

Natural gas often contains substantial amount of non-hydrocarbon gases, $N_2$ and $CO_2$ first of all. If the volume percentage of these is less than 8 percent for $N_2$ and 10 percent for $CO_2$, then the compressibility factor is most readily determined by a procedure suggested by Gráf (Szilas 1967): the hydrocarbons are considered to be a single component whose pseudocritical parameters and compressibility factors $z$ are determined separately by some suitable method. The compressibility factors

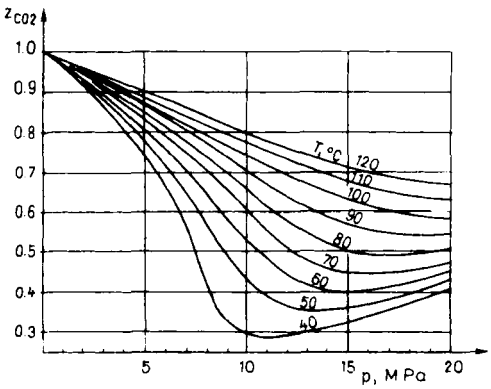


Fig. 8.1 – 3. Compressibility factor of $CO_2$ according to Reamer and Elters; after Török *et al.* (1968)

$z_{CO_2}$ and $z_{N_2}$ for $CO_2$ and $N_2$ are then read off *Figures 8.1 – 3* and *8.1 – 4*, and the value $z'$ for the mixed gas as a whole is calculated using the mixing rule

$$z' = y_{N_2} z_{N_2} + y_{CO_2} z_{CO_2} + (1 - y_{N_2} - y_{CO_2}) z \,.$$

In writing computer programs it is an advantage if the compressibility factor can be found by calculation, without having to resort to diagrams. Literature contains several calculation procedures. The relevant formulae are mathematical representations of more or less extensive domains of the families of curves constituting the

Table 8.1 – 2.

| $T$, °C | $k$ |
|---|---|
| 0 | $2{\cdot}65 \times 10^{-8}$ |
| 15 | $2{\cdot}04 \times 10^{-8}$ |
| 30 | $1{\cdot}65 \times 10^{-8}$ |

empirical diagrams. The French gas industry uses for pressures of below 70 bars at soil-temperature flow the formula

$$z = 1 - 2 \times 10^{-8} p \,. \qquad 8.1 - 5$$

(Société... *Manuel* 1968). A relationship accounting also for temperature, applicable below 60 bars, is

$$z = \frac{1}{1 + kp} \qquad 8.1 - 6$$

$k$ is listed for certain temperatures in *Table 8.1 – 2* (likewise from Société... *Manuel* 1968).

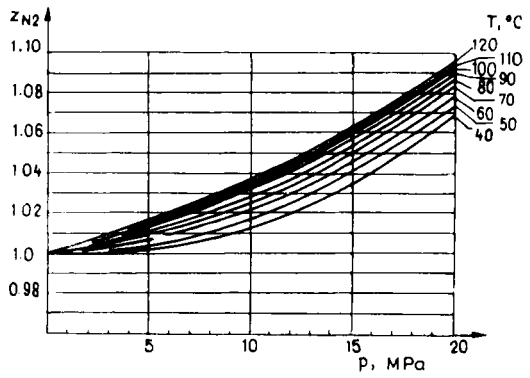


Fig. 8.1 – 4. Compressibility factor of $N_2$ according to Sage and Lacey; after Török *et al.* (1968)

Relationships for calculating the pseudocritical parameters of state have been given by Thomas *et al.* (1970)

$$p_{pc} = 4{\cdot}894 \times 10^6 - 4{\cdot}050 \times 10^5 \, \rho_r \qquad 8.1-7$$

$$T_{pc} = 94{\cdot}71 + 170{\cdot}7 \, \rho_r \, . \qquad 8.1-8$$

Wilkinson *et al.* (1964) gave for $p_r < 1{\cdot}5$ the formula

$$z = 1 + 0{\cdot}257 p_{pr} - 0{\cdot}533 \frac{p_{pr}}{T_{pr}} \qquad 8.1-9$$

where $p_{pr}$ and $T_{pr}$ are the values furnished by Eqs 8.1 – 3 and 8.1 – 4, respectively.

Gas density at pressure $p$ and temperature $T$ can be obtained putting $V = 1/\rho$ in Eq. 8.1 – 1:

$$\rho = \frac{pM}{zRT} . \qquad 8.1-10$$

If this equation is written up for the standard state, then $p = p_n$, $T = T_n$ and $z = z_n = 1$. Then

$$\rho_n = \frac{p_n M}{R T_n} . \qquad 8.1-11$$

Let e.g. $p_n = 1{\cdot}013$ *bar and* $T_n = 273{\cdot}2$ K. Since furthermore, $R = 8314$ J/(kmole K),

$$\rho_n = \frac{M}{22{\cdot}42} . \qquad 8.1-12$$

Rearranging we get, at the standard-state parameters stated above, the standard molar volume

$$V_{mol} = M \rho_n = 22{\cdot}42 \text{ m}^3/\text{kmole} . \qquad 8.1-13$$

Relative density is the standard-state density of the gas referred to the standard-state density of air:

$$\rho_r = \frac{\rho_n}{\rho_{an}}. \qquad 8.1-14$$

Now by Eqs 8.1 – 12 and 8.1 – 14,

$$\rho_r = \frac{M}{M_a} = \frac{M}{28{\cdot}96}. \qquad 8.1-15$$

Gravity is

$$\gamma = \rho g. \qquad 8.1-16$$

### 8.1.2. Viscosity

Gas viscosity, as distinct from liquid viscosity, increases as temperature increases, decreases as molecular weight increases, and is independent of pressure at medium pressures. At atmospheric pressure, viscosities of hydrocarbon gases vary linearly with temperature between 0 and 200 °C *(Fig. 8.1 – 5)*. The viscosity of hydrocarbon mixtures at atmospheric pressures is readily calculated using a relationship published by Herning and Zipper:

$$\mu_a = \frac{\sum_{i=1}^{n} \mu_{ai} y_i \sqrt{M_i}}{\sum_{i=1}^{n} y_i \sqrt{M_i}}. \qquad 8.1-17$$

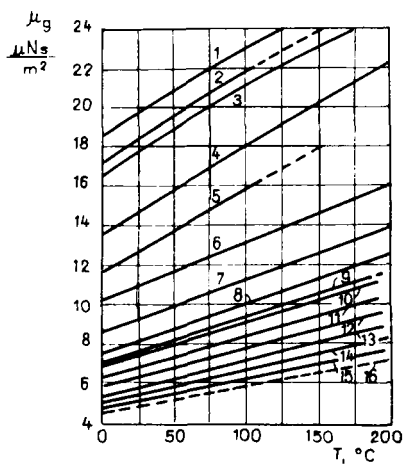


Fig. 8.1 – 5. Viscosities of natural gas components at atmospheric pressure; after Carr *et al.* (1954). *1* helium, *2* air, *3* nitrogen, *4* carbon dioxide, *5* hydrogen sulphide, *6* methane, *7* ethane, *8* propane, *9* isobutane, *10* n-butane, *11* n-pentane, *12* n-hexane, *13* n-heptane, *14* n-octane, *15* n-nonane, *16* n-decane

*Figure 8.1 – 6* is a plot of values furnished by this relationship, and, more generally, of measured viscosities of artificial hydrocarbon–gas mixtures. It permits us to find atmospheric pressure viscosity in terms of the molecular weight and relative gravity of the gas (Carr *et al.* 1954). The influence of non-hydrocarbon components may be taken into account by a viscosity-increasing correction

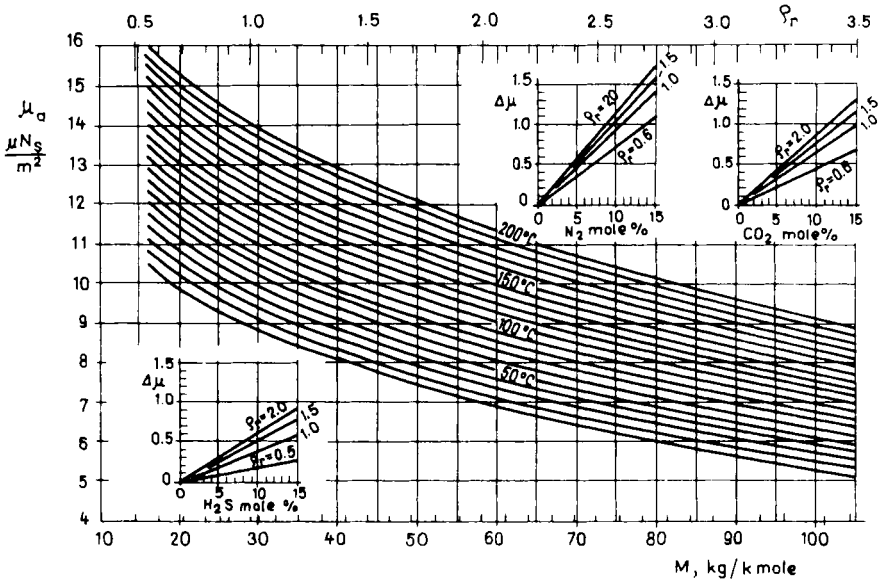


Fig. 8.1 – 6. Viscosity of natural gas at atmospheric pressure (Carr *et al.* 1954)

depending on relative density, provided the share of these components does not exceed 15 percent. A relationship between viscosity and pressure may be set up making use of the theorem of corresponding states. *Figure 8.1 – 7* allows us to find, in the knowledge of the pseudocritical pressure and temperature, the factor $k = \mu_p/\mu_a$ by which the viscosity at atmospheric pressure is to be multiplied in order to obtain the value that holds at pressure $p$ (Carr *et al.* 1954). The relationship is valid in the gaseous state only, and it is therefore necessary in critical cases to check by phase examinations whether or not a liquid phase is present.

### 8.1.3. Specific heat, molar heat, adiabatic gas exponent, Joule–Thomson effect

Specific heat is the heat capacity of the unit mass or molar mass of a substance or, in the case we are discussing, the ration of the heat $dQ$ imparted to a unit mass of gas to the resulting temperature change $dT$, provided no phase change takes place during the temperature change. The usual cases investigated in a gas are

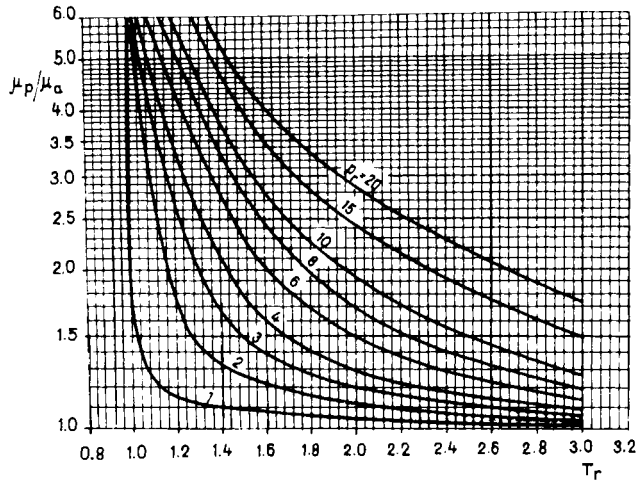


Fig. 8.1 – 7. Variation of $k = \mu_p/\mu_a$ v. the pseudo-reduced parameters of state (Carr *et al.* 1954)

temperature changes at constant pressure, on the one hand, and at constant volume, on the other, and accordingly, two distinct specific heats may be defined, the isobaric $c_p$ and the isochoric $c_v$, $c_p < c_v$, since part of the heat supplied to the system will expand the gas in the isobaric case. In ideal gases, the difference between the two constants equals the gas constant, that is,

$$c_p - c_v = R\,. \qquad 8.1-18$$

The difference between the characteristic specific heats in a real gas is not constant. *Figure 8.1–8* after Brown (1945) shows isobaric molar heats v. temperature of hydrocarbon homologues at atmospheric pressure. The $c_{pa}$ of gas mixtures can be determined on the basis of additivity, in terms of the components' specific heats and molar fractions, that is,

$$c_{pa} = \sum_{i=1}^{n} y_i c_{pai}\,.$$

The specific heat $c_{pp}$ of a gas mixture at pressure $p$ exceeds the value $c_{pa}$ at atmospheric pressure by $\Delta c_p$. *Figure 8.1–9* is a plot of $\Delta c_p$ v. pseudoreduced pressure $p_{pr}$ for various pseudoreduced temperatures $T_{pr}$ after Edmister (Perry 1969). Let us point out that $\Delta c_p$ is stated in molar terms, and has to be divided by the molar $M$ mass in order to transform it into a quantity having the nature of a specific heat.

The adiabatic gas exponent

$$\kappa = \frac{c_p}{c_v} \qquad 8.1-19$$

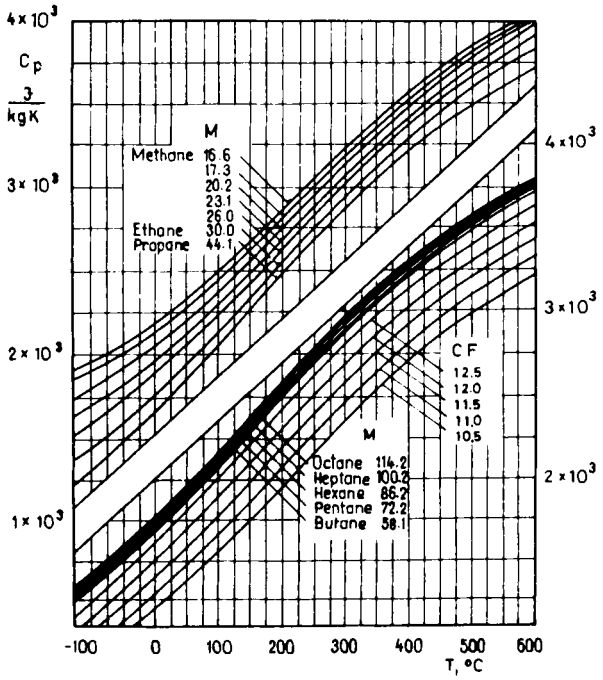


Fig. 8.1 – 8. Specific heats of natural-gas components at atmospheric pressure, after Brown (1945)

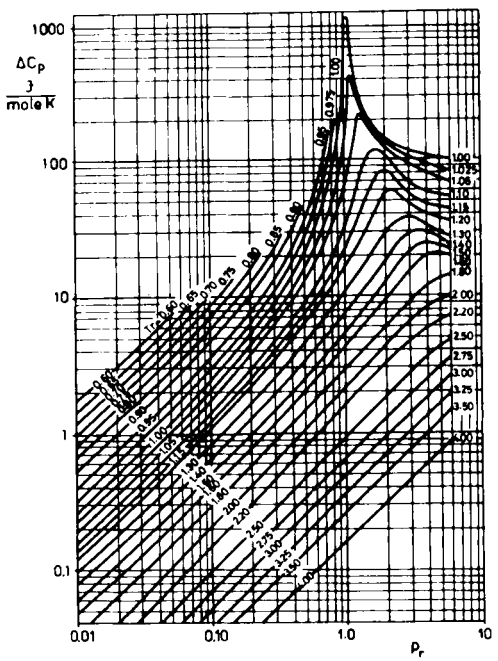


Fig. 8.1 – 9. Specific-heat correction, after Perry (1969)

is usually required in thermodynamic calculations. Its value can be determined, e.g., by reading the molar-heat difference $(c_p - c_v)$ off *Fig. 8.1 – 10* (after Perry 1969) and calculating $c_v$ in the knowledge of $c_p$. The use of the figure presupposes knowledge of the pseudoreduced parameters of state. The molar heat or specific heat is calculated for a certain temperature range rather than for a single pair of pressure and temperature values. The mean molar heat $c_p$ can be determined for instance by planimetering the specific heats calculated for various temperatures by the procedure outlined above. In a simpler procedure, one may read the enthalpy values

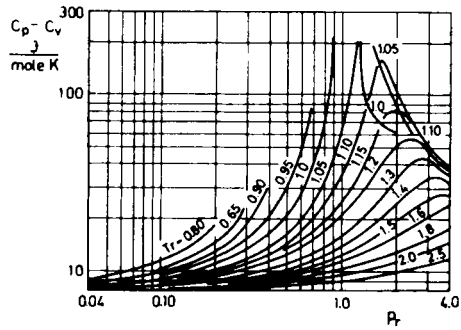


Fig. 8.1 – 10. $(c_p - c_v)$ of real gases v. the reduced parameters of state, after Perry (1969)

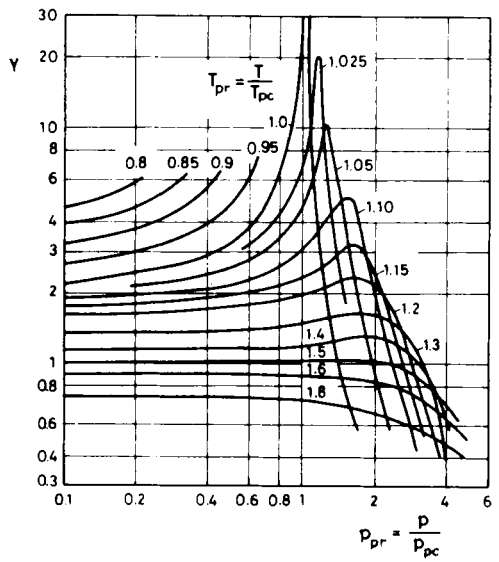


Fig. 8.1 – 11. Relationship for determining the choke effect, after Korchazhkin (1963)

$h_1$ and $h_2$ corresponding to the initial and terminal temperatures $T_1$ and $T_2$ off suitable diagrams or tables. Then

$$\bar{c}_p = \frac{h_2 - h_1}{T_2 - T_1}. \qquad 8.1-20$$

If the pressure of an ideal gas is lowered without the gas delivering energy, then, if the gas is ideal and the change of state is adiabatic, the total internal energy of the system remains unchanged, that is, the state change is isoenthalpic, and the temperature of the gas remains unchanged, too. If, however, the gas undergoing said change is real, then its volume change will differ from ideal gas behaviour. As a result, its internal energy and hence also its temperature will be affected (Joule–Thomson effect). Among the temperature changes taking place during gas flow, it is expedient to account for this effect by the Joule–Thomson coefficient $\mu_d$, which is a measure of temperature change per unity pressure change. $\mu_d \gtrless 0$, that is, expansion may increase, reduce or leave unchanged the temperature of the gas. Several relationships for determining $\mu_d$ have been derived. *Figure 8.1 – 11* gives the values [in J/(K kmole)] of the expression

$$y = 22{\cdot}425 \frac{p_{pc} c_p \mu_d}{T_{pc}}$$

in terms of the pseudoreduced parameters of state, and this expression may be solved to yield $\mu_d$ (Korchazhkin 1963).

### 8.1.4. Hydrocarbon hydrates

Hydrocarbon gas hydrate is a solid granular substance resembling snow or ice. It is composed of water and the molecules of one or more hydrate-forming gases. The molecules of this gas enter cavities in the $H_2O$ lattice, which is looser than the ice lattice, without entering into chemical bond with the water. The lattice thus forming may be one of two pentagonal dodecahedra. The conditions of hydrate formation and stability are: (i) sufficiently low temperature and high pressure; (ii) the hydrate-forming gas is held together by covalent bonds; its molecules are shorter than 8 Å; and when liquid, it is immiscible with water; (iii) during hydrate formation, water is liquid; (iv) hydrate is resistant to water and no Van der Waals forces arise between its molecules.

Hydrates include besides water methane, ethane, propane or butane, alone or mixed together. In addition to the hydrocarbons, other, non-hydrocarbon gas components such as nitrogen, carbon dioxide or hydrogen sulphide may also be hydrate-forming. Hydrate composition depends on the nature of the hydrate-forming gas but is not governed by the rules of stoichiometry. The least water-to-methane ratio in methane hydrate would be 4·5, in view of the number of methane molecules that can be accommodated in the water lattice. However, methane-unsaturated hydrates with more than 4·5 moles of $H_2O$ per mole of methane also

occur. The least water content of ethane hydrate is about 7·7 moles $H_2O$ per mole of ethane. The propane and butane molecules may enter but the largest cavities of the lattice, and hence, in propane hydrate, 17 moles at least of water are required per mole of propane.

*Figure 8.1 – 12* shows state diagrams of various two-component hydrocarbon hydrates after Willard (Orlicek and Pöll 1951). The upper temperature limit e.g. of propane hydrate formation is seen to be 5·6 °C, with a corresponding pressure of 5·6 bars. The point defined by these parameters of state is an invariant of the propane-water system, a four-phase point with no degree of freedom, where propane hydrate as the solid phase is at equilibrium with gaseous propane saturated with water vapour, water saturated with liquid propane and propane saturated with water. The figure shows which phases may coexist in the individual regions. In reality, it is usual for hydrates to involve more than one hydrocarbon component. The critical pressure of hydrate formation is substantially reduced e.g. if methane is

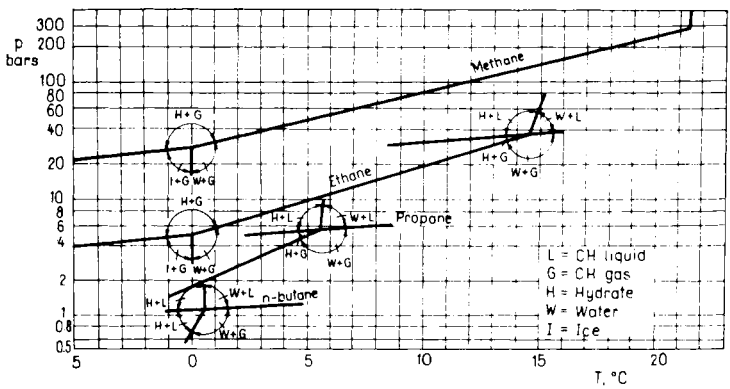


Fig. 8.1 – 12. State diagram of hydrocarbons according to Willard; after Orlicek and Pöll 1951, Table 118 (used with permission of Springer-Verlag, Wien/New York)

accompanied by some hydrocarbon of larger molar mass, propane or butane first of all. Even quite low concentrations of these may displace the phase diagram rather considerably. For approximate estimates one may use *Fig. 8.1 – 13*, which shows critical hydrate-formation pressures and temperatures for hydrocarbons of various relative densities. The presence of $CO_2$ and $H_2S$ at a given temperature may lower the critical pressure, whereas the presence of $N_2$ tends to raise it. The inset in *Fig.8.1 – 13* provides the correction factor $C_{N_2}$ which shows how many times the critical pressure of hydrate formation is higher in the presence than in the absence of a certain quantity of nitrogen.

Several more accurate procedures have been devised. For nitrogenless natural gas, up to about 280 bars pressure, Katz' procedure involving equilibrium constants

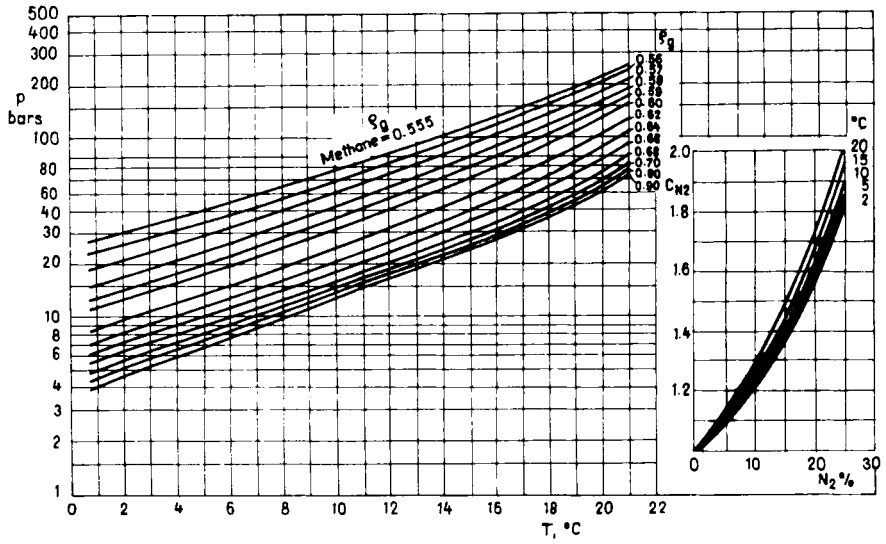


Fig. 8.1 – 13. Limits of gas hydrate formation, after Katz (1959, p. 213; used with permission of McGraw-Hill Book Company)

is best suited. The condition of hydrate formation is

$$\sum_{i=1}^{n} \frac{z_{hi}}{K_{hi}} = 1 .$$

The $K_{hi}$s are to be read off the $K_h = f(T)_p$ diagrams of the hydrate-forming components (Katz 1959). — Heinze (1971) prefers the modified McLeod–Campbell procedure for determining hydrate formation temperatures (hydrate points) of natural gas containing nitrogen up to about 400 bars pressure. The hydrate point is calculated using the relationship

$$T = \sqrt{\frac{K_h}{0{\cdot}445}} . \qquad 8.1-21$$

The values of $K_h$ for various pressures are contained in *Table 8.1 – 3*. The $K_h$ values falling between those given in the table may be found by linear interpolation. The hydrate factor for multi-component natural gas of known molar ratios may be found by applying the principle of additivity.

A broad survey was compiled by Berecz and Mrs Balla (1980) about the characteristics of hydrocarbon hydrates.

*Example 8.1 – 3* (Heinze 1971). Find the hydrate point at 147 bars pressure for the gas composition given in Column 2 of *Table 8.1 – 4*. Let us point out that, regardless of the quantity and nature of the longer-molecule non-hydrate-forming natural-gas

Table 8.1 – 3. Hydrate-equilibrium factors $K_h$ for hydrate-forming natural-gas components (modified after Heinze 1971)

| Components | $p$, bars | | | | | | | |
|---|---|---|---|---|---|---|---|---|
| | 50 | 100 | 150 | 200 | 250 | 300 | 350 | 390 |
| $CH_4$ | 34 543 | 35 949 | 36 719 | 37 357 | 37 814 | 38 204 | 38 531 | 38 767 |
| $C_2H_6$ | 45 535 | 47 101 | 48 078 | 48 704 | 49 316 | 49 772 | 50 140 | 50 435 |
| $C_3H_8$ | 85 060 | 83 970 | 79 836 | 75 610 | 73 150 | 71 340 | 70 103 | 69 154 |
| i-$C_4H_{10}$ | 102 096 | 94 310 | 89 319 | 82 481 | 78 791 | 75 569 | 74 533 | 73 304 |
| n-$C_4H_{10}$ | 57 979 | 51 133 | 47 648 | 45 032 | 43 846 | 43 328 | 43 276 | 43 234 |
| $N_2$ | 30 555 | 32 133 | 33 369 | 33 695 | 34 214 | 34 656 | 35 005 | 35 251 |
| $CO_2$ | 38 788 | 43 504 | 44 812 | 46 773 | 50 371 | 51 660 | 52 269 | 54 018 |
| $H_2S$ | 63 986 | 69 972 | 74 001 | 76 349 | 78 554 | 80 426 | 81 373 | 82 148 |

Table 8.1 – 4. Finding the hydrate formation temperature of Thönse gas (after Heinze 1971)

| Components | $z_{hi}$ | $K_{hi}$ at 147 bars | $z_{hi}K_{hi}$ |
|---|---|---|---|
| $CH_4$ | 0·865 | 36 673 | 31 722 |
| $C_2H_6$ | 0·073 | 48 020 | 3 505 |
| $C_3H_8$ | 0·028 | 80 084 | 2 242 |
| i-$C_4H_{10}$ | 0·013 | 89 618 | 1 165 |
| $N_2$ | 0·010 | 33 295 | 333 |
| $CO_2$ | 0·011 | 44 734 | 492 |

$$\sum_{i=1}^{n} z_{hi}K_{hi} = 39\,459$$

components, it is assumed that

$$\sum_{i=1}^{n} z_{hi} = 1 .$$

By the data in Column 4 of the Table, $K_h = 39\,459$ and hence, hydrate point is at

$$T = \sqrt{\frac{39\,459}{0{\cdot}445}} = 297{\cdot}8 \text{ K} = 24{\cdot}6 \text{ °C} .$$

Hydrate point may be substantially reduced by adding to the natural gas a hydrate inhibitor such as calcium chloride, methanol, ethylene glycol, diethylene glycol.

## 8.2. Temperature of flowing gases

In most long uninsulated pipelines, the temperature of flowing gas approaches soil temperature after a travel sufficiently short for flow temperature to be identified for all practical purposes with soil temperature over the full length of the pipeline. In certain cases, however, the flow temperature of gas may significantly differ from the temperature of the surrounding soil, and it may then be important to determine temperature traverses for the pipeline. The cases in question include the following. (i) It is necessary to decide in designing where the flow temperature drops below the hydrate point; (ii) it is desired to chill the gas by injecting liquified gas, in order to increase the throughput capacity of the pipeline (Gudkov *et al.* 1970); (iii) in arctic regions, the gas may cause an undesirable warming up of the permafrost soil in which the pipeline is laid.

*Figure 8.2 – 1* (after Smirnov and Shirkovsky 1957; and Török *et al.* 1968) is a temperature traverse of a given pipeline (Graph I). It permits us to delimit the line segment where there is a risk of hydrate formation. Graph II is the pressure traverse. The accurate calculation of the two traverses takes a successive-approximation procedure. In the knowledge of pressure, the hydrate-point traverse (Graph III) may be calculated in the manner explained in Section 8.1.4. At point *1*, where Graphs II and III meet ($l = 50$ km), the hydrate point $T_h$ is just equal to the temperature $T_g$ of gas flow. For hydrate to form, it is sufficient that there be some free water available

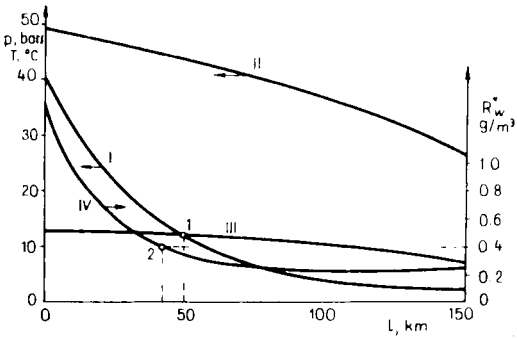


Fig. 8.2 – 1. Pinpointing hazard of hydrate formation in a pipeline, after Smirnov and Shirkovsky (1957) and Török *et al.* (1968)

at this line section. Graph IV is a water vapour saturation traverse along the pipeline. Points of this curve can be determined by means of auxiliary diagrams for corresponding pairs of $p$ and $T_g$ (e.g., Katz 1959). Assuming the water vapour content of the gas to be 0·4 g/m$^3$, the dew point of the gas turns out to occur at point *2*; from there on, the pipeline does contain condensed water: that is, this condition of hydrate formation is also satisfied at and beyond $l = 50$ km.

The temperature of gas flowing in the pipeline depends, for a given inflow temperature $T_1$ and soil temperature $T_s$, on the following factors: (i) heat exchange

with the environment, depending primarily on the heat transfer coefficient (cf. Section 7.6.3). The internal convection coefficient, $\alpha_1$, is infinite in a fair approximation. (ii) The Joule–Thomson effect due to friction, velocity increase and altitude change. (iii) Phase changes (condensation, evaporation) due to pressure and temperature changes. (iv) The energy loss of flow, which end up as heat.

These effects are accounted for in steady-state flow by the following equation (Pápay 1970), stating flow temperature at a distance $l_x$ from the head end of the line to be

$$T_{lx} = \frac{C_1^{\frac{C_2}{C_3}}\left[T_1 + \frac{C_4}{C_2} - \frac{C_1 C_5}{C_2(C_2+C_3)}\right]}{(C_1 + C_3 l_x)^{\frac{C_2}{C_3}}} - \frac{C_4 + C_5 l_x}{C_2} + \frac{C_5(C_1 + C_3 l_x)}{C_2(C_2+C_3)}, \qquad 8.2-1$$

where

$$C_1 = z_{V1} c_{pV} + (1 - z_{V1}) c_{pL}$$

$$C_2 = \frac{k}{q_m}$$

$$C_3 = \frac{z_{V2} - z_{V1}}{l}(c_{pV} - c_{pL})$$

$$C_4 = z_{V1} c_{pV} \mu_{dV} \frac{p_1 - p_2}{l} + (1 - z_{V1}) c_{pL} \mu_{dL} \frac{p_1 - p_2}{l} +$$

$$+ Q \frac{z_{V2} - z_{V1}}{l} + v_1 \frac{v_2 - v_1}{l} + g \frac{h}{l} - \frac{k}{q_m} T_s$$

$$C_5 = \frac{(z_{V2} - z_{V1})(p_1 - p_2)}{l^2}(c_{pV}\mu_{dV} - c_{pL}\mu_{dL}) + \left(\frac{v_2 - v_1}{l}\right)^2.$$

In deriving this equation, Pápay assumed pressure, flow rate and phase transitions to be linear functions of distance from the head end. It is therefore recommended in problems where a high accuracy is required to calculate temperature changes for shorter line segments. Let us point out that suffix 1 invariably refers to the head end and 2 to the tail end of the line of length $l$, except, of course, in the numbering of the constants $C$.

*Example 8.2 – 1* (after J. Pápay). Through a pipeline with $d_i = 0{\cdot}1$ m inner diameter and $l = 5$ km length gas with a rate $q_m = 1 \times 10^4$ kg/h is flowing. The pressures at the head end tail end of the pipe are $p_1 = 8{\cdot}5 \times 10^6$ Pa and $p_2 = 6{\cdot}0 \times 10^6$ Pa respectively. The flow velocities at the same points are $v_1 = 4{\cdot}5$ m/s and $v_2 = 6{\cdot}3$ m/s; the molar fractions of the gas phase $z_{V1} = 1{\cdot}0$ and $z_{V2} = 0{\cdot}9$. The flowing temperature at the head end $T_1 = 60$ °C, the undisturbed soil temperature in the depth of the pipe axis $T_s = 10$ °C, the difference of geodetical heights $h_2 - h_1 = 100$ m. The specific heat regarding gas- and liquid phases are $c_{pV} = 2{\cdot}94 \times 10^3$ J/(kg K) and $c_{pL} = 2{\cdot}10 \times 10^3$ J/(kg K) respectively, the Joule–Thomson coefficients $\mu_{dV} = 3 \times 10^{-6}$ K/Pa and $\mu_{dL} = -2 \times 10^{-7}$ K/Pa respectively, the phase transition heat $Q = 4{\cdot}2 \times 10^5$ J/kg.

Let us calculate the temperature at the tail end of the pipeline with Equation 8.2 – 1, a) taking into account all therms of this equation, b) neglecting the Joule–Thomson effect, c) neglecting the effect of change in velocities, d) supposing the pipe is horizontal, e) neglecting the effect of condensation.

The result of the calculation is listed as follows:

| case | characteristics | calculated value of $T_2$ in °C |
|---|---|---|
| *a* | all terms | 34·7 |
| *b* | $\mu_{dV}=0$; $\mu_{dL}=0$ | 39·4 |
| *c* | $v_1=v_2$ | 34·7 |
| *d* | $h_1=h_2$ | 34·9 |
| *e* | $Q=0$ | 25·2. |

It is visible, that in this case the effect of the change in velocities and heights is negligible but the impact of the Joule–Thomson effect and phase transition is considerable.

In the case when the phase changes are left out of consideration — that is, in single-phase flow — Eq. 8.2 – 1 simplifies to

$$T_{lx}=T_s+(T_1-T_s)e^{-alx}-\frac{\mu_{dV}(p_1-p_2)}{al}\times$$

$$\times(1-e^{-alx})-\frac{gh}{alc_{pV}}(1-e^{-alx})-g\frac{v_2-v_1}{alc_{pV}}\times$$

$$\times\left[\left(v_1-\frac{v_2-v_1}{al}\right)(1-e^{-alx})+\frac{(v_2-v_1)l_x}{l}\right] \qquad 8.2-2$$

where

$$a=\frac{k}{q_m c_{pV}}.$$

The first two terms of this equation describe heat exchange with the environment; the third one accounts for the Joule–Thomson effect, the fourth for the change in geodetic head and the fifth for the change in velocity head. In practical calculations, the last two terms may be neglected. The resulting error is usually less than the error due to uncertainties in the various parameters. If the pressure drop is small, then so is the temperature drop to expansion, and the third term may also be neglected, in which case Eq. 8.2 – 2 simplifies to Eq. 7.6 – 15.

## 8.3. Steady-state flow in pipeline systems

In the gas transmission pipeline network, strictly spoken, steady state flow never exists. There are some important cases however when we can assume, for fulfilling our task, the flow is of this type. This has the advantage, that the numerical simulation procedure is much simpler than to simulate the true transient flow. The two important fields of the steady state model application are the following:

a) Designing of a new *high-pressure gas transmission system* or of the development and the modification of the existent network respectively. Data of the future production and consumption are estimated. Set as an aim, the transmission system should transport the forecast gas streams from sources to the regulator station, at least, with minimum allowable pressure. The length of a transient period at real operating conditions comes to some hours. The reason for the existence of these transients at normal working order is the change of the consumption. (This can also occur by way of unexpected changes caused by failures in the system.) It is not possible to forecast such types of transients in the course of long term planning. Their magnitude and character are influenced beside the more or less determinable industrial demand by the alteration of the gas rate used for heating which is influenced by the daily change in the temperature of the environment; b) Consideration of the transient flow character in the course of designing the *middle- and low-pressure* gas network would be impossible and at the same time irrational, too. On the one hand the length of the pressure waves in the pipelines caused by the accidentally occurring fluctuation in the consumption is of a magnitude of minutes or seconds, on the other hand, the expected maximum gas demand does not equal the aggregated value of the maximum possible consumption of the gas equipment concerned. Experience shows the ratio of these values is $0{\cdot}7-0{\cdot}8$. The accuracy is rather satisfactory therefore if, taking into account the expected consumption districts, the demands characterized by the season of maximum consumption and the coincidence factor we design the network by means of the steady state flow model. This calculation method is, thus, important in the designing practice, and we assume it to remain so.

It should be noted that the pressure changes in the low pressure network do not react upon the operation of the higher pressure network separated by regulator stations. That is why the design of networks with different pressure-level may be performed independently of each other. This fact results in two advantages: on one hand the computing capacity, required for designing is smaller, on the other hand, it is not necessary to calculate the pressure changes of the low pressure network by the more labour-consuming and more complicated equations used for high pressure network designing (see the characteristics for the pressure drop, friction factor $\lambda$ and compressibility factor $z$ in Table $8.5-1$).

### 8.3.1. Fundamental flow equations

The two basic elements of a pipeline network are the *nodes* and the *node connecting elements* (NCEs). Nodes include those points where a pipeleg ends, or where two or more NCEs join, or where there is injection or delivery of gas. The pressure map of the network is determined by node pressures. The most important NCEs are pipelegs, compressor stations, regulators, valves, and underground gas storages. Prior to constructing a model of a a complex system it is necessary to establish mathematical models for individual NCEs. These models are in effect pressure v. throughput relationships valid at given parameters.

The characteristic equation of a *high-pressure pipeleg* is, by Eq. 1.2 – 7,

$$p_1^2 - p_2^2 = k_1 q^2 . \qquad 8.3-1$$

The gas flow expressed in standard volume units is

$$q = \left[\frac{p_1^2 - p_2^2}{k_1}\right]^{0.5} \qquad 8.3-2$$

where

$$k_1 = 1{\cdot}95 \times 10^{-4} \left(\frac{p_n}{T_n}\right)^2 \frac{lM\bar{T}\bar{z}\bar{\lambda}}{d_i^5} . \qquad 8.3-3$$

In a *low-pressure pipeleg*, with pressure close to atmospheric, we have $\bar{z} = 1$ and

$$p_1^2 - p_2^2 = (p_1 + p_2)(p_1 - p_2) \approx 2p_n(p_1 - p_2)$$

and the above equations modify to

$$p_1 - p_2 = k_2 q^2 \qquad 8.3-4$$

and

$$q = \left[\frac{p_1 - p_2}{k_2}\right]^{0.5} \qquad 8.3-5$$

respectively, with

$$k_2 = 0{\cdot}975 \times 10^{-4} \frac{p_n lM\bar{T}\bar{\lambda}}{T_n^2 d_i^5} . \qquad 8.3-6$$

*Compressor* characteristics are provided by the manufacturer. These may usually be approximated by a function of the type

$$q = \frac{P}{k_3\left(\frac{p_2}{p_1}\right)^{k_4} + k_5} \qquad 8.3-7$$

where $k_3$, $k_4$ and $k_5$ are compressor constants.

*Pressure regulators* may be described by the flow equations of chokes (cf. Section 1.4.3). If the pressure drop is less than critical (flow is subsonic), then Eq. 1.4 – 122

will hold if the gas is liquidless, that is,

$$q = k_6 p_1 \sqrt{\left(\frac{p_2}{p_1}\right)^{\frac{2}{\kappa}} - \left(\frac{p_2}{p_1}\right)^{\frac{\kappa+1}{\kappa}}} \qquad 8.3-8$$

where

$$k_6 = \sqrt{2R}\,\frac{\pi}{4}\,d_{ch}^2\,\frac{T_n}{p_n}\,\alpha\,\sqrt{\frac{1}{MT_1}\,\frac{\kappa}{\kappa-1}}\,. \qquad 8.3-9$$

If the pressure drop is above-critical (flow is sonic), then $p_2/p_1$ is to be replaced by the expression in Eq. 1.4−123 and the characteristic relationship is

$$q = k_7 p_1\,. \qquad 8.3-10$$

The production of wells tapping an *underground gas reservoir* can be described by the relationship

$$q = k_8 (p_1^2 - p_2^2)^n \qquad 8.3-11$$

where, as distinct from the usual productivity relationship (cf. Section 3.1) $p_1$ means formation pressure and $p_2$ means wellhead pressure; $k_8$ is a productivity index corresponding to this latter definition.

In the knowledge of the gas transmission system's elements, a mathematical-hydraulic model of the entire system may be constructed. In laying down the principles of modelling, the recognition of an analogy between gas flow in pipe networks and flow of electricity in electrical networks was extensively exploited. Kirchhoff's laws apply to gas flow, too. The first law applies to any node; the algebraic sum of gas flows entering and leaving the node is zero, that is

$$\sum_{i=1}^{m} q_i = 0 \qquad 8.3-12$$

where $m$ is the number of NCEs meeting at the node. Gas flowing into the node is given the positive sign. By Kirchhoff's second law, for any loop in the high-pressure system, the algebraic sum of pressure drops, taken with signs corresponding to a consistent sense of rotation around the loop, is zero, that is,

$$\sum_{i=1}^{n} (p_1^2 - p_2^2)_i = 0\,. \qquad 8.3-13$$

where $n$ is the number of NCEs in the loop, and $p_1$ and $p_2$ are, respectively, the head-end and tail-end pressures of said pipelegs, head and tail being taken with respect to the sense of rotation chosen. This relationship is also called the loop law. In low-pressure gas distribution networks, the compressibility of the gas is negligible and the loop law accordingly simplifies to

$$\sum_{i=1}^{n} (p_1 - p_2)_i = 0\,. \qquad 8.3-14$$

There are two fundamental types of gas transmission systems, loopless and looped.

### 8.3.2. Loopless systems

In a loopless system, NCEs joined by nodes form no closed loops anywhere in the system.

*Figure 8.3 – 1* shows a hypothetical loopless system. Gas enters through node I and leaves through Nodes II, III and IV. Pressures and throughputs in such a system, assuming all NCEs to be pipelegs, are calculated as follows. In the knowledge of the gas volumes respectively injected into and taken out of the nodes,

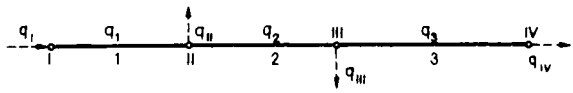


Fig. 8.3 – 1.

Eq. 8.3 – 12 furnishes the gas flows $q_i$ in the pipelegs. In possession of these latter, Eq. 8.3 – 1 yields pressure drops in the pipelegs and node pressures.

*Example 8.3 – 1.* Given the gas flows into and out of Nodes from I to IV of the pipeline shown in *Fig. 8.3 – 1* and the parameters of pipelegs from *1* to *3* and the prescribed terminal pressure $p_{IV} = 18$ bars for Node IV; find the injection pressure $p_1$ necessary to ensure the throughputs and the terminal pressure prescribed, and find the individual node pressures. The resistance factors calculated using Eq. 8.3 – 3 from the parameters of the pipelegs are listed in Column 3 of *Table 8.3 – 1*. The $k_{1i}$s have been replaced by $k_i$s. Node throughputs are listed in Column 4, and the prescribed terminal pressure appears in the last row of Column 9. In the possession of the node throughputs, the pipeleg throughputs listed in Column 5 were calculated using node law 8.3 – 12. Column 7 states the pressure drops in the pipelegs. Now with $p_{IV}$, and hence, $p_{IV}^2$, given, one may find the remaining node pressures using the

Table 8.3 – 1.

| Node $j$ | Pipeleg $i$ | $k_i$ $10^{10}\,\frac{N^2 s^2}{m^{10}}$ | $q_j$ $\frac{m^3}{s}$ | $q_i$ $\frac{m^3}{s}$ | $k_i q_i$ $10^{10}\,\frac{N^2 s}{m^7}$ | $k_i q_i^2$ $10^{10}\,\frac{N^2}{m^4}$ | $p_j^2$ $10^{10}\,Pa^2$ | $p_j$ $10^5\,Pa$ |
|---|---|---|---|---|---|---|---|---|
| 1 | 2 | 3 | 4 | 5 | 6 | 7 | 8 | 9 |
| I | | | +2·38 | | | | 3008·5 | 54·9 |
| | 1 | 249·0 | | 2·38 | 592·6 | 1410·4 | | |
| II | | | −0·38 | | | | 1598·1 | 40·0 |
| | 2 | 145·0 | | 2·00 | 290·0 | 580·0 | | |
| III | | | −0·80 | | | | 1018·1 | 31·9 |
| | 3 | 482·0 | | 1·20 | 578·4 | 694·1 | | |
| IV | | | −1·20 | | | | 324·0 | 18·0 |

relationship

$$p_j^2 = p_{IV}^2 + \sum_{i=j}^{3} k_i q_i^2 ; \qquad 8.3-15$$

$$j = \text{III; II; I}.$$

The calculation reveals that an injection pressure of $p_1 = 54{\cdot}9$ bars is required to ensure a terminal pressure of $p_{IV} = 18$ bar.

The situation is somewhat more complicated if the injection and terminal pressures are fixed, and so are the injection and delivery rates at the intermediate nodes, and the problem is to find the maximum gas output that can be ensured at the delivery end of the line. The solution involves a successive approximation (Hain 1968) in the following steps: (i) Estimate the maximum throughput $q_1^{(1)}$ of the first pipeleg. (ii) Using Eq. 8.3 – 12, find the first-approximation throughputs $q_i^{(1)}$ of the individual pipelegs. (iii) In possession of these latter find the pressure drops in the pipelegs using Eq. 8.3 – 1. (iv) Using the relationship

$$p_j^2 = p_1^2 - \sum_{i=1}^{j-1} k_i \mid q_i^{(k)} \mid q_i^{(k)} ; \qquad 8.3-16$$

$$j = \text{II; III; } \ldots, m$$

where $m$ is the number of nodes, find the node pressures belonging to the $q_i^{(1)}$s calculated in the first approximation. (v) If the square of terminal pressure $p_m$ deviates from the square of terminal pressure $p_m^{(1)}$ by more than the error permitted, then the throughputs determined in (ii) for the individual pipelegs are to be corrected using the expression $q_i^{(2)} = q_i^{(1)} + \Delta q$ where

$$\Delta q = -\frac{p_m^2 - p_m^{(1)2}}{2\sum_{i=1}^{n} k_i q_i^{(1)}} . \qquad 8.3-17$$

(vi) The procedure is repeated from Step (iii) on until the prescribed and calculated terminal pressures agree to within a prescribed tolerance.

*Example 8.3 – 2.* Find the maximum delivery rate at node IV in the pipeline characterized in the foregoing example, if $p_1 = 55$ bars and $p_{IV} = 16$ bars. — The main data of the solution are listed in *Table 8.3 – 2*. It shows that, at the given offtakes at intermediate nodes, the maximum delivery rate attainable at the delivery end of the pipeline is $1{\cdot}23\ m^3/s$.

In the two approximations employed to solve the problem, the values of the $k_i$s were unchanged although throughputs and tail-end pressures of the pipelegs were different. The reasons for this are, one, that flow is fully turbulent so that the friction factor is independent of the throughput-dependent Reynolds number and, two, the change in the mean pressures of the pipelegs is so slight that change in the compressibility factor $z$ is negligible.

If there is a booster compressor station installed somewhere along the pipeline, then the maximum throughput capacity of the pipeline can be calculated as follows

Table 8.3 – 2.

| Node | Pipeleg | $k_i$ | $q_j$ | $q_i^{(1)}$ | $k_i q_i^{(1)}$ | $k_i q_i^{(1)2}$ | $p_j^2$ | $p_j$ | $q_i^{(2)}$ | $k_i q_i^{(2)}$ | $k_i q_i^{(2)2}$ | $p_j^2$ | $p_j$ |
|---|---|---|---|---|---|---|---|---|---|---|---|---|---|
| | | $10^{10}\frac{N^2 s^2}{m^{10}}$ | $\frac{m^3}{s}$ | $\frac{m^3}{s}$ | $10^{10}\frac{N^2 s}{m^7}$ | $10^{10}\frac{N^2}{m^4}$ | $10^{10}$ Pa$^2$ | $10^5$ Pa | $\frac{m^3}{s}$ | $10^{10}\frac{N^2 s}{m^7}$ | $10^{10}$ Pa$^2$ | $10^{10}$ Pa$^2$ | $10^5$ Pa |
| 1 | 2 | 3 | 4 | 5 | 6 | 7 | 8 | 9 | 10 | 11 | 12 | 13 | 14 |
| I | | | | | | | 3025·0 | 55·0 | | | | 3025·0 | 55·0 |
| | 1 | 249·0 | | 2·38 | 592·6 | 1410·4 | | | 2·41 | 600·1 | 1446·2 | | |
| II | | | −0·38 | | | | 1614·6 | | | | | 1578·8 | 39·7 |
| | 2 | 145·0 | | 2·00 | 290·0 | 580·0 | | | 2·03 | 296·2 | 601·2 | | |
| III | | | −0·8 | | | | 1034·6 | | | | | 977·6 | 31·3 |
| | 3 | 482·0 | | 1·20 | 578·4 | 694·1 | | | 1·23 | 592·9 | 729·2 | | |
| IV | | | | | | | 340·5 | 18·5 | | | | 248·4 | 15·8 |

$\Sigma k_i q_i^{(1)} = 1461{\cdot}0 \times 10^{10}$

estimation (1):

$q_1 = 2{\cdot}38\ \text{m}^3/\text{s} \rightarrow q_{1V} = 1{\cdot}2\ \text{m}^3/\text{s}$

$$\Delta q = -\frac{(16\times10^5)^2 - (18{\cdot}5\times10^5)^2}{2\times1461{\cdot}0\times10^{10}} = 0{\cdot}029 \approx 0{\cdot}03$$

$\Sigma k_i q_i^{(2)} = 1489{\cdot}2 \times 10^{10}$

estimation (2):

$q_1 = 2{\cdot}41\ \text{m/s} \rightarrow q_{1V} = 1{\cdot}23\ \text{m}^3/\text{s}$

$$\Delta q = -\frac{(16\times10^5)^2 - (15{\cdot}8\times10^5)^2}{2\times1489{\cdot}2\times10^{10}} = -0{\cdot}0025$$

(Hain 1968): Steps (i) – (iii) of the calculation are as above. (iv) In the knowledge of the gas throughput, intake pressure and installed compressor capacity, the output pressure of the pump can be determined for the node examined. (v) The tail-end pressure of the pipeline is calculated in the knowledge of the output pressure and of pressure drops in the individual pipelegs. (vi) If the calculated tail-end pressure differs from the prescribed one, pipeleg throughputs are once more corrected using the relationship $q_i^{(2)} = q_i^{(1)} + \Delta q$, but the correction itself is now calculated by means of the relationship

$$\Delta q = -\frac{p_m^2 - p_m^{(1)2}}{2\left[\dfrac{(p_2)_c^2 - (p_1)_c^2}{q_c} + \sum_{i=1}^{n} k_i q_i^{(1)}\right]} \qquad 8.3-18$$

where $(p_1)_c$ and $(p_2)_c$ are the intake and discharge pressures of the compressor, respectively, and $q_c$ is compressor output.

### 8.3.3. Looped systems

The first procedure for modelling a low-pressure looped network was developed by Cross (1936); it was adapted with some modifications also to high-pressure systems (Hain 1968). Let us illustrate the application of this method on the loop shown as *Fig. 8.3 – 2*. The gas flows into and out of the nodes are known, and so is

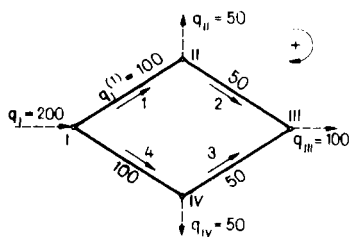


Fig. 8.3 – 2. Looped transmission system to Cross' method

pressure $p_I$ at Node I. We are to find the gas throughputs of the indivual pipelegs, as well as the pressures in the remaining nodes. The solution is based on the following consideration. Taking clockwise flow as positive, let us assume a first-approximation value $q_1^{(1)}$ for the throughput of pipeleg *1*. Let us then use the node law to find the gas throughputs $q_i^{(1)}$, whose signs will be according as flow is clockwise or counterclockwise. In the steady state, the loop law (8.3 – 13 or 8.3 – 14) will have to apply. If it is assumed that the first-approximation values of throughputs in the individual pipelegs differ by $\Delta q$ from the actual throughput, then

$$\sum_{i=1}^{n} k_i (q_i^{(1)} + \Delta q) \mid q_i^{(1)} + \Delta q \mid = 0\,,$$

where $n$ is the number of node-connecting elements (pipelegs). By this relationship, the correction is

$$\Delta q = -\frac{\sum_{i=1}^{n} k_i \mid q_i^{(1)} \mid q_i^{(1)}}{2 \sum_{i=1}^{n} k_i \mid q_i^{(1)} \mid} \qquad 8.3-19$$

provided $\mid \Delta q \mid \ll q_i$; the second-approximation values of the gas throughputs in the individual pipelegs can now be calculated as

$$q_i^{(2)} = q_i^{(1)} + \Delta q\,. \qquad 8.3-20$$

If after the $k$th successive approximation $\Delta q$ is within the tolerance admitted, then the node pressures can be calculated using the relationship

$$p_j^2 = p_1^2 - \sum_{i=1}^{j-1} k_i \mid q_i^{(k)} \mid q_i^{(k)}; \qquad 8.3-21$$

$$j = \mathrm{I}; \mathrm{II}; \ldots$$

for a high-pressure network or

$$p_j = p_1 - \sum_{i=1}^{j-1} k_i \mid q_i^{(k)} \mid q_i^{(k)} \qquad 8.3-22$$

for a low-pressure network; $k$ equals $k_1$ in Eq. 8.3 – 3 in the first case, and $k_2$ in Eq. 8.3 – 6 in the second.

If the system is composed of several loops, then, after a first-approximation estimation of the throughputs in the individual pipelegs, one calculates a $\Delta q$ for each loop, and then performs the correction of the pipelegs' throughputs loop after loop. The pipelegs common to two loops are corrected using the $\Delta q$s determined for both loops. Let us illustrate this procedure by an example referring to a low-pressure network.

*Example 8.3 – 3.* Given the gas flows into and out of the nodes of the network shown as *Fig. 8.3 – 3a*, and given the pressure $p_{\mathrm{I}(1)} = 3300$ Pa of node $\mathrm{I}_{(1)}$; find the gas throughputs of the individual pipelegs, and the individual node pressures. The loops are considered to be balanced if the condition $\left| \sum_{i=1}^{n} \Delta p_i \right| \leqq 5$ Pa is satisfied. A working model of the network is shown as part (b) of *Fig. 8.3 – 3*. The numbering, sizes and length of the pipelegs composing the loops in the Figure are given in Columns 2 – 4 of *Table 8.3 – 3*. The pressure drops in the individual pipelegs are calculated using the relationship

$$\Delta p_i = k_i \mid q_i \mid q_i \qquad 8.3-23$$

derived from Eq. 8.3 – 4; $k_i$ is furnished by Eq. 8.3 – 6, with $p_n = 1{\cdot}014 \times 10^5$ Pa, $T_n = 288{\cdot}2$ K, $M = 16{\cdot}03$ kg/kmole, $\bar{T} = 283$ K, and $\bar{\lambda}$ is obtained using Eq. 1.2 – 5.

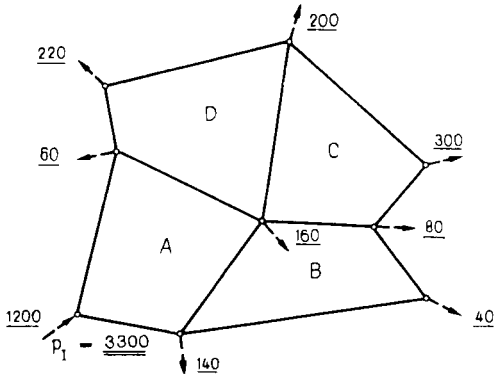


(a)

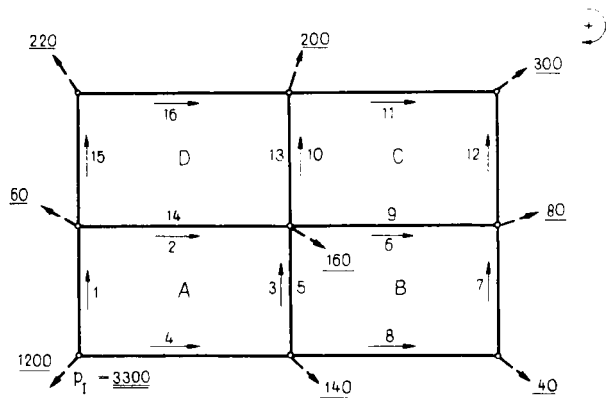


(b)

Fig. 8.3–3. Layout and hookup of low-pressure looped gas supply system

After substitutions,

$$k_i = 5{\cdot}079 \times 10^{-3} \frac{l_i}{d_i^{5{\cdot}333}}.$$

The values calculated in this way are listed in Column 5. Column 6 of the Table lists the first-approximation throughputs of the individual pipelegs, with clockwise rotation regarded as positive. In estimating these throughputs, the circumstance that the condition implicit in Eq. 8.3–12 must hold for each node separately was taken into due account. The pressure drops in Column 8 were calculated using Eq.

8.3 – 19. The $\Delta q$s for the individual loops were determined from Eq. 8.3 – 23; for instance, in loop *A*,

$$\Delta q_A = -\frac{26{\cdot}70}{2 \times 0{\cdot}5289 \times 10^4} = -2{\cdot}52 \times 10^{-3}\ \mathrm{m^3/s}.$$

The summed data of Column 8 show that $\left|\sum_{i=1}^{4} \Delta p_i\right|$ exceeds in each loop the tolerance of 5 Pa, so that the values listed in Column 6b have to be corrected. In the pipelegs which belong to one loop only, the corrected throughputs are supplied by Eq. 8.3 – 20. In the pipelegs common to two loops, the throughputs must of course be the same (Column 10). The corrected throughputs are calculated as shown in the example below. By the values for pipelegs *2* and *14* in Column 6b, the first approximation throughput was $5{\cdot}556 \times 10^{-2}\ \mathrm{m^3/s}$ with signs according to the sense of rotation. The absolute value of the corrected throughput, calculated by means of Eq. 8.3 – 21 but not stated in the Table, is $5{\cdot}304 \times 10^{-2}\ \mathrm{m^3/s}$ in pipeleg *2*. The throughput of pipeleg *14* is equated with this value, and then corrected using the correction for loop *D* and Eq. 8.3 – 21. The value obtained is $-4{\cdot}076 \times 10^{-2}\ \mathrm{m^3/s}$, and accordingly the throughput in leg *2* is $4{\cdot}076 \times 10^{-2}\ \mathrm{m^3/s}$. It is these values that are entered into the corresponding rows of Column 10. Iteration is pursued with the $q_i$s of Column 10. After seven steps of iteration, not given in detail, one obtains the last-step data and the final results listed in Columns 11 – 14. Clearly, by the data in Column 12, $\left|\sum_{i=1}^{n} \Delta p_i\right|$ is in every case within the tolerance of 5 $\mathrm{N/m^2}$. The data in Columns 13 and 14 are the $p_{\mathrm{I}i}$s and $p_{\mathrm{II}i}$s, the pressures at the head and tail ends, respectively, of the individual pipelegs, based on the pressure drop data in Column 12 and on the condition of $p_{\mathrm{I}(1)} = 3300\ \mathrm{N/m^2}$ at the node common to pipelegs *1* and 4.

The main advantage of the Cross method is its simplicity, whereas its main drawback is the slowness of the convergence, which renders this method uneconomical in many applications. In order to eliminate these drawbacks, Renouard developed a variant of the Cross method (Société . . . *Manuel* 1968). The Renouard method is suited for the modelling of steady-state operation in not-too-complicated looped networks. It takes into consideration the interaction of the connected loops, since if the two loops have a joint pipeleg, then the gas flow of this section changes the balance in both of the loops. Cross handles the loops as independent; thus the improvement of the balance of one of the connected loops may impair that of the other. That is why the convergence of this method is rather unfavourable. Renouard offers a system of equations, at which, by simultaneous solution, all the corrections are determined at the same time. To compare the two processes, in the followings we give the basic equations by Cross, and Renouard simultaneously, corresponding to *Fig. 8.3 – 4*.

The equations by Cross are

$$\left.\begin{aligned} a_{11}\Delta q_A &= -b_1 \\ a_{22}\Delta q_B &= -b_2 \end{aligned}\right\} \qquad 8.3-24$$

Table

| Loop | Pipeleg | $d_i$ | $l_i$ | $k_i$ | $q_i^{(1)}$ | $q_i^{(1)}$ | $k_i\|q_i\|^{(1)}$ | $\Delta p_i = k_i q_i^{(1)} \|q_i^{(1)}\|$ |
|---|---|---|---|---|---|---|---|---|
| | | m | m | $\frac{10^4\ \mathrm{Ns}^2}{\mathrm{m}^8}$ | $\mathrm{m}^3/\mathrm{h}$ | $10^{-2}\ \mathrm{m}^3/\mathrm{s}$ | $\frac{10^4\ \mathrm{Ns}}{\mathrm{m}^5}$ | Pa |
| 1 | 2 | 3 | 4 | 5 | 6a | 6b | 7 | 8 |
| A | 1 | 0·3071 | 450 | 0·1240 | 700 | 19·444 | 0·0241 | 46·87 |
| | 2(14) | 0·1541 | 420 | 4·5759 | 200 | 5·556 | 0·2542 | 141·23 |
| | 3(5) | 0·1541 | 370 | 4·0311 | −200 | − 5·556 | 0·2240 | −124·42 |
| | 4 | 0·2589 | 280 | 0·1917 | −500 | −13·889 | 0·0266 | − 36·99 |
| | $\sum_{i=1}^{4}$ | | | | | | 0·5289 | 26·70 |
| B | 5(3) | 0·1541 | 370 | 4·0311 | 200 | 5·556 | 0·2240 | 12·44 |
| | 6(9) | 0·1023 | 290 | 28·087 | 200 | 5·556 | 1·5604 | 866·89 |
| | 7 | 0·1023 | 240 | 23·245 | −120 | − 3·333 | 0·7748 | −258·27 |
| | 8 | 0·1023 | 660 | 63·923 | −160 | − 4·444 | 2·8410 | 1262·7 |
| | $\sum_{i=5}^{8}$ | | | | | | 5·4002 | −529·64 |
| C | 9(6) | 0·1023 | 290 | 28·087 | −200 | − 5·556 | 1·5604 | −866·89 |
| | 10(13) | 0·1541 | 480 | 5·2296 | 40 | 1·111 | 0·0581 | 6·46 |
| | 11 | 0·1023 | 480 | 46·489 | 60 | 1·667 | 0·7748 | 129·14 |
| | 12 | 0·1023 | 220 | 21·308 | −240 | − 6·667 | 1·4205 | −947·0 |
| | $\sum_{i=9}^{12}$ | | | | | | 3·8138 | −1678·3 |
| D | 13(10) | 0·1541 | 480 | 5·2295 | −40 | − 1·111 | 0·0581 | − 6·46 |
| | 14(2) | 0·1541 | 420 | 4·5759 | −200 | − 5·556 | 0·2542 | −142·23 |
| | 15 | 0·3071 | 180 | 0·0496 | 440 | 12·22 | 0·0061 | 7·41 |
| | 16 | 0·2051 | 500 | 1·1859 | 220 | 6·111 | 0·0725 | 44·29 |
| | $\sum_{i=13}^{16}$ | | | | | | 0·3909 | 95·99 |

Renouard's equations

$$\left.\begin{aligned} a_{11}\Delta q_A + a_{12}\Delta q_B &= -b_1 \\ a_{21}\Delta q_A + a_{22}\Delta q_B &= -b_2 \end{aligned}\right\}, \qquad 8.3-25$$

where

$$\begin{aligned} a_{11} &= 2(k_1|q_1| + k_5|q_5| + k_4|q_4|) \\ a_{12} &= -2k_5|q_5| \\ b_1 &= k_1 q_1|q_1| + k_5 q_5|q_5| - k_4 q_4|q_4| \end{aligned}$$

8.3 – 3.

| $\Delta q$ | $q_i^{(2)}$ | ... | $q_i^{(8)}$ | $q_i^{(8)}$ | $\Delta p = k_i q_i^{(8)} \lvert q_i^{(8)} \rvert$ | $p_{1i}$ | $p_{2i}$ |
|---|---|---|---|---|---|---|---|
| $10^{-2}\frac{m^3}{s}$ | $10^{-2}\frac{m^3}{s}$ | | $10^{-2}\frac{m^3}{s}$ | $m^3/h$ | Pa | Pa | Pa |
| 9 | 10 | | 11a | 11b | 12 | 13 | 14 |
| | 19·192 | ... | 20·960 | 754·6 | 54·47 | 3300 | 3246 |
| −0·252 | 4·076 | ... | 4·532 | 163·2 | 93·98 | 3246 | 3152 |
| | − 6·298 | ... | − 5·486 | −197·5 | −121·30 | 3152 | 3273 |
| | −14·141 | ... | −12·373 | −445·4 | − 29·35 | 3273 | 3302 |
| | | | | | − 2·20 | | |
| | 6·298 | ... | 5·486 | 197·5 | 121·30 | 3273 | 3152 |
| 0·490 | 3·846 | ... | 4·353 | 156·7 | 532·14 | 3152 | 2619 |
| | −2·843 | ... | −1·888 | −68·0 | − 82·81 | 2619 | 2702 |
| | −3·954 | ... | −2·999 | −108·0 | −574·75 | 2702 | 3277 |
| | | | | | − 4·12 | | |
| | −3·846 | ... | −4·353 | −156·7 | −532·14 | 2619 | 3152 |
| 2·200 | 2·083 | ... | 1·220 | 43·9 | 7·79 | 3152 | 3144 |
| | 3·867 | ... | 4·315 | 155·3 | 865·76 | 3144 | 2278 |
| | −4·466 | ... | −4·018 | 144·6 | −343·98 | 2278 | 2622 |
| | | | | | − 2·58 | | |
| | −2·083 | ... | −1·220 | − 43·9 | − 7·79 | 3144 | 3152 |
| 1·228 | −4·076 | ... | −4·532 | −163·2 | −93·98 | 3152 | 3246 |
| | 13·450 | ... | 14·762 | 531·4 | 10·81 | 3246 | 3235 |
| | 7·339 | ... | 8·651 | 311·4 | 88·74 | 3235 | 3146 |
| | | | | | − 2·22 | | |

$$a_{21} = -2k_5 \lvert q_5 \rvert$$
$$a_{22} = 2(k_2 \lvert q_2 \rvert + k_3 \lvert q_3 \rvert + k_5 \lvert q_5 \rvert)$$
$$b_2 = k_2 q_2 \lvert q_2 \rvert - k_3 q_3 \lvert q_3 \rvert - k_5 q_5 \lvert q_5 \rvert$$

With Renouard's method, by solving the equations similar in shape to Eqs 8.3 – 25, the gas-flow corrections may be computed. By using the corrected values we may check the fulfilment of the "loop law" (Eq. 8.3 – 13). If the resultant pressure drop exceeds the permitted tolerance, then the calculation must be repeated. In the author's opinion, by applying this method, we obtain suitable results after two or

three iterations even in the case, if the starting values have significantly differed from the proper values.

Stoner's method for solving looped-networks is based on the node continuity equation (Stoner 1970). It has the advantage that, whereas the Cross method can be used to establish throughput and pressure maps of the network only, the Stoner method will furnish any parameter (pipe size in a leg, compressor horsepower required, number of storage wells, size of pressure-reducing choke, etc.) of the complex system. It is, however, significantly more complicated than the previously mentioned methods, and it requires much more computer time. — The way of constructing the model is illustrated in *Fig. 8.3 – 5*. Node *II*, selected as an example,

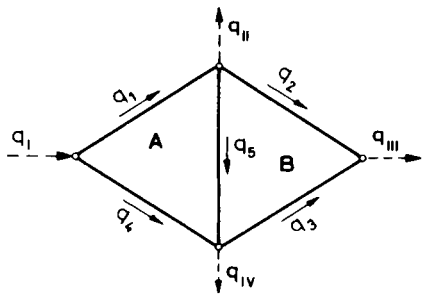


Fig. 8.3 – 4.

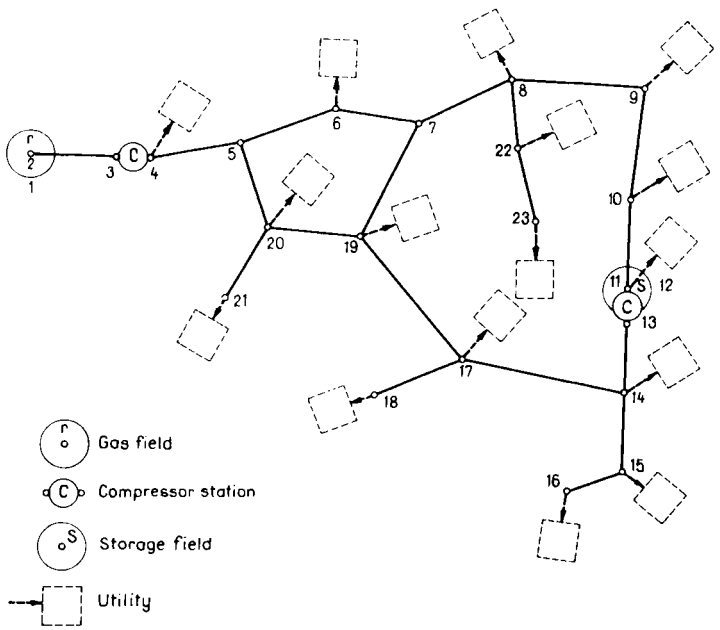


Fig. 8.3 – 5. Regional gas transmission system

receives gas from underground storage facility (*12 – 11*) and pipeleg (*10 – 11*), and delivers gas into the intake of pump (*13 – 11*), and into the consumer supply circuit directly attached to the node. By this model, the node equation 8.3 – 12 can be given the form

$$F_{11}=(q_{12-11})_s-(q_{13-11})_c+(q_{10-11})_p-q_{o11}=0 \qquad 8.3-26$$

where suffixes *s*, *p* and *c* respectively refer to storage, pipeleg and compressor, and $q_{o11}$ is the flow of gas out of node *11*. Flow into the node is positive. The measure of imbalance at the node is $F_{11}$; its value is zero if the node is balanced, that is, if the condition $|F_j|<\varepsilon$ is satisfied, where $\varepsilon$ is the tolerance. Introducing into this Equation the Relationships 8.3 – 1, – 7 and – 11, we get

$$F_{11}=J_{12-11}(|p_{12}^2-p_{11}^2|)_n S_{12-11}-\frac{p_{13-11}}{k_3\left(\frac{p_{13}}{p_{11}}\right)^{k_4}+k_5}+$$

$$+\frac{(|p_{10}^2-p_{11}^2|)^{0.5}}{(k_1)_{10-11}^{0.5}}S_{10-11}-q_{o11}=0 \qquad 8.3-27$$

where $S_{i,j}$ is a sign factor accounting for flow direction:

$$S_{i,j}=\text{sign}\,(p_i-p_j)=\begin{cases}+1 \text{ if } p_i\geq p_j\\ -1 \text{ if } p_i<p_j\end{cases}.$$

Writing up in a similar fashion *n* equations of continuity for the *n* nodes of the system, one obtains the non-linear system of Equations constituting the mathematical model of the system in the steady state.

The equations contain node pressures, inputs/outputs and the parameters of the NCEs (node connecting elements), altogether $(2n+m)$ parameters, where *n* is the number of nodes and *m* is the number of NCEs. The model of *n* equations will in principle yield any *n* unknowns of the $(2n+m)$ parameters, if the remaining $(n+m)$ parameters are given. These equations, similar to Eq. 8.3 – 27, can thus be written in the form

$$F_j(x_1, x_2, \ldots x_n)=0 \qquad 8.3-28$$

$$j=1, 2, \ldots, n.$$

The only criterion in choosing the *n* unknowns to be calculated is that the continuity equations of the type 8.3 – 27, written up for the nodes, must remain mutually independent. Since the value of the nodal gas throughput is independent in $(n-1)$ equations only, at least one of the values $q_{oj}$ must be known. It is likewise necessary to state at least one node pressure.

The solution of the non-linear system Equations 8.3 – 28 constituting the mathematical model of the network may be achieved by the Newton–Raphson technique.

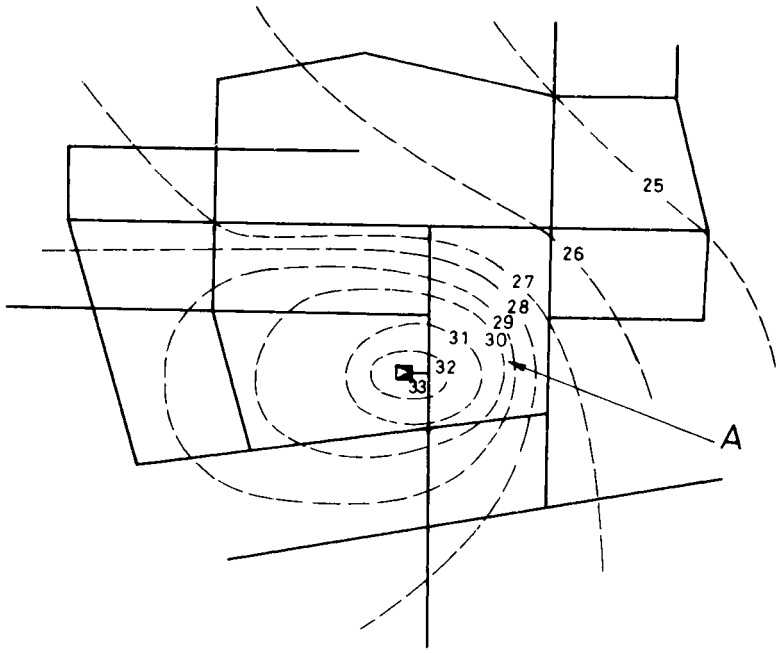


Fig. 8.3 – 6. Pseudo-isobar curves of a low pressure gas distribution system (I)

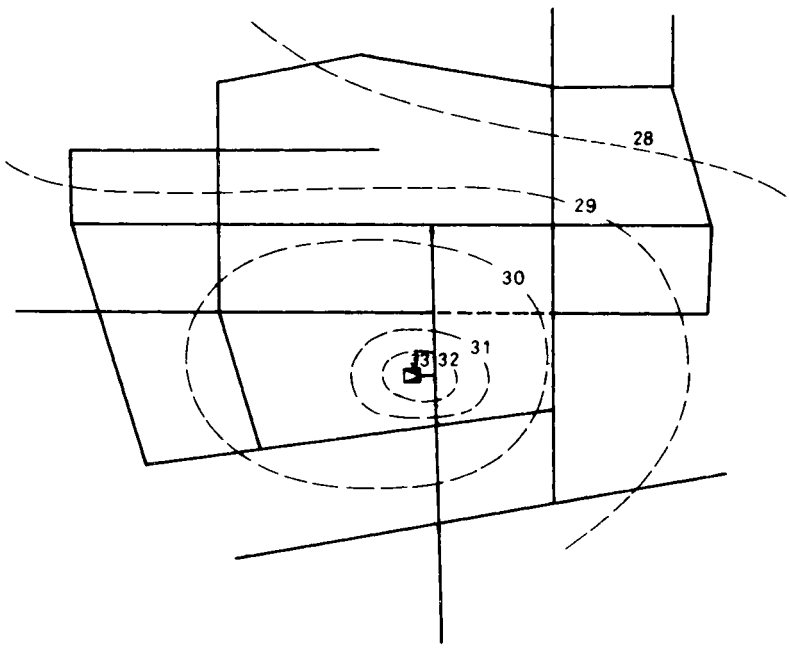


Fig. 8.3 – 7. Psuedo-isobar curves of a low pressure gas distribution system (II)

Stoner (1970, 1971), in a development of the above method, gave a procedure for determining the 'sensitivity' of the system in steady-state operation. The purpose of the calculation is in this case to find out in what way some change(s) in some parameter(s) of the system affect the remaining parameters. For instance, what changes in input pressures and flow rates, or compressor horsepower, are to be effected in order to satisfy a changed consumer demand?

The pressure distribution of the steady state flow in the gas networks is well represented by the pseudo-isobar map. A given isobar curve connects the points of equal pressure in the different pipelines of the network. They are called pseudo-curves because the pressure lines, at areas outside the pipelines, have no physical meaning. The pseudo-isobar maps may be used for the analysis of both high pressure looped systems (Patsch *et al.* 1974), and low-pressure looped gas-distributing systems (Csete and Soós 1974). In *Fig. 8.3–6* the pipelines (full line), and the pseudo-isobars (dashed line) of a low-pressure gas-distributing system are shown. It can be seen that first of all in field A the pseudo-isobar lines are "dense", the pressure drop is significant. If to this gas network the pipeline in *Fig. 8.3–7*, marked with thick dashed line, is fitted, then the pressure drop, in considerable part of the pipe network is reduced more advantageous and this circumstance may justify the building of the new line.

## 8.4. Transient flow in pipeline systems

The flow is transient in every pressure level gas transmission network, but its simulation has a practical significance in high pressure system design only (see the introduction of the Section 8.3). One of the aims of transient flow simulation is the numerical mapping of the flow characteristics of imagined or planned situation (e.g. the determination of maximum throughput capacity at given bounds, or the effect of a leak in a given pipeline leg). For the dispatch center it is a great help to incorporate a computer being able to evaluate unexpected situations and to suggest alternatives for solution by aid of a transient flow program (Gibbon and Walker 1978). Another task can be, to show, what will be the effect of a planned modification (e.g. of building a pipeline leg, or compressor station). Simpler problems can be solved approximately by use of a steady state model too. They do not take into account, however, the change of the mobile gas caused by the variation of the system pressure and hence the excess gas flowing through the regulator station from the high pressure system into the gas distribution network simultaneously with the pressure drop. By the transient model it becomes possible to know accurately the transport capacity of the system and to utilize it. As a result, sometime costs of a new investment increasing capacity may be spared. As an example *Fig. 8.4–1* after Tihanyi (1980) shows curves characterizing the transient operation of a pipeline of 200 km length and 0·8 m diameter. Curve *1* represents the gas stream flowing out of the pipeline (this will be the consumed gas), curve *2* models the gas rate injected into

the pipeline with constant pressure. Curve *3* represents the pressure prevailing at the tail end of the pipeline before the regulator station.

It can be seen the consumption is permanently increasing during the first six hours, than it remains constant in the next 12. The rate of the gas flowing into the pipeline is lower after a beginning equal value for about 14 hours than the offtake value. It becomes steady state thereafter, the intake and offtake values will be equal

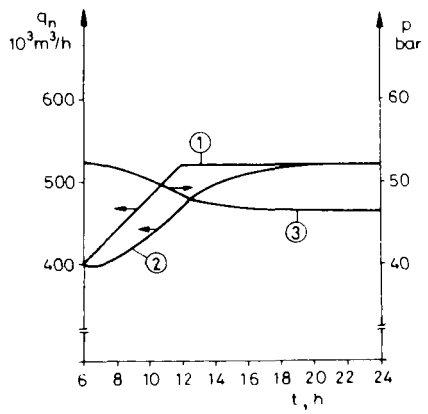


Fig. 8.4 – 1. Pipeline's operating characteristics v. time, after Tihanyi (1980)

again. During the same time the tail end pressure of the pipeline and so the average value too, decrease from the higher initial value to a lower final value. The quantity of the gas storaged in the pipeline decreases with a value proportional to the area between curves *1* and *2*. The same increase in consumption is realizable. This phenomenon, however, is impossible to be shown by aid of the steady state flow model.

### 8.4.1. Relationships for one pipe flow

The relationships describing flow in pipelines of finite length may be derived from four fundamental relationships; any differences in these are merely matters of formulation. The equation of continuity is

$$\frac{\partial q_m}{\partial x} + \frac{\partial(\rho A_i)}{\partial t} = 0. \qquad 8.4-1$$

The equation of energy or of motion is the transient form, accounting for the change of parameters in time, of Eq. 1.2 – 1:

$$\frac{\partial p}{\partial x} + \rho g \sin\alpha + \frac{\lambda v^2 \rho}{2d_i} + \rho \frac{\partial v}{\partial t} = 0. \qquad 8.4-2$$

The equation of state for a gas flow regarded as isothermal is, by Eq. 8.1 – 1

$$\frac{p}{\rho} = z\frac{R}{M}T.$$

The fourth fundamental relationship

$$z = \mathrm{f}(p)_T,$$

has several solutions employed in practice, one of which is Eq. 8.1 – 9. If $z$ is replaced by its average value and considered constant, then the number of fundamental equations reduces to three, and Eq. 8.1 – 1 may be written in the simpler form

$$\frac{p}{\rho} = B^2, \qquad 8.4-3$$

where $B$ is the isothermic speed of sound. Eqs 8.4 – 1 and 8.4 – 3 imply

$$F_1 = \frac{B^2\partial q_m}{A_i\partial x} + \frac{\partial p}{\partial t} = 0 \qquad 8.4-4$$

where mass flow is

$$q_m = \rho A_i v = \frac{p}{B^2} A_i v.$$

By Eqs 8.4 – 2, 8.4 – 3 and the above definition of $q_m$,

$$F_2 = \frac{1\partial p^2}{2\partial x} + \frac{p\partial q_m}{A_i\partial t} + \frac{p^2 g}{B^2}\sin\alpha + \frac{\lambda B^2 q_m|q_m|}{2d_i A_i^2} = 0. \qquad 8.4-5$$

Equations 8.4 – 4 and – 5 constitute a system of non-linear partial differential equations; then, on the assumption that $\bar{z}$ = constant, describe transient flow in the pipeline system.

In the approach to the numerical solution of the system of partial differential Equations 8.4 – 4 and 8.4 – 5, the system is transformed into a system of algebraic equations using the method of finite differences. This algebraic system is capable of solution. For the transformation, the method of central finite differences can be used to advantage. It consists in essence of replacing the function, continuous in the interval under investigation, by a chord extending across a finite domain of the independent variable. The slope of said chord is approximately equal to the slope of the tangent to the curve at the middle of the domain. It is subsequently simple to calculate numerically the derivative of the curve.

For solving the system of differential equations, literature (e.g. Zielke 1971) usually cites three methods: *the implicit method, the explicit method and the method of characteristics.* A common trait to the three methods is that calculation proceeds step by step, deriving pressures and flow rates prevailing at various points of the pipeline at the instant $t + \Delta t$ on the basis of the known distribution of pressures and

flow rates at the instant $t$. The differences are as follows. — In the explicit method, the partial differential equations are transformed into algebraic equations, so that the unknown pressures and flow rates at the instant $t+\Delta t$ depend only on the known pressures and flow rates of the preceding time step, which permits us to find their values one by one solving the individual equations for them. — In the implicit method, a system of algebraic equations results, which contains the unknown pressures and flow rates at the instant $t+\Delta t$ at the neighbouring points of the pipeline so as to be made available only by the solution of the entire simultaneous set of equations. The system of equations furnished by the transformation may, in both cases, be either linear or not. There is the fundamental difference that, whereas in the explicit system the time step is limited for reasons of stability, the only consideration that limits the time step in the implicit method is the accuracy required, but steps are usually significantly longer than what is admissible in the explicit method. — The method of characteristics is essentially an explicit method whose essence is to seek in the $[x, t]$ plane such directions along which the partial differential equation can be reduced to a common differential equation. This latter can be solved numerically by the method of finite differences. The time step is rather restricted also in this method.

Let us now discuss the transforming of the system of partial differential equations into one of algebraic equations by the method of finite differences as performed in the implicit method (Streeter and Wylie 1970, Zielke 1971). The pipeleg under examination is divided up into segments of length $\Delta x$. The time-variable flow rates and pressures of the line sections thus obtained can be assigned to the nodes of the lattice in *Fig. 8.4 – 2*, with a distance step $\Delta x$ and a time step $\Delta t$. *Figure 8.4 – 3* is a blow-up of the cell bounded by the lattice points $(i; i+1)$ in space and $(j; j+1)$ in time. On the basis of this Figure, approximate values for the derivatives figuring in the systems of partial differential Equations 8.4 – 4 and 8.4 – 5, relative to said cell, can be written up (with $q_m$ replaced by $q$) as follows:

$$\frac{\partial p^2}{\partial x} = \frac{p^2_{i+1,j+1} + p^2_{i+1,j} - p^2_{i,j+1} - p^2_{i,j}}{2\Delta x} \qquad 8.4-6$$

$$\frac{\partial p}{\partial t} = \frac{p_{i,j+1} + p_{i+1,j+1} - p_{i,j} - p_{i+1,j}}{2\Delta t} \qquad 8.4-7$$

$$\frac{\partial q}{\partial x} = \frac{q_{i+1,j+1} + q_{i+1,j} - q_{i,j+1} - q_{i,j}}{2\Delta x} \qquad 8.4-8$$

$$\frac{\partial q}{\partial t} = \frac{q_{i,j+1} + q_{i+1,j+1} - q_{i,j} - q_{i+1,j}}{2\Delta t}. \qquad 8.4-9$$

Regarding pressure $p$ and mass flow rate $q$ figuring in Eqs 8.4 – 4 and 8.4 – 5 as time and space averages that are constant within the cell, we get

$$q = \frac{1}{4}(q_{i,j} + q_{i+1,j} + q_{i,j+1} + q_{i+1,j+1}) \qquad 8.4-10$$

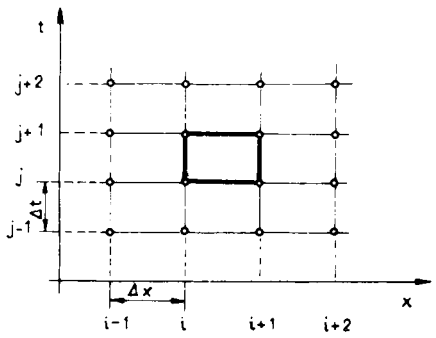


Fig. 8.4 – 2.

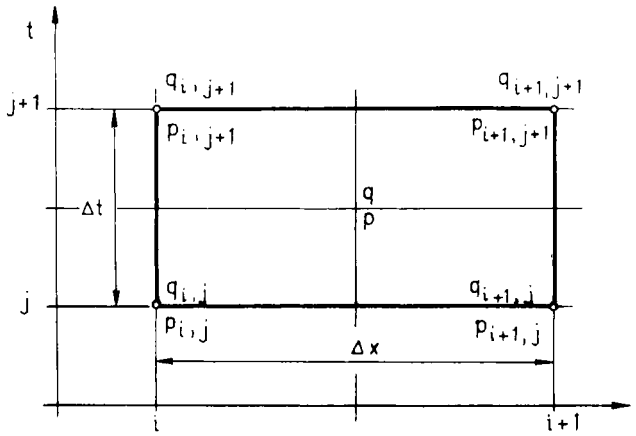


Fig. 8.4 – 3.

$$p = \frac{1}{4}(p_{i,j} + p_{i+1,j} + p_{i,j+1} + p_{i+1,j+1}). \qquad 8.4-11$$

Resubstituting Eqs 8.4 – 6 to 8.4 – 11 into Eqs 8.4 – 4 and 8.4 – 5, and rearranging, we have a system of non-linear algebraic equations:

$$F_1 = \frac{1}{\Delta t}(p_{i,j+1} + p_{i+1,j+1} - p_{i,j} - p_{i+1,j}) +$$

$$+ \frac{B^2}{A\,\Delta x}(q_{i+1,j+1} + q_{i+1,j} - q_{i,j+1} - q_{i,j}) = 0;$$

$$F_2 = \frac{1}{\Delta x}(p^2_{i+1,j+1} + p^2_{i+1,j} - p^2_{i,j+1} - p^2_{i,j}) +$$

$$+ \frac{1}{2A\,\Delta t}(p_{i,j} + p_{i+1,j} + p_{i,j+1} + p_{i+1,j+1}) \times$$

$$\times (q_{i,j+1} + q_{i+1,j+1} - q_{i,j} - q_{i+1,j}) +$$

$$+ \frac{g \sin \alpha}{4B^2}(p^2_{i,j} + p^2_{i+1,j} + p^2_{i,j+1} + p^2_{i+1,j+1}) +$$

$$+ \frac{\lambda B^2}{8dA^2}(q_{i,j} + q_{i+1,j} + q_{i,j+1} + q_{i+1,j+1}) \times$$

$$\times |q_{i,j} + q_{i+1,j} + q_{i,j+1} + q_{i+1,j+1}| = 0 . \qquad 8.4-12$$

If the values of the parameters $q_{i,j}$; $q_{i+1,j}$; $p_{i,j}$; $p_{i+1,j}$ at the instant $j$ are known, either because they figure in the initial conditions or as a result of the calculation for a preceding time step, then the pair of equations contains four unknowns in all: the parameters $q_{i,j+1}$; $q_{i+1,j+1}$; $p_{i,j+1}$; $p_{i+1,j+1}$, belonging to the instant $t + \Delta t$. The pair of Equations 8.4 – 12 may be written up in a similar manner for each one of the $n$ cells. Thus, in any time step, we have to solve $2n+2$ equations, including the two boundary conditions, for $2n+2$ unknowns altogether. For solving the $2n+2$ non-linear algebraic equations, Streeter and Wylie (1970) have proposed the Newton–Raphson method of iteration. The procedure of solution is influenced by the way the two boundary conditions are stated; it will differ according to whether the two boundary conditions refer to the same or to opposite ends of the pipe segment examined. Said boundary conditions are most often time functions of node gas flow rate or pressure. — The number of steps of iteration required to solve the system of equations depends to a significant extent on the choice of initial values for the variables. In order to accelerate convergence it is to be recommended to estimate the initial values by extrapolating from the values found for the preceding time steps. A solution of sufficient accuracy of the system of equations may thus be achieved in just one or two steps. The implicit method has the advantage of being stable even if the time steps $\Delta t$ exceed $\Delta x/B$ ($B$ is the isothermal speed of sound, m/s), and that, consequently, time-step length is limited by accuracy considerations only. There is, however, the drawback that the values of the variables for the instant $t + \Delta t$ may occasionally be furnished by a non-linear system of equations of almost-unmanageable size.

The method of characteristics has also been employed (Streeter and Wylie 1970) for the solution of Eqs 8.4 – 4 and 8.4 – 5. The advantages and disadvantages of this method resemble those of the explicit method; all there is to do in order to find the pressure and mass flow rate in the next instant of time is the solution of a system of two quadratic equations in two unknowns, but the time step, for reasons of stability, must be quite small: $\Delta t < \Delta x/B$. There is an advantage in simultaneously using the characteristic and the implicit method. This will increase the largest admissible time

step $\Delta t$ rather significantly against what is admitted by the sole use of the method of characteristics. Furthermore, the method of characteristics permits the breakdown of complex gas transmission systems into simpler elements. The implicit method, applied to the individual elements, will yield a smaller number of non-linear equations per system, and accordingly, time needed to solve these equations will be reduced rather substantially.

### 8.4.2. Flow in pipeline systems

If there is injection or offtake of gas at certain intermediate points of the transmission line, then these points are to be regarded as nodes and the node law must apply to them. The system of non-linear algebraic equations, written up for the implicit cells of the individual pipeline segments and composed of pairs of equations resembling Eqs 8.4 – 12, is then complemented by node continuity equations of the form

$$q_n + \sum_{i=1}^{m} q_i = 0,$$

where $q_n$ is the gas mass flow into or out of the node, and the $q_i$s are the mass flow rates in the pipelegs meeting at the node. It is the solution of this extended non-linear system of algebraic equations that furnishes the time-dependence of pressures and flow rates in a transmission line with injections and offtakes at intermediate points. Describing in this way the transients taking place in the transmission line system is fairly complicated; this is why, despite its accuracy, it is used to solve simpler, radial systems only (Wylie *et al.* 1970). Modelling the transients of more complicated, looped nets is usually performed by some simpler method resulting from certain neglections. The most usual neglections are as follows (Guy 1967).

In a gas transmission line system, neglecting the altitude difference between the system's nodes does not usually introduce a significant error. The third term on the right-hand side of Eq. 8.4 – 5 describing transient flow may therefore be dropped. It can further be shown that the term $(p/A_i)(\partial q/\partial t)$, describing the change per unit of time in the rate of mass flow on the right-hand side of Eq. 8.4 – 5, is in the majority of practical cases less by an order of magnitude than the friction term

$$\frac{\lambda B^2 q^2}{2 d_i A_i^2},$$

and is therefore negligible, too. These simplifications reduce the system composed of Eqs 8.4 – 4 and 8.4 – 5 to the following, much simpler, form:

$$\frac{\partial p}{\partial t} = -\frac{B^2 \partial q}{A \partial x}, \qquad 8.4-13$$

$$\frac{\partial p^2}{\partial x} = \frac{\lambda B^2}{\mathrm{d} A^2} q^2, \qquad 8.4-14$$

where we have changed the notation concerning internal cross-sectional area and $ID$ of the pipe ($A_i = A$; $d_i = d$). Equation 8.4 – 13 states the pressure change per unit of

time in an infinitesimal length of pipe dx, brought about by an infinitesimal change in the gas mass flow rate. The equation describes the capacitive property of the pipeline. — By Eq. 8.4 – 14, the flowing pressure drop in the infinitesimal length of pipe dx can be calculated using the relationship for steady-state flow. The equation expresses the flow resistance of the pipeline. The physical content of these equations can be generalized to systems of pipelines as follows.

One assigns to any node half the length of each pipeleg tying in to that node, and the half-legs thus obtained are summed. Let the volume thus assigned to node $j$ be $V_j$. The flows $q_{i,j}$ into and out of the node and the offtake $q_{o,j}$ at the node determine the change of the mass flow rate at the node. Equation 8.4 – 13 may, therefore, be rewritten for this node in the following form (Fincham 1971):

$$\frac{V_j \, \mathrm{d}p_j}{B^2 \, \mathrm{d}t} = \sum_{i=1}^{m} q_{i,j} - q_{o,j} \qquad 8.4-15$$

where $m$ is the number of pipelegs tying in to the node. — By Eq. 8.4 – 14, mass flow rates in the pipelegs assigned to node $j$ can be calculated using the relationship

$$q_{i,j} = \left[ \frac{d_{i,j} A_{i,j}^2}{\lambda_{i,j} B^2} \frac{|p_i^2 - p_j^2|}{l_{i,j}} \right]^{0.5} S_{i,j} \qquad 8.4-16$$

where the $l_{i,j}$s are the lengths of the individual pipelegs and

$$S_{i,j} = \operatorname{sign}(p_i - p_j).$$

Introducing Eq. 8.4 – 16 into Eq. 8.4 – 15, and employing the notation

$$K_j = \frac{B}{V_j} \text{ and } J_{i,j} = J_{j,i} = \left( \frac{\mathrm{d}A^2}{\lambda l} \right)_{i,j}^{0.5}$$

we get after rearranging the differential equation

$$\frac{\mathrm{d}p_j}{\mathrm{d}t} = K_j \sum_{i=1}^{m} [J_{i,j} (|p_i^2 - p_j^2|)^{0.5} S_{i,j}] - q_{oj}. \qquad 8.4-17$$

Applying the method of finite differences,

$$\frac{\mathrm{d}p_j}{\mathrm{d}t} = \frac{p_j(t + \Delta t) + p_j(t)}{\Delta t}.$$

Using this, Eq. 8.4 – 17 assumes after rearranging the form

$$p_j(t + \Delta t) = \Delta t \, K_j \left\{ \sum_{i=1}^{m} [J_{i,j} (|p_i^2 - p_j^2|)^{0.5} S_{i,j}] - q_{oj} \right\} + p_j(t). \qquad 8.4-18$$

Writing up similar equations for the other nodes we obtain a system of non-linear algebraic equations concerning the transients in the complex system. The solution of this system of equations furnishes the pressures prevailing at the individual nodes at the instant $(t + \Delta t)$. Differential equation 8.4 – 17 can be solved using the implicit or explicit method, as follows.

Let us introduce the notation

$$C_j = \Delta t K_j \left\{ \sum_{i=1}^{m} J_{i,j} (|p_i^2 - p_j^2|)^{0.5} S_{i,j} - q_{oj} \right\}. \qquad 8.4-19$$

Equation 8.4 – 18 may accordingly be written up in two ways:

$$p_j(t + \Delta t) = C_j(t) + p_j(t)$$

for the explicit method, and

$$p_j(t + \Delta t) = C_j(t + \Delta t) + p_j(t)$$

for the implicit method. If the node pressures at the instant $t$ are fixed by some initial condition, then the explicit method will directly furnish the pressures prevailing at the instant $(t + \Delta t)$. If, on the other hand, the implicit method is adopted, then said pressures may be obtained only by simultaneously solving the system of non-linear algebraic equations including an equation resembling 8.4 – 18 for each node.

The operation of the gas transmission system is significantly affected by the extant compressors, pressure regulators and valves. Their common feature is, that their storing volume is negligible, and, on the other hand they transmit external intervention and energy intake. The operation of the compressors and the valves may develop transients, while the pressure regulator can damp the pressure changes. Their operation is simulated by most the authors (Distefano 1970; Goacher 1969; Wylile *et al.* 1970) with the so-called black box method as against to hydraulic characterization of the pipeline. Substantially it means, that the input and output pressures of the compressors and regulators are given in the function of throughflowing gas rate and their operation is characterized by this relation. A simplifying bound of this method is, that either the value of the output pressure or the output gas rate is fixed (Fincham 1971). The power equation of the compressor, $P = f(p_1, p_2, q)$ is taken into account too. The valve has two characteristic conditions: it is totally closed or it is completely opened. These affect and modify the configuration of the pipeline network.

## 8.5. Numerical simulation of the flow in pipeline system by computer

The numerical simulation of the flow in pipeline system is so labour consuming, that both the computation of the steady state flow (see Section 8.3) and that of the transient flow (see Section 8.4) can be rationally solved only by using electronic computers. Mainly in the 1960s, the analog computer was also thought by the experts to have an important role in the design process. Its advantage is, that it can solve different problems without mathematical abstractions, with simple manual operation only, using practically no time for the calculation. That is why its usage proved to be fruitful in the rapid determination of several versions, and in selecting the optimum solution, both for designing a new system and in the analysis of the existing system operation. Due to its visualizing ability the analog computer can be

also very well used for the training of engineers dealing with maintenance of gas pipeline systems. Its main disadvantage is that the computer in question is a single-purpose device that can be used for network planning only. On the other hand, to simulate a complicated gas transmission system of several elements, a large and rather expensive device is needed. The largest analog computer, suitable for simulating gas transmission systems, was developed by SNAM in Metanopoli (Bonfiglioli and Crocc 1970). In the past decade no information has been received about the development of a new high capacity similar device. Today, for network calculation purposes digital computers are used almost solely. Up to the end of the seventies computing methods and computer programs were elaborated that are suitable for solving all the problems of practical importance (c.f. Section 8.5.3).

*Table 8.5 – 1* summarizes after Csete and Tihanyi (1978) the main characteristics of the numerical simulation methods of different pressure level gas networks.

Using the digital computer for system modelling a peculiar problem is the formulation of the fundamental parameters (e.g. of the existent configuration) and of the basic simulation rules into a mathematical language that can be "understood" by the computer. For solving this problem, a separate part of modern mathematics,

Table 8.5 – 1. Simulation characteristics of different pressure stage gas distribution networks after Csete and Tihanyi (1978)

| | Pressure stage | | |
|---|---|---|---|
| | high | medium | low |
| Characteristics regarding input data: | | | |
| — reliability of the node load estimation | high | moderate | low |
| — effect of the terrain level differences | negligible | negligible | not negligible |
| Computing features regarding | | | |
| — compressibility factor | $z = z$ (p, t) | $z = 1{\cdot}0$ | $z = 1{\cdot}0$ |
| — friction factor | $\lambda = \lambda(N_{Re}, k/d)$ | $\lambda = \lambda(N_{Re}, k/d)$ | appr. $\lambda$ relation |
| — pressure loss | $p_1^2 - p_2^2 = f(q_n^2)$ | $p_1^2 - p_2^2 = f(q_n^2)$ | $p_1 - p_2 = f(q_n^2)$ |
| Characteristics regarding output data: | | | |
| — maximum accuracy of calculated node pressures | 0·1 bar | 0·2 bar | 1 Pa |
| — calculation of flow velocity | not necessary | necessary | necessary |
| — pressure gradient as leg feature | not important | important | important |
| Problems regarding network transients: | | | |
| — damping time of transients | hours | minutes | seconds |
| — gas quantity stored in pipe-line network | considerable | not considerable | not considerable |
| — transient analysis relating to total network | needed in practice | mainly of theoretical importance | mainly of theoretical importance |

the graph theory (Haray 1969) offers a considerable aid. This will be briefly explained in the next Chapter.

It should be noted that the design methods using computers, generally have three typical stages of development, as follows: (a) Solution of calculation problems by computer, (b) computer-aided engineering design, (c) automated engineering design. In gas pipeline system design the stage (a) was achieved. Further development may be expected in the realization of stage (b), where the computer will not used for solving mathematical problems only, but for fulfilling other tasks of the design operation, such as data- and information storage and data handling. Such method, for the determination of strength behaviours of the pipeline, has been used for a relatively long time (Foord and Rowe 1981). The task of the stage, (c) is the pre-programing of the total design process decreasing considerably the number and significance of the human intervention during the work.

This stage will be probably achieved first of all in the hydraulic design of gas networks. I do not think, however, that the intuitive role of the engineer will ever become negligible, or superfluous in the designing of the complete system on the contrary, his duty will be to make decisions in all of the cases for which no computer program is preparable. This work will require an intellectual activity of higher level of the designer than it does now. A good summary of the theoretical problems of gas pipeline network design is given by Tihanyi (1982).

### 8.5.1. Principle of computation

The complex gas transmission system composed of nodes and NCEs may, with due attention to the known or assumed directions of flow, be regarded as a directed graph whose connection matrix **A** is rather simple to write up. Let the columns of **A** represent NCEs, that is, edges of graph, and let the rows represent nodes. Let element $a_{ij}$ of the matrix be

$$a_{i,j} = \begin{cases} +1, \text{ if edge } j \text{ emerges from node } i, \\ -1, \text{ if edge } j \text{ ends in node } i, \\ 0, \text{ if edge } j \text{ and node } i \text{ are unconnected.} \end{cases}$$

The connection matrix of the graph in *Fig. 8.5 – 1(a)*, representing the network in *Fig. 8.3 – 6*, is accordingly

| | 1 | 2 | 3 | 4 | 5 | 6 | 7 | 8 | 9 | 10 | 11 | 12 | |
|---|---|---|---|---|---|---|---|---|---|---|---|---|---|
| **A** = 1 | 1 | 0 | 0 | 1 | 0 | 0 | 0 | 0 | 0 | 0 | 0 | 0 | |
| 2 | −1 | 1 | 0 | 0 | 0 | 0 | 0 | 0 | 0 | 0 | 0 | 1 | |
| 3 | 0 | −1 | −1 | 0 | 0 | 0 | 0 | 0 | 0 | 1 | 1 | 0 | |
| 4 | 0 | 0 | 1 | −1 | 1 | 0 | 0 | 0 | 0 | 0 | 0 | 0 | |
| 5 | 0 | 0 | 0 | 0 | −1 | 1 | 0 | 0 | 0 | 0 | 0 | 0 | Nodes |
| 6 | 0 | 0 | 0 | 0 | 0 | −1 | 1 | 0 | 0 | 0 | −1 | 0 | |
| 7 | 0 | 0 | 0 | 0 | 0 | 0 | −1 | −1 | 0 | 0 | 0 | 0 | |
| 8 | 0 | 0 | 0 | 0 | 0 | 0 | 0 | 1 | −1 | −1 | 0 | 0 | |
| 9 | 0 | 0 | 0 | 0 | 0 | 0 | 0 | 0 | 1 | 0 | 0 | −1 | |

Node-connecting elements

8.5 – 1

This connection matrix uniquely defines system configuration. In network calculation, one requires in addition to the connection matrix also a definition of the loops — the senses of rotation — in the network, which may be performed with the aid of the so-called loop matrix. In order to derive the loop matrix from the connection matrix it is necessary to introduce the concept of a tree. This term denotes a connected graph in which there is one and only one trajectory between any two nodes. Thus, any loopless graph is a tree. If a graph is looped, it is possible to turn it into a tree by eliminating some of its edges. This may be performed automatically, by adding up the rows of the connection matrix. Let us designate on the tree chosen a so-called point of reference or base point, and let us drop the corresponding row from the connection matrix. Now rearranging the matrix so as to separate tree branches and chord branches (the latter are those which are to be eliminated to form the tree), we may write up the so-called matching matrix of the system. Let e.g. the reference point be node *1*, in the graph shown as *Fig. 8.5 – 1(a)*, and let us eliminate loops by dropping edges *3*, *6*, *8* and *10*. The matching matrix of the graph is, then, written in the form

$$\mathbf{B}=[\mathbf{B}_t\mathbf{B}_h]=\begin{array}{c} \\ 2 \\ 3 \\ 4 \\ 5 \\ 6 \\ 7 \\ 8 \\ 9 \end{array}\begin{array}{c}\begin{array}{cccccccc} 1 & 2 & 4 & 5 & 7 & 9 & 11 & 12 \end{array} \\ \left[\begin{array}{cccccccc} -1 & 1 & 0 & 0 & 0 & 0 & 0 & 1 \\ 0 & -1 & 0 & 0 & 0 & 0 & 1 & 0 \\ 0 & 0 & -1 & 1 & 0 & 0 & 0 & 0 \\ 0 & 0 & 0 & -1 & 0 & 0 & 0 & 0 \\ 0 & 0 & 0 & 0 & 1 & 0 & -1 & 0 \\ 0 & 0 & 0 & 0 & -1 & 0 & 0 & 0 \\ 0 & 0 & 0 & 0 & 0 & -1 & 0 & 0 \\ 0 & 0 & 0 & 0 & 0 & 1 & 0 & -1 \end{array}\right. \\ \text{Tree branches} \\ \mathbf{B}_t \end{array}\begin{array}{c}\begin{array}{cccc} 3 & 6 & 8 & 10 \end{array} \\ \left.\begin{array}{cccc} 0 & 0 & 0 & 0 \\ -1 & 0 & 0 & 1 \\ 1 & 0 & 0 & 0 \\ 0 & 1 & 0 & 0 \\ 0 & -1 & 0 & 0 \\ 0 & 0 & -1 & 0 \\ 0 & 0 & 1 & -1 \\ 0 & 0 & 0 & 0 \end{array}\right] \\ \text{Chord branches} \\ \mathbf{B}_h \end{array} \qquad 8.5-2$$

Clearly, in a graph of $n$ nodes and $m$ edges, the number of independent so-called basic loops is $k=m-n+1$. It can be shown that the transpose $\mathbf{C}^T$ of the matrix $\mathbf{C}$ of these basic loops is defined by the relationship

$$\mathbf{C}^T=\begin{bmatrix}\mathbf{C}_t^T \\ \mathbf{C}_h^T\end{bmatrix}=\begin{bmatrix}-\mathbf{B}_t^{-1}\mathbf{B}_h \\ \mathbf{I}\end{bmatrix}, \qquad 8.5-3$$

where $\mathbf{I}$ is the unity matrix.

$\mathbf{B}_t^{-1}$ is the inverse of matrix $\mathbf{B}_t$. It can be produced either by inverting matrix $\mathbf{B}_t$, or by writing up directly as follows. The rows of $\mathbf{B}_t^{-1}$ are the tree branches; its columns are the nodes. Let element $b_{ji}^{-1}$ of matrix $\mathbf{B}_f^{-1}$ be

$$b_{ji}^{-1}=\begin{cases} +1, & \text{if the trajectory from the base point to node } i \text{ includes} \\ & \text{branch } j, \text{ with the branch directed towards the base point,} \\ -1, & \text{idem, with the branch directed towards the node,} \\ 0, & \text{if the trajectory from the base point to the node does not} \\ & \text{include branch } j. \end{cases} \qquad 8.5-4$$

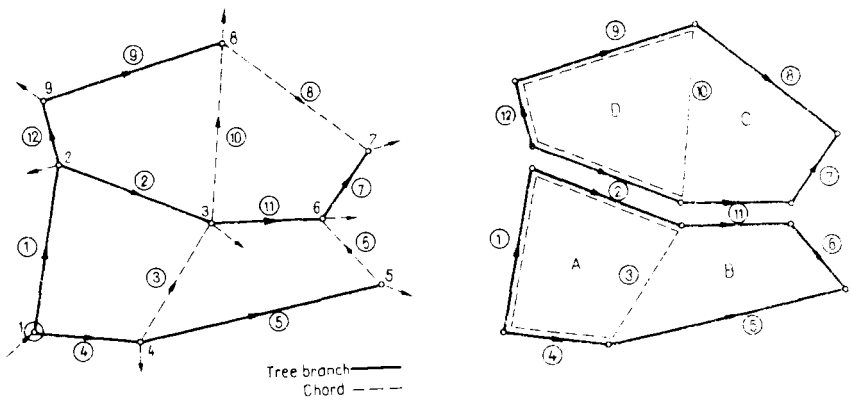


Fig. 8.5 – 1.

For an example, the inverse of matrix $\mathbf{B}_f$ referring to the tree shown in continuous line in *Fig. 8.5 – 1(a)*, written up according to Eq. 8.5 – 4, is

$$-\mathbf{B}_f^{-1} = \begin{array}{c} \\ 1 \\ 2 \\ 4 \\ 5 \\ 7 \\ 9 \\ 11 \\ 12 \end{array} \begin{array}{c} \begin{array}{cccccccc} 2 & 3 & 4 & 5 & 6 & 7 & 8 & 9 \end{array} \\ \left[\begin{array}{cccccccc} 1 & 1 & 0 & 0 & 1 & 1 & 1 & 1 \\ 0 & 1 & 0 & 0 & 1 & 1 & 0 & 0 \\ 0 & 0 & 1 & 1 & 0 & 0 & 0 & 0 \\ 0 & 0 & 0 & 1 & 0 & 0 & 0 & 0 \\ 0 & 0 & 0 & 0 & 0 & 1 & 0 & 0 \\ 0 & 0 & 0 & 0 & 0 & 0 & 1 & 0 \\ 0 & 0 & 0 & 0 & 1 & 1 & 0 & 0 \\ 0 & 0 & 0 & 0 & 0 & 0 & 1 & 1 \end{array}\right] \end{array}$$

Tree branches

Nodes

In possession of this inverse matrix, the transpose $\mathbf{C}^T$ of matrix $\mathbf{C}$ referring to the independent loops is obtained, after performing the matrix multiplication, written up in Eq. 8.5 – 3 in the form (cf. *Fig. 8.5 – 1(b)*):

Loops

$$\mathbf{C}^T = \begin{bmatrix} -\mathbf{B}_f^{-1}\mathbf{B}_h \\ \mathbf{I} \end{bmatrix} = \begin{array}{c} \\ 1 \\ 2 \\ 4 \\ 5 \\ 7 \\ 9 \\ 11 \\ 12 \\ 3 \\ 6 \\ 8 \\ 10 \end{array} \begin{array}{c} \begin{array}{cccc} \mathrm{A} & \mathrm{B} & \mathrm{C} & \mathrm{D} \end{array} \\ \left[\begin{array}{cccc} -1 & -1 & 0 & 0 \\ -1 & -1 & -1 & 1 \\ 1 & 1 & 0 & 0 \\ 0 & 1 & 0 & 0 \\ 0 & 0 & -1 & 0 \\ 0 & 0 & 1 & -1 \\ 0 & -1 & -1 & 0 \\ 0 & 0 & 1 & -1 \\ 1 & 0 & 0 & 0 \\ 0 & 1 & 0 & 0 \\ 0 & 0 & 1 & 0 \\ 0 & 0 & 0 & 1 \end{array}\right] \end{array}$$

NCEs

The system is uniquely defined by its connection matrix **A** and the loop matrix **C** derived from it. If in the following we agree to represent gas flow in the individual NCEs by $m$-dimensional column vector $q$, and the gas offtakes at the individual nodes by $n$-dimensional column vector $q_o$, then Kirchhoff's node law may be written in the form of a matrix equation

$$\mathbf{A}q = q_o ,$$

or, in more detail, of the relationship

$$\sum_j a_{ij} q_j = q_{oi} .$$

Kirchhoff's second law may be written up in a similar fashion, by representing pressure changes $\Delta p^2 = p_1^2 - p_2^2$ across NCEs by column vectors $\Delta P$. The loop law then assumes the form

$$\mathbf{C}\,\Delta P = 0 ,$$

or, in more detail,

$$\sum_j c_{kj}\,\Delta P_j = 0 ,$$

where $k$ is the subscript of loops.

It emerges from the above considerations that modelling gas transmission systems by means of directed graphs is fairly simple; description using matrices of such systems affords a clear insight into the essence of the problem; and the calculation is readily performed by computer. It should be noted, however, that if the system is extensive, the procedure takes a considerable storage capacity. Another problem is that matrices **A**, **B** and **C** are usually highly sparse; that is, a high percentage (up to 90 or even 98 percent in some cases) of their elements may be zero. In order to reduce storage capacity demand and to simplify calculation, special sparse-matrix solution methods have been devised.

### 8.5.2. Review of system-modelling programs

As a consequence of the fast-increasing popularity of the digital computer, numerous systems, simulation programs have been developed by the research teams involved with the problem. The most widely known programs were reviewed by Goacher (1969), who divided them in three main groups.

**(a) General programs suitable also for the modelling of gas transmission systems**

These are essentially programs suited for the solution of differential equations of various types. Several of these are included in the software of almost every medium and big general-purpose computer. The best-known such programs include CSMP (Continuous System Modelling Program (IBM 1130/360)); Digital Simulation Language (IBM 1130/7090/360); MIMIC; MIDAS (Modified Integration Digital Analog Simulation); KALDAS (Kidsrove Algol Digital Analog Simulation (ICL 1900 Series)); SLANG (Simulation Language (ICL 503/803/4120/4130/ATLAS)). These programs have the common drawback that the system of differential equations describing the process taking place in the system has to be formulated by the gas engineer, who must, in addition, bring the system to the most suitable form or, indeed, reduce it to the most fundamental operations (addition, subtraction), as the system of equations is fed to the computer as a basic data. Preparing the equations of the boundary conditions is not less cumbersome. Another disadvantage is that all programs named above employ the explicit method to solve the system of differential equations, and although the results for any time step are obtained rather fast, time steps must be quite short, which is a considerable disadvantage when handling transients of long duration.

**(b) Programs modelling steady states**

These programs are used for two distinct purposes: first, independently, to investigate one of the fairly large class of steady-state or nearly-steady-state technical and engineering problems, and secondly, to furnish initial conditions for the dynamic models.

The programs developed by the Gas Council London Research Station and by the Department of Petroleum Engineering (TUHI, Miskolc) are given in *Table 8.5 – 2*. The majority of these programs satisfy the requirement that the user need not know the structure and operation of the program. The input data including the network configuration, the parameters of the pipelegs, the pressures and flow rates of the sources, and the consumer demands can be readily compiled with reference to the set of instructions. In order to solve a loop it is sufficient to estimate the throughput in one pipeleg included in the loop. From these data, the computer will calculate the steady-state conditions by an iteration procedure. The program GFS-I computes the friction factor $\lambda$ from the Colebrook equation (Eq. 1.1 – 7), and takes into account the change of the compressibility factor $z$ by Wilkinson equation (Eq. 8.1 – 9). The pressures at the nodes are determinable with an accuracy of 0·1 bar by applying the Newton–Raphson iteration method. At GFS-III $\lambda$ is constant, while at GFS-II and GFS-III $z$ is constant, too. The accuracy of the pressure determination is 1 kPa at GFS-II while 1 Pa at GFS-III; in the first program the Newton–Raphson or the Cross method can be used, in the latter the Cross method is applied.

Table 8.5 – 2. Main features of steady state network analysis programs after Goacher 1969 (*a* – *g*) and Csete and Tihanyi 1978 (*h*, *i*)

| Program | | Pipelegs | Nodes | Pressure defined modes | Loops | Compressors regulators |
|---|---|---|---|---|---|---|
| 1 | | 2 | 3 | 4 | 5 | 6 |
| MANNA (8K) | *a* | 150 | 150 | 12 | 15 | None |
| MANNA (32K) | *b* | 300 | 300 | 40 | 50 | None |
| altogether | | | | 50* | | |
| MANNA I (32K) | *c* | 600 | 500 | 100 | 200 | None |
| altogether | | | | 200* | | |
| SONIC (8K) | *d* | 150 | 150 | 20 | 20 | 10 |
| altogether | | | | | 20* | |
| SONIC (32K) | *e* | 300 | 300 | 40 | 50 | 20 |
| altogether | | | | | 50* | at least 1 |
| DEVIL (32K) | *f* | 300 | 300 | 40 | 50 | 20 |
| altogether | | | | | 50* | at least 1 |
| SNAC (32K) | *g* | 400 | 300 | 25 | 150 | 25 |
| GFS I | *h* | 200 | 200 | No limit | 50 | 50 |
| GFS II, III | *i* | 600 | 600 | No limit | 150 | 50 |

MANNA — Matrix Algebra for Non-linear Network Analysis (IBM 1130)
SONIC — Steady-state of Networks Including Compressors (IBM 1130)
SNAC — Steady-state Network Analysis with Compressors
GFS — Gas Flow Simulation;
I high-, II medium-, III low pressure
* — Altogether

### (c) Programs modelling steady and transient states

In these programs, the part modelling the steady state serves to provide the initial conditions required for the transient calculations. The program is formulated also in this case so that the gas engineer in control of the system may use it as a 'black box' provided he observes certain instructions and rules of operation. Although the input data list differs from one program to the next, each program will require as a matter of course the data mentioned in connection with the programs simulating steady states. These must be complemented with the transient boundary conditions and with the parameters of the compressors, regulators, valves, etc. included in the system.

The main characteristics of some up-to date and in practice widely used programs are listed in *Table 8.5 – 3* after Goacher (1969), Goldwater *et al.* (1976) and Tihanyi (1980). No mention is made in the Table of the General Electric's (USA) fairly successful GE Simulator program, since its characteristic data are not available. This latter, similarly to CAP and ENSMP solves the differential equations by the implicit method, whereas PIPETRAN and SATAN use the explicit method. As a matter of fact SATAN is the combination of CAP and PIPETRAN. The three-stage operation provides the program with high flexibility (see later).

For solving the basic equations the PAN algorithm uses the Crank–Nicholson method. The program was tested partly by results obtained by the CAP method, and partly by data telemechanically measured in a gas transmission network. The correspondence was sufficiently good in both of the cases. For solving the differential equations the TGFS program uses a hybrid method that combines the speed of the explicit and the stability of the implicit methods. Its principle is that at each $\Delta t$ time-step for the determination of the change in pressure at the nodes it calculates explicit and implicit steps respectively according to a previously defined order. For an example as to the structure of a program simulating a complex gas transmission system, let us consider that of SATAN.

The program consists of three main units, which may be run separately if so desired. — *Phase 1.* Calculation of the steady state. Quite often, it is necessary to compare only the steady-state operation of various system configurations, or to furnish initial conditions for the transient calculation. In that case, running this program separately, one may examine up to 10 variants in succession. At the end of each run, in addition to the printout of the desired results, all data required for the transient calculation except the boundary conditions are stored in the background memory from where it may be called in as and when required. — *Phase 2.* This is the connecting phase in which the transient model is built up step by step out of the results of one or more variants of the previous phase, judged to be the most interesting, and out of the boundary conditions fed into the machine. The results are once more relegated to the background memory. Up to ten dynamic-model variants may be stored also in this case. — *Phase 3.* Transient analysis. The computer calls in the intermediate results, calculated in the foregoing phases, of one or several preferred variants, and calculates the transient flow rates and pressures.

The block diagram of the program is given after Goacher in *Fig. 8.5 – 2.* The program structure is such that routines providing higher accuracy, or a faster solution, or a more economical use of storage space can be introduced into the program without changing its structure, merely by exchanging certain segments.

#### (d) Programs solvable by simulation

In the prefatory parts of the Sections 8.3 and 8.4 the application fields of the steady state and transient flow simulation were discussed in general. The speediness of the computerized design makes it possible that the programs, already known, could be used for solving an ever increasing number of different problems. The next

Table 8.5 – 3. Main features of network analysis programs simulating steady and transient flows after Goacher 1969 (*a* – *d*), Goldwater *et al.* 1976 (*e*) and Tihanyi 1980 (*f*)

| Program | Pipe-legs | Nodes | Flow-defined nodes | Pressure defined nodes | Compressors | Regulators | Loops | Valves | Flow pressure profiles | Double or parallel pipes |
|---|---|---|---|---|---|---|---|---|---|---|
| 1 | 2 | 3 | 4 | 5 | 6 | 7 | 8 | 9 | 10 | 11 |
| CAP *a* | 150 | 150 may have upper and lower pressure limits | No limit | 5 | Not available | Not available | 10 | 10 | No limit | 150 |
| ENSMP *b* | 300 | 300 | No limit | 30 | 20 PCO | Not available | 10 compr. Does not include loops | Not available | 5 standard type. No limit on specific type | 300 |
| | | | | 30 altogether | | | | | | |
| PIPETRAN *c* | 105 | 106 | 30 | 5 | 10 PCO<br>PCI<br>FCO<br>FCI<br>HPC<br>HPM | 10 PCO<br>PCI<br>FCO<br>FCI | No limit | Not available | 30 | 105 |
| SATAN *d* | 300 | 300 may have upper and lower pressure limits | No limit | 25 | 50 altogether | | 150 | No limit | 50 | Not available |
| | | | | | PCO<br>FCO<br>HPM | PCO<br>FCO | | | | |

| | | | | | | | | | | |
|---|---|---|---|---|---|---|---|---|---|---|
| PAN *e* | 275 | 400 | No limit | 20 | 25 PCO<br>PCI<br>FCO<br>HPM<br>HPC | 25 PCO<br>PCI<br>FCO | No limit | Not available | No limit | Not available |
| TGFS *f* | 200 | 200 | No limit | No limit | No limit<br>PCO<br>PCI<br>FCO<br>HPM<br>HPC | No limit<br>PCO<br>PCI<br>FCO | No limit | No limit | 99 | Not available |

PCO – Pressure-controlled outlet
PCI – Pressure-controlled inlet
FCO – Flow-controlled outlet
FCI – Flow-controlled inlet
HPC – Horsepower control
HPM – Horsepower maximum
ENSMP – Extended Network Systems Modelling Program; Engineering Research Station of Gas Council (England)
CAP – Control Advisory Program; Engineering Research Station of Gas Council (England)
PIPETRAN – Pipeline Transients, Electronic Associates Inc. (USA)
SATAN – Steady and Transient Analysis of Networks; Gas Council, London Research Station
PAN – Program to Analyse Networks, British Gas (Great Britain)
TGFS – Transient Gas Flow Simulation, Petroleum Engineering Department, TUHI (Hungary)

sections give a comprehensive survey after Csete and Tihanyi (1978) about some typical soluble problems.

*High pressure networks.* Determination of the impact of a new-made pipeline (pipe-network) regarding the hydraulic characteristic of the system. Choice of the optimum solution from a number of possible network extension variants. Operation-analysis of a new-made compressor-station. Design of the main parameters of a compressor-station (the number of the units: the determination of

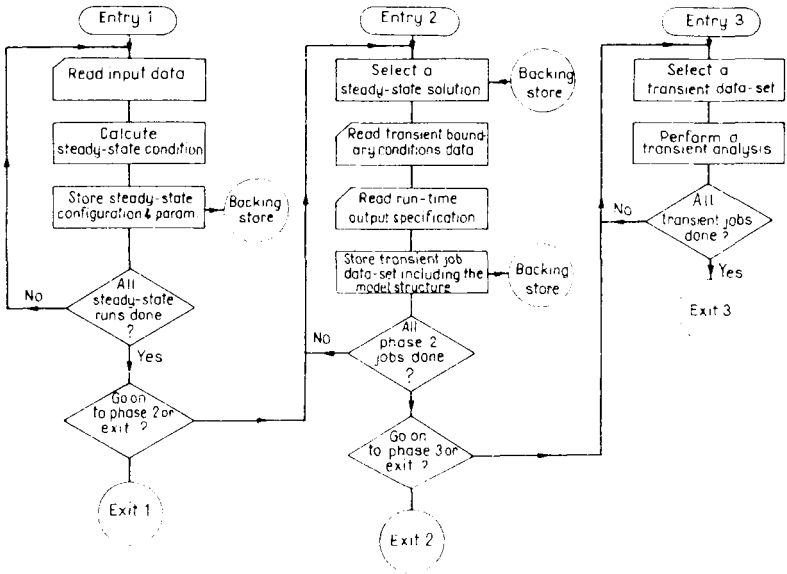


Fig. 8.5 – 2. The SATAN program, after Goacher (1969)

the power characteristics and that of the input and output parameters in function of the transport demand). Determination of the maximum deliverability of a given network considering the available limitations. Determination of the transport policy at a given network for transporting the demand with minimum energy consumption. In the case of joining different networks, calculation of the gas mixture composition at selected points. Preparing a transport schedule for the maintenance period. Finding the way of satisfying the consumer demand in the time of failure of source(s) inclusive of compressor units or compressor stations. Determination of the place(s) in the case of breakdown of different types.

*Middle-pressure network.* The modelling of the basic load map valid for the moment of simulation. Deciding the main transport demands of a complex network with given loads. Deciding if a new gas demand appearing at a given point or points can be fulfilled or not without network extension. Impact analysis of the effect of a load increase. In the case of several input points the determination of the supply

districts belonging to different sources at nearly horizontal terrain and if the network is created on a hilly surface with high level differences respectively. Determination of the transport capacity increase due to the increased input pressure. With several input points given the determination of the effect of the input pressures' change on the supply districts. Design of a network reconstruction. Determination of the network extension's impact on the hydraulic characteristics of the system. Impact analysis of the failure of a pipeleg. In the case of several sources the analysis of the failure of a district pressure regulator or of some sources respectively.

*Low pressure network.* The analysis of network extending variants, the choice of the optimum solution. The examination of the effect of a new district pressure regulator. Determination of the heat transport capacity of a network when changing from town gas to natural gas. Design of network reconstruction.

## 8.6. Pipeline transportation of natural gas; economy

In the previous Section, in connection with the flow simulation in gas transmission network, the optimum variant was mentioned several times. Here it was tacitly assumed that we intended to choose the network and mode of operation, that on one hand, is technically suitable to satisfy the consumer demands, and, on the other hand it requires the minimum possible transportation costs. It has been tacitly assumed too, that the gas volume demanded by the consumer is available at the required rate and fixed price. Such assumption is imaginable for imported gas, but not to such a degree if the source is a home gas field. The gas field and the gas processing plant are also parts of the gas supply system in this case. Rentability can also be influenced by the gas reserves of the fields, by the length of exploitation and by the production rate. The orders, and complementary technical methods, by which the daily or monthly rate of the production and transport can be stabilized all year round can also have a great economic significance. This will be discussed further on.

The duration of developing a gas field (drilling the gas wells, choosing the number of producing wells, the preparation and transmission equipment to be matched to them, the capacities and the construction and installation periods of these sets of equipment) may vary rather widely. Mayer-Gürr illustrates the economic importance of these factors on a simple example (Mayer-Gürr 1971). *Figure 8.6 – 1(a)* shows the first two sections of the typical production curve of a gas field, in three variants. The exploitable gas reserve of the field was assumed to equal 55 $km^3$. Three rhythms of exploitation have been invisaged. The first production period takes five years in all three. It is during this period that production is run up to full rated capacity. This latter is 4·5 $km^3$ in the first case, 3·0 in the second, and 2·25 in the third. This is the output that is desired to maintain over about 60 percent of the field's life. The period of level production is 10 years in the first case, 15 in the second

and 20 in the third. Part (b) of the Figure shows the drilling rates and numbers of wells required by the individual variants. The reason for drilling more wells even after the run-up period of five years is that, by the assumptions made, reservoir pressure and hence the productivity of the wells will decline during production. Part (c) of the Figure shows the first cost of wells and of production equipment in the field.

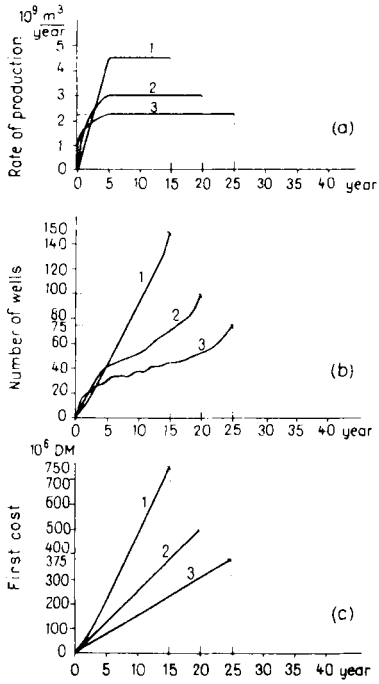


Fig. 8.6 – 1. Development costs of gas field, after Mayer-Gürr (1971)

First cost is seen to be exactly twice as high in the first case as in the third. The rhythm of development and the prescribed sustained level of production of the gas field does, then, substantially affect the economics of the regional gas supply grid.

The factors affecting the optimal operation of a gas supply system are, according to Graf (1971), as follows. (i) The load factor of the system should be as high as possible. (Load factor: ratio of mean to maximum hourly gas flow.) The load factor of the production system may differ from that of the supply system; the main reason for this is that one pipeline may convey gas coming from several gas fields. The gas supply company may, with a view to increasing the load factor, take the following measures: use the pipeline as a buffer storage facility (cf. Section 8.4); establish an underground stratigraphic storage capacity (storage field); use a reserve of liquefied gas, or propane injection, or high-pressure gas storage to ensure an excess supply

capacity for periods of peak demand. (ii) Of the above-enumerated measures, those are taken that ensure the most economical solution in any given case. (iii) Gas fields of various nature are to be produced in the most economical combination, possibly one after another. (iv) The system should ensure uninterrupted gas supply with a high degree of safety. The safety of supply can be measured by two factors. One is availability, which is the ratio of the aggregate length of uninterrupted supply periods to total time. The other is the reserve factor. The higher the availability the less reserve is needed in the form of parallel lines, underground storage capacity or standby peak-demand supply systems.

Underground storage in storage fields is a chapter of reservoir engineering. Here we shall just touch upon the essentials and the nature of the procedure. Natural gas may be stored in a gas reservoir, either exhausted or nearing exhaustion, in an exhausted crude oil reservoir, or in an aquifer. Requirements facing a reservoir are as follows. (i) It should have a cap-rock impervious to gas, (ii) it should have sufficiently high porosity and permeability, (iii) the storage wells should not establish communication between the formations traversed, that is, their casings should be cemented in so as to provide faultless packoff (isolation); (iv) it should be

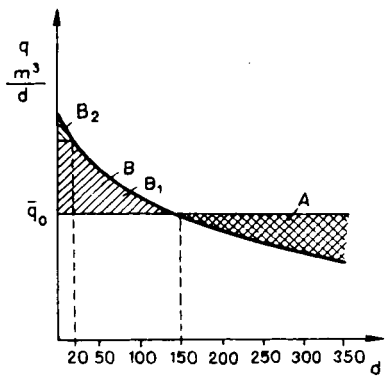


Fig. 8.6 – 2. Natural gas supply (after Kridner 1965)

situated close to the area of consumption, (v) the reservoir rock should be chemically inert vis-à-vis the gas to be stored. — The gas reservoir may be closed, with no inflow of water from below or laterally. The storage space may in such cases be regarded in a fair approximation as a closed tank whose volume equals the pore volume. In open reservoirs, decrease of pressure entails the inflow of water from below or from the periphery towards the centre of the reservoir. On the injection of gas into the reservoir, the gas-water interface will sink. The gas-filled volume of this type of underground reservoir is, then, variable. In the USA, underground storage reservoirs for the storage of natural gas have been in use since 1915, and G. C. Grow (1965) predicted the volume of such reservoirs to attain 35 percent of country-wide annual consumption by 1980.

The main purpose of an underground storage reservoir is to mitigate the economically harmful influence of seasonal fluctuations in demand. Such fluctuations are significant especially where one of the foremost uses of gas is in heating. In order to exploit the capacities of the production and transmission equipment more fully, a reserve is built up during the low-demand summer months in underground reservoirs (storage fields) close to consumption centres. This is where peak demand in the winter months is met from.

*Figure 8.6 – 2* is a typical diagram of natural-gas supply. The bold line shows the number of days on which daily consumption exceeds some arbitrary daily consumption $q_i$. The area below the curve equals the annual gas consumption, provided the axes are suitably calibrated. The average height of the area below the curve equals the mean daily consumption, $\bar{q}_o$. Assuming that the production equipment produces, and the transmission system conveys, a gas flow $q_o$ each day, the area $A$ indicates the volume of gas that can be stored up in the low-demand period. Area $B$, equal to area $A$, is proportional to the volume of gas to be taken out of the reservoir on high-demand days. The diagram reveals that, in the case

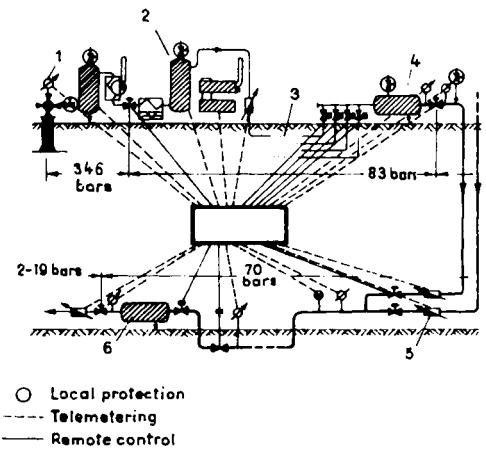


Fig. 8.6 – 3. The German Federal Republic's gas supply system, after Graf (1971)

considered, gas will have to be taken out of the reservoir over 150 days. Area $B$ is split in two parts. Gas volume $B_1$ is most expediently stored in a storage field, whereas the storage of volume $B_2$ by some other means may be more economical, because taking out $B_2$ of the storage field would need a fairly considerable increase of the gas production capability of the producing field, which is rather a costly affair. It may therefore be expedient to supply volume $B_2$ from, for example, high-pressure underground gas tanks, storage of liquefied gas, or of propane gas, etc. These methods have a copious literature.

Regional gas supply grids are usually too complicated to be operated optimally by unassisted men, in view of the continually changing demand and other conditions facing the system. This is why the process control of such systems is of so great an importance. Today's consensus is that joint off-line control by man and computer is to be preferred. One of the tasks of the computer is data acquisition and the presentation in due time of adequate information. In possession of this information, the dispatcher must be in a position to take optimal decisions and to

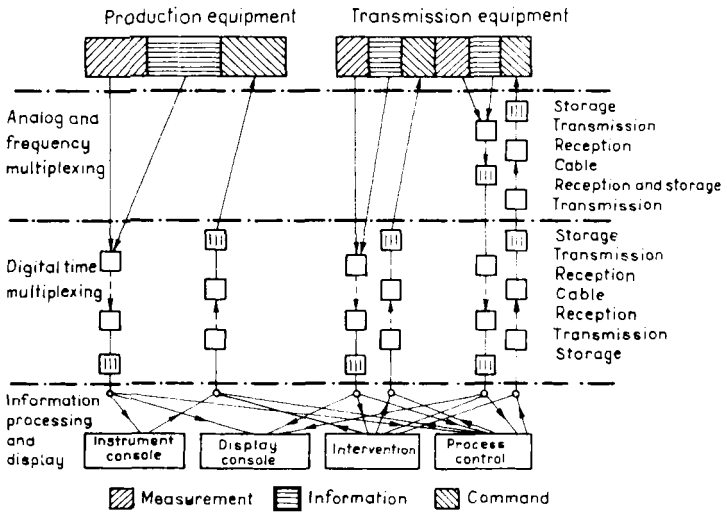


Fig. 8.6 – 4. Information transfer, display and control (Mittendorf and Schlemm 1971)

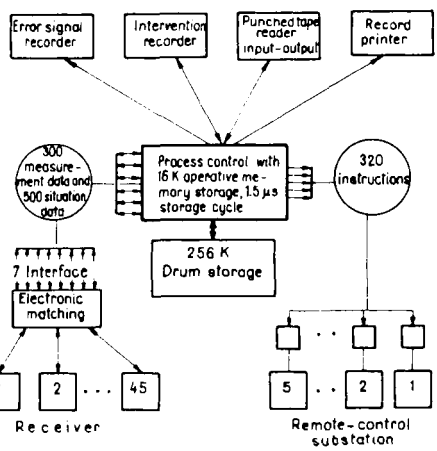


Fig. 8.6 – 5. Flow of information among telemetering, remote-control and program-control equipment (Mittendorf and Schlemm 1971)

implement them by remote control. The other main task of the computer is the on-line control of certain functions (Holland and Mix 1970). The first publication on off-line process control dates from 1966 (*Pipe Line News* 1966). Process control of gas supply systems has considerably spread since. Roberts (1970) describes the gas supply grid of Panhandle Eastern, controlled by a dispatcher assisted by an IBM-1800 computer. The grid incorporates pipelines of 2100 km aggregate length and supplies with natural gas 110 utilities catering to 22 million consumers. — Let us cast a brief glance on computer control, with the system realized at the Brigitta-Mobil Oil companies taken as an example. *Figure 8.6 – 3* is a schematic sketch of the journey of natural gas from the gas wells to the consumers. Gas is produced from wells *1*, and led through the dehydrators *2* installed next to each well into flowline *3* and through it into well centres *4*. From there, gas flows through transmission line *5* and enters the low-pressure utility at transfer station *6*. The data acquired all over the system is supplied to the central process control at Visbek. Critical points are provided with local automatic safety equipment (Graf 1971).

*Figure 8.6 – 4* is a schematic diagram of information flow and control (Mittendorf and Schlemm 1971). It is seen that both the dispatcher and the computer may give commands controlling both the production and transport equipment. *Figure 8.6 – 5* shows information flow between the computer, its peripheral units, and the remote-signalling and remote-control equipment.

# REFERENCES


ABRAMZON, L. S. (1968): Vybor temperatury podogreva nefti. *Transport i Khranenie Nefti i Nefteproduktov*, 4.

AHMED, S. (1984): Here are new approaches to tank farm construction. *Oil and Gas Journal*, Jan. 23.

ALIEV, R. A., BLEIKNER, E. M., KULKOV, V. A., LESHCHILIN, A. E. (1969): Opredeleniye raschetnykh reologicheskikh parameters smesei vysokozastivayushchei nefti s malovyazkimi razbavitelyami. *Transport i Khranenie Nefti i Nefteproduktov*, 8.

AMYX, J. W., BASS, D. M., WHITTING, R. L. (1960): *Petroleum Reservoir Engineering (Physical Properties)*. McGraw-Hill Book Comp. Inc., New York–Toronto–London.

ANDERSON, H. H. (1971): *Centrifugal Pumps*. The Trade and Technical Press Ltd Surrey, England.

ANDO, M., KAWAHARA, H. (1976): How skin effect tracing works. *Hydrocarbon Processing*, 12.

AUSTIN, J. E., PALFREY, J. R. (1963 – 64): Mixing of miscible but dissimilar liquids in serial flow in a pipeline. *Proc. Instn. Mech. Engrs.*

BABIN, L. A., VOLOKHOV, V. YA., KIM, B., RADYUN, L. V., DERTSAKYAN, A. K. (1972): Vybor optimal'noy trassy is sposoba prokladki magistral'nogo gazoprovoda. *Stroitelstvo Truboprovodov*, 1.

BALCKE, H. (1949): *Die Wärmeschutztechnik*. Verlag W. Knapp, Halle.

BARRETT, R. (1970): Unique "high efficiency" cyclone separator. *Europe and Oil*, 8.

BELHÁZY, T. Z. (1970): Die Entwicklung der Absperrorgane. *Gas und Wasserfach*, 3.

BERECZ, E., BALLÁNÉ, A. M. (1980): Gas Hydrates. Akadémiai Kiadó, Budapest and Elsevier, Amsterdam.

BÉRES DEÁK L., FILETÓTH A. (1975): The Analysis of the Pressure Surge in Pipeline-transport. *OLAJTERV*, Budapest, 11 (in Hungarian).

BLEAKLEY, W. B. (1970a): Humble takes a look at man's role in automated production. *Oil and Gas Journal*, Sept. 14 (1).

BLEAKLEY, W. B. (1970b): Pegasus automated to *n*th degree. *Oil and Gas Journal*, Nov. 2 (2).

BOBOK E. (1972): Determination of pressure losses in turbomachines. *Proc. 4th Conf. on Fluid Mech. and Fluid Machinery*, Akadémiai Kiadó, Budapest.

BONFIGLIOLI, G. P., CROCE, L (1970): Analog and numerical computers in the operation and design of gas network. *International Gas Union Conf.*, Moscow, Preprint C9-70.

BOTKILIN, A. I. MAJZEL', V. I. (1975): Trubi dlya gazoprovodov. *Gazovaya Promyshlennost*, 11.

BROD, M., DEANE, B. C., ROSSI, F. (1971): Field experience with the use of additives in the pipeline transportation of waxy crudes. *Journal of the Institute of Petroleum*, 3.

BROUSSARD, W. F., GRAVIS, CH. K. (1960): Three-phase separators. *World Oil*, 4.

BROWN, G. G. (1945): A series of enthalphy-entropy charts for natural gases. *Trans. AIME*, 160:65.

BURRELL, G. R., CORNETT, D. E., GREEN, B. F. (1970): Computerized multified data acquisition and control system. *SPE Preprint*, No. 2933.

BYERS, D. P. (1962 – 63): Handbook for LACT operation. *Pipe Line Industry*, 11:1962, 2:1963, 4:1963, 8:1963.

CABET, R. (1966): *L'économie du transport par conduite*. Société des Editions Techniques, Paris.

CAMPBELL, J. C. (1975): *Liquid pipeline leak detectors: how effective are in/out flow monitors?* Gas Pipeline Handbook, Energy Communications Inc., Dallas, Texas.

CAMPBELL, J. M. (1955): Elements of field processing. *Oil and Gas Journal*, Parts 2 – 5, 4 : 11, 5.9, 5.30, 6.20.
CAMPBELL, J. M. (1956): Separation of oil and water. *Oil and Gas Journal*, Oct. 29.
CANFIELD, F. B. (1971): Estimate K-values with the computer. *Hydrocarbon Processing*, 4.
CAPOT, M. (1966): *Les mesures*. Société des Editions Techniques, Paris.
CARR, N. L., KOBAYASHI, R., BURROWS, D. B. (1954): Viscosity of hydrocarbon gases under pressure. *Trans. AIME*, 201 : 264.
CARLSLAW, H. S., JAEGER, J. C. (1947): *Conduction of heat in solids*. Clarendon Press, Oxford.
CHANDRASEKHARAN, K. P., SIKDAR, P. K. (1970): Here's how waxy Indian crude is prepared for pipeline transit. *Oil and Gas International*, 10.
CHANISHEV, E. I., NECHVAL, M. B. (1971): Opredelenie ob'ema smesi po postledovatel'noy perekachke predvaritel'no podgretykh zhidkostey. *Izv. VUZ. NG.*, 12.
CHAPIN, R. L. WOODHALL, R. J. (1970): Analysis of an operating telemetring system at Elk Basin Field. *Journal of Petroleum Technology*, 4.
CHERNIKIN, V. I. (1958): *Perekachka vyazkykh i zastyuvayushchikh neftei*. Gostoptekhizdat, Moscow.
CHILINGAR, G. V., BEASON, C. M. (1969): *Surface Operations in Petroleum Production*. American Elsevier P. C., New York.
CHO, CH., HAMPEL, J., MCGINNIS, A. (1977): Modern control systems for liquid pipelines. *Pipeline and Gas Journal*, 7.
COHN, A. R., NALLEY, R. R. (1980): Using regulators for line pressure relief. *Pipe Line Industry*, 8.
CONRAD, P. G., GRAVIER, J. F. (1980): Peng-Robinson equation of state checks validity of PVT experiments. *The Oil and Gas Journal*, April 21.
COPIGNEAUX, P. (1980): Compare codes for relief valve calculations. *Hydrocarbon Processing*, 8.
COX, J. B., UNDERRINNER, C. F. (1970): Electronic-computer production management — a new era. *SPE Preprint*, No. 2934.
CRIDNER, C. W. (1974): Computer controls pipeline detection. *The Oil and Gas Journal*, Oct. 14.
CROSBY, J., BAXTER, W. (1978): Computer-aided pipeline scheduling increases system's flexibility. *The Oil and Gas Journal*. Feb. 6.
CROSS, H. (1936): Analysis of flow in networks of conduits or conductors urban. *Bulletin of University of Illinois*, 286.
CSETE, J. (1980): The strength calculation of the gas pipelines and the safety zone. *Bányászati és Kohászati Lapok, Kőolaj és Földgáz*, 8 (in Hungarian).
CSETE, J., SOÓS, I. (1974): The analysis of the carrying capacity of gas distributing networks of great level differences. *Energiagazdálkodás*, 11 – 12 (in Hungarian).
CSETE, J., TIHANYI, L. (1978): Modelling of gas networks of different pressure levels. *Energiagazdálkodás*, 6 (in Hungarian).
DAVENPORT, T. C., CONTI, V. J. (1971): Heat transfer problems encountered in the handling of waxy crude oils in large pipelines. *Journal of the Institute of Petroleum*, 5.
DEFELICE, CH. A. (1976): Flow simulator helps solve batch scheduling problems. *Pipe Line Industry*, 6.
DISTEFANO, G. P. (1970): *A digital computer program for the simulation of gas pipeline network dynamics*. PIPETRAN, Version IV, AGA, Catalog No. L20 000. 3.
DOBRINESCU, D., BULAU, L. (1969): Contribuţii la calculul termic al conductelor îngropate. *Petrol şi Gaze*, 2.
DUNHAM, C. L. (1977): A distributed computer network for oilfield computer production control. *Journal of Petroleum Technology*, 11.
EICHBERG, D. (1970): Zip-on jacketing insulates pipeline. *Oil and Gas Journal*, July 27.
ELLS, J. W., BROWN, V. R. R. (1971): The design of pipelines to handle waxy crude oils. *Journal of the Institute of Petroleum*, May.
ELPERIN, I. T., SMOLSKY, B. M., LEVENTAL, L. I. (1966): K voprosu umensheniya gidrodinamicheskogo soprotivleniya truboprovodov. *Inzhinerno-Fizicheszkiy Zhurnal*, 2.
FALK R. (1967): Mechanics I. Tankönyvkiadó, Budapest (in Hungarian).
FAYED, A. S., OTTEN, L. (1983): Comparing measured with calculated multiphase flow pressure drop. *Oil and Gas Journal*, Aug. 12.

FEIZLMAYR, A. H. (1975): Planung und Bau von Stationen für Mineralölfernleitungen. *Erdoel-Erdgas Zeitschrift*, 5, 6, 8.

FINCHAM, A. E. (1971): A review of computer programs for network analysis (developed at London Research Station). *The Gas Council Research Communications GC 189*, London.

FISHEL, F. D., HOWE, C. D. (1979): Cut energy costs with variable frequency motor drives. *Hydrocarbon Processing*, 9.

FOORD, A. G.,ROWE, T. S. (1981): 12 years of computerized piping design with ISOPEDAC. *Pipes and Pipelines International*, 8.

FORD, P. E. (1955): Pipelines for viscous fuels. *Proceedings of the Fourth WPC*, Section VIII.

FORST, T., SCHUSTER, H. G. (1975): Laengsnahtgeschweisste Grossrohre für Fernleitungen. *Das Gas- und Wasserfach. Gas Erdgas*, 3.

FRICK, TH. C. (1962): *Petroleum Production Handbook*. McGraw-Hill Book Co. Inc., New York, Toronto, London.

FROLOV, K. D., SEREDYUK, M. D. (1974a): Posledovatelnaya perekachka nefteproduktov s razdelitelnymi probkami iz ikh smesi. *Neftyanoye Khozyaistvo*, 9.

FROLOV, K. D., SEREDYUK, M. D. (1974b): Priem smesi v rezervuari pro posledovatelnoy perekachke s bufernym nefteproduktom. *Neftyanoe Khozyaistvo*, 12.

FULFORD, R. S. (1975): Oilwell paraffin prevention chemicals. *SPE Preprint*, No. 5614.

FUSSELL, D. D., YANOSIK, J. L. (1978): An iterative sequence for phase-equilibria calculations incorporating the Redlich-Kuong equation of state. *SPEJ*.

GAGEY, E. (1975): Leak detection with spheres. *Pipes and Pipe Line International*, 8.

GALATI, U., NAPOLITANO, C., CULZONI, F. (1979): Heated pipe line solves unloading problem offshore. *Pipe Line Industry*, 10.

GARRIS, N. A. (1984): O vozmozhnosti regulirovaniya raboti "goryachevo" truboprovoda v periodi sezonnoy nedogruzki. *Neft i Gas*, 3.

GAUTIER, M. (1970): L'expérience d'Elf Union sur le transport du fuel lourd par pipeline. *Revue de l'AFTP*, 11 – 12.

GERGELY, L., PANCZE, M. (1982): The computerized optimization of planning gathering systems on oil fields. *Bányászati és Kohászati Lapok, Kőolaj és Földgáz*, 9 (in Hungarian).

GIBBON, R. B., WALKER, A. (1978): Operational control of a natural gas transmission system. *The Institution of Gas Engineers*, Com. 1056, 5.

GOACHER, P. S. (1969): Steady and transient analysis of gas flows in networks. *The Gas Council Research Communication GC 157*, London.

GOLDWATER, M. H., ROGERS, K., TURNBULL, D. K. (1976): The Pan network analysis program — its development and use. *The Institution of Gas Engineers, Com. 1009*, London, 11.

GRAF, H. G. (1957): Vereinfachte Sammelstelle im Ölfeld. *Erdoel Zeitschrift*, 2.

GRAF, H. G. (1970): Stand der Automatisierung in der Öl- und Gasproduktion. *Erdoel-Erdgas-Zeitschrift*, 1.

GRAF, H. G. (1971): Dispatching von Erdgas. *Erdoel-Erdgas-Zeitschrift*, 9.

GRAVIS, CH. K. (1960): The oil and gas separator. *World Oil*, Jan.

GREATHOUSE, W. D., MCGLASSON, R. L. (1958): Progress in plastics for petroleum-production piping. *API Drilling and Production Practice*, Dallas.

GRIFFITH, R. A. (1970): Getty-operated 20-inch heated-crude pipeline. *Preprint SPE 3069*.

GROSSE, L. (1951): *Arbeitsmappe für Mineralölingenieure*. Deutscher Ingenieur-Verlag GmbH, Düsseldorf.

GUVIN, V. E., STEPANYUGIN, V. N. (1970a): Gidravlichesky raschet truboprovodov dlya perekachki neftei v smesi iz vodnym rastvorom PAV. *Neftyanoe Khozyaistvo*, 2.

GUVIN, V. E., STEPANYUGIN, V. N. (1970b): Optimalniye parametry dlya perekachki vysokovyazkikh i vysokozastyavyushchikh neftei v smesi s vodnym rastvorom PAV. *Neftyanoe Khozyaistvo*, 12.

GUDKOV, S. F., BENYAMINOVICH, C. A., ODISARIYA, G. E. (1970): Rational utilization fields of technological schemes for the natural gas large volumes transport. *International Gas Union Conf.*, Moscow, Preprint C-16-70.

GUY, J. J. (1967): Computation of unsteady gas flow in pipe networks. *Ind. Chem. Eng. Symposium*, London, No. 23.

HAARMANN, K. (1970): Metallurgical factors in producing steels for large diameter pipe. *World Petroleum*, 10.

HADDENHORST, H. G. (1962): Die Verpumpung von schwereren Erdölen durch Rohrleitungen. *Erdoel Zeitschrift*, 5.

HAIN, H. A. (1968): How to determine the maximum capability of a complex pipeline system. *Pipe Line News*, 9.

HARAY, F. (1969): *Graph Theory*. Addison Wesley, Massachusetts.

HARRISON, O. R. (1970): Planning and implementing a computer production control system. *Journal of Petroleum Technology*, 2.

HARVEY, I. O. (1980): Hand calculator program speeds flash calculation. *The Oil and Gas Journal*, March 31.

HATHAWAY, E. L. (1972): Overpressure protection is pipeline plus. *The Oil and Gas Journal*, Jan. 14.

HEINZE, F. (1971): Hydratbildung. *Lehrbogen 3.3 von Bergakademie Freiberg*.

HOLLAND, A. E., MIX, R. C. (1970): Computer aids gas dispatching. *Oil and Gas Journal*, Oct. 5.

HOPPMANN, G. (1976): Rechnergestützte Betriebsüberwachung einer Mineralölfernleitung. *3R International*, 9.

HOYT, J. W. (1972): The effect of additives on fluid friction. *Transaction of ASME. Journal of Basic Engineering*, 6.

Hydrocarbon leak detection with system pinpoints line breaks. *Pipe Line News*, 11. 1973.

JANSEN, J., COURAGE, G. (1977): Systemgerechte Berechnungen von Druckstossvorgaengen in Rohrleitungen. *3R International*, 2.

JONKER, P. E., PORTER, W. J., SCOTT, C. B. (1977): Control floating roof tank emissions. *Hydrocarbon Processing*, May 151.

KADYMOV, A. B., YUFIN, V. A., MUSAEV, V. G., MAGERRAMOV, F. G. (1984): Perehodniye processi v magistralnykh truboprovodakh pri regulirovanii rezhima raboty nasosnoy stantsii. *Neft i Gas*, 10

KARASSIK, I. J. (1977): Tomorrow's centrifugal pump. *Hydrocarbon Processing*, Sept.

KATZ, D. L. (1959): *Handbook of Natural Gas Engineering*. McGraw-Hill Book Co. Inc., New York, Toronto, London.

KATZ, D. L. (1972): Thermodynamic analysis of frictional heat effects in pipeline flow. *Oil and Gas Journal*, March.

KAUFMANN, T. G. (1968): A method for phase equilibrium calculations based on generalized Benedict–Webb–Rubin constants. *Industrial and Engineering Chemistry Fundamentals*, 2.

KEHOE, G. H. (1969): Advanced metering system runs U. K. products pipeline. *Oil and Gas International*, 3.

KISS, A. (1981): Continuous measurement of the water contents of hydrocarbons. *Automatizálás*, 12 (in Hungarian).

KOMICH, A. J. (1973): Proper selection of high capacity liquid meters. *Pipe Line News*, Apr. 7–8.

KORCHAZHKIN, M. T. (1963): Raschet protsessa drosselirovaniya prirodnogo gaza. *Gazovaya Promyshlennost'*, 7.

KREISS, M. (1972): Schnelle Erkennung von Leckagen an Rohrfernleitungen. *Erdöl und Kohle*, 7.

KREISS, H. (1976): Zur Simulation von Leckagen für die Überprüfung von Leckerkennungsanlagen. *3R International*, 7.

KRIDNER, K. (1965): What are needs for gas storage? *Pipe Line Industry*, 10.

KUBLANOVSKY, L. B., MURAVYEVA, L. I. (1970): Primenenie metoda konechnykh raznostei po "neyavnoi skeme" k recheniyu zadach neustanovivshegosya dvizheniya zhidkosti v napornykh truboprovodov. *Transport i Khraneniye Nefti i Nefteproduktov*, 10.

LAABS, H. (1969): Armaturen für den Transport von Erdöl, Erdgas und deren Produkten durch Pipelines. *Erdöl und Kohle, Erdgas, Petrochemie*, 12.

LAIRD, B. W. (1981): Inverting baseline increases gas-measurement accuracy. *Oil and Gas Journal*, March 16.

LAMB, M. J., SIMPSON, W. C. (1963): Pipeline transportation of waxladen crude oil as water suspension. *Sixth WPC*, Section VII, Paper 13.

LEHMANN, M. (1976): Mengen und Durchflussmessung mit Turbinenzählern. *VDI Berichte*, 254.

LESCARBOURA, J. A., CULTER, J. D., WAHL, H. A. (1970): Drag reduction with polymeric additive in crude oil pipelines. *Preprint SPE 3087.*

LESIC, A. (1973): Veliki cjevovodni sistemi kao integrativan faktor u naftnoj privredi. *Nafta* (Yug.), 8.

LESS, G. G. (1980): Standards for turbine meter measurement of fuel gas. *Pipe Line Industry*, 12.

LITTLE, L. F. (1963): Stock tank vapor recovery pays off. *World Oil*, June.

LIU, J. K. (1981): Use energy-efficient HVDs for mainline pump drives. *Pipe Line Industry*, 3.

MADDOX, R. N. (1963): Some properties of mixtures. *The Oil and Gas Journal*, March 4.

MAHER, J. L., COGGINS, R. W. (1969): How to estimate size, cost of producing equipment. Part 1. Separators and treaters. *World Oil*, Aug. 1.

MAKOWSKI, M. M., MOCHLINSKI, K. (1956): An evaluation of two rapid methods of assessing the thermal resistivity of soil. *Proceedings of the Institution of Electrical Engineers*, Oct.

MAPES, G. J. (1960): The low temperature separation unit. *World Oil*, Jan.

MARTIN, J. T. (1970): Low level automation for marginal leases. *Petroleum Engineer*, May.

*Mass flow Metering of Crude Oil.* Sereg Comptage des Liquides Industriels, 1978.

MATULLA, M. (1972): Die Durchmischung von schwarzen und weissen Mineralölprodukten, die in einer Rohrleitung hintereinander verpumpt werden. *Erdoel Erdgas Zeitschrift*, 9.

MAYER-GÜRR, A. (1971): Erdgas-Produzenten und Erdgas-Abnehmer. *Gasverwendung*, 10.

MCGHEE, E. (1957): How to get cheap daily tests on every well. *The Oil and Gas Journal*, April 8.

MENON, E. S. S. (1976): Design procedure can help select pumps for multiproduct pipelines. *The Oil and Gas Journal*, May 31.

MICHIE, T. W., PAGE, W. A., KIDD, A. H. (1970): Program for maintaining equipment reliability and data integrity in a large-scale computer production control project. *SPE Preprint*, No. 2935.

MITTENDORF, H., SCHLEMM, F. (1971): Prozessrechnereinsatz zur Leitungsüberwachung in Ferngasnetzen. *Erdoel-Erdgas Zeitschrift*, 11.

MOKHANOV, V. I. (1962): *Izmerenie razkhoda i kolichestva zhidkosty, gaza i para.* Gosenergoizdat, Moscow.

MORGAN, J. M. (1984): Gas pipeline building costs increase slightly. *Oil and Gas Journal*, Jan. 23.

MORSE, J. V. (1976): Field use of turbine meters in sand-laden oil. *Journal of Petroleum Technology*, 2.

MUKHOPADHYAY, A. I. (1979): Conditioning process solves crude transport problem. *Pipe Line Industry*, 6.

MUMA, W., HENRY, D. (1976): PLC system supervises crude pipeline. *The Oil and Gas Journal*, Nov. 22.

MURADOV, A., MAMETKLYCHEV, H. (1970): Opredelenie optimalnoi temperatury podogreva parafinovykh neftei pered perekachkoi. *Transport i Khraneniye Nefti i Nefteproduktov*, 6.

MÜLLER, W. (1977): Kunststoffrohre: Rohstoffe-Rohreigenschaften-Normung-Gütesicherung. *3R International*, 6.

MYERS, R. W. (1978): An electrically heated buried gathering system transports high-pour point crude oil. *Journal of Petroleum Technology*, 6.

Natural Gas Association of America (1957): *Equilibrium Ratio Data Book.* "K" values, Tulsa.

NAUDASCHER, E., MARTIN, W. W. (1975): Akustische Leckerkennung in Rohrleitungen. *3R International*, 12.

NEMATIZADEH, F. (1969): Silicone injection boosts separator capacity 40%. *World Oil*, May.

O'BRIEN, H. L. (1951): *Petroleum Tankage and Transmission.* Graver Tank and Mfg. Co. Inc., Houston, Texas.

O'DONNELL, J. P. (1968): Getty's new heated crude line is probably world's largest. *Oil and Gas Journal*, April 8.

O'DONNELL, J. P. (1973): Double-cup plunger finds use in fluid control. *Oil and Gas Journal*, Aug. 27.

*Oil and Gas Journal* (1956): Automatic custody transfer. June 11.

*Oil and Gas Journal* (1963): Treating plant will make high-wax crude transportable by pipeline. Feb. 25.

*Oil and Gas Journal* (1964): $500 000 automation investment. July 27.

*Oil and Gas Journal* (1969): Chemicals solve tank shortage. Jan. 27.

ORLICEK, A. F., PÖLL, H. (1951): *Hilfsbuch für Mineralöltechniker.* I. Band. Springer Verlag, Wien–New York.

ORLICEK, A. F., PÖLL, H. (1955): *Hilfsbuch für Mineralöltechniker. II. Band.* Springer Verlag, Wien–New York.

PÁPAY, J. (1970): Steady temperature distributions in producing wells and pipelines. *Kőolaj és Földgáz*, 11 (in Hungarian).

PÁPAY, J. (1971): Performance equations of oil reservoir, well and flowline. *Kőolaj és Földgáz*, 8 (in Hungarian).

PATSCH, F., CSETE, J., TIHANYI, L. (1974): Examination of the carrying capacity of the Hungarian high pressure gas network. *Bányászati és Kohászati Lapok. Kőolaj és Földgáz*, 2 (in Hungarian).

PEARSON, W. G. (1969): Is there a computer in your oil fields future? *Oil and Gas Journal*, May 26.

PEKTYEMIROV, G. A. (1951): Petroleum tankage handbook. NIK, Budapest. (Translation from Russian.)

PERKINS, T. K., TURNER, J. B. (1970): Starting behaviour of the gathering lines and pipelines when filled with gelled Prudhoe Bay oil. *Preprint, SPE 2997.*

PERRY, C. W. (1964): The modern ball valve. *Petroleum Times*, May 15.

PERRY, J. H. (1969): Chemical engineer's handbook. Műszaki Könyvkiadó, Budapest (in Hungarian).

Petroleum Extension Service (1955): *Oil Pipe Line Measurement and Storage Practice.* The University of Texas, Dallas.

Petroleum Extension Service (1956): *Field Handling of Natural Gas.* The University of Texas, Dallas.

*Pipe Line Industry* (1973): Ultrasonic device detects pinhole gas/oil leaks. 11.

*Pipe Line Industry* (1974): Big meter prover for Kiire terminal in Japan. 3.

*Pipe Line Industry* (1975): New concept-transport frozen oil slurry in LNG. 12.

*Pipe Line Industry* (1979): Surge relief system solves Soviet pipe line problem. 11.

*Pipe Line News* (1966): Pipe line news annual automation symposium. 10.

*Pipes and Pipeline International* (1976): Pressure surges in pipes. 10.

PLI Staff (1970): New triple action syphon pig leaves pipe lines clean and dry. *Pipe Line Industry*, 1.

PORAIKO, I. N., VASILENKO, S. K. (1975): O primenenii vodorastvorimykh polimerov dlya uvelicheniya proizvoditelnosti nefteproduktov. *Transport i Khranenye Nefti i Nefteproduktov*, 7.

PRESTON, T. S. (ed.) (1968): *Shell Flow Meter Engineering Handbook.* Waltmann Publishing Company, Delft.

PRICE, R. C. (1971): Flow improvers for waxy crudes. *Journal of the Institute of Petroleum*, 3.

PRUITT, G. T., SIMMONS, C. M., NEIL, G. H., CRAWFORD, H. R. (1965): A method to minimize the cost of pumping fluids containing friction-reducing additives. *Journal of Petroleum Technology*, 5.

RABINOVICH, E. Z., KUZNETSOV, P. B. (1970): Gidravlicheskie soprotivleniya magistralnykh nefteprovodov. *Transport i Khranenie Nefti i Nefteproduktov*, 7.

RABONE, N. S. (1979): Flow measurement and BGC — a "turbulent" affair. *Gas Engineering and Management*, 1.

REID, A. M. (1969): Valve design and selection. *Pipes and Pipelines International*, 4.

REINTSEMA, S. R. (1983): What's new in gas custody transfer measurement. *Pipe Line Industry*, 11.

*Report of the committee on the transmission of gases*, (1976): 13th World Gas Conference. C-76. London.

REPPISCH, I. (1958): Mengenmessung mit Ovalrad-Flüssigkeitzaehlern in der Erdölindustrie. *Erdoel Zeitschrift*, 8.

RESEN, L. (1957): Humble tries LACT, gives it stamp of approval. *Oil and Gas Journal*, March 4.

RITTER, R. A., BATICKY, J. P. (1967): Numerical prediction of the flow characteristics of thixotropic liquids. *Society of Petroleum Engineers Journal*, Dec.

ROBERTS, B. J. (1970): Pandhandle extends its automation. *Oil and Gas Journal*, July 23.

ROSE, S. C., MARSDEN, S. S. (1970): The flow of North Slope crude oil and its emulsions at low temperatures. *SPE Preprint* 2996.

ROWE, A. M. (1978): Internally consistent correlations for predicting phase compositions for use in reservoir composition simulators. *SPE* 7475.

ROY, C. E. (1984): Technological growth and future development will influence SCADA systems design. *Pipeline*, March.

SANDERS, J. M. (1969): Basic criteria for the sizing and selection of control valves. *Pipes and Pipelines International*, Oct. 12.

SAYE, H. A. (1958): Automatic well testing. *Oil and Gas Journal*, Jan.

SCOTT, R. W. (1965): Vacuum stabilizers boost income minimize production problems. *World Oil*, Jan.

SCOTT, J. (1967): Production automation breaks barriers. *Petroleum Engineer*, June.

SCOTT, J., CROSBY, G. (1970): What does industry expect of computer production control. *Petroleum Engineer*, May.

SEREG-SCHLUMBERGER (1978): *Mass flow metering of crude oil.* Sereg Comptage des Liquides Industriels.

SHAMIR, U. (1971): Optimal route for pipelines in two-phase flow. *Society of Petroleum Engineers Journal*, 215–22.

SHISHCHENKO, R. J., APRIESOV, K. A. (1952): Transport and storage of crude oil. NIK, Budapest. (Translation from Russian.)

SKINNER, D. R. (1977): Lightning protection for an oilfield automation and instrumentation system. *Journal of Petroleum Technology*, 11.

SMIRNOV, A. S., SHIRKOVSKY, A. I. (1957): *Dobicha i transport gaza.* Gostoptekhizdat, Moscow.

Société du Journal des Usines à Gas (1968): *Manuel pour le transport et la distribution du gas.* Paris.

SPEUR, A., JAQUES, A. W. H. (1977): Ein neuer Ultraschall-Molchmelder für Pipelines. *3R International*, 6.

SPEUR, A., MARKUSSE, A. J., VAN ARLE, L. G. M., VONK, F. J. (1975): Computer schedules Rotterdam-Rhine line. *The Oil and Gas Journal*, Nov. 8.

STANDING, M. B. (1952): *Volumetric and Phase Behaviour of Oil Field Hydrocarbon Systems.* Reinhold P. C., New York.

STANDING, M. B., KATZ, D. L. (1942): Density of natural gases. *Trans. AIME*, 146–159.

STARLING, K. E. (1973): *Thermodynamic Properties for Light Petroleum Systems.* Gulf Publ. Comp., Houston.

STEARNS, R. F., JOHNSON, R. R., JACKSON, R. M., LARSON, C. A. (1951): *Flow Measurement with Orifice Meters.* D. Van Nostrand Co. Inc., Toronto–New York–London.

STEPANOFF, A. J. (1948): *Centrifugal and Axial Flow Pumps. Theory, Design and Application.* Wiley, New York.

STONER, M. A. (1970): A new way to design natural gas systems. *Pipe Line Industry*, 2.

STONER, M. A. (1971): Sensitivity analysis applied to a steady state model of natural gas transportation systems. *SPE Preprint*, 3056.

STRADTMANN, F. H. (1961): *Stahlrohr Handbuch.* (6. Auf.) Vulkan-Verlag, Essen.

STREETER, V. L., WYLIE, E. B. (1967): *Hydraulic transients.* McGraw-Hill Book Co. Int., New York, Toronto, London.

STREETER, V. L., WYLIE, E. B. (1970): Natural gas pipeline transients. *Society of Petroleum Engineers Journal*, Dec.

STREETER, V. L., WYLIE, E. B. (1974): Transient analysis of offshore loading systems. *ASME publication*, Paper No. 74-Pet-2.

SZEREDAI, L. (1981): Continuous industrial measurement of viscosity. *Automatizálás*, 12 (in Hungarian).

SZILAS, A. P. (1966): *Erdölgewinnung.* Bergakademie Freiberg, Fernstudium.

SZILAS, A. P. (1967): Production, Handling and Transport of Natural Gas. Müszaki Könyvkiadó, Budapest (in Hungarian).

SZILAS, A. P. (1968): Startdruckaenderung eines in einer Erdölfernleitung abkühlenden strukturviskosen Öles. *Erdoel-Erdgas Zeitschrift*, 9.

SZILAS, A. P. (1979): *Optimum system of oil field production equipment.* Congresso Panamericano de Inginieria del Petrolio, Clave 3. 3.

SZILAS, A. P. (1980): Production system of oil field. *Bányászati és Kohászati Lapok. Kőolaj és Földgáz*, 1 (in Hungarian).

SZILAS, A. P. (1982a): Scientific bases of determining the industrial reserves of fluid reservoirs. *MTA X. Osztályának Közleményei*, 15/1–2 (in Hungarian).

SZILAS, A. P. (1982b): Interpretation of crude oil thyxotropy by gridshell structure. *Bányászati és Kohászati Lapok. Kőolaj és Földgáz*, 1 (in Hungarian).

SZILAS, A. P. (1983): Field-integrated production system cuts costs. *Oil and Gas Journal*, June 13.

SZILAS, A. P. (1984): Grid-shell theory, a new concept to explain thixotropy. *Rheologica Acta*, 1. 23.

SZILAS, A. P., NAVRATIL, L. (1978): Inversion of economy at non-isothermal flow of pseudo-plastic oil and solvent mixture. *Bányászati és Kohászati Lapok. Kőolaj és Földgáz*, 4 (in Hungarian).

SZILAS, A. P., NAVRATIL, L. (1981): Optimierung des Pipelinetransportes von hochviskosen, mit Fliessverbessern versetzten Erdölen. *Chem. Techn.*, 6.

SZILAS, A. P., OLÁH, M. (1978): The up-to-date control of oil transport. *Bányaipari Szakirodalmi Tájékoztató*, NIMDOK, Budapest, 3–4 (in Hungarian).

SZILAS, A. P., BOGNÁR, J., GERGELY, L., PANCZE, M. (1978): Computerized optimum design of the trace of pipelines. *Energia és Atomtechnika*, 2 (in Hungarian).

TAKÁCS, G. (1976): Comparison made for computer z-factor calculations. *Oil and Gas Journal*, Dec. 20.

TAKATSU, R., SUGAYA, S. (1977): Automatic pipeline control advances in Japan. *The Oil and Gas Journal*, Jan. 17.

TECHO, R. (1975): Product-line computer scheduling. *The Oil and Gas Journal*, Dec. 15.

TECHO, R. (1976): Pipeline hydraulic surges are shown in computer simulations. *The Oil and Gas Journal*, Nov. 22.

TECHO, R., HOLBROOK, D. L. (1974): Product pipeline scheduled using computers. *The Oil and Gas Journal*, Feb. 18.

TERRIS, J. (1965): How and when to automate oil producing facilities. *World Oil*, June.

THIELEN, H. (1971): Die Druckwellengeschwindigkeit in Pipelines unter dem Einfluss von Temperatur und Druck. *Rohre, Rohrleitungsbau, Rohrleitungstransport*, 11.

THIELEN, H. (1972a): Verfahren zur Ortung an Mineralölpipelines mit Hilfe der Laufzeitmessung von Druckwellen (Druckwellenortung). *Rohre, Rohrleitungsbau, Rohrleitungstransport*, 6.

THIELEN, H. (1972b): Druckstosserscheinungen in Rohrleitungen und ihre Berechnung. *Rohre, Rohrleitungsbau, Rohrleitungstransport*, 8.

THIELEN, H., BÜRMANN, W. (1973): Das Verhalten von Druckwellen beim Durchgang durch eine Pumpstation unter Berücksichtigung der Drosselung. *Rohre, Rohrleitungsbau, Rohrleitungstransport*, 4.

THOMAS, L. K., HANKINSON, R. W., PHILLIPS, K. A. (1970): Determination of acoustic velocities for natural gas. *Journal of Petroleum Technology*, 7.

THOMAS, N. L. (1965): Polyurethane foam insulates Australian heavy oil line. *Pipe Line Industry*, 5.

THOMPSON, D. D., NICKSIC, S. W. (1970): Frequency change can help improve bs and w monitor's accuracy. *Oil and Gas Journal*, Nov. 23.

THUMA, A., TÁNCZOS, L., BÁLINT, L. (1976): Application of simulation of pressure oscillation. *BME Vízgépek Tanszékének Közleménye*, 241.

TIHANYI, L. (1980): Simulation of flowing behaviours of gas transporting networks. *Energiagazdálkodás*, 4 (in Hungarian).

TIHANYI, L. (1982): Some problems of the computerized design of gas pipeline networks. *Bányászati és Kohászati Lapok. Kőolaj és Földgáz*, 3 (in Hungarian).

TÖRÖK, J., PÁPAY, J., HARASZTI, E., BERECZ, E., KASSAI, L. (1968): Phase equilibria and their application in petroleum engineering. NIMDOK, Budapest (in Hungarian).

TUGUNOV, P. Y. (1968): Opredelenie optimal'noy tolshchiny teplovoi izolatsii dlya magistral'nykh truboprovodov. *Neftyanoe Khozyaistvo*, 5.

VARACALLO, J. M. (1984): Changing to turbine meters can save money by reducing costs. *Pipeline and Gas Journal*, 11.

VERNOOY, B. (1980a): Fundamentals of pipe line pigging. *Pipe Line Industry*, 9.

VERNOOY, B. (1980b): Pipe line pigs have varied applications in operations. *Pipe Line Industry*, 11.

VERSCHUUR, E., DEN HARTOG, A. P., VERHEUL, C. M. (1971): The effect of thermal shrinkage and compressibility on the yielding of gelled waxy crude oils in pipelines. *Journal of the Institute of Petroleum*, May.

VIDA, M. (ed.) (1981): Plastic gas pipeline systems. OMFB tanulmány. *Műszaki Élet*, 3. 20 (in Hungarian).

VLADIMIRSKY, A. I., SAAKOV, YU. M., YUFIN, V. A. (1975): Posledovatelnaya perekachka neftei ili nefteproduktov s otborom chasti smesi na promezhutochnom punkte truboprovoda. *Neftyannoe Khozyaistvo*, 8.

VLADIMIRSKY, A. I., DRONGOVSKI, YU. M., ZAITSEV, L. A., IVANOV, YU. V. (1976): *Avtomatizatsiya i Telemekhanizatsiya Magistralnykh Nefteprovodov*. Nedra, Moscow.

VNIIOEHG (1969): *Sostoyanie i puty sovershenstvovaniya sbora i transporta nefti i gaza na promyshlakh Vostochnykh Rayonov SSSR*. Moscow.

WAFELMAN, H. R. (1969): Displacer operated level gauges most specified throughout Europe. *Europe and Oil*, 3.

WAGER, J. (1977): What's new in meter testing? *Pipeline and Gas Journal*, July.
WANG, C. B. (1972): Correlation of the friction factor for turbulent pipe flow of dilute polymer solutions. *Ind. Eng. Chem. Fundam.*, Vol. 11, No. 4.
WESTPHAL, K. (1952): Rohrleitungstransport von zaehflüssigen Rohölen mit hohem Stockpunkt. *Erdoel und Kohle*, 12.
WEYER, M. (1962): Über die Vermischung von Stoffen die in Rohrleitungen unmittelbar aufeinanderfolgen. *Brennstoff, Waerme*, Kraft, 6.
WHINERY, K. F., CAMPBELL, J. M. (1958): A method for determining optimum second stage pressure in three stage separation. *Journal of Petroleum Technology*, 4.
WHITE, G. L. (1964): Friction pressure reducers in well stimulation. *Journal of Petroleum Technology*, 8.
WIJDIEKS, J. (1971): Water hammer in large oil transmission lines. *Rohre, Rohrleitungsbau, Rohrleitungstransport*, 4.
WILKINSON, J. V., HOLLIDAY, D. V., BATEY, E. R. (1964): Analytic solution for gas flow. *Pipe Line Industry*, 11.
WITHERS, V. R. (1970): The expansion of an oil storage tank under the liquid head of its contents. *Journal of the Institute of Petroleum*, Jan.
WOOD, R. S. (1958): Capacitance-type B. S. and W. recorder. *Oil and Gas Journal*, Dec. 8.
*World Oil* (1970): Automation ideas improve marginal lease operation. June.
WRIGHT, R. E. (1981): Prime mover selection. *Oil and Gas Journal*, Feb. 16, 23.
WYLIE, E. B., STONER, M. A., STREETER, V. L. (1970): Network system transient calculations by implicit method. *SPE Preprint* 2963.
WYLIE, E. B., STREETER, V. L., STONER, M. A. (1972): Unsteady natural gas calculations in complex piping systems. *Society of Petroleum Engineers, Preprint 4004*, 7 p.
YOHO, M. L. (1978): Measuring thermal energy of fuel gases. *Pipe Line Industry*, 9.
YOUNG, H. A. (1975): Computersystem finds, reports pipeline leaks. *The Oil and Gas Journal*, 6.
YOUNG, T. R. (1960): Digital simulation of pipeline operation. *Pipe Line Industry*, 5.
YUFIN, V. A. (1976): *Posledovatel'naya perekachka neskolkykh nefteproduktov ili neftei odnomu truboprovodu.* Gubkin, Moscow.
ZACHARIAS, E. M. (1969): Sonic interface detector pays off in liquid lines. *Pipe Line Industry*, 7.
ZEINELOV, T. K., SARKISOV, E. T., BAGIRYAN, G. G. (1968): Teploizolatsiya neftegazoprovodov penopoliuretanom. *Gazovoe Delo*, 6.
ZIELKE, W. (1971): Einige Betrachtungen über die Berechnung in stationaeren Strömungsvorgaenge in Gasfernleitungen. *Das Gas- und Wasserfach*, 11.
ZONGKER, F. (1969): Testing program indicates advantages of polyurethane pipeline cleaning tools. *Europe and Oil*, 3.

# SUBJECT INDEX